November 2026

TECHNICAL AND REGULATORY GUIDANCE

Using Advanced Site Characterization Tools (ASCT-2)



Prepared By
The Interstate Technology & Regulatory Council (ITRC)
Advanced Site Characterization Tools Update Team

EXECUTIVE SUMMARY

The Interstate Technology & Regulatory Council's (ITRC) first guidance document on Advanced Site Characterization Tools (ASCT) was released in 2019. The guidance was developed to improve stakeholders' fundamental understanding of the application of ASCT and their role in acquiring and interpreting data to support conceptual site model (CSM) development, evaluate cleanup options, and meet the technical needs of projects. This updated guidance expands on the previous ASCT guidance to provide information that federal, state, and local regulators; contractors; and practitioners need to make decisions on the use of ASCT to collect high-resolution datasets to support traditional site characterizations or to implement a high resolution site characterization (HRSC).

The ASCT discussed in this guidance are divided into four general categories.

- Direct sensing tools
- Borehole geophysical tools
- Surface geophysical tools
- Remote sensing tools

In addition, an ASCT Selection Tool interactive spreadsheet and ASCT Technical Selection Matrices are provided to support the selection and evaluation of appropriate ASCT to meet the data needs of a project.

ASCT can play a cost-effective and beneficial role across a range of project sites, from small simple sites to larger or more complex settings. Descriptions and uses of a range of ASCT along with advantages and limitations of the tools are provided to help project teams select ASCT to support decisions during remedial investigations, as well as during subsequent remedial, feasibility, design, and implementation phases by obtaining quality site-specific data needed to improve understanding of the site conditions. ASCT can be used throughout the life cycle of an environmental project, which may reduce the backlog of case reviews, thereby saving time and money.

This guidance does not include all available ASCT but includes those most widely used and readily available. While this document contains extensive information on various ASCT, it is not a guide to designing a CSM or a user's manual for any specific ASCT.

ABOUT ITRC

ITRC is a national coalition focused on developing tools and strategies to reduce barriers to the deployment of innovative environmental technologies. ITRC produces documents and training to improve technical knowledge and expedite quality regulatory decision-making while protecting human health and the environment. With private and public sector members from all 50 states and the District of Columbia, ITRC truly provides a national perspective. More information on ITRC is available at **https://www.itrcweb.org**.

ITRC is a program of the Environmental Research Institute of the States (ERIS), a 501(c)(3) organization incorporated in the District of Columbia and affiliated with the Environmental Council of the States (ECOS). ECOS is the national, nonprofit, nonpartisan association representing the state and territorial environmental commissioners.

DISCLAIMER

The information provided in documents, guidance materials, fact sheets, training curricula, websites, webinars, videos, online tools, and other print or electronic resources created or distributed by the ITRC

(collectively “ITRC Materials”) is intended solely as a general reference to assist regulators, practitioners, and other stakeholders in evaluating and implementing environmental practices, technologies, and approaches.

ITRC Materials are developed through collaborative efforts involving representatives from government agencies, private sector organizations, industry, academia, nongovernmental organizations, and other interested parties. Participation in the development of ITRC Materials does not constitute endorsement of all content by any individual, employer, agency, organization, or affiliated entity.

ITRC Materials are provided for informational and educational purposes only and do not constitute legal, regulatory, engineering, scientific, technical, or other professional advice. ITRC Materials are not intended to serve as definitive guidance for any specific site, circumstance, or regulatory decision and are not a substitute for consultation with qualified professionals.

ITRC strives to provide information that is accurate and reliable as of the date of publication. ITRC Materials are provided “as is,” and users are solely responsible for evaluating the accuracy, completeness, relevance, and applicability of the information to their circumstances. Regulations, policies, scientific understanding, technologies, and industry practices may change after publication. Users should independently verify that information remains current before relying upon it.

ITRC Materials may not address all applicable health, safety, environmental, legal, or regulatory considerations associated with a particular technology, condition, site, or application. Users are responsible for determining compliance with applicable laws, regulations, ordinances, standards, permits, and other requirements. ITRC recommends consulting applicable statutes, regulations, standards, manufacturers, suppliers, safety data sheets, and qualified professionals regarding specific circumstances.

ITRC, ERIS, and ECOS make no representations or warranties, express or implied, regarding the accuracy, completeness, usefulness, merchantability, fitness for a particular purpose, or noninfringement of information contained in ITRC Materials. To the fullest extent permitted by law, ITRC, ERIS, and ECOS disclaim liability for any loss, claim, damage, injury, cost, expense, or other consequence arising from or related to the use of, reliance upon, or inability to use ITRC Materials.

Reference in ITRC Materials to any commercial product, process, technology, service, manufacturer, vendor, trademark, or trade name does not constitute or imply endorsement, recommendation, approval, or favoring by ITRC, ERIS, or ECOS. The inclusion of such references is for informational purposes only.

ITRC allows the use of artificial intelligence tools in the development of its materials, including brainstorming, research support, information synthesis, language editing, formatting, and the creation of illustrative graphics or figures.

All content included in ITRC Materials requires human review and oversight. Authors and contributors remain solely responsible for verifying the accuracy, completeness, appropriateness, and integrity of all content contained in ITRC Materials.

ITRC Materials may be revised, updated, replaced, or withdrawn at any time without notice.

FUNDING ACKNOWLEDGMENT

These materials were prepared as an account of work sponsored by an agency of the United States Government. Neither the United States Government nor any agency thereof, nor any of their employees, makes any warranty, express or implied, or assumes any legal liability or responsibility for the accuracy, completeness, or usefulness of any information, apparatus, product, or process disclosed, or represents

that its use would not infringe privately owned rights. Reference herein to any specific commercial product, process, or service by trade name, trademark, manufacturer, or otherwise does not necessarily constitute or imply its endorsement, recommendation, or favoring by the United States Government or any agency thereof. The views and opinions of authors expressed herein do not necessarily state or reflect those of the United States Government or any agency thereof.

This project has been funded wholly or in part by the United States Environmental Protection Agency under assistance agreement X5-84032001 to ECOS. The contents of this document do not necessarily reflect the views and policies of the Environmental Protection Agency, nor does the Environmental Protection Agency endorse trade names or recommend the use of commercial products mentioned in this document, as well as any images, video, text, or other content created by generative artificial intelligence tools, nor does any such content necessarily reflect the views and policies of the Environmental Protection Agency.

This material is based upon work supported by the Department of Energy EMCBC under Award Number DE-EM0005260.

Using Advanced Site Characterization Tools (ASCT-2)

Technical and Regulatory Guidance



November 2026

This document is a static PDF and is provided for informational purposes only. The content within is accurate as of the date of publication and will not be updated or maintained. Any references, links, or data contained herein may become outdated over time. For the most current information, please refer to the appropriate sources or contact the Interstate Technology & Regulatory Council. The Interstate Technology & Regulatory Council assumes no responsibility for any consequences resulting from the use of outdated or incorrect information.

Permission is granted to refer to or quote from this publication with the customary acknowledgment of the source. The suggested citation for this document is as follows:

ITRC (Interstate Technology & Regulatory Council). November 2026. *Using Advanced Site Characterization Tools.* ASCT-2. Washington, D.C.: Interstate Technology & Regulatory Council, ASCT Update Team. **https://itrcweb.org/**.

TABLE OF CONTENTS

1 INTRODUCTION 1

1.1 What Are ASCT? 1

1.2 Purpose and Scope 2

1.3 Document Organization 2

2 ASCT CHALLENGES AND PATH TO ACCEPTANCE 5

2.1 Survey of ASCT Usage 5

2.2 Challenges and Solutions 7

2.2.1 Cost 7

2.2.2 Lack of Understanding 8

2.2.3 Availability 8

2.2.4 Regulatory Issues 8

2.2.5 Potential Solutions 8

2.3 Site-Specific Regulatory Program Acceptance 9

3 ASCT IMPLEMENTATION 10

3.1 Conceptual Site Model 10

3.2 ASCT Application 11

3.3 ASCT Selection 12

3.3.1 ASCT Selection Considerations 12

3.3.2 Cost and Value Considerations 13

3.3.3 Important Outputs 16

3.4 Using Multiple ASCT Together 17

3.5 Comparison of Traditional Tools and Methods vs. ASCT 18

3.5.1 Supporting Tools 19

3.5.2 Additional Tools and Methods to Consider 19

3.6 Data Interpretation, Use, and Visualization 20

3.6.1 Effective Use and Communication of ASCT Data 20

3.6.2 Data Acquisition, Processing, and Interpretation 20

3.6.3 Data Quality 21

3.6.4 Data Management and Visualization 21

4 DIRECT SENSING 22

4.1 Selecting Direct sensing Tools 22

4.1.1 Access 23

4.1.2 Data Collection Design 24

4.1.3 Collection of Supporting Data 24

4.2 Cone Penetrometer Testing....28
4.2.1 What Is the Technology?....28
4.2.2 How Is the Technology Used?....29
4.2.3 What Are the Advantages?....32
4.2.4 What Are the Limitations?....32
4.3 Electrical Conductivity (EC) Probe....32
4.3.1 What Is the Technology?....32
4.3.2 How Is the Technology Used?....34
4.3.3 What Are the Advantages?....37
4.3.4 What Are the Limitations?....37
4.4 Hydraulic and Groundwater Profiling Tools....37
4.4.1 What Is the Technology?....37
4.4.2 How Is the Technology Used?....46
4.4.3 What Are the Advantages?....48
4.4.4 What Are the Limitations?....48
4.5 Membrane Interface Probe....50
4.5.1 What Is the Technology?....50
4.5.2 How Is the Technology Used?....54
4.5.3 What Are the Advantages?....61
4.5.4 What Are the Limitations?....61
4.5.5 Additional Information....64
4.6 Optical Image Profiler....65
4.6.1 What Is the Technology?....65
4.6.2 How Is the Technology Used?....68
4.6.3 What Are the Advantages?....75
4.6.4 What Are the Limitations?....75
4.7 Laser-Induced Fluorescence....77
4.7.1 What Is the Technology?....77
4.7.2 How Is the Technology Used?....80
4.7.3 What Are the Advantages?....91
4.7.4 What Are the Limitations?....92
4.8 Clear-Well....94
4.8.1 What Is the Technology?....94
4.8.2 How Is the Technology Used?....96
4.8.3 What Are the Advantages?....99
4.8.4 What Are the Limitations?....100

4.9 Borehole Liners 102
4.9.1 What Is the Technology? 102
4.9.2 How Is the Technology Used? 102
4.9.3 What Are the Advantages? 109
4.9.4 What Are the Limitations? 109
4.10 Passive Flux Meters 110
4.10.1 What Is the Technology? 110
4.10.2 How Is the Technology Used? 111
4.10.3 What Are the Advantages? 112
4.10.4 What Are the Limitations? 112
4.11 Point Velocity Probe 112
4.11.1 What Is the Technology? 112
4.11.2 How Is the Technology Used? 113
4.11.3 What Are the Advantages? 115
4.11.4 What Are the Limitations? 115
4.12 Distributed Fiber-optic Sensing Tools 116
4.12.1 What Is the Technology? 116
4.12.2 How Is the Technology Used? 117
4.12.3 What Are the Advantages? 119
4.12.4 What Are the Limitations? 119
4.13 Tools for Understanding Chemical and Biological Processes 120
4.13.1 NSZD Tools 120
4.13.2 Natural Attenuation Tools 122
5 BOREHOLE GEOPHYSICS 124
5.1 How to Select and Apply Borehole Geophysical Tools Using This Guidance Document 124
5.1.1 Tool Availability 126
5.1.2 Data Collection Design 126
5.1.3 Technical Advantages and General Limitations of Fundamental Logging Tools 127
5.2 Fluid Temperature 129
5.2.1 What Is the Technology? 129
5.2.2 How Is the Technology Used? 130
5.2.3 What Are the Advantages? 131
5.2.4 What Are the Limitations? 132
5.3 Fluid Resistivity (or Conductivity) 132
5.3.1 What Is the Technology? 132
5.3.2 How Is the Technology Used? 133

5.3.3 What Are the Advantages? 134
5.3.4 What Are the Limitations? 134
5.4 Mechanical Caliper 134
5.4.1 What Is the Technology? 134
5.4.2 How Is the Technology Used? 135
5.4.3 What Are the Advantages? 135
5.4.4 What Are the Limitations? 135
5.5 Optical and Acoustic Televiewer 136
5.5.1 What Is Optical Televiewer Technology? 136
5.5.2 What Is Acoustic Televiewer Technology? 137
5.5.3 How Is the Technology Used? 139
5.5.4 What Are the Advantages? 145
5.5.5 What Are the Limitations? 145
5.6 Natural Gamma Logging 146
5.6.1 What Is the Technology? 146
5.6.2 How Is the Technology Used? 147
5.6.3 What Are the Advantages? 148
5.6.4 What Are the Limitations? 149
5.7 Borehole Flowmeters 149
5.7.1 Heat-Pulse Flowmeter Logging 151
5.7.2 Impeller Flowmeter Geophysical Logging 156
5.7.3 Electromagnetic Flowmeter 158
5.8 Electrical Resistivity 161
5.8.1 What Is the Technology? 161
5.8.2 How Is the Technology Used? 162
5.8.3 What Are the Advantages? 164
5.8.4 What Are the Limitations? 164
5.9 Nuclear Magnetic Resonance 164
5.9.1 What Is the Technology? 164
5.9.2 How Is the Technology Used? 165
5.9.3 What Are the Advantages? 167
5.9.4 What Are the Limitations? 168
5.10 Borehole Video Survey 169
5.10.1 What Is the Technology? 169
5.10.2 How Is the Technology Used? 170
5.10.3 What Are the Advantages? 171

5.10.4 What Are the Limitations? 172
5.11 Other Borehole Geophysics Tools 172
5.11.1 Thermal Neutron 172
6 SURFACE GEOPHYSICS 175
6.1 How to Select and Apply Surface Geophysical Tools Using This Guidance Document 175
6.1.1 Tool Availability 176
6.1.2 Selecting Surface Geophysical Tools 177
6.1.3 General Geophysical Theory and Approach 177
6.2 Electrical Resistivity Imaging 179
6.2.1 What Is the Technology? 179
6.2.2 How Is the Technology Used? 179
6.2.3 Technology Implementation 182
6.2.4 What Are the Advantages? 188
6.2.5 What Are the Limitations? 189
6.3 Ground Penetrating Radar 193
6.3.1 What Is the Technology? 193
6.3.2 How Is the Technology Used? 193
6.3.3 Technology Implementation 196
6.3.4 What Are the Advantages? 201
6.3.5 What Are the Limitations? 201
6.4 Seismic Methods 202
6.4.1 What Is the Technology? 202
6.4.2 How Is the Technology Used? 202
6.4.3 Technology Implementation 203
6.4.4 What Are the Advantages? 209
6.4.5 What Are the Limitations? 210
6.5 Electromagnetic Surveys 212
6.5.1 What Is the Technology? 212
6.5.2 How Is the Technology Used? 212
6.5.3 Technology Implementation 215
6.5.4 Cost Issues 218
6.5.5 What Are the Advantages? 219
6.5.6 What Are the Limitations? 219
6.6 Other Surface Geophysics Tools 220
6.6.1 Gravity 220
6.6.2 Magnetotellurics 221

7 REMOTE SENSING 224
7.1 Introduction 224
7.1.1 Existing Remote sensing Data Availability 225
7.2 Sensors 226
7.2.1 RGB camera 227
7.2.2 Multispectral and Hyperspectral Cameras 229
7.2.3 Thermal Camera 234
7.2.4 LiDAR 235
7.2.5 Less Common Sensors 237
7.2.6 Data Processing, Storage, and Analysis 240
7.3 Remote sensing Platforms 243
7.3.2 Manned Aircraft 244
7.3.3 Unmanned Aerial Systems (Drones) 244
7.4 Drone-based Environmental Monitoring and Sampling 253
7.4.1 Environmental Media Sample Collection 253
7.4.2 Air Monitoring 255
8 CASE STUDIES 264
8.1 Case Study 1—Pre-excavation Scoping at the Satus Store, Washington 264
8.2 Case Study 2—Understanding Contaminant Pathways at Heflin's Garage, Fredericksburg, Virginia 265
8.3 Case Study 3—LNAPL Identification and Delineation, and Assessment of Petroleum Vapor Intrusion Risk at TJ's Quik Stop, Poplar, Montana 265
8.4 Case Study 4—Hydrogeologic Framework and Extent of Saltwater Intrusion in Kings, Queens, and Nassau Counties, Long Island, New York 266
8.5 Case Study 5—Use of Multiple Direct sensing Technologies and 3D Visualization to Complete a High Resolution Site Characterization of a DNAPL Pool 266
8.6 Case Study 6—Surface Geophysics: Electrical Resistivity 267
8.7 Case Study 7—Site Contamination Assessment of Legacy Groundwater Impacts to Inform Regulatory Action, Somerton Park, South Australia 268
8.8 Case Study 8—Managing a Catastrophic Release to Achieve Rapid Decision Making and Minimizing Long-term Impacts 268
ACKNOWLEDGMENTS 270
GLOSSARY 273
ACRONYMS 280
REFERENCES 284
APPENDIX A. SUMMARY AND SELECTION RESOURCE FOR THE PVP FAMILY OF TOOLS A-1
APPENDIX B. REMOTE SENSING DATA SOURCES B-1
APPENDIX C. REMOTE SENSING AIR SAMPLING TOOLS C-1

LIST OF EQUATIONS

Equation 4-1. Corrected HPT pressure. 41
Equation 4-2. Thiem equation. 105
Equation 5-1. Conversion of specific conductance from fluid resistivity. 132
Equation 5-2. Resistivity of subsurface materials to the flow of electrical current 161

LIST OF FIGURES

Figure 2-1. Breakdown of affiliation of survey responses. 5
Figure 2-2. Barriers to ASCT implementation. 6
Figure 2-3. Survey responses to what sorts of beneficial information to include in the document update. 6
Figure 2-4. Comparison of select state agency responses for barriers from the 2018 state survey and the 2025 team private and state surveys. 7
Figure 3-1. Expert individual and average cost impacts when using direct sensing tools for high resolution site characterization (HRSC) compared to traditional techniques alone across three petroleum underground storage tank (UST) release scenarios. 14
Figure 3-2. Expert individual and average estimates of changes to project durations when using direct sensing tools for high resolution site characterization (HRSC) compared to traditional techniques across three underground storage tanks (UST) release scenarios. 15
Figure 3-3. High resolution site characterization (HRSC) cost estimates for 3- and 5-day investigations (responses provided by state and federal regulators and technology providers and consultants). 16
Figure 3-4. Graphic representation of how the ASCT groups can be used together to develop a conceptual site model at different scales and degrees of precision. 17
Figure 3-5. Graphic representation of accuracy and precision: the difference between using ASCT and traditional tools. 18
Figure 4-1. Direct sensing tools. 23
Figure 4-2. Typical CPT configuration. 29
Figure 4-3. Soil behavior types (the interpreted lithology). 30
Figure 4-4. Typical CPT log. Total cone tip resistance (qt), sleeve friction (fs), friction ratio (Rf), pore pressure (u, pounds per square inch), soil behavior type (SBT). 30
Figure 4-5. Typical EC measurements for sand, silt, and clay. 32
Figure 4-6. Example of EC logs along a cross section. 33
Figure 4-7. EC probe with four-pole Wenner array (A) and simple dipole (B). 34
Figure 4-8. Geoprobe FI 6000 laptop display and field instrument. 34
Figure 4-9. EC log (right) with associated probe advancement rate log (left). 35
Figure 4-10. EC log (solid black line) and superimposed HPT pressure log (dashed purple line) corrected for hydrostatic pressure. 36
Figure 4-11. Capabilities of Geoprobe hydraulic and groundwater profiling tools. 38

Figure 4-12. Downhole probe components of the HPT. The pressure sensor is shown outside of the connection rod but is actually located inside the rod during use. 40
Figure 4-13. HPT-EC log with calculated K and SEC and comparison to offset lithology log from a confirmation sonic boring. 41
Figure 4-14. Example cross-section profile of HPT-EC logs across alluvial aquifer paleochannel to identify location and screen placement for production wells 42
Figure 4-15. Waterloo APS tool tip options (150, 175, and 225 versions) and instrument. 43
Figure 4-16. Waterloo APS operator purging groundwater from the sample interval, recording water-quality parameters, and preparing for sample collection. 44
Figure 4-17. The HPT-GWS probe shows 5 of the 20 injection and sampling ports, and the EC dipole at the tip of the probe. 45
Figure 4-18. A log from the HPT-GWS tool, including the corrected pressure, EC, and results of analytical dissolved anion/cation data from samples collected at 10-foot intervals. 45
Figure 4-19. Geoprobe hydraulic profiling tool and groundwater profiler (HPT-GWP). 46
Figure 4-20. Components of a typical MIP system. 50
Figure 4-21. The MIP probe. 51
Figure 4-22. MIP principles of operation. 51
Figure 4-23. Commonly used SRI gas chromatograph (left). On typical modern MIP systems housing three VOC detectors (right), from left to right, XSD, FID, and PID. 52
Figure 4-24. A MIP log collected at a former chemical manufacturing facility. 53
Figure 4-25. An example of a MIP log run at an oil field site with a pipeline condensate release 55
Figure 4-26. Interpreted low-level MIP log including HPT and EC data (LL-MiHPT) 56
Figure 4-27. Response test—method of introducing an aqueous standard to the membrane. 58
Figure 4-28. Example of soil sample confirmation sampling 59
Figure 4-29. MIP logs located at the same project site, one run in standard sensitivity mode (left) and the other in low-level sensitivity mode (right). 60
Figure 4-30. Common MIP detectors and example contaminants detected. 63
Figure 4-31. OIP controller instruments and data acquisition components. 65
Figure 4-32. The three currently available OIP tools include OIP-UV, OIP-UVR, and OIP-G. 65
Figure 4-33. OIP software display. 66
Figure 4-35. An OIP-HPT log with EC on left, HPT injection pressure in the middle, and percent area of fluorescence on right. 67
Figure 4-34. OIP probe with attached CPT cone. 67
Figure 4-36. NAPLs detected by the OIP suite of tools. 68
Figure 4-37. Spectra diagram showing the excitation wavelength of the UV LED light source, the range of emission wavelengths measured (375 nm–550 nm), and the blocked wavelengths above 550 nm. 68
Figure 4-38. Use of visible light on OIP-UV tool to produce continuous soil color strip logs. 69

Figure 4-39. OIP-G tool: Spectra diagram showing the excitation wavelength of the green LED excitation source at 520 nm, the blocked emissions from 375 nm to 590 nm, and measured emissions from 590 to 750 nm. 70

Figure 4-40. OiHPT-G log: Log collected as part of an investigation of MGP waste release 70

Figure 4-41. OIP-UVR tool: Spectra diagram showing the excitation wavelength of the UV (275 nm) LED light source, the range of visible fluorescence emission wavelengths measured (375 nm-550 nm) by the camera, the UV range fluorescence emission wavelengths (300–400 nm) measured by the photometer sensor, and the blocked emission wavelengths filtered above 550 nm. 71

Figure 4-42. OiPHPT-UVR log: This log comes from a jet fuel release investigation 71

Figure 4-43. Bench-scale test images of seashell chips as seen under visible (left) and UV (right) light using OIP sensor. 73

Figure 4-44. Examples of insitu mineral fluorescence under OIP-UV 73

Figure 4-45. Side by side images of visible (white) light and UV light mineral fluorescence versions of the same soil image 74

Figure 4-46. A confirmation core was collected in an offset boring to OIP-UV log 76

Figure 4-47. CSM with LIF logs plotted in 3D (colors are relative %RE with red being highest). 78

Figure 4-48. LIF tool and associated sensor (EC). 79

Figure 4-49. The three LIF systems and their associated NAPL types. 80

Figure 4-50. Composite UVOST log containing typical responses for gasoline, diesel, false positive soils, and kerosene. 81

Figure 4-51. Fluorescence photos (308-nm laser) with UVOST waveforms for common NAPLs in 20–40 mesh silica and quartz sand at 10% moisture. 82

Figure 4-52. UVOST response (%RE) of common fuels across a wide range of NAPL concentrations. 83

Figure 4-53. Example TarGOST log, with callout 2 (creosote NAPL lens), and callout 4 (natural organics), whose fluorescence is indiscernible with the exception of the tau trend behavior. 84

Figure 4-54. Example TarGOST responses versus heavy NAPL content (mg/kg). 85

Figure 4-55. Conceptual diagram showing a DyeLIF probe passing through a DNAPL-impacted soil formation. 86

Figure 4-56. Example DyeLIF log. 87

Figure 4-57. Well casing for field Installation (top) and field use of the portable surveying Clear-Well instrument (bottom). 94

Figure 4-58. Schematic diagram of well casing construction. Examples shown use 1 or 2 Clear-Well viewable sections 95

Figure 4-59. Clear-Well portable surveying unit (left) and details of the Clear-Well probe construction (right). 96

Figure 4-60. Illustration of operating principles of the Clear-Well technology 97

Figure 4-61. Images obtained under visible and UV (265 nm) light after the first identification of plant root growth (time 0) 98

Figure 4-62. Comparison of three surveys from a ~2ft interval at a pipeline spill over an 11-month period 98

Figure 4-63. Detailed white light images (top) and UV (265 nm) obtained at a former refinery over a period of 10 months 99
Figure 4-64. Comparison of surveys obtained using multiple excitations at the same soil location. 100
Figure 4-65. Differences in NAPL morphology upon water-saturated (left) and water-unsaturated (right) surveys 100
Figure 4-66. Simple eversion of flexible liner. 103
Figure 4-67. Acoustic televiewer logs recorded with and without a liner in the same borehole. 104
Figure 4-68. Examples of NAPL stains on the inside surface of a cover. 106
Figure 4-69. FACT components. 107
Figure 4-70. FACT results with transmissivity. 108
Figure 4-71. Passive flux meter monitoring well installation and PFM device. 111
Figure 4-72. (A) Computer rendering of the PVP components and design. (B) Plan view of schematic of the PVP illustrating tracer (red) movement across the surface of the probe and detection wires. 113
Figure 4-73. Schematic cross section of a fiber-optic installation in more than one borehole. 117
Figure 4-74. 3D perspective view of a DTS borehole network to monitor low-temperature biodegradation remediation of groundwater 118
Figure 5-1. Borehole geophysics tool summary. 125
Figure 5-2. View of the overall geologic framework using 2D representation. 127
Figure 5-3. View of the overall geologic framework using 3D representation. 127
Figure 5-4. Examples of downhole fluid temperature log and composite logs. 130
Figure 5-5. Example composite log of fluid temperature (blue line) along with fluid resistivity (red line), natural gamma, acoustic, acoustic caliper, and tadpole plots used to denote structural orientation of planar features. 131
Figure 5-6. Example borehole log including optical and acoustic televiewer, inferred structural characteristics (tadpole plots), fluid temperature (blue line), fluid resistivity (red line), and stressed HPFM measurements. 133
Figure 5-7. Optical televiewer. 136
Figure 5-8. Acoustic televiewer. 137
Figure 5-9. Acoustic log image. Darker intervals on the OTV and ATV indicate fractures and bedding planes. 138
Figure 5-10. Illustration of concepts of apparent dip vs. true dip. 139
Figure 5-11. Planar features such as fractures intersecting the borehole wall follow sinusoidal traces. 140
Figure 5-12. Down-dip well siting example (left); planar feature orientation along dip and implications for monitoring accuracy (right). 140
Figure 5-13. Unrolled format shows the borehole image, cut vertically at north and rolled out from left to right, often with vertical lines representing N (at the left), E, S, W, and N (again at the right). 141
Figure 5-14. Example of a structure log (incorporating both OTV and ATV). 142

Figure 5-15. Example stereonet plots commonly used to represent conditions throughout the borehole. 143
Figure 5-16. Example gamma log output with caliper log and lithology. 148
Figure 5-17. Flow within borehole. 150
Figure 5-18. HPFM. 152
Figure 5-19. Heat pulse flowmeter data presentation and analysis. 155
Figure 5-20. Impeller flowmeter probe. 156
Figure 5-21. Corehole Dynamic Flowmeter™ (manufactured by Century Geophysical, Inc.) is an example of an electromagnetic flowmeter. 159
Figure 5-22. Example electric log with spontaneous potential (left column), normal resistivity (16 inch and 64 inch), and single-point resistance outputs. 163
Figure 5-23. Sensitive shell (diameter from center of tool) where NMR data are collected. 165
Figure 5-24. Example NMR output. 166
Figure 5-25. Example borehole video camera systems. 169
Figure 5-26. Examples of screenshots from several borehole video surveys. 170
Figure 6-1. Surface geophysics tool summary. 175
Figure 6-2. Photo of ERI survey being conducted through a building (left). Photo of an ERI survey being conducted over a railyard (right). 180
Figure 6-3. Coal tar –impacted ERI image with water main perpendicular to image using higher-sensitivity GeoTrax Survey™ ERI. 181
Figure 6-4. Instrumentation commonly associated with collecting ERI data 183
Figure 6-5. Configurations and photos for (upper) temporary electrode stakes for ERI surveys and (lower) permanent cable installation for TERI monitoring. 184
Figure 6-6. Photo of ERI survey being conducted through a waterway (left). Photo of an ERI survey being conducted with a traffic crossing at a fueling station (right). 189
Figure 6-7. Water supply electrical imaging of mile section block of the Ogallala aquifer using higher-sensitivity GeoTrax Survey™ ERI. 191
Figure 6-8. Example of electrically resistive LNAPL anomalies (modified from data from Halihan et al. (2005)) using higher-sensitivity GeoTrax Survey™ ERI. 192
Figure 6-9. GPR implementation involves a pulse of EM energy traveling from a transmitter to a receiver antenna and contrasts in conductivity return a reflection in the GPR record. 194
Figure 6-10. View of the GPR technology decision-making process for the application of GPR technology. 195
Figure 6-11. Schematic of a GPR survey of sewer line 199
Figure 6-12. 3D GPR block view of response contrast for metallic objects in relation to 2D horizontal slices. 200
Figure 6-13. General seismic graphic depiction of an MASW field survey and field records imaging multiple types of seismic waves that can be distinguished and then showing how the data can be analyzed. 204
Figure 6-14. Simple seismic reflection record. 207

Figure 6-15. FDEM instrument components. 213
Figure 6-16. Example of duo central receiver coils with the WalkTEM system. 214
Figure 6-17. Example of an FDEM survey mapping variations in conductivity across a wetland impacted by leachate plumes from landfills. 215
Figure 7-1. Overview of sensors with example project use cases. 225
Figure 7-2. Electromagnetic spectrum. 226
Figure 7-3. Multispectral data vs. hyperspectral data. 230
Figure 7-4. The typical reflective spectra for various land surface materials from the ASTER Spectral Library. 231
Figure 7-5. Example of a drone-based thermal camera. 234
Figure 7-6. Example of a LiDAR sensor. 235
Figure 7-7. LiDAR pulse with different returns. 236
Figure 7-8. Schematic of drone-based GPR. 237
Figure 7-9. SPH Engineering SENSYS MagDrone R1 with rigid mount. 238
Figure 7-10. Geometrics MagArrow II 239
Figure 7-11. Magnetometer survey results as shown in geophysical software (Oasis-Montage). 239
Figure 7-12. Availability and spatial extent of the three types of platforms. 243
Figure 7-13. Water sampling using a drone. 254

LIST OF TABLES

Table 2-1. Summary of challenges and potential solutions. 8
Table 4-1. A guide to analyte detection levels in bulk formation using the MIP system and typical detectors. 62
Table 4-2. Inferring analyte category based on response(s) of MIP multidetector system. 62
Table 5-1. Typical electrical resistivities of earth materials. 161
Table 5-2. Example NMR tool specifications. 168
Table 7-1. Cloud-based versus desktop: Elements to consider when selecting cloud-based versus desktop data processing and storage. 241
Table 7-2. Estimates for standard photogrammetry. 242
Table 7-3 Platform attributes. 245
Table 7-4. Drone sizes and specifications. 247

1 INTRODUCTION

An effective site characterization begins with developing or updating a conceptual site model (CSM) based on a thorough review of existing information. Advanced site characterization tools (ASCT), selected appropriately and used wisely, will help quickly develop a more precise and accurate CSM. ASCT produce multifaceted datasets that strengthen the CSM, reduce uncertainty, and provide a defensible technical basis for more targeted and effective remedial strategies.

1.1 What Are ASCT?

ASCT are technologies that can rapidly collect detailed information about subsurface conditions, locations of contaminants of concern, and site geology. Through the use of an individual tool or a combination of tools, they provide geologic, hydrogeologic, and chemical data to support traditional and high resolution site characterization (HRSC) to delineate contaminant plumes, support remedial decisions, and reduce investigation time and costs. ASCT can enhance, supplement, or replace traditional characterization methods by delivering high-resolution data in the field, enabling quicker informed decision-making throughout the investigation process. Traditional characterization methods referred to herein generally involve the installation of multiple rounds of soil borings and monitoring wells and the direct collection of physical data (to characterize the subsurface, such as borehole logging) and environmental media samples for off-site laboratory analysis of target chemicals (to identify and evaluate the distribution of contaminants of concern) to provide data suitable for acceptance by most regulators.

ASCT are capable of rapid implementation and data generation and can be used to provide data for a more precise and accurate CSM. ASCT generate continuous, high-resolution datasets that characterize site conditions across two, three, or four (temporal) dimensions, revealing spatial and temporal relationships in geologic variability, preferential pathways, and contaminant distribution at scales that traditional data collection cannot resolve. These capabilities help target investigations and remedial actions in the most beneficial areas, potentially reducing characterization and monitoring costs while improving results. Many ASCT have multipurpose instruments or combinations of instruments designed to simultaneously collect geologic and contaminant data in a single deployment, producing an integrated dataset that strengthens the CSM, reduces uncertainty, and supports more effective remedial strategies.

ASCT have greatly expanded data types and data resolution and therefore the understanding of contaminant distribution, concentration, and mass, as well as the stratigraphy and physical characteristics of the contaminated media. Although these tools have been available for several years, they often are not used because users:

- perceive them to be expensive and unavailable
- do not understand how ASCT work
- do not know how to interpret the acquired data

Yet advances in computing and supporting technologies have vastly improved data analysis, visualization, and accessibility of ASCT data. The amount of data collected versus time invested exceeds that provided by more traditional approaches (such as laboratory analysis of soil samples, monitoring well installation, and groundwater sampling with laboratory analysis). ASCT are now more readily available as the number of companies offering these services in more locations has increased.

ASCT are typically used in HRSC but can also be used in traditional site characterizations to provide high-resolution data that can significantly reduce uncertainty, improve the delineation of contamination, improve remediation strategies, and support the design of more effective remediation strategies. ASCT complement traditional quantitative data collection by helping ensure that traditional quantitative data are

collected in the right place. This well targeted traditional data can be used to provide valid correlations and comparisons between ASCT and the traditional data.

1.2 Purpose and Scope

This guidance document expands on the previous ASCT guidance document to provide information that federal, state, and local regulators; contractors; and practitioners need to make decisions on the use of ASCT to collect the high-resolution datasets to support traditional site characterizations or to implement HRSC. This guidance document can be used throughout the life cycle of an environmental project, helping to identify and use ASCT. ASCT can play a cost-effective and beneficial role across a range of project sites, from small simple sites to larger or more complex settings. Descriptions and uses of a range of ASCT along with advantages and limitations of the tools are provided to help project teams select ASCT to support decisions during remedial investigations, as well as during subsequent feasibility and remedial design and implementation phases by obtaining quality site-specific data needed to improve understanding of the site conditions. Using real-world examples of ASCT use, such as at rural gas stations or convenience store sites, dry cleaners, and Superfund sites, this guidance document provides information to dispel the myth that these tools are too often prohibitively expensive. This guidance document also provides examples which demonstrate that by using an ensemble of specific ASCT tailored for site geology, geography, and contaminant type, investigative time can be considerably reduced, and remedial actions can achieve site closure sooner. ASCT can be used throughout the life cycle of an environmental project, which may reduce the backlog of case reviews, thereby saving time and money.

This guidance does not include all available ASCT but includes those most widely used and readily available. While this document contains extensive information on various ASCT, it is not a guide to designing a CSM or a user's manual for any specific tool.

1.3 Document Organization

The ASCT discussed in the guidance document are divided into four general categories: direct sensing tools, borehole geophysical tools, surface geophysical tools, and remote sensing tools. In addition, an ASCT Selection Tool and ASCT Technical Selection Matrices are provided to support the evaluation and selection of appropriate tools. The document is organized into eight sections. A summary of the section topics and additional tools is provided below.

Section 2 ASCT Challenges and Path to Acceptance

While the use of ASCT in site characterizations is increasing, there are still challenges to overcome. This section summarizes some of the potential challenges to implementing ASCT and potential solutions.

Section 3 ASCT implementation

The implementation of ASCTs involves selecting the appropriate tool, applying the tool in an appropriate location, and performing basic data interpretation. This section provides a general overview of the considerations for the application and implementation of ASCT. Topics covered include ASCT role in the conceptual site model; ASCT selection, including cost considerations; ASCT and traditional tools and methods; and data interpretation, use, and visualization.

Section 4 Direct sensing

Direct sensing tools measure a physical or chemical parameter of interest through direct contact or precise, discrete sampling. This section provides information on direct sensing ASCT that measure

physical properties such as porosity, resistance, radioactivity, groundwater flow, and permeability and chemical contaminants, such as volatile organic compounds (VOC) in groundwater.

Section 5 Borehole Geophysics

Borehole geophysics are used in open or cased wells or boreholes to collect data concerning the physical (lithology), hydraulic (flow zones and velocity), and chemical (dissolved solids) aspects of the subsurface in fractured bedrock or consolidated or semiconsolidated sediments. This section provides information on borehole geophysics ASCT that collect data on lithology, stratigraphy, and fluid properties; borehole integrity and structure; advanced structural imaging; and hydrogeology and flow dynamics.

Section 6 Surface Geophysics

Surface geophysics tools are nonintrusive and used to indirectly measure physical properties of subsurface materials over large areas from signals produced by natural or generated sources. This section provides information on borehole geophysics ASCT that collect subsurface data by electrical resistivity imaging (ERI), ground penetrating radar (GPR), seismic reflection and refraction, multichannel analysis of surface waves (MASW), and both time domain electromagnetic (TDEM) and frequency domain electromagnetic (FDEM) surveys.

Section 7 Remote Sensing

Remote sensing tools use active or passive sensors that are attached to aerial systems to detect electromagnetic emissions from the earth's surface. This section discusses the use of visible spectrum cameras, thermal sensors, multispectral and hyperspectral sensors, and light detection and ranging (LiDAR) sensors mounted on drone platforms. Information is also provided on environmental sensors (for example, air and water) and other less common sensors, such as ground penetrating radar, magnetometer, and bathymetry.

Section 8 Case Studies

Summaries of eight case studies are provided in this section with links to the case study documents. Case studies are included to provide examples of the use of these tools and aid in tool selection, data interpretation, and understanding of potential pitfalls or shortcomings related to individual tools.

Glossary, Acronyms, References

This document includes a glossary, a list of acronyms, and references. The user is encouraged to access each section and supplementary information and the most up-to-date sources of information on these topics.

ASCT-2 Selection Tool

The **ASCT-2 Selection Tool Macros** is a Microsoft Excel spreadsheet that can be downloaded from the ITRC ASCT-2 webpage (**https://itrcweb.org/using-asct-2/**). The Selection Tool uses macros; however, if macros cannot be enabled, a version of the **ASCT-2 Selection Tool Filters** using filters is also provided. The Selection Tool provides a process for a user to identify ASCT that may be suitable for a site by selecting the following characteristics appropriate for the site:

- **Data needed**—chemistry, geology, or hydrology
- **Subsurface/surface**—consolidated/bedrock, unconsolidated overburden, or surface

- **Data quality**—quantitative, semiquantitative, or qualitative
- **Data collection**—invasive or noninvasive

See the "How to Use" tab in the Selection Tool spreadsheet for more information.

Based on the selected characteristics, the ASCT-2 Selection Tool will provide a list of tools that meet these characteristics. Once a short list of tools has been identified, review information about each tool in the tool category introduction section, individual tool subsections, case studies, and the Technical Selection Matrices. The section numbers for the selected tools are provided in the Document Section column of the Selection Tool.

ASCT Technical Selection Matrices

ASCT-2 Technical Selection Matrices have been developed for the ASCT in the Direct sensing, Borehole Geophysics, and Surface Geophysics categories described in this document. These can be downloaded on the ITRC ASCT-2 webpage (**https://itrcweb.org/using-asct-2/**). The Technical Selection Matrices provide additional information to evaluate the applicability of each tool. A list of considerations typically associated with an investigation is provided for each category of ASCT, including depths of interest, subsurface CSM questions, site conditions/accessibility, and data quality/collection. For each tool, each consideration is identified as either almost always, sometimes, rarely, or never applicable to the tool.

2 ASCT CHALLENGES AND PATH TO ACCEPTANCE

Data from well-designed investigations using ASCT provide visual and accessible information that can help regulators, practitioners, and stakeholders understand and accept CSMs. The level of detail and the way the information is presented can increase the public's understanding of the CSM and the receptors potentially affected by the contamination at the site.

However, ASCT acceptance can be challenging due to complexities in data interpretation, lack of standardization, unfamiliarity among regulators and stakeholders, and accessibility issues (for example, flyovers are intrusive to neighboring sites or high security areas). These tools often produce large volumes of high-resolution data that require specialized expertise to analyze accurately. Without clear guidance or calibration protocols, the reliability of the data may be questioned. Additionally, perceptions of potential cost associated with integrating these data with traditional sampling results can pose barriers to widespread adoption, although the benefits of using the tools may outweigh the potential incremental costs associated with the tools.

Acceptance and common use of ASCT by practitioners and regulators who support and promote the technology generally leads to greater public acceptance. For regulatory programs that have a public participation component, the presentation of the data and information obtained from ASCT should be carefully considered by the team presenting the information. Direct sensing tools, for example, can significantly reduce the degree of uncertainty in the CSM by providing detailed three-dimensional data. In turn, a clearer understanding of the site for all stakeholders can facilitate agreement of the best path toward closure. The goal of this section is to discuss our findings of ASCT use among various stakeholders and discuss ways to overcome perceived barriers.

2.1 Survey of ASCT Usage

To better understand the barriers to using ASCT, along with what practitioners hope to gain from this guidance document, ITRC conducted a survey of federal and state agencies and private companies. The survey was sent to ITRC members in July 2025. **Figure 2-1** shows the breakdown of responses to the survey. Sixty-six responses were received, with a little more than half coming from state agencies.

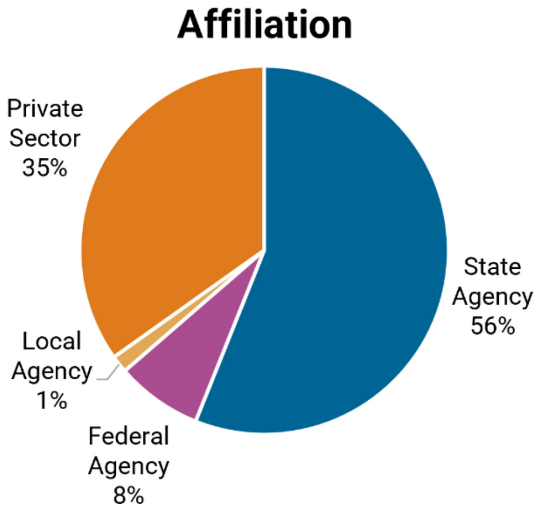


Figure 2-1. Breakdown of affiliation of survey responses.

Based on the responses, the main barrier to implementation of ASCT is the perceived higher cost associated with ASCT. The next two most significant barriers are understanding which tools are appropriate to use and how to use the data once acquired. **Figure 2-2** shows the range of responses broken out by public (agency) and private survey responses. While there was good agreement between public and private responses regarding barriers to ASCT use, some of the differences are instructive. While only 2% of regulators indicated there were regulatory barriers, 17% of private practitioners indicated regulatory acceptance was a significant barrier. While both private and public respondents indicated cost was a barrier, private practitioners were significantly more likely to report cost as a barrier. Finally, agency representatives were significantly more likely to find a lack of understanding of the tools and how to use the data as a barrier compared to private practice.

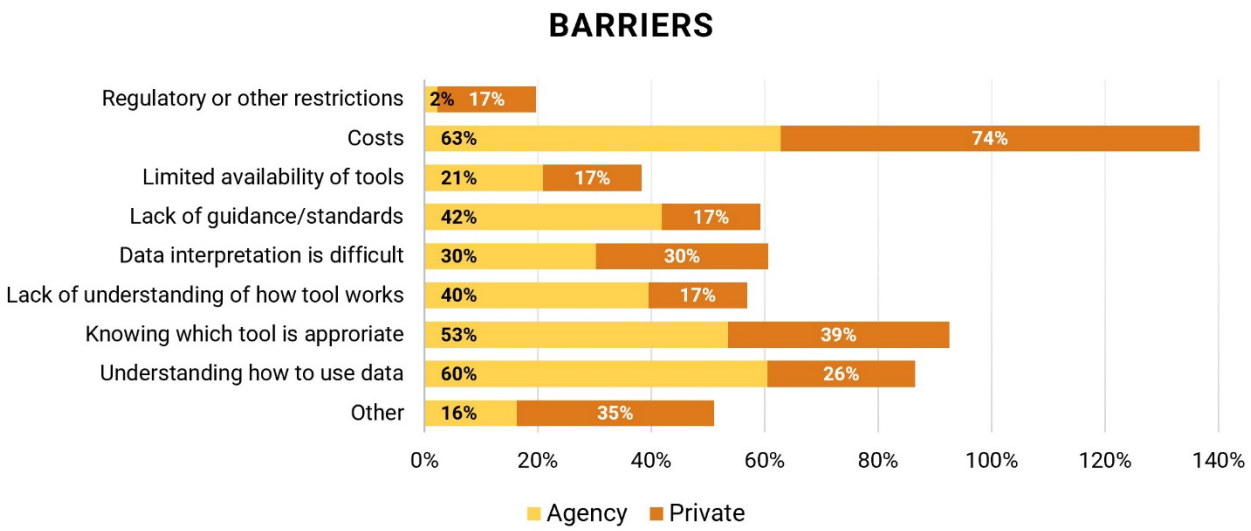


Figure 2-2. Barriers to ASCT implementation.

Likewise, there was also good agreement in regard to what sort of beneficial information was most wanted in the ASCT update document, as seen in Figure 2-3. Responders requested a better understanding of technical advantages and limitations of tools, along with a focus toward data interpretation.

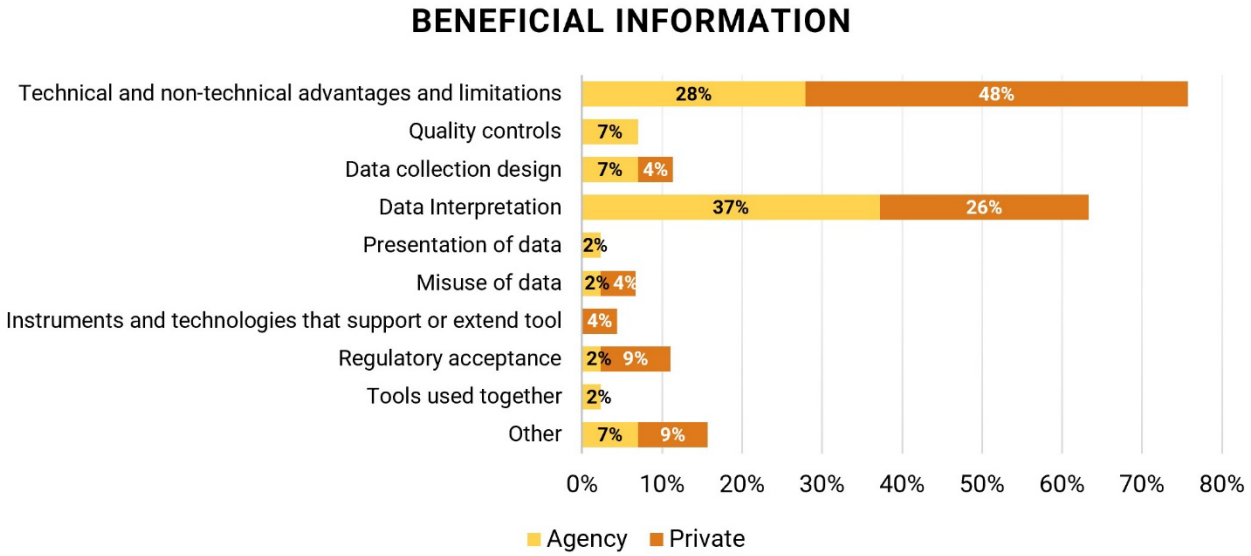


Figure 2-3. Survey responses to what sorts of beneficial information to include in the document update.

In 2018, the ITRC completed a state survey to gauge the extent of familiarity and use of ASCT by regulators and identify the limitations and barriers to achieving wider acceptance and use of these tools. Figure 2-4 shows a comparison of the major barriers to ASCT use identified in the 2018 and the 2025 surveys. In the intervening seven years since the original document was drafted, cost remains a primary barrier to the use of ASCT, although 20% fewer reported it as a barrier in the 2025 survey. There has been a significant increase in understanding of how the tools work. In 2018, 74% of agency respondents indicated this was a significant barrier, while in 2025 only 40% of respondents indicated this was a barrier. The other common barriers listed were tool availability, which showed some decrease, and regulatory other restrictions, which also decreased.

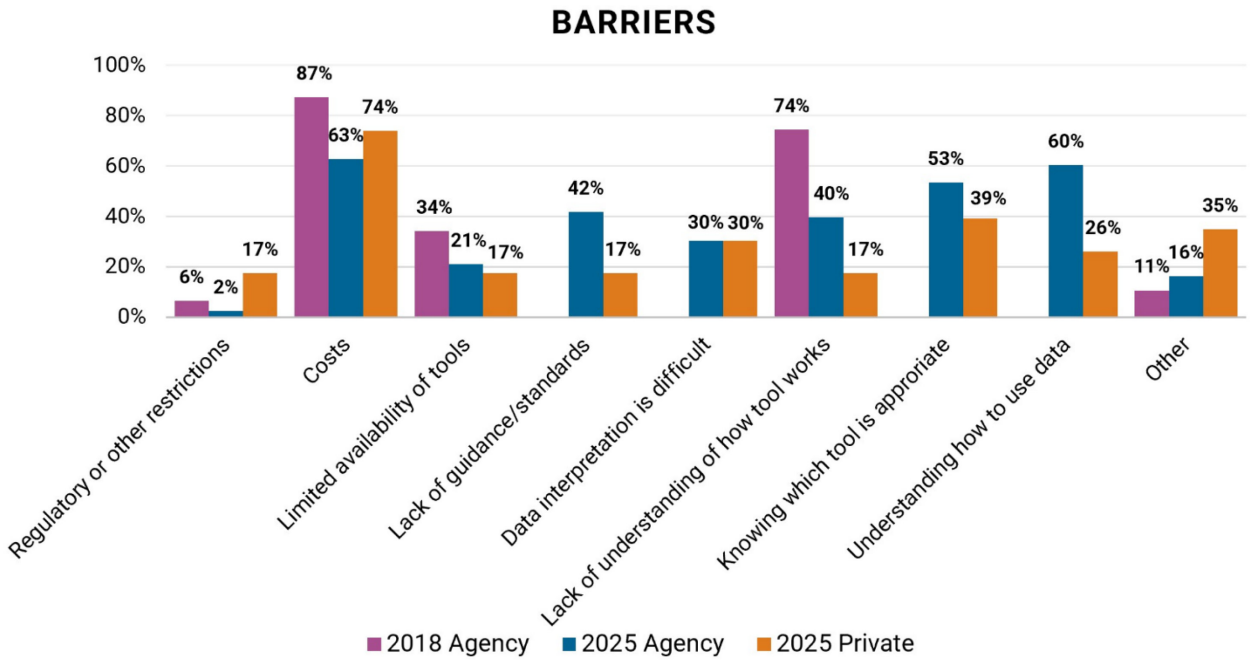


Figure 2-4. Comparison of select state agency responses for barriers from the 2018 state survey and the 2025 team private and state surveys.

2.2 Challenges and Solutions

Distinct challenges still remain to increase the use of ASCT. Resolving these challenges should be a consideration for all stakeholders. Despite the perception that using ASCT is beneficial, respondents noted the following barriers to their effective use: cost, understanding the proper tools to use to support investigations, understanding and integrating ASCT data into the development of more robust CSM, and tool availability. Respondents also noted that the two most important types of information they needed were descriptions of the technical and nontechnical advantages and limitations of each tool, and how to interpret the data from the tools. This document seeks to provide that information. The following sections review some of the barriers identified and outline ways the document helps address them.

2.2.1 Cost

Cost remained the most frequent barrier reported in the 2025 survey, as it did in the 2018 survey, but the number reporting it to be a significant barrier fell from 87% to 63%. In 2018, approximately half of the respondents reported that their state would reimburse or otherwise pay for using ASCT, and cost versus perceived benefit (reduced remedial time and cost) would be one of the most important considerations for selecting ASCT over more traditional methods, such as sample collection via soil borings and monitoring well installations. Some states have overcome cost uncertainty and avoided upfront investment by soliciting bids for contracts that include ASCT to establish per-ft or per-sample rates. Other possible solutions include drafting work plans to solicit prices on a case-by-case basis from companies using ASCT, requesting consultants to provide itemized cost comparisons for using ASCT as an alternative to more traditional methods, and controlling costs by limiting ASCT to specific scopes of work or certain types of sites. In addition, free or commercial tools (for example, USGS Earth Explorer or geographic information systems (GIS) software) can be used to access, process, and visualize datasets for many projects. See Section 7.1.1 for more information on existing remote sensing tools.

2.2.2 Lack of Understanding

Understanding of ASCT has improved significantly, but where there is a lack of understanding and knowledge of the tools, it appears to be equally shared among the regulatory community, consultants, and responsible parties. The main gaps in understanding are on which tool to use, interpreting the data, and understanding how to apply the data to the case. This creates an overreliance on the specialist provider and an inability to look beyond the "black box" of the data, creating a risk that information the regulator or consultant may be aware of is not incorporated into the overall data interpretation. By explaining how the data from each tool are interpreted and used, this document seeks to overcome that lack of understanding. In addition, more communication between community members and regulatory agencies may ease potential concerns associated with ASCT use. For example, pre-vetting neighbors and regulators before conducting aerial and/or drone surveys within and outside of property boundaries may allow greater understanding on the utility and benefits of remote sensing technologies.

2.2.3 Availability

A perceived lack of ASCT availability was identified in 2025 as a barrier by only 21% of regulators and 17% of private practitioners, down from 34% of regulators. This suggests that as understanding of the tools increases, suppliers are more easily identified and more willing to invest in the tools. Increasing understanding of the tools is likely to continue to increase demand for them to be used, creating more interest among suppliers to provide service over wider geographic areas. Increased usage should result in increased availability and decreased costs. This transition is likely to take at least a decade because each step is interrelated and interdependent. Perhaps if vendors offered incentives for ASCT use (for example, reduced mobilization fees, multiday discounts), there would be more motivation to propose ASCT use and prove their benefit. In addition, if regulators and consultants discussed the cost-benefits of ASCT to responsible parties, ASCT use may improve if they were aware of the reductions in project time and potential cost savings to the project life cycle.

2.2.4 Regulatory Issues

Survey respondents generally reported that their agency either suggests or recommends using ASCT. Only 2% of regulators reported regulatory issues as a primary barrier, but 17% of private practitioners did. Perceived regulatory issues by private practice may include some reimbursement funds not having an easy way to approve or pay for innovative technologies. In some cases, private practice may perceive that regulators require physical sampling and laboratory analysis to support regulatory decisions, which can lead to the perception that ASCT are unnecessary or not cost-effective. As described in Section 3.5, ASCT do not replace but *complement and enhance* the interpretation of data gathered by traditional methods.

2.2.5 Potential Solutions

Table 2-1 provides a summary of the challenges discussed and the potential solutions to address these challenges.

Table 2-1. Summary of challenges and potential solutions.

Challenges	Potential Solutions
Costs	Solicit contract bids with upfront costs for ASCT (for example, per-ft or per-sample rates)
	Cost itemization comparison between traditional tools and ASCT
	Limit the scope of ASCT use

Challenges	Potential Solutions
Lack of understanding	Provide education for the different ASCT available
	Improve data interpretation of ASCT
	Inform users how to apply ASCT data to inform the CSM/path to closure
Availability	Increased ASCT usage can improve availability to wider geographic areas
	Establish vendor incentives (for example, reduced mobilization fees and multiday discounts)
	Discuss cost-benefits of ASCT during project life cycle
Regulatory	Encourage more ASCT use for practitioners
	Build confidence among regulators regarding ASCT use (for example, ASCT do not replace but complement and enhance data from traditional methods)

2.3 Site-Specific Regulatory Program Acceptance

The 2025 survey showed that few regulators perceive there to be barriers to the use of ASCT at regulated sites. It is, however, important to consider project-specific and remedial phase data quality objectives when evaluating the use of ASCT. The use of ASCT should be communicated to a regulatory agency prior to deploying these tools in the field. The regulatory agency may have procedures, policies, or regulations regarding documentation, sampling, and analysis at remediation sites. The following questions are important to answer when interacting with regulatory programs about the possibility of using ASCT:

- Are there any legal (statutory or regulatory) barriers or hurdles in using ASCT within the regulatory program?
- Is quantitative data required as part of the regulatory process (for example, to calculate site-specific cleanup levels)?
- Does the regulatory program allow for the use of qualitative or semiquantitative data during the investigation or characterization phase?
- How much qualitative and semiquantitative data are needed to obtain higher quality quantitative data (for example, collection of proper qualified data with predefined sample density will reduce amount of high-quality quantitative data necessary for completing the CSM)?
- How will ASCT achieve data quality objectives (DQO) for the project?
- How will the ASCT data be used to inform the regulatory decision-making process?

Certain tools can also be applied to remedial design and optimization by providing data on potential effectiveness and performance of a selected remedy. The use of ASCT during the remedial phase may be subject to regulatory acceptance and concurrence.

Historical and traditional data previously collected should be used along with ASCT data to build a more comprehensive CSM and support site characterization and remedial action decisions. Multiple lines of evidence and the collection of more than one type of data are important in making effective regulatory decisions. Using both ASCT data and traditional data is the most effective way to evaluate specific characterization questions, evaluate the remedial design, and monitor the progress of remediation. If ASCT were used during the investigation phase of a project, deploying ASCT again to evaluate remedial actions will help with continuity of certain datasets or the evaluation of site decisions and recommendations (for example, using Laser-Induced Fluorescence (LIF) or Optical Image Profiler (OIP) direct sensing tools to map the extent of light nonaqueous phase liquid (LNAPL) before and after a remedial effort).

3 ASCT IMPLEMENTATION

Using ASCT requires thoughtful consideration of a range of technical, regulatory, logistic, and project-specific factors. Selecting the appropriate tool(s) involves not only understanding its capabilities but also ensuring it aligns with the overall investigation goals. These considerations help ensure that the selected tool(s) are not only technically and logistically viable but also add real value to the site characterization process.

The planning and implementation of ASCT involve selecting the appropriate tool, applying the tool (possibly with other ASCT or traditional methods), and interpreting the data. Considerations for use of an ASCT may include but are not limited to:

- What type of data does the ASCT yield (for example, real-time data, digital format) and will the data provide another line of evidence to aid in decision making for a project?
- Will the ASCT provide additional value to a project by filling data gaps, meeting data quality needs, and helping meet project time constraints?
- What are the data collection objectives (for example, screening (cursory or semiquantitative), delineation, pilot testing, monitoring, or remediation)?
- What contaminants are the ASCT suited for and are they sufficiently sensitive to meet the project's DQO?
- Will the raw data be useful or will it require further processing prior to analysis?
- Will it be technically feasible to use the ASCT for the project (for example, are there constraints on use of the ASCT, such as limitations due to area, site geology, and depth of coverage or availability of the tool)?
- What is the availability of trained and qualified contractors within the geographic area?
- Will the ASCT data assist regulators and stakeholders in making case decisions (for example, use may vary by purpose, such as a primary cursory screening versus investigation)?

3.1 Conceptual Site Model

The CSM is a written or visual description that integrates all known site data and information throughout all stages of the project life cycle, from investigation through cleanup (USEPA 2011). The CSM is iterative, evolves over time, and typically includes historical site use, previous investigations, geology and hydrogeology, intended reuse, decision criteria, pathway-receptor network, potential remedies, and completion strategy (USEPA 2018d).

ASCT support the development and updating of the CSM by providing high-resolution data to address data gaps and uncertainty and to determine the scope and goals of the next stage of investigation or remedy. Additional information gained from using ASCT can accelerate data collection, make the CSM more robust, and enable more informed project decision-making.

ASCT can be used to identify locations and depths where more quantitative data should be collected, to support the characterization of subsurface geology and hydrogeology, and to improve or complete the CSM. Applying ASCT is particularly effective at sites where:

- traditional tools are incapable of providing data of sufficient density or quality
- existing remedial strategies have not been effective

- remedial strategy effectiveness is sensitive to the precise distribution of contaminants in the subsurface

ASCT are also effective in complex hydrogeological conditions (for example, fractured bedrock, karst, intricate alluvial channel systems) where heterogeneity is prevalent and finer detail of a system is needed. They are useful during emergency response situations when timely decision making is required.

Having an accurate and robust CSM is integral to making efficient risk-based decisions for a site about both the investigatory and remedial paths. While this guidance document presents tools that can help in building a CSM, it details neither the components of a CSM nor best practices for building a CSM. The following documents provide further information on the development of a CSM, including DQO and risk assessment guidance, which are critical components of CSM development:

- Characterization and Remediation in Fractured Rock. FracRx-1 (ITRC 2017)
- Integrated DNAPL Site Characterization and Tools Selection. ISC-1 (ITRC 2015)
- USEPA Guidance on Systematic Planning Using the Data Quality Objectives Process (USEPA 2006)
- Expedited Site Assessment Tools for Underground Storage Tank Sites: A Guide for Regulators (USEPA 2016a)
- US Army Corps of Engineers. Environmental Quality: Conceptual Site Models (USACE 2023)
- Best Practices for Data Management Technical Guide (USEPA 2018a)
- ASTM Standard Guide for Developing Conceptual Site Models for Contaminated Sites (ASTM 2020b)
- USACE Engineer Manual 200-1-12 Environmental Quality Conceptual Site Models (USACE 2023)
- Smart Scoping for Environmental Investigations Technical Guide (USEPA 2018e)
- Environmental Cleanup Best Management Practices: Effective Use of the Project Life Cycle Conceptual Site Model (USEPA 2011)
- Guidance on Conceptual Site Models (USEPA 2023)
- Risk Assessment Guidance, Volume I Human Health Evaluation Manual (Part B, Development of Risk-based Preliminary Remediation Goals) (USEPA 1991)

3.2 ASCT Application

ASCT can be used to identify locations and depths where more quantitative data should be collected, to support the characterization of subsurface geology and hydrogeology, and to improve or complete the CSM. Applying ASCT is particularly effective at sites where:

- traditional tools are incapable of providing data of sufficient density or quality
- existing remedial strategies have not been effective
- remedial strategy effectiveness is sensitive to the precise distribution of contaminants in the subsurface

ASCT are also effective in complex hydrogeological conditions (for example, fractured bedrock, karst, intricate alluvial channel systems) where heterogeneity is prevalent and finer detail of a system is needed. They are also useful during emergency response situations when timely decision making is required.

3.3 ASCT Selection

Selection and proper use of any investigative tool is fundamental to a successful project and is the responsibility of the project team. The use of ASCT should be considered at the onset of an investigation. Final selection of appropriate investigation tools and techniques occurs once a CSM is developed, data gaps are identified, and data collection planning is complete. Keep in mind that developing a CSM is an iterative process. With the additional information gained from ASCT, the CSM will become more comprehensive and enable the project team to make informed decisions for the overall project.

The ASCT presented in this document include direct sensing tools, geophysics tools (borehole and surface geophysics tools), and remote sensing tools. Below is a brief summary of these tools:

- Direct sensing tools included in this guidance document measure a physical or chemical parameter of interest through direct contact or precise, discrete sampling. These tools are advanced into the subsurface and yield data logs that indicate lithology, permeability, the presence (or lack thereof) and magnitude of dissolved-phase contaminants (for example, VOC) or nonaqueous phase liquids (NAPL). These tools can also be combined with sensors for both contaminant detection and identification of lithologic or hydraulic properties in one device to provide insight into lithologic control of contaminant migration.
- Geophysics tools measure contrasts in the physical properties of different materials (through active or passive detection methods) that are used to indirectly infer or estimate parameters of interest. For example, contrasts observed in gamma radiation can be used to infer changes in lithology, while changes in temperature in a borehole can be used to infer groundwater flow direction and velocity. This guidance document divides geophysical methods into borehole geophysics and surface geophysics. Borehole geophysics tools are used in open or cased wells or boreholes to collect data that can be correlated to other nearby boreholes or wells or related site information. Surface geophysics tools are nonintrusive and used to evaluate the subsurface over large areas.
- Remote sensing tools use active or passive sensors that are attached to aerial systems to detect electromagnetic emissions from the earth's surface. These sensors can characterize objects, surfaces, or in some cases, subsurface areas. Four main sensors will be addressed in this guidance document for their advanced capabilities in site characterizations: visible spectrum cameras, thermal sensors, multispectral and hyperspectral sensors, and light detection and ranging (LiDAR) sensors. While these sensors can range in size depending on resolution quality and the limitation of the aerial platform to which they are attached, this guidance document will focus on unmanned aerial systems (UASs), or drones, as the primary platform for the more commonly used remote sensing sensors. Additionally, with the increased availability of drones for remediation, less frequently used payloads such as water samplers and magnetometers, which can be carried by drones, will be introduced as an alternative to capturing these types of data via more traditional methods. The other primary platforms include manned aircraft and satellites, which offer advantages that drones typically cannot achieve (wide area coverage and public/private data accessibility). It should be noted that although drones provide greater versatility in sensor types and data resolution, satellite data in particular has the advantage of government support, which often results in no-cost access to various data types.

3.3.1 ASCT Selection Considerations

Often, several different ASCT can be used to meet a specific data collection objective. In addition, many ASCT provide qualitative rather than quantitative data, which is important to consider. Selecting the optimum tool or combination of tools relies on several factors, including:

- capability of the tool to meet DQO

- ability of the tool to effectively provide data given site conditions
- required confirmatory data and data density
- availability and cost of the tool
- reliability of the tool
- familiarity with the tool
- expertise required to use the tool
- expertise required to interpret data from the tool
- acceptability to stakeholders of data generated by the tool

3.3.2 Cost and Value Considerations

ASCT are often perceived as expensive or unfamiliar compared to traditional methods. However, the amount, precision, and accuracy of data generated using ASCT are often greater than traditional sampling techniques (for example, soil borings, monitoring wells) and can result in cost savings over the life of the project. Whether used independently or in conjunction with traditional methods such as soil borings or monitoring wells, ASCT can reduce overall costs by reducing the reliance on these traditional methods for characterizing subsurface conditions. The value of an approach is not always monetary, but may also be measured based on time, convenience, social impact, or other qualitative impacts. As discussed in the USEPA document, Implementing Direct Sensing High Resolution Site Characterization at EPA UST Release Sites in Indian Country (USEPA 2025d), ASCT, specifically direct sensing tools, were used to improve outcomes at underground storage tank (UST) sites. Real-time or near real-time data generation in the field reduces mobilizations and sequential sampling, leading to more efficient, less disruptive investigations and quicker decision making. The data obtained can further improve the CSM (for example, providing additional details on hydrogeology and contaminant distribution), leading to better informed remediation strategies and potentially less overall costs toward additional investigations. Although the USEPA guidance focused on tribal communities, the impacts could be applicable to all communities. Specific case studies demonstrating the benefits of ASCT are discussed in USEPA 2025d and in Section 8. During the tool selection process, it is important to consider the monetary costs, the value added by the characterization, and whether the technology is appropriate for the site.

A cost-benefit analysis using the following approach allows the merits of ASCT and traditional characterization methods at a particular site to be evaluated:

- Outline all potential costs that will be incurred using a particular tool or approach for the lifetime of the project.
- Compare the potential costs to the total expected benefits to determine whether the proposed action is advisable. (Note: The overall benefit associated with a proposed action should outweigh the costs incurred.)
- Compare the potential costs to alternatives for which all potential costs are also outlined.
- Record all anticipated benefits associated with the potential action.
- Weigh the potential costs relative to the expected benefits to determine whether the positive benefits outweigh the negative costs.

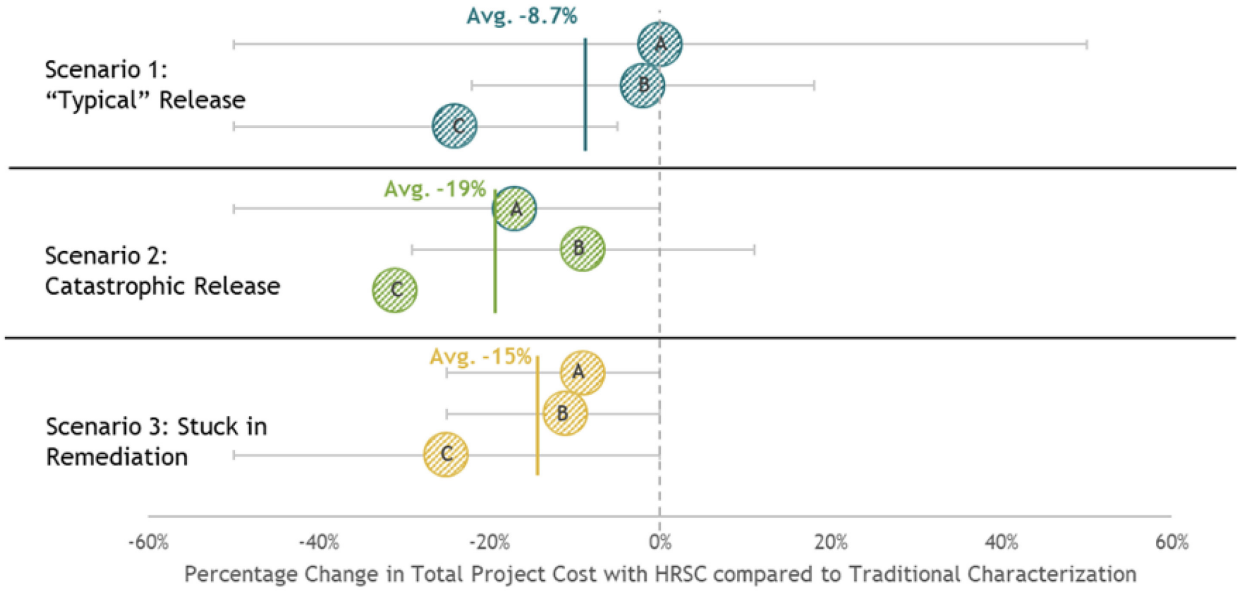
In 2023, USEPA released a report titled High Resolution Site Characterization at Petroleum Underground Storage Tank Release Sites–Applicability, Benefits, and Costs to summarize the time and cost implications of using high resolution site characterization (HRSC) at UST sites (USEPA 2023). The study investigated HRSC using direct sensing ASCT, such as laser-induced fluorescence, optical image

profiling, membrane interface probe, hydraulic profiling tool, and electric conductivity. The purposes of this study were to:

1) quantify the costs and benefits of ASCT investigations and their impact on overall project costs and time at UST sites
2) identify situations where ASCT could provide benefits in subsurface characterizations compared to traditional methods

Some of the cost impacts identified are summarized below. It is important to note that this report is only an example of potential savings that can be achieved based on experience and hypothetical scenarios. In addition, although the study focused on USTs, these impacts can be seen across various site settings.

As part of the USEPA study, three experts with decades of site characterization experience were asked to provide cost estimates for three hypothetical UST scenarios: typical release, catastrophic release, and stalled in corrective action. Refer to (USEPA 2023) for how the hypothetical scenarios were defined.



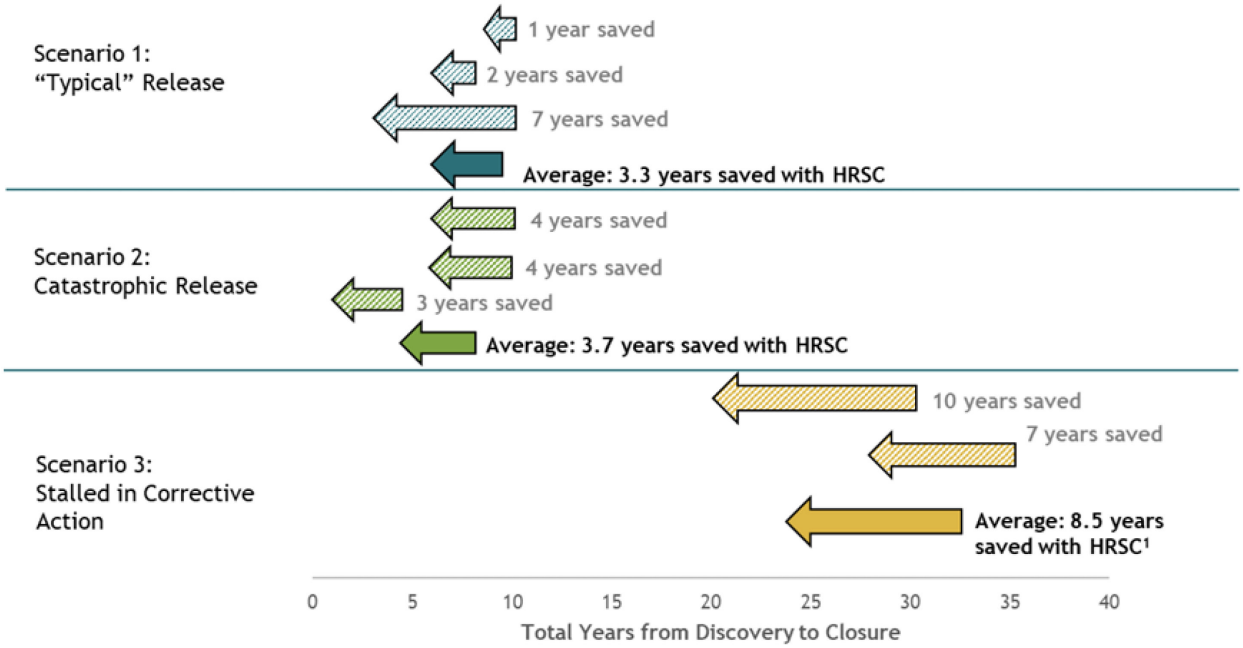
Notes: 1. Stripe-filled markers represent individual expert responses.
2. Brackets represent range of cost impacts that experts believed would encompass nearly all possible project outcomes (for example, Expert A believed costs at a single site when using ASCT for HRSC could range from +/-50% in total project costs when compared to use of traditional characterization methods). While experts believed site to site costs may vary, they expected the midpoints (dots) to represent the most frequent outcome and the likely overall cost impact across a portfolio of projects.
3. *Expert C did not provide a range for the catastrophic release scenario.*

Figure 3-1. Expert individual and average cost impacts when using direct sensing tools for high resolution site characterization (HRSC) compared to traditional techniques alone across three petroleum underground storage tank (UST) release scenarios.

Source: USEPA (2023).

The first objective the experts considered was cost differences between ASCT and traditional characterization methods. While cost savings in **Figure 3-1** are reported as the most likely scenarios for a given site, total project costs generally observed greater savings with ASCT (average range estimated at 8.7%–19% among the three scenarios) compared to traditional characterization methods. Some experts did point out that for sites with net-neutral or small-to-moderate cost savings, sites could still benefit from using ASCT because they increase site information and confidence in the CSM.

The second objective the experts considered was how long sites were active when ASCT were compared to traditional characterization methods. In **Figure 3-2**, all experts anticipated reductions in overall project duration (time from discovery to closure) for all three hypothetical scenarios, averaging 3–8 years with the use of ASCT. The study emphasized that because project duration and failure to close sites were major drivers of costs, ASCT use could be a potential major driver in reducing costs at a site.



Notes: 1. Expert C did not provide a duration estimate for the Stalled in Corrective Action scenario due to the complexity of the scenario. The average reflects the responses provided by experts A and B.
2. Right end of arrows represents the expert's estimates of total project duration using traditional characterization techniques, while left end represents duration when using direct sensing tools for HRSC (for example, Expert A estimated a 30-year duration with traditional characterization and 20year using direct sensing tools for HRSC in Scenario 3).
3. In each of the scenarios the top arrow represents the estimates for Expert A, the next Arrow represents the estimates for Expert B, the third arrow represents the estimates for Expert C, and the bottom arrow represents the average of the estimates of the three experts.

Figure 3-2. Expert individual and average estimates of changes to project durations when using direct sensing tools for high resolution site characterization (HRSC) compared to traditional techniques across three underground storage tanks (UST) release scenarios.

Source: USEPA (2023).

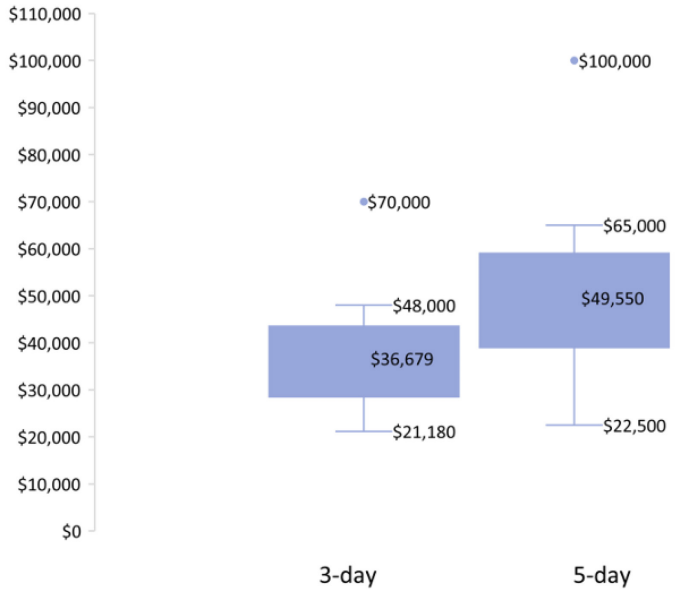
Aside from experts, ten participants from either regulatory agencies or consulting firms provided cost ranges for 3- and 5-day investigations to highlight the anticipated costs from ASCT use for a typical petroleum release scenario. One respondent did not provide cost estimates for the three-day investigation. **Figure 3-3** summarizes the responses from the ten participants. Although costs may vary based on the specific tools and site conditions, these cost ranges provide an estimate for those unfamiliar with ASCT.

As illustrated in **Figure 3-3**, site characterization cost estimates should compare using ASCT to traditional approaches to assess the most cost-effective method of filling the identified data need. Most ASCT described in the document provide real-time data evaluation (same-day data processing), and, therefore, reduce the need for multiple mobilizations by allowing the investigation scope to be adjusted in the field as data are collected. For some ASCT, that may require additional data processing. It may take 1–2 weeks to obtain usable information. The cost saved by avoiding multiple mobilizations should be

considered, particularly when mobilizing equipment to remote areas or areas without established equipment and personnel.

Cost considerations unique to a specific tool are discussed in the corresponding tool sections. Common cost considerations are included below:

- number and depth of borings being used for site characterization
- lump sum cost to mobilize the tool to the site, which varies depending on site location and proximity to tool suppliers and contractors
- daily tool rental rate to operate the tool
- data management or logging and data generation fee that is charged by the day or foot, including time to log the linear feet of drilling
- confirmation sampling (coring) and analysis for quality assurance and quality control (QA/QC)
- material costs
- oversight and labor costs
- data post processing and analysis costs that may also be associated with post processing and analysis of data, depending on project needs
- data management and completion report as a lump sum



Notes: 1. One respondent did not provide cost estimates for the 3-day investigation. The average reflects the responses provided by the remaining nine respondents.
2. Responses reflect individual responses. The highest-cost responses for 3- and 5-day investigation were provided by the same respondent.

Figure 3-3. High resolution site characterization (HRSC) cost estimates for 3- and 5-day investigations (responses provided by state and federal regulators and technology providers and consultants).

Source: USEPA (2023).

3.3.3 Important Outputs

Informative data and information outputs that support updates to the CSM and future decisions include:

- A summary of the tools and methods used and how effective they were
- A report that includes limitations that constrained the study physically (for example, interferences, safety considerations, access) or due to other reasons beyond control of the contractor
- Any limitations of the technology (for example, any suspected false negatives)
- Deviations from the scope and the justification for the deviations
- Post processing of the data and the methods and assumptions used
- Summary of the QA/QC, including data processing and interpretation performed and any deviations from the QA/QC plan
- Narrative summary of the findings and results

- Description of lines of evidence that support or refute project interpretations
- Recommendations for follow-up sampling locations if definitive confirmation was required and was not accomplished during the investigation
- Raw data files
- Summary tables of logs and results
- Logs presented in at least two appropriate scale resolutions (typically very low for absence or presence determinations and high for semiquantitative site-wide comparisons of impact and/or geologic and hydrogeologic characteristics)
- Plan view figure of the study area, sensing parameters and areas, and transect and investigation locations
- Graphics and visualizations to illustrate the findings (for example, 2D or 3D profiles of responses with adequate scale, color ramp definitions)

3.4 Using Multiple ASCT Together

It can be beneficial to combine two or more ASCT during an investigation to obtain complementary data that enhances the understanding of subsurface conditions. Each tool has unique strengths and limitations; thus, using them together can create a more complete and accurate CSM. This approach can reduce uncertainty, allow for real-time decision-making in the field, and confirm findings across tools. Ultimately, it leads to more informed, efficient, and cost-effective decisions for site management and remediation.

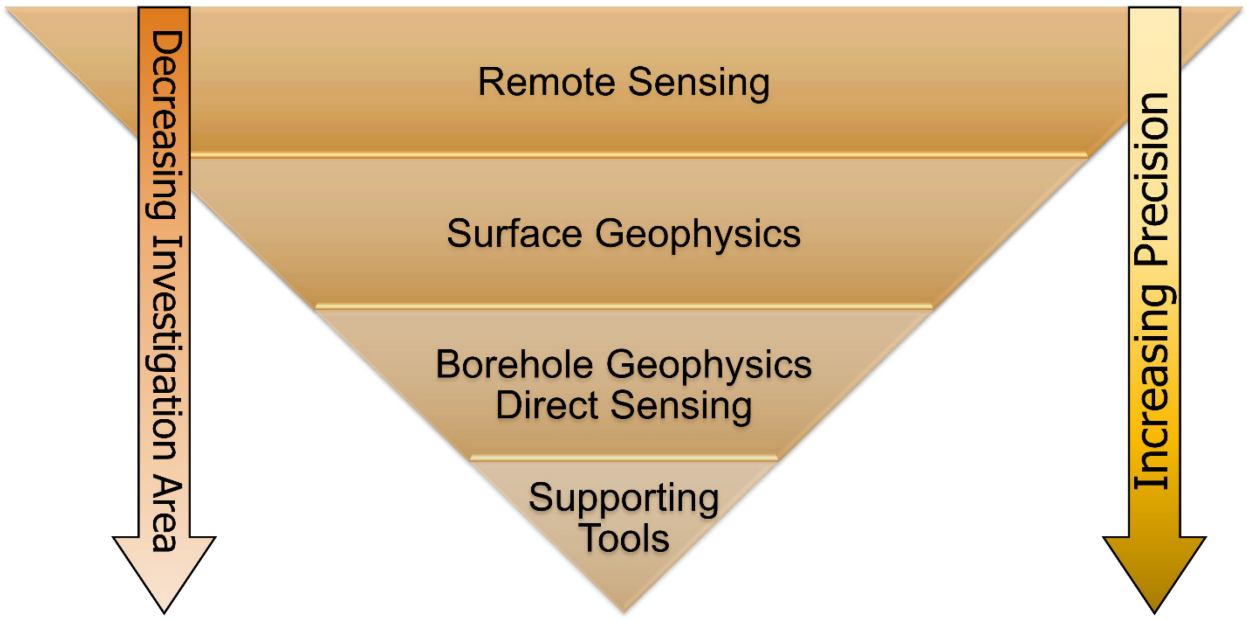


Figure 3-4. Graphic representation of how the ASCT groups can be used together to develop a conceptual site model at different scales and degrees of precision.

Using multiple ASCT from the core groups described in this guidance document together can help develop a refined CSM by first using tools that describe a broad area and then allowing specific areas of a site to be defined with increasingly precise ASCT (**Figure 3-4**). The location and depths where traditional samples should be collected using supporting tools (discussed in Section 3.5.1) to provide the most robust quantitative data can be decided in a way that minimizes the number of investigation points and

the number of needed mobilizations. Examples of this iterative use of multiple ASCT are described in case studies in Section 8.

3.5 Comparison of Traditional Tools and Methods vs. ASCT

Traditional site characterizations commonly involve tools and methods that advance soil borings for soil logging and discrete media sample collection, install groundwater monitoring wells for groundwater monitoring and media sample collection, or that involve the performance of some controlled field experiments (for example, aquifer slug testing) at preselected locations, depths, intervals, or times. These traditional tools and methods are used based on fixed investigation plans in which data are collected during one mobilization, evaluated after the field program, and used to plan a subsequent investigation phase. They generally require multiple mobilizations to provide sufficient spatial or temporal resolution to reduce uncertainty regarding contaminant distribution and the physical conditions controlling contaminant distribution. Historically, traditional tools and methods have been widely accessible, cost-effective, and relatively simple to implement.

Traditional tools and methods, however, typically require extended periods of time to complete site characterizations and have often provided data that are low-resolution and point-based, and can be time- and labor-intensive, often requiring multiple mobilizations. In contrast, ASCT, such as direct sensing technologies and borehole geophysics methods, offer high-resolution, continuous, and areal data collection with greater speed and precision than traditional methods. The USEPA has shown that 90% of mass flux contamination transport at Superfund sites occurs through 10% of the aquifer material (Carey 2016). Higher-resolution data can more readily identify these preferential contaminant flow paths and improve the CSM for remediation planning and execution. Although advanced tools may require higher upfront costs and trained personnel, they can significantly improve data quality, reduce field time, and be especially valuable for complex or large-scale site investigations where detailed subsurface information is critical.

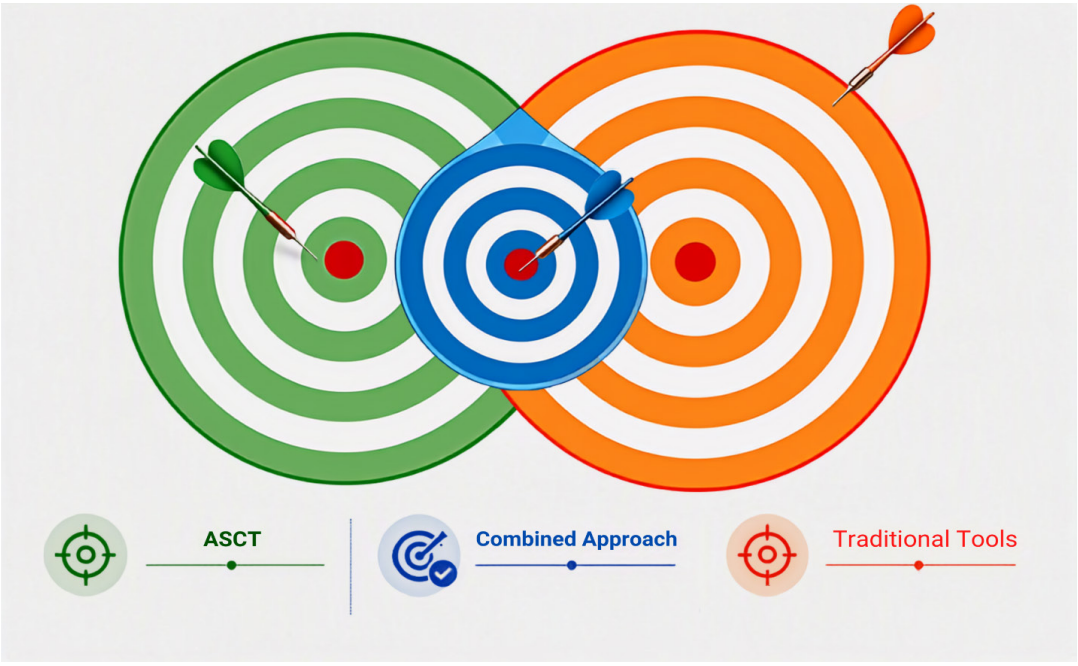


Figure 3-5. Graphic representation of accuracy and precision: the difference between using ASCT and traditional tools.

Source: Created by Ramboll.

In many cases the ASCT described in this guidance document provide semiquantitative data that can be accurate to the centimeter scale but typically do not provide high precision analytical data such as that often used to complete quantitative risk assessments. For cases where precise analytical data are needed, the ASCT ensure that the sampling is carried out only in the most appropriate locations and that the samples taken are representative of the media of concern (**Figure 3-5**). This minimizes the quantity and cost of traditional sampling and analysis.

In addition, traditional tools may be an important way to "ground truth" ASCT data, whether by comparing borehole logs to a surface geophysics survey or by lab analysis of a sample taken adjacent to a high direct sensing tool in situ measurement.

3.5.1 Supporting Tools

A variety of supporting tools may be used to support and confirm the results from the various ASCT described in this guidance document. Some supporting tools are considered primary screening tools in some situations, while others have been specifically designed to confirm cursory or semiquantitative "screening" data. Practitioners must understand the DQO of a project to ensure that the appropriate supporting tools and methods are selected for an investigation. The use of the right supporting tools can be vital in obtaining technical lines of evidence that meet these objectives. Some of these supporting tools can be used to determine media types, locations, depths, and analytical parameters for confirmation samples that then allow specific compounds to be identified in actual mass concentrations. Others can be used to simply confirm screening data (cursory or semiquantitative) collected using ASCT, such as lithology, the presence of impacted media, or the presence of NAPL. Using these data in conjunction with other tools guides additional sampling efforts, monitoring well placement, and well screen intervals. Representativeness, temporal consistency, and scale compatibility should be considered when evaluating supporting tools to confirm ASCT data. When using any tool, the user should be aware of the tool's limitations in all applications.

3.5.2 Additional Tools and Methods to Consider

While this guidance document presents several direct sensing, borehole geophysics, surface geophysics, and remote sensing ASCT, there are several additional tools and methods that can be used to efficiently conduct site characterization and complete a CSM. It is important for practitioners to be aware of these additional tools and how and when they can be used for a site. These tools include, but are not limited to, passive sampling of various media, modeling, digital plume mapping (3D plume mapping), the Triad method, real-time air and vapor monitoring, field gas chromatographs (GCs) for soil and groundwater, and semiquantitative analysis test kits. When considering any of these additional tools, practitioners can refer to the appropriate guidance documents for assistance in planning, use, and data evaluation of these tools. The following is a list of some applicable documents:

- Passive Sampling Technology Guidance Document (media sampling, biological and physical attenuation analysis) (ITRC 2024)
- Vapor Intrusion Toolkit (VI assessment, vapor and air sampling, real-time monitoring) (ITRC 2026)
- Environmental Molecular Diagnostics Guidance (ITRC 2013)
- LNAPL Update (LNAPL Technologies Appendix, NSZD Appendix) (ITRC 2018)
- Technical and Regulatory Guidance for the Triad Approach (ITRC 2003)
- Technical Bulletin for Management and Interpretation of Data Under a Triad Approach (USEPA 2007)
- Triad Issue Paper: Using Geophysical Tools to Develop the Conceptual Site Model (USEPA 2008)

- The Triad Approach to Managing Decision Uncertainty for Better Cleanup Projects (Crumbling 2004)
- High resolution Site Characterization (USEPA 2023)
- General Site Investigation Method, Tools, and Techniques (B. J. Nielsen 1995; USEPA 2025a)

3.6 Data Interpretation, Use, and Visualization

ASCT generate detailed, high-resolution, and often complex data about the properties of subsurface materials that require careful interpretation to extract meaningful insights, including those regarding lithology, stratigraphy, hydrogeology, and geochemistry. The tools measure properties of both naturally occurring and anthropogenic materials, compounds, and fluids present in the subsurface. Once properly interpreted, these data are then integrated to develop and update a CSM, guide further sampling, and inform and optimize remediation decisions, ultimately improving the accuracy and efficiency of environmental investigations. The intent of this report is to provide readers with a basic understanding of various tools available, but the selection, use, and integration of data provided should be informed by a variety of factors normally included in a project data management plan. It is beyond the scope of this report to provide detailed guidance on how to develop such plans. Readers should note that such plans are often subject to client-specific requirements. Such requirements should be considered in the selection and use of all tools.

3.6.1 Effective Use and Communication of ASCT Data

Effective data visualization through maps, 3D models, and graphs plays a crucial role in making this information accessible and understandable for project teams, regulators, and stakeholders, facilitating better communication and more informed decision-making throughout the site characterization and cleanup process. Without proper interpretation, valuable information about subsurface conditions and contamination could be misunderstood or overlooked, leading to ineffective cleanup strategies. Using the data effectively helps target efforts where they are needed most, saving time and resources while reducing risks to human health and the environment. Visualization ensures that complex data are clear and accessible to all stakeholders, supporting transparent communication and collaborative decision making. Overall, these processes help achieve safer, more cost-effective, and scientifically sound environmental outcomes.

3.6.2 Data Acquisition, Processing, and Interpretation

Modern data processing tools mean that data obtained from ASCT can often be interpreted and presented in minutes, hours, or days from acquisition, rather than in weeks or months. Data acquisition and processing are generally the responsibility of a specialized subcontractor (vendor) selected to perform those tasks, although it is useful for the primary contractor to have experienced personnel that can oversee and provide quality control during those phases of work. Although the primary contractor's responsibilities may vary depending on the client's specific acquisition process and policies, the primary contractor may often self-perform data acquisition and processing if they have appropriate experience and the necessary equipment to do so. If a vendor is used, they will in most cases generate a report with figures (logs or other visuals) that display the data in a useful format for the end user. There are data processing tools that the primary contractor may also acquire through public domain or purchased licenses to assist with reprocessing the data for quality control, data calibration, data analytics, or data visualization purposes. In many cases, the software allows the end user to reprocess the raw data files and reconfigure visual outputs, including building transects, to assist with data interpretation. Field staff who have access to that tool can analyze and interpret the data in real time to help guide the investigation.

Data interpretation is generally the responsibility of the primary contractor (and the project's team of SMEs) from the standpoint of using the acquired data for its intended purpose: to develop a robust CSM for the investigation, risk assessment, and remediation phases of an environmental program. This will include identification of contaminants of concern and characterization of sources, and the identification of migration pathways through various media as defined in the CSM (ASTM 2020b).

3.6.3 Data Quality

ASCT data quality can be affected by a number of factors generally associated with data acquisition and, in some cases, data processing. The primary contractor must often rely on their vendors to ensure that proper data quality procedures are followed. This may include calibration of tools, collection of repeat logs, and adherence to method-specific standard operating procedures (SOPs). For borehole geophysics, rate of logging can be variable and may be critical for some tools. The presence of experienced field staff who can monitor and document the data acquisition process is highly recommended. ASCT produce data that are quantitative, semiquantitative, or qualitative, which can significantly impact a tool's selection. For example, the Membrane Interface Hydraulic Profiling Tool (MiHPT) produces semiquantitative and qualitative data and is therefore not used to calculate risk.

Data processing for some tools is often performed using factory default settings the vendor selected based on historical use for various parameters but may require adjustment based on site-specific conditions. A discussion with the vendor regarding anticipated subsurface conditions such as lithology and depth to groundwater should be made prior to the start of work.

3.6.4 Data Management and Visualization

In addition to the vendor's report, all data acquired using direct sensing or borehole geophysical methods are stored in digital format files. It is recommended that the primary contractor request that the vendor provide the raw digital data files in addition to the final vendor report to support further data analysis and the interpretation of results. The digital data files can be used to reprocess the data in-house (for example, DI® Viewer) or conduct additional QA/QC of the data. The digital data can also be uploaded to a project database (for example, EQuIS). From there the data can be downloaded to various software programs and tools (for example, geographic information systems (GIS), WellCAD, Earth Volumetric Studio (EVS), Leapfrog, and RockWorks) to generate data tables, maps, cross sections, and 3D visualizations for analysis and reporting. The digital data can also be used to perform statistical analyses of the various parameters of interest that can later be used for things such as groundwater flow model discretization, remedial system designs, and remedial volume estimates.

4 DIRECT SENSING

Direct sensing ASCT are typically considered tools that can be used to rapidly and efficiently identify physical subsurface conditions (for example, lithology or hydrogeology) and the presence of dissolved-phase contaminants or NAPL. When some direct sensing ASCT are used together, physical and contaminant data can be obtained simultaneously. Based on a project's DQO and CSM data gaps, investigations that incorporate direct sensing technologies can be designed on a variety of scales to obtain the necessary data. The resulting data, which can be high resolution, can fill in data gaps and improve a practitioner's understanding of the CSM, potential cleanup options, and paths to closure.

Direct sensing data improve the development and updating of a project's CSM by characterizing a site and delineating a plume more efficiently than through extensive sample collection and analysis. The faster development of a robust CSM can then progress a site or project more rapidly by supporting investigation, cleanup, and closure decision making. Once a project is at a cleanup stage, the high-resolution data generated by direct sensing tools can aid in understanding exposure pathways, processes affecting fate and transport of contaminants, contaminant mass distribution and flux by phase and media, and how remedial measures will affect a given contaminant. This knowledge can significantly help practitioners in the development of a more robust remedial design that addresses mass distribution, heterogeneity, and hydraulics.

Direct sensing tools are typically deployed using direct-push drilling technology or open boreholes/existing groundwater wells. Most of the direct sensing ASCT are profiling tools that do not allow physical media samples to be collected, and many yield data that are considered qualitative or semiquantitative. However, these data can typically be validated and confirmed through the advancement of soil borings for the collection of confirmation soil, groundwater, and soil vapor samples.

The general adoption of direct sensing tools requires overcoming multiple barriers, such as misperceptions that the tools are not readily available or too expensive and beliefs that the resulting data are perplexing or subjective. The latter may result from a lack of knowledge of the basic principles underlying the function of direct sensing tools. Finally, the lack of guidance for the application of direct sensing tools and integrating them into a project to meet characterization and remedy objectives results in a hesitancy to use these tools.

4.1 Selecting Direct sensing Tools

As shown in **Figure 4-1**, the direct sensing tools evaluated in this section are categorized by the types of data collected. Physical tools measure properties such as porosity, resistance, radioactivity, groundwater flow, and permeability, while chemical tools detect and measure contaminants, for example, detecting VOC in groundwater. It should be noted that while the physical tools do not directly "measure" lithology, grain sizes and soil types are typically interpreted by some of the physical properties that are measured. Lastly, there are the tools that collect both physical and chemical data.

The direct sensing tools described in this section are generally available in North America and many countries worldwide. The systems associated with the tools are often portable and, with a trained operator, can be relatively easily transported if a local platform (for example, direct-push rig) to "drive" the sensors is available. Almost all of the direct sensing tools described in this section have proven histories of use and have been approved by regulators for use at sites across North America. Some regulators may not be familiar with the tools; however, this guidance document provides information to assist those regulators in understanding the use and limitations of these tools. Nevertheless, practitioners should be prepared to provide regulators with information, case studies, and field planning (such as data verification) to support the acceptance of a tool's use in the field.

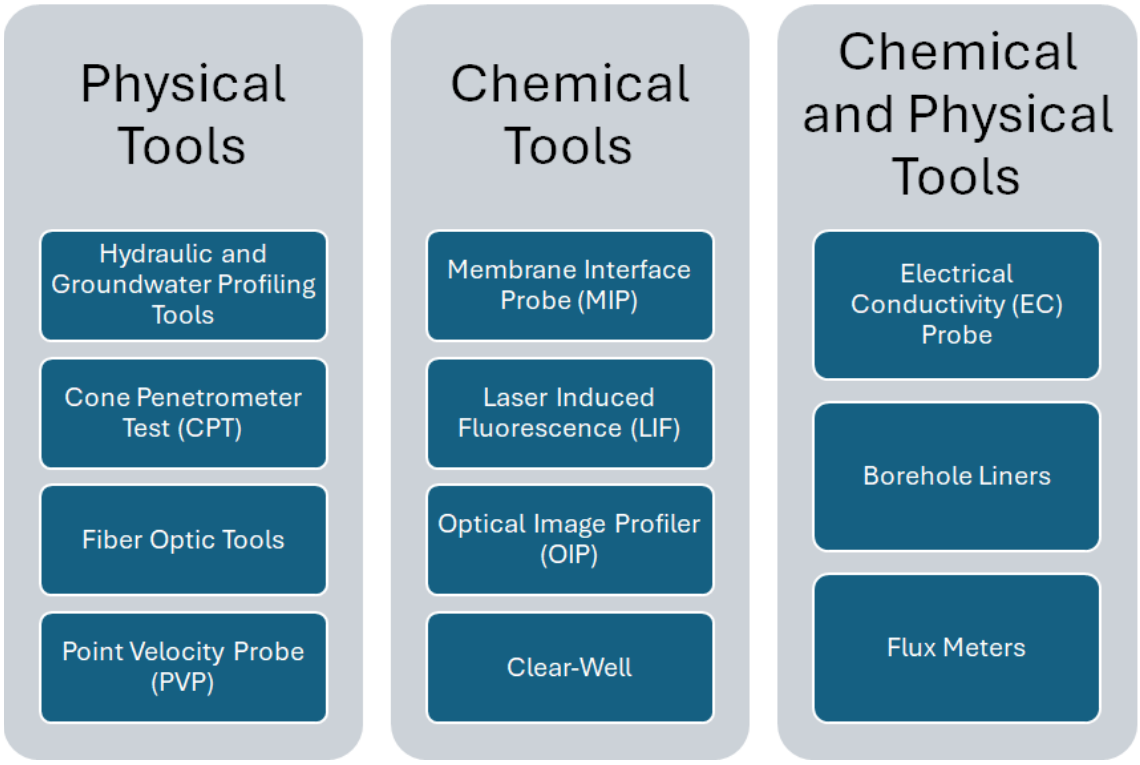


Figure 4-1. Direct sensing tools.

The ASCT-2 Technical Selection Matrices: DS Matrix allows the selection of direct sensing tools to satisfy characterization requirements for a specific topic of interest. This table can help identify the attributes and limitations of a selected tool.

4.1.1 Access

Most direct sensing tools use direct-push platforms to drive sensors and, therefore, need appropriate site clearance for this equipment. Probes can be advanced with smaller track-mounted direct-push-type drilling rigs (versus large truck-mounted drilling rigs) or limited-access direct-push rigs that allow access to areas with low overhead clearance limitations (for example, inside buildings) and soft or unstable ground. Most direct sensing tools can be operated remotely from the direct-push platform, providing significant versatility.

When a direct-push platform is used, the application of direct sensing tools is limited to use in unconsolidated sediments or partially consolidated to weathered bedrock. Unweathered bedrock, cobbles, and boulders can prevent the sensors from being driven into the subsurface. Direct-push drilling also has a practical depth limitation of approximately 100–120 ft below the ground surface in most unconsolidated materials, although greater depths (for example, 300 ft) can be achieved under favorable conditions. To investigate bedrock and other consolidated strata, direct sensing tools may be used in boreholes that were drilled using other methods (for example, sonic, air-rotary casing hammer), but these investigations must be custom designed and are not routine.

Direct sensing technologies that rely on a direct-push platform to deploy the tool, such as the membrane interface probe (MIP), hydraulic profiling tool (HPT), electrical conductivity (EC), and optical image profiler (OIP), are technically incompatible with frozen ground. The mechanical rigidity of nonstandard physical matrices (such as frozen soil and ice-cemented permafrost) causes immediate direct-push refusal and can severely compromise the sensors. Consequently, these technologies have rarely been successfully

deployed in permafrost environments, and empirical evidence regarding their effectiveness in permanently frozen soils is sparse to nonexistent.

4.1.2 Data Collection Design

To ensure that the data collected during the investigation using direct sensing tools are useful and cost-effective, it is particularly important to define the purpose of the investigation (for example, identifying locations for soil borings and monitoring wells, assisting in the design of a remedial system, geotechnical investigation). Some data that may be useful for enhancing the CSM prior to beginning any direct sensing investigation include:

- point(s) of release or source area(s) information
- historic use of the property
- location of underground utilities or structures
- available soil and groundwater sampling data
- depth to groundwater and bedrock

These data should be used to develop proposed boring locations, and measurements of depth to groundwater and depth to bedrock can assist in estimating the total depth of the proposed borings.

Direct sensing tools can be used in conjunction with either static or dynamic sampling approaches. If using a static sampling approach, boring locations are placed on a grid pattern so that resulting data aid in the understanding of the subsurface in an area of contaminant distribution and hydrologic conditions. If the project budget is limited, sampling transects across key areas helps develop a site-wide understanding of the subsurface geology. Dynamic sampling strategies can begin with a grid pattern and use the flexibility provided by these tools to adapt the sampling plan (for example, modify or add sampling locations) in real time to resolve uncertainties. This approach is more useful in areas where little is known regarding contaminant distribution and hydrological conditions at a site. The number of sampling locations needed for investigations using direct sensing tools varies from site to site and may be determined by defining the number of data points required to assess the geology, hydrogeology, and preferential migration pathways.

Like traditional drilling to advance soil borings and install monitoring wells, direct sensing tools carry the risk of cross contamination depending on the depth of penetration. Cross contamination occurs when two or more transmissive zones that are separated by a lower permeability barrier are connected. If one of the transmissive zones contains NAPL or high contaminant concentrations, it is preferable to stop the penetration at the top of the lower permeability barrier so that the potential to open a pathway for contaminants to migrate into a deeper, less contaminated or cleaner zone is limited.

During the advancement of a direct sensing ASCT, the contact between the tool and the borehole wall can act as a seal between the underlying and overlying intervals. However, this is not the case during tool retrieval. If a monitoring device is not installed, grouting the hole is the general best practice to prevent vertical migration of contaminants. Most states have rules or guidelines for sealing such boreholes under their water well drilling program.

4.1.3 Collection of Supporting Data

As stated in Section 4.1, many of the direct sensing ASCT do not allow physical media samples (for example, groundwater grab samples) to be collected, but rather, yield data that are considered qualitative or semiquantitative. These data, however, may be validated or confirmed through the collection of

supporting samples that are typically gathered by the advancement of soil borings for the collection of soil, groundwater, and soil-vapor samples. These supporting data can be used to determine sample types, locations, depths, and analytical parameters so that specific compounds are identified and actual mass concentrations can be measured. Thus, using the supporting data in conjunction with ASCT can help in decision-making for a project, such as supporting additional sampling efforts, monitoring well placement, and well screen intervals. The project scope should include the overall goals of the investigation and identify technical lines of evidence that need to be developed when methods and technologies are being selected.

It should be noted that where direct sensing tools cannot be used due to site geology, contaminant type, or other constraints, many of these supporting tools can be used to reach the same objectives as direct sensing tools. When doing so, practitioners can apply adaptive management strategies, such as the Triad approach (Crumbling 2004), by collecting a high density of physical media samples (soil, soil-gas, or groundwater) for laboratory analyses, allowing for real-time evaluations and data-driven adjustments to the scope of work that then leads to more efficient site characterization. It should be noted, however, that this approach can have a greater expense than traditional sampling methods, but can yield similar benefits to using the more advanced tools.

4.1.3.1 Sampling Tools

Sometimes, physical-media samples are required to obtain supporting data. A variety of tools may be used to collect these media samples. These tools use methods that allow sample collection (groundwater, soil, or soil gas) over discrete depths (from a few feet to a few inches) and generally are employed at multiple depth intervals in a boring to provide a high-resolution vertical profile of analyte concentrations or physical properties across a formation. The physical samples can then be further investigated for field or laboratory analyses. Many of these sampling tools are medium-specific. Like when using any tool, the user should be aware of the tool's limitations in all applications.

Soil and Bedrock Sampling Tools

Unless sampling is limited to the surface, the collection of soil and bedrock samples requires the use of one or more drilling technologies. Common drilling methods include hand auger, direct push, hollow stem auger, mud and air rotary, sonic technologies in unconsolidated sediments, and core drilling in bedrock. Some drilling methods retrieve soil or bedrock as the drill tooling is advanced, while others include the use of a sample "collector," such as a Shelby tube (thin-walled sampler), piston sampler, or double-tube core barrel. Environmental soil sampling has traditionally included methods originally designed for geotechnical sampling, such as hollow-stem auger and sampling with drop hammer split-spoon samplers. Drilling technology should be chosen based on project-specific details, such as the anticipated lithology, terminal depth, access, and waste. Some drilling methods advanced without coring, such as rotary, result in large data gaps and excessive waste soil. Alternatively, direct-push continuous dual-tube systems, such as Geoprobe DT22 and DT325, will collect longer core intervals while producing less waste. While hollow-stem auger drilling also produces more waste soil, core samples can be collected using tools such as a split-spoon sampler or continuous core barrel when the appropriate drill bit is used. It should be noted that hollow-stem auger and sonic dual-tube continuous-core systems are more appropriate in difficult drilling lithologies. Rotary, rock coring, and sonic drilling are preferred when collecting samples of bedrock and fractured rock, as most other methods will encounter refusal. Samples collected using rotary drilling, however, will be gathered from the cuttings rather than undisturbed cores.

Groundwater Sampling Tools

A variety of tools exist for the collection of groundwater samples; however, all involve the advancement of a borehole to access groundwater. Practitioners can use any of the drilling methods presented above in Soil and Bedrock Sampling Tools to advance a borehole for the installation of temporary or permanent

groundwater wells. The chosen drilling method will be determined by the medium (such as soil versus bedrock) and the physical attributes of said medium (such as finer grained versus coarser grained soils). Permanent groundwater wells should be installed in accordance with applicable state guidance. When multiple sampling depths are warranted, practitioners can install either nested wells (multiple well casings with different screen intervals) or well clusters (multiple well casings with different screened intervals installed in multiple neighboring boreholes. It should be noted that isolating multiple targeted intervals with proper seals may be difficult in a single borehole, thus nested wells may have a greater chance of cross-contamination migration. Temporary groundwater wells can be installed in an open borehole using screen and casing (often referred to as blank and screened casing) made from an inert material (such as polyvinylchloride (PVC)). Some drilling technologies allow for the collection of groundwater via the drill tooling. An example of such tools is the Hydropunch™, which is versatile and can be used with multiple drilling methods. Additional direct-push temporary well-point systems include Geoprobe Systems® Screen Point samplers (SP16, SP22, or SP60) and Sonic Screen Points.

Multilevel groundwater monitoring systems are additional sampling devices practitioners can use to collect a physical groundwater sample. Multilevel groundwater monitoring systems include the Solinst® Continuous Multichannel Tubing (CMT) system, Solinst Waterloo Multilevel Groundwater Monitoring System, and Flexible Liner Underground Technologies (FLUTe™) system. Groundwater well packers, or "packers," are tools that allows practitioners to collect samples from multiple depth intervals within a single well. Packers are expandable downhole tools that can isolate specific sections within a borehole or well, allowing said section to be sampled. It should be noted that piezometric testing or monitoring can also be conducted with some of these systems.

Once a temporary or permanent well is installed, practitioners have many tubing and pump options for collecting physical samples. Displacement pumps, such as electric or bladder pumps, are placed down well and send water to the surface via tubing. Others, such as a peristaltic pump, move water through the tubing using a mechanism at the surface. Groundwater samples can also be collected using the tubing or a bailer. When using these tools, both the tubing and bailer are affixed with a check valve at the bottom to allow water to be retained. Practitioners can refer to several external documents for more information on groundwater sampling, such the USEPA's Low Stress (Low Flow) Purging and Sampling Procedure for the Collection of Groundwater Samples from Monitoring Wells or Low-Flow (Minimal Drawdown) Ground-Water Sampling Procedures (Puls and Barcelona 1996; USEPA 2017). When using tubing as part of the sampling process, practitioners should ensure that inert material is being used.

Soil Vapor Sampling Tools

Like with groundwater, collecting soil vapor using active sampling procedures requires the use of a drilling method and the installation of a temporary soil gas probe or a permanent or semipermanent soil gas well to extract the physical soil gas sample.

Temporary probes generally consist of hollow steel probe rods driven with hand tools or direct-push rigs to the sampling depth. The rod is fitted with a sampling tool and a retractable or expendable drive point at the end of the rod, and clean inner tubing connecting the sampling tool to sampling pumps and vessels at the surface. The probe rod is retracted, dropping the drive point, and exposing the soil to the open tool, and a sample can be recovered. These methods collect a sample from disturbed soil, which is not in equilibrium with the soil gas. In accordance with USEPA guidance, grab soil vapor samples can be collected from these temporary probes without equilibrium purging; however, the data are limited to screening purposes.

Permanent or semipermanent soil gas wells or probes are completed by creating a boring via direct-push or auguring methods, then building the equivalent of a miniature monitor well in the boring, including tubing/casing, a screen or implant with a permeable sand pack, and a hydrated seal. It should be noted that in accordance with USEPA guidance, grab soil vapor samples can be collected from these temporary

probes without equilibrium purging; however, the data are limited to screening purposes. After installation, these installations can be purged but are given time to re-equilibrate with the surrounding soil gas after disturbing the soil. This allows data from these samples to be considered quantitative.

For more information on the installation and sampling procedures for active soil vapor probes, see ITRC's Vapor Intrusion Toolkit (ITRC 2026).

Supporting vapor samples can also be collected from the area just beneath the concrete slab of a building. These samples are collected from temporary or permanent sub-slab vapor probes that are installed using a rotary hammer drill. As with active soil vapor probes, sub-slab vapor probes require equilibrium time, leak checking, and purging. For more information on the installation and sampling procedures for active sub-slab vapor probes, see ITRC's Vapor Intrusion Guidance (ITRC 2026).

Finally, another tool for collecting supporting soil-vapor data is passive sampling. Passive soil vapor sampling typically requires shallow drilling, most often with a rotary hammer drill. The probes are typically set at depths ranging from 1 to 3 ft. Once the borehole is drilled, the passive sampler is set downhole for a designated period (typically 1–3 weeks), then retrieved. These samplers can also be placed in existing wells or utility conduits. Passive soil vapor data is considered semiquantitative, and most often used for screening; however, it is an option for obtaining lateral delineation of a VOC plume. For more information on the installation and sampling procedures for passive soil vapor probes, see ITRC's Passive Sampling Technologies Guidance (ITRC 2024) and Vapor Intrusion Guidance (ITRC 2026).

4.1.3.2 Laboratory Analysis

Once physical media samples have been collected, additional analyses must be completed to obtain the required supporting data. Many of these analyses are performed by either a fixed or mobile laboratory. The most common types of laboratory analyses include the evaluation of physical media samples for a site's target chemicals. Chemical analysis can provide concentration mass data that can be used to confirm results generated by ASCT. For each chemical (or group of chemicals) there is one or more analytical methods used by laboratories to detect concentration mass. Practitioners should become familiar with the analytical methods required for their project's contaminants.

Typically, practitioners send the collected media samples to a fixed laboratory for chemical analyses; however, mobile laboratories are available for various media. For example, soil vapor is commonly analyzed by mobile laboratories. Using a mobile laboratory can provide flexibility to a large-scale investigation, allowing the practitioner to adjust sampling locations and depths in real time.

Several direct sensing ASCT provide data about various physical parameters in the subsurface. Some of these parameters can also be confirmed by laboratory analyses. For example, cone penetrometer testing (CPT) provides valuable data on lithology and hydrogeology. The lithology at a specific depth interval can be confirmed by submitting a soil sample to a laboratory for a sieve analyses. These data can be vital in understanding fate and transport or predicting the effectiveness of potential remedial technologies.

4.1.3.3 Field Analyses

Similar to laboratory analyses (traditional or mobile), many field analyses can play a vital role in supporting data produced by direct sensing ASCT. Field analyses can be performed using various tools and methods, including field instruments, manual procedures, or test kits. Practitioners should choose an appropriate field analysis tool based on the type of confirmation data needed.

Many of these tools, such as handheld field meters or soil and water test kits for NAPL, generate additional qualitative or semiquantitative data. However, additional qualitative data may be enough to confirm ASCT data. For example, direct sensing tools such as UVOST® or OIP are used to identify the

presence of NAPL in soil and groundwater. To confirm UVOST peaks, a practitioner may only need to use a colorimetric soil test kit, which yields a "yes or no" answer, rather than a concentration. Confirming UVOST peaks in groundwater may also be done with a simple visual inspection of a collected groundwater sample. Some supporting field analysis tools, such as a portable gas chromatograph (GC) or a portable GC/mass spectrometer (MS), generate quantitative or semiquantitative data, such as mobile laboratory results. For example, a portable GC/MS can be used to measure real-time VOC concentrations at multiple soil vapor probes to confirm membrane interface probe (MIP) peaks.

It should be noted that some states may not accept data generated by certain tools for risk assessment purposes. This is particularly the case with tools that generate qualitative or semiquantitative data. Practitioners should always check with their oversight agency prior to selecting the appropriate supporting tool and analysis.

Here is a partial list of examples of supporting field analysis tools and methods:

- portable gas chromatograph (GC)
- portable gas chromatograph/mass spectrometer (GC/MS)
- handheld organic vapor detectors, such as a photoionization detector (PID) and flame ionization detector (FID)
- air and landfill gas meters (for example, O_2, CO_2, CH_4)
- radiation meters
- vapor-sensing colorimetric tubes
- handheld metal detectors, such as X-ray fluorescence (XRF)
- water quality meters (for example, pH, oxidation-reduction potential (ORP), conductivity, turbidity, temperature)
- water titration or colorimetric test kits
- soil and water test kits
- immunoassays and enzymatic assays

4.2 Cone Penetrometer Testing

4.2.1 What Is the Technology?

Cone penetrometer testing (CPT) is used to characterize geologic (lithology) and hydrologic properties in the subsurface, commonly in geotechnical applications. It is considered the "static" direct-push method of direct-push technologies (DPT)—that is, it uses the static weight of the vehicle to push the tools, rather than a hydraulic percussion hammer. It is generally applied to sites with unconsolidated lithology but may also be effective in soft rock. The detailed lithologic interpretation provided by CPT may be used to identify and distinguish soils with different grain sizes, the presence of groundwater, and zones of high or low permeability, making the tool useful for characterizing sites with discrete horizons or discontinuous lenses, or further defining groundwater migration pathways and potential groundwater storage zones.

CPT uses the weight of the vehicle to advance push rods affixed with a 60° cone penetrometer through the subsurface at a constant rate, usually 2 cm/sec. The cone penetrometer cross-sectional area varies in size, typically ranging from 10 to 15 centimeters squared (cm^2). The cone penetrometer can typically be advanced to depths up to 150 ft, but has been used as deep as 300 ft. Penetration depth is improved by using an expanded coupling behind the cone (friction reducer), which reduces friction on the rods by

enlarging the hole. CPT probes are designed for push-only applications and cannot be driven with a hammer or other percussion methods, which may limit the terminal penetration depth. Greater penetration depths may be achieved by predrilling through intervals where CPT data are not needed or subsurface conditions limit cone advancement.

A typical CPT platform is a hydraulic ram mounted in a box truck or tracked vehicle rated at 5 to 35 tons of downforce via the dead weight of the vehicle, or combined weight and anchoring. A string of 1-meter-long threaded rod segments is used to push probes into the subsurface. The system includes the following components:

- an electrical cone penetrometer
- a hydraulic pushing system with rods
- cable or data transmission device
- depth recorder
- piezoelectric element to measure pore pressure
- strain gauges to measure the tip resistance and sleeve friction
- data acquisition unit

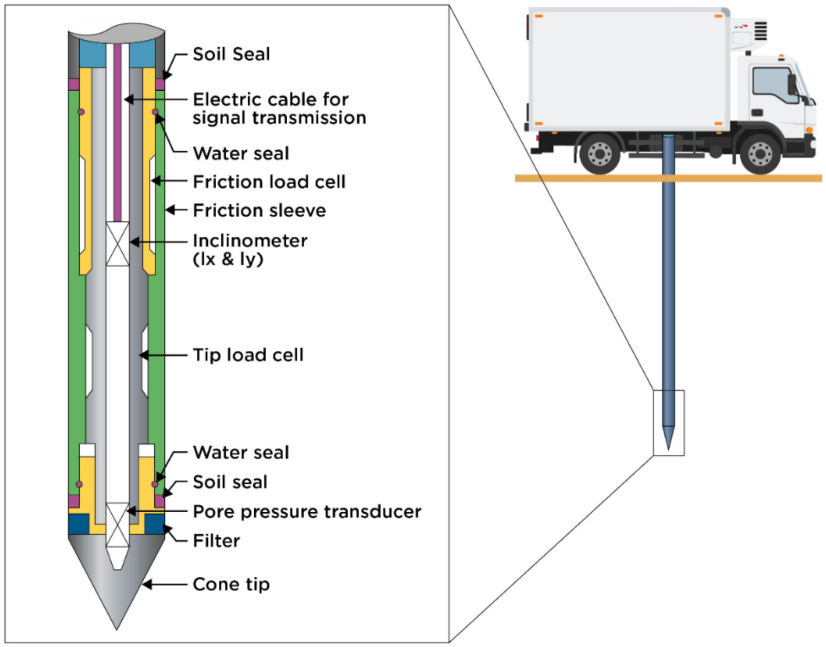


Figure 4-2. Typical CPT configuration.

Source: Adapted by Geosyntec Consultants, Inc., from Gregg Drilling & Testing, Inc. Used with permission.

Figure 4-2 illustrates a typical CPT platform and system (P. K. Robertson and Cabal 2008).

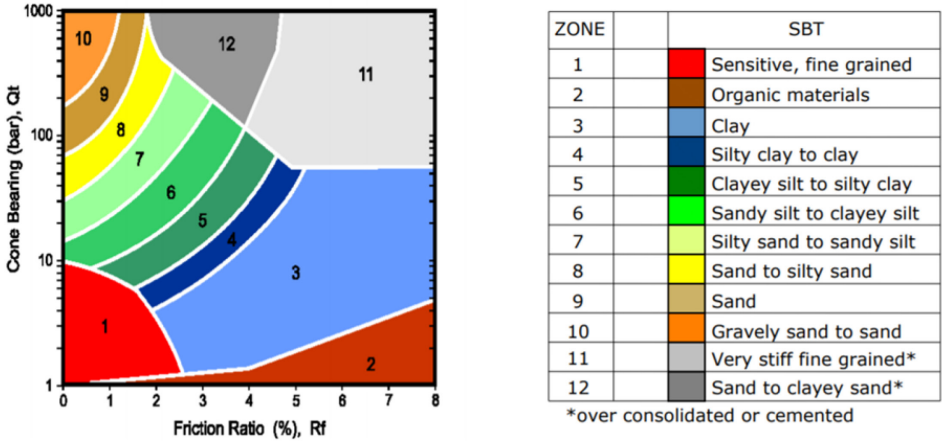
4.2.2 How Is the Technology Used?

CPT is used to evaluate the stratigraphy, soil types, water table, and engineering parameters of the subsurface. Data are logged directly to a field computer and can be assessed in real time by the on-site geotechnical engineer or scientist. CPT results should not be interpreted without reference to the CSM and, if available, other lines of evidence.

CPT measures tip resistance (qc) and sleeve friction (fs), typically at 1- to 5-cm intervals. Tip resistance is theoretically related to the shear strength of soils and is measured with an embedded load cell. The sleeve friction is related to the remolded shear strength of the soil being penetrated and is also measured using a load cell embedded in the sleeve (USDA 2009).

Tip resistance and sleeve friction are often plotted as the friction ratio (Rf) to aid in interpreting soil type (for example, sand, silt, clay; see Figure 4-3; defined as “soil behavior type” (P. K. J. Robertson et al. 1986; P. K. Robertson 1990)) based on various soil classification schemes. Generally, clay soils have a high friction ratio and sandy soils have a high tip resistance; however, values are dependent on individual soils

(ScienceDirect 2016). CPT probes may also be equipped with a pore-pressure sensor[1] (Lunne et al. 1997) to improve soil classification data. Dissipation tests conducted with a piezocone penetrometer (CPTu) also assist in estimating approximate hydraulic head and soil permeability or hydraulic conductivity at the point of measurement (P. K. Robertson et al. 2011). A typical CPT log is shown on **Figure 4-4**.



ZONE		SBT
1		Sensitive, fine grained
2		Organic materials
3		Clay
4		Silty clay to clay
5		Clayey silt to silty clay
6		Sandy silt to clayey silt
7		Silty sand to sandy silt
8		Sand to silty sand
9		Sand
10		Gravely sand to sand
11		Very stiff fine grained*
12		Sand to clayey sand*

*over consolidated or cemented

Figure 4-3. Soil behavior types (the interpreted lithology).

Source: Gregg Drilling & Testing, Inc. Used with permission.

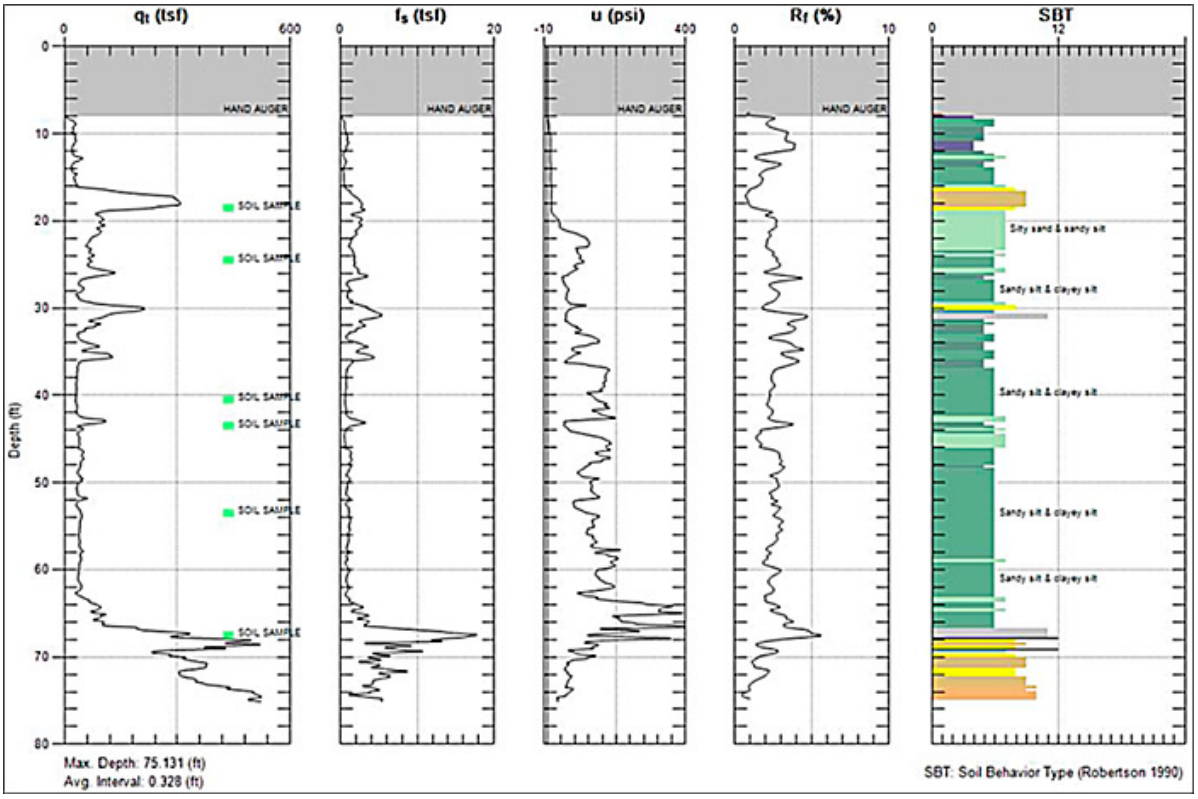


Figure 4-4. Typical CPT log. Total cone tip resistance (qt), sleeve friction (fs), friction ratio (Rf), pore pressure (u, pounds per square inch), soil behavior type (SBT).

Source: Gregg Drilling & Testing, Inc. Used with permission.

[1] A CPT cone equipped with a pore pressure sensor is referred to as a piezocone and CPT test using a piezocone is often abbreviated as CPTu).

4.2.2.1 QA/QC

CPT soundings should be performed in accordance with (ASTM 2012). CPT sensing devices should be properly calibrated using reference standards or by identifying readings considered reasonable by an experienced technician. Baseline readings (under zero load) should be measured before and after each sounding to assess measurement stability and consistency. Additional details are provided in the sections below.

Quality Assurance Prior to Use

Site conditions and objectives should be evaluated to determine the applicability of the CPT on site. Prior to use, lithology to be penetrated, potential interferences, and potential refusal depth must be evaluated to the extent practicable.

Quality Control During Use

Progress should be carefully observed, and the data (output on video screens in truck) should be viewed while advancing CPT. The advancement (push) rate must be monitored for deviations to account for associated response variations; the rate should not exceed method specifications. Slower advancement rates produce higher data densities, with minimal risk to data quality, but reduce daily production. An inclinometer on the probe is used to measure deviation from vertical, which should not exceed 2 inches.

Quality Control After Use

Targeted follow-up sampling (when data suggest the need) and comparison to existing logs, if available, may be used to validate CPT output. The results of dissipation tests and pore-pressure readings may require assistance from the CPT vendor for interpretation.

The CPT tool was designed primarily for measuring geotechnical soil/sediment properties for engineering applications. For environmental applications, it is used for identifying lithology types and hydraulic properties, and additional supporting tools have been added or stacked on the CPT tool to provide other sensing capabilities.

4.2.2.2 Supporting and Enhancing Instruments and Technologies

The following tools can be stacked on a CPT tool string (by some vendors) for environmental applications. These tools are described in detail in later sections:

- MIP (see Section 4.5 for a detailed description)
- OIP (see Section 4.6 for detailed description)
- Laser-induced fluorescence (LIF) (see Section 4.7 for a detailed description)
- HPT (see Section 4.4.1.1 for a detailed description)
- EC (see Section 4.3 for a detailed description)
- Gamma probe (Gamma techniques have been specifically developed for use in tandem with CPT; See Section 5.6 for a detailed description)

4.2.3 What Are the Advantages?

CPT data provide continuous profiles of soil information that can be used to provide an accurate CSM. Quantitative data on soil properties can be used to provide reliable strength and consolidation engineering design parameters and relevant environmental parameters for groundwater movement. CPT rigs may be able to drive direct sensing tools in soils too dense or consolidated for other direct-push rigs and may be able to reach greater depths.

4.2.4 What Are the Limitations?

Like other direct-push technology methods, CPT use is limited to sites with unconsolidated lithology and, possibly, soft or weathered bedrock, and cannot be used in competent bedrock or sediments with large gravel or cobbles.

The static push method requires either anchoring the rig to the ground or simply using the weight of the rig to overcome push friction. Smaller (lighter) and anchoring-type CPT rigs have shallower capabilities compared to larger (heavier) CPT rigs because rod friction during the static weight push gets greater with depth.

CPT does not provide direct grain-size measurement, and soils that do not conform to the expected behavior types may be misinterpreted.

When using CPT, soil behavior types may present an ambiguous representation when soil properties are nonstandard (for example, very dense or stiff soil) and omit grain-size information. These soils may have both elevated tip resistance and sleeve friction values and are not always handled accurately by the algorithm that calculates the soil behavior type. Experience suggests that dense fine-grained sand, for example, may not be accurately identified. Verification by collecting physical soil samples or comparing CPT results to existing lithologic logs may mitigate this phenomenon.

4.3 Electrical Conductivity (EC) Probe

4.3.1 What Is the Technology?

Electrical conductivity (EC) probes measure bulk conductivity or the ability of a particular material (for example, soil or sediment, or saturated sediments) to conduct an electrical current. Electrical conductivity is the direct inverse of electrical resistivity (ohm-meters (Ωm)) and is measured in millisiemens per meter (mS/m). The EC probe is typically deployed by direct-push methods (static or percussion) to measure the apparent EC of the bulk formation (solids and fluids) located adjacent to the advancing probe. The term “apparent conductivity” is used because the probe measures the bulk or average conductivity of materials near it.

As the probe is advanced, it produces a continuous log of apparent conductivity versus depth. Measurements of EC can be

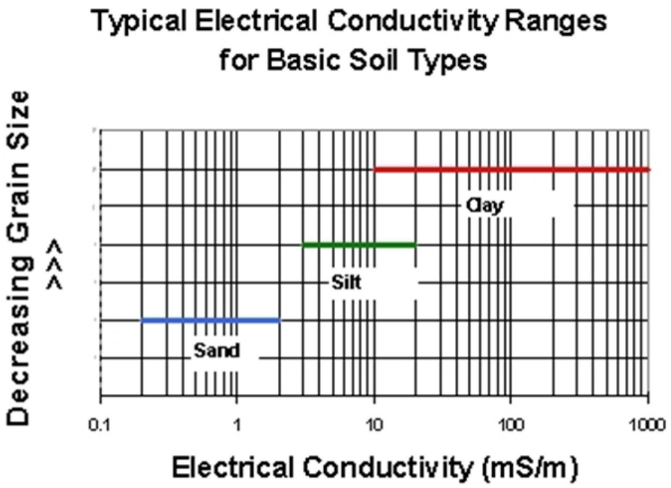


Figure 4-5. Typical EC measurements for sand, silt, and clay.

Source: Geoprobe Systems® Geoprobe (2015). Used with permission.

used to infer the presence of more highly conductive subsurface materials such as clays, but because EC can be influenced by several factors, EC probes are typically used in conjunction with other tools, such as the Hydraulic Profiling Tool (HPT) to better determine the true nature of the subsurface materials being investigated (USEPA 2016b).

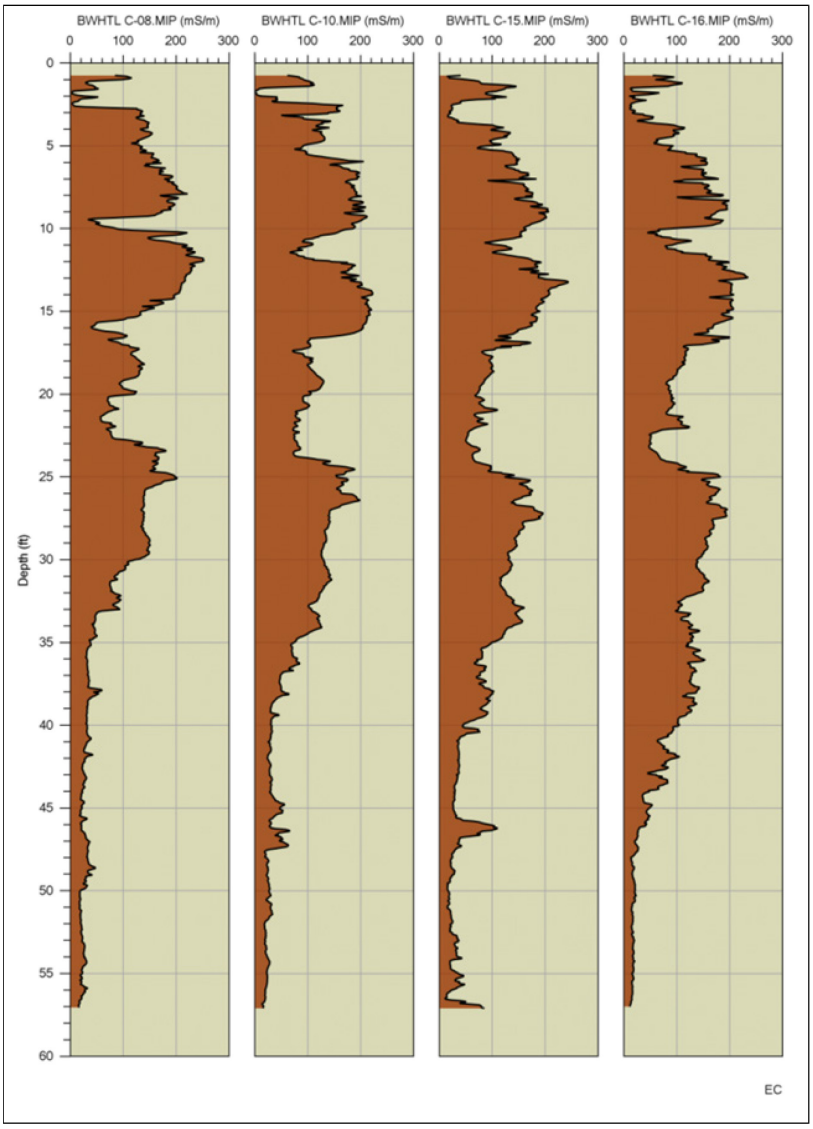


Figure 4-6. Example of EC logs along a cross section.

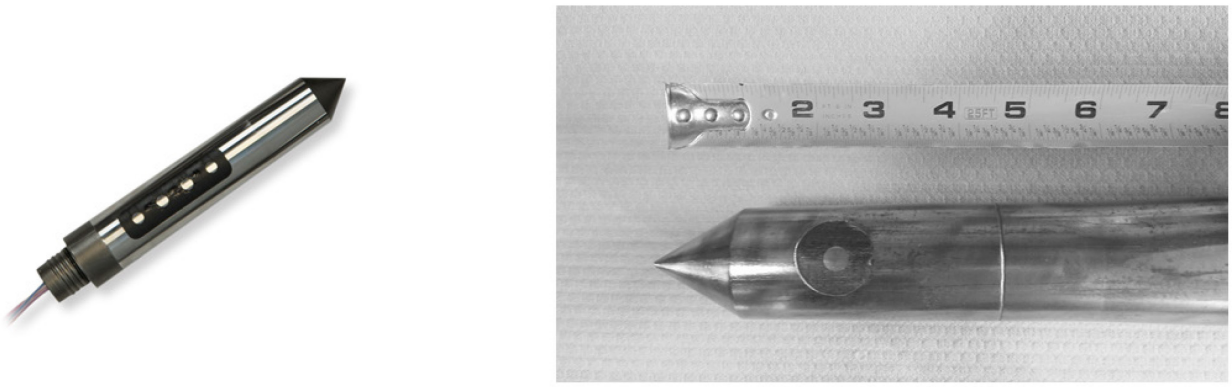
Source: Geoprobe Systems®. Used with permission.

Finer grained soils, such as silt or clay, have a higher surface-area-to-volume ratio than coarser grained sand and gravel, which promotes better particle-to-particle contact and can create finer, more interconnected, and water-saturated pore networks. As such, finer grained soils tend to produce higher EC signals. While specific values cannot be assigned to each soil type, each soil type typically provides a different response. The addition of ionic materials (salts), however, also increases the conductivity, and the tool can be used to look for high concentrations of, for example, brine spills. **Figure 4-5** shows the typical EC measurements for sand, silt, and clay.

An EC probe is frequently used to map potential contaminant pathways. Zones of lower EC usually indicate coarser grained, more permeable materials. These more permeable zones allow contaminants to migrate in the subsurface (path of least resistance). Finer grained sediments (for example, clays) can trap and store contaminants. The EC gives the investigator real-time, on-screen logs for on-site decision making. Once multiple logs are generated, a cross-sectional view of a series of logs is helpful to visualize how these preferential pathways connect across a site (**Figure 4-6**). On these example logs, coarser grained sediments are located near 10 ft to 11 ft and 16 ft to 24 ft below ground surface (bgs) and are also present near the bottom of the logs. More conductive, finer grained sediments are present elsewhere in the logs.

EC probes vary in design but in general appearance look like the probes in **Figure 4-7**. The volume of material being measured is fixed and does not extend far from the probe's surface. Of the two electrode configurations, the Wenner array measures a somewhat larger volume of the formation proportional to the length of the array. Using this configuration, more averaging is necessary to obtain the output signal

in the log, so small-scale features, such as a 1-inch-thick clay lens in a sand body, may not be as clearly distinguishable. Conversely, dipole arrays sample a smaller volume of the formation and therefore more easily distinguish the smaller-scale lithologic features. These probes measure bulk formation EC and provide a measure of the combined EC of the formation solids and any contained fluids and dissolved ions (Milsom and Eriksen 2011).



A B

Figure 4-7. EC probe with four-pole Wenner array (A) and simple dipole (B).

Source: Geoprobe Systems®. Used with permission.

The EC tool consists of the probe, a trunk line to connect the probe to the field instrument (**Figure 4-7**), a string potentiometer to measure sensor depth, and a laptop to process and view the EC versus depth and probe-advancement rate logs. As the probe is advanced into the ground, information from the field instrument is relayed to the field computer, which displays EC (in mS/m), depth of measurement, and probe advancement rate (**Figure 4-8**). The field instrument provides current to the probe and senses both downhole current and potential difference values. The probe is used in concert with a direct-push-type rig operated in either push or percussion mode.



Figure 4-8. Geoprobe FI 6000 laptop display and field instrument.

Source: Geoprobe Systems®. Used with permission.

4.3.2 How Is the Technology Used?

4.3.2.1 Data Collection Design

EC surveys are commonly used to help identify subsurface stratigraphic features that may be helping to control contaminant transport. If fine-grained deposits exist in the form of discontinuous lenses or as laterally continuous layers, then an EC survey combined with limited

soil coring could be useful in helping to refine the CSM. The amount of heterogeneity present determines the density of survey boreholes required at a given site. In many cases, a gridded approach to survey design may be used, especially if little is known about a particular site.

EC surveys can also be used to better identify the location or width of a conductive groundwater plume—for example, a brine release. In this case, course-grained, relatively nonconductive sandy or gravelly sedimentary environments may be ideal because EC would be mainly a function of the ionic content of the pore water. Under such circumstances, laying out a series of borings in the form of a transect(s) downgradient of the plume source may be advantageous. Regardless of the survey goal, using other tools or methods as multiple lines of evidence is often advantageous to support survey conclusions.

4.3.2.2 Data Interpretation and Presentation

Interpretation and presentation of EC logging data are straightforward. In many instances, elevated EC values indicate the presence of finer grained sedimentary layers (for example, silt or clay). Other tools can be used in conjunction with EC logging to identify situations where this relationship does not hold true. **Figure 4-9** shows an EC log obtained from the Arkansas River alluvial aquifer. From the interpretation provided (verified by targeted sampling), increasing EC values in freshwater formations typically indicate increasing clay content. Yet this is not always true, as clay mineralogy and the presence of brine can affect EC log response. Here the water table is visible where clean sand goes from dry to saturated at about 9 ft bgs. In finer grained materials, the water level is typically not discernible. When combined with the HPT, the HPT pressure correlates with the EC response unless ionic interferences are present (**Figure 4-9**). Various data presentation options are available, with the most common being to display individual EC logs side by side.

EC field logs are initially displayed on a laptop computer as conductivity versus depth. A separate log indicating probe advancement rate is also displayed, primarily for field use and may or may not be included in a final report. The EC probe should be advanced at a rate of approximately 2 cm/sec to ensure adequate contact between the probe and sediment and consistent results between adjacent boreholes. Because the probe is commonly used in tandem with other sensors that are more sensitive to advancement rate, advancement rates for each log should be confirmed to be close to the 2 cm/sec value.

If the ionic content of the soil and pore waters is believed to be consistent at a given site, then EC should be primarily a function of grain size and clay content, with higher EC values being associated with smaller grain size and more conductive clays. Silts and clays are less permeable than coarser grained sediments, which is why it is often advantageous to plot EC logs alongside hydraulic profiling logs obtained from the same borehole. When using this approach, a low-permeability clay should exhibit a similar

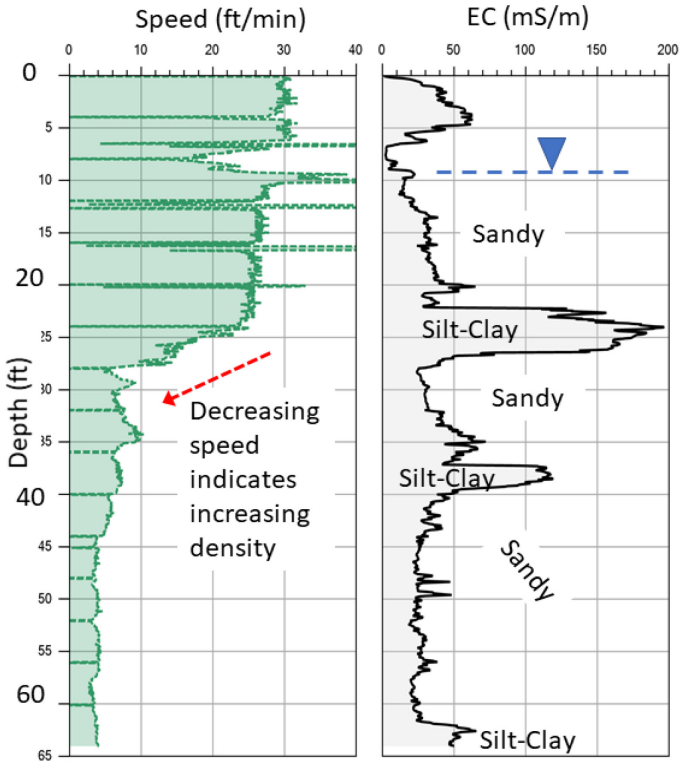


Figure 4-9. EC log (right) with associated probe advancement rate log (left).

Source: Geoprobe Systems®. Used with permission.

signature on both the EC and hydraulic profiling logs. An inverse relationship (for example, high EC and low pressure) may indicate coarser grained materials containing conductive pore water. **Figure 4-10** provides an example EC log that shows mostly sand and gravel present above approximately 23 ft and a clay layer below this depth, based on the abrupt pressure increase on the HPT log below 23 ft. Note that the EC log peaks above the clay layer. This effect is produced by the presence of sodium persulfate in the more permeable material located above the clay.

There are several different options when it comes to displaying EC data. Typically, EC data are simply presented as a log of conductivity versus depth with multiple logs being displayed in a cross-section format (**Figure 4-6**). If HPT is used in concert with the EC array, both sets of data (EC and corrected pressure curves) can be plotted on the same log or on adjacent logs to aid in data interpretation. While perhaps less common, plot plan view slice maps or even 3D images of EC can be created using appropriate software. Whatever the presentation style, EC data should not be viewed in isolation but should be presented with some form of supporting information (for example, HPT, natural gamma log).

4.3.2.3 QA/QC

Diagnostic tests should be run on the EC probe before and after each boring log. An EC load test confirms that the actual measured EC values are within 10% of the target values for three separate conductivity values. If the EC probe passes the load test, then the tool is ready for logging. If the EC probe fails the load test, then a separate set of tests must be run to troubleshoot the problem. If the EC probe is functioning as designed, then only pre- and post-load tests are required (Geoprobe 2015).

Because EC can be affected by multiple factors, it is common to collect at least a single sediment core near an EC boring to confirm log interpretation and allow correlation with strata identified in the core. Ideally, several core logs are available for a given site; other tools can be used in tandem with EC to assist with EC log interpretation.

4.3.2.4 Tool Suitability

Using the EC probe in areas known to contain mainly coarser grained, nonconductive soils (for example, coastal plain environments) may be of little benefit unless the survey goal is to map a zone of highly conductive pore water such as a saltwater intrusion. The EC probe is likely to be most useful in more heterogeneous unconsolidated environments where greater understanding of hydrostratigraphic relationships is required. It can also be useful for defining (in high resolution) acidic buried wastes, high-concentration total dissolved solid plumes (for example, brines) in groundwater, injected reagents, and buried material that has an EC different from the deposits that contain the buried waste.

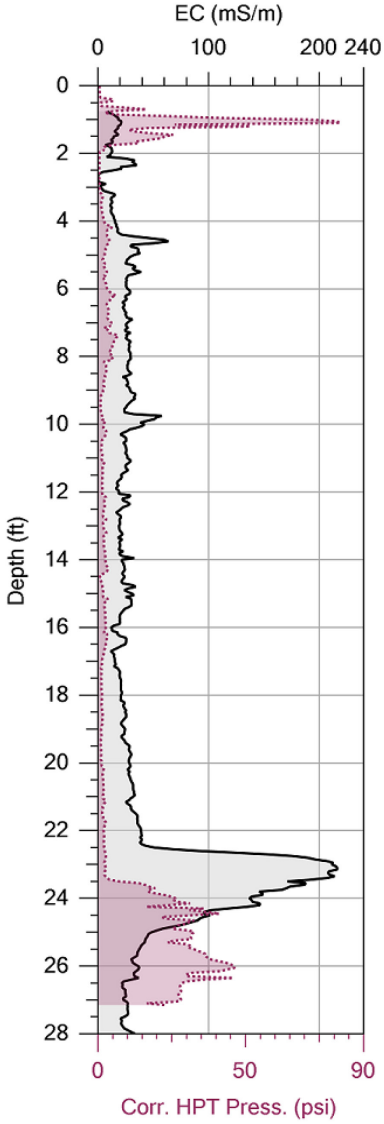


Figure 4-10. EC log (solid black line) and superimposed HPT pressure log (dashed purple line) corrected for hydrostatic pressure.

Source: Modified from McCall et al. (2014), Used with permission.

4.3.3 What Are the Advantages?

The simplicity and resilience of the EC probe make it a tool that can be used to quickly (and therefore cost effectively) differentiate fine- and coarse-grained materials at a centimeter level of precision. In homogeneous or well understood geology, it can be used to rapidly map conductive groundwater, such as might result from a leachate plume at a landfill, a brine release, or coastal saline intrusion. Used together with other tools such as HPT, it can confirm and fine tune stratigraphic sequences and even measure groundwater specific electrical conductance (SEC). The EC is rarely used alone with current configurations of direct sensing probes but may be a useful cost-effective option to use alone at some sites.

4.3.4 What Are the Limitations?

As with the other direct sensing tools, EC probes are limited to static or percussion direct push in unconsolidated sediments or highly weathered bedrock and cannot be used in competent bedrock applications or sediments with cobbles.

In freshwater formations, elevated EC readings often indicate increased clay content, but not all clays exhibit high EC. The presence of elevated dissolved ions (such as sodium, calcium, chloride, or ionic remediation fluids such as sodium persulfate) can further complicate EC log interpretation. High concentrations of dissolved ions can completely overwhelm and mask changes in EC due to lithologic variations. Because of these limitations, targeted soil and sometimes groundwater sampling should be conducted to verify log interpretation (McCall et al. 2017). The EC probe can also be used in conjunction with HPT (Section 4.4) as a means of addressing these limitations.

4.3.4.1 Detection Limits

EC logging resolution may depend upon several factors. The type of array configuration used (Wenner vs. dipole) may have some effect with respect to resolution, with the dipole configuration providing somewhat higher resolution (Geoprobe 1994). Using the Wenner configuration, clay layers as thin as 2.5 cm have been identified. Clay type can also be a factor. Clays with high cation-exchange capacity, such as smectite and montmorillonite, are more conductive and therefore more easily resolvable than kaolinite clays. Probes measure conductivity every 1.5 cm as the probe is advanced (Schulmeister et al. 2003). The instrument measures the bulk conductivity of soils, sediments, pore fluids, or other materials located in the proximity of the probe, generally within 5 cm to 10 cm (Beck et al. 2000).

4.3.4.2 Interferences

The EC probe is subject to certain interferences that may hinder or prevent it from detecting stratigraphic changes. It is possible that highly mineralized or otherwise conductive pore waters may overwhelm the ability of the EC probe to detect discrete changes in lithology that may be of interest. For instance, a thin conductive clay layer surrounded by sands or gravels filled with saline pore water may not be resolvable. If work is being performed in a disturbed area, buried debris, especially metallic debris, could affect readings if the debris were to come into direct contact with the probe array.

4.4 Hydraulic and Groundwater Profiling Tools

4.4.1 What Is the Technology?

Hydraulic and groundwater profiling tools are a group of injection flow-logging tools with the primary purpose to measure relative permeability or actual hydraulic conductivity. The advantage of hydraulic and

groundwater profiling tools is that they are capable of collecting a high density of hydrologic, lithologic, and groundwater data. The common feature is that they all measure pressure and flow as water is injected into the formation as the probe is pushed through the soil/sediment column. Injection pressure is inversely proportional to formation permeability, so relative permeability can be measured. The tools can be used independently, and some can be used in combination with other sensing tools on a single tool string. Some versions of these tools also perform discrete-interval groundwater sampling. These tools are used in conjunction with a direct-push platform and include the following:

- **Hydraulic profiling tool (HPT)**–an injection-flow logging tool that measures downhole injection pressure, injection flow, hydraulic conductivity, and bulk electrical conductivity (EC) and can be used alone or integrated with MIP, OIP, and (Cascade 2026; Geoprobe 2026a) laser-induced fluorescence (LIF). Under certain conditions, it can also perform dissipation tests to measure piezometric head and uses these values to estimate hydraulic conductivity (K_{est}), and report groundwater specific electrical conductance (SEC), which is related to total dissolved solids (Geoprobe 2026b).
- **Waterloo Advanced Profiling System (Waterloo APS)**–an integrated injection-flow logging and discrete interval groundwater sampling tool that measures pressure and flow, and calculates the index of conductivity (I_k), a relative permeability indicator.
- **Hydraulic profiling tool–groundwater sampler (HPT-GWS)**–an integrated injection-flow logging and discrete interval groundwater sampling tool (2.25" diameter) that measures pressure, flow, hydraulic conductivity, and EC. Under certain conditions, it can also perform dissipation tests to measure piezometric head and uses these values to estimate hydraulic conductivity (K_{est}), and report groundwater SEC, which is related to total dissolved solids.
- **Hydraulic profiling tool–groundwater profiler (HPT-GWP)**–a smaller version of the HPT-GWS tool (1.75" diameter) that measures injection pressure and flow and collects discrete groundwater samples but does not include the EC or downhole pressure sensor (Geoprobe 2026b).

Figure 4-11 summarizes the capabilities of the hydraulic and groundwater profiling tools.

These multipurpose tools generate real-time logs of formation permeability while advancing through the subsurface. The tools operate in unconsolidated formations, commonly to depths of 100 ft and sometimes deeper. The value of these tools is the lithologic and hydrologic data generated, which allows contaminant mass relationships to formation permeability, flow zones, confinement, and sorbed storage to be understood and identified.

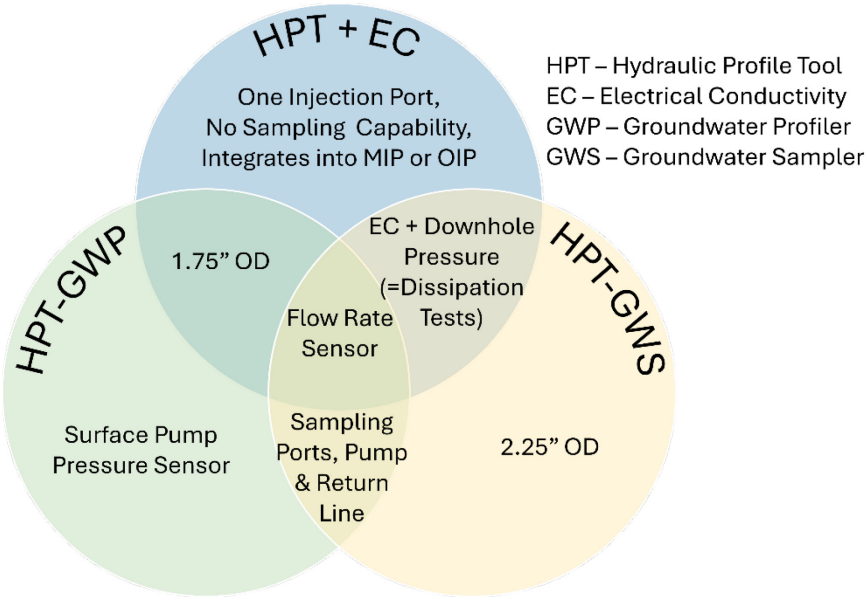


Figure 4-11. Capabilities of Geoprobe hydraulic and groundwater profiling tools.

The primary benefits of hydraulic and groundwater profiling tools are that they:

- optimize site characterization and remedial efforts by providing a high-resolution, real-time depiction of formation permeability, including potential contaminant flow pathways and potential confining layers, which can be used to optimize well and well screen placement
- identify the water table, infer lithology, identify confined or semiconfined aquifers, and estimate hydraulic conductivity in the saturated zone
- integrate with MIP, OIP, or LIF tools to understand the depth and distribution of contaminant mass relative to formation permeability and infer relative mass flux
- collect discrete groundwater samples from a short screen interval (2 inches to 6 inches) in identified permeability intervals to generate a vertical quantitative groundwater data profile of dissolved non-VOC or semivolatile organic compound (SVOC) contaminants that cannot be detected with the chemical sensing tools (MIP, OIP, LIF, etc.)
- rapidly characterize site contaminant impacts and hydrogeologic conditions without installing permanent monitoring wells, and with the data gathered can aid in optimizing monitoring well network installation and screen interval placement

Applications for hydraulic profiling tools include:

- site characterization (hydrostratigraphy–relative confinement, confining beds [aquitards], contaminant pathways, hydraulic conductivity)
- sampling and well design (optimized well placement–screen intervals, physical sampling locations)
- contaminant delineation (dissolved brine or metal ion [total dissolved solids (TDS)] plumes–vertical and lateral extent, NAPL as related to confining zones)
- enhance remedial design and monitoring (design characterization–reagent tracking, pumping system effects, performance monitoring, map emplaced fractures)
- groundwater resource investigations (identify production zones, artesian [confined] conditions, pumping effects, profile water quality)

Hydraulic and groundwater profiling tools are typically operated by trained professionals employed by a drilling company or other specialty vendors. No specific training is required for an environmental professional to use these tools, but it is recommended that a scientist familiar with site geology oversee tool operation to direct the contractor where to terminate borings and collect samples (if applicable) and assist the operator with the interpretation. Some tool vendors offer software for viewing log data and creating other custom outputs (for example, creating logs in custom formats, creating simple cross sections, overlaying logs).

Injection-flow logging tools measure the pressure required by a water pump to inject a flow of clean water (generally clean tap water) into the soil, through small screen port(s) on the side of the tool, as the probe is advanced into the subsurface. The tool produces a graphical log of injection pressure and flow with depth, which can be used to infer formation permeability and to calculate semiqualitative values of hydraulic conductivity with depth. Injection flow logging is useful for understanding the heterogeneity of formation permeability, which often varies over short vertical, and to a lesser extent, horizontal distances.

The sampling version of these tools (HPT-GWS, HPT-GWP, and Waterloo APS) combines injection-flow logging with discrete interval groundwater sampling. Because the groundwater samples collected are submitted for laboratory analysis, these tools are not limited to detecting a certain type of contaminant. Deionized injection water may be required for certain applications, such as metals analysis, for purging

the sampling lines prior to sampling. Once groundwater samples are evaluated by a laboratory, the collective dataset includes formation permeability and quantitative groundwater analytical data.

Together, hydraulic and groundwater profiling tools are capable of generating a powerful high-resolution dataset that can be used to understand contaminant mass in relation to formation permeability.

4.4.1.1 HPT

The HPT is an injection-flow logging tool manufactured by Geoprobe Systems that measures the pressure required to inject water into the soil, and the flow rate, as a probe is advanced into the subsurface. The tool includes an EC Wenner array to measure bulk soil conductivity and a downhole pressure transducer to measure piezometric head. The downhole components of the tool include (**Figure 4-12**):

- probe equipped with an injection screen port and EC Wenner array
- pressure sensor (transducer) to measure combined ambient, injection, and hydrostatic pressure
- trunk line consisting of electrical wires and a water-injection line
- connection tube and drive head with the pressure sensor, electrical wires, and water-injection line
- probe rods (1.75- or 1.5-inch-diameter rods are typically used, and successive rods are added as the probe is advanced with depth)

The aboveground components of the tool are similar to the instruments shown in **Figure 4-8** and consist of:

- data acquisition instrument—measures EC and acquires data from other instruments (such as MIP) if the HPT is being used in conjunction with another tool
- computer—receives data from acquisition instrument, displays logs, and saves all data and operating parameters
- controller—regulates the flow of injected water and measures surface injection pressure and flow rate to the HPT trunk line and probe

The injection-pressure log produced by the HPT is an indicator of relative formation permeability; higher injection pressures correspond to lower formation permeability (silts and clays) and lower injection pressures correspond to higher formation permeability (sands and gravels). The HPT operates by continuously injecting water as the tool advances, which creates a real-time log of average HPT pressure and flow at depth every 0.05 ft.

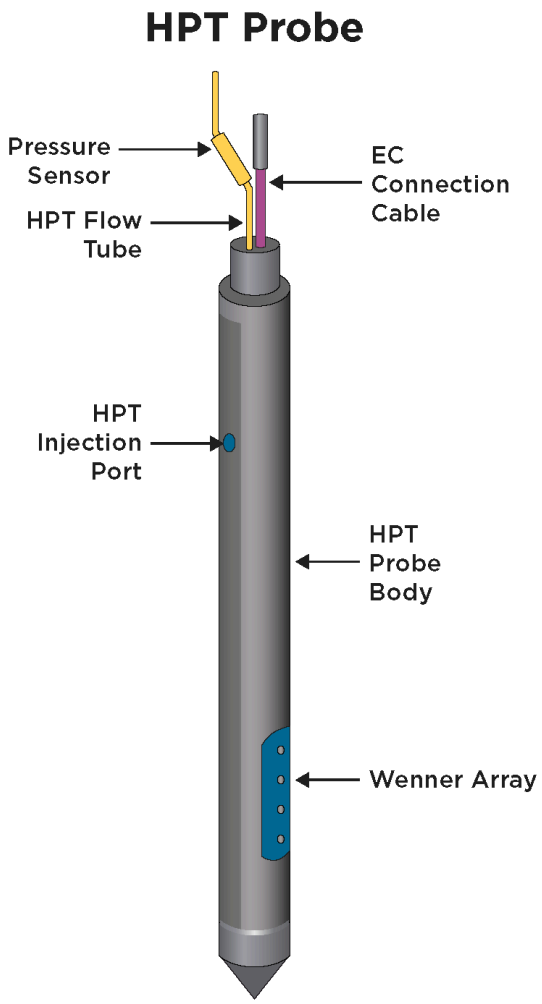


Figure 4-12. Downhole probe components of the HPT. The pressure sensor is shown outside of the connection rod but is actually located inside the rod during use.

Source: Modified by Geosyntec Consultants, Inc., from Geoprobe Systems® (Geoprobe 2026b). Used with permission.

Following completion of the boring, HPT pressure data are corrected at each depth interval using a graph of absolute hydrostatic pressure, which is calculated from a dissipation test. The corrected HPT pressure graph can be used along with the HPT injection flow rate to calculate and plot estimated hydraulic conductivity (McCall 2010). Additional information about calculating estimated hydraulic conductivity is provided in McCall (2010). The correction equation is provided in **Equation 4-1**.

Corrected HPT pressure = Average HPT pressure – Absolute hydrostatic pressure

Equation 4-1. Corrected HPT pressure.

To conduct a dissipation test, the operator identifies a depth below the water table in a permeable zone to temporarily pause tool advancement and pause injection of water. The operator turns off the water pump, which allows the pressure of the ambient formation to dissipate until it reaches the hydrostatic head at the depth of the tool. Typically, the pressure-dissipation tests should be completed in relatively high-permeability zones to allow full dissipation of ambient formation pressure over a relatively short duration of time.

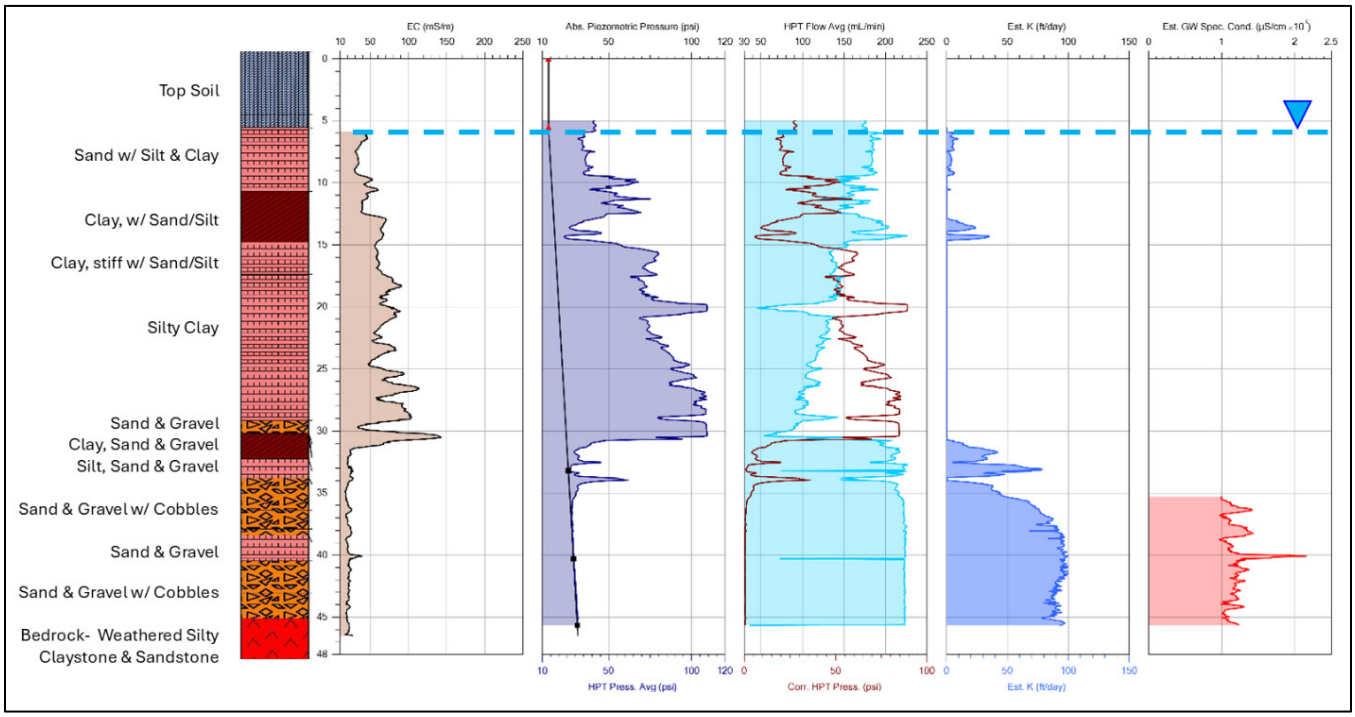


Figure 4-13. HPT-EC log with calculated K and SEC and comparison to offset lithology log from a confirmation sonic boring.

Source: Vista GeoScience LLC, & HRS Water Consultants.

As shown on **Figure 4-13**, injection-flow logging from the HPT can be combined with EC (black line in first column) in one tool. It can also be combined with other sensing tools such as the MIP, OIP, or LIF. The combined tool is advanced into the subsurface, creating an output log showing both injection pressure and flow rate from the HPT, and bulk electrical conductivity from the EC tool. Other parameters are then calculated post-log run. **Figure 4-13** provides an example HPT-EC log showing:

a) 1st column - a lithologic description log of an offset sonic boring core

b) 2nd column–electrical conductivity (black line, brown shading)

c) 3rd column–injection pressure (blue graph) and absolute piezometric pressure (black line) showing ambient pressure above water table, contact with water table (red triangle), increasing piezometric head with depth, and the location of the dissipation test (black square)

d) 4th column–Injection flow rate (light blue), corrected injection pressure (dark red)

e) 5th column–calculated estimated hydraulic conductivity (K_{est})

f) 6th column–calculated groundwater specific electrical conductance (SEC)

g) Depth of water table represented by horizontal dashed blue line

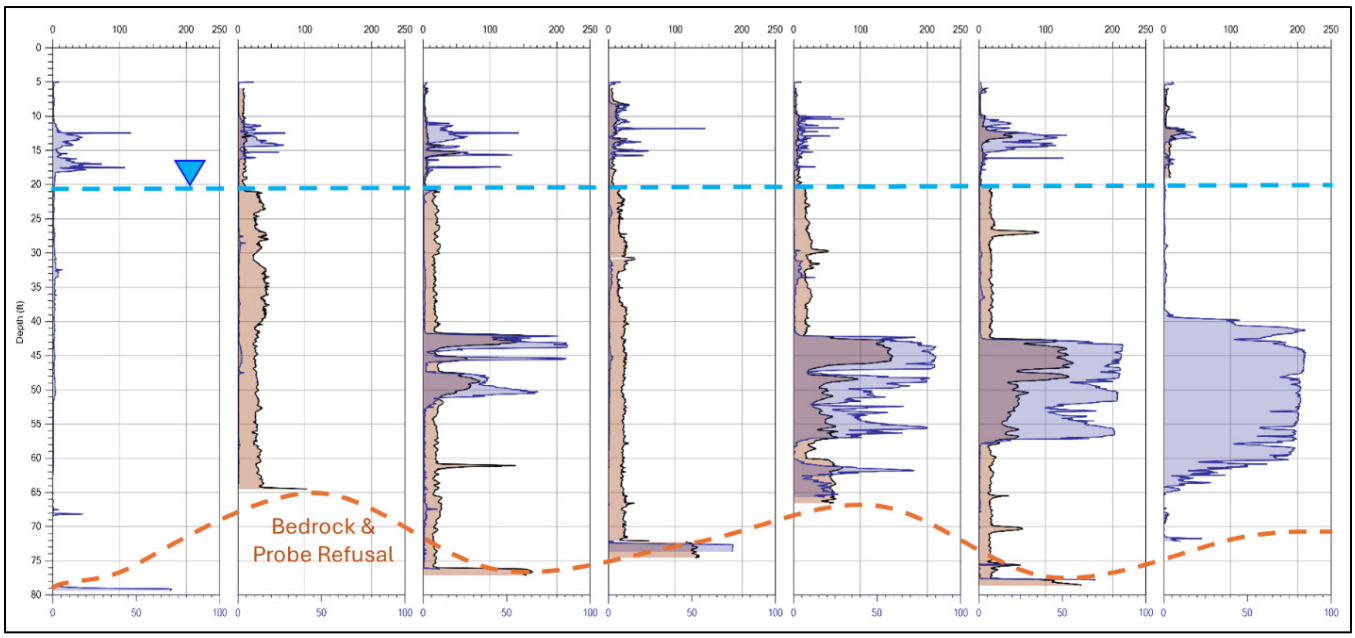


Figure 4-14. Example cross-section profile of HPT-EC logs across alluvial aquifer paleochannel to identify location and screen placement for production wells. The brown graph is bulk electrical conductivity (EC) and dark blue graph is corrected HPT pressure.

Source: Vista GeoScience LLC & HRS Water Consultants.

Figure 4-14 is a cross section generated by Geoprobe's DI Viewer software shows a cross section of seven EC and corrected HPT-pressure logs oriented perpendicular across an alluvial paleo-channel. The logs were used to determine the placement of production well screen intervals. Typically, EC cannot be used to detect groundwater due to variable and higher conductivity of most sediments, but in the coarser grain sediments (sands and gravels) with low bulk EC, a positive shift in EC can be seen where the water table is encountered due to a slightly higher ionic content. The EC component failed on the tool on the first log on the left side of the profile, so the EC data were not plotted on that log. Bedrock contact was interpreted from the probe refusal depth combined with a spike on the EC response.

4.4.1.2 Waterloo Advanced Profiling System

The Waterloo APS is an integrated injection-flow logging and discrete interval groundwater sampling tool that is driven into unconsolidated soils using direct-push rods. It is a proprietary tool currently operated by Cascade Technical Services (Cascade 2026). The tool was developed and tested extensively at the University of Waterloo and was introduced to investigation and remediation professionals in 1994.

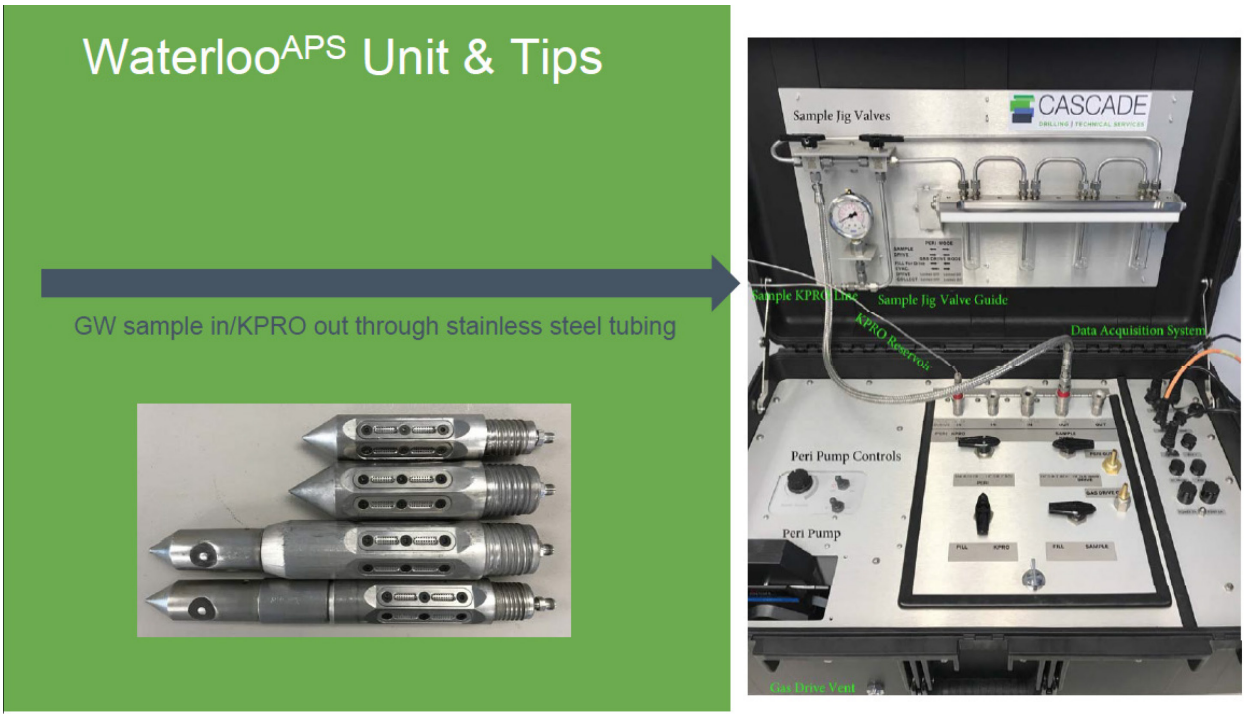


Figure 4-15. Waterloo APS tool tip options (150, 175, and 225 versions) and instrument.

Source: Cascade Environmental. Used with permission.

The downhole components of the Waterloo APS (**Figure 4-15**) are:

- profiler tip consisting of a drive point with stainless-steel screened ports
- conventional direct-push rods
- up to three stainless-steel lines running through the drilling rods and connecting the profile head to the ground surface:
- KPRO line–injects water at a consistent pressure into the subsurface, allowing flow to fluctuate
- sample line–conveys groundwater up through the drill rods to the surface via peristaltic or gas drive pump
- gas line–conveys nitrogen to operate the downhole pump
- nitrogen gas positive displacement pump for when the water table is below the suction limit of a peristaltic pump

The aboveground components of the tool are:

- peristaltic pump
- multiparameter water-quality meter used to measure pH, temperature, oxidation-reduction potential (ORP), electrical conductivity, and turbidity of purged groundwater
- sensor and laptop computer equipped with software to measure and log the index of hydraulic conductivity, which is the flow response to inject a flow of water into the subsurface at a consistent pressure

The Waterloo APS 225 (2.25-inch outer diameter (OD)) version is the most robust model, built to be used with the Geoprobe 8040 rigs for maximal depth penetration. The tip has more open area for higher sampling rates and reduced clogging. The 225 can be used with either a peristaltic pump or with the downhole nitrogen drive positive displacement pump.

The Waterloo APS 175 is a 1.75-inch OD version and is the same diameter as the original Waterloo Profiler but uses a more durable direct push rod and has a unique APS tip design.

The injection-flow logging component of the tool operates like the HPT except that the tool logs relative formation permeability, reported as the "index of conductivity," in real time by using a consistent injection pressure and allowing flow to fluctuate. Dissipation tests are not completed, and the index of conductivity data are not corrected. In relatively high-permeability formations such as sands and gravels, flow is required to maintain injection pressure, but in relatively low-permeability formations such as silts and clays, lower flow is required to maintain injection pressure into the subsurface. The operator or consultant reviews the real-time log of relative formation permeability and directs the driller to stop advancing once the profile tip is at a permeable interval within the target sampling unit.



Figure 4-16. Waterloo APS operator purging groundwater from the sample interval, recording water-quality parameters, and preparing for sample collection.

Source: Cascade Environmental. Used with permission.

To collect a groundwater sample, drilling temporarily stops and groundwater is purged to the surface via a peristaltic or gas-drive pump and is monitored for geochemical parameters to determine stability (**Figure 4-16**). Once stabilization is achieved, samples are collected for laboratory analysis, and the profiler tip is advanced to the next targeted sample depth. The Waterloo APS is commonly fitted with a stainless-steel sample holder used to collect zero-headspace groundwater samples in 40 mL volatile organic analyte (VOA) vials, but the tool can be used to collect any type of groundwater sample.

The Waterloo APS profiler tip is available in two sizes, 2.25-inch and 1.75-inch, and is attached directly to the same-diameter direct-push rods used on the direct-push drilling platform. The larger diameter tip can be used on a larger drill rig for maximal depth penetration and higher sampling rates; the smaller tip is used with smaller drill rigs to access tighter spaces where larger drill rigs cannot operate.

4.4.1.3 Hydraulic Profiling Tool - Groundwater Sampler (HPT-GWS)

The Geoprobe HPT-GWS combines the injection-flow logging of the HPT with discrete interval groundwater sampling and operates in a similar manner to the Waterloo APS. It injects water and measures both fluctuating pressure and flow, which are then used in combination with piezometric head to calculate estimated hydraulic conductivity (K). The HPT-GWS is designed for use on a 2.25-inch-diameter probe rod for advancement into the subsurface using direct-push methods (**Figure 4-17**). The

tool components are generally the same as the HPT described in Section 4.4.1.1, with the addition of a ¼-inch-OD sample line. The probe tip is equipped with 20 screened ports, each about ½-inch in diameter, installed in four vertical rows of five each around the probe circumference. The ports are distributed over a 4-inch vertical segment of the probe, providing for a discrete sample interval.

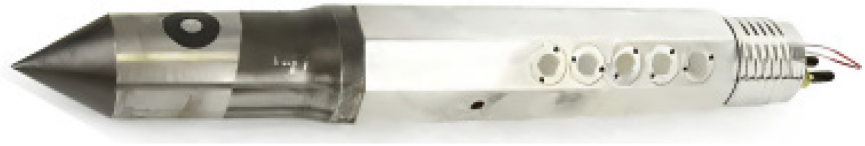


Figure 4-17. The HPT-GWS probe shows 5 of the 20 injection and sampling ports, and the EC dipole at the tip of the probe.

Source: Geoprobe Systems®. Used with permission.

As with the HPT, it measures the pressure resistance, and flow response required to inject the water into the formation. The pressure is logged by a downhole pressure transducer located just above the sampling ports, and flow is measured in the surface instrument. An EC dipole is positioned at the end of the probe to provide a log of bulk formation EC, and the EC, injection pressure, and flow rate are logged every 0.05 ft (about 15 mm) of log depth. The log data guide selection of permeable zones for sampling. Once the HPT-GWS has reached a desired sampling depth, advancement of the tool pauses temporarily, and the operator may conduct a dissipation test prior to sampling. To sample, groundwater is purged through the sample line using either a peristaltic or a mechanical bladder or syringe pump. Parameters can be measured for stabilization at the surface using a standard multiparameter meter. Following sample collection, the operator resumes HPT logging, and the tool is advanced to the next sample depth.

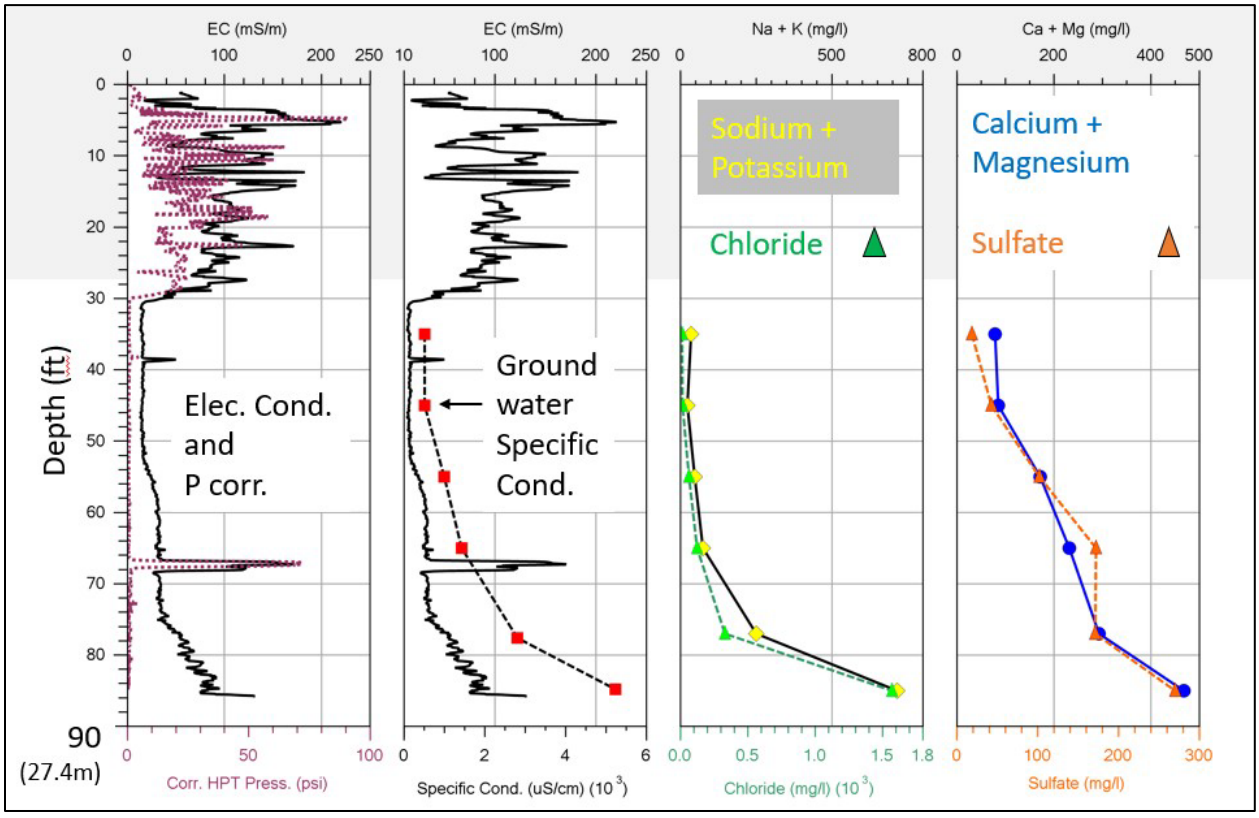


Figure 4-18. A log from the HPT-GWS tool, including the corrected pressure, EC, and results of analytical dissolved anion/cation data from samples collected at 10-foot intervals.

Source: Geoprobe Systems®. Used with permission.

The Waterloo APS and the HPT-GWS are both operated by an operator with training and experience on the equipment who typically works for an HRSC contractor. As such, no specific training is required for an environmental professional "using" the tool, but it is recommended that a scientist familiar with the tool data output, site geology, contaminant release information, and project objective oversee the tool operation and direct the operator on the frequency and where to sample.

Figure 4-18 is an example HPT-GWS log with side-by-side plotted samples analyzed for dissolved cations and anions.

4.4.1.4 Hydraulic Profiling Tool - Groundwater Profiler (HPT-GWP)

The HPT-GWP is a smaller diameter (1.75 inch) version of the HPT-GWS that lacks the EC dipole and downhole pressure transducer (**Figure 4-19**). It measures injection flow and pressure (surface pump pressure) and has the 20-screen port arrangement for collecting groundwater samples at discrete intervals. Compared to the HPT-GWS, it is a simpler and more robust design because it only has two water lines. The HPT-GWP is used to collect multiple discrete groundwater samples from predetermined intervals.

One strategy for using this tool is to use a MiHPT, OiHPT, LIF, or HPT-EC tool to log a continuous boring and locate sampling target intervals, and then offset using the HPT-GWP to collect the discrete groundwater samples from those target samples, which may also be used to analyze for compounds not detected by the other sensors.



Figure 4-19. Geoprobe hydraulic profiling tool and groundwater profiler (HPT-GWP).

Source: Geoprobe Systems®. Used with permission.

4.4.2 How Is the Technology Used?

4.4.2.1 Data Interpretation and Presentation

Logs provided by the contractor are often grouped together to form cross sections. The vertical variations in formation permeability are correlated horizontally and shaded to help the reader visualize the geologic strata. Laboratory analytical data are added to the cross section.

Boring log data provided by the contractor can be requested in spreadsheet format and input into visualization and modeling programs such as Earth Volumetric Studio (EVS), ArcGIS, or Leapfrog so that cross sections or 3D visualization models can be created using other software programs as needed.

As site characterization progresses, additional types of data can be added to the cross sections, including monitoring wells and associated groundwater analytical data and soil borings and associated soil analytical data.

4.4.2.2 QA/QC

QA/QC standards must be established and followed to ensure reliable data. In addition to comprehensive operator training (which may be verified prior to commencing work) and an operator track record of successful use, approved field procedures must be understood and followed before, during, and after profiling activities. The manufacturer's SOPs must be reviewed prior to initiating fieldwork.

Quality Assurance Prior to Use

Prior to beginning investigation activities, the operator should calibrate and test hydraulic and groundwater profiling tools. Depending on the tool, testing may be conducted daily during a field program or at the beginning of each boring. The project team should ask the operator about the quality control procedures specific to the tool and request that testing and calibration results be communicated to the field team and included within the final data report. For example, before and after each log run, the HPT-EC tool is pressure tested by submerging the sensor in a tube of water and changing the water level by 6 inches, equivalent to 0.22 psi. The EC dipole is tested with a resistance jig. The parameters must pass within +/-10% of the required readings.

Quality Control During Use

Once data collection has begun, the operator must monitor the equipment throughout the data collection process. For most hydraulic and groundwater profiling tools, the operator monitors the rate of advancement, depth, EC, and injection pressure to ensure equipment responses are within normal ranges. Maintaining a constant rate of advancement (typically around 2 cm/sec) produces a representative log; a slower rate gives a more detailed log but affects the rate of production. A rate that is too fast can miss smaller stratigraphic features. Daily productivity varies greatly depending on desired drilling depth and the number of times that drilling is stopped to either complete a dissipation test (if applicable) or collect a sample for laboratory analysis (if discrete interval samples are being collected). Generally, with the profiling tools, the factor that limits productivity is the number of samples collected per day for laboratory analysis.

Prior to beginning work, the depth of the local water table from a nearby well or temporary piezometer should be estimated, because it is not always evident from the pressure injection log. Understanding the approximate depth of the water table helps the operator interpret the injection pressure log and generate contaminant screening data. If the tool is being used to collect discrete interval groundwater samples (Waterloo APS or HPT-GWS), the water table depth must be estimated to direct the depth at which sampling can begin.

For sampling tools, some trial and error may be necessary to determine the site-specific conditions under which groundwater samples can be efficiently collected. Sample flow may be directed through an in-line flow-through cell with a multiparameter water-quality meter, and a sample interval is purged until stabilized criteria are met, which typically involves purging 400 mL to 1,000 mL. If deionized water is used for the injection fluid, a good contrast between the natural formation water and the deionized water is easily observed with the water-quality meter. If a water-quality meter is not being used, three system volumes should be purged before collecting samples for laboratory analysis. A purge water blank should be included with the laboratory sample analysis.

After sample collection, sample-specific tubing is changed. Following completion of a boring, the drill rod, stainless-steel tubing, and profiling probe or tip are decontaminated between each profiling point with clean water or by following project-specific decontamination procedures.

Quality Controls After Use

Depending on investigation objectives, co-located groundwater and soil samples may be collected following completion of a hydraulic and groundwater profiling investigation to make defensible statements regarding the accuracy and precision of the data collected. For example, if HPT or index of conductivity (I_K) logs are being used to inform remedy design, it may be important to advance targeted soil borings within the low permeability zones where contaminant mass is retained to correlate injection pressure log data to a specific soil type. In another scenario, soil analytical samples may be collected to

determine contaminant mass within the low permeability layers where groundwater samples have not been collected.

The investigation may also be supplemented with a select number of permanent monitoring wells if multiple rounds of groundwater data from a monitoring well are required for risk characterization or site closure. In this case, the hydraulic and groundwater profiling investigation can significantly reduce the scale and cost of the monitoring well network by informing the well network design so that well screens are placed within specific hydrogeologic units identified by the hydraulic and groundwater profiling investigation.

4.4.2.3 Data Misuses

Samples collected from groundwater profiling tools are different from monitoring well screen samples because they are collected from a much smaller discrete interval. Samples from a 5- or 10-ft-long submerged well screen can originate from multiple lithological zones within the well screened interval. These zones may exhibit different contaminant concentrations. Therefore, monitoring well data may represent a weighted-average concentration within the screened interval, which is often less reliable when developing a CSM. Weighted-average concentrations within a screened interval should not be compared directly to discrete intervals sampled by profiling tools without considering the potential dilution factors within the screened interval of the monitoring well.

4.4.2.4 Supporting and Enhancing Instruments and Technologies

An EC array is standard equipment on most hydraulic profiling tools. EC is discussed in detail in Section 4.3.

4.4.3 What Are the Advantages?

The HPT provides a rapid and data-rich method for characterizing subsurface hydrogeologic conditions by generating high-density data in real time. As the tool is advanced through unconsolidated formations, it continuously measures formation permeability and produces detailed logs that reveal variations in hydraulic conductivity, groundwater storage zones, and preferential flow pathways. These data provide a high-resolution depiction of the subsurface that helps identify the water table, infer lithologic changes, and distinguish confined or semiconfined aquifers. Because the system operates in real time, it allows investigators to make immediate decisions in the field regarding sampling intervals, investigation depth, and well placement.

A key advantage of HPT investigations is the ability to integrate hydrogeologic tools with contaminant detection and sampling tools on a single direct-push tool string. When combined with technologies such as MIP or OIP, HPT data allow contaminant distribution to be interpreted relative to formation permeability, improving understanding of contaminant transport and relative mass flux. Some HPT configurations also allow discrete groundwater sampling from short-screened intervals, providing quantitative analytical data to complement the hydraulic profile. Together, these capabilities enable rapid HRSC, optimize monitoring well and sampling locations, and support more effective remedial design and performance monitoring without the immediate need for permanent well installations.

4.4.4 What Are the Limitations?

As with the other direct sensing tools, HPTs are limited to static or percussion direct push in unconsolidated sediments or highly weathered bedrock and cannot be used in competent bedrock applications or sediments with cobbles.

The technical limitations associated with hydraulic and groundwater profiling tools are associated with applicability and accessibility such as formation permeability, tip clogging, and freezing conditions. These limitations are described in the subsections below.

4.4.4.1 Formation Permeability

The HPT system can resolve soil permeability within a hydraulic conductivity range of about 0.1 ft/day (3.5×10^{-5} cm/sec) to 75 ft/day (2.7×10^{-2} cm/sec), approximately three orders of magnitude in range. The lower end of the range varies depending on flow rate, effective pressure, and the specific nature (density, grain size, moisture content) of the soil or sediment being penetrated. At the upper end of the range, formation permeability becomes sufficiently high to reduce the pressure required to inject fluid into the formation to relatively low. Under high hydraulic conductivity conditions, the injection pressure may be equal to or less than the pressure resulting from the internal friction due to fluid flow in the HPT probe. Under these conditions, the hydraulic conductivity of the formation is effectively above the upper limit of what the HPT can discern. Simply increasing flow rate to the probe does not alleviate this problem; it also increases the internal friction and pressure. In aquifer zones where the estimated hydraulic conductivity is near the upper limit, temporary piezometers (Geoprobe 2006; ASTM 2012) can be installed across these intervals and slug tests (ASTM 2013; Butler Jr 2019) can be performed to more precisely define higher hydraulic conductivity zones.

These systems have limitations for pressure measurement. The HPT is currently designed with a 100 psi (about 700 kilopascal) pressure transducer. Including ambient air pressure at sea level, the effective upper operating limit is about 80 psi (550 kilopascal) or about 180 ft (about 55 m below the water table in an unconfined aquifer. When approaching significant depths, there is not as much room for differentiation in pressure resistance between very tight and more permeable formations. For example, if operating at a depth where the ambient and head pressure is 80 psi, the pump can only hit about 110 psi, or a 30 psi differential (corrected pressure), which could be a silt or fine sand.

The Waterloo APS also has a similar upper limit for differentiating relative formation permeability within high-permeability zones. Due to these upper limits, the estimations of K, or the index of conductivity logs, may not be able to differentiate between the most permeable zones, such as coarse sand and gravel.

For all hydraulic and groundwater profiling tools, sample collection is limited by formation permeability because groundwater samples cannot be collected unless there is sufficient groundwater flow within the formation. Unlike a monitoring well, which can sometimes be sampled under low-recharge conditions (for example, purging the well dry and returning later to collect a sample), a groundwater sample cannot be collected unless there is sufficient flow. If a particular depth interval does not produce sufficient flow for sample collection, it can be inferred that mass flux within that zone would be relatively low. Then, the tool can be advanced deeper to collect samples from subsequent depth intervals.

4.4.4.2 Tip Clogging

In silty geologic conditions, the HPT screen ports may clog, preventing sample collection. To unclog, the tool typically has to be removed from the hole to remove the clog from the tip. Additionally, the tip may clog when advancing through a viscous dense nonaqueous phase liquid (DNAPL).

4.4.4.3 Freezing Conditions

Groundwater profiling tools can be challenging to operate in subfreezing conditions because the injection-flow-logging component of the tool relies on a steady flow of water from the surface to the subsurface, and the profiling component of the tool requires groundwater to be pumped back up to the surface. In subfreezing conditions, tubing may freeze and prevent water from flowing in either direction.

Heated tents can be used when profiling in subfreezing conditions, but additional health and safety precautions must be taken, and productivity will likely be slower.

4.5 Membrane Interface Probe

4.5.1 What Is the Technology?

The membrane interface probe (MIP) is an ASCT that is deployed using a direct-push drilling platform. The MIP generates real-time logs of detector responses to VOC and some SVOC in the subsurface vadose and saturated zones. The resulting data are semiquantitative and are typically used to assess relative concentrations of hydrocarbons and chlorinated compounds in the subsurface and the depth of their occurrence. The MIP data can assist practitioners in overcoming the challenges associated with fully understanding contaminant distribution in heterogeneous unconsolidated or semiconsolidated materials. The MIP is rarely used as a stand-alone tool and the current version of the probe is combined with the hydraulic profiling tool (HPT) (Section 4.4) and electrical conductivity (EC) sensor (Section 4.3), allowing for a more thorough understanding of subsurface contaminant distribution and potential migration pathways. This combination of tools is typically referred to as MiHPT. In the interest of simplicity, this section focuses on the MIP tool. Additional tools commonly used in tandem with the MIP are discussed in other sections.

The MIP can significantly reduce the amount of data gaps in the CSM because it provides a detailed dataset along the borehole (typically at 1-ft intervals), rather than at the coarser intervals typically associated with traditional soil-sampling methods. MIP data can be used to create one-dimensional (1D) profiles, two-dimensional (2D) transects, and three-dimensional (3D) interpolated visualizations and interactive maps. Each method of presentation can help refine the CSM, leading to a clearer understanding of the site so that all stakeholders can support a common path forward and develop a remedial approach.

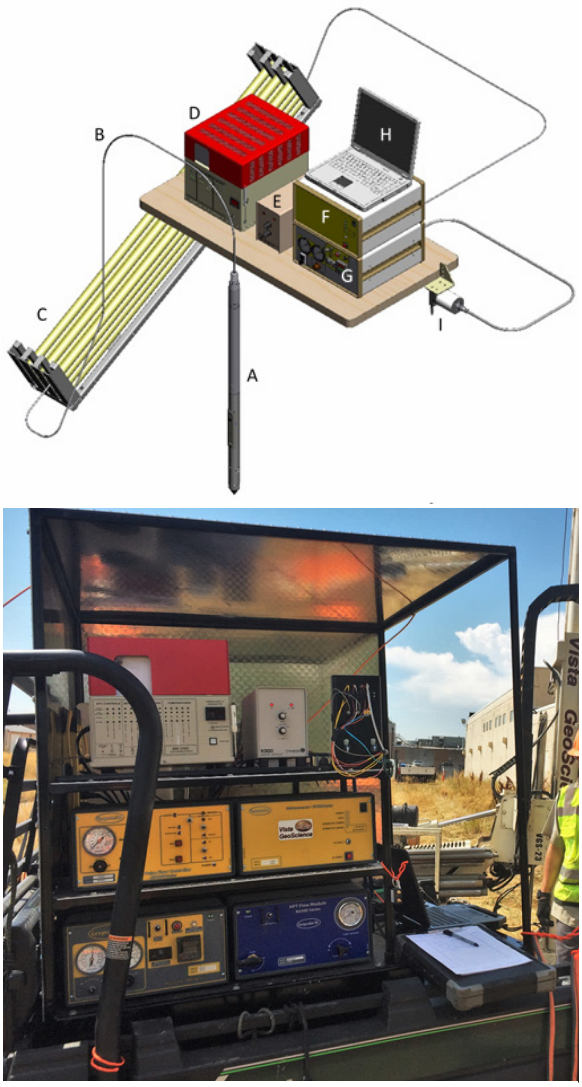


Figure 4-20. Components of a typical MIP system.

Source: Geoprobe Systems®. Used with permission (top), Vista GeoScience, LLC. Used with permission (bottom).

The MIP was developed by Geoprobe Systems as a direct-push-deployed logging tool to detect the presence of VOC in situ (Christy 1996).

The MIP system shown in **Figure 4-20** consists of A) the MIP probe, B) prestrung trunk line within the probe, C) probe rods organized in rack, D) GC with gas-phase detectors, E) detector controller, F) field instrument that converts analog signal to digital data, G) MIP control, H) laptop computer, and I) string

potentiometer that measures depth and rate of probe advancement. Not shown in the diagram is the low-level controller module, but it is shown in the photo as the center left component.



Figure 4-21. The MIP probe.

Source: Geoprobe Systems®. Used with permission.

The MIP tool is a 24-inch (60-centimeter (cm)) long steel probe with a maximum diameter of approximately 1.75 inches (45 millimeters (mm)) (Figure 4-21). It is driven into the soil using a 1.5-or 1.75-inch OD probe rod. It is also available in a 2.25-inch-diameter probe version, which is driven into the ground using a 2.25-inch OD probe rod. A semipermeable membrane about ½ inch (12 mm) in diameter is fixed to a heater block located on the side of the probe. The membrane is reinforced with stainless-steel mesh, allowing advancement into soil and unconsolidated (and some poorly consolidated) formations with direct-push methods. A polymer-clad trunk line is prestrung through the drive rods and connects the downhole probe and sensors to the uphole instrumentation (Figure 4-20). The tool also contains a small electrical conductivity (EC) dipole array, and currently manufactured tools include an HPT 0.375" (10 mm) water-injection port on the upper section of the probe and on the opposite side of the heated-membrane section.

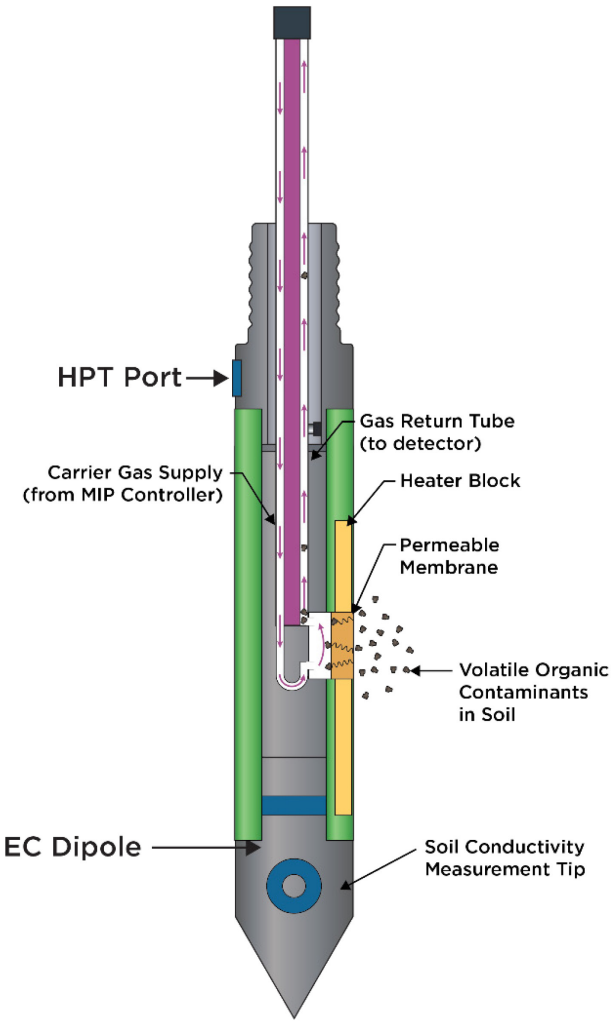


Figure 4-22. MIP principles of operation.

Source: Modified by Geosyntec Consultants, Inc., from Geoprobe Systems®. Used with permission.

Basic MIP tool operation is as follows: VOC cross the semipermeable membrane and enter the carrier gas flow to be swept up the trunk line to gas-phase detectors at the surface (Figure 4-22) (Christy 1996). Volatilization of subsurface contaminants is enhanced by heating the soil, groundwater, and vapor in the soil pore space adjacent to the membrane with the heater block. Lag time is measured by performing response tests, and depth of the response is measured using a string-pot system connected to the rig derrick. The MIP log data acquisition software corrects for the lag time and records the detector response versus depth in real time, allowing the operator to observe the logs drawn in real time on the computer display.

In standard MIP sensitivity operation, the probe is nominally advanced in 1-ft increments, stopping at each interval to heat the soil, water, and vapor for a consistent period to ensure the surrounding VOC in the subsurface are volatilized and, therefore, detected consistently with increased sensitivity. This also mimics the procedure for conducting a response test of submersing the membrane in a

liquid standard for 45 seconds. However, the probe can be advanced continuously at 1ft per minute without stopping at 1-ft increments if lower sensitivity is not required, such as sites with very high contaminant concentrations. VOC data are collected every 0.05 ft, but the most representative VOC measurements are collected at the 1-ft increments in which the MIP stops. Tandem EC and HPT sensors provide lithologic data every 0.05 ft (about 15 mm) as the probe is advanced. Site lithologic characteristics dictate how fast the probe can be advanced and the refusal penetration depth. The type of contaminant and its associated boiling point and vapor pressure dictate the length of the heating cycle at each depth, typically 45 to 60 seconds (sec). Compounds miscible in water are generally not detectable. These parameters should be established in the field by conducting performance testing and determining the time required for contaminants of concern to travel across the MIP membrane prior to deployment (Geoprobe 2021a; ASTM 2017).

Geoprobe developed an add-on valve module to operate the MIP system in low-level MIP sensitivity mode. The same downhole probe is used, but the control valve pauses, or pulses, the carrier gas flow that sweeps the membrane. While the flow sweeping the membrane is paused, pure carrier gas is sent to the GC detectors. The probe typically advances and pauses at the 1-ft intervals as above or can be paused at shorter intervals for greater resolution. The length of pause and lag time for the signal to hit the detectors is programmed into the valve control system for consistent measurements, and this is estimated to increase detection sensitivity by approximately a factor of 10. For typical analytes this means that a properly operating system can see compounds in the 10–100 micrograms per liter (µg/L) range versus the low milligram per liter (mg/L) range for standard sensitivity mode. Since clean carrier gas is sent to the detectors between intervals, the responses between the pause peaks are simply detector background or baseline, and the actual detector response to the compounds is the difference between the response peak and the baseline reading.

Total VOC are typically detected using a photoionization detector (PID), flame ionization detector (FID), and halogen-specific detector (XSD) (**Figure 4-23**). Older system versions may also include an electron capture detector (ECD) in place of or in addition to the XSD.

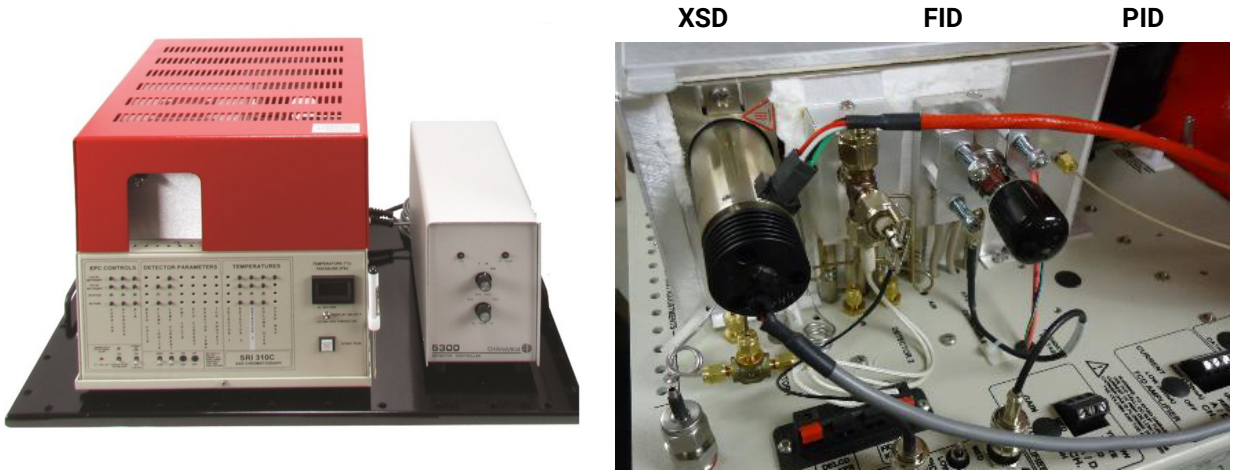


Figure 4-23. Commonly used SRI gas chromatograph (left). On typical modern MIP systems housing three VOC detectors (right), from left to right, XSD, FID, and PID.

Source: Geoprobe Systems®. Used with permission.

An EC sensor (Section 4.3) located on the probe measures the bulk electrical conductivity of the soil adjacent to the probe while a downhole HPT pressure transducer measures the soil's pressure response to a continuous injection of water. The flow of the water is also measured in the pump controller at the surface and recorded in the log data.

Post processing of EC and HPT data will also allow continuous log graphs of estimated hydraulic conductivity, and groundwater SEC.

Graphic logs of VOC detector responses are recorded as the MIP is advanced with depth. The PID responds to VOC molecules with an ionization potential below 10.6 electron volt (eV), which includes aromatic hydrocarbons and molecules with carbon double bonds [tetrachloroethene (PCE); trichloroethylene (TCE); and benzene, toluene, ethylbenzene, and xylenes (BTEX)]. The FID generally responds to VOC molecules with a carbon-hydrogen bond, which includes most VOC that combust in the H_2-air flame, including methane. The XSD responds only to halogenated (fluorine, chlorine, bromine) VOC and has largely replaced the older ECD for detecting these compounds in modern systems.

Figure 4-24 shows a MIP log collected at a former chemical manufacturing facility in an alluvial setting underlain by glacial lake deposits. EC, HPT, and K_{est} data shown are displayed in the three columns on the left, while MIP detector responses from the FID, PID and XSD are shown in the three columns on the right, respectively. FID and PID detections consistent with fuel hydrocarbon impacts are shown in the upper 7 ft near the water table. XSD detections from about 13 to 25 ft indicate the presence of halogenated hydrocarbons—in this case, PCE and daughter products. Maximum XSD detections occur in the least permeable soils as indicated by the HPT, suggesting mass is being stored.

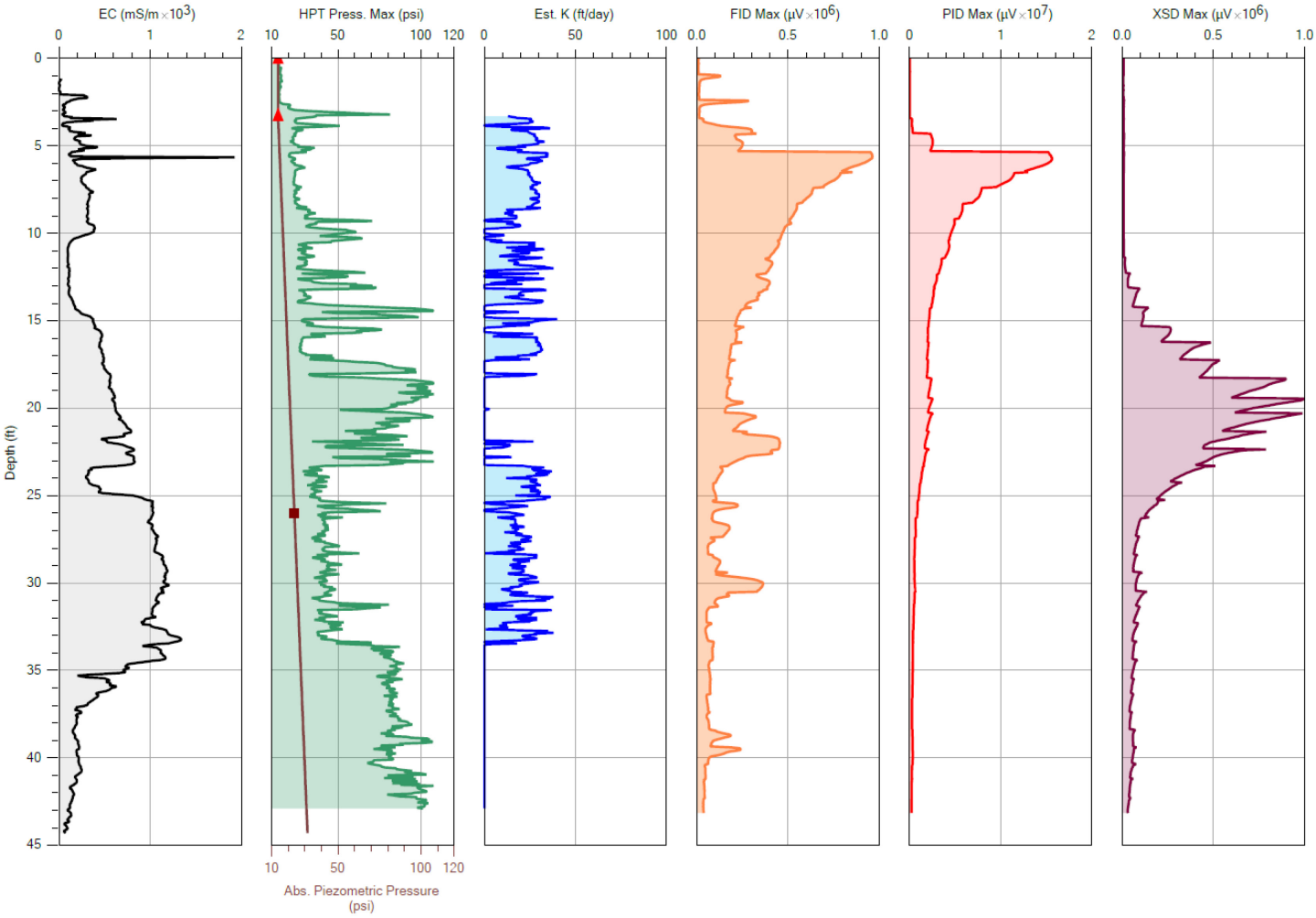


Figure 4-24. A MIP log collected at a former chemical manufacturing facility.

Source: S2C2 LLC. Used with permission.

4.5.2 How Is the Technology Used?

The MIP provides a timely and cost-effective method for detecting VOC (combined sorbed, vapor phase, and dissolved) in saturated and unsaturated zones by recording qualitative to semiquantitative levels of total VOC in situ with depth. It provides data to identify and delineate a VOC source zone to delineate a VOC groundwater plume. With some limitations, the MIP can infer the presence of light nonaqueous phase liquid (LNAPL) and dense nonaqueous phase liquid (DNAPL).

The MIP can significantly reduce the amount of data gaps in the CSM because it provides a detailed dataset along the depth of the borehole (typically at 1-ft intervals), rather than at the coarser intervals typically associated with traditional soil sampling methods. MIP data can be used to create 1D profiles, 2D transects, and 3D interpolated visualizations and interactive maps. Each method of presentation can help refine the CSM and develop a more effective remedial approach, leading to a clearer understanding of the site, so all stakeholders can support a common path forward.

Since multiple sensors are typically used and readings are recorded at 0.05-ft intervals, investigations using MIP generate a significant quantity of data. If available, field notes recorded during an investigation using a MIP should include an interpretation of the sensor results for each log run. A more rigorous analysis should follow shortly after each day or mobilization and may include the generation of maps, cross sections, 3D figures or animations, and other types of data displays. Data can be used to update the working CSM in the field to allow the CSM to evolve in real time in the field as additional data are generated. The final data presentation includes the interpreted MIP results as well as relevant CSM components (for example, source locations, geologic strata and properties, groundwater elevations and flow, mass flux). The following subsections provide summaries of the stages of data interpretation and presentation for an investigation using MIP.

4.5.2.1 Field Log Interpretation

As the investigation proceeds, the field team should view a graphical presentation of the sensor results on a computer monitor as the MIP is advanced. Depending on the sensors used, the field investigator may be able to determine, in real time, the:

- relative level of impact at the boring location compared to other boring locations
- vertical distribution of impacts
- location of the groundwater table (when used with HPT, see Section 4.4.1.1)
- vertical distribution of lithologic units. Step-out locations can be selected in the field based on this initial real-time data review.

It is possible to use the level of detector response or lack of response from the different detectors in the MIP system to tentatively identify the category of VOC present. For example, when the XSD and PID give strong responses, but the FID has a weak response, the analytes being detected are most likely chlorinated ethenes such as PCE or TCE. More examples are provided in **Table 4-2**. To confirm an analyte category or to identify a specific analyte, co-located samples of environmental media need to be collected and submitted for laboratory analysis.

While logs are visible on a laptop screen as work progresses, printed or electronic logs are typically made available by the operator at the end of the log run, end of the day, or by the following morning (**Figure 4-25** and **Figure 4-26** for example logs). **Figure 4-24** is an example of a MIP log run at an oil field site with a pipeline condensate release**.** The site was in an alluvial stream valley, and the EC and HPT curves indicated relatively permeable interbedded silts and sands**.** The condensate contained high levels of BTEX compounds that dissolved in groundwater and are reflected in the PID response**.** The FID

responded to high levels of methane in the lower part of the log, possibly unrelated to the release, but related to the gas-charged sediments in the basin. Methane can cause quenching of the PID response, indicated as negative drifts below the PID baseline response.

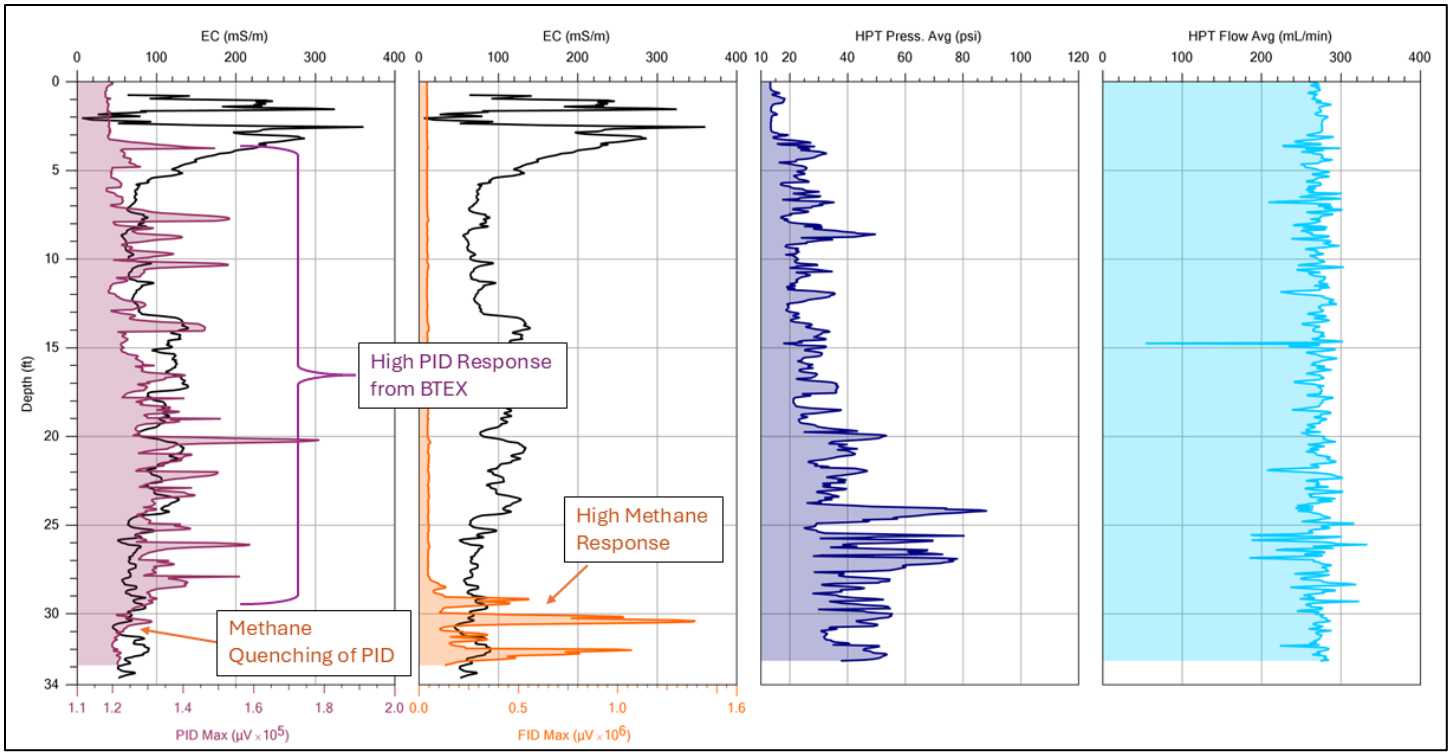


Figure 4-25. An example of a MIP log run at an oil field site with a pipeline condensate release. The FID and PID responses are differentiating BTEX type responses from higher level methane responses.

Source: Vista GeoScience LLC. Used with permission.

Figure 4-26 is a MIP log at a chemical plant. High EC and HPT-pressure zones define finer grain materials, while low EC and HPT-pressures define highly permeable sand zones. Different chemical classes such as chlorinated compounds (based on the XSD response) move through the permeable zones below 20 ft deep and sorbed to finer grain materials below 45 ft, whereas aromatic petroleum compounds (based on the PID and FID response) exist above 23 ft in finer grain soils and in the vadose zone above the water table.

Following post-log QA/QC, off-site team members may access logs from the field via a shared cloud folder or by email, using Wi-Fi, cellular, or satellite connectivity as available. Overlays of two or more logs can be created for comparison, and simple cross sections may be created using the field logs to evaluate site hydrogeology and potential contaminant migration pathways or contaminant storage zones. Such information can be useful when implementing adaptive sampling plans. Logs can be used in the field to help answer the following questions:

- Have all relevant geologic layers been investigated (that is, have the MIP borings penetrated to the bedrock or a sufficient distance below the impacted zone to confirm vertical extent)?
- Are additional borings required to complete horizontal and vertical delineation?
- Where should confirmatory soil and groundwater samples be collected?
- Where is the optimal placement of future monitor wells, and what screen intervals?

These questions and other DQO are established in the planning phase prior to mobilization.

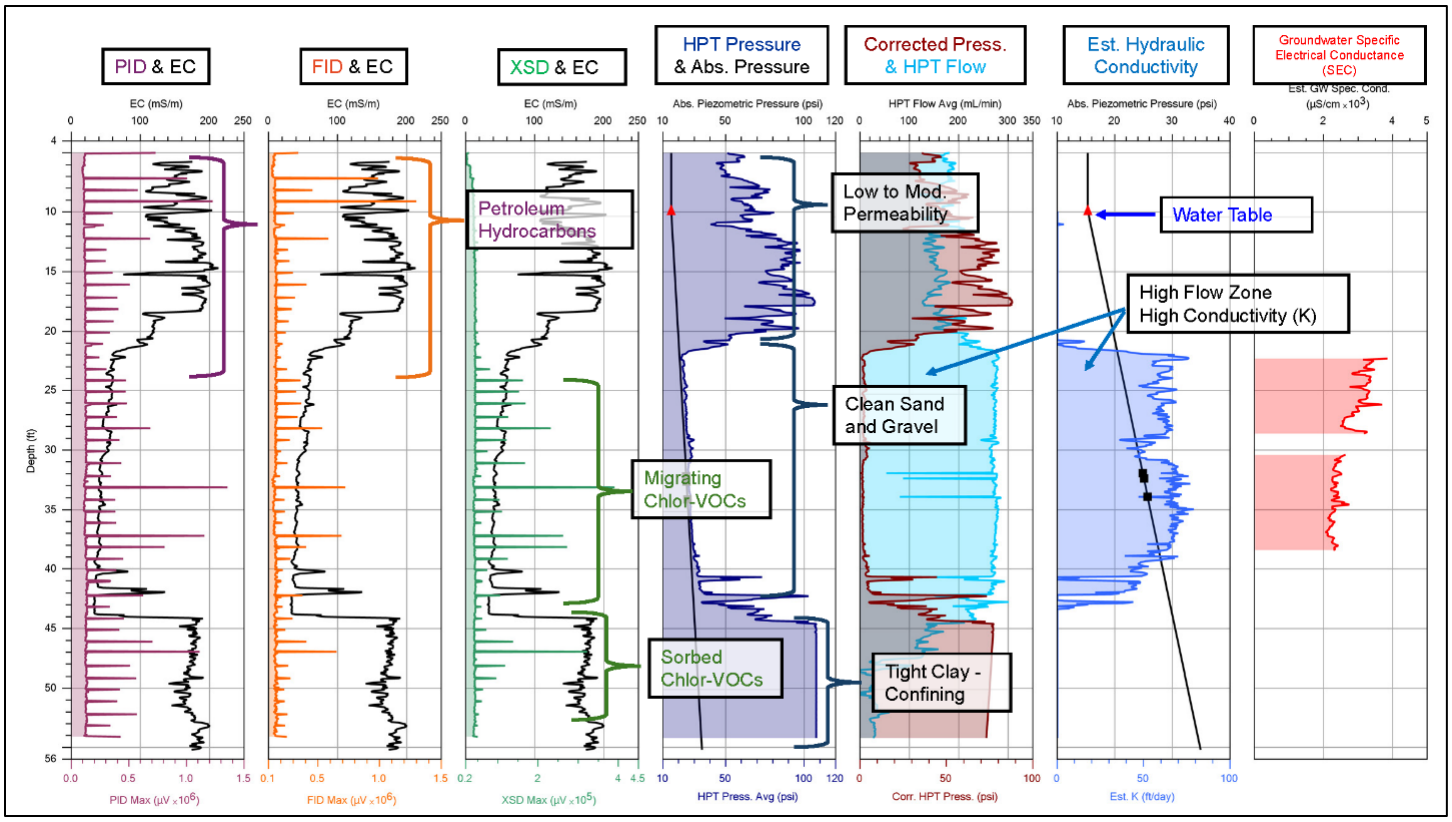


Figure 4-26. Interpreted low-level MIP log including HPT and EC data (LL-MiHPT). Postprocessed variables include head pressure, corrected pressure, estimated hydraulic conductivity (K), and groundwater specific electrical conductance (SEC).

Source: Vista GeoScience LLC, Used with permission.

1.1.1.1 Data Collection Design

General information pertaining to data collection and design for direct sensing tools is provided in Section 4.1.2. Additional considerations to design effective MIP investigations are as follows:

- Select appropriate detectors and supporting technology.
- Determine verification requirements.
- Plan to collect confirmation samples.

Selecting the appropriate complementary tools can help define contaminant migration pathways, geologic barriers, flux, and other parameters of interest. Appropriate detectors should be selected based on the contaminants at a site (**Table 4-1**). Although it is not necessary to use multiple detectors simultaneously at all sites, it is typical. Typical systems are set up so the carrier gas flows through the PID, then to the FID and XSD. Since the FID and XSD destroy the compounds being analyzed, it is necessary to split the MIP carrier gas stream upstream of those detectors. Current MIP probes are built in tandem with an EC array and HPT or CPT sensor. It is important to note that the CPT sensor can be used only on CPT-type direct-push rigs, not percussion-driven direct-push rigs. Complementary tools should be selected based on known and anticipated hydrogeological properties of the site.

Because data produced by the MIP is qualitative to semiquantitative and susceptible to interference (Section 4.5.4.2), it is important to supplement MIP data with quantitative data from an adequate number of confirmation samples collected and analyzed on site or in a laboratory. In general, multiple laboratory confirmation samples should be collected from areas of high, low, and medium response to verify the ability to detect the target contaminants in all desired concentration ranges. Verification sampling should also consider the number and location of geologic layers, as detector response may be affected by subsurface geology. In addition, regulatory agencies may have specific requirements for verification sampling.

4.5.2.2 Data Presentation

Deliverables from the operator at the end of the project may include a field report, digital copies of the log files for use in the Direct Image Viewer software, and text files of the raw sensor data. Some providers are also experienced users of various 2D and 3D visualization software packages and will often generate a 3D CSM as part of their reporting. The required deliverables should be specified in the contract before fieldwork is initiated.

The field report may vary from company to company, but should describe the sensors used, include response test procedures and final logs for each boring, provide a table of borings drilled, and provide basic boring information such as boring ID; total depth, date, and time; and a location map or coordinates. An experienced service provider should be able to provide a summary report that includes a quality control review of all logs and describes issues associated with individual log runs, along with an interpretive narrative summary. The consultant or site owner should request a copy of the raw or final edited logs files for recordkeeping purposes. Data from these logs can be reviewed for quality assurance later, and the data can be exported into other databases and mapping or visualization software. Scaling of the log graphs is an important consideration when comparing results from multiple locations, as several factors other than concentration can influence peak responses and sensor responses can span several orders of magnitude. Many providers will provide two sets of logs prints—one set with common sensor scaling for all the boring logs, and another set where each boring log is scaled individually to show the most detail for each sensor in that individual boring.

4.5.2.3 QA/QC

Proper operator training in using the MIP system is critical to obtaining logs that represent subsurface conditions. Training includes proper operation of MIP system electronics, GC, and operating software, as well as understanding MIP advancement methods and component maintenance. It is helpful to understand the analytical chemistry part of the operation in terms of the GC components, such as the detectors and their responses in field conditions. Although not as critical, it is beneficial for the MIP operator (versus the driller) to also have a thorough understanding of mechanics of direct-push operations. Improper operation and lack of maintenance can result in poor quality, reduced productivity, and even inaccurate, nonrepresentative data.

Chemical-response testing is an important QA measure used to validate each log by demonstrating the integrity of the GC detectors and MIP system. A response test must be performed before and after each log. The response test standard should be made from one or more VOC found at the site under investigation. A MIP-response test is performed by preparing a working standard in a 40-milliliter (mL) volatile organic analyte (VOA) vial, inverting it over the membrane, and leaving it in place for 45 sec to 60 sec. A clean vial with deionized water may be used to run a blank test in the same fashion (**Figure 4-27**). Additionally, multiple concentrations of multiple analytes can be tested to gain a better understanding of how the system responds. For example, at a site where both gasoline and PCE were released, the stock standard may be made with benzene and PCE to verify performance of the MIP system and GC detectors for these analytes. Generally, stock standards must be kept cold and should be considered expired after one month, while working standards should be prepared daily. Gas standards of

much lighter VOC (such as methane) can also be applied to the membrane using a test jig combined with a Tedlar® bag, pressurized gas, or other means.

In a laboratory setting, precision is usually assessed by comparing the results of duplicate analyses; however, because MIP samples are obtained in situ, it is not possible to collect true duplicate samples. Instead, an estimate of the instrumental precision can be obtained for the entire system by evaluating the results from multiple measurements of response test samples, which are analyzed before and after each push. Offset or replicate log runs insitu can also serve as a "duplicate" run to measure reproducibility, as described below.



Figure 4-27. Response test—method of introducing an aqueous standard to the membrane.

Source: Geoprobe Systems®. Used with permission.

Quality control is performed during and after each log is generated. Log quality control addresses the following concerns to ensure that the log data are valid (Geoprobe 2021a):

- Proper functioning of the MIP system. Does the log look correct? Does anything in the MIP log and detector responses indicate that the MIP system was not working correctly (for example, sudden changes in pressure, flow, or temperature that correspond with a shift in detector response)?
- Consistency between chemical response tests. As more logs are completed, do they show general consistency between chemical response tests?
- Significant changes in the response factors. As multiple logs are completed, are there significant changes seen in the response factors that do not appear related to these variables? Response factor is defined as the amount of signal response divided by the signal response increase on a response test. Control charts of response test results over time can be used to gauge typical MIP system and detector response factor variations; however, response factors vary due to numerous variables, including the membrane condition and age, trunk line type and length, and ambient temperatures.
- Log repeatability and system consistency. Review log overlays or a cross section of logs in the log viewing software to evaluate log repeatability and system consistency. Replicate logs may be run every 10–20 locations to verify repeatability. Run replicate logs with a 0.5-m to 1.5-m spacing (approximately 3-ft offset from original borehole) for optimum results. Small-scale variability is common; large-scale patterns are usually consistent.
- Low-level mode operations. This mode is especially complicated and requires constant tracking of changes in lag time during log runs to ensure that the sample capture timing does not miss the signal response.

Confirmation Sampling: While simultaneously referring to the completed MIP log for both chemical detections as well as differences in soil characteristics indicated by the EC and HPT data, targeted soil cores and groundwater samples (as described in Section 4.1.3) should be collected (see **Figure 4-28** for a comparison example). Core samples can be analyzed in an on-site mobile laboratory or sent off-site for rapid turnaround analysis. A statistically significant number of samples should be collected from each continuous core in nondetect, moderate, and high response areas. Cores may have more distortion in terms of precise depth location of the sample, so one should be mindful of that during comparison to the

more precise MIP logs response depths. The frequency of offset core samples should be at least 10–20% of the MIP locations, but can be more based on project goals, such as a remediation design, which may require more quantitative concentration data.

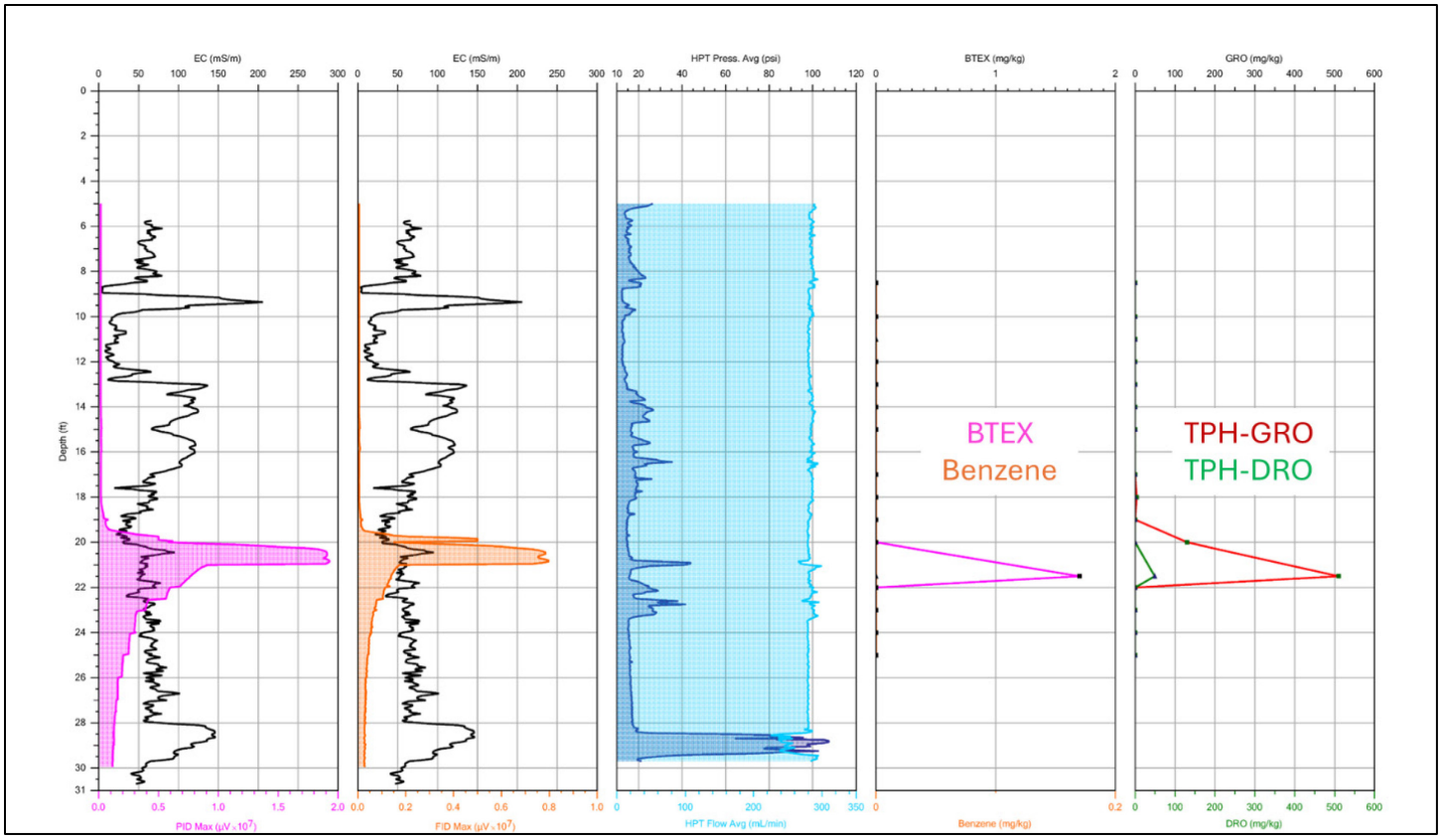


Figure 4-28. Example of soil sample confirmation sampling. A confirmation core was collected in an offset boring to a MIP log run at a gas station site. A total of 16 soil samples were collected at 1-ft intervals and were analyzed for VOC and total petroleum hydrocarbons (TPH). Selected results are plotted at the same vertical scale on the log using the DI Viewer software.

Source: Vista GeoScience LLC. Used with permission.

4.5.2.4 Data Misuses

Lithology, saturation, the presence of multiple compounds, and other factors make direct correlation of MIP response to compound concentrations problematic. Detection levels measured in volts may not correlate directly to concentrations. In some cases when compared with physical sample analyses, MIP results have poor quantitative correlation, especially if limited samples were collected and/or the ECD was the only chlorinated VOC detector used (Quinnan 2010; Adamson et al. 2014). Improved correlation with physical samples can be achieved with the use of the now standard XSD detector (McCall et al. 2014). MIP values may vary by orders of magnitude from one location to another and are not absolute or unique to a specific compound or concentration. MIP data should primarily be used to establish relative contaminant concentrations and guide the placement of confirmation borings, rather than attempting direct correlation with absolute concentration values.

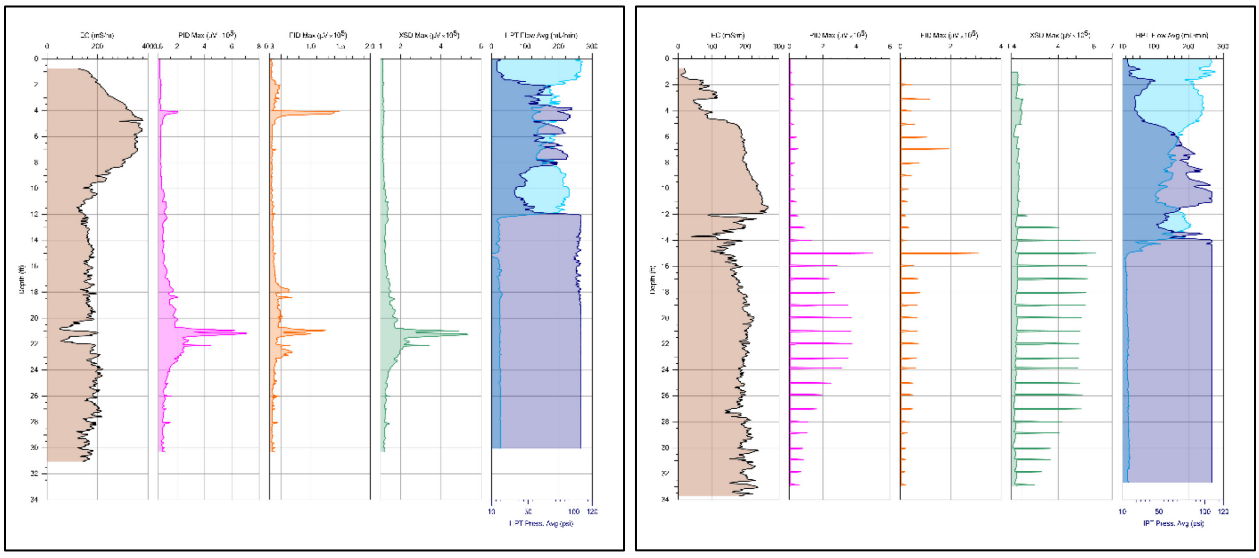
A lack of MIP response does not necessarily indicate that the soil column investigated is free of VOC or SVOC because MIP detection limits (**Table 4-1**) may be above regulatory action levels. The MIP cannot,

therefore, be used to directly determine whether health-based levels have been exceeded in a particular media. This should be done with confirmation sampling.

4.5.2.5 Supporting and Enhancing Instruments and Technologies

Attempting to use the standard MIP configuration to characterize low-level or high-level contaminated sites can be challenging. In some cases, modified field procedures or slightly modified versions of the tool allow characterization at these sites. The low-level MIP system is used to detect lower VOC concentrations by pausing the return carrier gas to concentrate the VOC signal seen by the detectors by approximately an order of magnitude. **Figure 4-29** compares standard and low-level run logs at the same site. The first graph is the EC response. The next three graphs are the PID, FID, and XSD sensors. Note the difference in the continuous curve on the standard mode log, which is recording continuous sensor, and the spikes on the low-level log, which are the depth intervals at which the concentrated sample is acquired—every 1-ft in this case. The far-right graph on each log is the HPT injection pressure and flow graph.

Heated transfer line MIP (HTL-MIP) incorporates a heated trunk line to minimize trunk line analyte retention that occurs with high-level analyte concentrations, particularly analytes with higher molecular weights such as chlorobenzene. The heated trunk line can also increase sensitivity. More soluble compounds, such as tert butyl methyl ether (MTBE), can be detected better by removing the Nafion dryer in the GC system, which removes water vapor from the gas flow. These methods require hardware modifications to the standard MIP by an experienced operator.



Standard MIP log **Low-level MIP log**

Figure 4-29. MIP logs located at the same project site, one run in standard sensitivity mode (left) and the other in low-level sensitivity mode (right).

Source: Vista GeoScience LLC. Used with permission.

The MIP is typically used in conjunction with other direct sensing tools to allow as much subsurface information to be gathered as possible during a single push. The current production MIP (also referred to as MiHPT) is equipped with a small dipole EC array (Section 4.3) near the end of the probe and an HPT port on the opposite side of the heater block. The EC array is used to acquire a log of bulk formation EC as the probe is advanced while the HPT port is used to conduct injection logging. Tandem HPT logging

provides an injection flow and pressure log versus depth to help evaluate formation permeability (Section 4.4). Used together, the EC and HPT logs can help better define stratigraphic and hydrostratigraphic characteristics of the subsurface, including estimated hydraulic conductivity (K) and groundwater SEC. Plotting MIP detector logs with HPT and EC logs can help identify contaminant migration pathways or low permeability back-diffusion sources of VOC. The MIP can also be advanced in tandem with a CPT cone (Section 4.2) to obtain geotechnical information on soil type and material strength. Targeted sampling of sedimentary layers is recommended to confirm MIP log data for VOC distribution and lithologic interpretation.

4.5.3 What Are the Advantages?

The MIP offers substantial advantages for environmental site characterization and remedial planning. By providing real-time data collection, MIP enables dynamic adjustment of work plans in the field, allowing teams to respond immediately to observed conditions. Its ability to deliver a rapid, high-resolution depiction of contaminant distribution in the subsurface facilitates identification of discrete targets, such as “hot spots,” which in turn supports more effective placement of sampling points, monitoring well screens, and soil vapor probes, as well as targeted remediation efforts. When combined with other direct-push sensors, such as EC, HPT, and CPT, MIP also yields valuable information about local geologic conditions, further enhancing the CSM.

MIP is particularly effective for the vertical delineation of VOC in soil vapor, and when used with multiple detectors, it can distinguish between different classes of VOC, such as halogenated versus no-halogenated compounds. In addition, MIP minimizes worker exposure to impacted media and produces minimal to zero investigation-derived waste, making it a safer, more sustainable alternative to traditional sampling methods.

4.5.4 What Are the Limitations?

The MIP system provides qualitative to semiquantitative results for total VOC levels (combination of sorbed, vapor, and dissolved VOC) in the bulk formation. Because a chromatography column is not typically used to separate analytes in the sample gas stream before their introduction to the gas-phase detectors, specific analyte identification is not possible. Using multiple detectors that are selective to different groups of contaminants (for example, aromatic hydrocarbons, chlorinated alkane or alkene VOC) helps to identify the type of contaminant(s) present. In some modified systems, the MIP gas stream can be sampled for further analysis with additional assay methods (for example, GC/MS) (Costanza and Davis 2000; Considine and Robbat 2008; Van de Putte et al. 2012). The MIP should not replace soil sampling and monitoring wells but is a means to optimize a reduced number of boreholes and monitoring wells and better target well screen and sampling intervals to achieve site characterization and long-term monitoring objectives, and support remediation design.

The MIP can be used to infer the presence of subsurface concentrations indicative of fuel NAPL (residual or saturated). However, when fuel NAPL is directly encountered during MIP operation, the membrane, carrier-gas tubing, and detectors may become overloaded. This overload (and carryover) can lead to artificially elevated background readings as the tool is advanced beyond the NAPL zone. Once the system components become saturated, purging the lines and detectors can require significant time and may require removing the tool from the borehole. The heated trunk line (HTL-)MIP can help reduce these effects, but at sites with known or suspected fuel-related NAPL releases, the Ultraviolet Optical Screening Tool® (UVOST) (Section 4.7.2.1) or the Optical Image Profiler–Ultraviolet (OIP-UV) (Section 4.6.2.1) is generally recommended.

4.5.4.1 Detection Limits

As with the other direct sensing tools, they are limited to static or percussion direct push in unconsolidated sediments and cannot be used in bedrock applications or sediments with large gravel or cobbles.

MIP detection limits depend on many factors, including, but not limited to, the analyte characteristics (boiling point, volatility, solubility), soil type, temperature at the membrane face, and detector used. Additionally, operational and instrumentation differences between providers may affect detection limits, and those limits should be verified and maintained during the project using appropriate quality assurance measures described above. Table 4-1 provides estimated lower limits of detection in bulk formation for several contaminant classes for commonly used detectors.

Table 4-1. A guide to analyte detection levels in bulk formation using the MIP system and typical detectors.

Detector	Analyte detection limits [parts per million (ppm)]								
	BTEX	Gasoline	Diesel	TCE, PCE	CCl_4	DCE	VC	DCA, TCA	CH_4
PID*	0.5–5	3–10+	10– >25	0.5–3	N/A	5–10	>5	N/A	N/A
FID†	1–10	1–5	3–10	>500	>500	25–50+	>50	10–25	100 (ppm-v)
XSD‡	N/A	N/A	N/A	0.2–0.5	0.2–0.5	0.2–0.5	0.2–0.5	0.2–0.5	N/A
ECD§	N/A	N/A	N/A	0.2–0.5	0.1–0.5	25–50	>100	1–25	N/A

Notes: *PID–photoionization detector; †FID–flame ionization detector; ‡XSD–halogen-specific detector; §ECD–electron capture detector BTEX–benzene, toluene, ethylbenzene, and xylenes; CCl4-- carbon tetrachloride; DCE -- dichloroethylene; VC -- vinyl chloride; DCA -- dichloroethane; TCA–trichloroethane, ppm: parts per million CH4: methane, ppm-v: parts per million by volume in air N/A: not applicable, this detector is not sensitive to this analyte.

Source: Geoprobe Systems®. Used with permission.

The MIP and associated detectors are generally appropriate for investigating common VOC, including chlorinated solvents, light oil and fuel mixtures, and those VOC that are not fully miscible in water and have low-to-moderate boiling points (Table 4-2). Multiple detectors are available for analyzing the effluent gas, including the PID, FID, XSD, and ECD. If a detector option is available, then the detector, or more likely, combination of detectors should be selected based on the properties of the compounds being investigated (Figure 4-30).

Table 4-2. Inferring analyte category based on response(s) of MIP multidetector system.

MIP detector	Chlorinated or fluorinated ethenes	Chlorinated alkanes	Gasoline, diesel, or similar petroleum fuel	BTEX, naphthalene	Methane	Mixed petroleum fuel or BTEX and halogenated VOC
	Relative detector response(s) to analyte categories					
PID	Moderate to high	None to low	Moderate to high	High	NA	Moderate to high
FID	Low (*see notes below*)	Low	High	High	High	Moderate to high
ECD	Low to high	High	NA	NA	NA	Low to high
XSD	Moderate to high	High	NA	NA	NA	Moderate to high

Notes: FID often responds in chlorinated DNAPL. A PID can detect chlorinated alkenes, allowing the user to distinguish them from chlorinated alkanes, which do not respond on PID, when ECD or XSD results indicate either may be present. Relative PID- FID response will vary with degree of weathering. Other nonchlorinated VOC may give similar response pattern. Useful for tracking landfill gas plumes and releases of natural gas, or for monitoring methane produced by anaerobic in situ bio projects.

Source: Modified from Geoprobe Systems®. Used with permission.

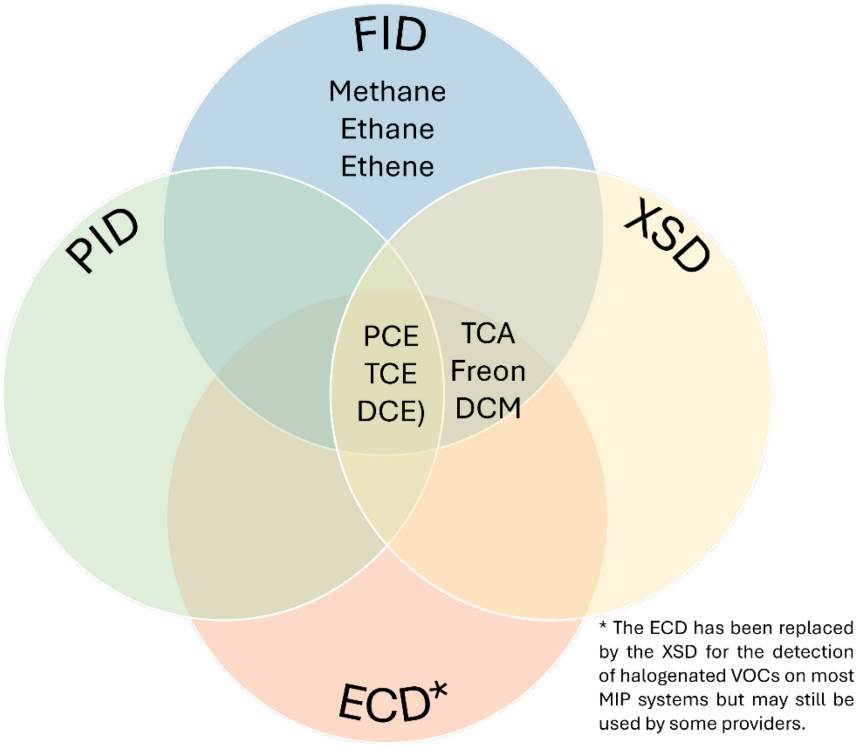


Figure 4-30. Common MIP detectors and example contaminants detected.

It is worth noting that the FID detects all hydrocarbon VOC, including methane, which is common when anaerobic degradation is occurring. The other two detectors (PID, XSD) do not detect methane. If a response is present on the FID and not on the PID or XSD, then methane may be present. At significant concentrations, methane also has a quenching effect on the PID, which can reduce response or even cause a negative shift on the PID baseline. Ethanol is another common VOC that responds only on the FID and also has a PID quenching effect on other compounds. The quenching effect could be considered a potential "false negative" response issue.

If the instruments are operated properly and within specifications, then there are no false positives known. However, since detection is not compound-specific, VOC unrelated to target compounds could be misinterpreted as the target compound. This is where confirmatory sampling and analysis are required as part of the QA/QC.

Soil type, saturation level, and proximity of contaminants to the surface of the probe can significantly affect the ability of the MIP to detect subsurface contamination. Different soil types and variations in degree of saturation can influence the ability of the MIP probe to volatize compounds and may result in variability in detection levels that are unrelated to the mass concentrations present.

Low-level MIP systems can be used when lower detection limits (for example, below the ppm level) are required, such as when halogenated VOC are the contaminant. A low-level MIP system includes an additional carrier gas flow modulating controller to start and stop the carrier gas flow at desired times and depths. Using the low-level system increases the detection level of the MIP system by approximately an order of magnitude for many contaminants.

4.5.4.2 Interferences

In zones with high concentrations, carryover or cross contamination of the membrane sampling port and return carrier gas line may occur as the MIP is advanced. Carryover or cross contamination results in slow bleeding off of the signal response for an extended depth below the interval where the high concentrations were encountered. Complex mixtures (for example, weathered gasoline) containing lower volatility and higher molecular weight compounds travel through the gas line at a slower rate, arriving at the detector(s) sometime after the more volatile contaminants, resulting in a delayed or shifted response. These effects can result in detector responses being plotted at greater depth than where the analytes were located in the formation. This carryover effect (Bumberger et al. 2011; Adamson et al. 2014; McCall

et al. 2014) often has been mischaracterized as a physical drag down of contaminants. Actual physical drag down of contaminants while logging appears to be much less common than carryover effects. In certain cases, probe advancement may be suspended beyond the highly impacted interval to allow additional time for insitu gas-line purging. However, discrete soil sampling across the affected interval often provides the most reliable means of resolving such interferences and may be included as part of the confirmatory sampling plan.

Because the MIP provides for total VOC detection without analyte separation and specificity, interference between analytes is common. Interference can be most pronounced on sites with co-mingled releases of multiple compounds, such as chlorinated VOC TCE and PCE, as well as BTEX compounds. In this case, depending on concentration, TCE, PCE, and BTEX compounds could all be detected by the PID and FID detectors, while the XSD would detect only TCE and PCE (**Table 4-1**). Using multiple detectors helps identify classes of contaminants and reduces interferences.

Additionally, some natural and anthropogenic compounds are nonhazardous but cause a detector response. Natural pine oil or similar natural aromatic compounds from pine tree or juniper roots may yield a response if touched by the MIP membrane at depth. The site should be investigated to assess the potential presence of nonhazardous VOC and, if identified, these interferents should be included in the data interpretation, if they cannot be eliminated.

4.5.5 Additional Information

Alaska Department of Environmental Conservation, Division of Spill Prevention and Response Contaminated Sites Program, Field Sampling Guide (ADEC 2024)

Montana Light Non-Aqueous Phase Liquid (LNAPL) Recovery and Monitoring Guidance (MDEQ 2013)

Senate Bill 96 (2015) Status of $7,000,000 Appropriation from the Orphan Share Account Environmental Quality Council – Final Report (MDEQ 2017)

Final Proposed Plan, Former Kirksville Air Force Station Missouri, Fuds Project No. B07MO023204 (USACE 2008)

Final Supplemental Groundwater Characterization Report, Bishop Tube Site, East Whiteland Township, Chester County, Pennsylvania (M. Baker 2004)

A Study of Managing Decision Uncertainties using the Triad Approach (SDPRCF 2005)

Virginia DEQ's Northern Region Petroleum Program current understanding of the Robinson Terminal North – the former Washington Post paper depot (VDEQ 2017)

High Resolution Site Characterization: A Sustainable Risk Management Approach (Fiacco 2010)

The Triad Approach to Managing Decision Uncertainty for Better Cleanup Projects (Crumbling 2004)

Membrane Interface Hydraulic Profiling Tool (MiHPT) (Geoprobe 2026b)

Membrane Interface Probe (MIP) Standard Operating Procedure (Geoprobe 2021a)

USEPA CLU-IN, Membrane Interface Probe (MIP) (USEPA 2018c)

4.6 Optical Image Profiler

4.6.1 What Is the Technology?

The Optical Image Profiler (OIP) system is a field-screening tool used for characterizing the subsurface distribution of products (NAPL) containing polycyclic aromatic hydrocarbons (PAHs). The system provides qualitative to semiquantitative results for product and PAH levels in the bulk formation. The OIP is deployed using a direct push drilling platform and detects the visible fluorescence of NAPL products and PAH. The system consists of a probe, the field instrument, optical interface, and laptop computer (**Figure 4-31** and **Figure 4-32**). All three OIP tool types are operated using the same data acquisition instruments and software. The field instrument interfaces with, provides power to, and allows data transfer from an EC dipole mounted on the probe and a string potentiometer located at the surface. The string potentiometer is mounted to the direct-push unit and provides information on probe depth and push rate. The optical interface delivers power to the downhole camera and light-emitting diode (LED) and transmits images to the laptop computer for analysis. A trunk line connects the probe directly to the optical interface (McCall et al. 2018). The HPT pump controller is also required to control the built-in HPT component of the tool.

The OIP probe is advanced using direct push percussion

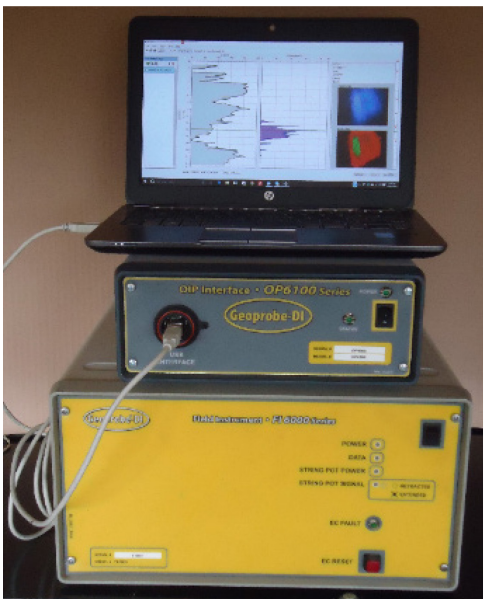


Figure 4-31. OIP controller instruments and data acquisition components.

Source: Geoprobe Systems®. Used with permission.

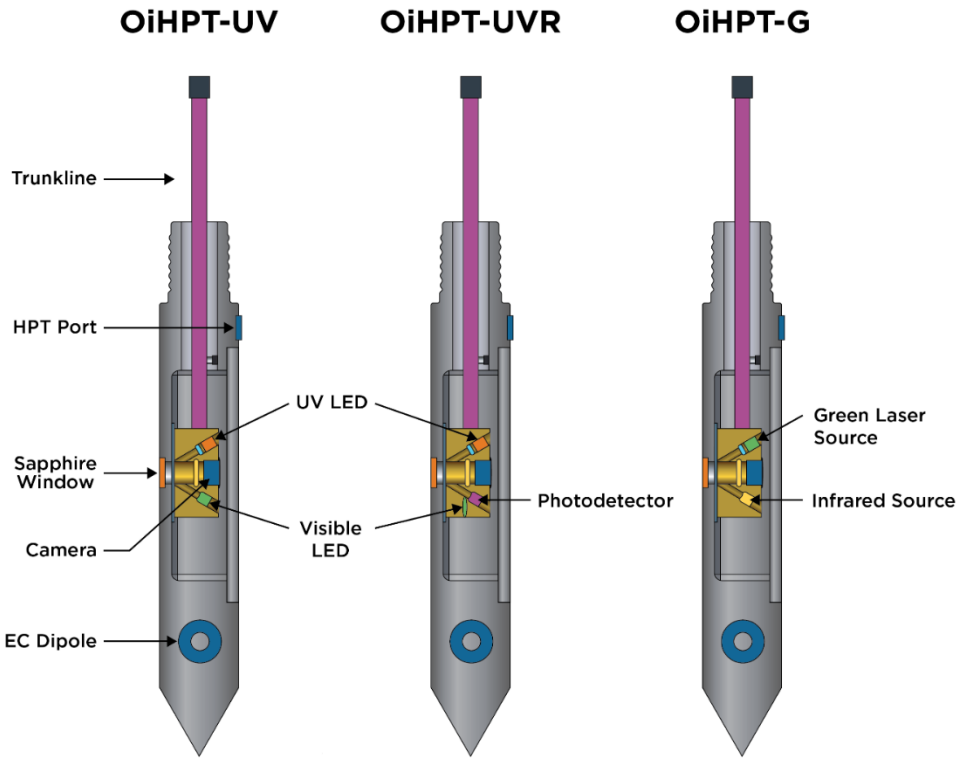


Figure 4-32. The three currently available OIP tools include OIP-UV, OIP-UVR, and OIP-G. All three tools are currently manufactured to include an HPT injection port and EC dipole array.

Source: Modified by Geosyntec Consultants, Inc., from Geoprobe Systems®. Used with permission.

probing methods into soils and unconsolidated formations at a rate of approximately 2 cm/sec (4 ft/minute). The standard probe (Figure 4-32) used during petroleum NAPL investigations is equipped with both a UV LED (275 nm) and a visible spectrum (VIS) LED stationed behind a sapphire window. Either of these LEDs may be used to illuminate the formation outside the sapphire window. To capture the illuminated image, a small complementary metal–oxide semiconductor camera is mounted behind the window, inside the probe. As the probe is advanced, the camera captures images of fluorescence at 30 frames/sec. One image is saved for every 0.05 ft (~15mm) of probe advancement. The system operator can halt probe advancement at any depth and capture a still fluorescence or VIS image. Still images provide better clarity and detail than images captured as the probe is advancing. VIS images may help to define formation texture, structure, and color. As the probe is advanced, an integrated EC array provides real-time readings of the EC of the formation while a downhole HPT pressure transducer measures the soil's response to a continuous injection of water.

The left side of Figure 4-33 shows the EC and percent area of fluorescence logs versus depth; the right-side presents captured still images. The UV images, both still and dynamic, are analyzed by software and displayed on a laptop computer for interpretation in the field. As seen in Figure 4-33, the captured image represents the unfiltered image as detected by the complementary metal–oxide semiconductor sensor. The analyzed image is what remains of the unfiltered image following the application of digital filters. These filters eliminate pixels that are unrepresentative of fuel fluorescence. The average area illuminated per frame is calculated using multiple filtered frames obtained over a 0.05-ft interval to calculate the percent area of fluorescence, which is then plotted on the log.

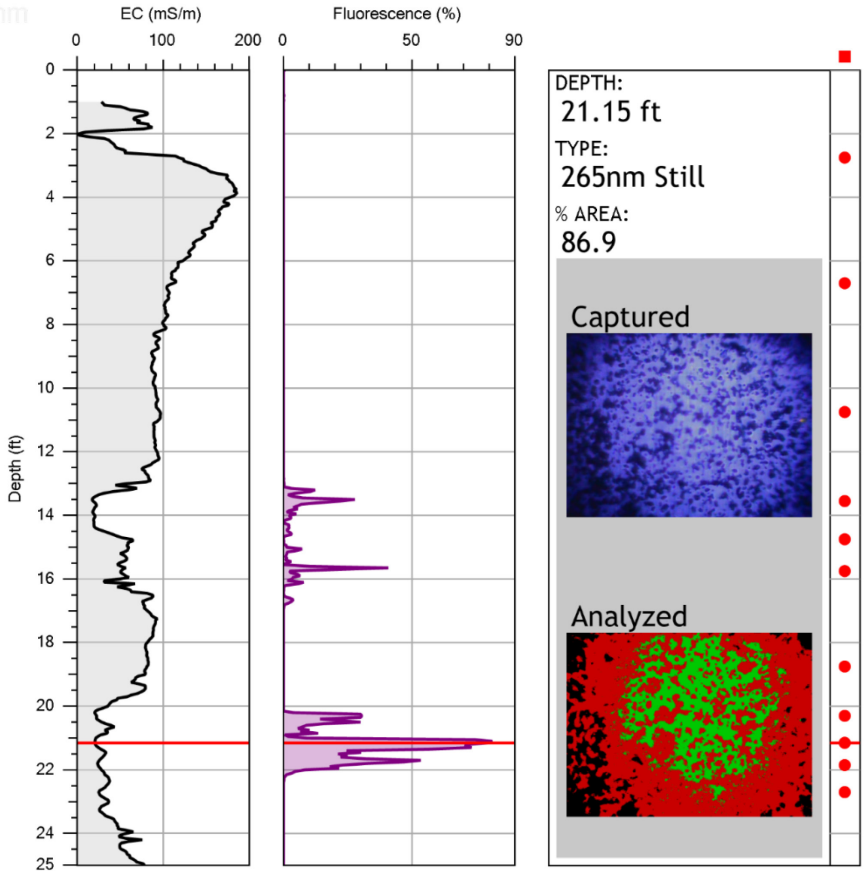


Figure 4-33. OIP software display.

Source: Geoprobe Systems®. Used with permission.

OIP data are rarely viewed in isolation but combined with information obtained from complementary sensors. All OIP probes are equipped with a small dipole EC array near the end of the tool to acquire logs of bulk formation EC and an HPT port to conduct injection logging as the probe is advanced (Sections 4.3 and 4.4). Information from these sensors can be viewed together with the OIP percent area of fluorescence data and EC log information. In addition, OIP probes can be fitted with a CPT cone (Section 4.2) to obtain information on soil type and material strength (Figure 4-34).



Figure 4-35. OIP probe with attached CPT cone.

Source: Geoprobe Systems®. Used with permission.

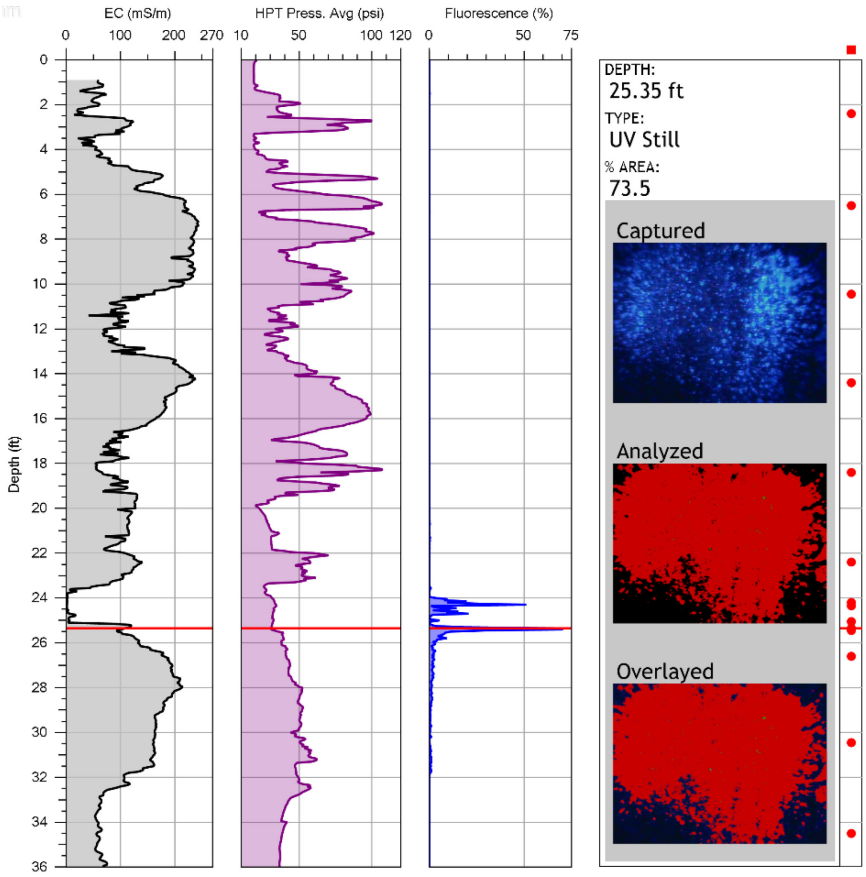


Figure 4-34. An OIP-HPT log with EC on left, HPT injection pressure in the middle, and percent area of fluorescence on right.

Source: Geoprobe Systems®. Used with permission.

Tandem HPT logging is used to provide a pressure log versus depth to help evaluate formation permeability (Section 4.4.1.1). Viewing these logs alongside the OIP fluorescence logs can help to better define contaminant migration pathways or low permeability back-diffusion sources. In **Figure 4-35**, the low EC (Section 4.3) and low HPT pressure (Section 4.4) from about 23.5 ft to 25 ft indicate the presence of a dry sand (not water wet). The image of fluorescence at 25.35 ft indicates the presence of LNAPL globules in the formation. The percent fluorescence log shows that NAPL is present in the sandy layer bounded above and below by silty clays. The data indicate that the sandy layer is behaving as a migration pathway for the LNAPL at this site.

4.6.2 How Is the Technology Used?

Coal tars, creosote, and some heavy fuels do not fluoresce consistently under UV illumination but do fluoresce under green wavelength light. An OIP probe, the OIP-green (OIP-G), has been designed with a green (525 nm) laser diode for investigation of these contaminants. Three versions of the tool are manufactured, each with varying response depending on the NAPL of interest (Figure 4-36):

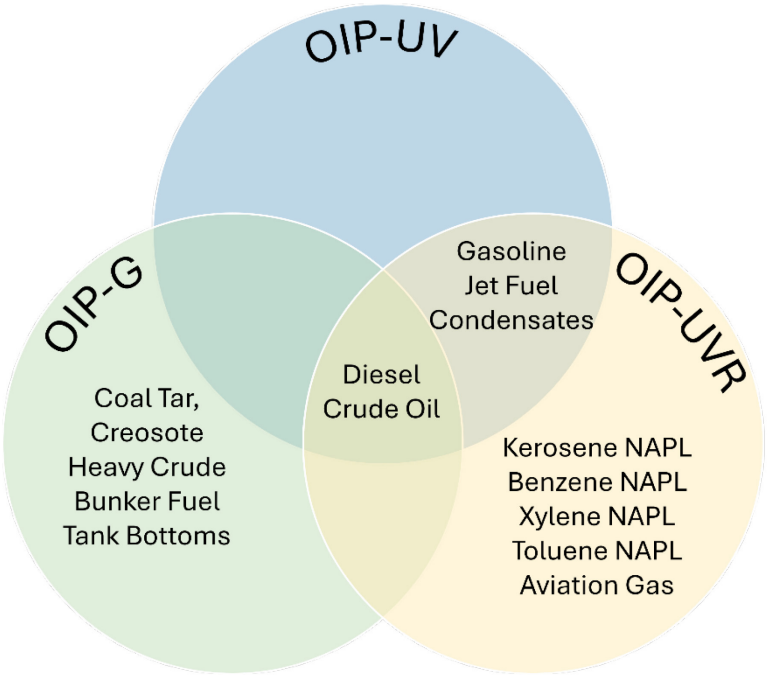


Figure 4-36. NAPLs detected by the OIP suite of tools.

- The OIP-UV is a UV-LED and camera-based system optimized to detect visible fluorescence of most petroleum NAPL products, gasoline, diesel, oils, and lubricants.
- The OIP-G is a green laser diode and camera-based system used to detect the longer wavelength fluorescence of heavier PAHs, including coal tars and creosote.
- The OIP-UVR adds a photodetector (photometer) to the OIP-UV system for optimized detection of jet fuel and gasoline, as well as benzene, toluene, xylene, and other NAPLs. These compounds fluoresce in the ultra-violet spectrum, which the photodetector can measure.

4.6.2.1 OIP-UV

The OIP-UV system employs a 275-nanometer (nm) UV light-emitting diode (LED) to induce fluorescence in PAHs, a visible (white) light (VIS) LED to examine the media, and an integrated camera to capture images of both. Each of these instruments is housed opposite a sapphire window within a 2-ft-long, 1.75-inch-diameter probe. Fluorescence is logged as a percent area of the camera's field of view or "percent area of fluorescence." The system is deployed using either direct-push technology with hydraulic hammer or a CPT unit.

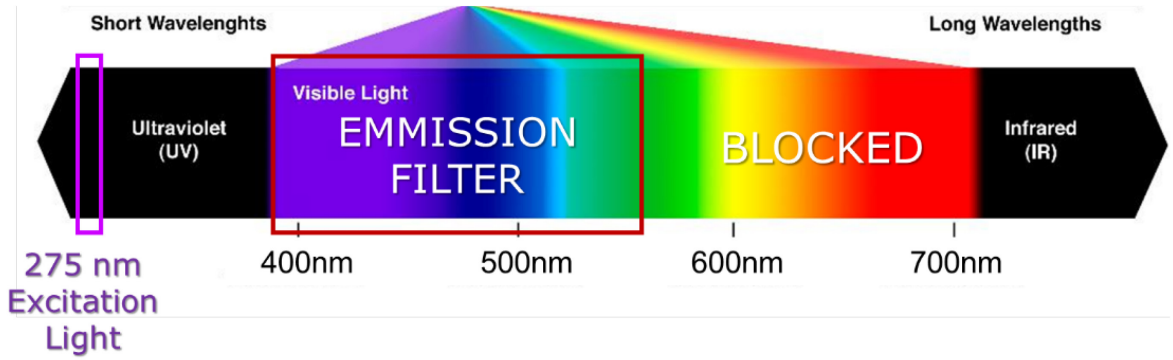


Figure 4-37. Spectra diagram showing the excitation wavelength of the UV LED light source, the range of emission wavelengths measured (375 nm–550 nm), and the blocked wavelengths above 550 nm.

Source: Vista GeoScience LLC. Used with permission.

The OIP-UV takes advantage of PAH fluorescence in the presence of UV light (Lakowicz 1999). UV light causes electrons in the molecules to jump to a higher energy state, and after a short period of time, the electrons return to the normal, lowerenergy state by releasing a photon of light (fluorescing). Light is released by these molecules at specific wavelengths depending on the compounds being excited. Smaller PAH molecules, such as naphthalene, emit shorter wavelengths, while larger molecules emit longer wavelengths. In all cases, the light emitted by these molecules is of a longer wavelength than the exciting source (Aldstadt 2002). Naphthalene emissions are primarily in the UV range. For mixtures containing larger PAH molecules, fluorescence occurs at visible wavelengths (Berlman 1971; Dixon 2005) (Section 4.7 for a more in-depth description). The OIP camera cannot detect most UV emissions but is sensitive to emissions in the visible portion of the electromagnetic (EM) spectrum (**Figure 4-37**).

The OIP-UV is primarily used to identify the presence and distribution of lighter hydrocarbon LNAPL, such as gasoline, diesel fuel, used motor oil, and similar compounds in contaminated subsurface soils and sediments. OIP-UV can also be used to estimate certain physical properties of overburden materials. The device is equipped with a VIS LED to provide images of soil texture and color at selected depths, which allows grain-size distribution and permeability to be estimated (**Figure 4-38**). Normally while pushing the OIP-UV tool the UV LED is on, continuously capturing UV fluorescence images. However, the system has the option to run the visible (white) light and capture continuous soil images. The latest software version of Geoprobe's DI Viewer allows the creation of a strip log of either set of images. The system does not allow the user to discriminate between types or mixtures of LNAPL present (for example, gasoline versus diesel versus jet fuel); therefore, some prior knowledge of the type of release is required (McCall et al. 2018).

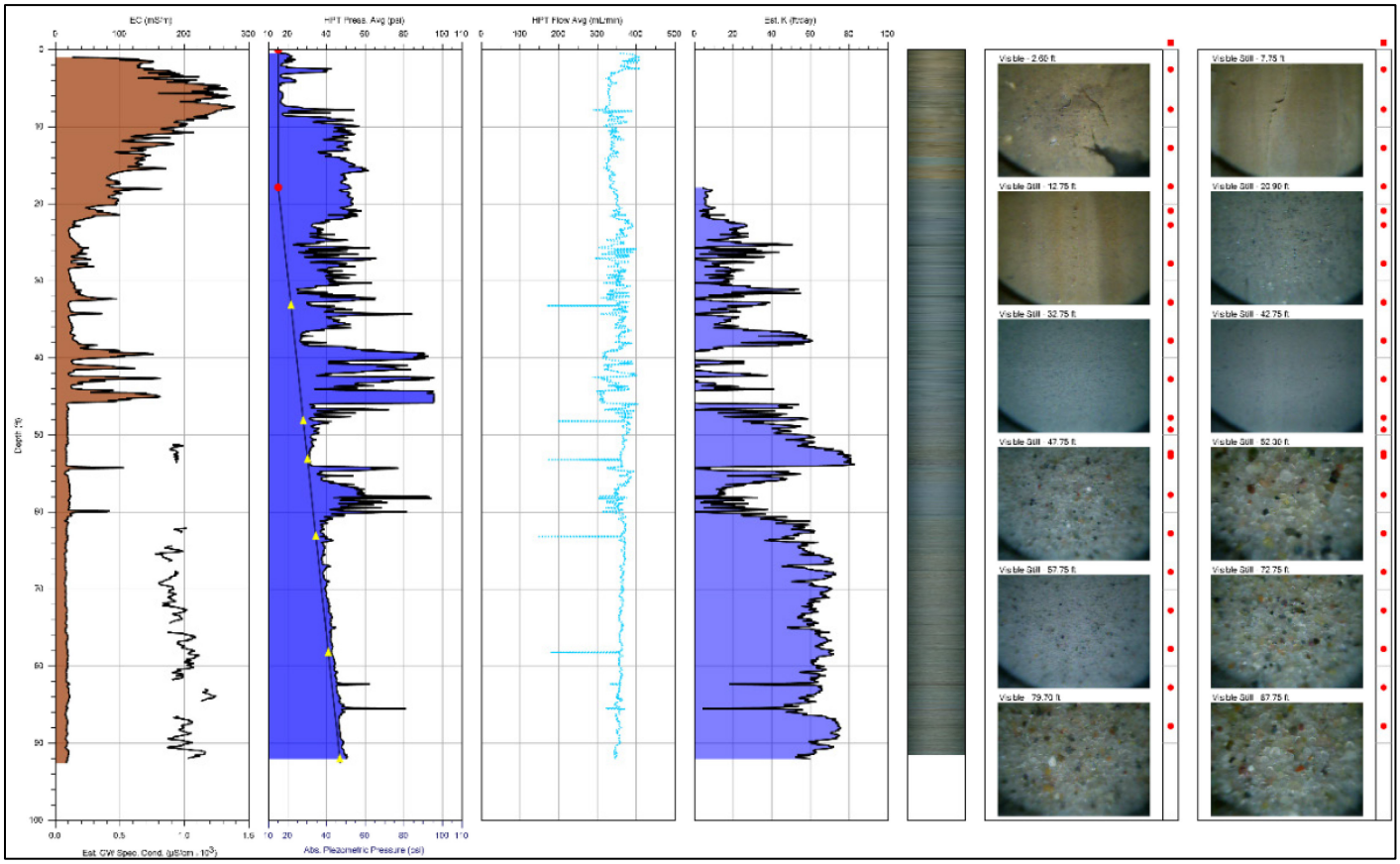


Figure 4-38. Use of visible light on OIP-UV tool to produce continuous soil color strip logs.

Source: Geoprobe Systems®. Used with permission.

4.6.2.2 OIP-G

An OIP-G probe is equipped with a green wavelength (520 nm) LED excitation source and is available to detect coal tars and creosote. These heavier compounds do not fluoresce or fluoresce only weakly under UV light but do fluoresce well under the green light source, typically in the red-orange wavelength range (**Figure 4-39** below). A low pass optical filter over the camera excludes reflected green light from the laser from reaching the camera. As such, the OIP-G probe is equipped with an infrared (IR) LED in place of the VIS LED on the OIP-UV to view soil texture and structure at selected depths. See **Figure 4-40** for an example OIP-G log.

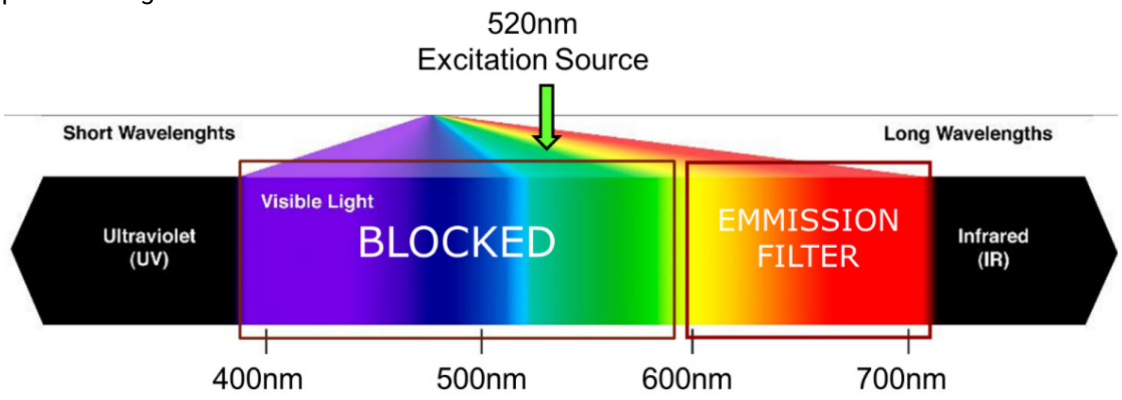


Figure 4-39. OIP-G tool: Spectra diagram showing the excitation wavelength of the green LED excitation source at 520 nm, the blocked emissions from 375 nm to 590 nm, and measured emissions from 590 to 750 nm.

Source: Vista GeoScience LLC. Used with permission.

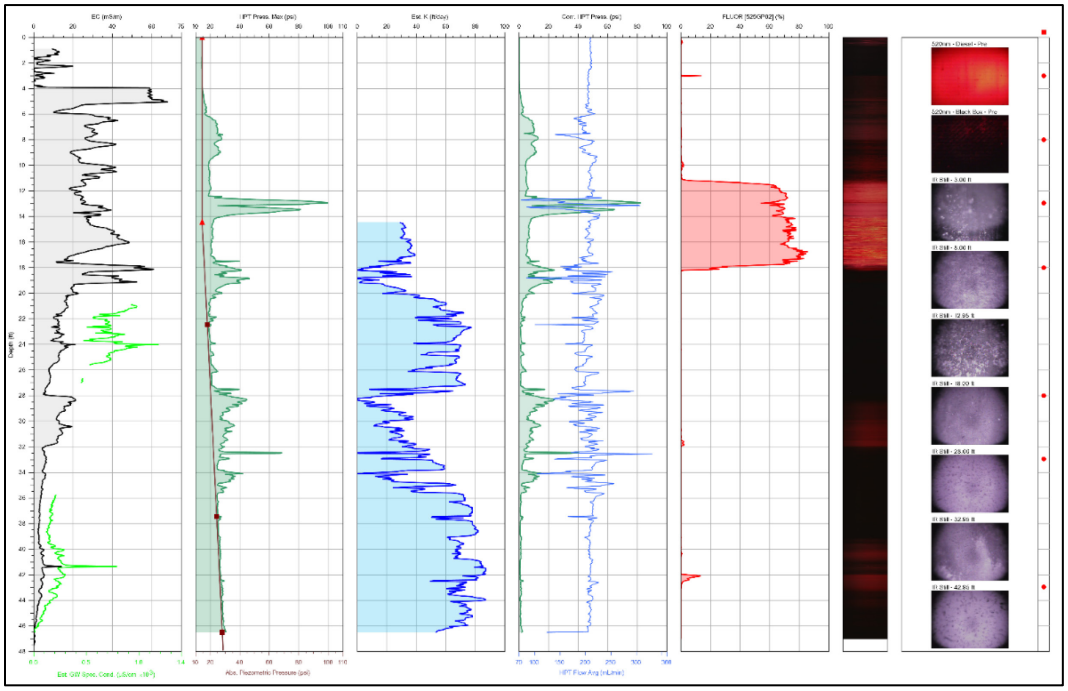


Figure 4-40. OiHPT-G log: Log collected as part of an investigation of MGP waste release. Measured emissions are shown in red and a highly impacted zone is indicated from ~11 ft to 18 ft, while a less impacted zone is shown at ~42 ft.

Source: S2C2 LLC. Used with permission.

4.6.2.3 OIP-UVR

The OIP-UVR probe is a modification of the standard Optical Image Profiler (OIP-UV) that expands detection capabilities by incorporating measurement of fluorescence outside the visible spectrum. As with the conventional system, the probe uses UV light to induce fluorescence in petroleum hydrocarbons and a downhole camera to record visible-wavelength responses, generating a continuous log of NAPL distribution with depth. However, the OIP-UV camera is inherently limited to visible wavelengths, meaning that fluorescence occurring solely in the UV range (<400 nm) is not captured.

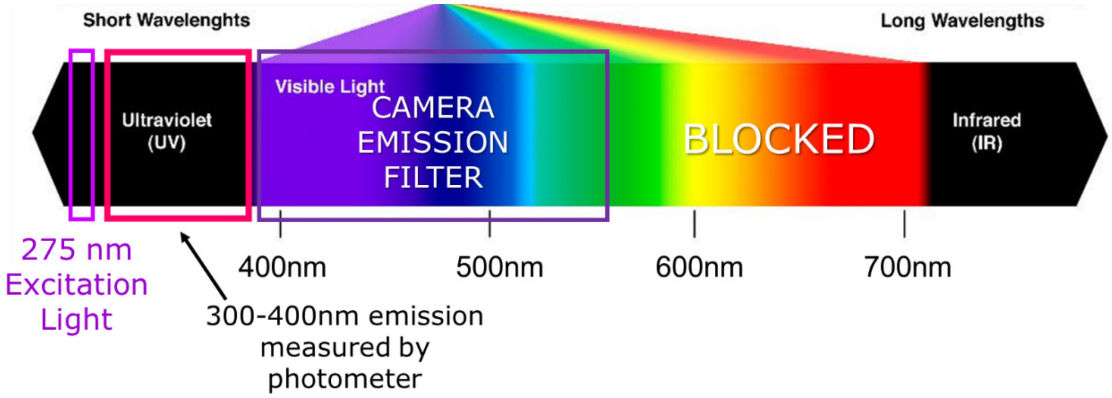


Figure 4-41. OIP-UVR tool: Spectra diagram showing the excitation wavelength of the UV (275 nm) LED light source, the range of visible fluorescence emission wavelengths measured (375 nm-550 nm) by the camera, the UV range fluorescence emission wavelengths (300–400 nm) measured by the photometer sensor, and the blocked emission wavelengths filtered above 550 nm.

Source: Vista GeoScience LLC. Used with permission.

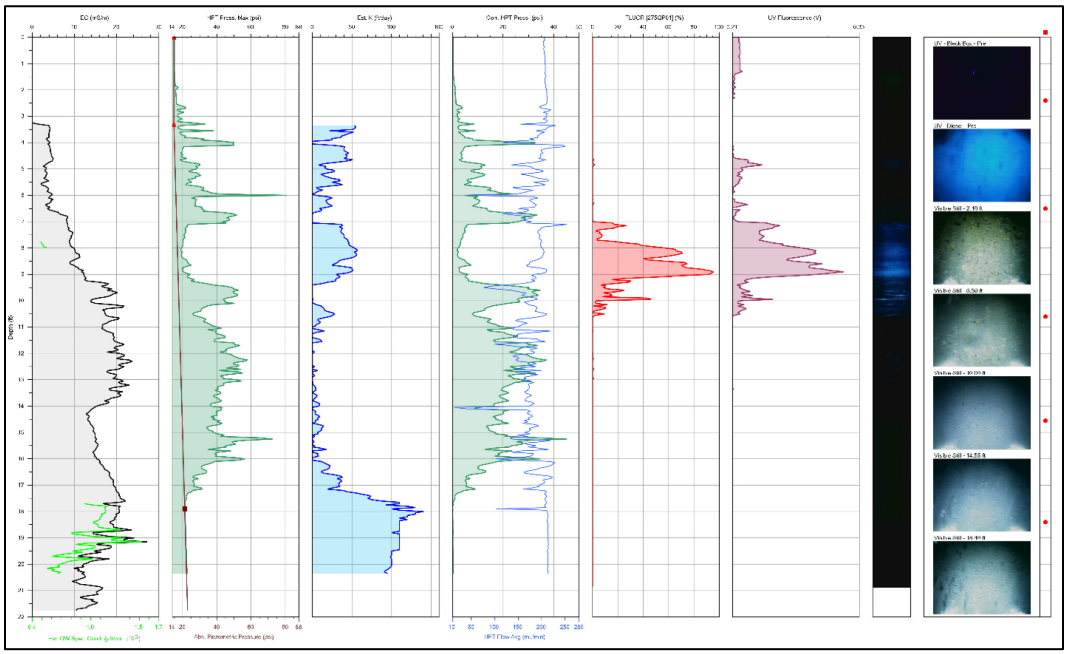


Figure 4-42. OiPHPT-UVR log: This log comes from a jet fuel release investigation. OIP-UV fluorescence is displayed in red while the OIP-UVR photodetector is displayed in purple. False positive readings in the top 2 ft of the log are attributed to ambient light entering the borehole. The UVR photodetector exhibits increased sensitivity to jet fuel NAPL from ~4–7 ft.

Source: S2C2 LLC. Used with permission.

To address this limitation, the OIP-UVR includes an additional photodetector tuned to approximately 300–400 nm, with optical filtering to minimize interference from the excitation source (**Figure 4-41**). This allows the probe to register UV-range fluorescence that would otherwise not be detected by the camera alone. The added sensor improves the consistency of response for hydrocarbons that exhibit weaker or partially UV-shifted fluorescence, such as BTEX and lighter refined fuels. While these NAPLs can still be detected by standard OIP-UV under many conditions, the UVR configuration provides a more complete representation of their fluorescence behavior, supporting more reliable interpretation across a broader range of fuel types.

As shown in **Figure 4-42** in the field log from a jet fuel release investigation, the UVR photodetector exhibits increased sensitivity relative to the standard OIP-UV fluorescence response at shallower depths, highlighting its ability to better resolve jet fuel impacts in the subsurface.

4.6.2.4 QA/QC

QA/QC standards must be established and followed to ensure reliable data. Quality control should be performed during and after each log is generated and care should be taken to ensure that the operator is performing the necessary quality control tasks. In addition to comprehensive operator training (which may be verified prior to commencing work) and an operator track record of successful use, approved field procedures must be understood and followed before, during, and after OIP logging activities. The manufacturer's SOP must be reviewed prior to initiating fieldwork (Geoprobe 2021b).

Quality Assurance Prior to Use

Site conditions, the type of subsurface contamination, and the project objectives should be evaluated to determine whether OIP is the appropriate tool. One such evaluation can include collection of NAPL and soil samples prior to initiating fieldwork to test and assess NAPL response and the potential for false positives and background interference. Another important premobilization consideration is determination of how probe refusal will be defined for the site. Many investigations using direct-push technologies define refusal as an advancement rate (plotted on screen) below 0.5 ft/minute.

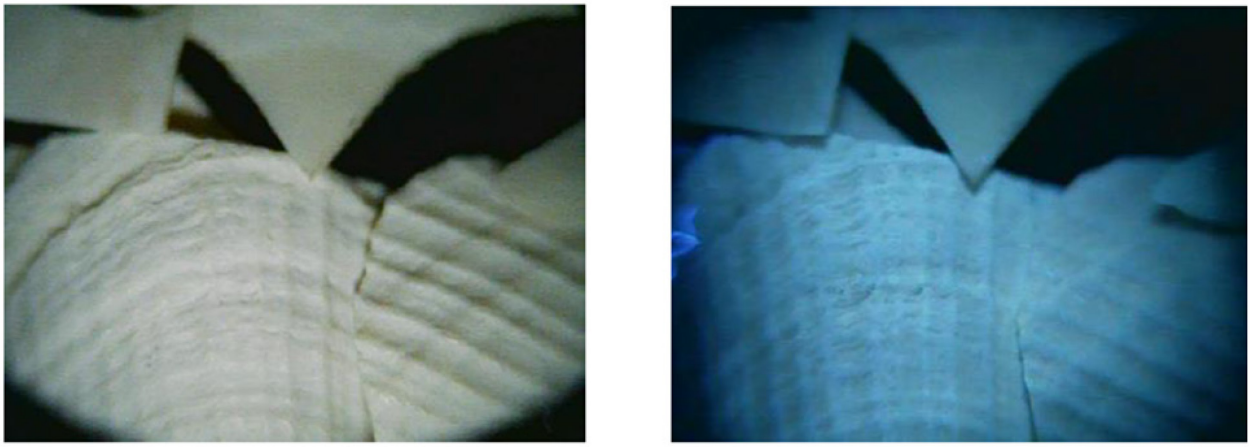
The equipment operator should complete all required quality assurance tests prior to advancing the OIP in accordance with the manufacturer's SOP (Geoprobe 2021b). These tests verify that the probe is undamaged prior to use, that interferences are absent, and that the probe sensor is responding appropriately to reference standards. Quality assurance test data obtained prior to beginning work should be saved to a log file and should include all images and fluorescence responses to known products tested. The file may be reviewed any time after logging is completed. Typically, the same quality assurance test sequence is performed after each log is completed (or at least after the last log of the day) to verify data quality for the final log. Quality assurance test data obtained after logging should also be saved to a log file.

Quality Control During Use

When using the OIP, frequent communication between the probe machine operator and OIP operators is the primary key to success. The OIP and probe operators should agree on verbal commands and hand signals to alert the probe operator when to halt probe advancement so still images can be captured. Good still images in zones of high fluorescence (UV and VIS) or where lithology changes occur (VIS) are valuable when reviewing logs and ultimately developing the CSM.

Real-time images of fluorescence are displayed on screen as the OIP probe is advanced. These images may be used to confirm the indicated presence or absence of fluorescence plotted in the percent area of the fluorescence log. The fluorescence images on screen (and saved to file) are dark if fluorescence is absent. For fuel investigations, the OIP-UV-generated images show blue light typical of fuel fluorescence.

Occasionally, fluorescent light of a wavelength outside of that defined for fuels under OIP-UV may be observed but the digital filters in the software do not recognize this fluorescent light as a contaminant of concern. Unfiltered images are captured at a rate of 30 frames/sec and saved at a rate of one image/0.5 ft of probe advancement. Multiple (unsaved) images obtained over the 0.05 ft interval are processed (filtered and averaged) to obtain the percent area of fluorescence for that interval .



Visible light image

Fluorescent light image
(Instrument registered 64% area fluorescence)

Figure 4-43. Bench-scale test images of seashell chips as seen under visible (left) and UV (right) light using OIP sensor.

Source: Geoprobe Systems®. Used with permission.

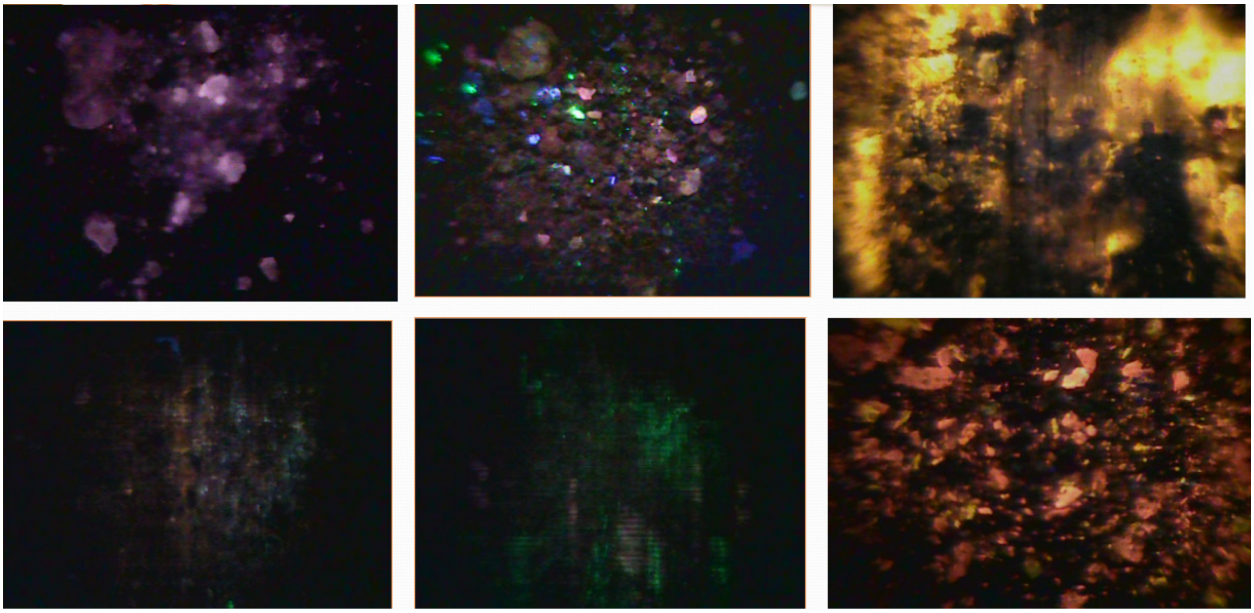


Figure 4-44. Examples of insitu mineral fluorescence under OIP-UV. Generally mineral fluorescence is an undesired effect, but it can be used to identify solid phase contaminants with fluorescent properties. There are publications that cite the use of the tool for identifying mineralization from injections or the use of fluoresceine dye as a tracer.

Source: Vista GeoScience LLC. Used with permission.

In some cases, viewing the images of fluorescent light and visible (reflected) light or infrared images may help to identify materials causing false positive responses. The UV and tandem VIS (OIP-UV only) or infrared (OIP-G only) images may help identify objects with identifiable shapes or patterns in the subsurface, such as paper or seashells (**Figure 4-43**, **Figure 4-44**, and **Figure 4-45**). Caliche nodules in soils can develop and may have a characteristic shape and size that differs from fluid products. Targeted sampling at some locations may be needed to verify materials suspected of causing false positive responses.

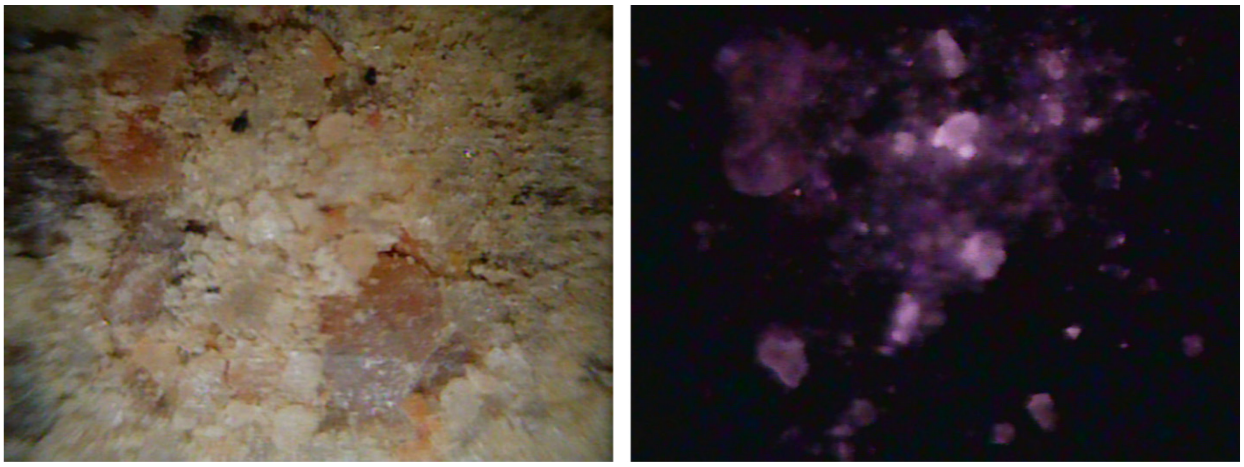


Figure 4-45. Side by side images of visible (white) light and UV light mineral fluorescence versions of the same soil image. Note how certain mineral grains of the items fluorescing can be seen in the visible light image.

Source: Vista GeoScience LLC. Used with permission.

Quality Control After Use

A response check is run before and after each log run, including the last run of the day. Quality control tasks after using the OIP include inspecting the tool window for damage and contamination, checking to ensure that the camera frame rate is not consistently low, checking consistency between response tests, and verifying that no contamination is present on the optical window or inside the optical cavity by checking the focus and clarity of the visual image test, and verifying a nondetect response on the black box test (Geoprobe 2019).

In addition, occasionally performing replicate log runs to verify repeatability and collecting targeted confirmation soil samples for analysis and comparison to the fluorescence response is part of the post-log quality control process. The frequency and number of confirmation samples collected for comparison can be part of the project objectives; for example, more samples may be required for a remediation design versus just a site characterization verification.

4.6.2.5 Tool and Data Misuse

The OIP provides photographic images of NAPL fluorescence in situ. These images can provide photographic verification of PAH fluorescence in the subsurface and some indication of the relationship between the fluorescent NAPL and the formation matrix and the NAPL distribution in the formation (for example, suspended droplets, blebs, ganglia, massive saturation in the pore space). The OIP is unable to detect NAPL that are significantly PAH-deficient (for example, chlorinated NAPL) and should not be used for this purpose.

Because various factors can affect OIP response, care should be taken to prevent overly simplistic interpretations when reviewing logs. The formation and any contained NAPL are disturbed and compressed when the probe is advanced into the formation. This disturbance and compression may lead to local increases in NAPL-saturated pore space at the sapphire window. Thus, the images (and resultant percent area of fluorescence log) may overestimate the amount of NAPL observed at any given depth. Conversely, soft clays may smear over the sapphire window and block the fluorescence of small amounts of NAPL. Confirmatory sampling can help to verify these misrepresentations if they occur.

4.6.3 What Are the Advantages?

The Geoprobe OIP system provides high-resolution, real-time vertical delineation of PAHs in soil, generating detailed subsurface data that supports dynamic work plan implementation and refinement of the CSM. By providing a detailed depiction of PAH distribution with depth, the OIP system supports site characterization and remedial planning by delineating impacted zones and informing decisions related to targeted sampling, monitoring well screen placement, and remediation design.

In addition to contaminant characterization, secondary downhole lighting integrated into the OIP system provides visual information to support interpretation of subsurface conditions. The OIP-UV and OIP-UVR configurations allow direct observation of soil texture and color, whereas the OIP-G configuration provides information on soil texture only. When combined with other direct-push sensors such as EC, HPT, and CPT, these observations contribute to improved characterization of geologic heterogeneity, sorption behavior, and contaminant transport pathways. Data logs can be securely transmitted using cloud-based, real-time data management systems to support collaborative visualization and decisionmaking, and when multiple borings are combined, the results can be interpreted in 2D and 3D formats. Compared to traditional sampling methods, the OIP system presents significantly less potential for worker exposure to impacted media and produces minimal to zero investigation-derived waste.

4.6.4 What Are the Limitations?

As with the other direct sensing tools, OIP systems are limited to static or percussion direct push in unconsolidated sediments and cannot be used in bedrock applications or sediments with large gravel or cobbles.

The ability of the OIP to detect various contaminants depends on a variety of physical and chemical factors. Interferences, such as mineral fluorescence, can cause false positive results. Confirmatory sampling and analysis are needed when using the OIP data to assist with interpretation of these potential interferences, as well as to compare soil sample concentrations to the fluorescence response results.

Whenever possible, a sample of the target NAPL should be obtained for pretesting on the particular OIP tool (-UV, -UVR, or -G) to ensure it is responding to the correct excitation wavelength and emission range of that OIP tool, and to compare to other interferences (for example, mineral fluorescence) in the soil matrix.

These technical limitations are discussed in the subsections below.

4.6.4.1 Detection Limits

OIP sensitivity depends on chemical characteristics, the soil type, and other factors. The OIP cannot detect disseminated or dissolved contaminants; it only detects NAPL phase. NAPL that is PAH -deficient may exhibit little to no fluorescence signature. The detection level for gasoline is higher than that for diesel, crude oil, or motor oil due to lower PAH concentrations in gasoline (McCall et al. 2018). Weathering and biodegradation of the product often result in lower levels of fluorescence and, therefore,

higher detection limits. With the OIP-UV system, products that are PAH-rich with heavier molecular weight compounds may also exhibit reduced fluorescence due to quenching.

LIF response tends to be stronger in coarser grained materials and weaker in fine-grained materials such as clay (Apitz et al. 1993) (Section 4.7). The OIP, as a fluorescent-based detection tool, is likely to be similarly affected by grain size. OIP fluorescence data do not provide an indication of product type (for example, gasoline versus diesel versus jet fuel); sampling and analysis are required to specifically identify the product present in the subsurface.

Pure chlorinated contaminants are invisible to the OIP because pure chlorinated DNAPL does not fluoresce under UV unless they are mixed with PAHs (such as degreasing wastes). Chlorinated DNAPL can be detected with DyeLIF™ (Section 4.7.2.3), and chlorinated VOC, including DNAPL, can be detected with the MIP (Section 4.5).

4.6.4.2 Interferences

Some natural and human-made materials fluoresce and can potentially result in false positive results. Probably the most common natural interferant is calcite, a mineral in limestone, seashells, and caliche soils. Although it is common, calcite fluoresces weakly under OIP-UV illumination. Many human-made materials (for example, paper and plastics) fluoresce, so investigations at landfills or similar facilities may need to assess those materials as potential false positives. Often, a review of the fluorescence distribution in the captured images can confirm if observed fluorescence is a false positive. Soil sampling is required to verify if false positive fluorescence is observed with the OIP system.

4.6.4.3 Confirmatory Sampling

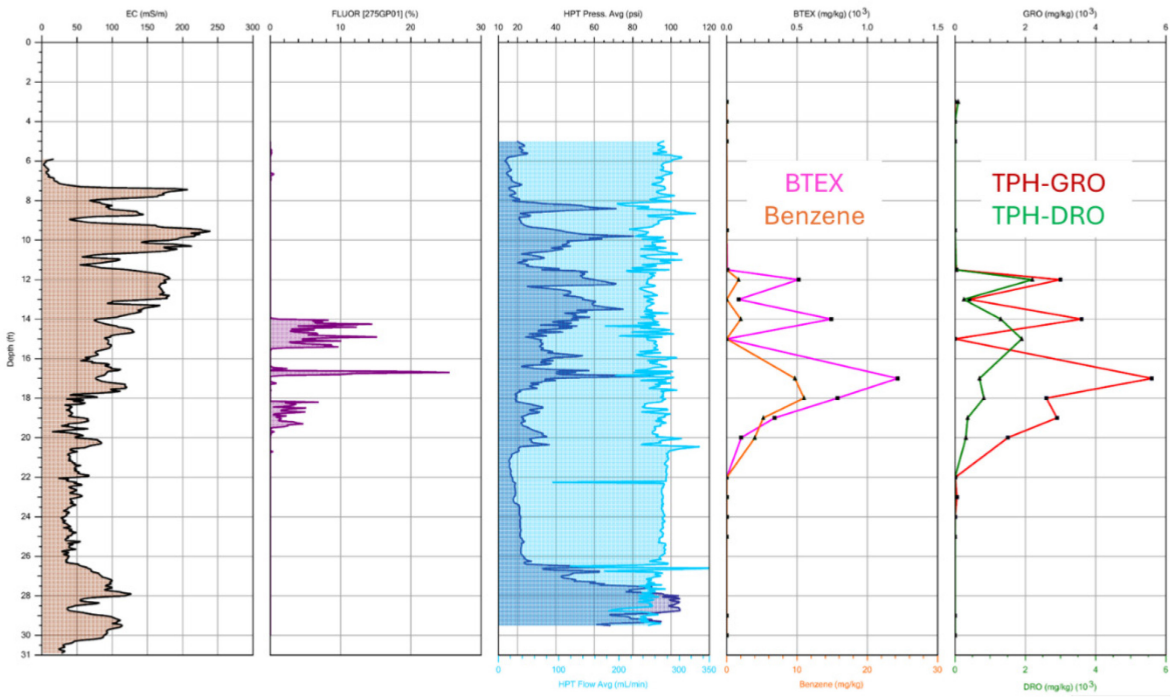


Figure 4-46. A confirmation core was collected in an offset boring to OIP-UV log. A total of 19 soil samples were collected at 1-ft intervals and were analyzed for VOC and TPH. Selected results are plotted at the same vertical scale on the log using the DI Viewer software.

Source: Vista GeoScience LLC. Used with permission.

Because the OIP is a screening-level (qualitative to semiquantitative) tool, confirmatory soil sampling and analysis is recommended. Using log data to target specific locations and depth intervals to collect confirmatory samples is recommended. Multiple samples should be collected from high, moderate, and low fluorescence intervals, as well as a few nondetect zones. Confirmation of OIP results using fixed-based sampling methods may be problematic because NAPL distribution tends to be in the form of diffuse ganglia or through preferential pathways in heterogeneous materials. In most cases, the goal is to determine whether the OIP results indicate the presence of product in the same area as samples collected and analyzed in a laboratory. A specific OIP sample cannot be used to determine site contamination; a larger picture of contamination based on multiple samples is the goal. Therefore, confirmatory samples should be collected to confirm the presence of NAPL generally and, perhaps, not to directly compare paired, collocated samples due to known uncertainties in their correlation. Quantitative correlation of OIP and other chemical log data to laboratory analysis of samples is often low due to several factors, including, but not limited to, the differences in analytical methods and qualitative nature of in situ tests compared to rigorous quantitative laboratory procedures. Furthermore, a core sample taken only 0.5 m from the log location may have a different NAPL distribution due to heterogeneity challenges discussed previously, as well as vertical coring sample distortion, depending on the sampling methods used. These issues can be improved by taking samples at a higher frequency interval as in the example in **Figure 4-46**.

4.7 Laser-Induced Fluorescence

4.7.1 What Is the Technology?

Laser-induced fluorescence (LIF) is a field-portable system that detects NAPL in the subsurface, including most refined fuels through heavy crude petroleum. LIF employs laser light to excite fluorescent molecules in NAPL, including jet fuel, kerosene, petroleum fuels and oils, coal tars, and creosotes. In addition, LIF detects fluorescent compounds added to nonfluorescent NAPLs. The system is deployed using either direct-push technology with hydraulic hammer or a CPT unit and provides qualitative to semiquantitative, real-time results. LIF does not typically respond to dissolved- or vapor-phase PAHs that result from the presence of NAPL. Fluorescence is logged as a response percentage of a reference emitter (%RE) calibration standard.

LIF works by using a laser to excite PAH electrons in the NAPL to a higher-energy state. The excited PAH electrons return to ground state, releasing photons with wavelengths longer than the excitation laser. The resulting fluorescence is recorded by a detector. PAHs are fundamental components of most fossil fuels and tar-like substances. They are multiple aromatic ring structures, with the simplest being naphthalene (two rings). Gasoline contains less PAH than diesel. Tar-like substances such as asphalt and creosote contain far greater weight percentages of both smaller and larger PAH molecules. Light is emitted by PAHs at specific wavelengths that are indicative of their size and degree of substitution. Smaller PAH molecules such as naphthalene emit shorter UV wavelengths; larger PAHs emit increasingly longer wavelengths that extend out into the red and even infrared spectrum.

Under optimal conditions, the intensity of fluorescence is proportional to the quantity of the NAPL present. In addition, different PAHs continue to emit fluorescence after excitation more or less quickly (differing lifetimes). Some NAPLs fluoresce for a short time [1 nanosecond (ns) to 2 ns] following excitation (for example, coal tar), whereas other NAPLs (for example, diesel) fluoresce for longer (50 ns to 100 ns) following excitation (St. Germain 2024 - 8.6.3).

When LNAPL and DNAPL are present in the subsurface environment, it can be difficult to delineate their occurrence by collecting soil samples, especially in heterogeneous geology. To gain a comprehensive understanding of the subsurface contaminant distribution, many soil samples need to be collected and analyzed at great cost. Modified forms of LIF have been successful at detecting chlorinated compounds

(which are often DNAPL) as described above, and, in some cases, chlorinated DNAPL contains sufficient fluorophores (fluorescent chemical compounds of interest) to allow LIF detection without modification.

When used in conjunction with direct-push delivery, LIF can rapidly obtain high-density diagnostic data over a wide area and to sufficient subsurface depth to provide a cost-effective delineation of NAPL phase "body." The large amounts of information gathered can be displayed on a borehole-by-borehole basis or site-wide using 3D visualization software (**Figure 4-47**). Multiple LIF logs from NAPL release sites provide a basis for a detailed CSM (St. Germain 2011). In the case of some refined fuels, LIF can help the investigator discriminate between weathered and nonweathered LNAPL based on the fluorescence's spectral (color) and lifetime properties (St. Germain 2024). Stakeholders are encouraged to seek guidance from the LIF vendor and consider results of any validation sampling or benchtop testing when determining a proper NAPL threshold for the site. Downhole geophysical tools such as CPT, EC, or HPT are popular add-ons to LIF and give investigators insights into how site geology is controlling the NAPL distribution and pathways.

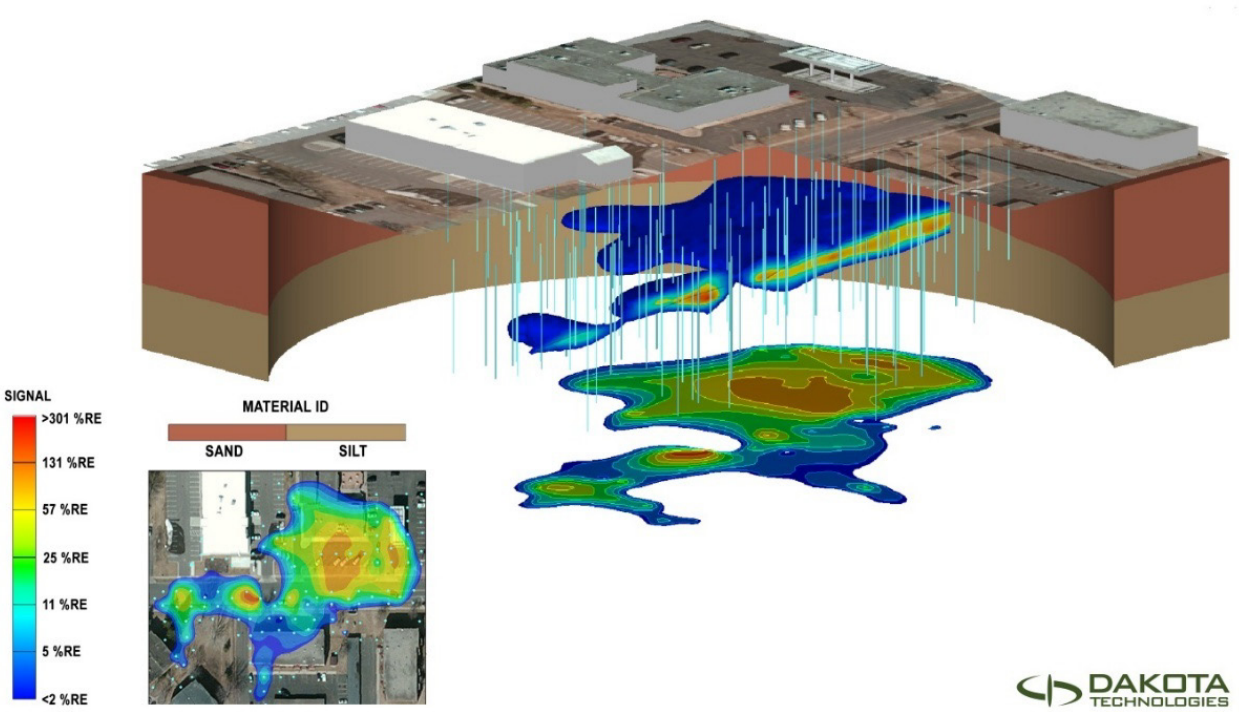


Figure 4-47. CSM with LIF logs plotted in 3D (colors are relative %RE with red being highest).

Source: Dakota Technologies, Inc. Used with permission.

LIF system consists of several components: a direct-push (either percussion or static) system with attached sapphire-windowed probe, a pulsed laser, a wavelength selection module, a photomultiplier tube, an oscilloscope, and a computer to control the components and record the data (Aldstadt 2002). The probe containing the sapphire window is pushed or hammered into the ground at a rate of about 2 cm/sec (ASTM 2010), with a measurement obtained approximately every 0.05 ft. A fiber-optic cable transmits the pulsed laser light downhole to the window where the light exits the probe and illuminates the adjacent soils and sediments and NAPL, if present (**Figure 4-48**). The laser excites aromatic compounds in the NAPL, which emit photons (fluorescence). A portion of the soil-scattered laser excitation along with a portion of detected fluorescence are returned to the surface through a second fiber-optic line, and results are displayed in real time.

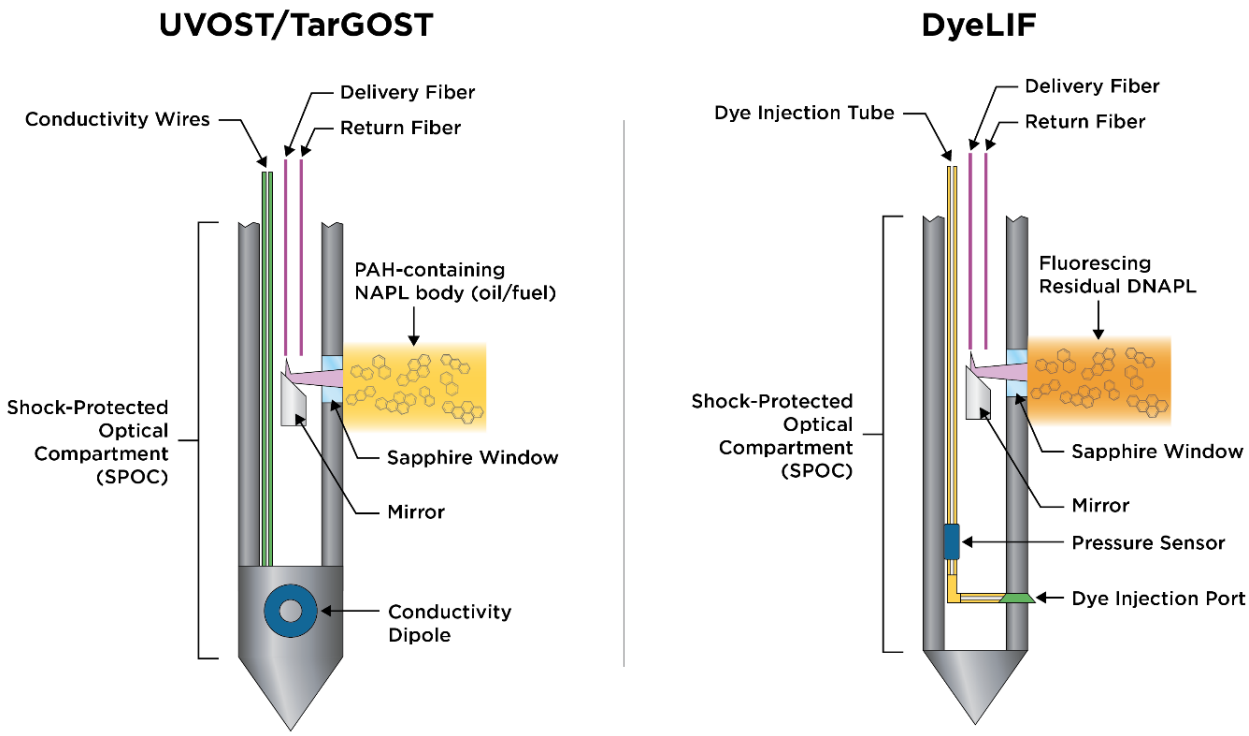


Figure 4-48. LIF tool and associated sensor (EC).

Source: Modified by Geosyntec Consultants, Inc., from Dakota Technologies, Inc. Used with permission.

LIF's versatility originates from its use of *pulsed* laser light as the excitation source. The laser light's narrow excitation range and high power produce very low detection limits, while the pulsed nature of the light provides LIF the ability to measure fluorescence decay times. This ability to simultaneously detect the intensity, color, and lifetime of the fluorescence outside the probe provides LIF with the capability to identify target fluorophores while simultaneously identifying nontarget fluorophores (for example, false positives such as peat or minerals). Careful selection of excitation lasers also optimizes its ability to respond to certain target chemistries while ignoring others.

Optimizing detection capabilities for the unique chemistry of one class of NAPL means other NAPLs cannot be properly detected with the same LIF system. LIF technology developers have crafted a family of LIF systems that strikes a balance between optimized detection of some important classes of NAPL and the ability to detect other NAPL classes. Although a universally responsive tool is technically feasible, its high cost and complexity is currently beyond industry's ability to pay for its implementation. The three currently available LIF systems strike a balance between specialization and broad applicability. **Figure 4-49** illustrates how these LIF systems relate to each other and the various NAPL types commonly encountered in the subsurface.

This LIF tool description is divided into three parts according to three major NAPL classes and LIF systems that were designed to detect them. The section headings mirror the elements described in **Figure 4-49**.

The UVOST and Rapid Optical Screening Tool (ROST)® LIF systems are nearly identical UV-laser-based systems optimized to detect most petroleum products, oils, and lubricants. They detect LNAPL common to most releases at gas stations, refineries, pipelines, and bulk-handling facilities.

TarGOST® is a visible-wavelength laser system that was designed to detect heavier hydrocarbons. These heavy NAPLs are commonly DNAPL due to their higher density, and include coal tars, creosote, tank bottoms, bunker (marine) fuel, and chlorinated solvents that were used for degreasing (used for cleaning items contaminated with hydrocarbons).

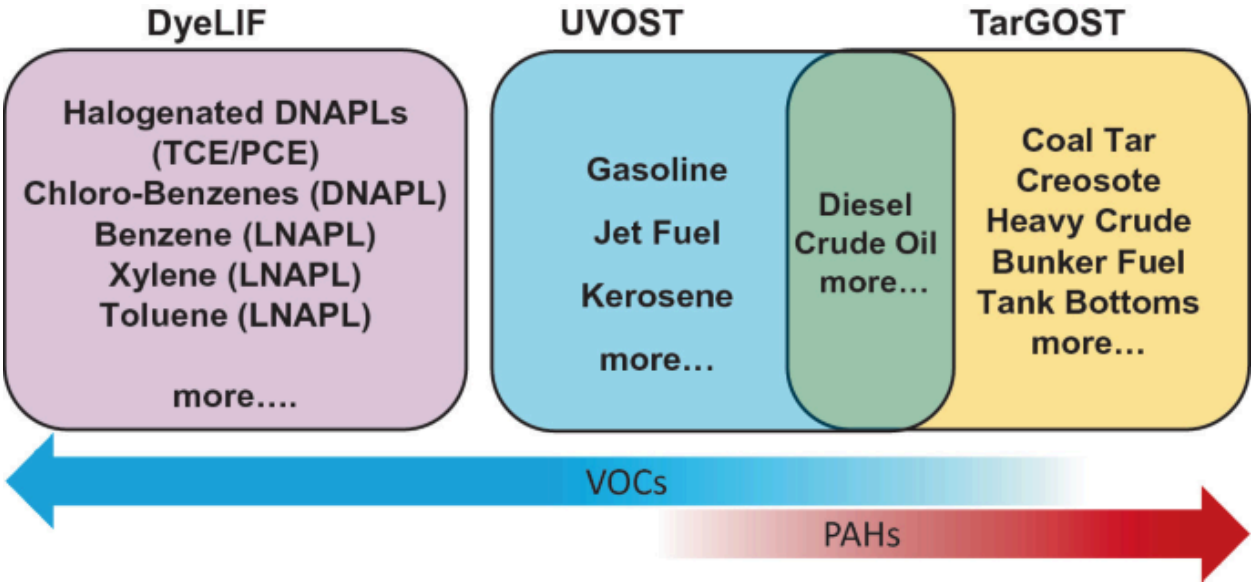


Figure 4-49. The three LIF systems and their associated NAPL types.

Source: St. Germain (2024), Figure 8.8. Used with permissions.

DyeLIF™ is a dye-enhanced laser-induced fluorescence system designed for chlorinated solvents and similar compounds that do not naturally fluoresce. DyeLIF is similar to TarGOST but involves the injection of a fluorescent marker dye that renders the NAPL fluorescent prior to the arrival of the LIF probe.

UVOST and ROST were the first time-resolved LIF systems to be commercialized and are closely associated with the generic label "LIF." The description in Section 4.7.2.1 uses this class of LIF to discuss the general hardware and tool functions shared by all LIF systems. The subsequent sections describing TarGOST and DyeLIF systems focus on the unique attributes of those systems, challenges typically encountered when characterizing their unique classes of target NAPL, and best practices for success in deployment.

4.7.2 How Is the Technology Used?

4.7.2.1 UVOST

As discussed in the tool description, a portion of the LIF is returned to the surface through a second fiber-optic line, and results are displayed in real time. The scattered laser light used for UVOST is filtered out from the fluorescence return fiber, after which the light is split into four wavelength channels, each of which responds to different size distributions of PAHs. Using different lengths of fiber optics, these four channels are delayed in time before being directed to the photomultiplier tube detector for conversion from light intensity to electric current. The current from the photomultiplier tube is sent to a digital oscilloscope that measures the intensity and the decay rate of the four wavelength channels to generate what is called a waveform (St. Germain 2024). The waveforms are analyzed and displayed graphically versus depth in real time with signal strength; waveforms are normalized to the %RE waveform (Aldstadt 2002). Increasing NAPL in the soil pores results in increasing fluorescence, causing increases in the size

of the waveform. Figure 4-50 presents an example of a UVOST log. The shape of each collected waveform is representative of both the color and lifetime of the fluorescence, which provides insight into the fuel type (Figure 4-51). Differing NAPL types in the log can be recognized by their waveforms in Figure 4-50. Labeled a-d, they are: a (Callout 1) consisting of fluorescence of weathered gasoline, a (Callout 2) is intact gasoline, b is caused not by fuel but by clay (false positive), c is diesel, and d is kerosene (jet fuel).

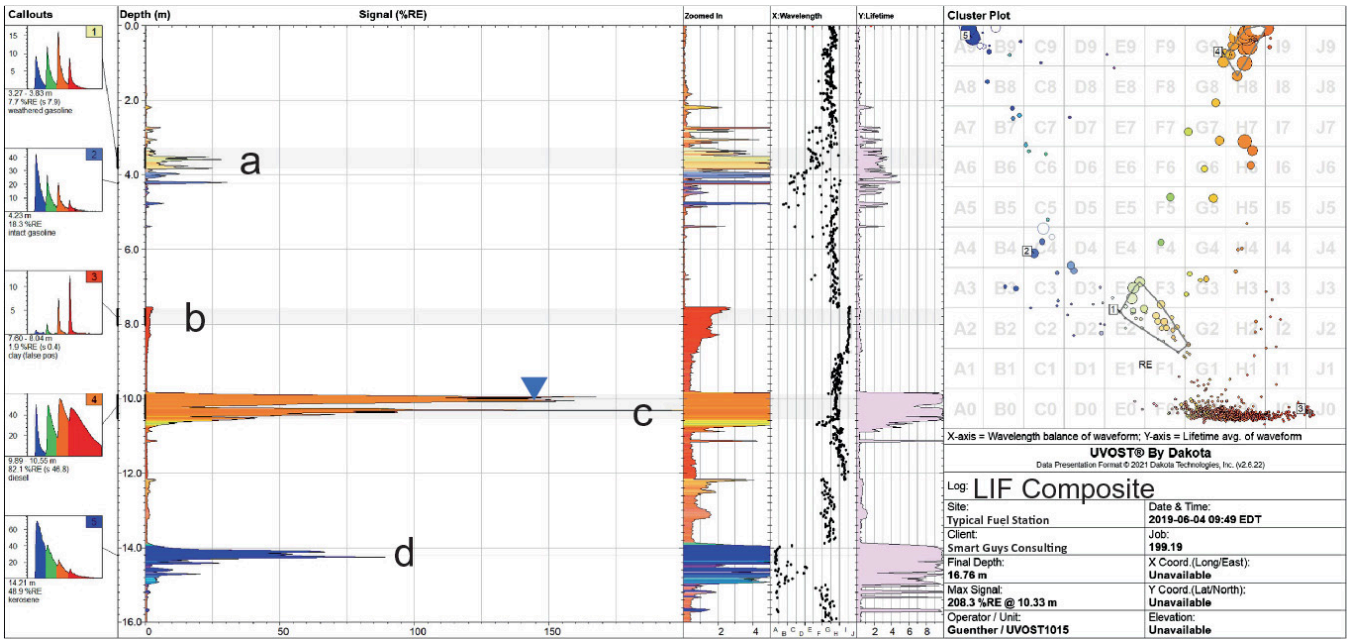


Figure 4-50. Composite UVOST log containing typical responses for gasoline, diesel, false positive soils, and kerosene.

Source: St. Germain (2024), Figure 8.25. Used with permission.

In general, the intensity of the total fluorescence response is expected to increase with increasing NAPL pore saturation. In benchtop tests (where the soil and NAPL are held constant), the behavior between NAPL content and %RE is typically linear across three to four orders of magnitude depending on the NAPL and %RE is typically linear (monotonic) across three to four orders of magnitude depending on the NAPL and soil types (Coleman 2006; St. Germain and Martin 2008). Such monotonic performance through several orders of magnitude is typical across all LIF systems, until the NAPLs become too rich in PAHs and internal quenching mechanisms begin to dominate. At that point the response begins to weaken; plateaus across all concentrations; and, in many cases, decreases with increasing NAPL concentration. A monotonic relationship between fluorescence intensity and NAPL pore saturation is assumed but is not guaranteed due to a host of other factors that can enhance or quench this ideal behavior. It is, therefore, important to fully understand the numerous factors affecting the fluorescence response prior to interpreting LIF logs. Figure 4-52 illustrates the monotonic (linear) response of the same data shown on Figure 4-51.

LIF logs accurately represent the conditions, but it is important to realize that the fluorescence emanates from the very surface of the soil immediately against the window in fine sediments, and perhaps as deep as several mm into clean sands with relatively few fines. This c high fidelity for sensing even small globules or seams of NAPL (often chaotically distributed in the formation), combined with a very limited reach out into the formation, is a recipe for poor correlation between dual LIF logs or confirmation sampling adjacent to the LIF log.

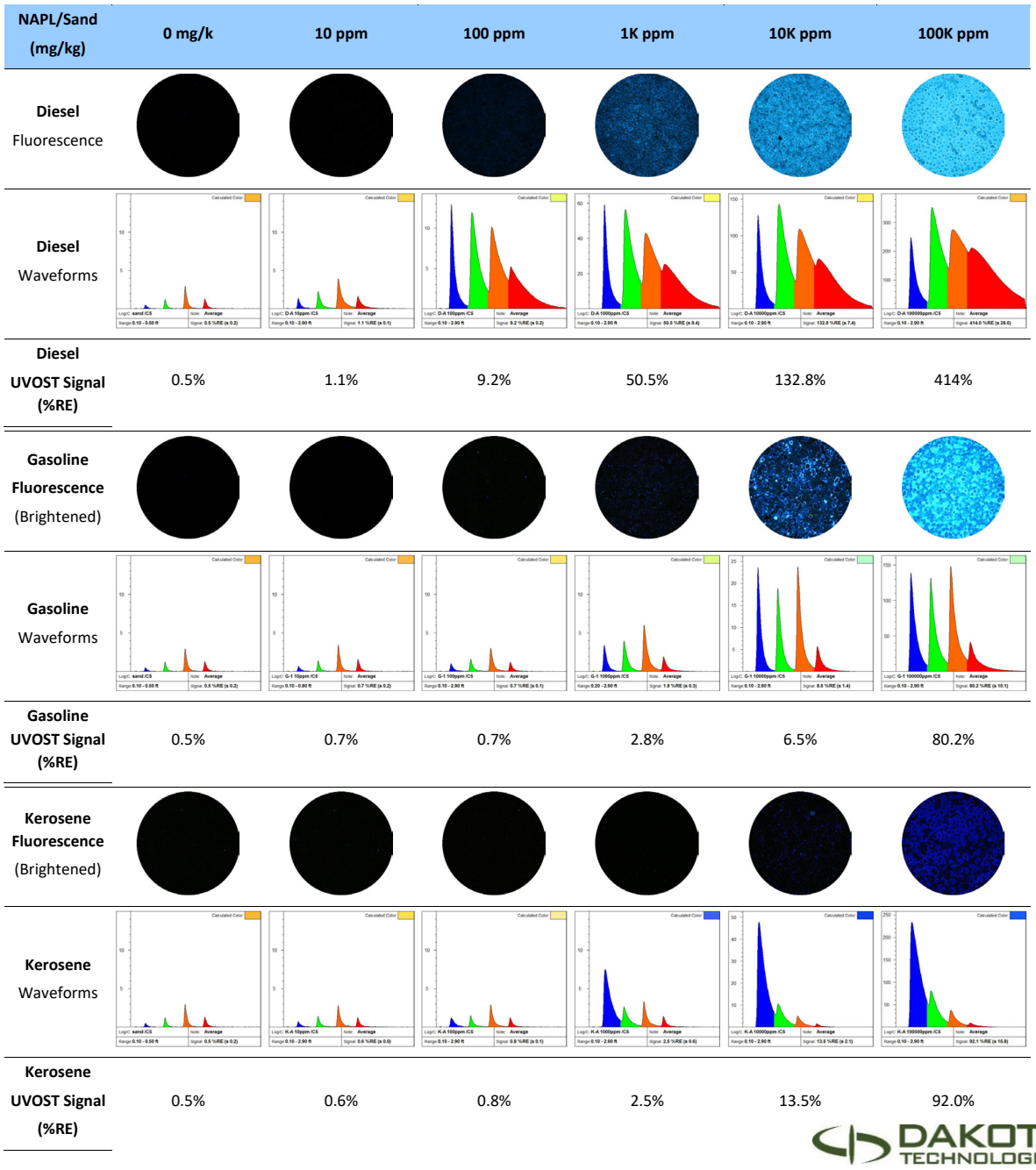


Figure 4-51. Fluorescence photos (308-nm laser) with UVOST waveforms for common NAPLs in 20–40 mesh silica and quartz sand at 10% moisture.

Source: Dakota Technologies, Inc. Used with permission.

Since LIF's introduction in the mid-1990s, this propensity for generating seemingly inconsistent results between two different methods (for example, LIF versus coring) or between repeats of LIF at the same location has created endless opportunities for debate of whether LIF results can be "trusted." Human psychology dictates that the method that produced soil in hand (soil cores) is the "right" result, so LIF is often accused of having "missed it," responded to NAPL that was not there, or otherwise gotten things wrong. Readers are encouraged to review (Randy St. Germain 2024, 2025) to familiarize themselves with

the challenges that await anyone hoping to confidently validate readings produced by insitu sensors of nearly any HRSC method, not just LIF.

Careful confirmation methodology, including placement splits of collected soil samples back onto the LIF sensor for confirmation, is key to managing the chaos almost inevitably introduced by NAPL's inherent spatial heterogeneity. The Collocated Soil Borings (Week 2) section on page 38 of Einarson et al. (2018) is an excellent resource for anyone planning on confirming LIF sensor results prior to trusting its results to guide them on risk or remedy design. Trust, but verify is strongly advised for anyone using HRSC to develop their CSM, including LIF.

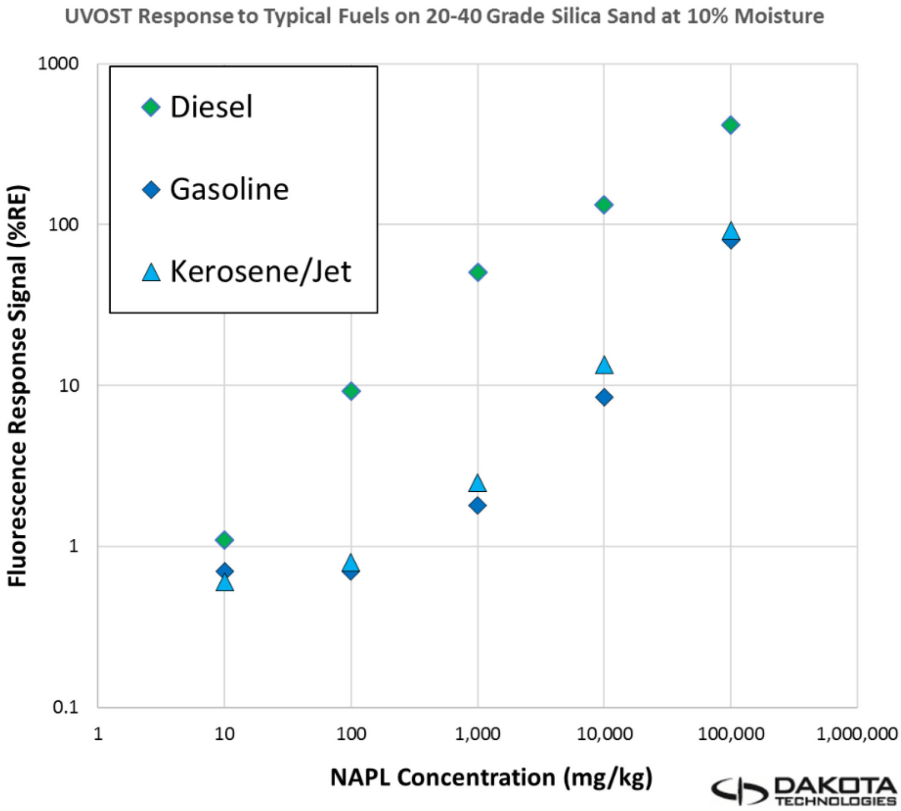


Figure 4-52. UVOST response (%RE) of common fuels across a wide range of NAPL concentrations.

Source: Dakota Technologies, Inc. Used with permission.

4.7.2.2 TarGOST

Field trials of existing UV excitation LIF tools were found to consistently under-report the NAPL content (logs show very low fluorescence in NAPL-saturated soil) when applied to "heavy NAPL" such as coal tars, creosotes, and bunker fuels. Most of this poor responsivity is due to energy transfer of smaller excited-state PAHs to larger PAHs after the laser pulse is absorbed. Dakota Technologies, Inc., developed the TarGOST(St. Germain 2024) to overcome these confounding behaviors. The first successful field trials of TarGOST delineating coal tar at manufactured gas plants are documented by (Coleman 2006).

Shifting the excitation laser to longer wavelength (weaker energy) light targets the larger PAH molecules directly, since 2- and 3-ring PAHs do not absorb this longer wavelength light. In addition, TarGOST shifts to detecting the longer wavelength fluorescence emitted by very large PAH molecules, which eliminates some, but not all, of the quenching. Even with this optimization, multiple-wavelength waveforms (and their associated lifetime decay) remain a crucial component in differentiating between target NAPL

fluorescence and false positive fluorescence of peat, meadow mat, wood, calcites, and the like. The TarGOST system has been used at hundreds of coal tar, creosote, and heavy fuel projects to date. An example TarGOST log is presented as **Figure 4-53**.

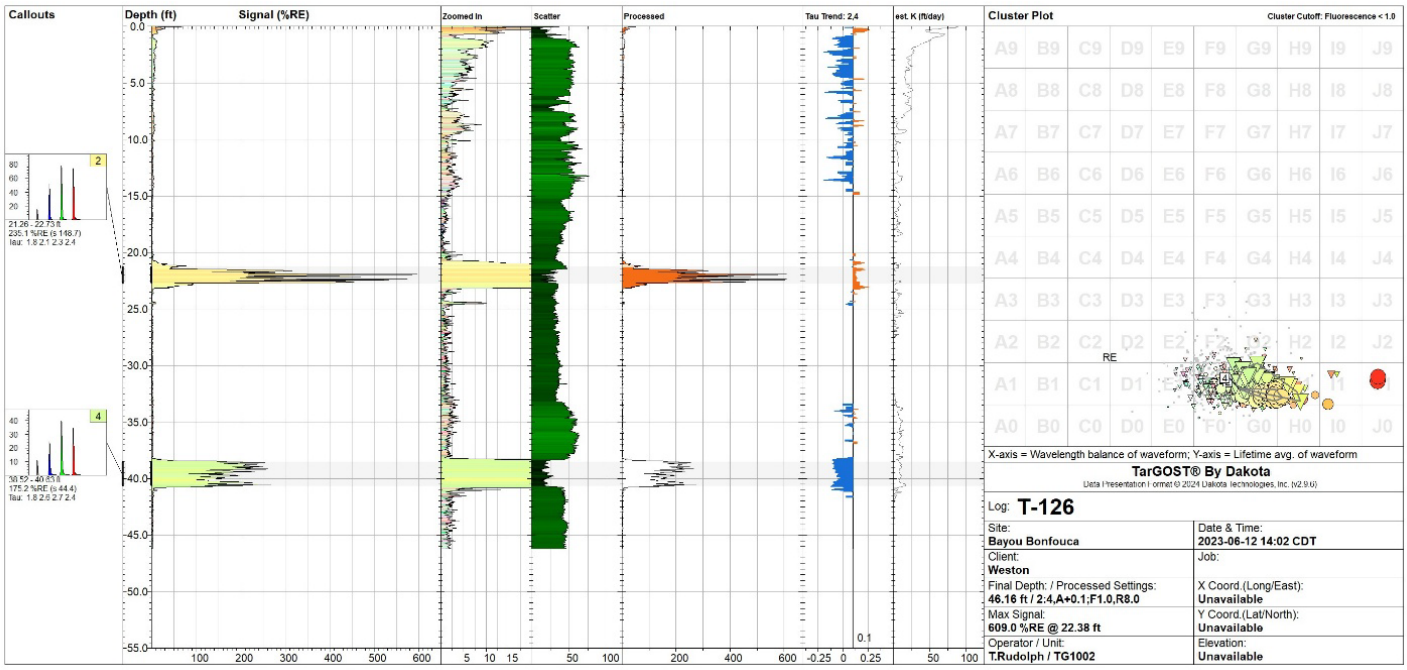


Figure 4-53. Example TarGOST log, with callout 2 (creosote NAPL lens), and callout 4 (natural organics), whose fluorescence is indiscernible with the exception of the tau trend behavior.

Source: Dakota Technologies, Inc. Used with permission.

The presence of false positives that have rivaling or even brighter intensities as the target NAPLs, but have matching color and average lifetimes, often complicates interpretation of fluorescence logging at heavy NAPL sites. At many sites, this would make concise interpretation practically impossible without extensive confirmation sampling.

But a relatively recent discovery (St. Germain 2025) is that molecularly heavy NAPLs such as coal tars, creosotes, and crude oils exhibit increasing lifetimes with increasing wavelength (they show a positive lifetime trend in subsequent waveform channels from left to right). This innate property of heavy NAPLs (but not exhibited by false positives or LNAPLs) has revolutionized the vendor's and stakeholder's ability to recognize, and subsequently isolate, NAPL fluorescence from highly problematic false positive fluorescence at virtually all sites.

The advantages of the TarGOST system over UVOST LIF for heavy NAPL include:

- a robust response to most coal tars and creosotes
- excellent linearity of response for coal tars and creosotes (**Figure 4-54**) across many orders of magnitude
- no possibility of response to dissolved-phase PAHs since the TarGOST laser is incapable of exciting water-soluble PAH.

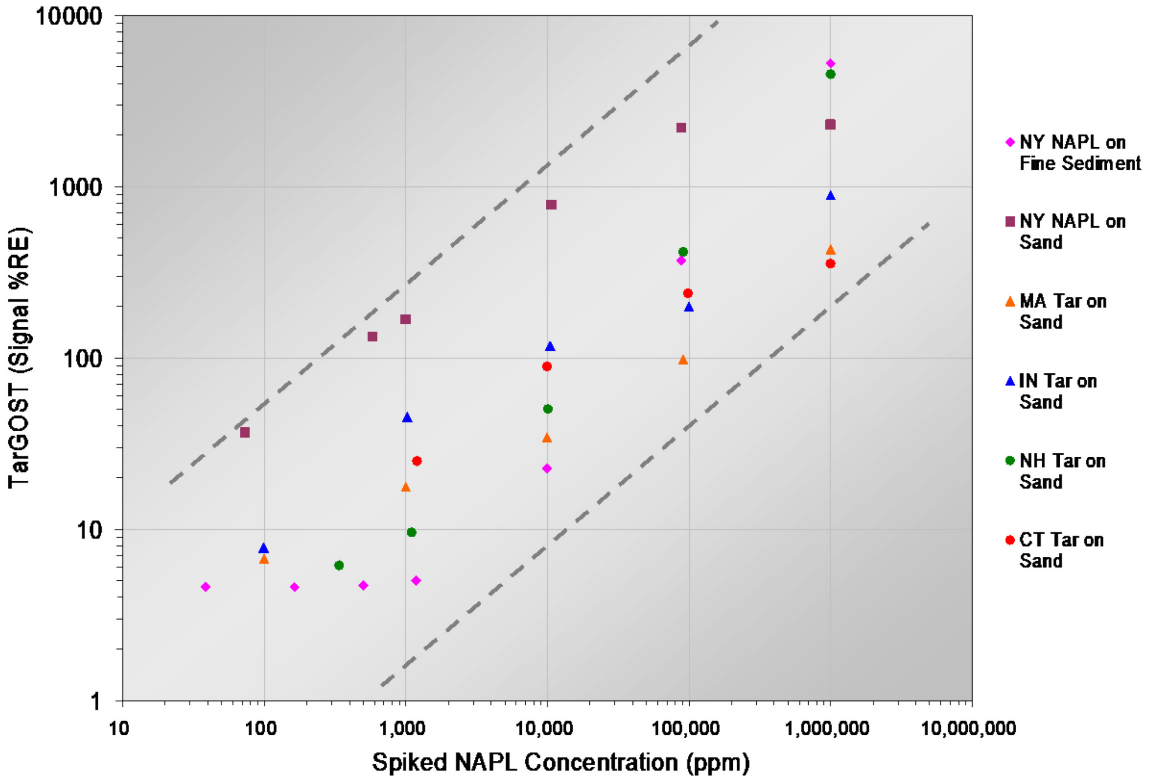


Figure 4-54. Example TarGOST responses versus heavy NAPL content (mg/kg).

Source: Dakota Technologies, Inc. Used with permission.

The following facts are important to keep in mind when characterizing heavy NAPL with a system such as TarGOST:

- Coal tars, creosotes, bunkers, and other DNAPLs distribute themselves in highly heterogeneous fashion.
- NAPL denser than water is typically found to have traveled much deeper than LNAPL.
- Wood treatment sites and manufactured gas plants are typically located along waterways, so the likelihood of encountering highly problematic false positive fluorophores such as wood, calcareous sands, shell hash, peat, meadow mat, and associated wetland debris is very high.
- A typical range of the detection limit for most mixed-component DNAPL (for example, coal tars and creosotes) is 100 mg to 1,000 mg NAPL per kg soil. This limit of detection is close to human observation.

The following actions are recommended when implementing the TarGOST system:

- Contact the TarGOST vendor to arrange for benchtop testing of representative NAPLs from the site.
- Do not apply too high of a %RE threshold to the site. While the long-term average threshold indicative of tar and creosote has ranged from 7% RE to 50% RE, each site is unique and requires site-specific interpretation.
- Budget for limited targeted validation sampling in conjunction with the NAPL threshold determination.
- Average the %RE over a selected depth range rather than choosing narrow peak TarGOST values spanning just one or two readings.

4.7.2.3 DyeLIF

The DyeLIF tool is a specialized form of LIF that was developed to improve the detectability and reliability of LIF for chlorinated NAPLs (Randy St. Germain 2025; Randy St. Germain et al. 2014; Einarson et al. 2018). The DyeLIF tool injects a small amount (<1 g per 50-ft log) of a noncarcinogenic and relatively nontoxic proprietary fluorescent dye into the formation several centimeters ahead of the LIF sensor. The dye mixes with and elicits a response from the nonfluorescing NAPL, as described in more detail below. In addition, dye injection pressure and flow are monitored to produce estimated hydraulic conductivity values, similar to the HPT (Section 4.4.1.1).

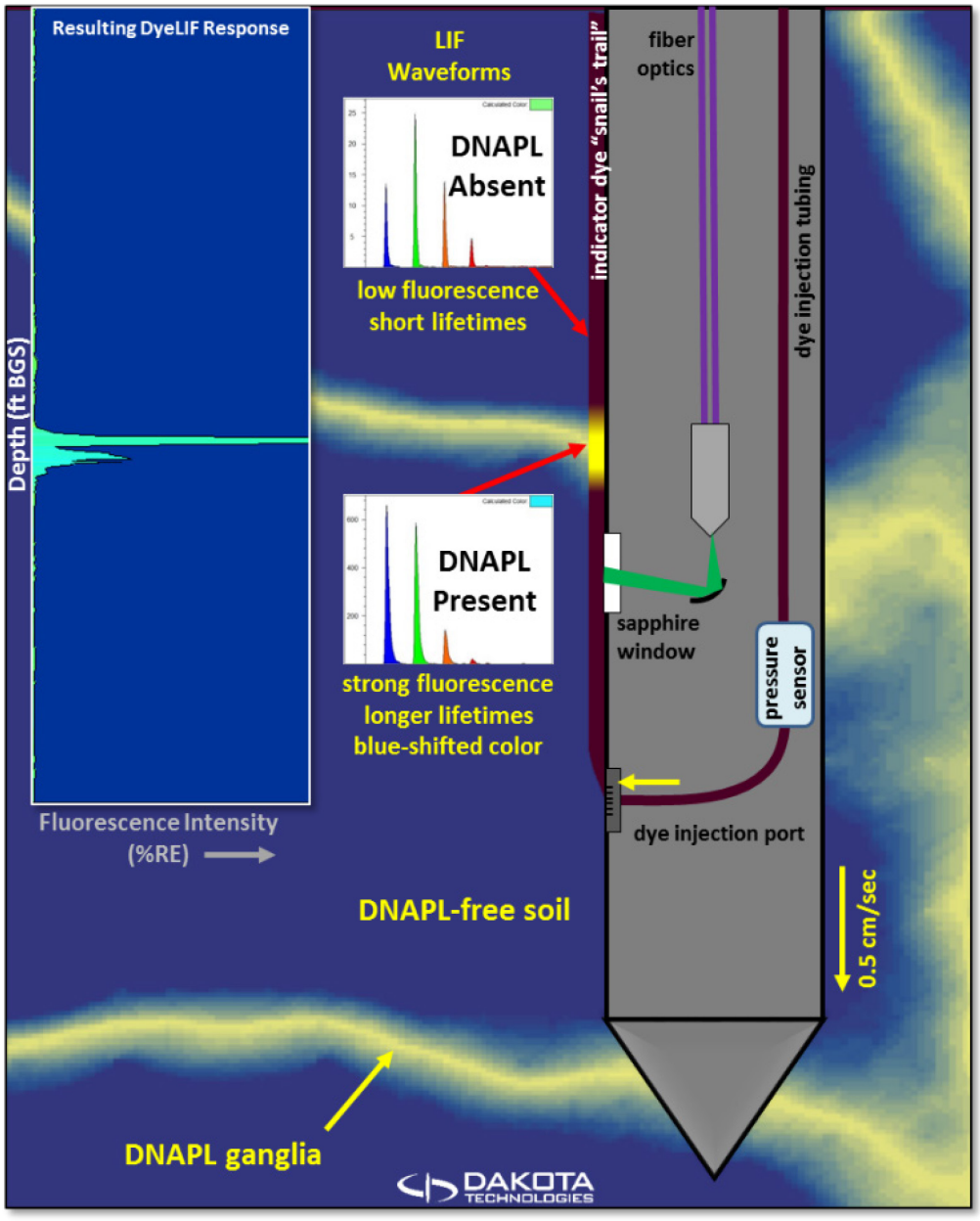


Figure 4-55. Conceptual diagram showing a DyeLIF probe passing through a DNAPL-impacted soil formation.

Source: Dakota Technologies, Inc. Used with permission.

As previously described, NAPL fluorescence depends on conditions such as PAH content, solvent-body conditions, and fluorescence excitation and emission energies. The molecular structures of chlorinated DNAPLs such as PCE and TCE lack aromaticity and therefore do not fluoresce. However, chlorinated NAPLs can contain remnant PAHs from manufacturing processes (for example, picked up while cleaning or degreasing), and naturally occurring fluorophores solvated after release can fluoresce sufficiently to allow for detection (M. L. Kram et al. 2004). Unfortunately, false negatives remain likely; therefore, UVOST and TarGOST should not be used for chlorinated NAPL detection without first establishing that the site-specific NAPL fluoresces sufficiently by bench testing of site DNAPL, if available.

Figure 4-55 illustrates the concept of injecting dye below the LIF sensor to render NAPL fluorescent for subsequent detection. Rather than changing from a black to red color such as Oil Red O or Sudan IV dye shake tests (Cohen et al. 1992), the DyeLIF dye fluoresces orders of magnitude more intensely when it contacts NAPL. It also changes color and the fluorescence lifetimes increase, all of which are recorded in the DyeLIF waveforms. The dye currently used in the DyeLIF tool fluoresces more intensely and is more universally effective than the original dye, which was robustly responsive to TCE and PCE but lacked sufficient response to reliably detect some other classes of DNAPL. The current dye performs well with monoaromatics such as benzene and toluene as well as chlorobenzenes, dichloroethane, trichloroethane, TCE, PCE, and chloroform. DyeLIF is expected to respond to nearly all halogenated solvents, but conducting site-specific NAPL bench testing is always advised. Nitrobenzenes are a notable exception, having been found to quench both versions of DyeLIF indicator dye fluorescence significantly.

Figure 4-56 shows a typical DyeLIF field log. The darker blue responses indicate fluorescence due to TCE at the site. The results of a non-negative least squares (NNLS) analysis of the fluorescence waveforms, plotted in coral red, indicate those responses with very high confidence for being the target TCE NAPL fluorescence (the calcareous sea sand false positives and indicator dye are removed via NNLS analysis.

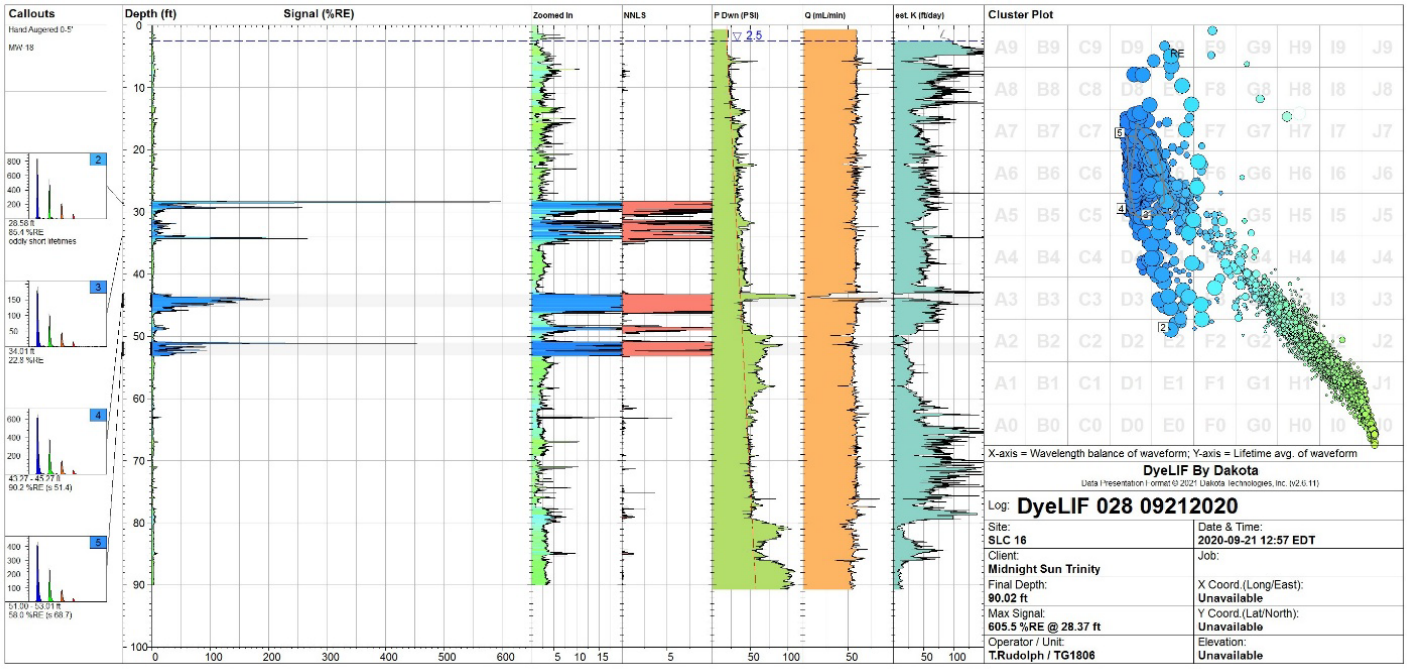


Figure 4-56. Example DyeLIF log.

Source: Dakota Technologies, Inc. Used with permission.

The following actions are recommended when implementing the DyeLIF system:

- Because investigating chlorinated NAPLs is generally more challenging than LNAPLs, time should be invested in discussing the applicability of the DyeLIF tool to the site with the vendor prior to initiating work.
- It is important to note that DyeLIF is unresponsive to dissolved-, vapor-, or adsorbed-phase chlorinated solvent contamination, making it truly NAPL-specific in its behavior.
- This tool, like TarGOST, is relatively unresponsive to light molecular weight NAPLs such as kerosene and gasoline.
- DyeLIF responds well to diesel and heavier fuels, which can interfere when specifically targeting chlorinated solvent NAPLs.
- DyeLIF responds monotonically to chlorinated NAPL saturation when the soil grain size is fixed. Finer soil particles dampen the response while coarser grained soils enhance the response.

4.7.2.4 Proper LIF Selection

Selecting the proper LIF tool to target specific NAPL is essential. Some LIF systems are blind to certain NAPLs, many of which carry higher risk than the target NAPL. For example, UVOST is designed to characterize light-fuel LNAPL and is unresponsive to many coal tars, which are DNAPLs with potentially hundreds of times more toxicity and recalcitrance than diesel. The TarGOST system, on the other hand, is designed for coal tar delineation but fails to detect gasoline. Selecting the inappropriate LIF tool may result in overlooking contaminants and wasting money, effort, and remediation efficacy. Before selecting a LIF system for a project, we recommend contacting the developers of LIF systems. They can answer questions, provide guidance in selecting the appropriate system, and provide complimentary testing services for target NAPL(s) or advise whether LIF is generally appropriate for a site.

4.7.2.5 Data Collection Design

General information about ASCT data collection and design is provided in Section 4.1.2. Additional considerations for LIF include NAPL type (for example, gasoline, diesel, kerosene, jet fuel, crude oil) and the age of the release.

4.7.2.6 Quality Control

Quality control standards must be established and followed to ensure reliable data. In addition to comprehensive operator training (which may be verified prior to commencing work) and an operator track record of successful use, approved field procedures must be understood and followed before, during, and after LIF activities.

Quality Control Prior to Use

During project planning stages, site conditions and the project objectives should be evaluated to determine whether LIF is the appropriate tool. If desired, NAPL and soil samples can be collected and tested to assess NAPL response and the potential for false positives and background interference. It should be noted that benchtop NAPL analysis can also be performed after fieldwork, but this delay eliminates the possibility of factoring these responses into real-time interpretation of the logs.

Prior to beginning work, discuss with the operator how hard they should push when advancing becomes difficult so that the likelihood of breaking equipment or getting the equipment stuck is reduced. Prior to advancing LIF tools and systems, the equipment operator should complete the following:

- Test the equipment and verify it is in good working order.
- Ensure proper setup and alignment of the shock-protected optical compartment and evaluate and mitigate fogging, if necessary.
- Record and evaluate the %RE.
- Record and evaluate the system background response (nothing on the sapphire window). Foreign materials inside the probe can fluoresce, masking the response occurring from outside the window in the formation. Background should never exceed 1% RE, with <0.5% preferred, if possible. This makes small responses outside the window easier to detect and interpret.

Acquire baseline soil response from, for example, carbonate-rich soils to understand whether small contaminant responses may be masked. This is usually in an area of the site where no previous impacts have been reported. If such an area has not been identified, the background response usually can be determined during LIF advancement from intervals that do not appear impacted.

If product sample(s) are available, apply the NAPL to sapphire window to log on-site response in benchtop fashion. Low-viscosity NAPLs such as gasoline need to be applied to a small volume of moist sand piled onto the probe window to prevent thin-sheeting and evaporation that may produce artificially low fluorescent responses.

Quality Control During Use

During fieldwork, the equipment operator must repeat the following quality control measures prior to every log:

- Verify the shock-protected optical compartment is in good working order and there is no fogging.
- Record the %RE to calibrate the tool for that log.
- Record the system background response (clean window). Again, background should never exceed 1% RE, with <0.5% preferred, if possible.
- Evaluate the waveforms and other concurrent outputs throughout the LIF advancement to identify potential non-NAPL materials, potential background interference, or evidence that a previously unidentified form of NAPL exists at the site.
- Monitor the advancement (push) rate, typically about 2 cm/sec, for deviations to account for associated response variations. The rate should not exceed that specified for the method. Although advancement rates slower than the standard rate produce higher data densities with minimal risk to data quality, these slower rates negatively impact daily production.

Quality Control After Use

Following each LIF push, the operator should inspect the sapphire window for fogging, chips, cracks, or other issues.

Soil samples may be collected (or existing samples used) to confirm potential non-NAPL or unidentified NAPL signatures and to understand lithology that may affect response (for example, porosity effects from clayey versus sandy material) and natural soil fluorescence interference, as described in Section 4.7.4.4. These results are incorporated into the final report from the LIF operator.

Targeted follow-up soil sampling (when data suggest the need) is exceedingly useful. However, sample results may not always correlate well with LIF results due to localized heterogeneity, which is the rule, not the exception. Multiple lines of evidence are necessary, including lithology, other soil and groundwater

samples, visual observations, and field testing. To achieve this goal, the LIF operator should place recovered materials onto the LIF system, either on-site or by sending samples to the vendor post investigation.

After completing the investigation, it is critical that an individual with LIF data interpretation experience (for example, technology developer) assists in reviewing the LIF data in a site-wide context. The LIF waveforms contain a wealth of information that can provide insights into fuel types, weathering, false positives, and unknown NAPL existence and can be the key to differentiating NAPL from mineral fluorescence. If no individual on the project team has the experience necessary, do not hesitate to contact the LIF technology developer for assistance.

4.7.2.7 Tool and Data Misuse

Like results from similar investigation methods, LIF results should not be interpreted without understanding the overall CSM and, if available, multiple other lines of evidence. Because of the potential for interferences and sequestered NAPL (in fine-grained materials), results must be maintained in the context of available information and investigation requirements. For example, monotonic behavior between fluorescence intensity and NAPL pore saturation may be assumed but is not guaranteed. In addition, applying an inappropriate fluorescence method may result in lack of NAPL detection.

Possible misinterpretations of LIF data may result during data transformation or interpolation. Statistical methods may incorrectly represent datasets if the data condition is not well understood or the wrong method is used.

The following actions reduce common misinterpretations during LIF implementation and data evaluation:

Premobilization

- Have the LIF vendor perform testing on NAPL samples to ascertain that the site NAPL has an appropriately bright fluorescence response and to select the most suitable LIF technology (typically most intense and most unique waveform possible).
- Make certain that the vendor understands what other NAPLs or false positives might also be present, even though they are not the target NAPL.
- Budget for and prepare to screen cores for NAPL from a limited number of locations.
- Plan to conduct validation sampling based on the LIF results in real time—usually only if and when new or unusual LIF responses are encountered. The information gained allows for confident data interpretation in real time as the investigation proceeds, thus enabling adaptive site characterization—one of HRSC's greatest strengths.

Field Operations

- It is critical that any false positives are identified by comparing other lines of evidence (coring, drillings logs, NAPL in wells, etc.) to waveforms, clustering diagrams, and log fill color in the logs. This prevents expending time and money chasing false positives that are not target NAPL.
- Remember that different NAPLs have inherently different fluorescence intensities (for example, applying diesel intensity values to gasoline LIF causes an underestimation of gasoline NAPL impacts. It is easy to get so used to seeing bright diesel fluorescence (300–400 %RE) in the log that it may be tempting to ignore or downplay gasoline fluorescence of only 2–3%, even though 2–3% RE represents highly actionable levels of gasoline NAPL.

- Do not apply too high of a %RE threshold to gasoline sites (using 5%, 10%, or 20% RE as indicative of NAPL). Even the smallest response indicates gasoline NAPL as long as the waveform (blue-shifted with long lifetimes) supports its being present.
- Gasoline weathers rapidly and its fluorescence covers a wide spectrum of signatures, eventually fading to an orange fill and waveform, so be careful not to confuse weathered gasoline with shorter lived calcareous sands, clays, crushed limestone fill, and the like.
- Base limits of detection on benchtop tests of site-specific NAPLs or multiple lines of evidence. There are no fluorescence intensities or thresholds that are applicable to all sites and all NAPLs.
- Push the LIF well below the groundwater surface. Overlooking substantial amounts of NAPL trapped below the groundwater surface is a very common mistake.
- Regard any extremely short-lived and red-shifted responses (UVOST) with extreme prejudice. Such a waveform may well indicate the existence of unreported dramatically high PAH-content NAPL, such as creosote or coal tar, but will generate only an easily ignored fluorescence of just a few percent RE. Sample that location, if at all possible, as soon as possible during the investigation.

Post investigation

- Try not to "cherry pick" the single highest LIF value in a log. Consider averaging the RE over some minimum depth range. For example, a single cluster of ~13% RE readings across, say, 0.2 ft equates to far less NAPL than a 2.0 ft thick series of ~5% RE readings. But if the maximum is chosen, the log with a 13% maximum will show over twice the impact on a site map versus the more impacted 5% maximum location.
- Dig deeply into the LIF data. It is far more common for clients to underappreciate their LIF data's value to their project than it is for them to over-interpret the data.
- Schedule the data review with the vendor and be sure to interpret the data as soon as is practicable, hopefully even before the field team transitions to acquiring validation samples. It is surprising how often a consultant might wait six months or more to schedule a review.

4.7.3 What Are the Advantages?

LIF responds preferentially to the NAPL phase, logging its relative presence continuously, without sloughing and with "100% recovery." At the same time, LIF is practically unresponsive to the dissolved, sorbed, or vapor-phase "cloud" of contaminants that emanates from NAPL. LIF's selective response to the source term's true architecture ensures that the resulting CSM is not inflated by the more broadly distributed secondary contamination.

LIF is frequently deployed after traditional tools have produced an incomplete NAPL delineation and an initial remedy has been implemented; rebound observed during performance monitoring often prompts stakeholders to invest in LIF-based characterization to improve efficacy of future remedies.

LIF's key advantages include:

- Waveforms—a data type that records both emission spectrum and fluorescence lifetime. These measurements enable:
    - continuous differentiation of NAPL chemistry with depth
    - mathematical deconvolution of mixed fluorescence signals into separate NAPL bodies

    - assessment of weathering extent, supporting targeted remediation of the highest priority NAPL types and their depth intervals
    - robust rejection of false positive soil fluorescence via simple “at a glance” lifetime filtering
- Monotonic LNAPL response spanning three to four orders of magnitude (generated by the photomultiplier-tube detector). This wide range affords:
    - sensitivity to low NAPL saturations, even in false-positive soils
    - reliable delineation of high-saturation zones that control mobility and recovery
- Availability of expert waveform analysis and interpretation assistance of LIF data to any/all regulators/consultants (through Dakota). This ensures optimal value is derived from the LIF data, regardless of the data holder’s size or affiliation.
- Rigorous documentation of the science behind LIF data online (open access) (St. Germain 2024)

4.7.4 What Are the Limitations?

The technical limitations of LIF systems are similar to those of other direct-push technologies that are constrained by problematic geology, detection confirmation issues, and NAPL detection and interferences.

4.7.4.1 Geologic Setting

LIF is typically advanced through unconsolidated overburden where it has the same limitations as other direct-push tools. However, LIF has been successfully used in harder bedrock by advancing direct-push technology with LIF in a previously cored borehole filled with a sand and organoclay mixture (Hale 2011).

Additionally, even unconsolidated soils can become consolidated when frozen. Dakota personnel have, on rare occasions, met near-refusal while probing in Alaska in what site personnel regarded as permafrost. But by either preprobing with a dummy rod, or by sustained hammering, they were able to get through any frozen soils and achieve the desired depths. With respect to the frozen soil’s ability to influence fluorescence intensity, fluorescence intensity generally decreases and lifetimes generally shorten, with increase in temperatures. But even in frozen or near-frozen soil, temperature plays such a minor role versus other factors such as soil grain size, degree of weathering, and even localized heterogeneity’s effects that its small effect on intensity can be ignored.

4.7.4.2 Confirmatory Sampling

Confirmation sampling for NAPL is more difficult than expected. Geologic heterogeneity and contaminant variability, combined with limitations in sampling equipment and methodologies, complicate correlation or misdirect interpretations (Randy St. Germain 2022, 2023).

Whenever possible:

- Advance the confirmatory soil boring within 1–2 ft of the LIF log.
- Meet with the vendor online to discuss which locations might yield the most benefit if sampled. For instance, one location might apply to a large number of similar locations, thus killing multiple birds with one stone. Or one location might answer questions related to both NAPL and false positives. Setting up over that single location and sampling two horizons avoids setting up over two locations to sample a single horizon at each location.

- Collect continuous core samples (or screen with a PID or visually) across the target interval (the heightened LIF response) to visually correlate observed NAPL with the LIF response.
- Use oil-red-o, glove tests, jar shakes test, or other NAPL-specific techniques.
- Soil cores cannot be over documented. Use photography and placards religiously. Once that core goes into the waste barrel, it is too late to correct mistakes or solve mysteries that only make themselves known later during review.
- Place samples back onto the LIF to confirm that the target soil was successfully harvested. It is not at all rare for the drilling team to "miss" the NAPL-impacted horizon due to NAPL heterogeneity or difficult-to-sample soils. Placing the soil back on the LIF system will confirm the "miss" by its lack of response. This prevents misinterpretation of the two seemingly conflicting lines of evidence (an altogether too common occurrence).

Confirmatory soil sampling to LIF results can prove unsuccessful for the following reasons:

- Sampling in NAPL-friendly geology (such as sands, gravels) can result in poor correlation between sample results and the subsurface NAPL location, possibly due to mismatching depths between sampling methods (especially when NAPL occurs in thin horizons).
- Coarser materials, which often contain substantial NAPL, can be more difficult to sample or retain in a sampling device. Be prepared for sampling or recovery difficulty exactly where it is critical to get good recovery (where the NAPL resides).
- Confirmation samples are often collected from different boreholes, and, although the boreholes may be close to the LIF being confirmed, natural lithologic heterogeneity can be significant over short distances. To control this, laboratory confirmation sample splits should be reanalyzed with LIF (benchtop testing) to ensure the same sample is measured by both the LIF and confirmatory lines of evidence (for example, visual, PID, and NAPL-indicating dyes). This approach is recommended to ensure the two methods are analyzing the exact same sample.
- Confirming a NAPL-specific screening tool's response is an atypical activity for most drillers and consultants. While it is not difficult to do it properly, it requires a different mindset and discipline that, unless it is carefully planned for and conducted, will lead to misinterpretation of the direct sensing tool data's veracity and value. (St. Germain 2023)

4.7.4.3 Detection Limitations

LIF does not generally detect dissolved- or vapor-phase impacts related to NAPL. Unusual NAPLs that have not been classified as detectable or NAPL for which there is no information on the LIF response should always be sent to the vendor for testing. This is critical to success, because false negatives (NAPL in the subsurface that do not respond to LIF) result in an uncharacterized contaminant mass unless there is significant co-sampling—a potentially daunting and expensive task at NAPL release sites. Knowing the limitations of the ability of a technology to detect all NAPL types that might exist at a site is critical to success for any sensor, including LIF. Aviation gasolines are a notable example for all fluorescence systems, having failed to generate a satisfactory LIF response at a number of sites and in laboratory testing.

4.7.4.4 Interferences

False positives are fluorescence emitted by organic matter, seashells, peat, calcite (limestone), clays (for example, montmorillonite and kaolinite), and calcareous sands. These false positives are identified during data evaluation because they generate a short lifetime and signature (waveform) that varies from most NAPLs (heavy NAPLs can closely resemble false positives). Recognizing and excluding false positives prior to CSM development or revision prevents misrepresentation of contaminant distribution and other

cascading effects. Sites with fill contain anthropogenic materials that often fluoresce (for example, wood, plastic, and paper), which interferes with LIF. Other materials that can cause false positives include peat and meadow mat, asphalt, stiff and viscous tars, tree roots, sewer lines, coal, and quicklime (St. Germain 2008).

Positive tau trend behavior (St. Germain 2025) has made rejection of false positives a far more consistent and concise affair at heavy NAPL sites, where false positives can fluoresce more brightly than the target NAPL and cause as much as one-half the total fluorescence across the entire site. Keep in mind that even the waveforms from much older TarGOST surveys can be reprocessed to generate tau trend responses, vastly improving target NAPL recognition, even for decades-old datasets.

Fine-grained, organic-rich sediments are challenging. High surface area and small grain size soils (for example, clays) can hide NAPL so that it cannot be detected by LIF; under these conditions, the NAPL in the interstitial spaces of clay is not visible to the sensor unless there is clear line of sight. LIF sensitivity to petroleum hydrocarbons in soil has been shown to be inversely proportional to the available surface area of the soils. Sandy soils tend to have a much lower total available surface area than clay soils, so hydrocarbon compounds in sandy soils generally yield a higher fluorescence response than they do in clay-rich soils. These environments can result in high background readings and wandering baselines that can be deleterious to proper interpretation and can mask smaller signals, often requiring advanced data analysis.

Other factors related to soil type that can affect fluorescence response include mineralogy, degree of soil aggregation, and moisture content(Apitz et al. 1993). Increasing water content tends to impede LIF response in sand but enhances response in clay, while having negligible effect in sand-clay mixtures where their respective effects offset one another (Apitz et al. 1993).



Figure 4-57. Well casing for field Installation (top) and field use of the portable surveying Clear-Well instrument (bottom).

Source: E-Flux, LLC. Used with permission.

4.8 Clear-Well

4.8.1 What Is the Technology?

Clear-Well is a proprietary system that allows for repeatable soil imaging surveys through transparent sections of a stabilized port in the ground that stays permanently in place to monitor time-dependent changes (J. Zimbron 2020). The stabilized port consists of sections of standard PVC pipe joined with modified viewable sections of pipe. Viewable sections are lined with borosilicate glass exposed to the soil column through precut windows in the PVC. A digital imaging instrument, or probe, surveys the soil column by collecting images through the borosilicate glass windows (**Figure 4-57**). Typical direct push drill rig techniques are used to install the stabilized port in the ground.

The Clear-Well system allows for repeated imaging of the soil column under multiple optical excitations to reveal different soil features, including soil type, NAPL soil contamination, and plant roots. Images collected in the field are processed with filters to remove image distortions caused by a combination of the cylindrical geometry of the probe and the lens, to generate a single large picture corresponding to each glass window. Surveys designed to capture NAPL contaminant saturations (the fraction of the pores filled with NAPL (under UV light)) are processed to generate a contaminant saturation vs. soil elevation profile. This tool was first field-deployed in 2023. As of December 2025, it has been implemented in 11 locations, some with multiple 5-ft-long viewable sections. The current version of the technology includes a probe with a 12 MP camera and multiple sets of light-emitting diodes (LEDs) that can be used to collect information in the same survey. The difference in this technology with respect to other imaging ASCT such as LIF and OIP is that after installation of the stabilized port in the ground, surveys are intended to be repeatable using a portable instrument. Currently, the probe contains LEDs that emit the following types of light:

1) Visible (white) light. Images obtained under visible light provide detailed lithology information, such as soil texture, particle size, and transitions between zones with different properties. Other information observable under visible light includes soil color, the presence of tree roots, and soil color changes induced by geochemical changes, such as sulfide precipitates.
2) UV light (275, 310, and 365 nm). The general principles of fluorescence applicable to other UV-based tools (LIF and OIP) also apply to this part of the technology. UV light elicits a response from chromophore groups, typically conjugated double bonds, that generate a visible response. The photons from UV lights excite the subatomic electronic structure of the molecules and then they are released from the molecules as an optical signal, with a higher wavelength than the wavelength of the excitation light. Compared to the excitation using a single light source, the use of multiple exciting LEDs within the same survey probe increases the chances of contaminant detection. The relative response to the multiple wavelengths provides information related to the chemical structure of the contaminant mixture. For example, monoaromatic compounds are known to respond at the lower wavelengths, whereas polyaromatic compounds respond to higher wavelengths. This technology allows differentiation of NAPL composition caused by different weathering mechanisms at different elevations in the soil column. For example, aerobic NAPL degradation occurs at shallow depth (in the presence of ambient oxygen), as opposed to anaerobic degradation occurring at depth.
3) 520 nm (green lights). This wavelength is used to detect heavy compounds (coal tar and creosote) with a weak fluorescence response (to UV lights, see previous section).

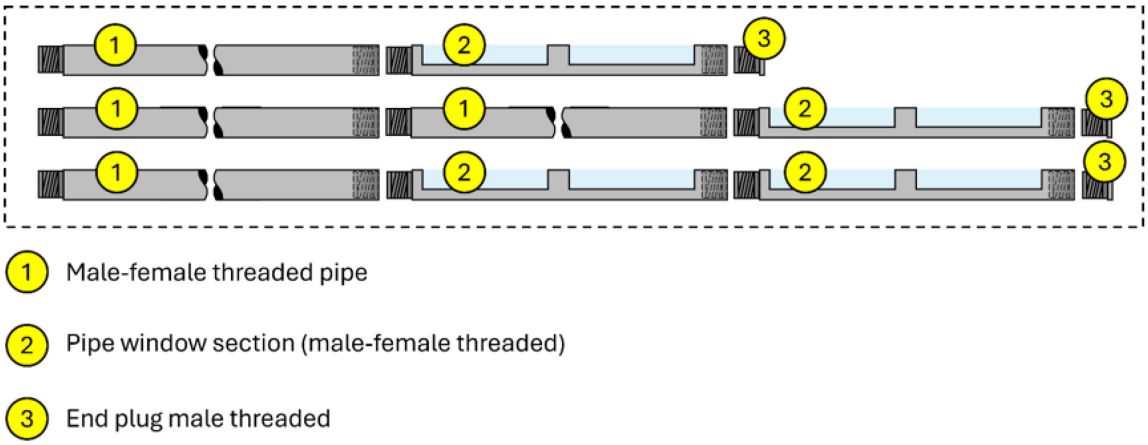


Figure 4-58. Schematic diagram of well casing construction. Examples shown use 1 or 2 Clear-Well viewable sections. Each viewable section is approximately 5 ft long and includes 50”-long sections with exposed glass (divided into two 25-inch subsections).

Source: E-Flux, LLC. Used with permission

A key part of the technology relies on the installation of permanent ports in the ground. The bore hole is stabilized using standard solid PVC (non-slotted) casing, jointed using threaded connections. The viewable sections of the PVC pipe are created by hosting a solid section of borosilicate glass within and exposing sections of this transparent material in precut sections of the hosting PVC. The joints of the glass and PVC are watertight, and the inside of the Clear-Well is intended to be dry, while the exterior (the formation) can be either saturated or unsaturated. Furthermore, installation of the PVC Clear-Well casing is expected to include both unsaturated and saturated (below the water table) sections of the soil column. The pipe is currently 2.5-inch schedule 80 PVC. Viewable sections are 5 ft long (with two 25-inch windows for a total viewable length of 50 inches). Multiple 5-ft-long viewable sections can be stacked. Other nonviewable sections consist of 5- and 10-ft-long standard PVC casing (**Figure 4-58**) to adjust the reach of viewable sections to predetermined depths of interest. This technology has been deployed to variable depths from 10 to 45 ft bgs.

4.8.2 How Is the Technology Used?

The Clear-Well system requires field installation using standard drilling methods. Once the monitoring port is installed, surveys can be conducted on the same port using a portable field instrument, enabling repeated imaging of the same soil locations. The field portable instrument is an electronic device that lowers an imaging probe using a cable spool within the preinstalled Clear-Well casing. The probe surveys these viewable sections in approximately 0.5-inch increments under a preset number of light sources (currently up to five different light sources). The same soil pores can be surveyed repeatedly over an extended time, along with other changes in related processes (**Figure 4-60**). The 12 MP imaging camera used allows a resolution of approximately 15 microns (near or below the thickness of a human hair (J. A. Zimbron and Rayo 2025).

The imaging probe (**Figure 4-59**) includes the imaging camera and two sets of lights on each side to reduce glare and properly illuminate the section of soil in front of the camera. The probe is kept from rotating to line up with the field installation using a proprietary magnetic system. The probe has a quartz clear window to allow interaction with the target formation. Each set of lights includes up to five LEDs (each one with different purposes, as described in the figure). The imaging probe advances 0.5” at a time within the preprogrammed interval (to match the Clear-Well construction

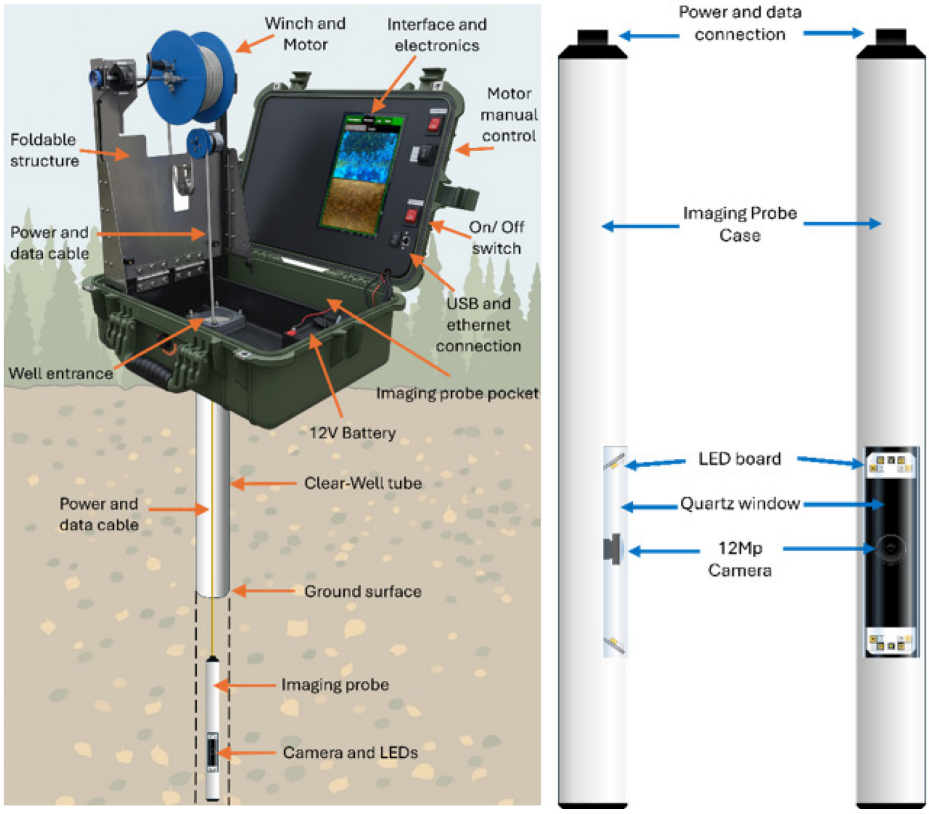


Figure 4-59. Clear-Well portable surveying unit (left) and details of the Clear-Well probe construction (right).

Source: E-Flux, LLC. Used with permission.

underground), taking multiple preprogrammed images under each of the different light sources at the same location. A survey using five different excitations of an approximately 5-ft viewable section requires approximately 1 hour, resulting in a surveying velocity of about 5 ft per hour. Reducing the number of images taken at each location will increase the surveying speed. An image preview of the last location surveyed is available on the aboveground controller unit screen (near real time, with a delay of a few seconds) to provide feedback to the operator. The image obtained under white light conditions shows detailed pore size and lithology, while other types of light reveal other soil features (contaminant distribution). Side by side images obtained using multiple excitations are key to identifying detailed NAPL distributions and potential interferences (**Figure 4-60**).

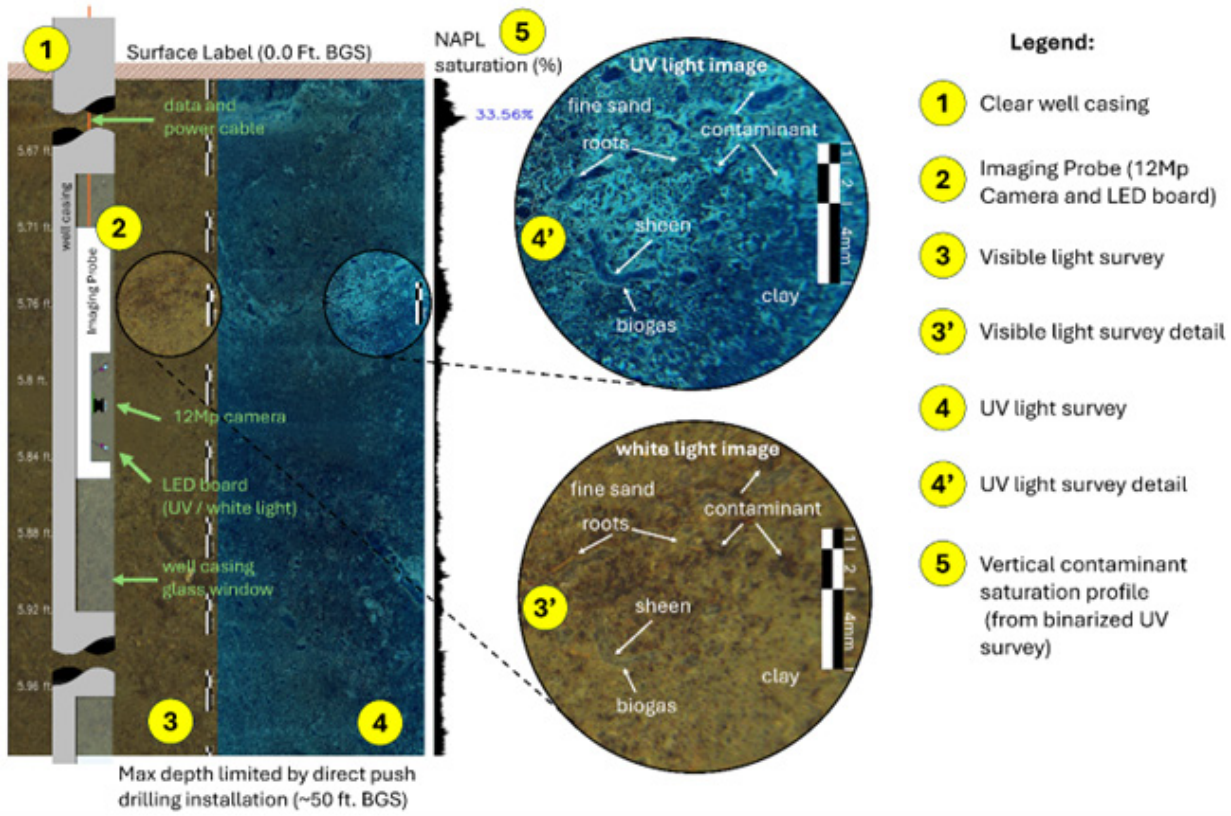


Figure 4-60. Illustration of operating principles of the Clear-Well technology. Images from actual field surveys. Image details noted might be viewable only under one type of light (NAPL sheens are viewable only under UV lights).

Source: E-Flux, LLC. Used with permission.

The resolution of the current 12 MP camera allows identifying soil features down to 15 µm. **Figure 4-60** shows field images of soil section obtained using white and UV lights. The white-light image in **Figure 4-60** reveals soil grains and plant roots, while the UV-light image reveals biogas bubbles from natural source-zone depletion (NSZD) coated with NAPL thin films or sheens. Sheens are formed when NAPL spreads as a water-wetting fluid between water-coated surfaces and air (in the water unsaturated zone) (ITRC 2018).

4.8.2.1 Data Examples

This section describes three examples of data collected with Clear-Well related to plant root growth, contaminant redistribution within the soil column, and contaminant redistribution at the porescale. These will be described in further detail below.

Plant root growth

A short-term plant root growth experiment was conducted in a laboratory setup. A plant was planted on a soil column that contained a Clear-Well borosilicate section and provided water and supplemental lights. Once the plant was established, repeated surveys using the Clear-Well probe were conducted twice per week. The first plant growth was identified approximately 2 weeks after planting (day 0). **Figure 4-61** below shows multiple pictures obtained at days 7, 10, and 14, using both UV (365 nm) and visible lights. A close-up picture at 14 days shows details of the plant roots. This plant root study is illustrative of applications of phytoremediation to soil remediation and the high level of resolution that this technology can provide.

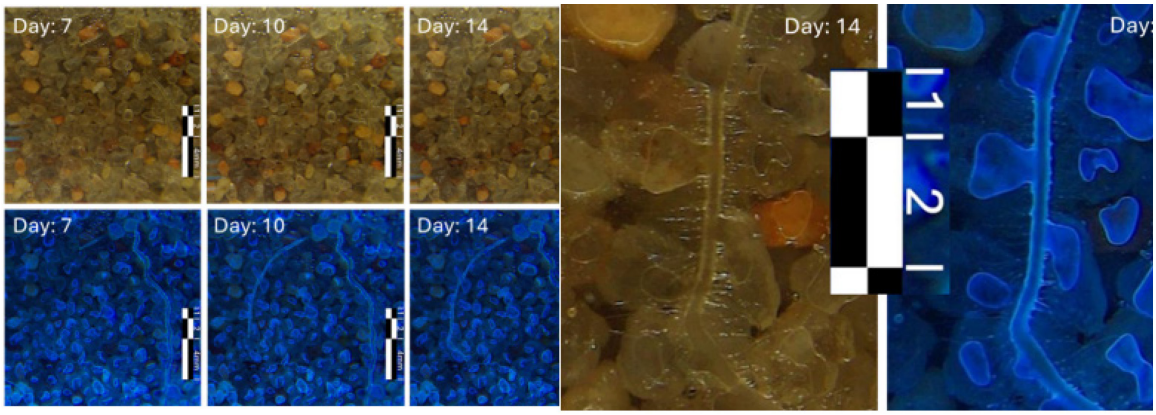


Figure 4-61. Images obtained under visible and UV (265 nm) light after the first identification of plant root growth (time 0). The right part of the image is a zoom in to reveal primary and secondary root structures 14 days after time 0.

Source: E-Flux, LLC. Used with permission.

Measurement of variable contaminant distribution profiles at a pipeline spill of petroleum crude

Two Clear-Well installations were field-installed in the summer of 2023 at a heavy crude pipeline confidential spill. These were repeatedly surveyed multiple times from 2023 to 2025. **Figure 4-62** shows the different contaminant distribution profiles measured throughout three different surveys on the same installation using white lights and UV (365 nm) at a depth from 5.93 to 7.76 ft bgs.

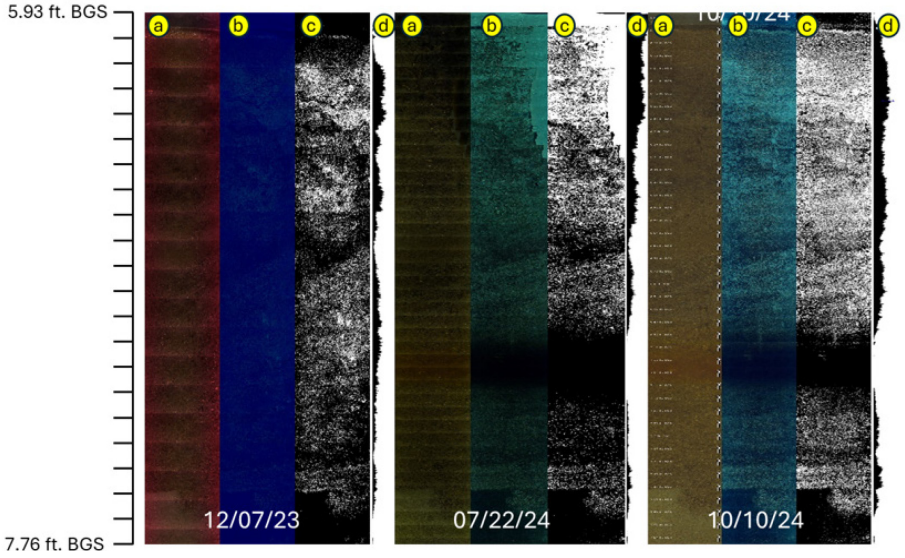


Figure 4-62. Comparison of three surveys from a ~2ft interval at a pipeline spill over an 11-month period. Legends (yellow circles) indicate a) white light images, b) UV (265 nm) images, c) binarized images showing NAPL, and d) NAPL vertical concentration profile.

Source: E-Flux, LLC. Used with permission.

Changes in contaminant distribution resulted from interactions between the formation NAPL with water levels and infiltration from snow melt.

4.8.2.2 Measurement of Pore-scale NAPL Redistributions at a Former Refinery

Two Clear-Well casings were installed at a former refinery at a total depth of 45 ft bgs and surveyed repeatedly for a period of nearly a year. The images shown in **Figure 4-63** reveal a detail at an approximate depth of 39 ft bgs showing the same formation feature (a pore within clay) with changing LNAPL distributions within, reflecting complex interactions between soil water and NAPL concentrations.

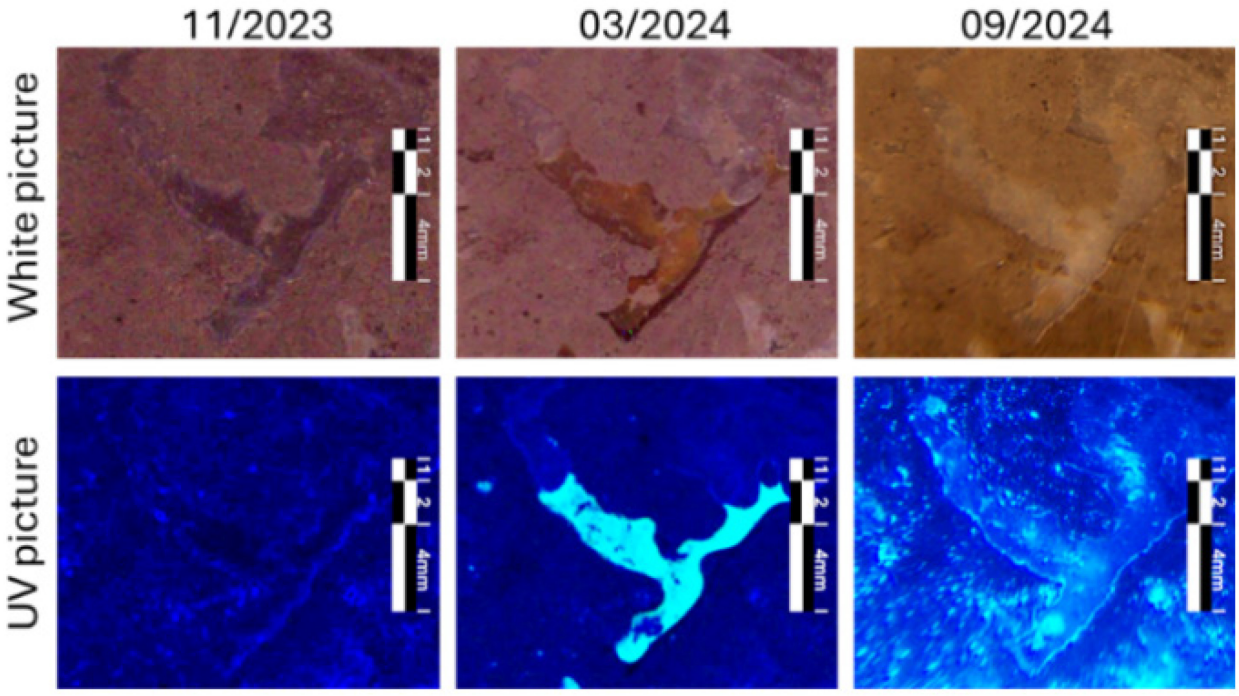


Figure 4-63. Detailed white light images (top) and UV (265 nm) obtained at a former refinery over a period of 10 months. White images show the same formation features (a small crevice) changing NAPL concentrations.

Source: E-Flux, LLC. Used with permission.

4.8.3 What Are the Advantages?

This tool is designed to enable multiple surveys of the same soil sections, suitable for characterizing dynamic soil processes. These include NAPL soil redistributions due to changes in water content due to water table changes, surficial drainage, or mass removal upon remedy implementation, a process known as remedy performance. The tool allows detailed tracking of fluid composition of small soil pores down to the imaging resolution of 15 µm, as well as NAPL saturations throughout the surveyed intervals (such as the final output of other imaging tools over the long term). This high resolution is the result of the use of the high-definition camera, and the use of the optically transparent borosilicate glass. The other probe-mounted imaging technologies might have to trade off optical clarity for hardness—for example, using sapphire. **Figure 4-64** shows two surveys of a soil section under water-saturated and water-unsaturated conditions (J. A. Zimbron and Rayo 2025). Clear-Well technology requires an initial, one-time mobilization, while repeated surveys can be conducted afterward using the portable instrument (**Figure 4-65**).

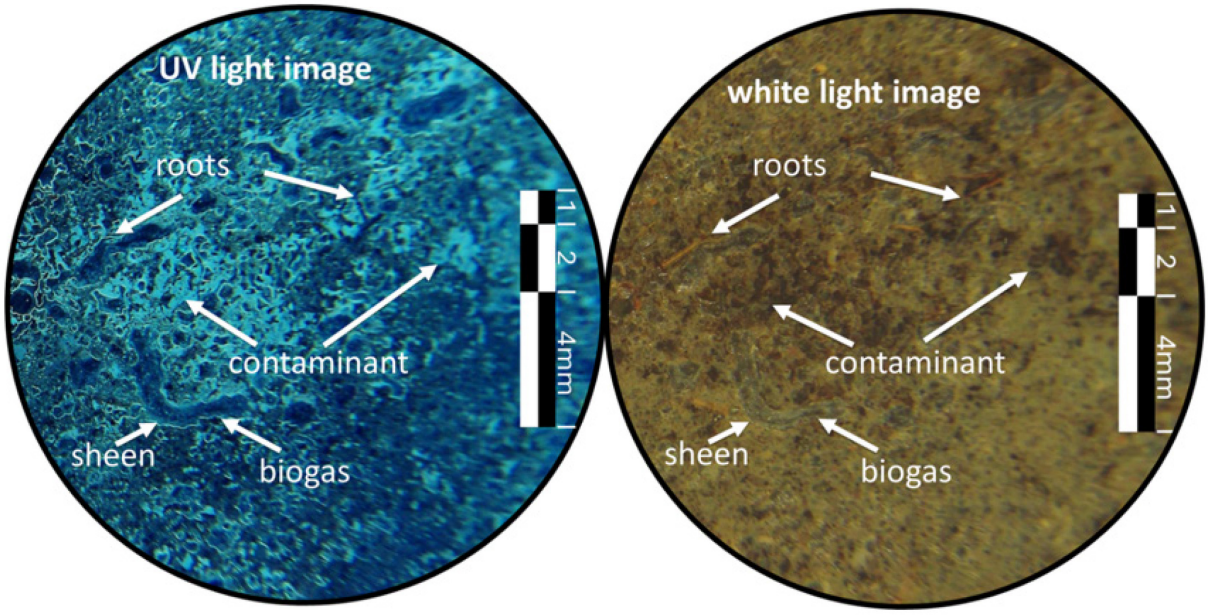


Figure 4-64. Comparison of surveys obtained using multiple excitations at the same soil location.

Source: E-Flux, LLC. Used with permission.

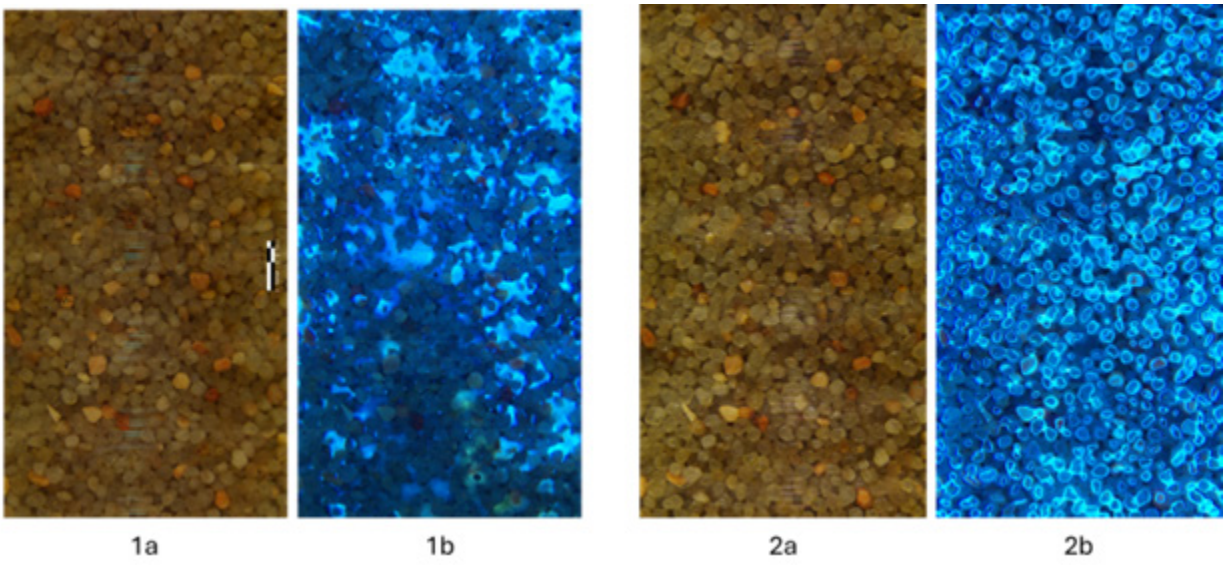


Figure 4-65. Differences in NAPL morphology upon water-saturated (left) and water-unsaturated (right) surveys. In both surveys, the survey obtained at the same camera position under white (visible) lights is shown to the left (a) of the image obtained under UVlights (b).

Source: J. A. Zimbron and Rayo (2025). Used with permission.

4.8.4 What Are the Limitations?

Limitations of this technology include those related to field installation, optical limitations, and data interpretation. Each of these will be further described below.

4.8.4.1 Limitations Related to Field Installation

Due to the specific dimensions of the Clear-Well tool, the required direct push drilling tool must be at least 3.0-inch inner diameter (corresponding to a nominal 3.75-inch drilling tool).

After installation, the formation is intended to collapse around the viewable sections of PVC casing. At most drilling installations, this occurs within a day or two of drilling, although other formations might require longer periods.

Due to the coupling unions between different clear sections, imaging covers only approximately 90% of each viewable section. Compared to other imaging tools that are probe-mounted, Clear-Well installation requires additional hardware, which results in a temporary shorter yield (length of soil surveyed per day). This is a tradeoff to being able to survey the same soil in the future.

In general, other tools, including other ASCT, might be used prior to the use of this tool to formulate a suitable CSM before deciding which areas would require the higher resolution provided by the Clear-Well tool.

4.8.4.2 Optical Limitations

Clear-Well technology is limited to the response of the NAPL to the UV light wavelengths used. Testing the actual NAPL response to the available UV lights is strongly suggested. Furthermore, comparison of contaminant concentration profiles from boring logs to those from Clear-Well imaging surveys can be conducted, depending on the data quality required. In general, the response is stronger at lower wavelength (275 nm) for monoaromatics, while the presence of PAHs will shift the response to higher wavelengths.

The camera currently used is a visible camera (with a capacity to detect light in the range of 400–700 nm). The technology manufacturer has plans to add a spectrometer within the imaging probe in the near future (to extend the sensitivity of the sensor beyond the current wavelength range).

The use of this technology for NAPL that do not fluoresce (chlorinated solvents) can be limited. However, even small amounts of impurities (either fumic/fulvic acids or aromatic NAPL) can make chlorinated solvent spills fluoresce (M. Kram et al. 2019). A simple bench test using field-collected NAPL can help assess this limitation. If present, this limitation can be overcome by injecting a fluorescent tracer to partition into the NAPL (if present), as is done by other ASCT technologies (DyeLIF).

4.8.4.3 Limitations Related to Data Interpretation

As with other imaging tools, certain minerals can interfere with the optical response of the instrument. For example, calcite can fluoresce upon excitement with UV lights. The collection of multispectral data can help differentiate the signal from these interfering minerals with those of the NAPL. Additionally, the white light survey can offer further insight into the geometry of an object related to the signal and help differentiate a particle from a pore. Note that NAPL will change morphology depending on whether it is in water-saturated and water-unsaturated conditions (**Figure 4-65**). The algorithm used to determine the presence of NAPL on a pixel-by-pixel basis and ultimately to generate vertical NAPL saturation profiles is sensitive to the input parameters (which determine what combination of colors in the collected images is related to the NAPL). The final selection of these inputs should be carefully justified, depending on consistency of the data with presurveying tests and the conceptual site model. As with other ASCT that offer depth-dependent signals, each survey is a 2D dataset. Integration of multiple 2D surveys will enable 3D datasets. This tool can expand the multidimensionality into time, by repeating multiple surveys at different times on the same ports.

4.9 Borehole Liners

4.9.1 What Is the Technology?

Flexible liners in the context of ASCT technology as discussed here refers to commercially available borehole liners using Flexible Liner Underground Technology (FLUTe™) devices. While the same liner technology is also a key element of the FLUTe multilevel well systems, these are not discussed further in this guidance document. Flexible liners fundamentally serve the purpose of temporarily sealing a borehole—for example, to reduce potential cross-hole contamination if the borehole would otherwise be left open for some period between completion of drilling and subsequent well installation or abandonment.

The liner technology has been adapted to conduct various high-resolution screening measurements from qualitative to semiquantitative, including fracture interconnectivity, hydraulic conductivity, direct and indirect groundwater pressures, and water quality, including dissolved and free-phase NAPL distribution within a borehole. A flexible liner and its insertion into a borehole are shown in **Figure 4-66**.

Flexible liner measurement methods are simple and have been aided by the development of strong impermeable fabrics and the availability of data-recording pressure transducers. Because liners are deployed in open boreholes, they are typically used in bedrock, although it is also possible to deploy them in unconsolidated materials for certain applications.

Flexible liners can have multiple applications depending on the data needs of the investigation. A high-resolution dataset is generated at a borehole spatial resolution typically on the order of inches. Some applications can be performed with minimal training; others require trained FLUTe personnel to perform the installations and data reduction. The following core applications of flexible liners are described in more detail in this section:

- vertical distribution of NAPL (NAPL FLUTe)
- vertical distribution of dissolved-phase contaminants [FLUTe Activated Carbon Technique (FACT)]
- borehole transmissivity profiles (FLUTe T profiler)
- sealing boreholes with liners and associated fracture interconnectivity mapping

These applications often follow a combination of the numbered sequence above because they reuse the same flexible liner. Throughout the eversion and subsequent inversion process, the outside of the liner never comes in contact with the interior side. Consequently, there is no direct path for cross contamination between the borehole and the water inside the liner.

4.9.2 How Is the Technology Used?

4.9.2.1 Sealing Boreholes with Blank Liners (FLUTe)

The liner is used to seal the borehole to prevent cross connection between zones of different hydraulic heads. Blank liner installation can be performed without prior experience. However, while the method is fundamentally simple, it relies on good understanding of certain principles to achieve successful results and to avoid critical pitfalls. The blank liner seals the borehole until it is removed. Therefore, it is considered a temporary seal as opposed to permanently abandoning the borehole using a grout seal.

FLUTe liners are used to seal a borehole. The advantages of this method are:

- ease of installation and removal
- continuous seal quality
- support from the liner to protect the borehole wall against slough
- tracer arrival detection because of transparent liner
- ability of certain geophysics technologies to "see" through the liner from the protected interior
- installation of liner without heavy equipment
- use of the same liner for multiple methods (NAPL FLUTe, FACT, FLUTe T profile, and the reverse-head profile)
- liner removal for repair or replacement, if needed. Information and videos are available online from FLUTe to illustrate how to deploy liners, or a trained technician can be provided by FLUTe.

The blank liner is installed using eversion; the liner is attached to the top of the well casing and filled with water, which advances a liner downhole by turning it right sideout, thus it does not slide along the borehole wall. To facilitate the process, the liner is shipped inside out to the site on a reel. The installation or removal process is as follows:

1) Liner is pulled from the reel and secured to the borehole casing with a clamp after cutting a slit at the top of the liner to create an opening for pumping equipment or pressure transducers as needed.
2) Liner is pushed down inside the casing, forming an annular pocket in the liner.
3) Water is poured into the annular pocket; the weight of water in the liner causes the liner to evert down into the borehole, pulling the liner from the reel (**Figure 4-66**). A minimum height of water of a couple feet is needed to drive the everting liner to the water table. Water may be removed from the borehole below the liner, typically by using an electrical or air lift pumping method.
4) Liner eversion stops at the water table, and more water is required to restore an excess head in the liner to continue eversion.
5) Liner eversion below the water table displaces borehole water into the formation unless it is removed by pumping.

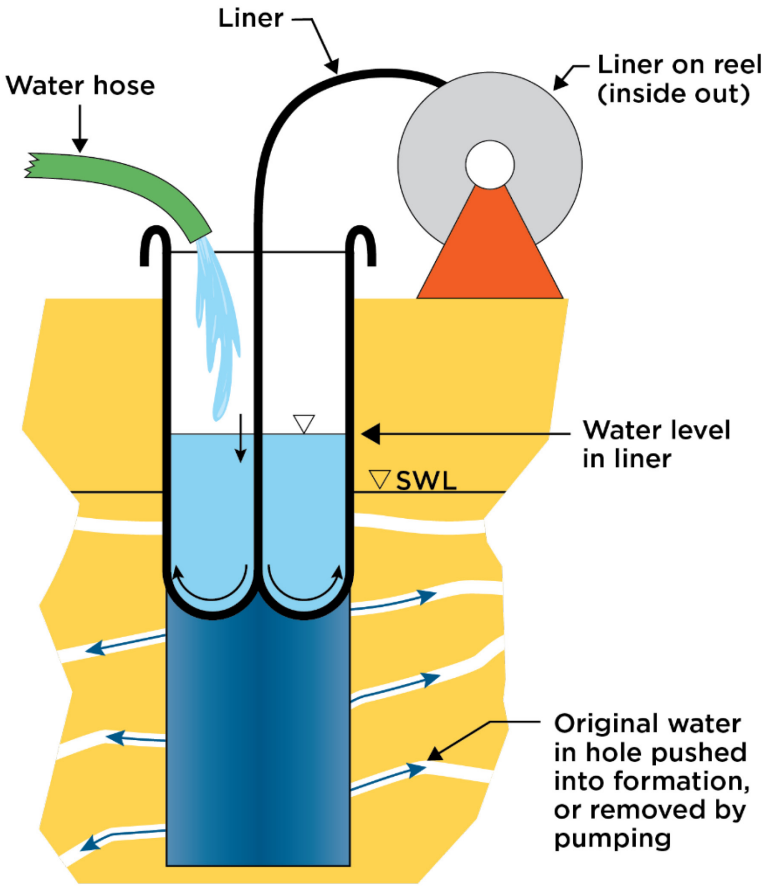


Figure 4-66. Simple eversion of flexible liner.

Source: Adapted by Geosyntec Consultants, Inc. from Flexible Liner Underground Technologies. Used with permission.

6) Liner descent by eversion continues at a progressively slower rate until there is insufficient formation transmissivity beneath the everting liner to permit its further descent; at that time, the borehole is effectively sealed by the pressure inside the liner.
7) The liner is manufactured with a tether line attached to its lower end. This tether is used to secure the liner to the top of the well, which avoids further eversion deeper into the borehole.
8) To invert (remove) the liner, the operator pulls upward on the tether using a winch system and water is drawn into the borehole from the formation until the liner is fully removed.

Water-filled liners effectively seal boreholes by tightly conforming to the borehole wall and sealing around cavities and fractures in the formation. The seal of the liner with its conforming capability is better than that of most inflatable well packers, which are made from stiffer materials.

The excess water head against the everting end of the liner causes tension to develop on the liner and the tether attached to the inside end of the liner. This tension is used for various applications, such as towing logging tools into angled and horizontal boreholes or carrying tubing and other devices into the borehole. Water is the common driving fluid for liner eversion, but other fluids (such as heavy mud or air) may be used. Liners have been everted through crooked pipes and upward in boreholes from inside mine tunnels. Gamma, neutrons, and sonic and electrical signals may be measured through the seal-coated nylon fabric, allowing geophysical tools to be deployed in the protective interior of the liner, which prevents borehole collapse and contamination of the tools.

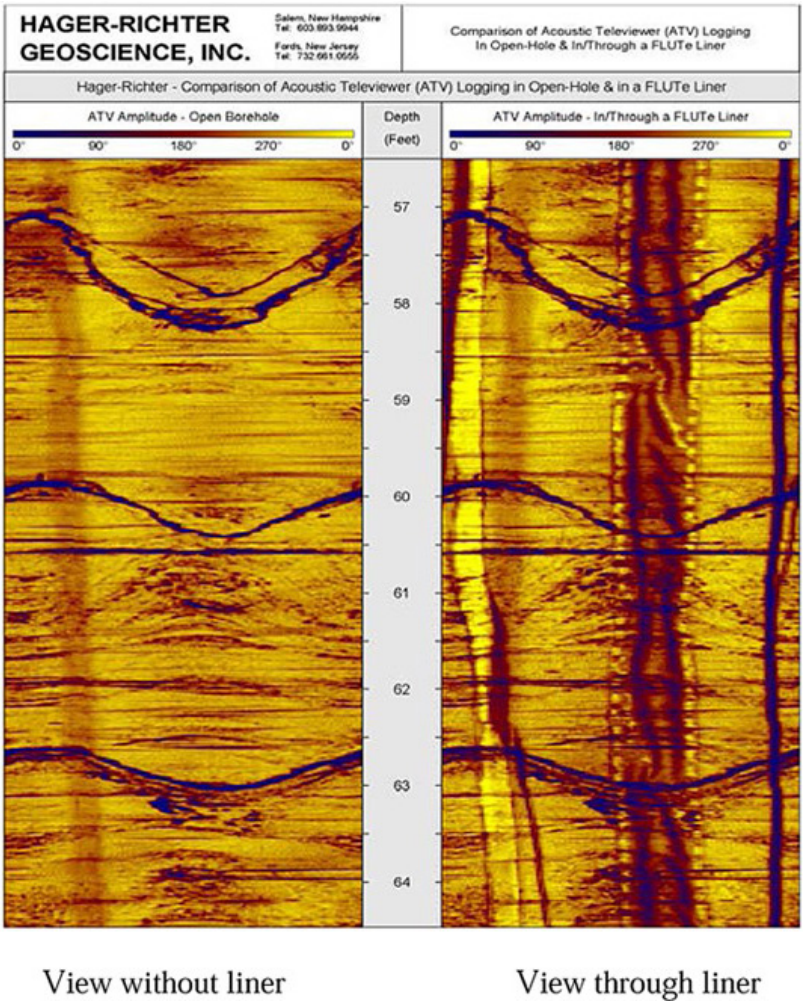


Figure 4-67. Acoustic televiewer logs recorded with and without a liner in the same borehole.

Source: Flexible Liner Underground Technologies. Used with permission.

An image of a borehole can also be obtained through both opaque and clear liners. In the case of opaque liners, an acoustic televiewer can be used to obtain the image. Figure 4-67 shows views of an acoustic televiewer log (Section 5.5) with (left) and without a liner (right). An interior sleeve (dark strip) and tether (right-most shadow) are visible in the view through the liner at right, but obscuration of the borehole wall by the liner is minimal; fracture locations are equally clear in both views. Transparent liners are also

available, and they may be useful, for example, to visually monitor the arrival of injected potassium permanganate within a borehole with a downhole camera.

The displacement of borehole water into the formation as the liner everts into the borehole creates a pressure pulse that propagates away from the borehole via fracture features. Installing pressure transducers to continuously log water levels in any nearby monitoring wells allows for studying fracture interconnectivity. Monitoring well screens that are connected to the open borehole via fractures will show increased water levels until the respective fracture is sealed, at which time the water level returns to ambient conditions. Mapping out well screens that are connected to borehole fractures at a certain depth can greatly improve the understanding of the CSM.

4.9.2.2 FLUTe Transmissivity Profiler

The liner descent rate in a water-filled borehole can be used to map the location and flow rates of water in the fractures intersecting the borehole. However, the procedure requires that the excess head driving the liner and the tension on the liner be maintained relatively constant. Under these conditions, the liner suffers a drop in its descent velocity each time a flowing fracture is sealed by the descending liner. The velocity change multiplied by the cross-sectional area of the borehole is the flow rate of the water in the fracture before it was sealed.

The transmissivity of the interval traversed by the liner in one recording time step is calculated using the Thiem **Equation 4-2**):

$$\Delta T = \Delta Q/\Delta H_h \ln(r_a/r_h)/2\pi = (v_i - v_{i+1})\, A \ln(r_a/r_h)/(2\pi(H_h - H_a))$$

Equation 4-2. Thiem equation.

where ΔQ is the change in velocity (v_i) multiplied by the borehole cross section (A), ΔH_h is the difference between the borehole pressure (H_h) and the ambient pressure (H_a) in the formation at a distance (r_a) from the borehole center, and r_h is the borehole radius. Since r_a is often not well known, it is estimated. The ratio r_a/r_h is assumed to be constant.

The spatial interval depends on the recording time step (typically 0.5 sec) and the velocity of the liner. In other words, the faster the liner descends, the longer the interval is traversed in onetime step. For example, when integrated over 1-ft intervals, the result is similar to that obtained from a series of 1-ft-long straddle packer tests.

Intervals with large transmissivity and, fractures with significant yield may accommodate the borehole water that would otherwise have exited through smaller fractures at a shallower depth. This is an important limitation to consider when interpreting the transmissivity profiler results because a large fracture at depth may obscure the transmissivity of smaller fractures above it.

Upon completion of the transmissivity profile, the blank liner may be left in the borehole as a temporary seal.

4.9.2.3 The NAPL FLUTe Liner

The NAPL FLUTe maps the distribution of free-phase NAPL present at the borehole wall. It consists of a blank liner fitted with a hydrophobic cover that is pressed against the borehole wall upon eversion of the liner. Upon contact, the NAPL produces a stain on the white surface of the hydrophobic cover. Stain colors vary from purple to dark brown or nearly black based on the composition of the NAPL. The hydrophobic cover works with both light NAPL, such as gasoline or diesel range organics, or dense NAPL,

such as chlorinated solvents or coal tar. The hydrophobic cover reacts only with pure NAPL, not dissolved-phase contaminants, creating a visual log of free-phase product within the borehole, if present.

The NAPL FLUTe is usually left in the borehole from a couple of hours up to a day. Depending on the volume of NAPL available in a fracture, the NAPL cover will wick the product at different rates. Leaving the NAPL FLUTe in the borehole for an extended period could generate a stain several feet long, making it challenging to identify the exact depth of a specific NAPL fracture.

When everting the NAPL FLUTe liner into a borehole, one borehole volume of water is pumped from beneath the liner during installation to reduce the injection of water into the fractures (the injection effect may displace NAPL from the borehole vicinity). Pumping should not be excessive so that significant mobilization of NAPL is avoided. It is important to note that water displaced into fractures during the eversion is likely extracted from the same fractures during the inversion (removal) of the liner from the borehole.

After a minimum of one hour, the liner is inverted from the borehole as shown in **Figure 4-66**. The dye-stripe liner cover is now inside of the inside-out liner. The liner cover is held as the liner is slipped off the liner cover, exposing the normally white inside surface of the liner. Visible stains on the white surface of the liner indicate where NAPL has contacted the liner cover. A tape measure is placed next to the cover, and the stains are photographed to record the depth in the hole where NAPL contacted the liner cover.

Because the liner and liner cover are inverted from the borehole, the liner cover does not contact any other portion of the borehole than where it was everted against the borehole wall. The NAPL FLUTe cover is often installed on the blank liner for the initial emplacement to seal the borehole. Upon removal of the NAPL FLUTe cover, the liner is replaced to seal the borehole or perform other measurements.

Figure 4-68 shows stains from TCE, coal tar, xylene, and gasoline on the inside surface of a cover. The first three stains were obtained in open-fractured rock boreholes, which are the conditions where this method is most commonly used. The LNAPL stain was the result of a thin gasoline film on water in a tube.

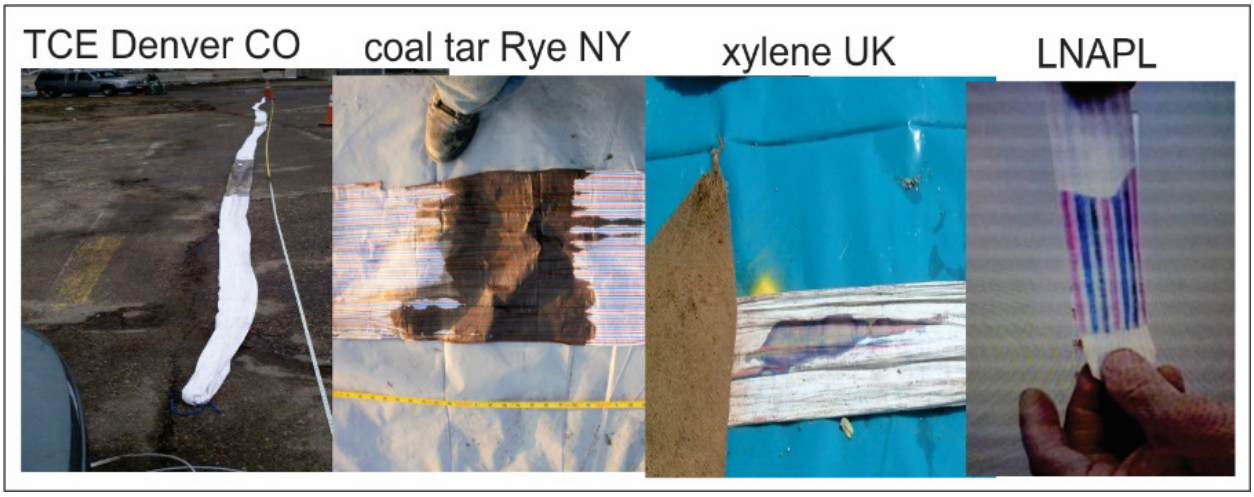


Figure 4-68. Examples of NAPL stains on the inside surface of a cover.

Source: Flexible Liner Underground Technologies. Used with permission

Rather than being deployed downhole, the NAPL FLUTe cover material may also be used as a bag to detect NAPL in extruded core material that is placed inside the bag. This technique is used if the borehole is not expected to remain open when casing is removed or if only a small section of core is to be tested.

Similar to the liner, contact of NAPL in the core with the dye on the inside surface of the bag will produce a visible stain on the outside of the bag.

Advantages of the NAPL FLUTe liner are:

- Stains observed are a reliable indication of the presence of NAPL at any depth within the borehole.
- Stains indicate the presence of NAPL not apparent through visual observation of a rock core.
- Stains are easy to observe and photograph and require minimal interpretation.
- Spatial resolution of NAPL is approximately 1–2 inches and presents a full 2D map of the presence of NAPL.
- The NAPL FLUTe liner is a relatively inexpensive addition to a sealing liner used to prevent cross connection.

Many compounds have been tested for reactivity with the NAPL FLUTe liner; a list is available online from the manufacturer. To confirm reactivity, a confirmation staining test of the target NAPL with the FLUTe liner material should be conducted prior to employing a FLUTe liner investigation program.

4.9.2.4 FLUTe Felt Activated Carbon Technique

The NAPL FLUTe liner, described above, detects only free-phase NAPL in direct contact with the cover. The FLUTe Activated Carbon Technique (FACT) can detect relative concentrations of dissolved-phase contaminants in the pore water and in fractures of the formation at the borehole wall. The NAPL FLUTe liner and FACT are deployed together by design, generating two simultaneous datasets from the same borehole. The FACT is a screening methodology that provides relative measurements, which may be affected by multiple variables. Therefore, FACT analytical results should be considered a line of evidence in the process of refining the CSM on the borehole scale. In the FACT, an activated carbon felt strip is pressed against the borehole wall when the sealing liner is everted into the borehole. The FACT strip is left in the borehole for up to two weeks, during which the carbon adsorbs the dissolved phase of the contaminants.

The construction of the FACT is shown in Figure 4-69. The FACT carbon-felt strip (about 1.5inches wide and 0.125inches thick) is contained between the outer NAPL FLUTe cover material and a diffusion barrier that is sewn into the inside surface of the thin (about 1 mil) cover material. The pressurized liner presses the diffusion barrier, the carbon felt, and the NAPL FLUTe cover against the borehole wall.

After 2 weeks in the borehole, the liner is inverted from the borehole with the NAPL FLUTe cover. As described in Section 4.9.2.3, the liner is slipped off the inverted cover, and NAPL stains, if present, are photographed. The diffusion barrier, which is now on the outside of the inverted cover, is slit and the carbon felt strip is removed, cut to desired lengths, and

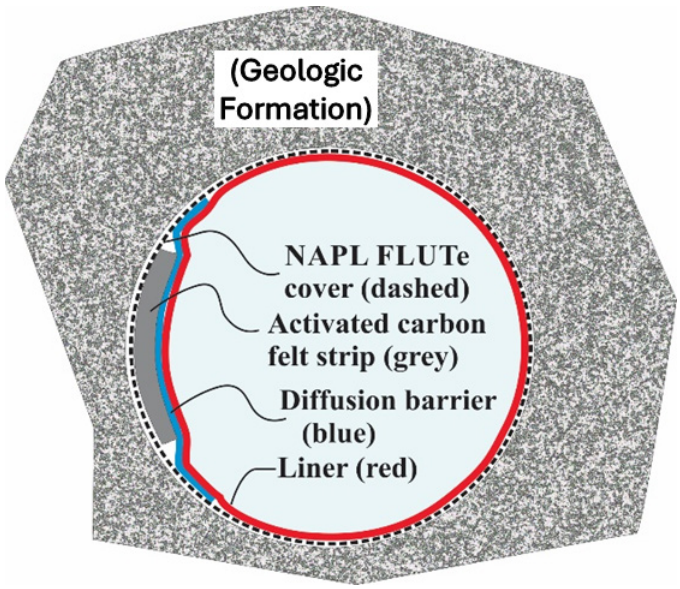


Figure 4-69. FACT components.

Source: Flexible Liner Underground Technologies. Used with permission.

inserted into sample jars filled with deionized water. Carbon-felt samples are shipped to a laboratory for analysis according to USEPA Method 8265. Acceptable performance for the carbon-felt matrix should be demonstrated by matrix spikes or laboratory control samples with analytes spiked onto the carbon felt.

The spatial resolution of data is determined by the length of each carbon-felt strip, which is determined by the user. For a high-resolution dataset, the carbon strips may be cut into small (6-inch) pieces; for a lower resolution dataset, the carbon strips may be cut into larger (1–2 ft) pieces. Analyzing larger sections of FACT is less costly because fewer samples are generated, but a dataset with lower resolution results. Regardless of sample length, the entire carbon strip sample must be analyzed because contaminants do not migrate in the carbon; failure to analyze the entire length of carbon can result in an interval of elevated contamination being missed. An alternative streamlined sampling method is to split a longer sample along its length and cut the remaining half into smaller subsamples. The long sections can be used as initial screening samples while keeping the subsamples on hold. The initial samples that show relevant concentrations can then be analyzed in greater detail via the subsamples.

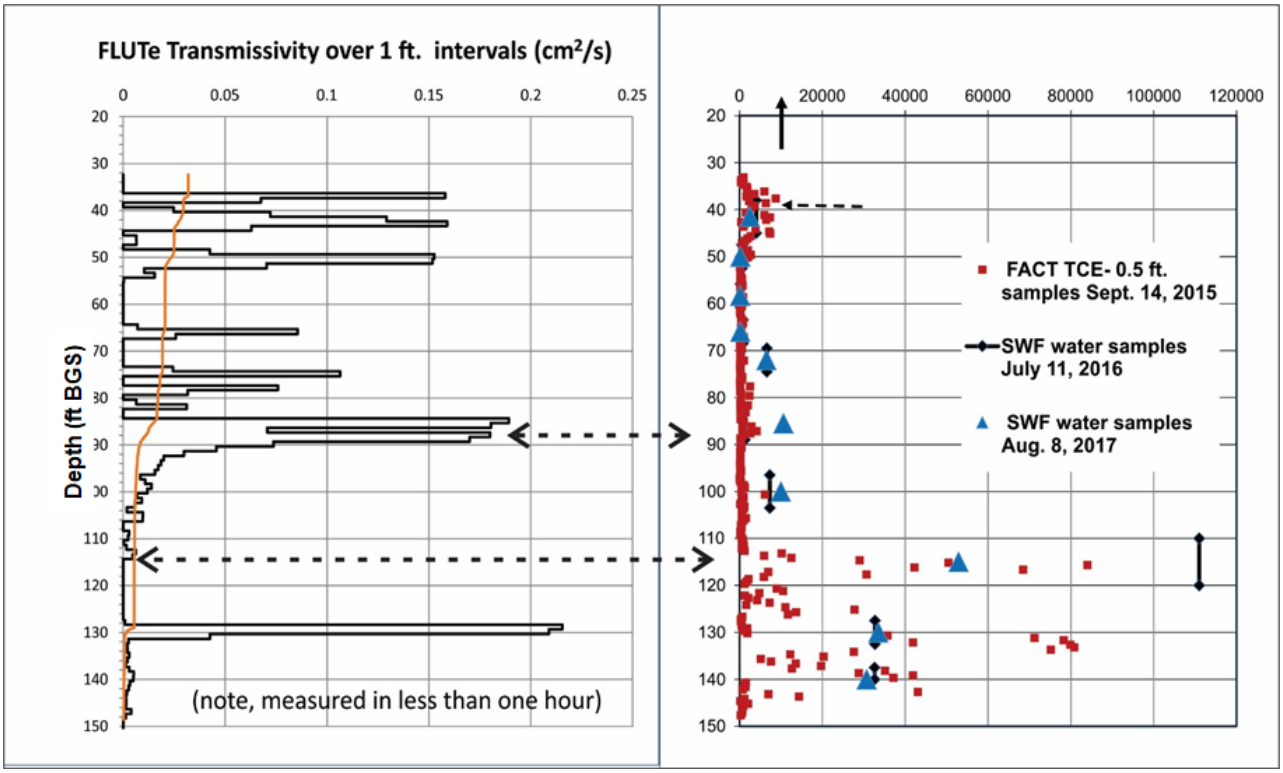


Figure 4-70. FACT results with transmissivity.

Source: Flexible Liner Underground Technologies. Used with permission.

The right side of **Figure 4-70** shows measurements of TCE (in mg/L of carbon) in 6-inch carbon-felt segments from a 150-ft borehole using the FACT. The graph also shows corresponding groundwater concentrations [in micrograms per liter (µg/L)] obtained from 10 sample intervals 300 days (black bars in **Figure 4-70**) and 700 days (blue triangles in **Figure 4-70**) after the FACT carbon strip was removed. Water samples are plotted on the same scale regardless of unit, which shows the distribution similarity. The data comparison between the FACT and water sample results shows the accuracy of the measurements from the FACT and how the liner prevents borehole cross connections between different contaminated zones. The water samples are derived mainly from fracture flows, suggesting that the FACT is also sensitive to fracture flow concentrations. Because the FACT produces a diffusion-based measurement, contaminant concentration gradients are expected to be highest for water flowing past the FACT carbon

strip as compared to water trapped in the pore space of the matrix. Thus, the mass of diffusion is directly dependent on the concentration gradient.

Relative measurements from the FACT generally agree with the contaminant concentration distribution in the core, but not necessarily with all locations in the borehole. The FACT draws from pore water and fracture water, whereas a core assessment measures the pore water of selected samples, not the entire core, or intervals of lost core. FLUTe is often a component of a discrete fracture network (DFN) investigation (Section 4.1.3.2), so a high-resolution comparison may be performed when both investigation methods are used.

The left side of **Figure 4-70** shows transmissivity over the intervals, providing a side-by-side comparison of the FACT results and the transmissive intervals measured. The arrows correlate two example high concentration intervals to corresponding transmissivity intervals. The highest concentrations are not always in the high flow zones. The highest concentration at 115 ft occurs within a low-transmissivity interval, and the relatively low concentration at 87 ft occurs within a high-transmissivity interval.

The FACT uses carbon-felt strips, which contain toluene that is known to be leached from the urethane-coated liner fabric. Leaching is unlikely to impact future water samples because the toluene dissipates relatively quickly from the liner, but not in the time frame of the FACT installation and therefore will be seen in the analysis of the carbon strip.

4.9.3 What Are the Advantages?

General considerations of sealing a borehole with a blank liner include:

- The cost advantage of using FLUTe versus individual tools to achieve the same results is the multiple data streams that are derived from a single borehole and liner. In addition, FLUTe liners are readily removed, unlike permanent subsurface installations.
- Gamma, neutrons, and sonic and electrical signals may be measured through the seal-coated nylon fabric, allowing geophysical tools to be deployed in the protective interior of the liner, which prevents borehole collapse and contamination of the tools.

The advantages of the FACT liner include the following:

- Provides a continuous vertical map of the dissolved-phase contaminants (the entire length of the borehole is evaluated, so no intervals are missed).
- Is not dependent on prior judgment of where contaminants reside.
- Results correlate to groundwater samples.
- Is sensitive to both pore-space and fracture contamination.
- Can be added to the NAPL FLUTe cover at a relatively small additional cost.
- Carrier liner can be reused to seal the borehole or to perform other high-resolution measurements.

4.9.4 What Are the Limitations?

General considerations of sealing a borehole with a blank liner include:

- If the liner is exposed to extremely high concentrations of VOC (NAPL), the VOC diffuse through the liner into the liner interior water. Upon removal, the water must be treated as contaminated.

- Some compounds such as potassium permanganate degrade nylon liners; polyester liners are available for sites with potassium permanganate in groundwater.
- For extreme downward gradients (>50 ft over the borehole depth), a stronger liner is required to prevent the liner from bursting.
- Although liners can be punctured by sharp rocks in the borehole wall, puncturing has occurred in fewer than 1% of liner installations.
- Low transmissivity may necessitate installation of a pump tube to expedite the installation by removing water from below the liner. Conversely, water will need to be added if similarly expedited removal times are to be expected.
- It is important to secure the tether line once the liner velocity has slowed to the near stop. The liner would otherwise continue to advance until it reaches zero transmissivity, which can take a long time. The same amount of time is required to remove the liner.
- Adherence to installation methods is critical. Too low driving pressure (adding water too slowly) may allow formation water to buckle (collapse) the liner. Not keeping sufficient tension on the tether may cause the liner to bunch up.
- Using excessive force to pull out the liner —for example, with a truck or a drill rig —will inevitably destroy it.

The limitations of the NAPL FLUTe liner include:

- An open stable hole or installation through drill casing is required.
- The dissolved phase is not detected by the liner, and it must contact NAPL for a stain to develop.
- Solvents migrate in the cover material and, therefore, the size of the stain is not indicative of NAPL thickness.
- The NAPL type cannot be identified by the stain.
- Stains represent current NAPL locations; NAPL may be redistributed by the drilling process, resulting in scattered staining. (Scattered small stains usually occur in boreholes with large stains from the source of the scattered NAPL).

4.10 Passive Flux Meters

4.10.1 What Is the Technology?

The passive flux meter (PFM) has been developed to measure groundwater and contaminant fluxes in the saturated zone (Hatfield and Rao 2006b; Hatfield and Rao 2006a). The PFM can be applied for the following site characterization uses:

- Quantify the source strength and identify hot spots and distribution of contaminant mass to inform remedial decisions.
- Determine mass attenuation rates between transects and evaluate remedy effectiveness.
- Evaluate contaminant distribution, and whether contaminant mass is primarily contained within high- or low-conductivity zones.
- Compare the mass discharge of electron donors, electron acceptors, and contaminant mass to evaluate biodegradation.

The PFM is a nylon mesh sock that contains both a permeable sorbent and soluble tracers. The PFM is placed in a borehole or monitoring well within the saturated zone to intercept groundwater flow. After a known exposure period, the concentration of dissolved constituents in the sorbent and remaining tracer is measured and used to estimate groundwater and contaminant fluxes. The ITRC guidance document Use and Measurement of Mass Flux and Mass Discharge (ITRC 2021) presents the concepts and approaches of fluxes and is not discussed further here; however, the PFM is included as an ASCT because it provides direct and high-resolution measurement of groundwater velocity and chemical concentrations.

4.10.2 How Is the Technology Used?

A PFM is deployed in a well or borehole and exposed to the groundwater flow from a few days to a month. It is designed for the specific application as follows (Figure 4-71):

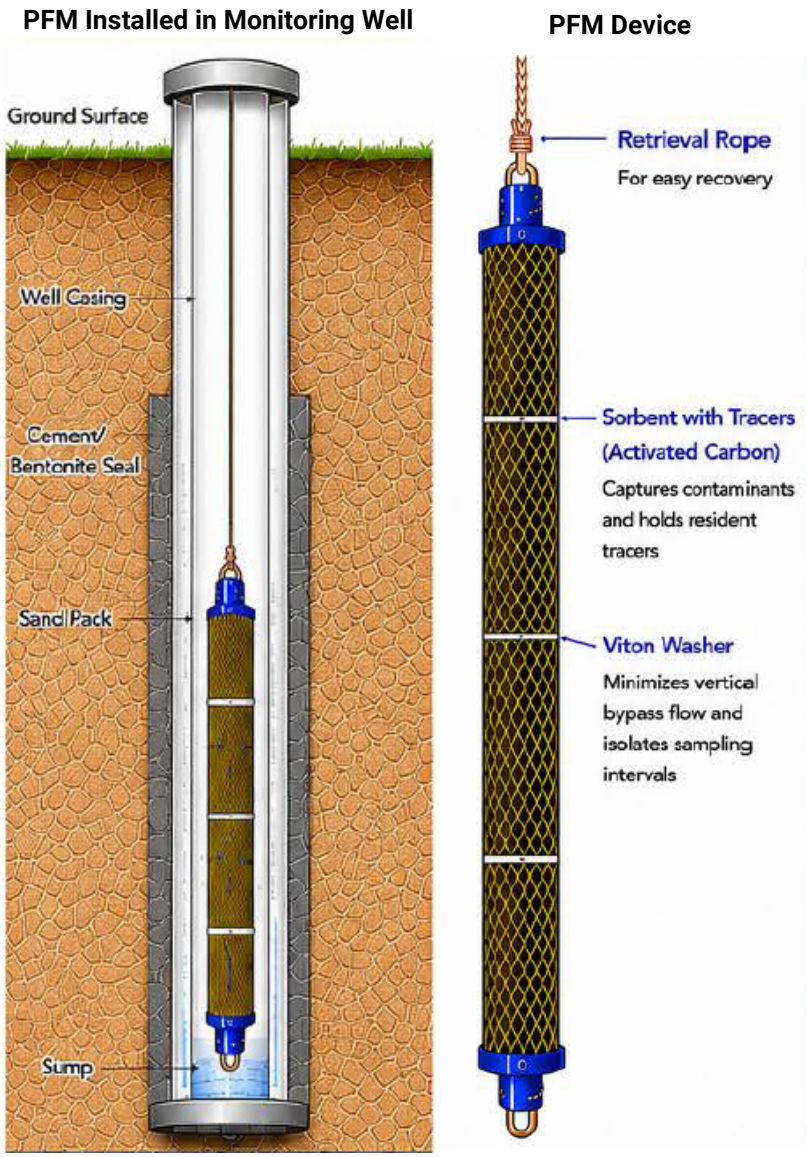


Figure 4-71. Passive flux meter monitoring well installation and PFM device.

Source: EnviroFlux. Used with permission.

- The diameter of the PFM needs to be the same as the diameter of the borehole or monitoring well in which it is installed to help ensure groundwater flow is through the PFM.
- The number of sampling locations within an individual site can be varied; spacing should be based on the geology and groundwater flow characteristics of the aquifer.
- The PFM may be separated into different vertical zones isolated by impermeable barriers, such as rubber or neoprene washers.
- The sorbent can be varied based upon the contaminant.
- The exposure period can be varied; the optimum time would allow for one-half of the initial groundwater tracer to be removed from the PFM. Estimates of contaminant concentration and Darcy flux should be used to determine the optimum deployment time (ITRC 2021).

During the PFM deployment, soluble tracers are released, and contaminants are sorbed. After retrieval of the PFM from the well, high-resolution sampling and analysis of the sorbent and remaining tracer are conducted at

discrete-depth intervals to provide a direct measurement of groundwater velocity and contaminant concentration.

The PFM can be used to evaluate a variety of different chemical types, including hydrophobic organic compounds (chlorinated solvents; 1,4-dioxane; hydrocarbons) and organic or inorganic ionic compounds (hexavalent chromium and perchlorate). The vertical resolution of measurements with a PFM can vary from very fine (centimeters) to larger (feet) scale, though PFMs are commonly sampled and analyzed at 1-ft intervals (Hatfield and Rao 2006b, 2006a; Hatfield et al. 2006a, 2006b).

4.10.3 What Are the Advantages?

The PFM allows for a time-integrated, simultaneous measure of both groundwater velocity and chemical concentration at a monitoring well or borehole. This approach has the potential to reduce errors by integrating the measurements over time. The PFM provides a detailed vertical profile of groundwater velocity and chemical concentration to evaluate the vertical variation over the thickness of the aquifer. The PFM is fast and easy to deploy and requires only two trips to the site (one for deployment and one for retrieval). Because there is no groundwater purging or sampling, minimal investigation-derived waste is generated.

4.10.4 What Are the Limitations?

PFMs are only available for a subset of chemicals and are only appropriate for dissolved-phase chemicals. The duration of the deployment must be considered to ensure that the capacity of the sorbent is not exhausted. There is potential for competitive or rate-limited sorption of chemicals to occur during deployment, which may result in the PFM underestimating the actual chemical concentration and flux. Some chemicals and high concentration of chemicals can impact desorption of internal tracers, reducing the accuracy of groundwater flux measurements (Hatfield and Rao 2006b).

The measurements provided by the PFM are not accurate at sites where vertical gradients are substantial. Additionally, if the horizontal groundwater flow direction changes substantially during the time of deployment, the flux estimates may no longer be valid (ITRC 2010a). At sites where active bioremediation is occurring, concerns may exist about the integrity of the tracers used to evaluate groundwater flux. These tracers, typically alcohols, may be degraded or otherwise affected by enhanced biodegradation processes, which could result in an overestimation of groundwater velocity. The PFM has typically been used to evaluate mass flux in relatively permeable, unconsolidated formations, but the PFM can be deployed in fractured rock.

4.11 Point Velocity Probe

4.11.1 What Is the Technology?

The direct sensing point velocity probe (PVP) measures groundwater velocity by pushing a probe to the required depth, or placing the tool into a well screen, and conducting a “mini tracer” test. Groundwater velocity is a fundamental concept in understanding various hydrogeological processes, including contaminant transport. Typical velocity estimates are made using Darcy’s law and measured hydraulic gradients, hydraulic conductivity, and water elevation measurements in wells. Parameter measurements in wells can miss small-scale subsurface variations and only provide average flow across broad areas. For example, there are situations where the gradient is very flat or low and difficult to measure accurately, even over distances of tens of meters (Devlin and McElwee 2007). Direct groundwater velocity measurement offers a solution to this limitation. This resulted in the development of the PVP, which consists of a cylindrical shell with multiple detectors and injection ports, allowing for three-dimensional velocity measurements in unconsolidated sediments or well screens depending on tool configuration. It

can be deployed in various configurations, including single or multilevel setups. Unlike typical methods that rely on hydraulic gradients and conductivity, the PVP provides direct measurements of groundwater velocity.

PVPs have been used to validate the CSM, quantify flux across compliance boundaries and barriers, and monitor transient flow phenomena (for example, bioremediation-induced changes). Their independence from Darcy's law makes them especially valuable where K is large and gradients are difficult to measure reliably; in highly conductive aquifers, conventional head-based gradient estimation may require tens of meters of well spacing (for example, ~31 m to resolve 1 m/day), making direct velocity measurements the practical option at the treatment scale (Devlin et al. 2012).

A PVP consists of:

- Probe body: Cylindrical PVC or stainless-steel housing (~3–4 cm OD, ~25 cm long) with one or more injection ports and paired electrical conductivity detectors mounted on the outer surface (Figure 4-72).
- Injection port: Delivers a brief, low-volume pulse of saline (for example, NaCl; typically, 0.01–1 mL at ~1 g/L, adjusted to ambient TDS) to the probe surface. The tracer travels with ambient flow along the cylinder.
- Detectors and wiring: Short stainless wires (or copper leads) configured as half-bridge circuits connected to a datalogger. As tracer passes, resistance and voltage changes produce breakthrough curves.

Datalogger and acquisition: Alternating current (AC) excitation, voltage measurement, time-stamping, and storage for multiple detectors (commonly up to 16 channels per probe array).

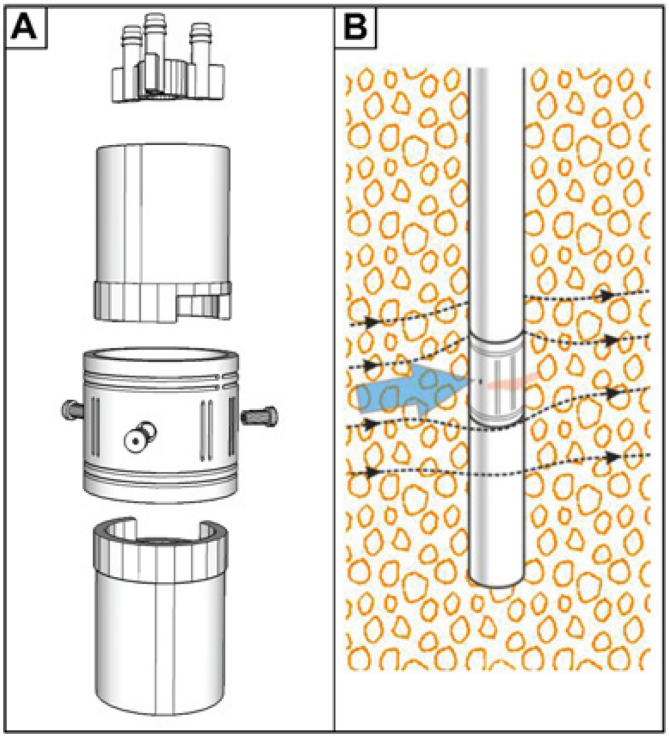


Figure 4-72. (A) Computer rendering of the PVP components and design. (B) Plan view of schematic of the PVP illustrating tracer (red) movement across the surface of the probe and detection wires.

Source: Ozark Underground Laboratory. Used with permission.

4.11.2 How Is the Technology Used?

The PVP tools operate on the basis of a mini-tracer test that occurs on the probe surface (Figure 4-72). As the tracer passes over the probe surface, paired detection wires track changes in electrical resistivity over time. Tracer selection is therefore focused on creating a clear resistivity contrast between the tracer solution and the native groundwater, while avoiding density-related flow effects. The resulting resistivity time series is used to define the tracer breakthrough curve (Ozark 2021).

PVPs provide direct, local estimates of groundwater flow used to:

- refine the CSM with high-density velocity profiles (vertical and lateral)

- quantify flux across property lines, PRBs, and engineered treatment zones
- monitor transient changes in flow (for example, clogging or bioactivity during remediation).

Deployment configurations: Probes can be used singly or in multilevel arrays (for example, four probes per stand, several stands forming a "fence") to resolve vertical and lateral variability over time. Arrays are often installed by jetting open casing and allowing the subsurface to collapse around the probes for intimate contact with the aquifer(Devlin et al. 2009)..

Breakthrough curves from the detectors placed at known angular offsets (γ_1, γ_2) from the injection port are fitted to an advection–dispersion solution to obtain apparent tracer velocities. These are then converted to ambient groundwater speed and flow direction using closed-form relationships. Accuracy is best when detectors are positioned ~45° and ~75° from the injection port and the incident flow approaches α≈40–80 (Labaky et al. 2007; Schillig 2012).

Proper PVP Design and Selection

- Detector geometry (γ angles): Place paired detectors at 45° and 75° from the injection port to minimize sensitivity to small placement errors and to maximize the solvable range of flow direction (up to ~100–105° from a single port). Use three-port probes spaced 120° apart where flow direction is variable in time; at least one port will be well oriented for a measurement.
- Tracer choice and concentration: Use saline differing from ambient TDS; concentrations up to 5 g/L NaCl are acceptable in sands when density effects are managed. In high-TDS waters, deionized water can be used as an inverse (reduced conductivity) signal.
- Signal quality and logging: Select dataloggers capable of stable AC excitation and high-resolution voltage measurement; wire detectors in half-bridge configurations; confirm low baseline drift and steady sampling intervals.
- Array strategy: For barrier monitoring, fence-line compliance, or transient studies, use multilevel fences (for example, 4 depths × 5 stands) to contour velocity magnitude and direction in cross section.

4.11.2.1 Data Collection Design

- Installation: Avoid compacting or smearing the formation adjacent to the probe.
- Test setup: Preload tracer lines; define launch times; record detector distances (used to compute detector geometry precisely from outer diameter and wiring layout).
- Injection pulse: 0.01–1 mL; Ensure clean, single-pulse delivery to avoid pulse splitting (which qualitatively indicates low flow direction but complicates quantitation).
- Sampling rate and duration: Match to site velocities (seconds to minutes per breakthrough curve); maintain consistent timing across detectors.
- Replicates: Acquire multiple breakthrough curves per port and repeat across depths to quantify variability.

Five unique tools were designed for direct groundwater velocity measurements across a wide range of geologic settings as summarized in the table ~~in~~ **Appendix A. Summary and Selection Resource for the PVP Family of Tools**. These tools function on the same principle as the original PVP described here but have varying details in application, advantages, and limitations as shown in Appendix A. PVP = direct emplacement on a direct push technology tool; in- well PVP (IW-PVP); fractured rock in- well PVP

(F-IWPVP); HRX-PVPV for use in horizontal wells; and stream bed PVP (SB-PVP; measures *in situ* groundwater velocities at the groundwater-surface water interface without reliance on hydraulic conductivity, porosity, or hydraulic gradient information).

4.11.3 What Are the Advantages?

The design and inexpensive nature of the PVP instrument makes it possible to deploy these devices in multilevel fashion. A multilevel PVP has the advantage over other methods of velocity estimation of providing detailed vertical information about the velocity profile. This profile can be re-evaluated through time. PVP instruments provide the following-:

- The design of the PVP is low cost and supports multilevel deployment. They use cost-effective and simple hardware (probes < $50 in DIY builds, excluding drilling).
- They provide a cost-effective method; simple hardware with array deployment supports spatial mapping.
- The PVP provides detailed vertical velocity profiles not achievable with current available methods.
- The PVP deployed over time supports evaluation of transient flow conditions.
- The PVP tool provides direct, local measurement of a velocity vector (rate and direction) at the centimeter scale, supporting fine-scale profiles and coupled chemistry and flow studies.
- PVPs provide an independent check on traditional Darcy based calculations and model predictions, especially where hydraulic conductivity is high and at most sites with average hydraulic gradients are calculated.

4.11.4 What Are the Limitations?

Geologic Setting–PVPs are best suited to granular, noncohesive aquifers (sands, fine gravels) where the formation can collapse snugly around the probe. They are less effective in cohesive clays and silts or fractured media where collapse and intimate contact are not achieved. Variations in the tool have been developed to overcome some of these limitations.

Confirmatory Sampling–Correlation with conventional samples may be relative because PVP measures local velocity, while samples integrate different intervals or boreholes. Multiple lines of evidence confirm PVP results.

Measurement Limitations

- Uncertainty floor (inherent): With good breakthrough curves, expect ± 4–10% speed uncertainty at flow direction≈50°, increasing to ~± 15% at very low (~20°) or high (~100°) flow direction; direction uncertainty is ~± 9–12° in worst cases.
- Solvable flow direction range: From a single port with detectors at 45°/75°, flow direction is typically solvable up to ~100–105°; beyond that, tracer may not reach both detectors. Use multiport designs.

Interferences

- Electrical noise and drift can occur on baselines.
- High ambient TDS can reduce contrast; adjust tracer accordingly.

- Temporal flow variability during tests can distort breakthrough curves; repeat runs to confirm.

4.12 Distributed Fiber-optic Sensing Tools

4.12.1 What Is the Technology?

Distributed fiber-optic sensing comprises distributed temperature sensing (FO-DTS), distributed acoustic sensing (DAS), and distributed strain sensing (DSS). Fiber-optic sensing relies on the physical properties of light traveling along a fiber, and it can detect changes in temperature, vibration (strain-rate), strain, and other parameters. The fiber acts as a sensor, providing thousands of sensing points along it (the fiber acts as the distributed sensor ["intrinsic fiber sensing"]), although measurement is essentially continuous along the fiber. "Interrogators" are used to measure the changes detected along the fiber. These measurements can be used to monitor parameters accurately over tens of kilometers. Standard telecommunications fibers can be used if the temperature remains below 100° C and the fiber is protected from chemical and mechanical interference. A thorough description of the technology and its uses can be found in The Groundwater Project's Distributed Fiber-Optic Hydrogeophysics (Tyler et al. 2022).

The phenomenon measured for fiber-optic sensing is photon scattering (or backscattering)—that is photons are absorbed and re-emitted. The measurement of temperature, strain, or vibration uses Raman, Brillouin, or Coherent Rayleigh backscattering for DTS, DSS, and DAS, respectively:

- Raman scattering results from temperature-induced molecular vibrations in the fiber so photons are scattered back to the source with lower or higher energy than the source (inelastic scattering). Measuring the difference between the lower and higher intensity (than the original) backscattered light allows the temperature to be accurately quantified at any location along the fiber. Multimode fiber (larger core size), allows multiple light modes to travel simultaneously, best for short distances (less than 500 m) is most often used for Raman measurements).
- Brillouin scattering is also an inelastic scattering process where the light in the optical fiber interacts with acoustic waves in the fiber in a predictable way. Acoustic waves result in density variations in the fiber, and these variations cause scatter. Brillouin scatter is affected by both temperature and mechanical strain and must be separated by independent monitoring (for example, DTS when strain is needed). The Brillouin reflection profile can be compared over long periods of time to determine differential strain in wells, structures, tunnels, and pipelines. Single-mode fiber (small core size, allows only one light mode, good for long-distance transmission (10s of kilometers)) is most often used for Brillouin measurements.
- Rayleigh scattering, caused by small-scale heterogeneities in the fiber-optic cable (for example, where the refractive index or chemical content varies), can be used to detect vibrations and acoustic waves through a measurement of strain rate. Rayleigh scatter is elastic (energy is not changed or is conserved) so the signal to noise ratio is usually much higher than in Brillouin and Raman scattering. By analyzing light phase shifts caused by vibrations and acoustic waves at two locations along the length of the fiber (the virtual gauge length), strain rate can be located along the fiber. Rayleigh scattering is also sensitive to temperature, so strain rate and temperature must be separated in the measured signal response. Single-mode fiber is most often used for Rayleigh measurements.

Because this is relatively new technology in subsurface investigations, it is expected that an expanded description and examples will be included in future ASCT guidance updates.

4.12.2 How Is the Technology Used?

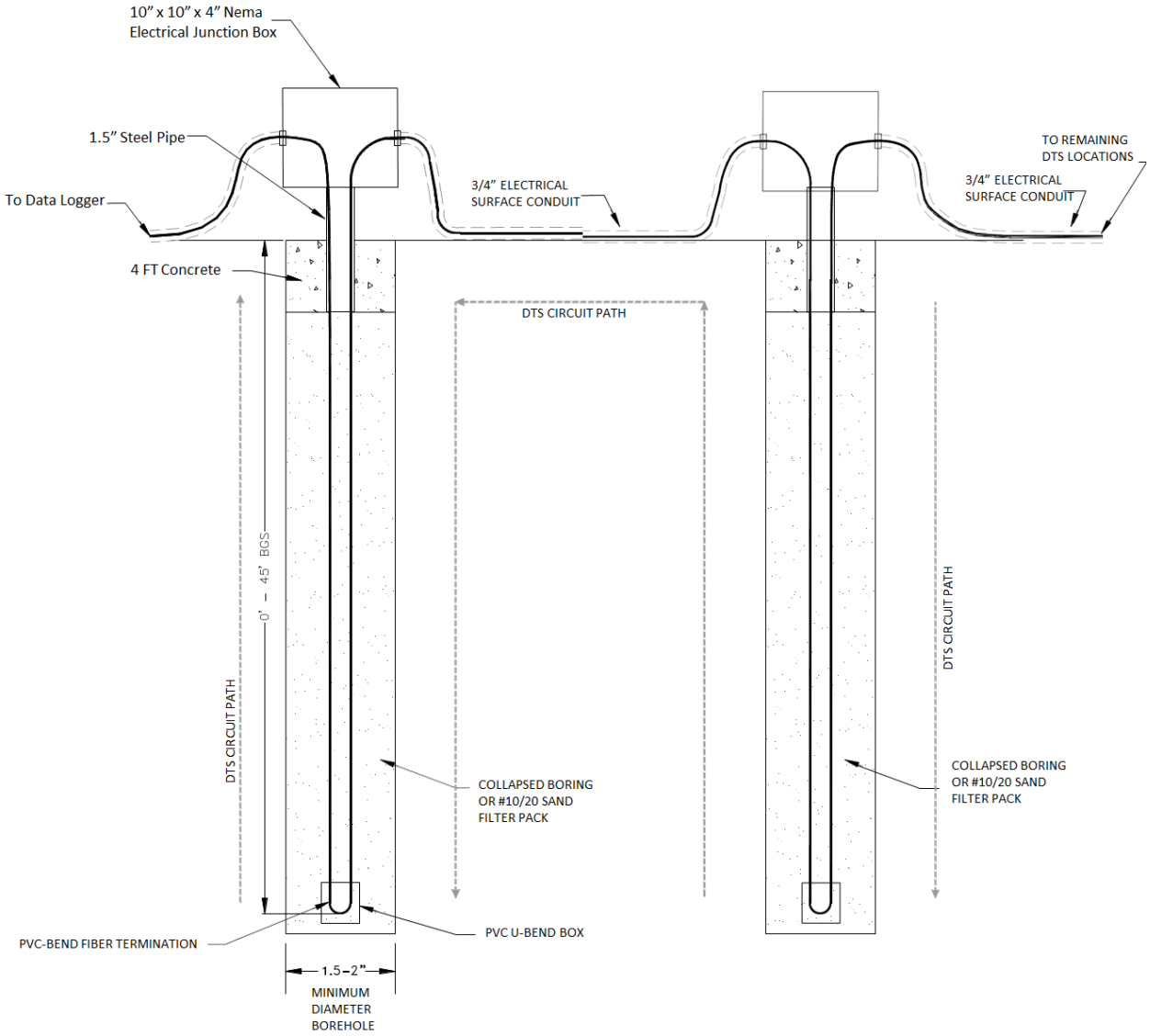


Figure 4-73. Schematic cross section of a fiber-optic installation in more than one borehole.

Source: Courtesy of Jonah Munholland, Arcadis.

Like any other geophysical technique, distributed fiber-optic sensing measures indicators of the parameter of interest—for example, heat as a tracer of water movement, or strain-rate as a measure of fluid pressure changes. In some case— for example, in thermal monitoring or subsidence measurement, the parameter of interest may be measured direction (for example, strain). In the context of advanced site characterization and direct sensing tools, this guidance document is focused on DTS, which can be used to measure temperature of unsaturated and water-saturated media. With addition of a heat source (active DTS), it can measure dissipation of heat as a tracer to evaluate conductive zones and zones of water exchange. Heating of the subsurface for enhanced biodegradation can also be monitored using DTS (Becker et al. 2025). DTS has also been used to measure stream-aquifer interaction (USGS 2019b) and in groundwater settings (fractured and unconsolidated aquifers) to evaluate seawater intrusion (Folch et al. 2020), flow paths, fracture connectivity, and other aquifer characteristics. Temperature precision is

generally around 0.02 °C and spatial resolution can be sub-meter. The light signal must be calibrated in the field with sources of known temperature (for example, water baths) measured using an independent device. Downhole temperature measurement is also recommended for calibration.

It is possible to monitor existing fiber-optic cable to measure parameters, but this practice has been adopted mostly by the seismic community (DAS). A key concern is coupling the fiber to the material to be measured. For example, in a downhole or well deployment, fiber-optic cable may be attached to the outside of well casing (for example, with cable ties) or placed within a backfilled borehole. Direct-push applications are also used to deploy fiber downhole inside a drill casing, which is then retracted to allow formation material to collapse around the fiber. **Figure 4-73** shows a schematic section of a direct-push fiber-optic installation in boreholes within which the soil was allowed to collapse around the fiber. **Figure 4-74** shows a 3D image of a DTS system installed to monitor thermal treatment of contaminated groundwater. Monitoring is accomplished through one fiber-optic cable that is routed through all the boreholes. In addition to deployment during direct-push drilling (where the fiber is advanced with the drill pipe and then left in the borehole following its retraction), fiber can be deployed in wells by attaching it to casing as it is lowered into a well. In other cases, fiber can simply be lowered into an existing well.

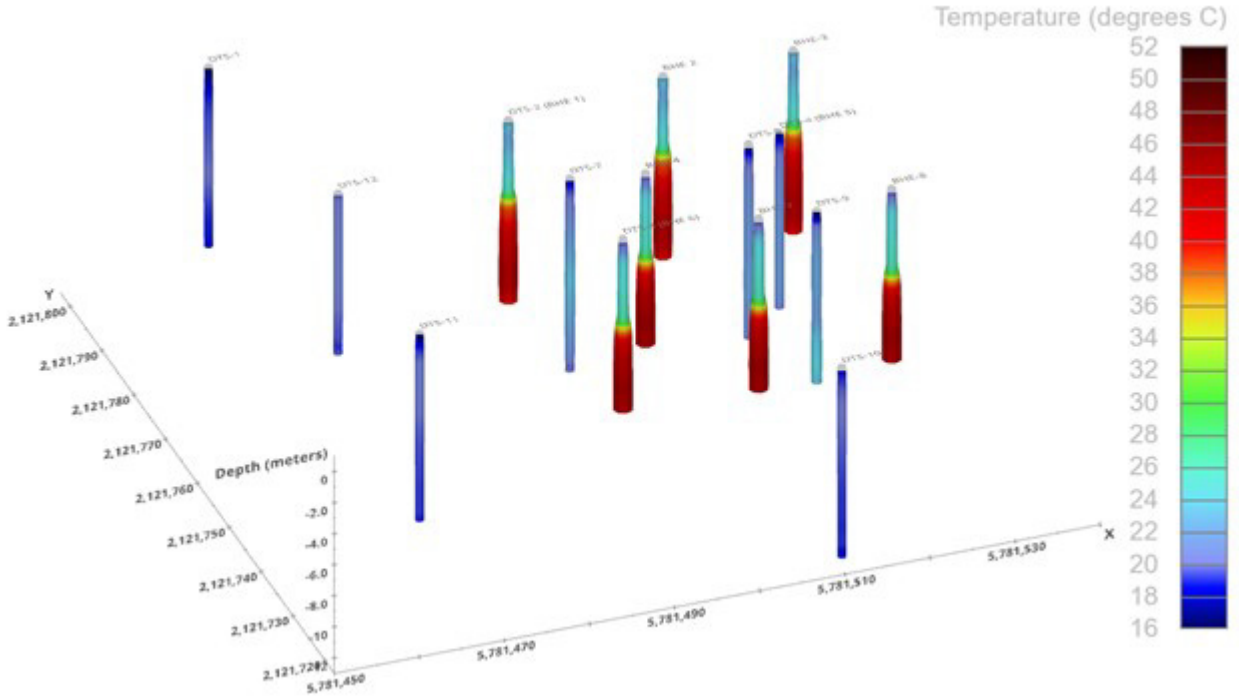


Figure 4-74. 3D perspective view of a DTS borehole network to monitor low-temperature biodegradation remediation of groundwater. DTS-X indicates a DTS borehole fiber and BHE-X indicates the co-location of borehole heaters.

Source: Courtesy of Jonah Munholland, Arcadis.

4.12.2.1 Data Interpretation and Presentation

Interpretation and presentation of fiber-optic DTS data require expertise and are often best suited for more sophisticated graphics (for example, 3D) to display the results. Large datasets are evaluated and interpreted with other technologies to characterize subsurface conditions (for example, preferred groundwater flow and transport pathways, distribution of heat during thermal remediation). Data are

processed through specialized programs and require additional processing time compared to other real-time data collection methods. Results of distributed fiber-optic sensing can be presented for a single borehole (vertical or horizontal), in section (along a transect), or in 3D to show results for a volume of the subsurface.

4.12.3 What Are the Advantages?

Fiber-optic sensing is a high-resolution, high sensitivity method for measuring temperature and strain over significant distances and depths (> 5 km) at sampling rates of milliseconds (DAS) to a few minutes (DSS, DTS). It is best suited to applications where dense measurements in both time and space are required or where environments are too harsh for electronic sensors. It is also valuable when variable gradients are required. For example, it may be cost-effective to install a series of thermistors to measure thermal gradients, but drift and accuracy of the thermistors will limit their effectiveness. Hence, applications that require distributed measurement may benefit from distributed fiber-optic sensing.

The technology can be employed for multiple hydrogeologic applications, including contamination investigations, flow evaluation in unconsolidated and fractured aquifers, and stream-aquifer interaction, as well as others. It can be used to develop detailed 3D understanding of subsurface conditions, including temporal changes. Most instruments can be deployed in the field using a 12V power source.

4.12.4 What Are the Limitations?

While established for use in applications such as petroleum and pipeline monitoring, fiber-optic sensing in other fields (for example, environmental) is a relatively new technology and use outside of academia and scientific government agencies is not common, although increasing. Limited availability may, therefore, be an issue until acceptance and familiarity grow. Regulatory acceptance may be limited until more widespread use is established.

Although the interrogator technology is becoming more robust and lower cost, installation of fiber-optic cables can be challenging, and experienced practitioners should be involved in the selection and installation of the fiber-optic cable. Datasets produced from these installations can be large (>1 TB/day for DAS), which may result in data storage and transfer limitations. The dynamic time/space density of the data is the strength of the technology, but this requires data-science skills to interpret and communicate, as well as potential coding skills, although these limitations may be at least partially overcome using AI (artificial intelligence) tools. A lack of skilled practitioners is currently a bottleneck to the dissemination of the technology into practice.

Technical limitations include cases (Folch et al. 2020) where the fiber-optic cable may need to be cut and re-fused (spliced), which can result in reading and interpolation difficulties. Damage to fibers may also occur due to pinching or at fusion points and sharp bends. Selection of appropriate fiber and installation is critical for the success of installation. Cable must be protected from damage, tripping, and animal damage when installed on the surface. When installed correctly, fiber-optic cable can run for decades, even in saturated environments.

The fiber-optic cable generally costs a few dollars per meter but can be more for harsh environments. Interrogators can cost $50K to $100K for purchase, with costs currently elevated due to tariffs, and can be more for research-grade instruments. Interrogators can be rented/leased for approximately $1,500-$2,500 per week. Costs for interrogators are expected to decline as the technology gains more widespread use.

4.13 Tools for Understanding Chemical and Biological Processes

Evaluating chemical and biological processes of contaminants is a critical component of the CSM. Natural source zone depletion (NSZD) and natural attenuation of contaminants occur through a variety of processes, including physical processes such as dilution, sorption, and diffusion; chemical processes such as abiotic degradation; and biological degradation. The following sections are meant to provide an awareness of some ASCT that can be applied in the evaluation of NSZD or natural attenuation, but this guidance document does not describe attenuation processes, NSZD processes, or tool details, because such information is provided in the following:

- ITRC's 2018 LNAPL Update (LNAPL Technologies Appendix, NSZD Appendix) provides detailed information on the evaluation of NSZD for LNAPLs (ITRC 2018)
- ITRC's 2010 Decision Framework for Applying Monitored Natural Attenuation Processes to Metals and Radionuclides in Groundwater details the application of EPA's three-volume technical background series on attenuation for metals and radionuclides in groundwater (ITRC 2010a)
- ITRC's 2007 Decision Flowchart for the Use of Monitored Natural Attenuation and Enhanced Attenuation at Sites with Chlorinated Organic Plumes (ITRC 2008)
- ITRC's 2013 Environmental Molecular Diagnostics Guidance and 2011 Environmental Molecular Diagnostics Fact Sheets provide detailed information on the application of molecular diagnostic tools for the evaluation of natural attenuation of VOC (ITRC 2013)
- American Petroleum Institute (API) Publication #4784 Qualification of Vapor Phase-related Natural Source Zone Depletion Processes (API 2017)
- Cooperative Research Centre for Contaminated Site Assessment and Remediation (CRCCare 2018)
- Technical Report 44: Technical Measurement Guidance for LNAPL Natural Source Zone Depletion (CRCCare 2018)
- ASTM Standard E3361-22, Standard Guide for Estimating Natural Attenuation Rates for Non-Aqueous Phase Liquids in the Subsurface (ASTM 2022)

4.13.1 NSZD Tools

Natural source zone depletion (NSZD) refers to the natural biodegradation of NAPL, including both immobile residual and mobile fractions, which occur through the combined action of natural processes to change the composition of NAPL and reduce NAPL mass in the subsurface over time. Key NSZD processes include volatilization, dissolution, and biodegradation of dissolved and vapor phase constituents, as well as the direct microbial degradation of the NAPL itself. Tools presented in this section for determining NSZD activity measure surficial CO_2 efflux, biogenic heat generation, and vertical soil gas gradients from consumption of O_2 and production of CO_2 and CH_4. Details regarding tools and measurement methods can be found in guidance listed in Section 4.13.

4.13.1.1 Dynamic Closed Chambers

The dynamic closed chamber (DCC) system measures CO_2 efflux using a shallow-embedded, ground surface-based flux chamber, typically equipped with a circulation pump and real time gas detector (an infrared gas analyzer). In general, DCC systems are capable of short- or long-term measurements. For NSZD assessments, it is common to perform rapid surveys on the order of several minutes at multiple site locations over the course of several days, providing one snapshot in time of the spatial variation of CO_2 efflux. DCC systems use the rate of increase of CO_2 concentration in a measurement chamber to

estimate the efflux. For such an estimate to be valid and representative, pressure conditions must be similar inside and outside the chamber. To maintain ambient pressure during the various possible weather conditions, the chambers use a patented pressure vent. It is assumed that all petroleum hydrocarbon vapors, including methane, in the unsaturated soil zone are converted to CO_2 and that the LNAPL degradation rate can be estimated from stoichiometric considerations for the biodegradation of a representative petroleum hydrocarbon compound.

4.13.1.2 Fossil Fuel Trap

The fossil fuel trap (also referred to as a passive CO_2 flux trap) captures the CO_2 emanating from the soil surface over a multiday or multiweek duration of time. After field deployment (shallow embedded), the traps are collected, capped, and then shipped back to the vendor for laboratory analysis. Knowing the cross-sectional capture area and the deployment time, the cumulative CO_2 mass released by the soil (and captured by the trap) is then used to calculate the flux. Similar to the DCC, it is assumed that all petroleum hydrocarbon vapors, including methane, in the unsaturated soil zone are converted to CO_2 and that the LNAPL degradation rate can be estimated from stoichiometric considerations for the biodegradation of a representative petroleum hydrocarbon compound. The standard practice for passive flux traps is to analyze both total carbon and ^{14}C (radiocarbon dating by atomic mass spectroscopy) to differentiate the contributions to the sample from modern CO_2 (background generated from natural organic matter in the soil) and fossil fuel CO_2 (generated from biodegradation of LNAPL contaminants).

4.13.1.3 Heat Sensing

The heat released from vadose zone microbial degradation can result in a two-dimensional temperature profile that peaks in the heart of the CH_4 oxidation zone (temperature anomaly) when compared to background locations or modeled subsurface temperatures.

Vertical subsurface temperature profiling can be accomplished using temperature monitoring devices such as off-the-shelf temperature loggers or thermocouples capable of measuring temperature changes on the order of 0.1°C, assembled in a vertical multilevel arrangement. For a snapshot picture of NSZD activity at a site, a string of loggers and thermocouples can be deployed short term (on the order of hours) in existing site wells to collect vertical temperature profiles, allowing a site to be assessed in days to weeks. For longer term evaluations, a string of dedicated loggers or thermocouples can be installed in existing wells, or a network of multidepth devices can be installed directly in the ground so that there is direct thermal communication with subsurface soils. Quantification of the NSZD rate from the biodegradation heat signal (temperature gradient) involves evaluation of the heat flux followed by conversion to an NSZD rate using the heat released from the biodegradation reaction.

4.13.1.4 Direct Gas Measurement

The confirmation of methanogenic conditions (O_2 depletion, CH_4 and CO_2 production) in the vadose zone provides a line of evidence of NSZD activity. The flux of the gases (mass flow per unit area per unit time) can be determined from soil gas measurements taken at discrete depths. Because NSZD directly impacts both O_2 and CO_2, either the diffusive flux of O_2 (consumption) or CO_2 (production) can be stoichiometrically equated to an NSZD rate (equivalent LNAPL mass loss rate) (CRCCare 2018). Multidepth soil gas probes installed directly into the soil provide one method of measurement for soil gas concentration profiles. Additionally, soil gas measurements can be collected at multiple depths in existing wells using a multigas analyzer (or combination of analyzers) for O_2 (0%-25% vol), CO_2 (0%–100% vol), and CH_4 (0.5 ppm–100% volume). It may be necessary to use a CH_4-specific meter, such as the Landtec SEM5000, for the required CH_4 measurement range.

4.13.2 Natural Attenuation Tools

Natural attenuation processes are those that effectively reduce contaminant concentrations in groundwater. Natural attenuation relies on naturally occurring destructive mechanisms such as biodegradation and chemical reactions and nondestructive mechanisms such as sorption, dispersion, dilution, and volatilization to reduce contaminant concentrations in groundwater. Tools mentioned in this document for assessing natural attenuation activity measure presence of microbes or activity of biodegradation, transformation of chemicals in the environment, degradation of contaminants, and chemical changes. Detailed information regarding tools and measurement methods can be found in guidance listed in Section 4.13.

4.13.2.1 Molecular Diagnostic Tools

Many natural attenuation and enhanced remedies rely on biological processes to degrade contaminants to achieve remedial goals. Molecular diagnostic tools are laboratory-based techniques to evaluate microbial communities in environmental samples, such as soil or groundwater, to provide direct or indirect lines of evidence for the degradation potential. Molecular diagnostic tools analyze biological molecules such as deoxyribonucleic acid (DNA), ribonucleic acid (RNA), enzymes, proteins, or lipids and include analyses such as quantitative polymerase chain reaction (qPCR), meta-omics, phospholipid fatty acid (PLFA), fluorescent insitu hybridization, microarray, proteomics, metabolomics, and enzyme activity probes. ITRC's 2013 Environmental Molecular Diagnostics Guidance and 2011 Environmental Molecular Diagnostics Fact Sheets provide detailed information on the application of molecular diagnostic tools for the evaluation of natural attenuation of VOC.

4.13.2.2 Stable Isotope Techniques

Stable isotope techniques quantify the isotopic composition of individual elements within chemicals. Commonly used examples include carbon, hydrogen, nitrogen, oxygen, and chlorine. There are many applications for stable isotope techniques, including to distinguish between physical, chemical, and biological attenuation and to quantify the extent of chemical and biological degradation.

Compound-specific isotope analysis (CSIA) is a laboratory-based method for the determination of the isotopic composition of individual elements within multiple chemicals present in the water sample. Field sampling can be completed using standard methods, and the analysis is available through several commercial laboratories. The evaluation of the CSIA results is complex and is not discussed further. ITRC's 2013 Environmental Molecular Diagnostics Guidance and 2011 Environmental Molecular Diagnostics Fact Sheets provide detailed information on the application of CSIA.

Stable isotope probing involves "spiking" with an isotopically labeled chemical and measuring the change in isotopic composition over time to directly measure the extent of degradation. Field sampling requires deploying and retrieving the spiked chemical in a BioTrap or similar, and specialty laboratory analysis. Further considerations for sample collection, sample handling, quality control, and analysis are presented in ITRC's 2013 Environmental Molecular Diagnostics Guidance and 2011 Environmental Molecular Diagnostics Fact Sheets. (ITRC 2013).

4.13.2.3 Iron Content Determination

Abiotic degradation has been demonstrated to occur under a variety of conditions due to the mineralogy of the subsurface, specifically iron mineral content. One method for the quantification of iron minerals is magnetic susceptibility (Wiedemeier et al. 2017), which is a technique used to screen for the presence of magnetite. Field-portable detectors are available and laboratory-based commercial analyses are also available. Another laboratory-based analysis that is available commercially is X-ray diffraction (XRD). The

2009 USEPA guidance document Identification and Characterization Methods for Reactive Minerals Responsible for Natural Attenuation of Chlorinated Organic Compounds in Groundwater provides further detail on the abiotic processes and methods for characterization.

4.13.2.4 Min-Trap

The Min-Trap is an insitu passive monitoring sampler that collects mineralogical data to inform natural attenuation and enhanced biodegradation processes that rely on the formation, dissolution, and transformation of solid-phase minerals (Divine et al. 2023). For example, the abiotic degradation of chlorinated volatile organic compounds through interaction with reactive minerals is a recognized important process, and Min-Traps are well suited to document the formation of these minerals during remediation (Divine et al. 2023).The Min-Trap consists of a solid porous medium contained within a nylon mesh that is deployed in a monitoring well. The porous medium serves as the solid substrate upon which minerals form, and chemical, microscopic, or other techniques can be applied to quantify the minerals that formed insitu (Ulrich et al. 2021). See ITRC PSU-1 Passive Sampling Technologies—Passive Sampling Technologies Update Section 5.3.6 for more information on Min-Trap Samplers (ITRC 2024).

4.13.2.5 CoreDFN

Contaminant distribution in low-permeability zones, preferential migration pathways, groundwater plume retardation, and contaminant mass storage serving as a secondary source are all important aspects of natural attenuation. Evaluation these factors leads to better understanding of dissolved-phase plumes, as each factor influences long-term plume behavior and remedial timeframes, but these factors are challenging to evaluate at fractured-rock sites. In particular, back diffusion has been recognized as a significant process that can serve as a secondary source of groundwater contamination (Parker 2007). Chemicals diffuse into low-permeability zones such as clay or bedrock due to concentration gradients when groundwater concentrations are high and then act as a secondary source when groundwater concentrations are low. Core Discrete Fracture Network (CoreDFN) is a propriety sampling and analysis approach that relies on high-frequency sampling of bedrock to assess contaminant distribution in both the secondary porosity (fractures) and primary porosity (matrix) (Parker and Cherry 2011). It was developed by Dr. Beth Parker at the University of Guelph and is offered commercially.

5 BOREHOLE GEOPHYSICS

Borehole geophysical tools provide high-resolution geologic and hydrogeologic data that aid in developing the CSM. These tools have been applied for decades to improve site characterization but are generally underused due to lack of understanding or awareness, but advancements in data accessibility and visualization capabilities have reduced this awareness gap. Borehole geophysics is best applied for obtaining structural geologic features, for finding groundwater and characterizing hydrogeologic properties of the subsurface materials in fractured bedrock or consolidated or semiconsolidated sediments, and to a lesser degree, for obtaining characteristics of the borehole fluids. Some borehole geophysical tools can also be used to assess conditions in wells to support selection of well maintenance and optimization measures or for the selection of well screen intervals or overall well design. Most of the borehole geophysical tools discussed can be used in existing bedrock, consolidated to semiconsolidated sediment boreholes, or cased wells as a cost-effective alternative to drilling.

The tools presented in this guidance document can provide information concerning the physical (lithology), hydraulic (flow zones and velocity), and chemical (dissolved solids) aspects of the subsurface. Borehole geophysics can provide relatively quick subsurface information without incurring significant additional costs. Typically, a suite of tools is deployed either simultaneously or in sequence, and the results of each are integrated to infer subsurface characteristics. Combinations of tools (see USGS Fractured Rock Geophysical Toolbox Method Selection Tool (USGS 2016a) are appropriate for particular geologic environments and to describe the particular geologic properties that affect contaminant distribution, transport, and fate that inform decisions regarding remedial approaches.

The following are resources for describing and selecting borehole geophysical tools for various applications:

- ASTM Standard D5753-18. Standard Guide for Planning and Conducting Borehole Geophysical Logging (ASTM 2018)
- A Fractured Rock Geophysical Toolbox Method Selection Tool. Groundwater (Day-Lewis et al. 2016)
- ITRC 2017 Characterization and Remediation of Fractured Rock (FracRx-1) (ITRC 2017)
- Borehole Geophysics Applied to Ground-water Investigations (Keys 1988)
- Selecting Geophysical Logs for Environmental Applications (Keys et al. 1993)
- Review of Geophysical Techniques to Define the Spatial Distribution of Subsurface Properties of Contaminants (Murray et al. 2005)
- ASACE Engineering and Design: Geophysical Exploration for Engineering and Environmental Applications (USACE 1995)
- Use of Airborne, Surface, and Borehole Geophysical Techniques at Contaminated Sites (USEPA 1993b)

5.1 How to Select and Apply Borehole Geophysical Tools Using This Guidance Document

The borehole geophysics tools evaluated in this section are categorized by the types of data collected, as shown in **Figure 5-1**.

The **ASCT-2 Technical Selection Matrices: BG Matrix** is meant as a quick guide to point to the specific downhole tool(s) needed to fill data gaps in the CSM. The specific tools discussed in this section are

presented as columns, and subsurface CSM questions with limitations are presented as rows. Color coding of the intersecting cells indicates the acceptability of the tool to the condition or limitation (green for "yes," red for "not recommended" or "not suitable").

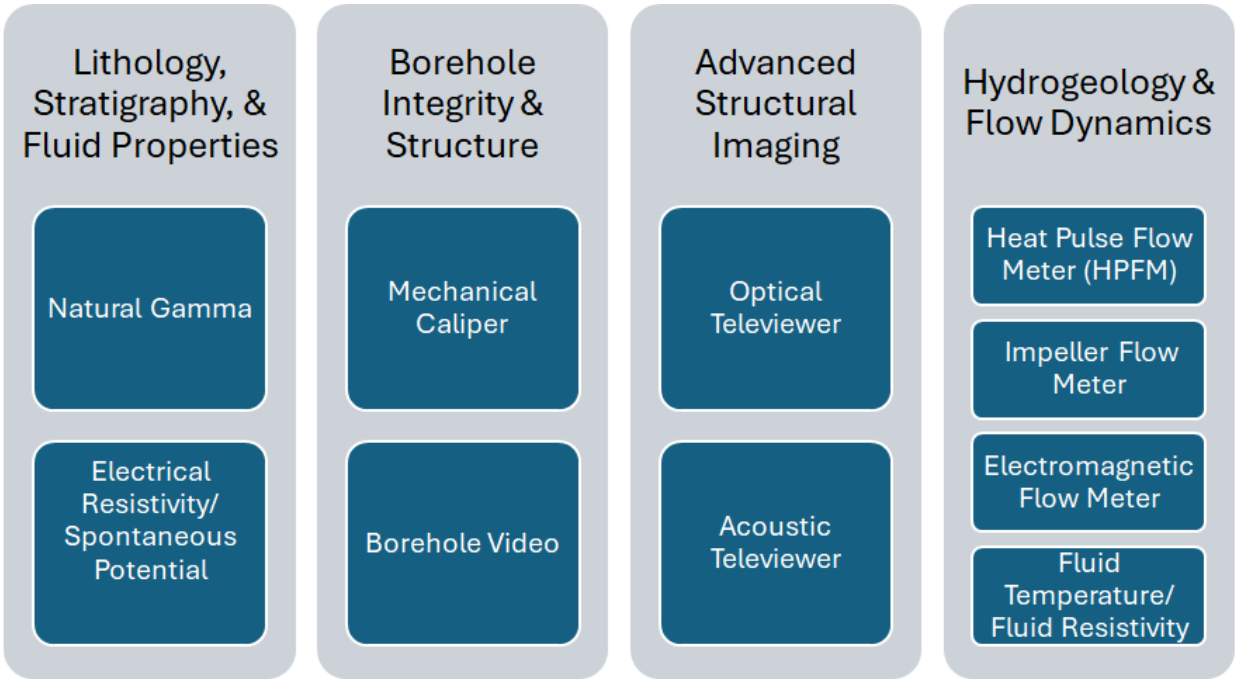


Figure 5-1. Borehole geophysics tool summary.

Preparing a borehole geophysical tool logging program includes identifying the key project parameters and objectives, selecting the most appropriate geophysical tools, and communicating with the geophysicist. Before selecting a borehole geophysical tool, it is important to understand the parameters the tool can measure and the site-specific conditions the tool requires to acquire the data. Each of the tools listed in the columns of the Borehole Geophysics Technology Selection Matrix is discussed in the subsections of this section. However, a suite of commonly used tools for hydrogeologic analysis of fractured bedrock includes the following tools: fluid temperature, fluid resistivity, mechanical caliper, optical televiewer, acoustic televiewer, natural gamma, heat pulse flowmeter, and impeller flowmeter.

The borehole geophysical program development and tool selection should consider the following:

- project and DQO
- local and regional geology
- site-specific logging logistics
- drilling methodology
- anticipated borehole conditions
- log analysis
- cost

The following subsections present several borehole geophysical tools, including their advantages, disadvantages, usage, and how to interpret the resulting data. In almost all instances, more than one tool will be necessary to provide the data required, and a number of the tools described below can be used

concurrently. By using different tools to collect similar data, supporting evidence is provided and data confidence for site characterization is improved.

5.1.1 Tool Availability

The majority of borehole geophysical investigations involve the application of multiple tools, most of which are readily available. As noted in the **ASCT-2 Technical Selection Matrices: BG Matrix**, a standard suite of downhole tools is commonly employed for borehole characterization. Less commonly used tools (for example, nuclear magnetic resonance (NMR)) may require extra coordination with the geophysicist to confirm tool availability and application. It is critical to communicate with the geophysical contractor or operator to ensure project objectives are met, data of known quality are collected, and an accurate schedule and cost is received. Critical site information must be provided to the geophysicist, such as geology, depth to groundwater, borehole conditions, well construction, estimated logging footage, field schedule, and site accessibility.

5.1.2 Data Collection Design

Data collection and reporting are important components of geophysical logging programs. Data acquisition and processing are typically provided by a geophysical contractor or qualified practitioners who can purchase or rent the necessary equipment and perform the work themselves. Data processing includes establishing a set datum for depth or elevation matching between geophysical logs, correcting borehole effects, converting log measurements to parameters of interest, and merging logs into a presentable format. A geophysical contractor may not provide data analysis and interpretation unless explicitly requested to do so. Hence, it is important to discuss expectations prior to initiating work so that budgets can be adjusted accordingly.

To effectively communicate with the geophysicist on appropriate tool selection and ensure quality data are collected in a cost-effective manner that meet the project objectives, a good basic understanding of each tool's physical limitations, data processing methods and limitations, and data analytical methods is recommended.

Borehole logging results may vary depending on the skill and experience of the field personnel. Borehole geophysical logs are typically generated from continuously acquired, objective, and repeatable data from which desired parameters can be qualitatively or quantitatively derived. Geophysical logs provide a significant amount of high-resolution data on lithology, hydrogeologic parameters, and pore fluid characteristics in or near the borehole. While these borehole logs represent detailed vertical interpretations, they must be compared to other on-site borehole logs to provide a planar or horizontal interpretation that can potentially be extrapolated across the site. Multiple parameters can be measured using different tools and the results validated using multiple lines of evidence along with other investigative data for site interpretation.

Borehole geophysical logs can (and should) be correlated between multiple borehole locations, providing stratigraphic and structural information, and can be corroborated with lithologic data from standard drilling techniques. This correlation allows the overall geologic framework to be portrayed in 2D and 3D representations (**Figure 5-2** and **Figure 5-3**). These tools can identify and quantify various bedrock structural features, such as formation contacts and fracture location and orientation. These data can then be correlated between wells. In sediments and sedimentary bedrock, the correlation process uses characteristic curve matching and relies on principles of stratigraphy and sedimentary depositional processes such as original horizontality and Walther's law. These principles state that stratigraphic facies and facies sequences commonly display characteristic compositional and textural changes in the vertical profile that can be observed on geophysical logs and correlated over distances between logs. Once the various facies or facies sequences are identified and correlated, intervals of interest (such as fluid transport pathways) can be assessed and mapped at a site-wide scale.

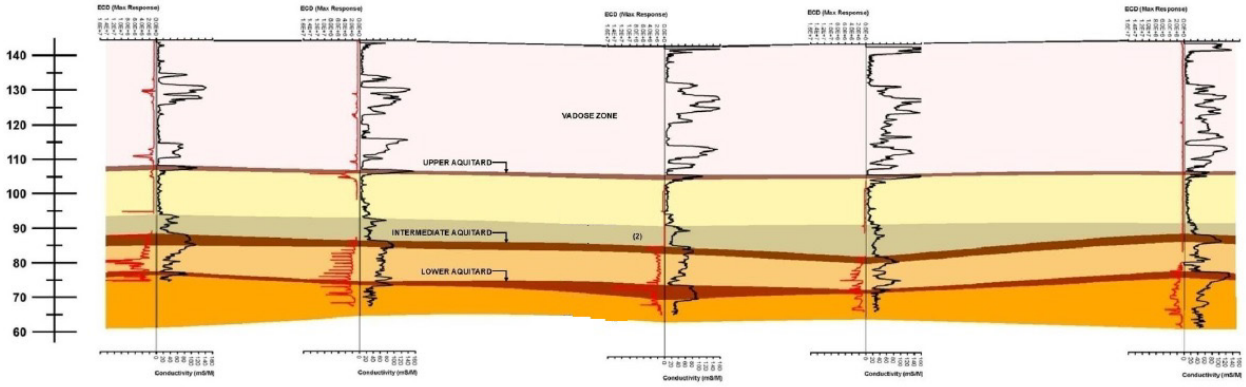


Figure 5-2. View of the overall geologic framework using 2D representation.

Source: ERM. Used with permission.

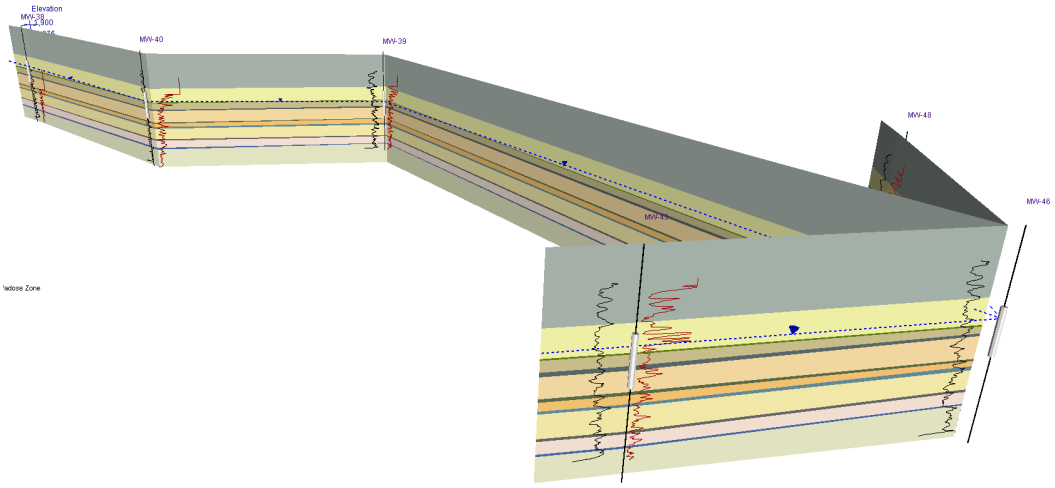


Figure 5-3. View of the overall geologic framework using 3D representation.

Source: ERM. Used with permission.

Whether in sediments or bedrock, the spacing of log data dictates the ability to resolve and correlate features of interest. At the local level, and where closely spaced geophysical logs are available, correlating individual stratigraphic or structural features is usually feasible. For projects where geophysical logs represent locations that are several hundred feet or more apart, only larger scale features that are laterally continuous can generally be correlated. A critical part of data acquisition planning is understanding the spacing needed to resolve and characterize geologic features of interest based on the conceptual model for the local geology (the representative scale for the site).

5.1.3 Technical Advantages and General Limitations of Fundamental Logging Tools

The suite of fundamental borehole logging tools is a comprehensive set of tools intended to enhance characterization of bedrock and fractured rock systems. All of these tools are widely available for use by qualified geophysicists and logging personnel. The tools are intended to be used in a collaborative fashion, as shown in several of the “composite log” examples below. Amalgamation of data returned from individual tools builds a conceptual framework for fluid flow in fractured bedrock aquifer systems or

contaminant migration in consolidated or semiconsolidated sediments or rock and is a critical CSM component. Many of these tools are readily deployed during a single day's worth of logging and do not involve significant independent costs beyond daily rates offered by geophysical service providers. Key technical advantages of these tools include the following:

- Post processed data offer a visually familiar record understood by many.
- High-resolution data are easily and rapidly obtained at sub-cm (or lower) accuracy.
- Use of these tools and supplements may replace or reduce the need for rock-core collection and visual logging during bedrock characterizations.
- Downhole tooling and surface cables allow the rapid interchange of probes, sondes, and detectors during logging.
- Select tools can be deployed in both cased and uncased hole settings, which can be advantageous at some sites.
- The combination of tools collectively supports lithologic and structural determinations of bedrock or sediment structure and hydraulic conditions.
- Iterative deployment of tools provides detailed information that assists in the interpretations of other logs. For instance, use of the caliper tool assesses borehole diameter in advance of gamma logging.
- Under certain circumstances, key information may be obtained across air-filled zones.
- Several of the tools provide a useful first step toward determining flow into or out of the borehole independently of more detailed borehole flowmeter assessments.
- They can provide rapid and continuous logs along the length of a borehole, improving spatial resolution compared to point sampling.

While there are inherently more technical advantages associated with the fundamental borehole logging tools described herein, there are a few notable limitations that should be considered when planning a borehole investigation program or interpreting logs. These general limitations include:

- Proper downhole tool performance requires the borehole to be at equilibrium with removal of drilling fluids and residual groundwater. A minimum of 24 hours is recommended subsequent to well completion, development, or pumping prior to well logging to ensure that representative data are obtained. In some formations, it may take longer to establish equilibrium, and an extended period of fluid level monitoring may be necessary to demonstrate that static conditions exist prior to geophysical tool deployment.
- Inadvertent damage to sensitive probes or potential drag-down of contaminants can result from the presence of residual NAPL.
- Well pumps, cables, and other potential infrastructure require removal to allow tools to be lowered and raised in a borehole.
- Certain tools require use of centralizers, which may present a challenge with irregular borehole wall conditions.
- Poor well construction can cause degradation of image and data quality.
- An adequate column of water must be present to allow for proper tool function.
- Select tools require a minimum borehole diameter.
- Well construction can limit some tools (for example, cased versus uncased boreholes, PVC versus metallic casings).

- Electromagnetic interference from nearby infrastructure, power sources, pumps, or metallic components can affect certain logging measurements.
- Radioactive, nuclear magnetic resonance, or other specialized logging methods may be subject to regulatory, permitting, site-access, or health-and-safety restrictions.
- Practitioners should always take care to identify and understand the implications for any materials that are introduced into wells or boreholes.

Contractors typically report planar features orientation data relative to magnetic north. A correction to true north may be required using local magnetic declination. In addition, adjacent subsurface conditions can prevent accurate magnetic measurements (for example, basaltic dikes, magnetite precipitation in LNAPL sites, metallic debris).

Interpretation of individual tools may be less accurate in highly variable or complex lithologies, unless supplemented by additional data from multiple tools.

A field geologist familiar with the local geology and hydrogeology should be present during data acquisition to assist in evaluating real-time data and identifying potential issues. As with other borehole logging tools, site-specific information (such as location, elevation, well construction details) should be recorded in the log headings for future reference.

5.2 Fluid Temperature

5.2.1 What Is the Technology?

Fluid-temperature logging involves using a downhole probe to continuously record the temperature of fluids in a borehole. During logging, a probe is incrementally lowered to directly measure changes in temperature using a thermistor or platinum sensor to estimate geothermal gradients of groundwater or other fluids in direct contact with the probe. Temperature logging is commonly used in fluid-filled bedrock boreholes to assess flow into or out of the borehole under either static or dynamic conditions. During field application, fluid temperature is routinely logged concurrently with fluid resistivity (or conductivity), based on the current configuration of most commercially available tools that combine both tools on the same sonde, and are commonly used during the first run. Refer to Section 5.3 for a description of the fluid-resistivity tool; **Figure 5-4**).

Under static conditions, borehole fluid temperature equilibrates with the surrounding formation and reflects the local geothermal gradient. Deviations from the expected geothermal gradient (approximately 1°F per 100 ft) indicate fluid movement within the borehole. Reduced gradients with minimal temperature variation suggest vertical flow, whereas elevated gradients can denote inflow or outflow at transmissive zones.

A continuous profile of borehole temperature is also a useful first step prior to deploying a borehole flowmeter or caliper to identify potential zones of flow into or out of a borehole (Section 5.7).

5.2.1.1 Data Collection Design

Fluid-temperature logging is typically one of the first tools to be used in borehole logging. Because temperature logging generally occurs downward in a borehole, fluid-temperature logging is performed prior to using tools that are logged upward to minimize water-column disturbance.

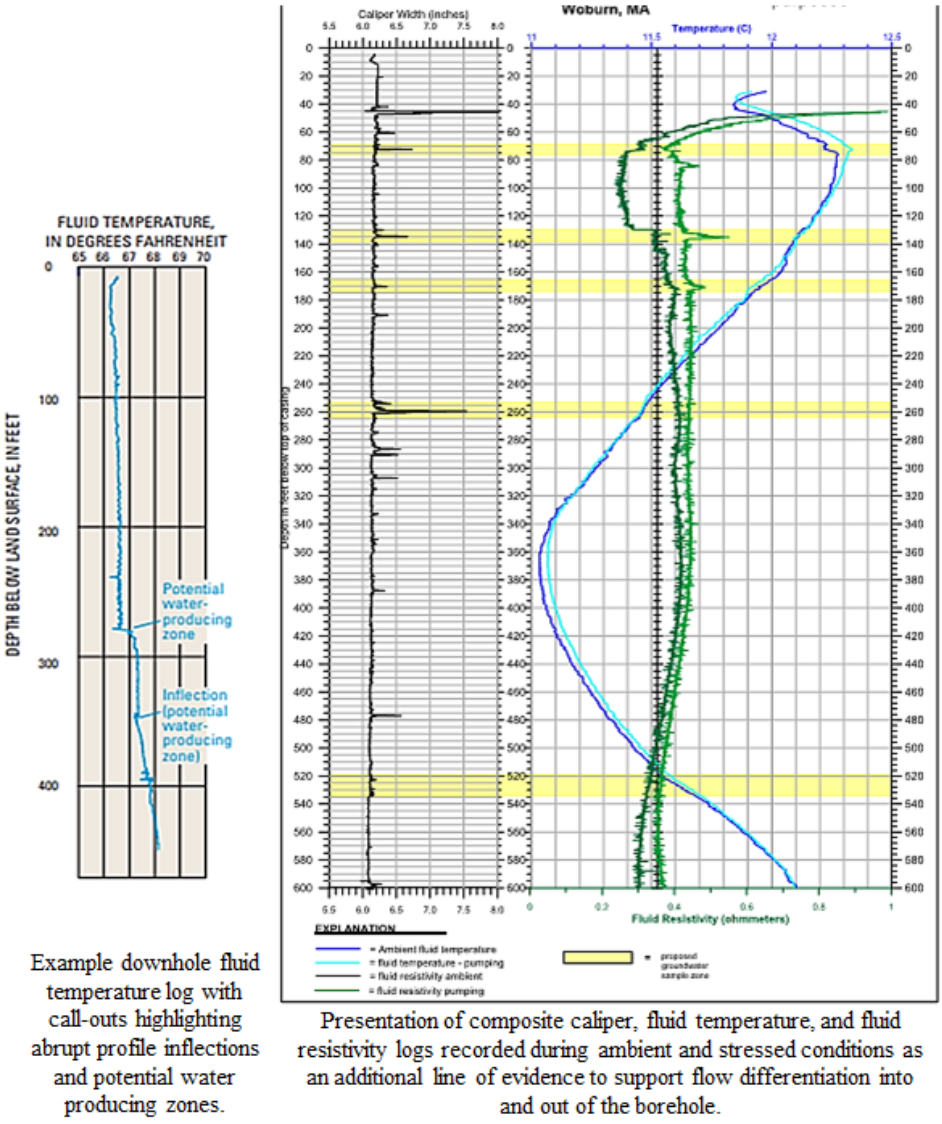


Figure 5-4. Examples of downhole fluid temperature log and composite logs.

Source: Left–Borehole Geophysical Logging of Water-Supply Wells in the Piedmont, Blue Ridge, and Valley and Ridge, Georgia (USGS 2007) and Right–Woodard & Curran. Used with permission.

5.2.2 How Is the Technology Used?

Fluid-temperature logging helps quantify geothermal changes and assess the flow of groundwater within a borehole (**Figure 5-5**). The tooling is easily deployable using a downhole winch and pulley system with a depth encoder to determine vertical accuracy. To minimize fluid disturbance while the borehole is at equilibrium, the tool should be lowered, rather than raised, while gathering data.

Abrupt changes in fluid temperature may correspond with zones with a discrete inflow or outflow of water from the borehole. Plotting the continuous-temperature profile as one track or strip along with results and data from other traditional logging tools corroborates interpretations using multiple lines of evidence.

Fluid temperature data are often used to identify potential flow zones that can be subsequently evaluated using additional tools, including caliper, heat pulse flowmeter, optical or acoustic televiewer tools, or any of the electrical property tools, all of which are discussed in subsequent sections of this guidance document. Additionally, fluid temperature logging can occur while the borehole is under stress (dynamic conditions) by pumping to potentially enhance water-bearing zone identification.

5.2.2.1 Log Interpretation

Fluid-temperature logs provide an index of temperatures in a borehole. Groundwater temperatures often vary based on flow conditions, and small-scale changes are a useful indicator to assess inflections on a downhole basis. The sub-centimeter accuracy of temperature logging may be used to estimate where flow is occurring, and corroboration by similar deviations in other logs and borehole wall images can suggest fracture locations. Thus, side-by-side comparison of multiple tool logs is a critical component of data interpretation.

Figure 5-5 provides an example composite log of fluid temperature along with fluid resistivity, natural gamma, ATV (borehole image developed from ultrasonic frequency), acoustic caliper (application of ATV travel times to generate acoustic borehole log based on borehole diameter), and tadpole plots used to denote structural orientation of planar features.

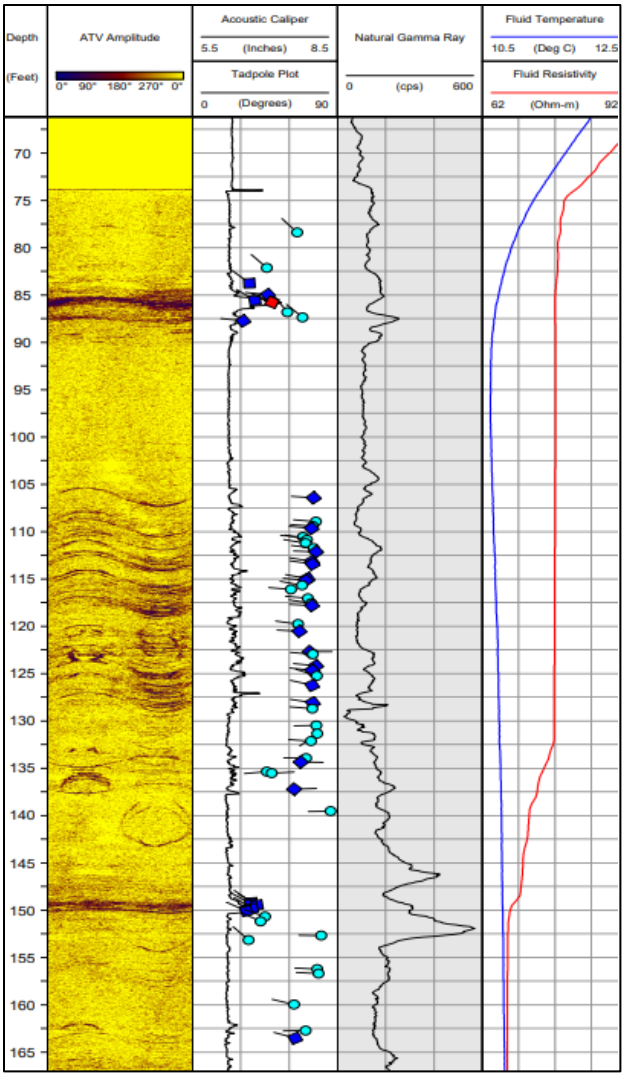


Figure 5-5. Example composite log of fluid temperature (blue line) along with fluid resistivity (red line), natural gamma, acoustic, acoustic caliper, and tadpole plots used to denote structural orientation of planar features.

Source: Image adapted from borehole geophysical logs included in the Remedial Investigation Report for the Savage Municipal Water Supply Superfund Site, Milford, NH, prepared by Weston Solutions Inc., March 2014). Used with permission.

5.2.3 What Are the Advantages?

Fluid temperature is an inexpensive, quick, and durable method to initially characterize potential flow intervals into and out of the borehole to guide the need or techniques for additional investigation and to assist in CSM development.

Temperature sensor requires little to no ongoing maintenance and calibration depending on the site-specific DQOs.

5.2.4 What Are the Limitations?

There are several conditions that can limit the use of fluid temperature tools. To collect temperature measurements, boreholes must have sufficient fluid-filled volume. Although it is preferred to be completed before the borehole is cased, nonmetallic casing (PVC) may be used. Additionally, clean borehole conditions are preferred; therefore, well development is recommended prior to using the tool. Fluid temperature tools provide gross measurement of borehole fluid transfer into and out of the borehole, so there must be sufficient fluid flow into or out of a borehole for temperature changes to be measured. As such, it should be used with other borehole geophysical ASCT.

5.3 Fluid Resistivity (or Conductivity)

5.3.1 What Is the Technology?

Fluid-resistivity logging uses a downhole probe to continuously record the electrical resistance of the fluid in a borehole using a series of electrodes. The downhole resistivity sounding incorporates multiple electrodes for real-time measurement. The electrodes are configured in a stacked array to minimize interferences during logging. Based on interpretations of the generated fluid-resistivity logging profile, areas of inflow or outflow to/from the formation into or out of the borehole are differentiated and then corroborated by changes in fluid temperature, caliper measurements, and other downhole geophysical measurements and readings.

Fluid resistivity notably is the inverse of fluid conductance or fluid conductivity and provides a record of changes in the dissolved-solids concentration measured as ohm-meters (Ωm). Many of the tools currently in use have reverted to logging fluid conductivity, typically measured as microsiemens per centimeter (µS/cm). It is important to establish the preferred convention prior to logging. Many practitioners prefer to retain the convention of expressing logging results as fluid conductivity for consistency with direct-instrument reading (if such a tool is employed). Expressing logging results as fluid conductivity is also preferred for comparison with other direct-read multiparameter instruments used during groundwater investigations, where specific conductivity is measured prior to groundwater sample collection. Specific conductance (SC) can be converted from fluid resistivity as provided in **Equation 5-1**.

$$SC\ (uS/cm) = 10{,}000 * (1 / \text{fluid resistivity}(\Omega m))$$

Equation 5-1. Conversion of specific conductance from fluid resistivity.

Electrical current flow (and its resistivity) within a formation is governed primarily by fluid-filled pore spaces and the relationship of pore interconnectivity, volume, fluid composition, and temperature. Formation lithology also affects resistivity properties based on mineralogic assemblage and geochemical changes resulting from hydrothermal alteration. The interrelationship of these formation properties and the general ease of fluid-resistivity logging using traditional and commercially available tools has led to resistivity logging in support of various applications, including mineral explorations, oil and gas evaluations, and hydrogeologic assessments. Similarly, due to the strong dependence of fluid resistivity on the presence of dissolved solids, logging is often used to evaluate salt water and freshwater interaction in coastal aquifers.

5.3.1.1 Data Collection Design

Fluid-resistivity logging is conducted using wireline methods in a similar manner as most other borehole geophysical logging tools and is generally acquired in open (uncased), fluid-filled boreholes; however, although not preferred, nonmetallic-cased boreholes can be used as long as there is direct contact with the water column (screened interval).

Fluid-resistivity logging should be performed early in the logging process along with other primary tools (caliper and fluid temperature) to capture the static and undisturbed state of the borehole. Additionally, logging fluid resistivity early best represents the ambient conditions in the boring.

As with other borehole geophysical tools, logging at a single location provides parameter data only in the immediate vicinity of that location. By logging multiple locations, data can be correlated over greater distances and provide 2D (cross-sectional) and 3D conceptual models. The density of well locations to be logged should be based on the stratigraphic framework and the nature of features that the investigation is attempting to resolve.

5.3.2 How Is the Technology Used?

Fluid-resistivity logging is conducted in primarily fluid-filled open boreholes. Prior to fluid resistivity logging, the borehole should be flushed of drilling fluids and borehole fluid additives and given time to equilibrate. Fluid resistivity logging can also be conducted while the borehole is under stress from pumping to facilitate identification of intervals where water is entering the borehole.

Fluid resistivity is commonly logged concurrently with fluid temperature as an additional line of evidence to delineate hydraulically active zones and identify flow conditions within a borehole. This parameter is generally recorded earlier in the logging process to gain a relative understanding of flow in and out of the borehole before the water column has been disturbed by other logging tools. Downhole resistivity probes are typically combined with a temperature thermistor in one probe. Fluid resistivity logs are also used in hydrophysical logging investigations that require borehole fluid replacement with deionized water (as mentioned below in Section 5.7) to identify and monitor where water enters or exits

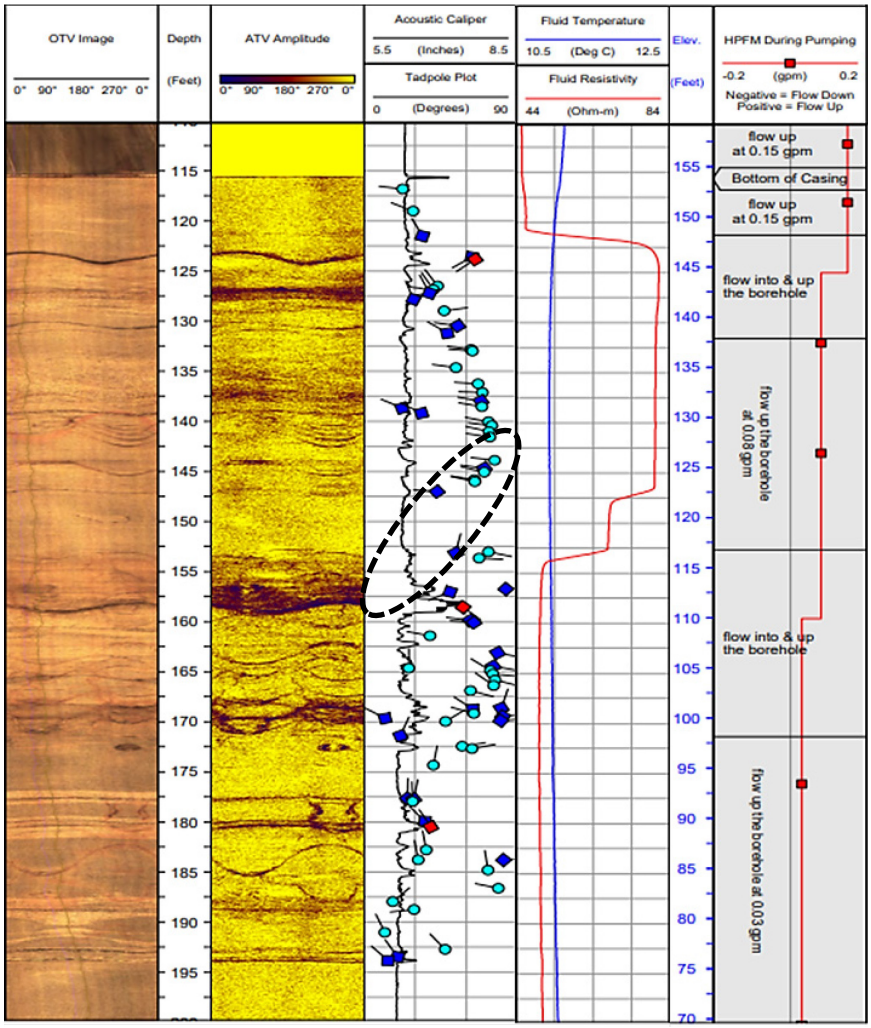


Figure 5-6. Example borehole log including optical and acoustic televiewer, inferred structural characteristics (tadpole plots), fluid temperature (blue line), fluid resistivity (red line), and stressed HPFM measurements.

Source: Image adapted from borehole geophysical logs included in the Remedial Investigation Report for the Savage Municipal Water Supply Superfund Site, Milford, NH, prepared by Weston Solutions Inc., March 2014). Used with permission.

the borehole based on contrasts in resistivity.

5.3.2.1 Data Interpretation and Presentation

Resistivity log data are usually processed and can be displayed in real time. An example log is provided in Figure 5-6, along with a subset of key geophysical logging parameters. The dashed oval in the figure highlights the fluid-resistivity deviation that occurs above a notable fracture at a depth of approximately 158 ft and concurrent with a change in flow in the heat-pulse flowmeter (HPFM) log.

5.3.3 What Are the Advantages?

Fluid resistivity (or conductivity) logs are influenced by a number of parameters of the fluid in the borehole. Principally, measurements are related to the quantity of total dissolved solids (TDS) or total suspended solids (TSS) in the formation fluid. For example, salt water has a very low resistivity (high conductivity) and vice versa for fresh water. Hydrocarbons will also have very high resistivities. Additionally, while slower logging speeds allow for longer equilibration time for the probe within a formation, fluid resistivity logging can be accomplished at typical logging speeds of up to 40 feet per minute (USEPA 2025b).

5.3.4 What Are the Limitations?

Fluid resistivity logs should not be interpreted by themselves. Simply knowing the resistivity of fluid in a formation does not provide sufficient information to identify lithology or fluid types. Typically, at a minimum, resistivity logs are collected alongside fluid temperature, spontaneous potential (SP), and caliper logs, which together provide enough data to begin making scientific interpretations and develop a CSM. Fluid resistivity should be logged in open boreholes after borehole stabilization (after drilling fluids have been flushed from the borehole). Measuring fluid resistivity in existing cased borings is not the preferred methodology, as it may not be representative of actual conditions. Additionally, for the same reason, it is not recommended in older, disturbed borings.

Resistivity logs measure electrical resistivity, which is affected by a number of factors, including temperature, drilling-fluid resistivity, borehole diameter, mud cake, and drilling-fluid invasion. To use resistivity logs for quantitative analyses, these factors must be documented during logging and recorded in the log headings so they can be factored into the evaluation of the data.

5.4 Mechanical Caliper

5.4.1 What Is the Technology?

A mechanical caliper tool provides a vertical profile of borehole diameter often using either a three-armed or four-armed device. During field application, the caliper is lowered to the bottom of the borehole (or lowest desired depth of measurement) and the arms are opened via direct connection to a laptop computer and pulled upward at a steady rate to record data. The spring-loaded arms reach outward against the edges of the borehole wall and the distance from each arm is recorded on the laptop computer in real time. The total spacing from each arm is aggregated to determine average borehole diameter on a depth basis.

Caliper logging is a common geophysical measurement used to evaluate the physical features of a borehole. Caliper logging characteristics can be important measurements to identify washouts, cave ins or voids, swelling, soft spots, etc., within a bedrock formation. These features can be used to identify areas of potential fractures, bedding planes, and preferential flow zones.

5.4.1.1 Data Collection Design

Caliper logging is often among the first geophysical tools to be deployed because of its durability and lower cost compared to video, electrical, or acoustic tools. Caliper logging is performed upward from the bottom of the borehole to the ground surface. As noted below, caliper logs are typically presented with other outputs to readily compare borehole features. The tool can be independently deployed; thus, it can be run at any time during the downhole investigation.

5.4.2 How Is the Technology Used?

5.4.2.1 Use and Application

Mechanical calipers are effective at identifying voids, fractures, and similar openings in borehole walls, but cannot provide information on the orientation or lateral extent of such features. For this reason, the mechanical caliper is commonly used to identify vertical zones where enlargement has occurred. These zones are qualitatively interpreted as intervals where fractures may be present, alterations of the formation along the borehole wall occurred during drilling, or lithologic and depositional voids may be present.

Calipers are also effective, with or without corollary downhole tools, in locating the bottom of well casings, confirming drill casing diameter, and identifying casing breaks.

5.4.2.2 Log Interpretation

A caliper log often includes a corresponding geologic section to demonstrate the possible or likely caliper responses to given strata. Most data interpretation is performed with other standard downhole tool outputs, including natural gamma, fluid temperature, fluid resistivity, and electrical logs (**Figure 5-4**). Aligning complementary log outputs supports the multiple lines of evidence approach emphasized by correlating individual strip logs. When interpreting caliper logs, borehole-diameter deviations alone may not be indicative of fluid flow; therefore, correlation with other logs, notably fluid temperature or resistivity, is required to identify flow into or out of a borehole.

5.4.3 What Are the Advantages?

Mechanical calipers are a simple, cost-effective, wireline technology that collects continuous measurements in most well conditions, including those with high turbidity. Like many other geophysical tools, they are sensitive to borehole deviations and diameter. Calipers containing more arms can easily provide a comprehensive borehole measurement. They can help with early detection of issues associated with borehole instability, including washouts or collapse. As such, mechanical caliper data are essential for log corrections and verifying the accuracy of the other geophysical measurements.

5.4.4 What Are the Limitations?

Since borehole calipers are by definition mechanical, several limitations are associated with that aspect of the technology.

- Caliper tooling is performed from the bottom up and may create disturbance or turbid conditions that could create challenges for optical equipment deployed immediately after.
- Caliper arm type (for example, rod or pad) and number may produce inaccurate readings and affect log results in certain formations (for example, caving holes, unconsolidated sediments,

karst) and irregular or caving holes as they cut or glide along the borehole. Therefore, centralizers are recommended.

- Fracture orientation cannot be determined by caliper logging.
- Mechanical nature does not provide real-time data such as electronic borehole geophysical tools; however, newer types of logging while drilling (LWD) calipers can log in real time, but they are sometimes deemed more unreliable than mechanical calipers.
- Wear of the device is common from the constant motion against the borehole wall and harsh downhole conditions can affect its accuracy; therefore, it is imperative to make sure the caliper is in good working condition.
- Borehole calipers should be used with other borehole geophysical tools.

5.5 Optical and Acoustic Televiewer

5.5.1 What Is Optical Televiewer Technology?

The optical televiewer (OTV) collects a series of ring-shaped optical images at closely spaced discrete vertical spacings as the tool is moved vertically along the path of the borehole (Figure 5-7). Coincident with OTV data acquisition, data are collected by orientation sensors (a magnetometer and accelerometers) within the tool. Acquisition and processing software are used with data from these orientation sensors to produce accurate, precisely oriented, cylindrical images of the borehole (Section 5.5.3.3). The OTV results in a familiar photographic image, as shown in Figure 5-7, which many practitioners refer to as an image log or virtual core.

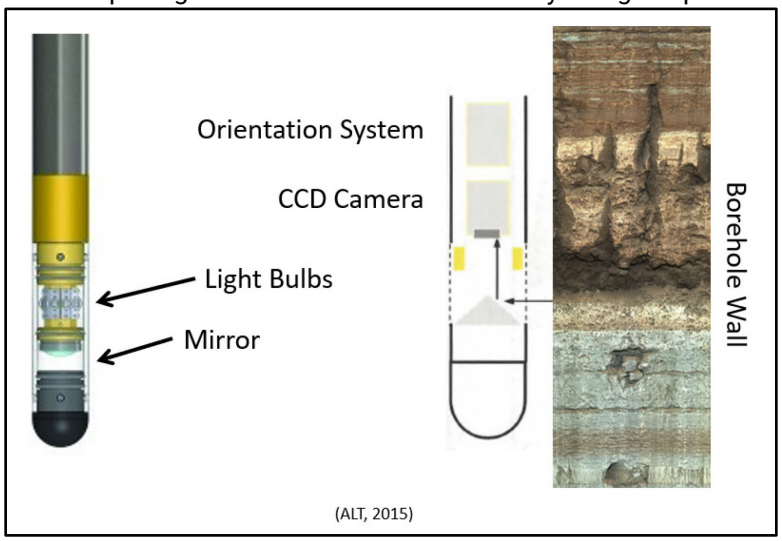


Figure 5-7. Optical televiewer.

Source: Mount Sopris Instruments. Used with permission.

The OTV probes are used during borehole investigations to produce vertically continuous, static images representing conditions at the borehole wall and cased interval in a well.

5.5.1.1 Optical Televiewer Data Collection Design

The quality of OTV data obtained within the water-filled portion of the hole varies significantly with turbidity. As such, logging should be planned to allow time for suspended materials to settle following disturbances resulting from drilling activities, pump removal, or use of other downhole tools.

Chemical precipitation and biological growth may obscure features on the borehole wall; therefore, redevelopment may be appropriate to ensure the best possible image quality in older wells.

In situations where the hole is first cored and subsequently reamed, the smaller diameter core hole may provide a better OTV image, depending on many factors including lithology and drilling characteristics. In some circumstances (such as soft rocks that may be eroded by drilling-fluid movement during coring), a

rapidly drilled air-rotary hole may yield a smoother borehole and a superior image. Consulting with the geophysical logging and drilling contractors during project planning can help identify the best approach at a particular site.

OTV logging speed depends on the selected vertical and horizontal resolution and the system design and cable type. Typical logging speeds for early-generation OTV systems were on the order of 1 m/min (3.3 ft/min) (Williams and Johnson 2004), while the latest generation of tools can be run at 2 m/min to 16 m/min (6.6 ft/minute to 52.5 ft/minute) (Mount Sopris Instruments 2026). Although the latest generation of OTVs are capable of running at higher speeds, the speed is a function of image resolution as well as borehole diameter and the wireline/surface system technology used. Higher speeds produce lower resolution images, so the tradeoff of speed versus resolution should be decided up front in any program. Also, it should be noted that standard OTVs use conventional visible light (RGB) and white LEDs to capture 360° images of a borehole wall; however, advanced models are equipped with specialized UV imaging systems.

Color calibration can be achieved using calibration kits supplied by the manufacturer of the OTV probe. The magnetometer and accelerometers are factory calibrated. Field checks on the magnetometer can be made using a compass and oriented cylinder (Williams and Johnson 2004).

5.5.2 What Is Acoustic Televiewer Technology?

The acoustic televiewer (ATV) uses pulses of ultrasonic acoustic energy to generate an image of the borehole wall. A fixed transducer creates high-speed pulses that are directed to a rotating surface or acoustic mirror within the probe. Energy reflected off the mirror travels through the borehole fluid to the borehole wall. Some of the energy reflects back to the mirror and is reflected to a transducer, where it is detected (Figure 5-8). For each reflected pulse, the amplitude and travel time are recorded. Amplitude is a measure of energy retained in the returning pulse; low amplitudes indicate loss of energy at the borehole wall as a result of soft or fractured rock. Higher amplitudes suggest harder, unfractured rock. Travel time is proportional to distance traveled by the acoustic pulse; where the borehole fluid density is known, borehole diameter can be accurately determined and an acoustic caliper log generated.

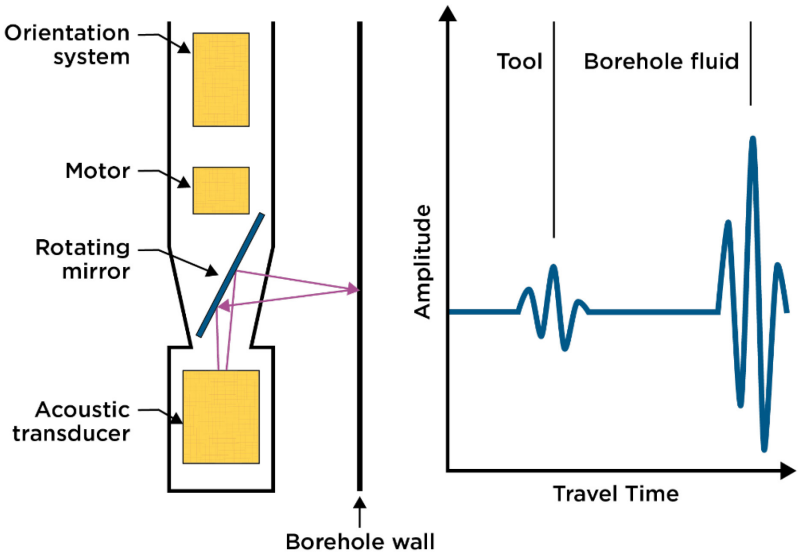


Figure 5-8. Acoustic televiewer.

Source: Adapted by Geosyntec Consultants, Inc., from Mount Sopris Instruments. Used with permission.

The ATV collects up to 360 pairs of amplitude and travel time measurements in each circumferential scan as the tool is moved vertically along the path of the borehole. The vertical spacing between scans depends on tool speed inside the borehole; acquisition software guides selection of logging speed to provide optimal horizontal to vertical resolution. As with the OTV, data are collected by orientation sensors (a magnetometer and accelerometers) within the tool. Acquisition and processing software are used with data from the orientation sensors and the transducer to produce accurate, precisely oriented cylindrical images of the amplitude and travel time (Section 5.5.3.5).

5.5.2.1 *Acoustic Televiewer Data Collection Design*

A key consideration during ATV deployment is the project requirements for vertical and horizontal resolution of the borehole image; this resolution greatly depends on logging speed. Typical logging speeds for early-generation ATV systems were on the order of 1 m/min (Williams and Johnson 2004); the latest generation of tools can be run at 2 m/min to 5 m/min or (ALT 2023)more . Acquisition software should be used to evaluate and adjust logging speed as logging proceeds.

Prior to initiating ATV logging, factors such as the borehole fluid type and level, as well as the borehole condition, should be considered. In general, a better ATV record is obtained in a borehole filled with water instead of drilling mud, so flushing the hole clean before logging may be desirable. Also, adding water to the borehole may allow portions of the borehole above the static water level to be logged, especially for a hole completed in low-transmissivity units.

Probe centralization is especially important for good-quality image data and accurate structure orientation during ATV logging, as shown in **Figure 5-9**. Decentralization on ATV images is indicated by vertically striped transit-time and amplitude images. Adjustable centralizers should be deployed based upon inspection of a mechanical caliper log. Using adjustable centralizers provides a more direct representation of actual borehole diameter compared to the nominal diameter of the tool used during borehole advancement.

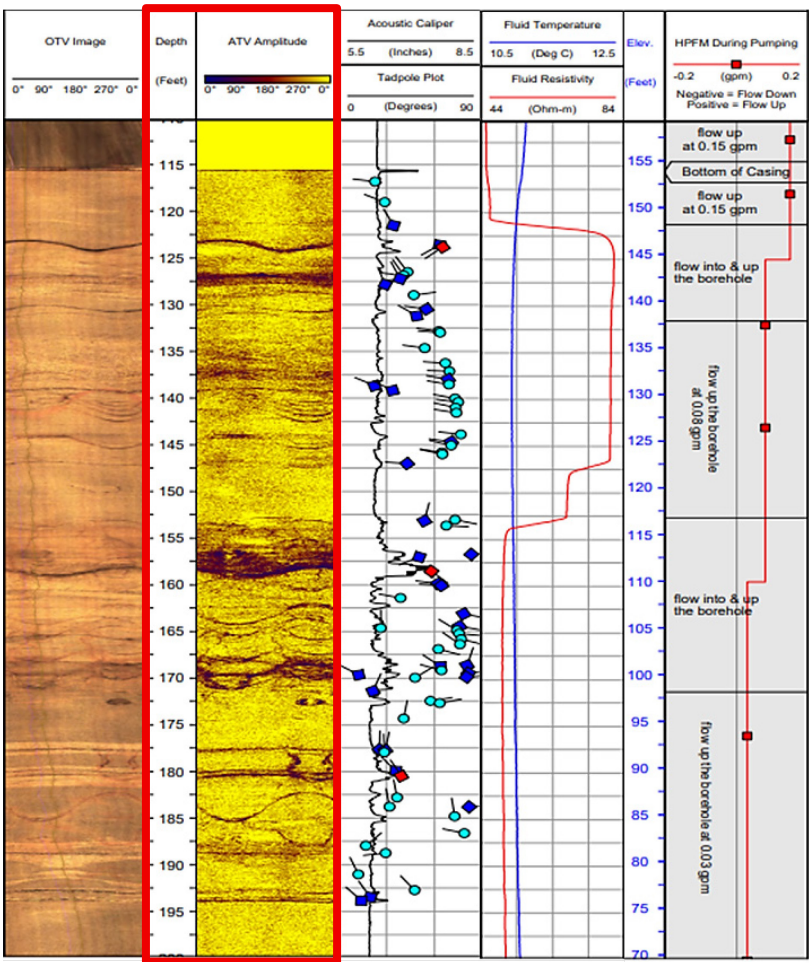


Figure 5-9. Acoustic log image. Darker intervals on the OTV and ATV indicate fractures and bedding planes.

Magnetometers and accelerometers are used to provide data on tool orientation during logging. The magnetometer and accelerometers are factory calibrated. Field checks on the magnetometer, however, can be made using a compass and oriented cylinder (Williams and Johnson 2004).

It is important to note that the presence of the steel casing interferes with image orientation. Williams and Johnson noted that imaging in a fractured-rock aquifer borehole just below the base of steel surfacing casing is important because the magnetometer is affected by steel casing (Williams and Johnson 2004). Therefore, the interval between the steel casing and borehole plus some overlap should be rerun with the magnetometer turned off. Then the rerun image is matched and spliced into the oriented image for the rest of the borehole.

5.5.3 How Is the Technology Used?

5.5.3.1 Optical Televiewer Use and Application

The OTV tool can be deployed in air- or water-filled open boreholes to assess consolidated formations or in wells completed with screen and casing to evaluate the general condition of the well. The OTV provides a photographic image that is used to assess formation properties, such as stratigraphic bedding, contrasting lithologies, and geologic contacts. Fractures are often easily discernible and can reflect regional interpretations involving joints or faults, as well as washed out or karstic zones. OTV logs may provide an indicator of groundwater flow within a borehole based on evidence of oxidative staining. If the borehole has been impacted by NAPL, stains or residues from these contaminants may also be observed.

5.5.3.2 Acoustic Televiewer Use and Application

The ATV is deployed within fluid-filled portions of boreholes, where the fluid (water or drilling mud) transmits the acoustic energy needed to generate the borehole record. The ATV is most commonly used in open boreholes to assess competent, consolidated formations and to provide acoustic caliper and virtual core logs. In addition to the basic elements used for other geophysical logging (winch and wireline, data acquisition unit, field computer with monitor), metal- or plastic-band centralizers are installed on the probe to guide the probe along the central axis of the borehole to maintain consistent proportionality. Using centralizers also on the tools helps provide accurate estimates regarding the strike and dip of planar and subplanar features. With appropriate processing, the ATV may also be used to evaluate the thickness and corrosion of the steel casing and to assess less competent consolidated formations prone to collapse when a centralized PVC liner is emplaced within the borehole. ATV logs can be used to assess casing or well screen conditions.

Consistent with the OTV, the ATV provides an image-based output of the borehole wall that is used to interpret stratigraphy, lithology, and the presence of geologic contacts. Evidence of subsurface fracturing as well as washed-out zones in karst (for example, limestone) environments is also possible based on acoustical differences across void spaces.

5.5.3.3 Optical Televiewer Log Interpretation

Structural interpretations generated based upon OTV are sensitive to conditions such as borehole deviation and variations in diameter. Borehole deviation, the departure of the borehole from vertical (measured in degrees), and the concepts of apparent dip vs. true dip are illustrated on **Figure 5-10**. Obviously, a probe run in a deviated borehole does not provide accurate dip (relative to horizontal); therefore, during log processing, deviation measurements collected by orientation sensors within the OTV (and ATV) probe should be used.

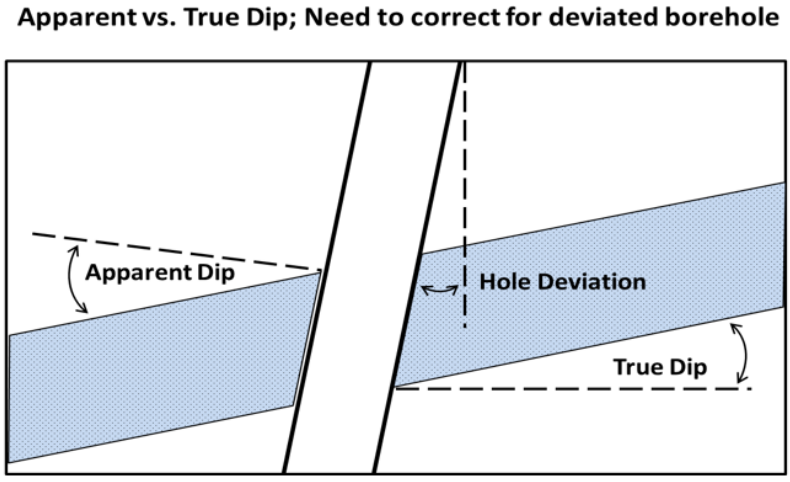


Figure 5-10. Illustration of concepts of apparent dip vs. true dip.

Source: Peterson (2017). Used with permission.

5.5.3.4 Acoustic Televiewer Log Interpretation

ATV logs are post processed using specialty software to quantify the orientation of features identified on the recorded image. The precise orientations of planar features (for example, fractures, sedimentary bedding) identified by the log analyst may be determined and presented in a variety of formats.

To facilitate structural analysis (Section 5.5.3.5), the cylindrical image is presented in an unrolled format, cut vertically at north (true or magnetic) and rolled out from left to right, often with vertical lines representing N (at the left), E, S, W, and N (again at the right). In this format, planar features such as fractures intersecting the borehole wall follow sinusoidal traces, as shown on **Figure 5-11**.

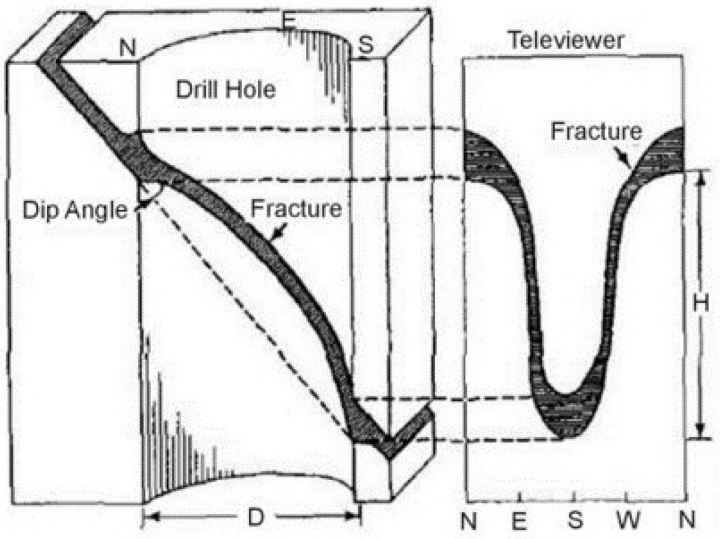


Figure 5-11. Planar features such as fractures intersecting the borehole wall follow sinusoidal traces.

Source: USACE (1995), Figure 7-30.

Structural interpretations generated based upon ATV are sensitive to conditions such as borehole deviation and variations in diameter, previously summarized in **Figure 5-10**. As illustrated in **Figure 5-12**, where planar features intersect a portion of the borehole with an enlarged diameter, a correspondingly higher amplitude feature trace results on the sinusoidal structure plot. As a result, if corrections are not made to properly account for the off-gauge condition of the borehole, dips will be overstated through caving or soft-rock intervals where the hole diameter is enlarged. Experience shows that even a 1-inch enlargement of hole diameter can result in overstatement of dip by several degrees, which is further supported by trigonometric principles. The correction requires reference to a continuous log of borehole diameter (mechanical or acoustic caliper); therefore, either mechanical caliper or ATV logs should also be run when OTV is used to evaluate structure.

5.5.3.5 Virtual-Core Presentation of OTV and ATV Logs

As previously indicated, OTV and ATV probes include orientation sensors (magnetometer and accelerometer) to translate borehole wall images into a 360° wrapped image referred to as a virtual core. This presentation format provides a consolidated and simplified image of conditions that are useful during log interpretation. Similarly, advances in post processing software used to develop virtual cores also allow these logs to be presented adjacent to strip logs from other tools. This section outlines the technical complexity

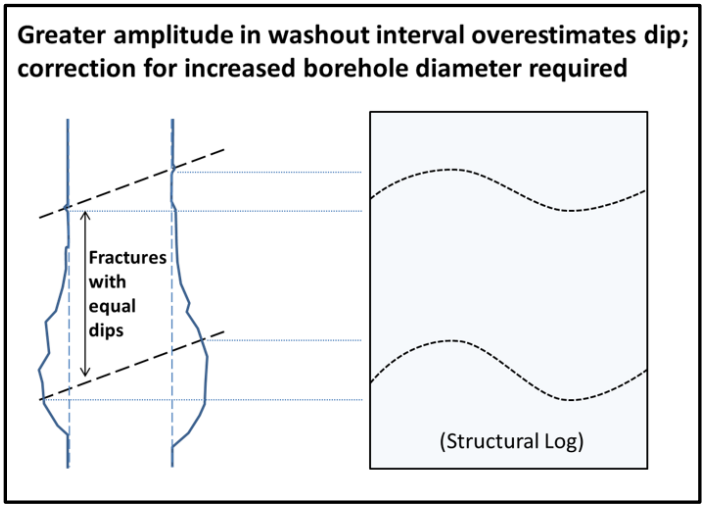


Figure 5-12. Down-dip well siting example (left); planar feature orientation along dip and implications for monitoring accuracy (right).

Source: Peterson (2017). Used with permission.

associated with translating borehole images into 2D projections and key details about presenting structural information.

Uninterpreted Data

Using processing software, oriented, uninterpreted image logging data can be presented in several formats, each represented as a single column on the well log. These include the unrolled, virtual-core, and slab-core logs. The unrolled format (**Figure 5-13***)* shows the borehole image, cut vertically at north (true or magnetic) and rolled out from left to right, often with vertical lines representing N (at the left), E, S, W, and N (again at the right). In this format, planar features such as fractures intersecting the borehole wall follow sinusoidal traces. During interpretation (discussed subsequently), these traces allow the log analyst to determine the attitude (orientation) of the planar features. The low point of the sinusoid corresponds to the compass direction (azimuth) of the dip for the planar feature, while the amplitude (peak to trough distance) is directly proportional to the magnitude of the dip.

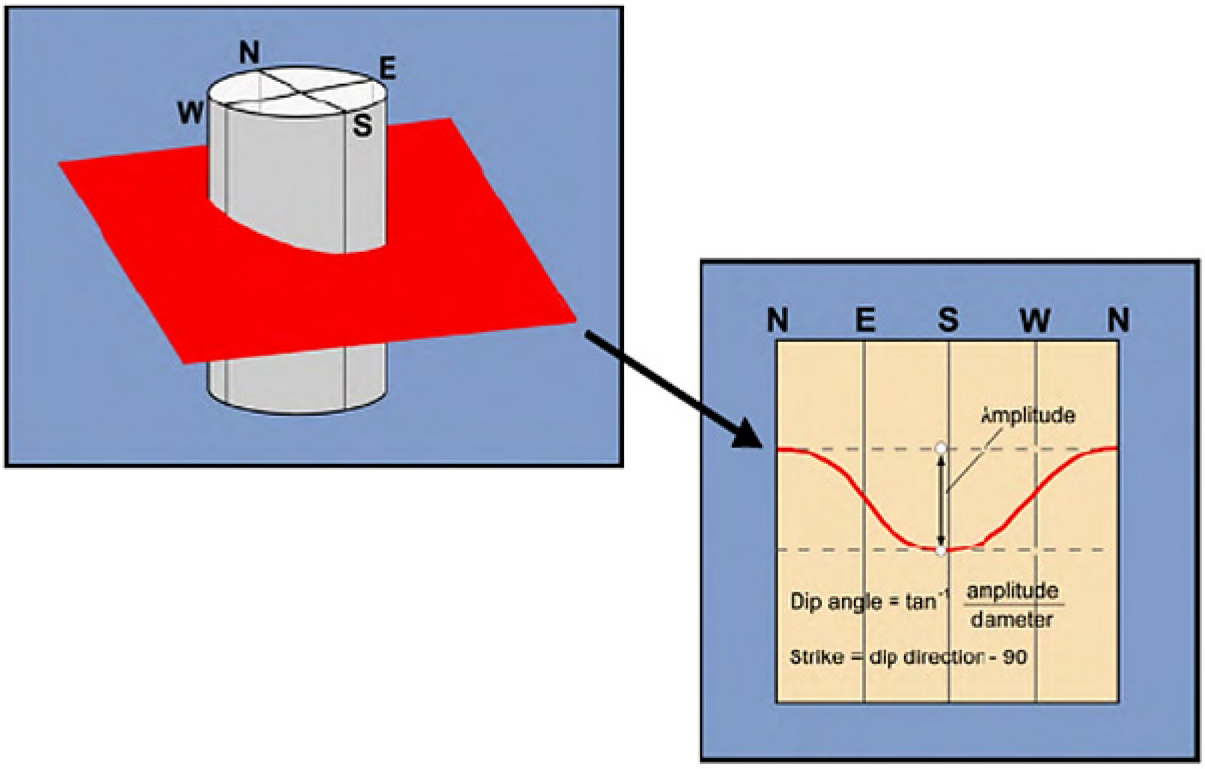


Figure 5-13. Unrolled format shows the borehole image, cut vertically at north and rolled out from left to right, often with vertical lines representing N (at the left), E, S, W, and N (again at the right).

Source: Weston (2014).

The virtual-core format for OTV or ATV provides a 3D view of the borehole as viewed externally. When viewed in the processing software, the core-like image may be rotated to view from all directions. The slab-core format depicts features evident on the viewed side of the borehole as they would appear projected onto a flat surface, mimicking the expected appearance of a slabbed-core or outcrop view. As with the virtual-core format, the slab core is typically shown in reports oriented either on prevailing structure or arbitrarily aligned (for example, toward north).

Interpreted Structure Logs

A log analyst may use the image log output and processing software to prepare interpretive logs, such as a structure log depicting the attitude (strike and dip, or dip, or dip azimuth) of each planar feature identified. Commonly, the log analyst uses the output of the image-logging probes (and other probes, discussed below), processing software, and significant professional judgment to prepare an interpretive structure log depicting the attitude of each planar feature. The structure log is usually presented as a plot of colored sinusoidal lines over or next to a copy of either the unrolled OTV or ATV logs, along with accompanying tadpole plots and notes. Tadpole plots represent the azimuth and magnitude of the dip of planar features as follows: dip azimuth is shown by the compass direction in which the tail on the tadpole is pointing, and dip magnitude is shown by the left-to-right position in which the tadpole is placed on a scale from 0° to 90° of dip. Notes are used to describe key features of the well, including the attitude (orientation) of planar features, such as interpreted sedimentary bedding and fractures. An example of a structure log (incorporating both OTV and ATV) is shown on **Figure 5-14**.

These interpretive logs incorporate significant judgments made by the log analyst, often considering data from more than one logging tool. For example, if both OTV and ATV are used, both are considered when developing the structure log. If the structural-feature classifications employed by the log analyst make reference to apparent capacity of a feature to yield water to the well, the interpretive log depicts the apparent water-yielding fractures or intervals. The analyst's interpretation is based on considering not only the tools used to create the structural log, but also those indicative of potential fluid movement (fluid temperature, fluid resistivity, and heat-pulse flowmeter).

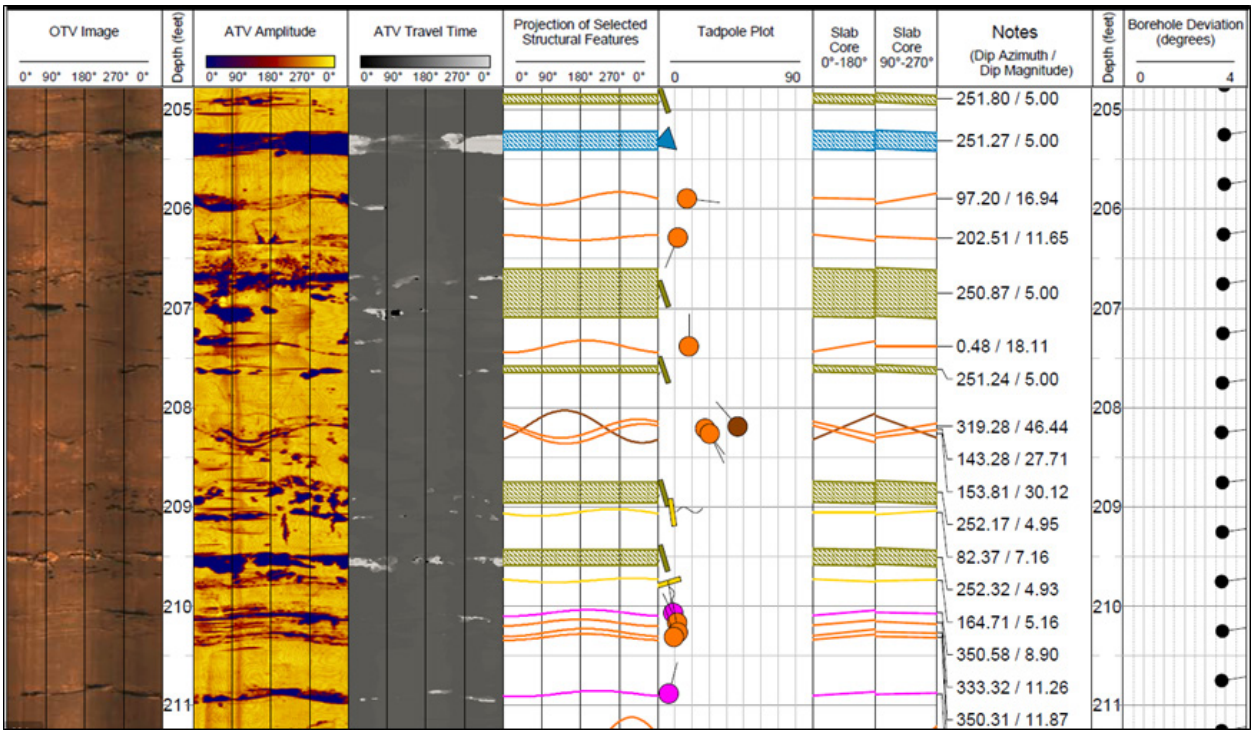


Figure 5-14. Example of a structure log (incorporating both OTV and ATV).

Source: Peterson (2017). Used with permission.

Planar-feature orientation is described using the dip azimuth, dip magnitude convention. The dip azimuth is the compass direction (measured from true north) pointing toward the direction of maximum dip. The dip magnitude is the angle down from horizontal of a line in a planar feature pointing down dip. For

example, a designation of 316, 12 refers to a planar feature whose maximum dip is 12° from horizontal, pointing toward azimuth 316° degrees (in the northwest compass quadrant). Colors selected for plotted sinusoids and tadpoles correspond to the specific feature classifications applied by the log analyst.

Structure plots showing lower hemisphere, equal area (or Schmidt) stereonet plots of dip azimuth for interpreted planar features may also be provided, either in a column of the structure log or on separate pages, employing the same feature classification color scheme. When plotted on the structure log, the stereonets can be shown to represent populations of planar features occurring within individual depth intervals (perhaps corresponding to lithologic units). In **Figure 5-15**, four separate stereonets are provided to show all features interpreted as bedding, banding, or foliation (left column); all identified fractures (center column, top); inferred bedding-parallel fractures (in this case, those fractures with orientations within +/-25° of the bedding dip azimuth and within +/-3.5° of expected bedding dip based on area geological mapping (center column, bottom); and a rose plot showing dip azimuths of all fractures interpreted from the ATV logs (right column).

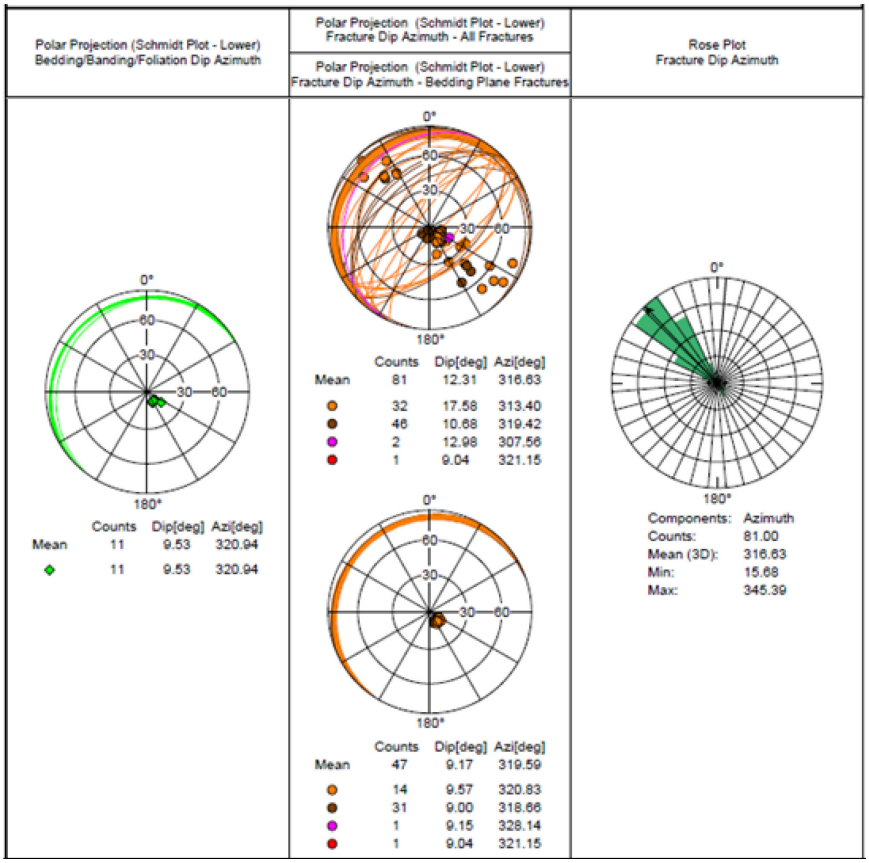


Figure 5-15. Example stereonet plots commonly used to represent conditions throughout the borehole.

Source: Peterson (2017). Used with permission.

Geologists have devised a number of plotting conventions to graphically depict bedrock fabric data and allow for statistical evaluation of these data. The two types used by most geophysical service providers include the compass rose and stereonet plots. The compass rose (shown in **Figure 5-15** at right) shows the strike of a planar feature on a 360° circular compass. The number of measured planes that fall within a specified azimuth arc (typically, every 10°) is indicated by the length of the colored pie-shaped ray comprising the azimuth range. A compass rose plot does not specify planar dip and is therefore a 2D depiction. The value of this display may be lessened for shallow-dipping or subhorizontal features.

Three-dimensional planar attitudes are represented on a stereonet diagram whereby a line bisecting a plane is shown as a single dot (or pole) projected onto a lower hemisphere. The lower hemisphere is constructed with both compass and angular dip angles represented by lines of latitude and longitude. Equal area stereonets are constructed to contain an equal projection area for each angular field represented by all possible planar orientations. This construction allows the determination of planar orientations by statistically analyzing pole density plotted in a given stereonet cell. Thus, a steeply dipping plane is represented as a single dot near the perimeter of the circular stereonet plot, and the planar strike

is normal to the compass heading of the dot. Conversely, a flat-lying plane is plotted near the center (or south pole) of the stereonet projection.

It should also be noted that most geophysical service providers report planar orientation from OTV and ATV logging in a dip-azimuth and dip-angle format. Dip azimuth is perpendicular to planar strike and requires data conversion to present the orientation of the plane as a standard strike and dip symbol typically used on geologic maps.

Key Considerations for Virtual-Core Interpretation

The familiar (image) format of OTV and ATV logs can lead to errors or misuse when inexperienced users become overconfident. Common problems include:

- assuming that fracture aperture evident in the borehole image is the same as in undisturbed formation (damage during drilling tends to enlarge fractures at the borehole)
- assuming that all thin, planar features are fractures (while comparison to other logs may reveal them to be filled)
- assuming that all apparently open fractures are hydraulically conductive (while comparison to fluid or HPFM logs may indicate otherwise)
- failing to apply quality control measures (for example, not correcting for vertical deviation or borehole diameter), resulting in structure log data of unknown accuracy

When adjusting raw magnetic north data to true north for log presentation, the log analyst must be careful to ensure that the correct direction for the adjustment is applied. It is easy to make the mistake of applying the correct magnitude of declination but wrong direction (introducing dip-azimuth error equal to twice the magnetic declination). Therefore, checking dip-azimuth data against what is known from other on-site or regional studies is always a good idea.

Other considerations relate to how the image log (and other log) data are used in the overall site characterization. The first consideration pertains to the underutilization of geophysical logging data. At times, multiparameter logging projects are conducted at numerous wells on a site, but the resulting data are used only for limited purposes (for example, to support packer testing or well-screen placement). Project objectives in these cases are further advanced by correlating log results between wells to develop a site-wide framework. The second consideration relates to the scale of the site and problem at hand. Structural data collected at single locations may be suitable to evaluate a small site (for example, a small BTEX plume at a UST site). Investigating more complex conditions over a larger area (for example, a chlorinated VOC plume at a DNAPL site) may warrant a site-wide evaluation that employs multiwell log correlation and three-point structural evaluations. In this case, a structure log from a single borehole probably is not sufficient to characterize the aquifer matrix.

When analyzing data derived from distinct sources or methods, the genesis and population of the data should be considered. A typical outcrop study may result in a dozen or fewer measurements of planar features over a moderately sized area, whereas a single borehole can generate 50 or more such data points from a single point on a site plan. Conversely, it is important to consider that a vertical boring is less likely to intersect vertical and steeply dipping fractures than horizontal and shallow dipping fractures present within the bedrock formation that may be readily observable in an outcrop. Mixing these data types produces results skewed toward the borehole data, overpowering field measurements and making distinctions difficult to recognize. Other situations may arise where vertical changes in a borehole (such as formation change, fault) may result in distinct data populations from a single borehole. In both cases, the distinct datasets should be analyzed separately to evaluate results and collectively identify similarities and differences in the datasets. These decisions regarding data analysis can be somewhat

subjective and require informed expertise regarding the regional and local site geology and data procurement methods.

5.5.4 What Are the Advantages?

5.5.4.1 Advantages of OTV

Though interpretation can sometimes be tricky, with an experienced geophysical services provider, OTV provides several advantages:

- High-resolution, color, and continuous 360° imaging of a borehole
- Precise identification and measurement of fractures, joints, and bedding planes, including dip and direction
- Accurate orientation of geologic features
- Identification of thin features such as bedding, fine fracture, and clay seams
- Ability to deploy in dry or clear fluid–filled boreholes
- Ability to give orientation reference of physical core samples
- Cost-effective way to reduce handling and storage of core samples

5.5.4.2 Advantages of ATV

Advantages associated with use of ATV technology, especially in poor-recovery situations, include the following:

- Continuous 360° imaging of a borehole
- Potential deployment in existing wells, because some advanced ATV tools can scan through PVC casing
- Production of high-quality data even in cloudy water or with some coatings on the borehole walls
- Excellent for use in dark-colored bedrock formations
- Production of 3D caliper log using travel-time data
- Ability to assess corrosion in cased holes, unlike OTVs
- Accurate determination of fractures, joints, and bedding planes, including dip and direction

5.5.5 What Are the Limitations?

5.5.5.1 Limitations of OTV

As described in *Key Considerations for Virtual-Core Interpretation* above, it is important to recognize the types of errors or misuse of OTV data and virtual-core interpretation that may occur. It is also important to recognize some of the limitations of OTV technology. These can include:

- OTVs are purely visual tools. As such, cloudy, turbid, or murky water can prevent OTV cameras from capturing a clear image of the borehole features.
- Borehole needs sufficient illumination to capture clear images.

- Mud-cake, bacterial growth, or chemical precipitates coating the borehole wall can limit the OTV camera from identifying bedrock fractures or features.
- Distorted images can occur if the tool is not properly centered in the borehole.
- Steel casing or magnetic minerals can interfere with borehole images, although post processing may sometimes be able to address this.
- Cold temperatures can affect OTV function. Check the tool manual for specific requirements.
- Resolution can be affected by logging speed.

5.5.5.2 Limitations of ATV

There are several limitations associated with the ATV, and as such, an approach using multiple tools is best. Limitations include:

- Tools are sensitive to borehole conditions (for example, deviations, borehole washout). Assessment requires verification with other geophysical tools such as mechanical caliper to validate or adjust readings.
- Density of fluid in the borehole must be known or calculation of borehole diameter may be affected and negate the use of acoustic caliper function.
- ATV requires a fluid-filled borehole; performs poorly in dry holes.
- This technology may be affected by magnetic interference from casing or minerals.
- ATV has lower resolution compared to optical televiewers.
- Rough borehole walls can scatter the acoustic signal and may affect resolution.
- Cold temperatures can affect ATV function. Check the tool manual for specific requirements.
- Data processing for fractures can be complex, and large fractures can be problematic.
- Distorted images can occur if the tool is not properly centered in the borehole.

5.6 Natural Gamma Logging

5.6.1 What Is the Technology?

Gamma logging uses a passive detector lowered in a borehole via wireline to measure natural gamma radiation in the borehole. Gamma radiation is emitted from common radioisotopes, primarily potassium-40 and daughter products of uranium and thorium decay, which are useful indicators of lithology. The strength of the natural gamma radiation decreases with distance from the borehole wall. Thus, the larger the diameter of the borehole, the lower the resolution of the natural gamma log.

Earth materials have varying amounts of naturally occurring gamma emitters. Potassium-40 and, to a lesser extent, uranium and thorium, tend to be more concentrated in clays and fine-grained materials. Clean silica sands generally contain few gamma emitters. Many factors affect the radioactivity of soil and rock materials and need to be considered when interpreting gamma logs. Sands that contain high amounts of potassium feldspar emit higher gamma radiation due to the potassium content. The potential for uranium deposition in certain regions and environments must also be considered when interpreting logs.

5.6.1.1 Data Collection Design

Gamma logs are acquired in a similar manner as most other borehole geophysical logs but do not require fluid-filled boreholes or casing. When logging in existing monitoring or extraction wells, certain well construction features that could affect data quality, including the original borehole diameter, annular fill outside the casing, and casing material, should be considered. Smaller borehole and casing diameters provide higher-quality results with better vertical resolution.

As with other borehole geophysical tools, logging at a single location provides parameter data only in the immediate vicinity of that location. By logging multiple locations, data can be correlated over greater distances and provide 2D (cross-sectional) and 3D conceptual models. The density of well locations to be logged should be based on the stratigraphic framework and the nature of features that the investigation is attempting to resolve.

5.6.2 How Is the Technology Used?

5.6.2.1 Use and Application

The most common application of gamma logging is for lithologic characterization and stratigraphic correlation. Gamma-logging results are objective and repeatable, and, when viewed in vertical profile, stratigraphic information can be derived and used to develop the CSM through characteristic curve-matching and cross-borehole correlations. Where clay minerals contribute to a significant portion of the gamma response, gamma logs can be used to estimate the fraction of clay present, represented by the clay volume divided by the total rock volume.

In igneous and metamorphic rocks, gamma response is generally dependent on minerals in the rock, although water-bearing fractures can exhibit high gamma response due to the precipitation of uranium or other radioactive minerals along fracture walls. Under certain circumstances, gamma logs can be a good indicator of water-bearing fractures.

Key considerations during gamma logging are logging speed and distance from the source to the detector. Based on background conditions, logging speeds can be optimized to observe variations between clay-bearing and clean sandy soils. Slower logging rates may be required to obtain a higher resolution of data across a site and identify smaller variations in lithology; higher logging rates, which increase the footage rate of data collected, may be sufficient to characterize geologic lenses that are of greater thickness. A consistent borehole diameter is optimal in reducing the variability caused by the distance between the detector and the soil matrix. Gamma logging should always be accompanied by a caliper log when logging in open boreholes. The accompanying caliper logging is used to identify potential variabilities of the borehole wall diameter that might impact data quality. A centralizer is also recommended to keep the gamma detector within the center of the borehole. Where borehole washouts are present, the gamma response is reduced regardless of soil or rock type.

5.6.2.2 Log Interpretation

Gamma log data are usually processed and can be displayed in real time. Geophysical reports may present the gamma logs for different borings on different response scales for counts per second, especially if logging occurs over multiple field events. When interpreting gamma responses and correlating logs between boreholes, verify that the response scaling is the same. Some geophysical contractors color code the response curve with a filled hatch pattern, which can be useful for rapid visual correlations, but misleading if the response scalings differ. Data interpretation is straightforward, as

shown in the example log displayed below (Figure 5-16). Other example logs are available on the USGS geophysical logs–Gamma logs web page (USGS 2000a).

5.6.2.3 Spectral Gamma

Spectral gamma logs (also known as spectral gamma ray or SGR) are a variation of natural gamma logs that measure the natural gamma radiation spectra caused by the decay of uranium, thorium, and potassium-40, along with anthropogenic radioactive isotopes. Spectral gamma logs are used primarily in oil-field evaluations. Whereas natural gamma ray logs provide a total count of gamma emissions, the spectral tool measures the distinct, characteristic energy level of these isotopes. Using post processing tools, the relative concentrations of the radioactive sources can be determined.

The data collected can be used to differentiate shales and potassium salts, compute shale percentages, determine lithology and clay mineral types, correlate structure and stratigraphy, identify clay depositional environments, and help analyze rock-water interactions (USGS 2019a).

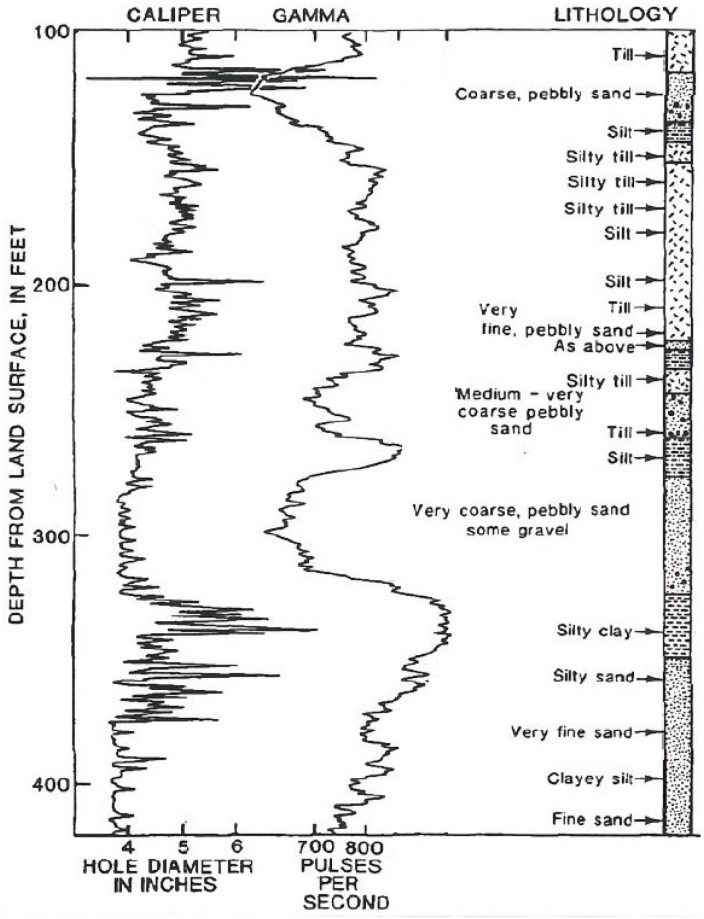


Figure 5-16. Example gamma log output with caliper log and lithology.

Source: Adapted from USACE (1995), Figure 7-8.

As such, spectral gamma can provide large amounts of data for undisturbed rock compared to physical core sampling. It can be effective in a borehole with dry or wet conditions and can be deployed in cased boreholes, allowing for logging of existing wells.

5.6.3 What Are the Advantages?

Natural gamma is one of the most useful and frequently used geophysical technologies used in boreholes to distinguish lithology and correlate stratigraphy. Advantages of natural gamma include:

- simple and cost-effective logging method
- high resolution
- deployable in cased boreholes allowing for logging of existing wells
- excellent at differentiating lithology, particularly between shales and sands
- passive logging method that does not require contact with the borehole wall
- effective in a wide range of boreholes, including both fluid-filled and dry conditions

5.6.4 What Are the Limitations?

Although natural gamma logging is versatile, there are some limitations associated with the technology, including:

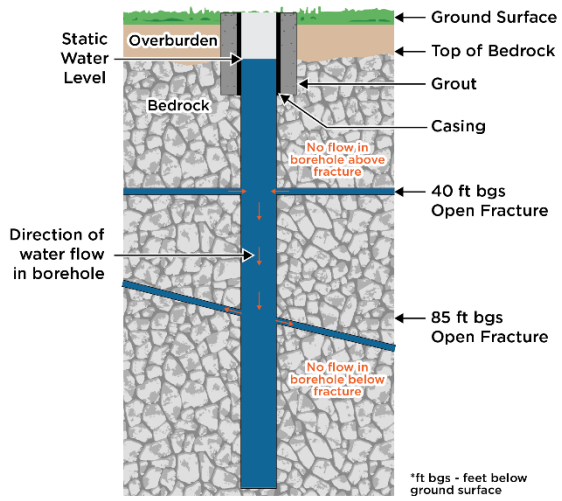
- Logging speed may affect resolution and results.
- This is not the best technology for resolution of thin beds.
- Borehole diameter, casing type, and fluid conditions in the well may affect readings and measurements.
- Smaller casing sizes may limit use of the probe.
- Although centralizers help in deviated holes, errors can be introduced.
- Natural gamma logging should be deployed with other technologies to confirm results.
- This technique is not useful if natural radioactivity is not present (clean sandstones).
- SGR requires calibration.

5.7 Borehole Flowmeters

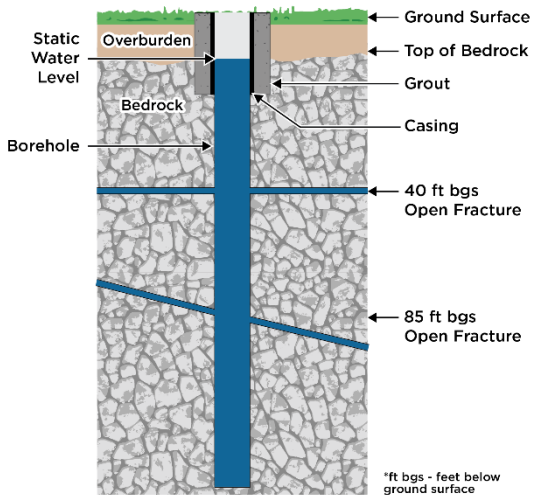
Borehole flowmeters are used to measure the rate and direction of water flow within a borehole, and how rate and direction vary with depth in the borehole. The primary utility of borehole flowmeters is to identify hydraulically active (transmissive) zones intersected by the borehole and determine the direction of the vertical hydraulic gradient between transmissive zones. It is important to understand that they do not directly measure the rate or direction of groundwater flow *within* a transmissive water-bearing zone. Additionally, flowmeter results can be used to estimate transmissivity and hydraulic head in transmissive water-bearing zones intersected by the borehole. Borehole flowmeters are commonly used in fractured rock systems where groundwater flow is largely controlled by discrete open fractures or fracture zones in a relatively low permeability rock matrix. However, they can be applied in other situations as well, such as karst systems or porous media systems, if conditions allowing the flowmeter to be used are present (for example, open, stable borehole). Borehole flowmeters can also be used in wells. Some examples of this include identifying which portions of the well screen or open interval provide the most flow to the well, assessing if a well is cross-connecting hydrostratigraphic zones with different hydraulic heads, and identifying leaks in a well casing. When using a borehole flowmeter in a well, the potential effect of well construction on measurements (for example, flow within the filter pack between the borehole and the screen) must be considered in interpreting results.

For flow to occur in a borehole, differences in hydraulic head need to be present in the borehole such that the water will flow from an interval of higher head to an interval of lower head. For example, consider a situation where two transmissive fractures intersect a 150-ft-deep bedrock borehole wherein the rock matrix has a very low hydraulic conductivity with one fracture intersecting the borehole at 40 ft bgs, and another intersecting the borehole at 85 ft deep (**Figure 5-17A**). If the hydraulic head in the fracture at 40 ft bgs is greater than in the fracture at 85 ft bgs, water will flow downward through the borehole from that fracture and into the fracture at 85 ft bgs. Below 85 ft, there will be no flow in the borehole, because in this scenario there are no transmissive fractures for water to enter or exit the borehole in that interval. If the hydraulic head in the fracture at 40 ft bgs and 85 ft bgs is the same, then there would be no flow within the borehole under ambient conditions (**Figure 5-17B**).

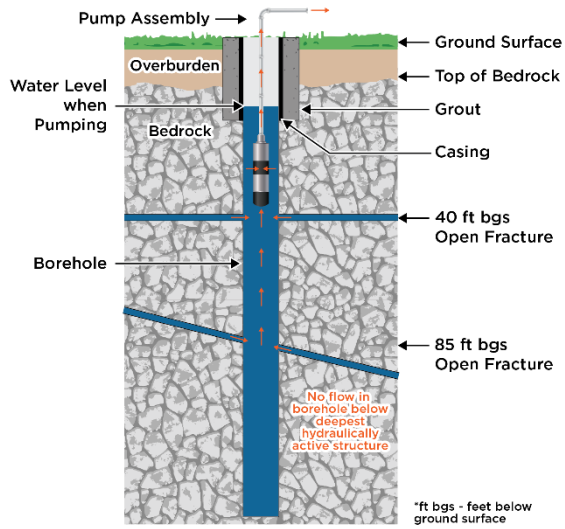
Note that with a borehole that intersects multiple water-bearing intervals with different hydraulic heads as described above, there is a potential for cross contamination of groundwater between these intervals. This potential needs to be considered in planning a drilling program and deciding whether to use a borehole flowmeter.



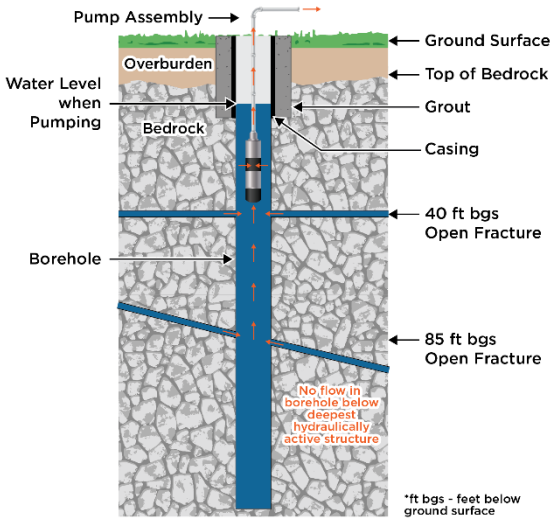
A: Flow within borehole: Ambient conditions, head in shallower fracture greater than in deeper fracture



B: Flow within borehole: Ambient conditions, head in deeper fracture equal to head in shallower fracture



C: Flow within borehole: Pumping conditions, head in shallower fracture greater than head in deeper fracture



D: Flow within borehole: Pumping conditions, head in deeper fracture equal to head in shallower fracture

Figure 5-17. Flow within borehole.

Source: Bob O'Neill, Brown and Caldwell. Used with permission.

Oftentimes, two flowmeter logging runs are performed on a borehole—one under ambient conditions (as in the conditions in the examples described above), and a second with the water being pumped from the borehole at a constant rate that is well within the operational measurement range of the particular

flowmeter, and with a stabilized water-level drawdown that ideally remains well above the section of interest in the borehole. Logging under pumping conditions:

- facilitates detection and evaluation of transmissive fractures when there is little or no flow in the borehole under ambient conditions, such as is depicted in **Figure 5-17**
- facilitates identifying fractures that contribute a relatively small proportion of the flow in the borehole under ambient conditions, and for which the flow contribution under ambient conditions is below the resolution range of the flowmeter being used
- provides additional evaluation of the relative transmissivity and yield of fractures intersecting the borehole

However, logging under pumping conditions does not allow for assessing the direction of the vertical gradient between transmissive zones, as with logging under ambient conditions. **Figure 5-17C** and **Figure 5-17D** illustrate borehole conditions when water is being pumped from the borehole.

Borehole flowmeter logging is typically conducted after the borehole has been completed to its target depth and flushed of cuttings and after other borehole geophysical tools have been run and analyzed to select potentially transmissive features (targets) in the borehole (for example, fractures, bedding planes, joints). Examples of other borehole geophysical tools here include caliper, fluid temperature, fluid resistivity, ATV, and OTV. Other information that can facilitate selection of target intervals for flowmeter logging includes examination of rock cores, packer test results, and observations during drilling, such as intervals that gain or lose water or where drilling footage rates change.

In the following sections three types of borehole flowmeters used for site characterization are discussed: heat-pulse flowmeters (HPFM), impeller (spinner) flowmeters, and electromagnetic flowmeters (EMFM). All three of these flowmeters measure flow rate and direction in a borehole. Other borehole tools are available that are aimed at further characterizing groundwater flow in water-bearing zones, such as the hydrophysical tool, which combines EMFM technology with electrical conductivity and temperature sensors, along with borehole fluid replacement with deionized water, to characterize aquifers, and the colloidal borescope, which tracks the movement of colloids in a borehole or well to measure groundwater velocity and direction. However, the discussion below is focused on the three above listed tools that are frequently applied to evaluate groundwater flow within a borehole.

5.7.1 Heat-Pulse Flowmeter Logging

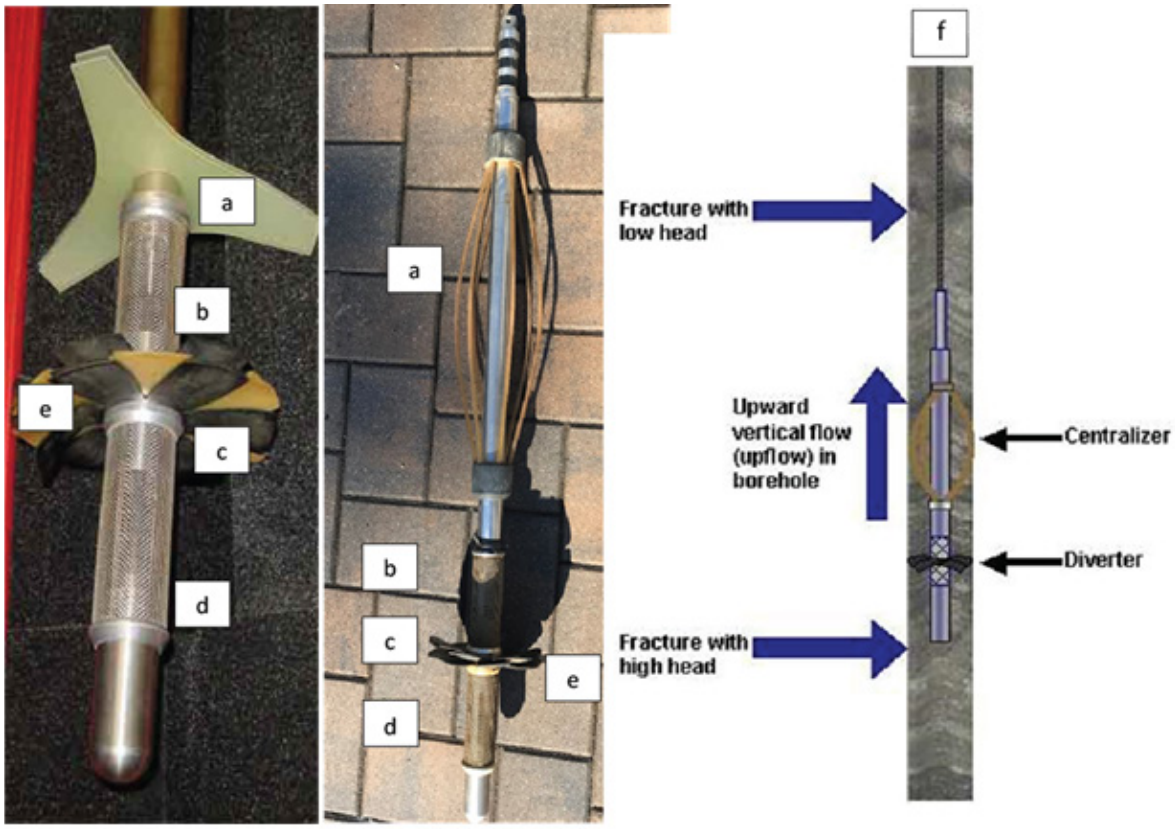
5.7.1.1 What Is the Technology?

An example of a heat-pulse flowmeter is pictured in **Figure 5-18**. The diameter of the depicted tool is about 41 mm (1.63 inches); it is about 1.2m (48 inches) long and weighs about 5 kilograms (12 pounds). The HPFM requires centralization and uses a diverter to channel vertical flow in the borehole through the body of the instrument (**Figure 5-18**). The typical flow measurement range of this instrument is approximately 0.15 to 13 ft/min [equating to approximately 0.03 to 1.0 gallon per minute (gpm) (0.113 to 3.785 L/m) if flow is fully diverted through the chamber in the body of the tool].

The HPFM uses a pulse of heated water to detect vertical groundwater flow, hence the name of the tool. On the tool, a small heating grid is positioned between two heat sensors (thermistors), one above and one below the heating grid. If flow is occurring in the borehole, the heated water will move either up or down the borehole from the heating grid to one of the sensors. The HPFM is run after the borehole has been completed to its target depth and flushed of cuttings, and after other logs (Section 5.7 and 5.7.1.1 *Data*

Collection Design) have been run and analyzed to select potentially transmissive features (targets) in the borehole (for example, fractures, bedding planes, joints). The HPFM works as follows (**Figure 5-18**):

- It is run in the water-filled interval of an open borehole.
- The instrument is positioned at a station above or below a target and held stationary in that position until the test is completed. Care must be taken by the operator when selecting a station to position the instrument close to the target and in a section of borehole wall where the diverter can form a good seal with the borehole wall (a caliper log is valuable for this assessment).
- A diverter with a diameter flush with the borehole wall channels vertical groundwater flow through the instrument.
- The instrument is triggered by the operator and an electric element in the center of the instrument rapidly heats up a small volume of water to generate a pulse of heated water.
- Vertical groundwater flow carries the heated water up or down, where it is detected by thermistors positioned above and below the heating element.
- After data are collected, the reading can be repeated, or the instrument is moved to the next station.



a) Centralizer, b) upper thermistor chamber, screened to allow water to pass through it, c) flexible diverter petals (channel flow through the HPFM), d) lower thermistor chamber screened to allow water to pass through it, (e) heating element located in the center of the HPFM body, and (f) HPFM measuring upward vertical flow in an open bedrock borehole.

Figure 5-18. HPFM.

Source: Left and right images: USGS (2016b); middle image: Robert Garfield, Hager Richter Geosciences. Used with permission.

Heat-pulse data are collected in the borehole under ambient, or natural, flow conditions and then under pumped conditions. Under pumped conditions, a submersible pump is installed in the well near the top of the water column and run at a low flow rate, typically about 1 gpm. The HPFM log is then repeated at the same stations as the ambient flow log. The results developed from the pumped conditions may identify transmissive features that were not detected by the ambient log because the head in the borehole and the fracture were the same under ambient conditions (Section 5.7).

HPFM data are typically collected in only one direction, either starting at the deepest target interval and moving upward to progressively shallower target intervals or starting at the shallowest target interval and moving to progressively deeper target intervals. The HPFM is run separately from other borehole geophysical tools. If other borehole geophysical tools are to be used, they are used on a separate logging run from the HPFM.

Tool Availability

HPFM tools are available from most geophysical contractors that offer borehole geophysical logging services. Typically, geophysical logging contractors perform HPFM logging due to the specialized nature of the HPFM and the expertise and experience required to use the associated software.

Quality Control

The HPFM should be calibrated by the operator or contractor before mobilizing to the field. Field quality control measures when using the HPFM consist of the following elements:

- Before, during, and after use, document that the instrument is working and accurately measuring flow. To test operation, position the HPFM near the top of the water column, ideally in the casing; install a pump above the HPFM, and run the pump at a specific flow rate (for example, 0.5 gpm). Measure the discharge from the pump to confirm the flow rate and then check the flow rate reported by the HPFM. The two values should match within the accuracy and resolution of the instrument.
- Allow fluid flow to stabilize after the HPFM is moved to a specified depth in the borehole before proceeding with flow measurements. Moving the HPFM can cause vertical flow that is unrelated to the flow caused by head differences in the borehole.
- Collect multiple measurements at individual target intervals to allow for the differentiation between tool-induced flow and borehole flow.
- Monitor the water level in the borehole during logging under ambient and pumped conditions.
- Under pumped conditions, allow the water level in the borehole to stabilize (stabilized drawdown) before beginning the logging run and collecting measurements. During logging, maintain a constant flow rate to facilitate consistency in data interpretations.

To determine whether the flow rate is outside of the range of detection for the HPFM (<0.03 gpm or >1.0 gpm):

- Move the instrument, stop it, and trigger it immediately to detect if flow is caused by instrument movement.
- If flow is detected, keep the instrument stationary and trigger the instrument again. Repeat this process. If the flow rate is zero, each subsequent pulse takes longer to reach the thermistor because the movement of water caused by the motion of the instrument is dissipating.
- If flow should be present based on other logs and previous flow measurements and is not at the time of the HPFM deployment, modify the diverter to increase bypass around the instrument and

decrease flow through the instrument into the range the HPFM can detect. Document the modifications in the geophysical report and consider them when interpreting results.

Data Collection Design

The HPFM is typically used as part of a suite of borehole logging tools and is used after other logs, such as caliper, ATV, OTV, and fluid temperature and conductivity, have been completed and analyzed to identify potentially transmissive (water-bearing) features (Section 5.7). These potentially transmissive features are termed targets. Stations for HPFM readings are identified above and below each target where the borehole wall is relatively smooth. Readings are collected at each station and then compared to assess whether water is entering or exiting the borehole at the feature.

5.7.1.2 How Is the Technology Used?

The value of the HPFM is that its resulting data reveal features in the borehole that are transmissive—that is, where water is entering and exiting the borehole. HPFM data also reveal the relative head distribution in the borehole—for example, features where water entering the borehole has a higher head than features where water is exiting the borehole (**Figure 5-18**). This information, coupled with data from other logs, is used to define the site geologic framework, the hydrogeologic framework, and potential groundwater contaminant migration pathways. Additionally, flowmeter results can be used to estimate transmissivity and hydraulic head in transmissive water-bearing zones intersected by the borehole.

Data Interpretation and Presentation

Figure 5-19 illustrates the interpretation and presentation of HPFM data, outlined in red, in context with output from other geophysical logs that are often run in conjunction with, and prior to, the HPFM, including OTV; ATV with acoustic caliper; natural gamma; single point resistance; spontaneous potential (SP); borehole fluid temperature; and borehole fluid conductivity. These tools are run first and then evaluated to identify targets and stations for HPFM readings. The HPFM ambient log is then run followed by the HPFM pumping log. To facilitate analysis, the HPFM logs (ambient and pumping conditions) are overlain on one another, using the same horizontal (flow in gpm) and vertical (depth in ft) scales. Zero flow is in the middle of the horizontal scale. Upward flow is indicated by positive values to the right of zero, and downward flow is indicated by negative values to the left of zero. In this example, the ambient log (shown by blue squares at measurement stations) showed inflow to the borehole at about 59 ft (between measurement stations at 63 and 56 ft). This position is adjacent to a fracture dipping at shallow angle to the northeast as indicated on the OTV or ATV tadpole plot. Below 59 ft there was no flow within the borehole. Above 59 ft the water in the borehole flowed upward, and then exited the borehole at approximately 16 ft, at a possible fracture positioned at or near the base of a casing that is set at 16 ft. This indicates an upward gradient within the borehole from the deeper water-bearing fracture to the shallower fracture under ambient conditions. No flow is indicated by the HPFM within the cased portion of the borehole, as any water-bearing fractures would be isolated from the borehole by the casing. Note that the borehole fluid temperature and conductivity logs, which are run under ambient conditions, both showed an inflection at about 16 ft, corresponding to the position of the water outflow. The pumped log (shown by red squares at measurement stations) also showed a water-entry interval at about 59 ft, but at a slightly higher rate due to the pumping from the top of the borehole. The pumping HPFM log indicated upward flow from 59 ft, similar to the ambient log, but did not show the outflow from the borehole at 16 ft as seen in the ambient log; rather, the water continued to flow upward into the casing toward the pump. This may be because the head in the fracture at 16 ft is similar to the water level in the borehole during pumping. The HPFM data can be used to estimate transmissivity and hydraulic head in transmissive water-bearing zones that intersect the borehole using readily available modeling code, such as the USGS's flow-log analysis of single holes (FLASH) (USGS 2018a).

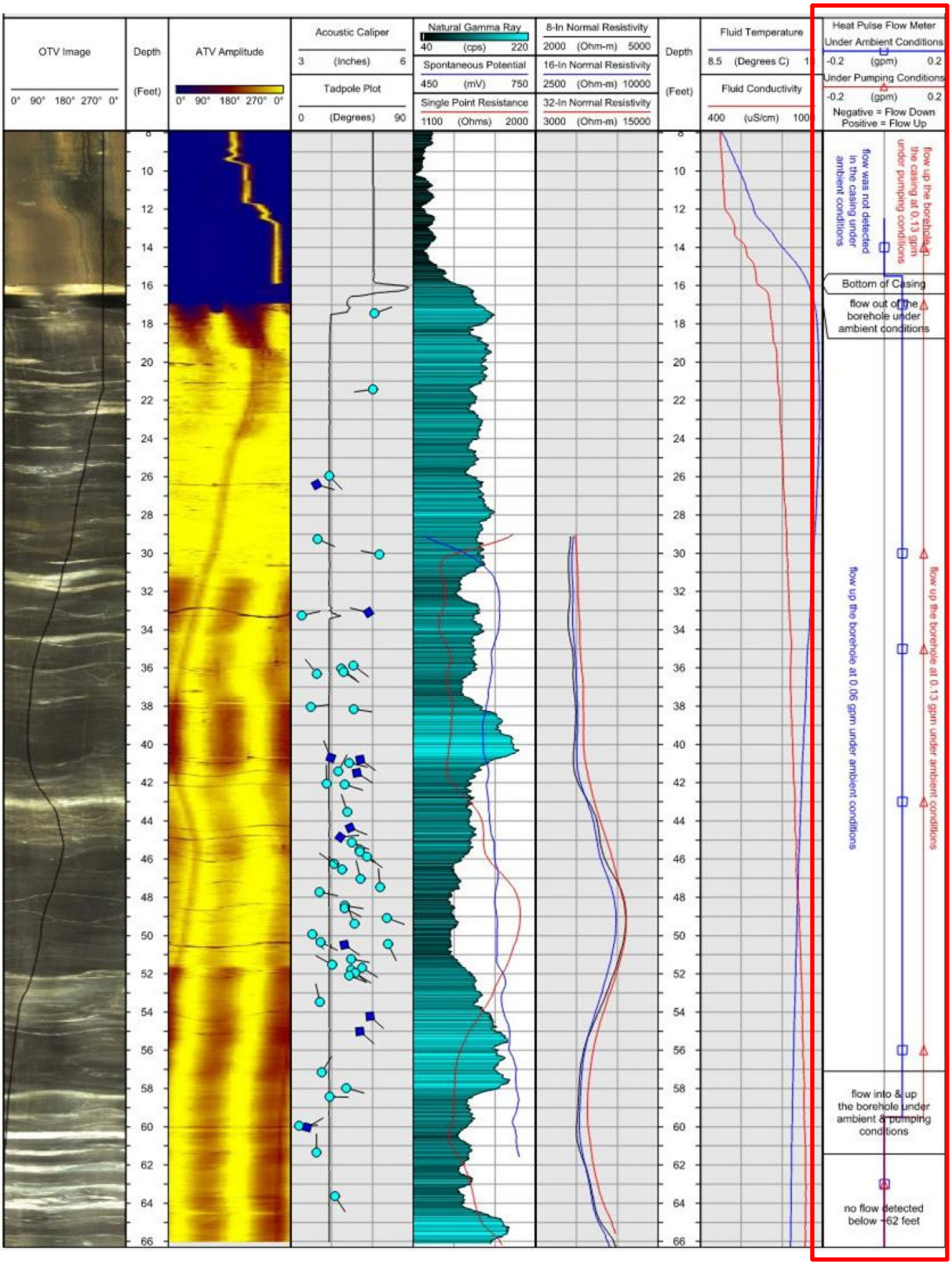


Figure 5-19. Heat pulse flowmeter data presentation and analysis.

Source: Hager-Richter Geoscience. Used with permission

5.7.1.3 What Are the Limitations?

The limitations of the HPFM are that it detects the most transmissive features in a borehole due to its range of operation. The minimum flow rate it can detect is about 0.03 gpm; therefore, a reading of zero flow should be interpreted as flow <0.03 gpm. It is important to note that transmissive features may be present outside the range of detection of the HPFM. Likewise, the maximum flow rate the HPFM can detect is about 1 gpm, which is sufficient for many site investigations. (An impeller (spinner) flowmeter can be used to measure higher flow rates; see Section 5.7.2) Another limitation of the HPFM is associated with the diameter of the borehole. Because flow must be diverted through the instrument, it is best to conduct the log in boreholes ranging from 4 inches to 8 inches in diameter. Measurements can be made only when the HPFM is stationary, unlike the impeller flowmeter (Section 5.7.2) and the electromagnetic flowmeter (Section 5.7.3), which can be used to make flow measurements while stationary or while the instrument is moving up or down the borehole. The depth to which HPFM can be used is based on the pressure and temperature ratings of the specific tool, as well as cable and winch capacity. Accordingly, the depth objective for logging should be discussed with the geophysical contractor and/or equipment manufacturer when planning the logging program.

5.7.1.4 What Are the Advantages?

The technical advantage of the HPFM is that it measures the direction and rate of vertical groundwater flow in the borehole. This, coupled with data from other logs, can be used to define the site geologic framework, the hydrogeologic framework, and groundwater contaminant migration pathways. Compared to the commonly used impeller flowmeters (discussed below), the HPFM has better resolution for lower flow rates. Also, the HPFM tool has no moving parts that could be blocked or otherwise interfered with, which is not the case with the impeller flowmeter.

5.7.2 Impeller Flowmeter Geophysical Logging

5.7.2.1 What Is the Technology?



Figure 5-20. Impeller flowmeter probe.

Source: Photo courtesy of Mount Sopris Instruments. Used with permission.

As with the other flowmeter tools described in this section, the impeller, or spinner, flowmeter (**Figure 5-20**) is used to measure the rate and direction of vertical fluid movement in a borehole produced by a difference in hydraulic head between two transmissive water-bearing zones. This tool was developed over 70 years ago for the petroleum industry and is one of the oldest borehole logging tools for measuring fluid flow in a borehole. Impeller flowmeters may be made out of various materials, such as stainless steel, plastic, brass, or titanium, and there are multiple sizes and configurations. Additional components include centralizers and a protective basket or cage around the impeller. The sensor for the tool is a mechanical impeller mounted on a vertical shaft that revolves in response to fluid flow. As the impeller revolves, the unit generates electrical pulses that are converted to counts per second or per minute. The count rate is related to the fluid velocity and converted to fluid flow rate by use of a calibration curve. The two most common technologies for rotation sensors are Hall-effect sensors (magnetic) and optical sensors. An overview of this tool and associated literature references is available on the USGS Vertical Flowmeter Logging (USGS 2016b) web page . The measurement range for the impeller flowmeter is variable based on the configuration and make, but its lowest range is higher than the HPFM and the EMFM; it is not suited for detecting flows less than about 2 to 4 ft/minute (note that the measured velocity can be converted to volumetric flow rate [for example, gpm] based on the diameter of the borehole or casing and configuration of the tool). It is better suited for higher flow ranges.

Tool Availability

Impeller flowmeters are produced by most borehole logging tool manufacturers and usually come with multiple sizes of impellers, cages, and centralizers to accommodate a range of borehole diameters. When selecting an impeller flowmeter to use, choose the one with the largest impeller blades and lowest friction bearings that produce the highest number of pulses per revolution. Most impeller flowmeters can be run on a single or four-conductor logging cable and require a logging winch with a tripod and an uphole electronic panel or controller to interface to a computer.

Quality Control

The impeller flowmeter should be calibrated by the operator or contractor before mobilizing to the field. The impeller should always be run centralized so that it is positioned in a zone in the center of the borehole where flow has a greater potential for being laminar. When using the tool in trolling mode, the logging speed should be maintained constant and recorded with the flowmeter data. A caliper log should be run in conjunction with the flowmeter. Caliper logging data should be presented with the flowmeter data for borehole and casing diameter corrections. Runs should be made logging down and logging up for a select suite of logging speeds and repeat runs should be made. Calibration data should be recorded in the cased portion of the well, when possible, logging up and logging down for at least three different logging speeds to generate a calibration curve.

Data Collection Design

The impeller flowmeter can operate under ambient conditions and under stressed conditions (pumping or injecting) while moving down or up or while the impeller is held stationary at a specific depth. When planning an open-hole impeller flowmeter test, it is important to know the water level in the borehole or well, and the configuration of the borehole or well (for example, bottom of the borehole or well, bottom of surface casing, position of the well screen or open interval). As with the HPFM, supporting borehole geophysical logs, such as caliper, fluid temperature and conductivity, and televiewers, provide insight in identifying potential transmissive zones. When logging the impeller flowmeter under pumping or injecting conditions, it is critical to maintain a constant pumping or injecting rate and monitor the rate to obtain usable quality data.

The impeller flowmeter can be used to measure flow at individual stations within the borehole, similar to that described for the HPFM (Section 5.7.1.1). Measurements can also be made as the tool is moving at a constant speed either up or down the borehole to provide a continuous profile of flow measurements (trolling). Note that trolling induces flow through the tool in a direction opposite to the tool motion, so this needs to be accounted for via tool calibration (which incorporates borehole diameter) and considered in the evaluation of the data. As with stationary measurements, the trolling can be conducted under both ambient and pumping conditions. The continuous profile produced from trolling can be used to identify transmissive zones that can be targeted for more accurate stationary flow measurements.

5.7.2.2 How Is the Technology Used?

The impeller flowmeter can be run in a cased well and in an open borehole. It can be used to measure the rate and direction of vertical fluid movement produced by a difference in hydraulic head between two permeable units. It can also be used to measure relative hydraulic gradients, identify transmissive units or fractures, identify leaking casing, or characterize the flow within a screened interval. The value of the flowmeter is that its resulting data reveal features in the borehole that are transmissive—that is, where water is entering and exiting the borehole. As described in Section 5.7.3.2, in addition to stationary measurements, the impeller flowmeter measurements can also be made as the tool is moving up or down the borehole (trolling) at a consistent rate to provide a continuous profile of flow measurements. The continuous profile produced from trolling can be used to identify transmissive zones that can be targeted

for more accurate stationary flow measurements. Impeller flowmeter data also reveal the relative head distribution and hydraulic gradients in the borehole. For example, intervals and features where water is entering the borehole have a higher head than intervals and features where water is exiting the borehole (**Figure 5-20**). This information, coupled with data from other logs, is used to define the site geologic framework, the hydrogeologic framework, and groundwater contaminant migration pathways. Additionally, flowmeter results can be used to estimate transmissivity and hydraulic head in transmissive water-bearing zones intersected by the borehole.

Data Interpretation and Presentation

Impeller flowmeter data can be viewed and plotted in standard borehole logging software packages and processed in Microsoft Excel. It can be presented in a format with other borehole information as shown for the HPFM in **Figure 5-18**. Additionally, flowmeter results can be used to estimate transmissivity and hydraulic head in transmissive water-bearing zones that intersect the borehole using readily available modeling code, such as the USGS's FLASH (USGS 2018a).

5.7.2.3 What Are the Limitations?

The impeller flowmeter is generally considered a low-resolution tool. The low-threshold velocity of a typical impeller flowmeter is around 2 to 4 ft/min, which limits its use to conditions with higher flow rates. It is not suitable for measuring flows in the lower part of the HPFM detectable flow range. The logging speeds for this tool can be quite high, so attention must be paid to the location in the well or borehole in relation to the bottom and to the placement of the pump. The Hall-effect sensor and optical rotation sensor are both subject to malfunctioning if the borehole fluid contains debris, sediment, grease, or sand. Moreover, if the tool is assembled with too much pressure on the impeller bearing, the rotation will be impaired and provide incorrect data. Another interference source can come from variations in the viscosity of the borehole fluid, such as can be caused by gas bubbles. The depth limitations for an impeller flowmeter vary with the tool construction but should be discussed with the geophysical contractor and/or equipment manufacturer when planning the logging program. Some impeller flowmeter tools are designed for operation at depths of thousands of feet, but the capacity of the associated equipment must also be considered in assessing the planned logging depth.

5.7.2.4 What Are the Advantages?

The impeller flowmeter can measure higher flows than HPFM or EMFM. It can be used to make flow measurements while stationary or while the instrument is moving up or down the borehole (trolling), unlike the HPFM. There is no requirement for the borehole fluid to be conductive for the impeller flowmeter to operate, as is the case with the EMFM.

5.7.3 Electromagnetic Flowmeter

5.7.3.1 What Is the Technology?

An electromagnetic flowmeter (EMFM) is pictured in **Figure 5-21**. The diameter of this tool typically is about 51 mm (2 inches); it is about 1.42–1.54 meters (56–61 inches) long and weighs about 6.1 kilograms (13.5 pounds). The EMFM requires centralization and often, depending on the size of the borehole, a diverter is used to channel vertical flow in the borehole through the body of the instrument (**Figure 5-21**). The typical flow measurement range of this instrument is approximately 0.2 to 250 ft/min (0.01 gpm to 10 gpm if flow is fully diverted through the chamber in the body of the tool).

The EMFM detects and measures flow in a borehole using the principle of Faraday's law, wherein a conductor (in this case water containing dissolved ions) moves through a magnetic field at a right angle to the field, inducing a voltage perpendicular to the flow, and to the magnetic field, that is proportional to the flow velocity of the moving conductor. Water flow is directed through a hollow cylindrical chamber within the tool. The cylinder has two electrodes for measuring the generated voltage, one on each side of the cylinder (180° apart), and an electromagnet that generates a magnetic field oriented 90° to the alignment of the electrodes and perpendicular to the flow within the cylinder. For the EMFM to function properly, the fluid in the borehole needs to have a specific conductance of 5 microsiemens per centimeter (µS/cm) or greater. The voltage polarity of the electrodes is used to determine the direction of flow (up or down) in the borehole.

The EMFM can be used to measure flow at individual stations within the borehole, similar to that described for the HPFM (Section 5.7.1). Measurements can also be made as the tool is moving at a constant speed either up or down the borehole to provide a continuous profile of flow measurements (trolling). Note that trolling induces flow through the tool in a direction opposite to the tool motion, so this needs to be accounted for via tool calibration (which incorporates borehole diameter) and considered in the evaluation of the data. As with stationary measurements, the trolling can be conducted under both ambient and pumping conditions. The continuous profile produced from trolling can be used to identify transmissive zones that can be targeted for more accurate stationary flow measurements.



Figure 5-21. Corehole Dynamic Flowmeter™ (manufactured by Century Geophysical, Inc.) is an example of an electromagnetic flowmeter.

Source: Photo courtesy of COLOG, Inc. Used with permission.

5.7.3.2 How Is the Technology Used?

Tool availability

EMFM is currently not as widely available as the HPFM or impeller flowmeter. Typically, a geophysical logging contractor performs EMFM logging due to the specialized nature of the EMFM, the required calibrations, and the expertise and experience required to use the associated software.

Quality Control

The EMFM should be calibrated by the operator or contractor before mobilizing to the field. Field quality control measures are similar to those described for the HPFM and impeller flowmeter. When collecting data via trolling, it is important to maintain constant logging speed.

Data Collection Design

The design of the data collection is similar to the HPFM and the impeller flowmeter. The EMFM can operate under ambient conditions and under stressed conditions (pumping or injecting) while moving down or up or while the tool is held stationary at a specific depth. When planning an open-hole EMFM logging run, it is important to know the water level in the borehole or well, and the configuration of the borehole or well (for example, bottom of the borehole or well, bottom of surface casing, the position of the well screen or open interval, and diameter(s) of casing, screen, and open borehole). As with the HPFM, supporting borehole geophysical logs, such as caliper, fluid temperature, and conductivity, as well as televiewers, provide insight for identifying potential transmissive zones. When

logging the EMFM under pumping or injecting conditions, it is critical to maintain a constant pumping or injecting rate and monitor the rate to obtain usable quality data.

As with the HPFM and the impeller flowmeter, the EMFM can be run in a cased well and in an open borehole. It can be used to measure the rate and direction of vertical fluid movement produced by a difference in hydraulic head between two permeable units. It can also be used to measure relative hydraulic gradients, identify transmissive units or fractures, identify leaking casing, or characterize the flow within a screened interval. The value of the EMFM is that its resulting data reveals features in the borehole that are transmissive—that is, where water is entering and exiting the borehole. As described in Section 5.7.3.1, in addition to stationary measurements, the EMFM measurements can also be made as the tool is moving up or down the borehole (trolling) to provide a continuous profile of flow measurements. The continuous profile produced from trolling can be used to identify transmissive zones that can be targeted for more accurate stationary flow measurements. EMFM data also reveal the relative head distribution and hydraulic gradients in the borehole. For example, intervals and features where water is entering the borehole have a higher head than intervals and features where water is exiting the borehole (**Figure 5-17**). This information, coupled with data from other logs, is used to define the site geologic framework, the hydrogeologic framework, and groundwater contaminant migration pathways. Additionally, flowmeter results can be used to estimate transmissivity and hydraulic head in transmissive water-bearing zones intersected by the borehole.

Data Interpretation and Presentation

EMFM data can be viewed and plotted in standard borehole logging software packages and processed in Microsoft Excel. It can be presented in a format with other borehole information as shown for the HPFM in **Figure 5-19**. Additionally, flowmeter results can be used to estimate transmissivity and hydraulic head in transmissive water-bearing zones that intersect the borehole using readily available modeling code such as the USGS's FLASH (USGS 2018a).

5.7.3.3 What Are the Limitations?

The EMFM measures a broad range of flows 0.2 to 250 ft/min (0.01 gpm to 10 gpm) but does not detect the lower range of flows detectable by the HPFM. For the EMFM to function properly, the fluid in the borehole needs to have a specific conductance of 5 µS/cm or greater. The other tools described—the HPFM and impeller flowmeter—do not have this specific conductance requirement. Currently, the EMFM is not as widely available as the HPFM or the impeller flowmeter. The depth to which EMFM can be used is based on the pressure and temperature ratings of the specific tool, as well as cable and winch capacity. Accordingly, the depth objective for logging should be discussed with the geophysical contractor and/or equipment manufacturer when planning the logging program.

5.7.3.4 What Are the Advantages?

The EMFM provides a broad measurement range between the lower flow rates that can be resolved by the HPFM and the higher rates that can be measured by the impeller flowmeter. The EMFM tool has no moving parts that could be blocked or otherwise interfered with, which is not the case with the impeller flowmeter. In addition to stationary measurements, the EMFM measurements can also be made as the tool is moving up or down the borehole (trolling) to provide a continuous profile of flow measurements. The continuous profile produced from trolling can be used to identify transmissive zones that can be targeted for more accurate stationary flow measurements. The HPFM measurements can only be made at fixed stations in the borehole.

5.8 Electrical Resistivity

5.8.1 What Is the Technology?

Resistivity logging is most commonly used in bedrock or deep boreholes where high-resolution data cannot be collected using direct sensing methods. Resistivity logging includes several downhole wireline tools that measure the degree to which subsurface materials resist the flow of electrical current. Tools are available to measure the resistivity of various downhole materials, including borehole fluids in the invaded zone and deeper volumes of the formation beyond the invaded zone. The invaded zone is the area in the immediate vicinity of the borehole where native fluids have been displaced by the drilling fluids. Resistivity is the direct inverse of electrical conductivity (EC) and is measured in ohm-meters (Ωm). It is a fundamental property of the material sampled (**Equation 5-2**).

$$R = r*S/L$$

Equation 5-2. Resistivity of subsurface materials to the flow of electrical current.

where R = resistivity (Ωm), r = resistance (Ω), S = the cross-sectional area being measured (m^2), and L is the length (m)

The resistivity of formation materials is affected by properties of the matrix material (for example, mineralogy, porosity, permeability) and of material occupying the pore spaces (such as gas or pore fluids). Clay minerals and metallic minerals (for example, smectite, magnetite, hematite, pyrite) are typically more conductive than other minerals, such as quartz. In water-saturated pores, resistivity is a function of the concentration of dissolved electrolytes in the water (salt water is highly conductive whereas fresh water is less conductive). Deionized water and air are infinitely resistive, as are many hydrocarbons. Because of these differences, resistivity can often be used as a lithologic indicator, as well as an indicator of formation porosity, permeability, and pore fluid chemistry. The relative resistivity of various earth materials is shown in **Table 5-1**.

Table 5-1. Typical electrical resistivities of earth materials.

Material	Resistivity (Wm)
Clay	1-20
Sand–wet to moist	20-200
Shale	1-500
Porous limestone	100-1,000
Dense limestone	1,000- 1,000,000
Metamorphic rocks	50-1,000,000
Igneous rocks	100-1,000,000

Source: (Wightman et al. 2004).

Resistivity is measured by several methods. Normal resistivity is the most commonly used resistivity-logging method, wherein the tool incorporates four electrodes set at two electrode spacings (usually 16 inches and 64 inches), enabling variable depths of investigation. The shorter electrode spacing measures resistivity of the invaded zone, and the longer electrode spacing measures resistivity of both the invaded zone and deeper native formation. The tool measures apparent resistivity, which must be converted to true resistivity for quantitative interpretations. Another resistivity logging tool is the lateral log, which incorporates electrodes in a different configuration designed to measure only the resistivity of the native formation beyond the invaded zone. In addition, focused resistivity logging tools, such as the guard log, have an even greater depth of investigation and can provide higher resolution and thin-bed detection. Additional resistivity tools include focused resistivity meters, single-point resistivity meters, microresistivity meters, and dipmeters. These tools are listed here for completeness but are not discussed further in this document.

Resistivity logs must be collected in fluid-filled open boreholes. An alternative to resistivity logging is induction logging, which measures formation conductivity (the inverse of resistivity). Induction logging is accomplished by transmitting an alternating current (AC) that generates a magnetic field that induces eddy currents in conductive materials. The eddy currents result in a secondary magnetic field that induces a voltage in a receiving coil. The magnitude of the voltage is a function of the conductivity of the formation material. An advantage of induction logging is that it can measure formation conductivity (and thus resistivity) with or without fluid in the borehole and through plastic casing in existing wells.

5.8.2 How Is the Technology Used?

5.8.2.1 Quality Control

Resistivity-logging tools are calibrated using fixed resistors between electrodes. A field geologist familiar with local hydrogeology should be present during data acquisition to assist in evaluating real-time data and identifying potential issues, such as atypical lithology for the region. As with other borehole logging tools, site-specific information (such as location, elevation, well construction details) should be recorded in the log headings for future reference.

5.8.2.2 Data Collection Design

Resistivity logging is conducted using wireline methods in a similar manner as most other borehole geophysical logging tools and must be acquired in open, fluid-filled boreholes. Alternatively, induction logs can be acquired with or without fluid in the borehole and in existing wells with plastic casing. Resistivity logs measure apparent resistivity within the zone of investigation and are influenced by a number of factors, such as temperature, drilling-fluid resistivity, borehole diameter, mud cake, and drilling fluid invasion. To use resistivity logs for quantitative analyses, these factors must be considered during logging and recorded in the log headings.

The requirement for open, fluid-filled boreholes means that geophysical logging should be conducted soon after the borehole is completed and stabilized by the driller. This approach requires communication and coordination with the geophysical service provider to minimize costs for standby time. Logging is usually conducted on a borehole-by-borehole basis rather than logging multiple boreholes in a single mobilization. In cases where the well design requires telescoping casing, mobilization and logging must be conducted prior to setting each casing string.

As with other borehole geophysical tools, logging at a single location provides parameter data only in the immediate vicinity of that location. By logging multiple locations, data can be correlated over greater distances to provide 2D and 3D conceptual models. The density of well locations to be logged should be based on the stratigraphic framework and the nature of features that the investigation is attempting to resolve.

The most common application of multi-electrode-resistivity logging is lithologic characterization and pore-water quality determination. Due to the many factors that contribute to apparent resistivity measurements, experience interpreting resistivity logs is advantageous when performing quantitative analyses. The methods and algorithms used for quantitative interpretation are beyond the scope of this guidance document but can be obtained from a number of available sources.

Like other lithologic characterization tools, resistivity logs can serve as a correlation tool (where multiple logs are available within reasonable proximity to each other) to resolve desired stratigraphic features. Resistivity logs can also be useful when investigating saltwater and freshwater issues associated with aquifers.

Downhole-resistivity logging is a useful method to assess lithology and pore-fluid characteristics. It is one of the most common borehole geophysical logging methods used and is widely available from most geophysical services providers. Qualitative interpretation is facilitated by an understanding of the primary factors that influence apparent resistivity responses. Quantitative interpretation can provide insight into parameters of interest, such as formation pore-water quality and porosity. The type and configuration of the resistivity-logging tool selected depends on site-specific conditions and the investigation goals. Multi-electrode-resistivity logs are often acquired with other logs (spontaneous potential, single-point resistance) as part of a suite of tools providing multiple lines of evidence.

5.8.2.3 Data Interpretation and Presentation

Resistivity-logging data are usually processed and displayed in real time. A typical log suite, referred to as an electric log, is shown in **Figure 5-22** with lithologic interpretation.

In **Figure 5-22**, lithologic interpretations are based on inflections of the resistivity curves to the right of the baseline, indicating an increase in resistivity associated with nonclay-bearing sediments. Clay intervals have an apparent resistivity of <5Ωm, while the alluvial aquifer interval has an apparent resistivity between 20 Ωm and 50 Ωm. In this example, the pore fluid in the alluvial aquifer is fresh water. If saline or brackish water were present, the apparent resistivity would be significantly lower, which would make determining lithology more difficult. When a large variance between short (16”) and long (64”) resistivity measurements exist, this may indicate to the user increases in grain-size heterogeneity or increases in transmissivity. Another example of a resistivity log result is available on the USGS Geophysical logs—Spontaneous-potential log web page (USGS 2000b).

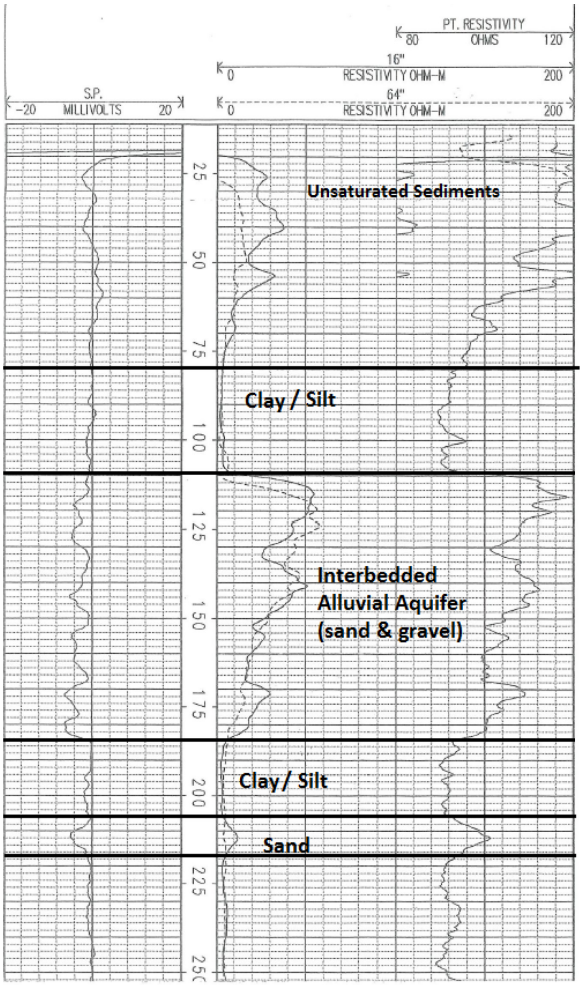


Figure 5-22. Example electric log with spontaneous potential (left column), normal resistivity (16 inch and 64 inch), and single-point resistance outputs.

Source: ERM. Used with permission.

Quantitative interpretation of resistivity logs involves making corrections to apparent resistivity (logged values) by applying various correction factors for such measurements as borehole diameter, drilling-fluid resistivity, depth of drilling-fluid invasion, and bed thickness. Logging manuals with correction charts are readily available on the internet and elsewhere to assist with log analysis (Schlumberger 2009).

5.8.2.4 Data Misuse

Many factors affect material resistivity within the zone of investigation and the apparent resistivity log response. While qualitative interpretation can be straightforward for most near-surface investigations in freshwater-saturated sediments, quantitative interpretation requires experience and a thorough understanding of log responses to a number of variables. Reference materials are readily available to facilitate log interpretation, although familiarity with resistivity logging and the local geologic and hydrogeologic framework are critical.

5.8.3 What Are the Advantages?

Advantages of resistivity logging include:

- cost-effective method of continuous logging bedrock
- efficient and much faster than other geophysical tools
- can help identify saline intrusion within a formation.

5.8.4 What Are the Limitations?

Limitations include:

- The primary limitation of resistivity logging is that quantitative interpretation can be complicated by a number of variables. Collectively, these variables result in nonunique solutions to established analytical approaches.
- Corrections for temperature, drilling-fluid resistivity, borehole diameter, mud cake, and drilling-fluid invasion may be necessary to convert apparent resistivity to true resistivity.
- Normal logs can be affected by bedding thickness as a function of electrode spacing and provide erroneous results. As such, quantitative interpretation requires experience and a thorough understanding of the regional and local geologic framework so that the proper assumptions for analytical solutions are made. Collecting ancillary data, such as water-quality sampling at sites in proximity to the area of interest, can facilitate quantitative interpretations.
- Resistivity readings are fluid-dependent and typically cannot be collected in dry boreholes.
- For accurate readings, the borehole fluids should be at equilibrium with the surrounding bedrock.

5.9 Nuclear Magnetic Resonance

5.9.1 What Is the Technology?

Nuclear magnetic resonance (NMR) has been adapted from use in deep oil and gas exploration to shallow subsurface investigation. NMR uses an active detector that can be lowered on a wireline into existing cased or uncased wells or deployed via direct push technology. As a geophysical method, NMR technology is unique in its ability to quantitatively estimate formation fluid content, porosity, and pore structure.

NMR probes take advantage of a quantum physical property of hydrogen atoms (known as nuclear spin) and the response of hydrogen atoms to magnetic field perturbations, similar to magnetic resonance imaging used in the medical industry. First, the probe emits a static magnetic field that polarizes the spinning nuclei of hydrogen atoms within a fluid (such as water or hydrocarbons). The polarized hydrogen atoms then emit a small magnetic field parallel to the static field, sometimes called “nuclear magnetization,” that is too small to be measured apart from the static field. To measure the nuclear magnetization, a second magnetic field is induced at an angle to the static field. This induced field applies a net torque to the nuclear magnetization, turning it away from the static field. After a short time, the induced field is turned off, and the “echo time” begins. At the beginning of the echo time, the nuclear magnetization begins to turn back, “decay,” or “relax” toward the static field. The NMR probe can measure the magnitude of nuclear magnetization and speed of decay during the echo time, often noted as “T2.” The magnitude of nuclear magnetization and decay speed are both directly correlated to the volume of

fluid and the surface area to volume ratio of the geologic material. NMR probes pulse the induced field many times per second to generate high-quality data.

Traditionally applied, NMR provides quantitative estimates of total porosity, pore-size distribution, permeability, and relative pore-fluid saturations of oil and water. The oil-field NMR tools were developed for deep subsurface bedrock applications and are typically expensive and cumbersome to deploy, making them impractical for near-surface investigations. In recent years, modified NMR logging tools have been developed that are easily and cost effectively used to acquire high-resolution hydrogeologic parameter data for shallow unsaturated (vadose) zone and aquifer investigations. NMR logging provides continuous, high-resolution data throughout the interval logged using either wireline or push-tool data acquisition methods. Surface NMR geophysical methods are also available but are not discussed in this guidance document. Wireline data acquisition can be applied in stable open boreholes or in existing groundwater monitoring or extraction wells, provided the casing materials are nonmetallic. Data are acquired from multiple narrow bands of soil matrix at various radii from the center of the NMR logging tool (called the sensitive diameter; **Figure 5-23**). This method allows formation conditions beyond the disturbed area in the vicinity of the borehole or well to be assessed.

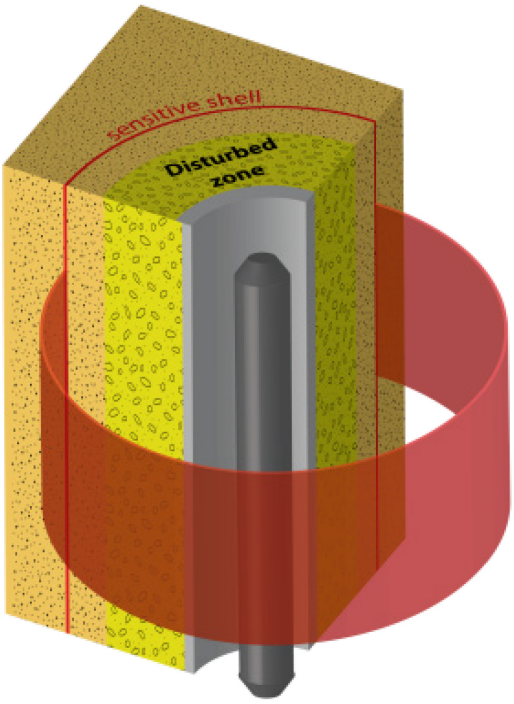


Figure 5-23. Sensitive shell (diameter from center of tool) where NMR data are collected.

Source: Vista Clara, Inc. Used with permission.

5.9.2 How Is the Technology Used?

Quality Control

NMR tools are calibrated by the manufacturer prior to use in the field. The processing software also includes calibration files that are used prior to each logging run to establish data acquisition specifications and procedures relevant to site conditions. The calibration files also specify appropriate logging speeds. Industrial noise such as power lines and electric generators near logging equipment can interfere with NMR signals. The equipment should be grounded, and a reference coil box must be used when logging to measure background noise. Background noise can be minimized during data processing to improve the signal-to-noise ratio. NMR probes that measure multiple sensitive shells (radius around the borehole) have a higher signal to noise ratio. For assessing data quality during data acquisition, the signal-to noise-ratio can also be monitored in real time using the processing software provided by the manufacturer.

Data Collection Design

NMR logging is a fairly slow process compared to other borehole geophysical methods. Logging rates of 150 m/h (approximately 500 ft/h) are typical, and for some applications the logging rate is slower. Considering time for mobilization, demobilization, and decontamination between wells, 60 m to 75 m (200 ft to 250 ft) is the maximum log production expected in a typical workday for most near-surface applications. For deeper wells with a single mobilization, greater log production is feasible.

When logging in existing monitoring or extraction wells, certain well construction considerations must be considered, including casing material (nonmetallic only), casing diameter, and the original borehole

diameter. The casing diameter determines which tool can be used. In larger-diameter casings, a larger NMR tool can be used to increase the maximum sensitive diameter and improve vertical resolution. The sensitive diameter must be greater than the original borehole diameter to avoid logging the annular material outside the casing. Conversely, if the nature of the annular material of the well is of interest, a tool with a sensitive diameter can be selected to measure parameters within the annular space.

When implementing NMR logging using direct-push tool advancement technologies, data collection follows similar protocol to other direct sensing methods (Morozov et al. 2024). In this case, a small-diameter casing is advanced to the maximum depth to be logged and the tool is inserted into the casing. The casing is then retracted in stages to expose the tool to the soil matrix. Following logging at each stage, the tool is raised into the casing and the casing is retracted, ready for the next logging stage. Alternatively, a blank PVC casing (permanent or temporary) can be installed in an open borehole for logging purposes.

As with other borehole geophysical tools, logging at a single location provides parameter data only in the immediate vicinity of the location. By logging multiple locations, data can be correlated over greater distances to provide 2D and 3D conceptual models. Based on mobile- and bound-water porosity information, transport pathways and storage intervals can be identified and mapped. The density of well locations to be logged should be based on the stratigraphic framework and the nature of features that the investigation is attempting to resolve.

Parameters that can be quantified include residual-water saturation (vadose zone), total porosity, mobile porosity, bound porosity (clay and capillary bound), hydraulic conductivity, and multiphase saturations for certain NAPL that are present in the aquifer. Based on pore-size distributions and relative mobile versus bound water content, lithology can be indirectly inferred. Some lithology data are likely already available for any given site, lending context for and weight to NMR-based lithologic interpretations. As stated previously, NMR can be deployed in stable boreholes, existing groundwater monitoring or extraction wells, or advanced using push-tool methods to collect high-resolution data over the interval logged.

Data Interpretation and Presentation

The laptop computer provided by the supplier includes software for processing and displaying the data in real time. Data interpretation is straightforward, as shown in the example log displayed (**Figure 5-24**).

The left column in **Figure 5-24** shows the transverse relaxation time (T2) distribution of excited hydrogen molecules derived from composite spin echo trains measured by the NMR tool. The integral of the T2 distribution reflects total water content, and the distribution along the T2 axis is indicative of water mobility. The center column shows the

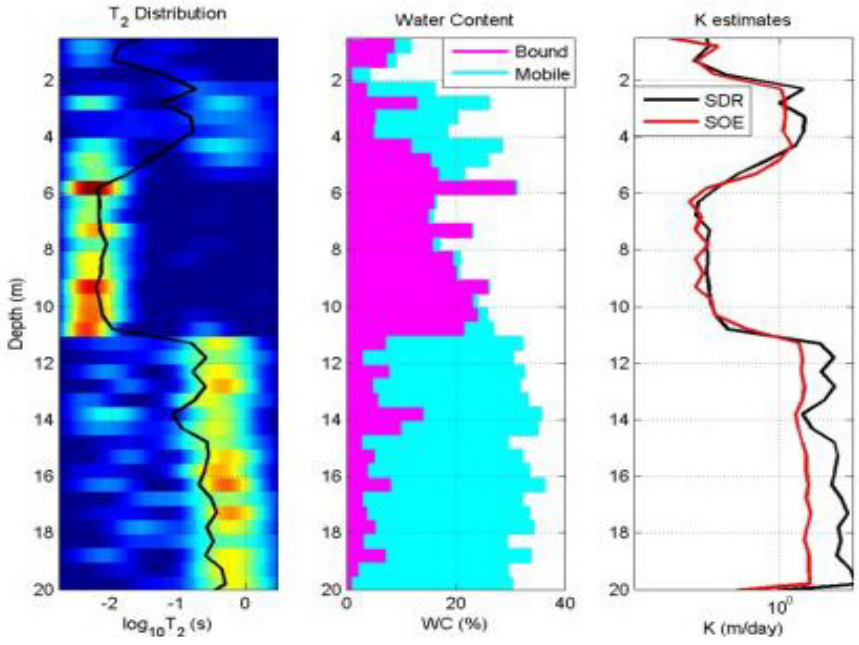


Figure 5-24. Example NMR output.

Source: Vista Clara, Inc. Used with permission.

relative amounts of mobile and bound water, and the combination of these represents the total water content. In unsaturated media, total water content reflects the residual-water saturation. In saturated media, the total water content reflects the total porosity of the matrix material. Intervals with a high percentage of mobile water are indicative of highly permeable coarse-grained soils, and intervals with a high percentage of bound water are indicative of low permeable clays and fine-grained soils. The right column shows the estimated hydraulic conductivity distribution for the logged interval. Hydraulic conductivity is estimated from total porosity and pore-size distribution using multiple algorithms developed and empirically tested on various soil and rock types.

Other properties of pore fluids that can be measured by the NMR tool are hydrogen index and fluid diffusivity. Fluid diffusivity is the extent to which molecules move at random in the fluid. There is little difference between the hydrogen index of water and that of petroleum hydrocarbons, although the presence of petroleum hydrocarbons affects fluid diffusivity and has an inverse effect on T2 relaxation times. Using oil-field NMR technology, NMR data can be processed to evaluate those properties and derive estimates of hydrocarbon saturation within the pore space. Testing this analytical method (Spurlin et al. 2019) has shown that hydrocarbon saturations of less than 5% can be detected and semiquantitatively estimated within a reasonable margin of error. This analysis can be performed in stages within intervals of interest identified following initial NMR logging.

Data Misuse

The primary considerations when using NMR data are the vertical resolution and the sensitive diameter where data are collected. Vertical resolution is defined by the vertical length of the stage where data are collected and represents average properties of the soil matrix over the interval. If the sensitive diameter is close to or less than the original borehole diameter (and potentially disturbed zone beyond the borehole), the results obtained may not accurately reflect native soil matrix conditions. It is best to use a tool with a sensitive diameter that extends 2 inches or more beyond the original borehole wall. If the original boring was drilled with mud, the invaded zone may impact formation properties even more deeply.

Tool Availability

Currently, only a few geophysical service providers offer turnkey near-surface NMR logging; however, NMR logging equipment can be rented and shipped by the manufacturer to most locations in the US, as well as globally. This option allows users to perform the logging themselves or have the equipment shipped to their preferred geophysical service provider. The basic equipment required includes the logging tool, a tripod and sheave wheel, a cable spool and winch, an electronics unit and laptop computer, a reference coil to detect background noise, and a generator. The system is designed to be easily set up and operated via user-friendly interfaces on the laptop. Following data acquisition, software installed on the laptop processes the data to provide viewable output of results in real time.

5.9.3 What Are the Advantages?

Advantages of NMR include:

- Unlike neutron porosity tools, does not require a radioactive source
- Can be implemented on existing PVC-cased wells
- Can be implemented at locations without wells using available direct-push NMR probes
- Can provide details on hydrocarbon type within a borehole
- Provides excellent information on effective porosity and permeability

NMR is the only available borehole geophysical tool that quantitatively measures porosity, pore-size distribution, and hydraulic conductivity concurrently. Based on the pore-size distribution, NMR can also differentiate between mobile porosity and bound porosity (silt and clay) fractions. In comparison, neutron logging yields quantitative estimates of total porosity but requires using a radioactive source. This requirement can raise concerns when investigating near-surface and drinking-water aquifer systems **ASCT-2 Technical Selection Matrices: BG Matrix**. Another advantage of NMR is its ability to detect and differentiate between water and certain petroleum hydrocarbons in pore fluids and provide quantitative estimates of the relative saturations of each.

A key advantage of NMR logging is that it can be conducted in existing PVC-cased monitoring wells, eliminating the need for additional intrusive drilling and derived-waste handling. The depth of investigation is not limited by soil conditions that preclude tool advancement, as can be the case with direct sensing tools. In addition, variations in parameters over time, such as hydrocarbon saturation or reductions in porosity due to biofilm formation, can be monitored by periodically relogging wells. The NMR tooling can also be deployed using direct-push methods, if desired.

5.9.4 What Are the Limitations?

Limitations include:

- Equipment is expensive.
- Users cannot log NMR in steel-cased wells due to the magnetic field generated from the equipment. Similarly, metallic centralizers may interfere with NMR measurements.
- Data can be complex and time-consuming to process and may require verification/validation with other geophysical or drilling or sampling methods.

Table 5-2. Example NMR tool specifications.

Category	Tool Name	Tool Diameter (inches)	Tool length (inches)	Weight (lbs)	Pressure Rating (psi)	Vertical Resolution (inches)	Sensitive Shell Diameters (inches)
Max	JPX350F	3.5	70	60	1700	18	F1-12"; F2-13.5"; F3-15"
	JPX525F	5.25	65	90	1700	18	F1-16"; F2-18"; F3-21"
Slim	JPY238N	2.38	65	25	2350	8	F1-9"; F2-11"
	JPY238J	2.38	62	27	2350	4	F1-9"; F2-11"
	JPY300N	3.0	69	40	1700	11	F1-13"; F2-15"
	JPY350N	3.5	72	55	1700	18	F1-13"; F2-15"
Micro (Dart)	JPZ175E	1.75	69	14.5	830	15	F1-9"; F2-10"
	JPZ175A	1.75	69	15.5	1700	15	F1-7"; F2-8"
	JPZ175D	1.75	52	11	1700	6	F1-5"; F2-6"
	JP140G (Geoprobe)	1.4	68	12	380	9	F1-5"; F2-6"

Source: Vista Clara, Inc. Used with permission.

NMR vertical resolution is somewhat limited compared to other borehole geophysical methods. Data are generally acquired in stages based on tool specifications (coil spacing) and are averaged across each

stage. Some NMR tools generally provide approximately 0.5 m (approximately 1.5 ft) of vertical resolution; direct-push NMR tools provide approximately 1.5 to 6 inches of vertical resolution. Tools typically log between one and four sensitive shells simultaneously, with the maximum sensitive diameter varying between 5 inches and 21 inches, depending on which tool is used. It is important to know the original borehole diameter to ensure that the sensitive diameter of the tool being used is measuring undisturbed soil matrix beyond the borehole wall. It is also important to note that the sensitive shells are typically only 1–2 millimeters thick. **Table 5-2**. provides a summary of the various tools and associated features but naturally is not an exhaustive list of available tools. Additionally, a practitioner must be aware of the designed depth of investigation for a specific probe, which varies from probe to probe, and must be considered during investigation design.

5.10 Borehole Video Survey

5.10.1 What Is the Technology?

Borehole video surveys provide a visual record of the actual condition of a well and allow the viewer to see the actual condition of the borehole walls firsthand. Under adequate conditions, the viewer can explore a wide range of subsurface environments—from 2-inch diameter monitoring wells to open boreholes and production wells exceeding 12 inches in diameter. Dual-viewing (both downhole and 360° side view), high-resolution cameras allow the viewer to identify and classify geologic features, well construction details, and obstructions, if present. Digital video recordings can be saved to a variety of electronic media or uploaded to a cloud-based platform in the field.



Figure 5-25. Example borehole video camera systems.

Source: Photos courtesy of Mount Sopris Instruments. Used with permission.

Borehole video camera systems range from portable systems that can reach 1,000 ft in depth to truck-mounted units capable of reaching 5,000 ft or more. Most borehole cameras are fitted inside stainless-steel housings and pressurized with nitrogen. Some models are reportedly waterproof up to 2,500 psi, which is equivalent to submersion to a depth of 5,880 ft underwater. The housing typically ranges from 1.6 inches to 3.5 inches in diameter (**Figure 5-25**) and up to 22 inches in length. Digital video feeds are transmitted over single-conductor (coaxial) wireline, wrapped with armored cable.

In addition to the descriptions in the following paragraphs, see the example temperature log on the USGS Geophysical logs–Temperature log web page (USGS 2000c).

5.10.2 How Is the Technology Used?

5.10.2.1 Quality Control

The following activities are recommended to control data quality:

- Check camera diagnostics such as internal temperature, pressure, humidity, and voltage and amperage during each survey, in real time, to ensure safe camera operation, or for troubleshooting purposes.
- Reset the on-screen depth measurement prior to conducting each borehole video survey to maintain project-specific reference points. This depth measurement can be calibrated as frequently as necessary.
- Prior to performing a borehole video survey, the viewer should confirm with the operator the exact location on the camera where the depth is being referenced. It is important to note that during each portion of the video—both downhole and side view—the reference depth does not change, and the side-viewing window is often located slightly above the downhole camera lens.
- Before logging, identify the diameter of the well casing and borehole and the camera's centralizer bands should be adjusted to fit loosely against the borehole or casing wall.
- Note the relative size of the borehole or well and account for the camera's proximity to the borehole wall. The viewing window may exaggerate the size of certain features. For example, a void that might appear cavernous may only be a couple of inches in length. It is important to note the relative size of the borehole or well and account for the camera's proximity to the borehole wall. Additionally, other geophysical probes, such as a mechanical caliper or acoustic televiewer, can more accurately estimate the size of the features in question.
- Before logging, confirm with the operator the planned logging speed and adjust as necessary to meet the goals of the survey.
- Check recording devices at regular intervals to confirm the collection (and storage) of video files.

5.10.2.2 Data Collection Design



Downhole view of casing joint



Downhole view of borehole wall. Note groundwater flow on right side of image.

Figure 5-26. Examples of screenshots from several borehole video surveys.

Although the SOP for obtaining borehole videos may change from vendor to vendor or by operator and client preferences, the common practice is to record the first portion of the survey moving downward through the borehole, viewing through the downhole lens. Newer cameras allow the operator to pan and tilt the lens, but the lens continues to point downward during this initial portion of the survey. The

operator notes features of interest until the total depth of the well is reached. During this process, care should be taken to avoid borehole disturbance, which could reduce camera visibility.

The second portion of the video survey is conducted while pulling the camera upward, recording through a side-viewing window. The camera lens is rotated 360° to view each side of the borehole wall. This rotation can be performed while the camera is in a static (stopped) position or while the camera is moving vertically through the hole. Because of the limited speed of the lens's 360° rotation, a side-viewing survey is typically conducted at a slower speed than the downward-viewing survey.

Video surveys are typically viewed on a monitor or laptop computer screen provided by the operator or camera rental company. The software necessary for video display and processing should also be included. Examples of screenshots from a number of borehole video surveys are included in **Figure 5-26**.

Video surveys can be recorded as MPEG video files, which could become large files. Wi-Fi capabilities in the field may allow the operator to upload video files to a cloud-based platform for easy distribution.

Borehole video surveys can be used to perform the following activities:

- inspect well casing and screen
- document well construction
- identify and classify fractures
- identify seeps from fractures in the vadose zone
- identify water-bearing zones
- characterize lithologic or geologic features
- identify obstructions
- confirm changes in conditions before or after work
- document regulatory compliance and pre-well abandonment

An important aspect of conducting a successful borehole video survey is the ability of the camera's light source to reach the borehole walls. With the advancement of LED technology, modern borehole cameras are outfitted with more powerful and efficient LED light rings or forward-facing bulbs (pictured above). Note that halogen lighting techniques also remain in use.

Centralizer bands (thin lengths of bowed metal or plastic affixed to collars that slide over the camera) are used to keep the camera centered in the borehole or well casing throughout the survey. Real-time adjustments to the camera's focus, light intensity, and rotation (during the side-viewing portion of the survey) are controlled remotely at the surface.

A depth encoder, often located at or near the camera system's winch, provides the depth of the camera's lens, from a reference point selected by the user, to the nearest tenth of a foot, on screen. Camera diagnostics, such as internal temperature and humidity, are also available to monitor the condition of the unit or for troubleshooting purposes.

5.10.3 What Are the Advantages?

Borehole video surveys have the following advantages:

- Surveys can be conducted in submerged or open-air environments.

- The viewer is able to observe the condition of the borehole walls firsthand, which is useful for classifying the subsurface geology and lithology and planning subsequent tasks (for example, hydraulic packer testing and well construction).
- If present, inflowing and outflowing features are clearly defined to an exact depth.
- The tool can be used to remove well obstructions (for example, small hand tools, piping and tubing, sampling equipment dropped or lost down a well).
- This tool is readily available for rent, purchase, or contract through a vendor.
- Surveys can often be completed in a matter of hours for wells up to 500ft deep.
- Surveys are electronic and can be uploaded and downloaded, reproduced, or distributed quickly after completion.

5.10.4 What Are the Limitations?

Borehole video surveys have the following limitations:

The clarity of the image depends solely on the amount of light reaching the borehole walls. If the water is or becomes turbid, the camera does not receive sufficient light, and the image is compromised or lost. If permitted, constantly running clean water into the well or removing water via pumping before or during the survey usually resolves the turbidity issue.

In wells that are deviated, the camera may favor one side of the borehole wall, compromising the image.

Many cameras are not equipped with a compass, which limits the viewer's ability to reference or orient the features observed. Using an ATV or OTV, which includes internal magnetometers (for orientation) and inclinometers (for tilt), along with a borehole video survey compensates for this limitation.

Borehole video surveys are often conducted with specialized borehole retrieval tools, which are separate tools not discussed in this document.

Potential interference during the survey may include electrical issues caused by the power source or the physical hazards associated with open rock wells (for example, collapse, loose material, obstruction).

5.11 Other Borehole Geophysics Tools

Several tools, such as neutron logging, sonic logging, spontaneous potential (SP) logging, magnetometric resistivity (MMR), colloidal boroscope, saline tracing, in-well heat tracing with fiber optic monitoring, active line source (ALS) logging, and hydrophysical logging (HPL), are considered applicable in specific instances and under special conditions. Some of these require open hole logging, or are specific for fractured bedrock conditions, or open bedrock boreholes. These are also considered supporting tools for environmental investigations. Several of these are better suited for hydrocarbon exploration than environmental investigation. Detailed discussion on these tools is beyond the scope of this document. One such tool is discussed in the following section.

5.11.1 Thermal Neutron

5.11.1.1 What Is the Technology?

Neutron borehole logging uses a radioactive source to emit neutrons into subsurface materials. As neutrons interact with atoms in the surrounding formation, the energy of the neutrons decreases through

collisions and absorption. The main purpose of this technology is to estimate hydrogen content, which often reflects pore water, making neutron logs valuable tools for assessing porosity and water saturation in environmental investigations. All neutron-logging tools involve radioactive materials and generally require special handling and permits.

Neutron logging tools emit high-energy neutrons using a radioactive source, typically americium-beryllium or plutonium-beryllium. As neutrons travel within the formation they lose energy mainly by elastic collisions with hydrogen atoms. Because neutrons and hydrogen nuclei have similar mass, more energy is transferred, making the tool very sensitive to hydrogen content. Neutrons move through three key energy states: fast neutrons (initial high energy), epithermal neutrons (intermediate energy, continue to scatter), and thermal neutrons (low energy, easily absorbed by surrounding atoms, typically heavy elements which emit gamma photons on absorption).

5.11.1.2 How Is the Technology Used?

Neutron logs help determine porosity and water content in saturated and unsaturated formations, supporting aquifer studies, remediation planning, and contamination monitoring. Thermal neutron technology is used to identify permeable zones, track changes in saturation, and assist in delineating fluid migration pathways within the open borehole. In environmental applications, neutron logging is often paired with other geophysical methods to cross-verify hydrostratigraphic interpretations.

Formations with more hydrogen (water, hydrocarbons) slow down and capture neutrons more rapidly. Therefore, high neutron counts can indicate low hydrogen content while low neutron counts can indicate high hydrogen content.

In saturated formations, neutron count data can be used to estimate porosity. In unsaturated zones, the method estimates volumetric water content.

A thermal neutron tool is a sidewall tool and often employs a mechanical arm to maintain contact with the borehole wall and collect ancillary caliper data.

5.11.1.3 What Are the Limitations?

Thermal neutron tools have the following limitations:

- Special permits and safety procedures are needed due to the radioactive sources used in these tools.
- Water content or porosity estimates can be impacted by elements such as chlorine or boron, and in some cases, lithologic variations (such as clay or hydrated salts).
- The thermal neutron tool cannot distinguish between water and other hydrogen-bearing fluids (such as hydrocarbons) without supporting information.
- Operators need special clearance to use on military installations or moving across country borders.
- Several complicating factors, including mineralogy, borehole size, fluid, and casing, can affect hydrogen content and thus formation-porosity estimates. Neutron logs often require corrections, most commonly for borehole size and the shale effect. The shale effect, caused by shale's high immobile water content that inflates porosity readings, can be corrected using complementary logs such as gamma or NMR.

5.11.1.4 What Are the Advantages?

Thermal neutron tools have the following advantages:

- Data can be collected quickly, with tools typically lowered into boreholes for real-time logging and immediate interpretation.
- They are highly sensitive to hydrogen, making this an effective method for estimating water and hydrocarbon content regardless of lithology in many cases.

6 SURFACE GEOPHYSICS

Surface geophysical tools are a class of nonintrusive geophysical instruments used to evaluate the subsurface. They indirectly measure physical properties of materials from signals produced by natural or generated sources and rely on contrasts in the properties of different materials. Their purpose is analogous to medical imaging: in the same way that CT scans, ultrasounds, MRIs, etc., can be used to look beneath the skin to identify an area needed for biopsy or surgery, surface geophysical tools can look beneath the ground surface to identify key features and target drilling or remedial locations.

6.1 How to Select and Apply Surface Geophysical Tools Using This Guidance Document

This section addresses only those geophysical methods more commonly applied in the environmental industry for the purpose of site characterization and remedial design: electrical resistivity imaging (ERI), ground penetrating radar (GPR), seismic reflection and refraction, multichannel analysis of surface waves (MASW), and both time domain electromagnetic (TDEM) and frequency domain electromagnetic (FDEM) surveys (**Figure 6-1**). Where appropriate, other methods are briefly addressed in related sections; spontaneous potential and induction polarization, for example, are mentioned under the electrical resistivity section.

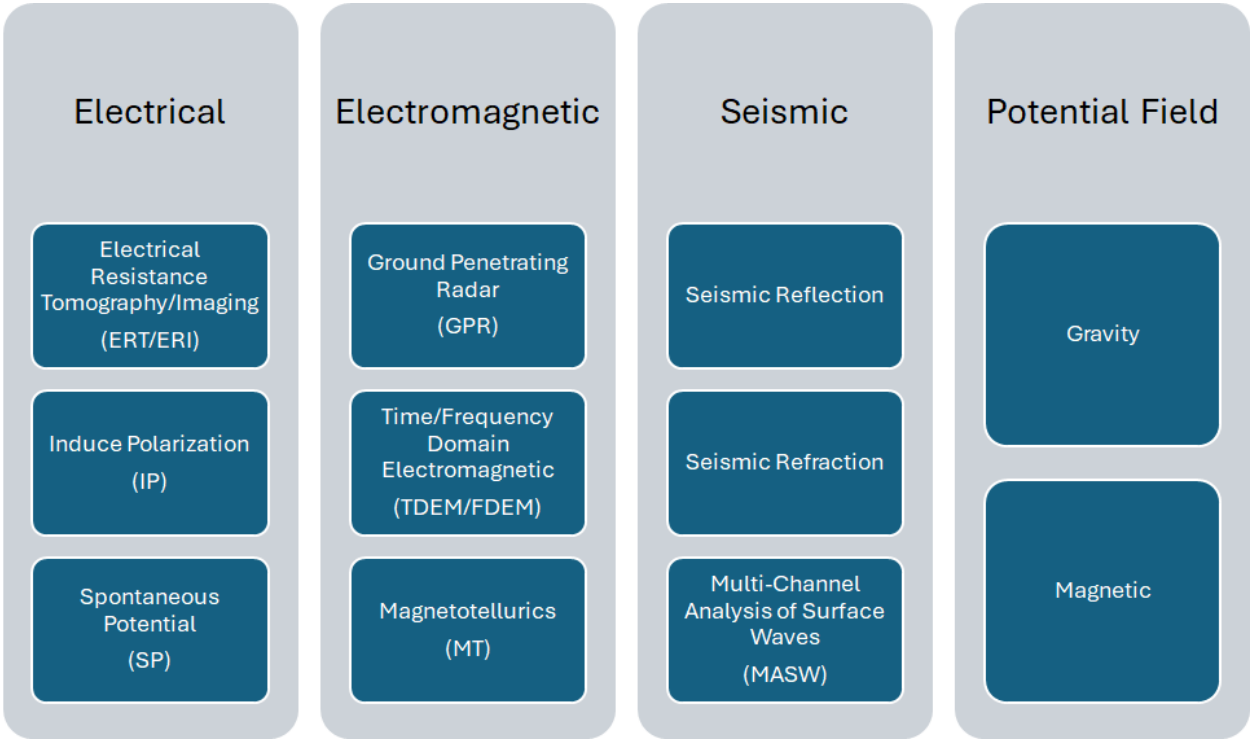


Figure 6-1. Surface geophysics tool summary.

General advantages to using surface geophysics include:

- Ability to visualize the subsurface problems (between boreholes) that need to be solved, thereby reducing the costs of characterization and monitoring

- A better understanding of complex geology, preferential pathways, and contaminant extents compared to data produced using point samples (groundwater monitoring wells)
- Enhanced lateral coverage and resolution due to continuous data coverage
- Collection of data in areas that are difficult to access with a drill rig, such as through buildings, across utility corridors, under power lines, over uneven terrain, or across water bodies (abilities dependent upon the specific method)
- Ability to cover large sites quickly
- Robust, high-density datasets that lend themselves to developing a 3D CSM
- Potential for integration with existing and future datasets (for example, boring logs, chemical samples) to calibrate the geophysical data to site-specific conditions and maximize other datasets
- Provision of a roadmap for additional investigation and remedial design characterization (ITRC 2020) by identifying critical subsurface targets (for example, contaminated zones where monitoring wells, injection wells, or other remediation systems should be installed)
- Ability to monitor a site over time (temporal visualization of a site) to see subsurface changes such as plume migration, dissolution features developing, or recharge zones

General considerations when using surface geophysics include:

- Surface geophysical tools are an indirect method, meaning they can be used to image subsurface features that control contaminant transport and, under optimal conditions, sense proxies of contamination, but cannot measure concentrations of specific contaminants.
- Correlation with existing datasets (for example, boring log geology or groundwater samples), drilling and sampling the geophysical anomalies (called ground truthing), and interpretation by those with local site knowledge are required to understand the subsurface conditions.
- Results of geophysical investigations are nonunique, meaning multiple scenarios can produce the same geophysical signal (an electromagnetic (EM) tool, for example, can record a highly conductive signature that results from a small, shallow object or a large, deep object), hence the need for data integration and ground truthing.
- Data processing usually includes a smoothness constraint that can result in a "blurry" representation of the subsurface, making it difficult to discern the exact shape and size of anomalies, especially when stations are not close enough to reveal all details of the signal (Mussett and Khan 2012).
- Vertical resolution is lower than is possible with borehole geophysical and direct push methods.
- Above- and belowground site features can interfere with the techniques and generate noise that can degrade data quality and/or result in anomalies. Some sources of interference include nearby infrastructure, power sources, buried utilities, pumps, subsurface temperature variations, and/or objects (fences, buildings, vehicles). While one source of noise can impact one geophysical method, it may have no impact on a different one, so refer to the matrix (**ASCT-2 Technical Selection Matrices: SG Matrix**) for tool-specific noise sources.

6.1.1 Tool Availability

Surface geophysical tools are generally portable, can cover a large area, can "see" between wells, require minimal intrusion, and provide the best means to observe the subsurface in three dimensions. The portability of the tools and technological advances in computing power allow surface geophysical

methods to be efficiently used in large-scale investigations (for example, regional area geology) and small-scale site characterizations (for example, identifying a UST at a corner retail store). Surface geophysical tools can also be used as part of remote sensing investigations and can be paired with other tools discussed in this guidance document (see the **ASCT-2 Technical Selection Matrices: SG Matrix**). While surface geophysics tools are available globally, North America is leading the global market in the use of surface geophysical tools due to the comprehensive environmental regulatory requirements across multiple industries, such as environmental characterization, mining, oil and gas, and construction (Fortune 2026).

6.1.2 Selecting Surface Geophysical Tools

Surface geophysics is most beneficial to a project and offers the greatest return on investment when used early (before several rounds of drilling or any remediation have occurred) because it can narrow the targeted areas for investigation and treatment (analogous to a doctor ordering an MRI before collecting a biopsy or performing surgery). It is particularly beneficial for projects with the following conditions:

- Site is 2 or more years old (Winner 2025).
- Site is in a cycle of advancing borings and drilling additional wells for site characterization with no clear path to delineation.
- Complicated site logistics prohibit a drill rig in key areas.
- Complex geology, transmissive layers, or preferential pathways are suspected.
- Contamination is suspected in bedrock (weathered, fractured, or otherwise).
- Contamination is deep (more than 100 ft bgs).
- Current total project costs are estimated to be approximately three times the cost of the geophysical investigation (Winner 2025).
- One or more remedial actions have been implemented without success or a clear path to site closure.

The **ASCT-2 Technical Selection Matrices: SG Matrix** provides rough guidance as to which geophysical tool will provide the most value to the project and in which conditions the tool can be most effective. The different geophysical tools are listed across the top and different CSM considerations, and site conditions are listed along the left. The intersecting cell color will tell if that technique is almost always (green), sometimes (yellow), or rarely (red) effective for those questions or conditions. A detailed discussion on each method is available later in this section. It is important to note that multiple ASCT can often be deployed on a site to provide synergistic information and value.

Additional resources for selecting an appropriate geophysical tool to support tool selection and use and project management can be found in the USGS Fractured Rock Geophysical Toolbox Method Selection Tool (USGS 2018b) and in the **ASCT-2 Selection Tool**.

6.1.3 General Geophysical Theory and Approach

Geophysical projects typically have the following phases: forward modeling, data acquisition, data processing, data visualization, integration, and interpretation. The final interpreted results can then be used to inform the CSM and remedial action. General descriptions of these phases include:

> **Forward modeling:** Forward modeling takes a model for the distribution in subsurface properties (such as a geologic cross section) and uses a mathematical algorithm to approximate the geophysical response that might be seen with a tool (for example, given some set of variables,

what is the result). It is often done prior to survey design and data acquisition and can sometimes be helpful in assessing if a target will be sensed by a specific method. It is nearly impossible, however, to accurately account for the subsurface heterogeneity that is likely to be encountered. Therefore, forward modeling is not a required first step. It can also be used after data collection to test hypotheses and compare against the collected data.

Data acquisition: The tool sends an impulse along a linear transect or across a 3D grid. The signal propagates through the subsurface and is picked up by the tool's receiver. A single transect typically has constant sensor spacing, which affects resolution and target detection. Transects are preferably run perpendicular to the target. When multiple transects are combined, a 3D grid of stations and contoured results can be formed. The signal (the data that is desired) to noise (unwanted fluctuations in the measured data that may be spatial or temporal) ratio is improved by repeated measurements.

Data processing: The raw data from the data acquisition transect (or survey) must be corrected for geometric effects controlling signal transmission and attenuation or inverted to transform indirect geophysical measurements of the earth's subsurface into quantitative models of geological structures and properties. This can include correcting data for unwanted variations unrelated to the variation in subsurface properties (for example, topographical corrections are critical for accurate interpretation of most datasets).

Data visualization: The results of a geophysical survey vary depending on the method employed. Dimensionality of the results depends on the data coverage. It may be a 1D vertical profile from a sounding around a single point, a 2D cross section from a single profile of data, or a 3D model or contour map generated from a set of parallel transects.

Integration: Oftentimes, a wide collection of data could be available for the same area of the geophysical survey and leveraging this data during interpretation will assist with understanding the geophysical response. Helpful datasets include regional geologic maps, potentiometric surface maps, boring logs and/or lithologic cross sections, groundwater parameters, and groundwater and soil analytical data. These data should be integrated with accurate geospatial referencing so that no anomalies are improperly interpreted.

Interpretation: Following visualization and existing data integration, the results are interpreted into a geological or site characterization context. Targets are recognized as an "anomaly" in the data (values are above or below the surrounding data averages). For example, a region of higher electrical conductivity (EC) could indicate the presence of higher salinity groundwater. The geophysical model must be combined with all available data (including geologic, outcrops, geophysical, and chemical data) to update the (Mussett and Khan 2012) CSM . Best practice is for interpretation to be performed by an experienced practitioner with sufficient certifications.

CSM updates: After integration of existing data with the geophysical data, hypotheses can be made regarding the source of geophysical anomalies and their potential place in a site's CSM. Invasive techniques can then be used to target those anomalies, the results of which can be used to fine-tune the calibration of the geophysical data for site-specific conditions. The geophysical survey results can continue to provide a roadmap for future action and remediation. For example, if a particular electrical resistivity anomaly was found to correspond with high TPH impacts, those zones, as they appear throughout the datasets, can be targeted for remediation.

QA/QC protocols might not be provided by the equipment manufacturer, so it is important to ask the geophysical provider about their QA/QC protocols. Data processing is important, but no amount of processing can fix data that were collected poorly. It is also critical that all geophysical surveys

performed include some land survey work so that the results can be accurately integrated geospatially with existing datasets and provide accurate targets for follow-up work.

6.2 Electrical Resistivity Imaging

6.2.1 What Is the Technology?

Electrical resistivity imaging (ERI)/electrical resistivity tomography (ERT)/multi-electrode resistivity is one of the most versatile surface geophysical methods as it can be applied to a full range of geologic conditions and can acquire data over water, across varying terrain, and through buildings. The names are all similar technology whether ERI or ERT or multi-electrode resistivity. The differences originate from electrode placement and geometry, but the names are generally used interchangeably now. A noninvasive technique that does not require a drill rig or excavation, ERI uses electric current actively applied via an array of electrodes at the ground surface to map the distribution of electrical resistivity in the subsurface. While the voltage and current can be adjusted, ERI surveys often use less than one ampere (amp) of current for less than one second during a measurement, which is considered safe for humans and pets. Electrical resistivity (ER) is the intrinsic property of a material to oppose the flow of current through it, and its variations in the subsurface can inform a multitude of parameters that it is a function of, including lithologic composition, grain-size distribution, porosity, fluid saturation and chemistry, presence of metallic features, and biogeochemical processes.

While ERI can be deployed in a grid pattern or a nonlinear geometry, it is commonly performed along linear transects of electrodes that produce 2D electrical profiles of the subsurface. These static cross-sectional electrical images can provide good quality data to depths of hundreds of meters, covering the depth of interest for most environmental concerns. ER methods can be used for a variety of applications, including detection of NAPL or saline fluids, mapping of preferential flow paths, groundwater well siting, geohazard mitigation, lithologic mapping, archeological investigation, and geotechnical site characterization. As a monitoring technique, temporal or transient electrical resistivity imagery (TERI) provides a stable method to compare datasets across events or seasonal variations. TERI applications include evaluating effectiveness of remedial applications, aquifer recharge and recovery, dam seepage, saltwater intrusion, and monitoring geohazards such as sinkholes or slopes that pose landslide risks.

6.2.2 How Is the Technology Used?

6.2.2.1 Water Supply and Aquifer Management

ER methods can target water supply objectives by finding channels in porous media (commonly electrically resistive targets for coarser grained channels) or fractures in bedrock (commonly electrically conductive targets). In this way, ERI has been used to site high-yield water supply wells in areas with low or variable yields in the past. Additionally, variations in downhole groundwater electrical conductivity (EC) measurements can be further evaluated with ERI to map water quality changes such as delineating a freshwater lens or identifying the saltwater-freshwater interface in coastal areas (Panthi et al. 2024). As saline fluids are typically orders of magnitude more electrically conductive than fresh water, it is a valuable tool for detecting and monitoring saltwater intrusion into freshwater aquifers. While static ERI is more ambiguous about water table location, TERI can build an understanding of where airfilled voids extend in order to observe water table conditions. However, it should be noted that the observation of water table conditions provided by TERI is possible only under certain site conditions and is lower resolution than well data. TERI can serve as a useful tool to help regulators oversee groundwater protection by monitoring aquifer depletion and recovery and can likewise help gauge the effectiveness of aquifer storage and recovery and managed aquifer recharge projects (Fields et al. 2022).

6.2.2.2 Urban Settings

Given their noninvasive nature, ER methods can be used in urban settings to acquire information about sites where drilling is difficult or impractical. Public and private utility locators should be used to design the survey locations to understand where electrode placement might be limited or restricted for safety and access concerns. Further, an understanding of known utility locations can be essential to ERI data interpretation. As features such as metallic infrastructure and surface obstacles can be more prevalent in urban environments, proper planning (such as avoiding placing surveys immediately parallel to uncoated metallic pipelines and turning off cathodic protection) should be performed in advance to avoid a reduction in data quality. Because significant metallic interference with current flow is obvious in most datasets, if cathodic protection or other features cannot be altered, a dataset may be determined to be poor and some or all of the data will not be usable to achieve the project objectives as the electrical current could not bypass the surface features. With advanced planning, this is a relatively rare occurrence.

Modern utility trenches tend to be electrically resistive structures because modern pipe coatings prevent current from entering the utility, and the surrounding backfill material from when the utility was excavated and filled in is often coarser grained and therefore more electrically resistive than the surrounding soil. In much the same way, ERI can be used to locate prior excavations that correspond to other anthropogenic features such as graves, tunnels, or former underground storage tank pits. Older utilities or metal well casings can show up in the datasets, generally as more electrically conductive features. Running ERI surveys perpendicular to uncoated metallic utilities allows imaging of these locations. Industrial installations using surface grounding grids such as transformer yards prevent the electrical current from getting to depth and limit the use of geophysical methods over these metallic grids.

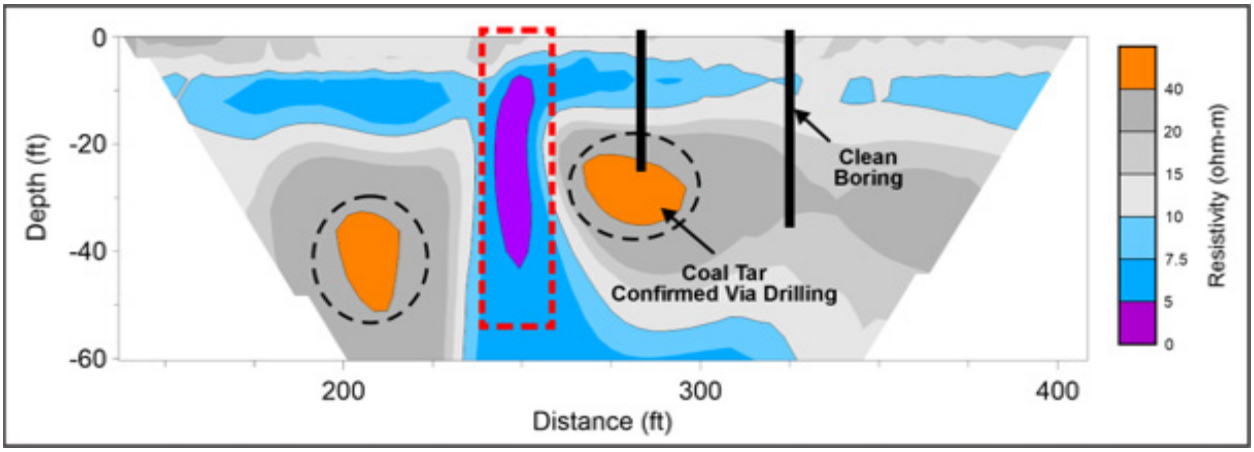


Figure 6-2. Photo of ERI survey being conducted through a building (left). Photo of an ERI survey being conducted over a railyard (right).

Source: Photos courtesy of Aestus, LLC. Used with permission.

Settings such as industrial buildings, refineries, and railyards can be successfully surveyed using ERI techniques (**Figure 6-2**). Planning for these sites requires greater logistics but does not limit the ability to collect quality data. Good QA/QC is needed to distinguish targets if the surface properties are unknown. Drilling through concrete or asphalt in these locations to insert electrodes is recommended, because there are often air-filled voids beneath the slabs. Agreeing to a patching protocol for the electrode holes in advance is recommended.

An example of urban interference is provided in **Figure 6-3**. In this case, a town's water main was in the center of the image in a coal tar –impacted site. The utility was old (not coated) metal and was electrically coupled to the ground. The anomaly is a vertically conductive stripe in the dataset. Drilling adjacent to the noise feature into a resistive target still resulted in coal tar detection. Drilling near the conductor would result in piercing the water main, so the level of impacts directly below the water main is unknown. The horizontal nature of the bedding is apparent in the dataset as well with clear layering shallow in the dataset.



- The vertical conductive feature in the center of the image with the red dashed box is an electrically conductive "shadow" generated by a water main. For the anomaly to be a strong vertical conductor, the water main must be uncoated metal.
- The resistive feature adjacent to the water main is a coal tar anomaly that was confirmed by drilling. The horizontal nature of the background geology is apparent in the shallow layers of the dataset.
- Color scheme changes from cool as electrically conductive to warm as electrically resistive because nontechnical readers do not visualize cool colors such as blue or green as negatively impacted areas.

Figure 6-3. Coal tar –impacted ERI image with water main perpendicular to image using higher-sensitivity GeoTrax Survey™ ERI.

Source: Courtesy of Aestus, LLC. Used with permission.

6.2.2.3 Geotechnical Engineering and Mining

ER methods have been proven effective for a variety of engineering applications. This is a helpful site characterization tool that can provide information such as groundwater levels and rock and soil properties that could inform slope stability and load-bearing capacity. It can be used to detect karst features and potential sinkhole risks, and to evaluate the integrity of structures such as tunnels and levees by revealing structural anomalies such as cracks and voids (Fabregat et al. 2017). TERI can monitor changes in groundwater movement and soil compaction over time, which allows for the evaluation of structural integrity of features as they age or before and after major events such as earthquakes. Natural features such as sinkholes and hillsides that pose landslide risks can also be monitored using TERI to evaluate their hazard to the public and environment. ERI is a valuable tool to the mining industry not only due to its abilities to locate voids and to characterize geologic strata, but also in its ability to directly detect metallic ore bodies because of their electrically conductive nature.

6.2.2.4 Contaminants

ER methods have been applied at a range of contaminated sites to either characterize hydrogeology and lithologic variation or to directly detect contaminant sources. ERI is able to locate and map preferential flow paths for contaminant migration that are characterized by coarser grained lithology (more

electrically resistive), increased fluid electrical conductivity (EC) flow (more electrically conductive), or electrical signatures consistent with the type of contaminant present. High sensitivity ERI methods have been shown to detect electrically resistive NAPL materials at both LNAPL and DNAPL (light and dense nonaqueous phase liquids, respectively) sites (Halihan et al. 2012, 2017; Meng et al. 2023). TERI could be used to monitor changes in the lateral and vertical migration of a plume body over time.

Various contaminants exhibit different electrical properties in the subsurface. Coal ash, also known as coal combustion residuals (CCRs) or the residual waste that remains from the combustion of coal, is typically several orders of magnitude more electrically resistive than native material and therefore results in a strong electrical contrast easily detectable by ERI. On the other hand, saline spills and landfill leachates are typically significantly more electrically conductive than native material, making ERI a strong candidate for their characterization as well.

6.2.2.5 Bioactivity

ER methods can be used to evaluate colony structure in sites with significant subsurface bioactivity (Stonecipher and McDonald 2011). The approach led to the development of biogeophysics research (Atekwana and Atekwana 2010; Atekwana et al. 2024). The colony structure, typically more electrically conductive than surrounding material, will extend beyond areas of impact, so targeting of anomalies must account for the structures extending to depth and to the surface. On NAPL contaminated sites, highly electrically conductive features indicative of bioactivity often coincide with the NAPL body as the microorganisms use the NAPL (often hydrocarbons) as a nutrient source or as an electron acceptor (chlorinated solvents). Biogenic gases such as methane and carbon dioxide that can be generated by prolific bioactivity in the subsurface typically exhibit electrical signatures several orders of magnitude more resistive than native material.

6.2.3 Technology Implementation

6.2.3.1 Detailed Description

ER methods have been used since the 1800s to evaluate geologic variability of the electrical resistance of the subsurface, both spatially and temporally. ER values of subsurface materials are highly variable across several orders of magnitude, making it a valuable tool for observing subsurface changes (Van Nostrand and Cook 1966; Binley et al. 2015). The ER measurement (in ohm-meters) is obtained using four electrodes: two for inducing current flow (commonly called A and B) and two for measuring the difference in electric potential (commonly called M and N). Developments in the 1990s led to instrumentation that allows the deployment of electrodes at the surface for automated data collection that generates an ERI when deployed at the land surface or ERT when deployed in the subsurface, typically down boreholes. This approach is used as static imaging to collect a snapshot of site conditions. Additionally, electrodes or cables can be deployed in the field that can acquire data over time as temporal or transient ERI (TERI) for monitoring events or seasonal changes.

While ERI sends current into the ground for a steady-state measurement of potential generated due to the induced current, two other methods can be employed with the same cables with additional data collection time. Spontaneous potential (SP) data can measure what potential exists in the ground without induced current. Induced polarization measurements can measure the transient decay of potential due to the current signature being cut off and watching the potential values decay. Adding this method to a survey can add significant data acquisition time, so users must evaluate whether it will add significantly to understanding subsurface conditions.

ER units (ohm-meters) are for bulk electrical properties of the subsurface and are the inverse of bulk conductivity (formerly mho/meter, commonly siemens/meter). This bulk measurement incorporates the matrix properties as well as fluid electrical conductivity (EC), which is commonly measured in the field in

wells (units of millisiemens/centimeter). To avoid confusion between bulk measurements and fluid measurements, bulk ER data are kept as resistivity and fluid measurements are kept as conductivity, although the units themselves are simply the inverse of each other.

ER data vary as a function of lithology, fluid properties, contaminants, remediation efforts, and subsurface bioactivity. The lithologic variability for porous media is strongly related to porosity and the amount of fine-grained material. For competent rock, the cementation and weathering provide strong controls on the ER signature as well as fracturing, which generally makes the rock body more electrically conductive. Fluids generate variations based on fluid EC, with higher ion content providing lower electrical resistivity while air in the vadose zone generates higher electrical resistivity. NAPLs are generally liquid resistors with high resistivities that can generate resistive signals at 1–10 mg/L. Remedial compounds vary widely in their electrical properties. Finally, most bioactivity in the subsurface generates conductive material that can be detected with ER techniques. The exception is the generation of biogenic gases, which, if trapped, generate resistive pockets in the subsurface.

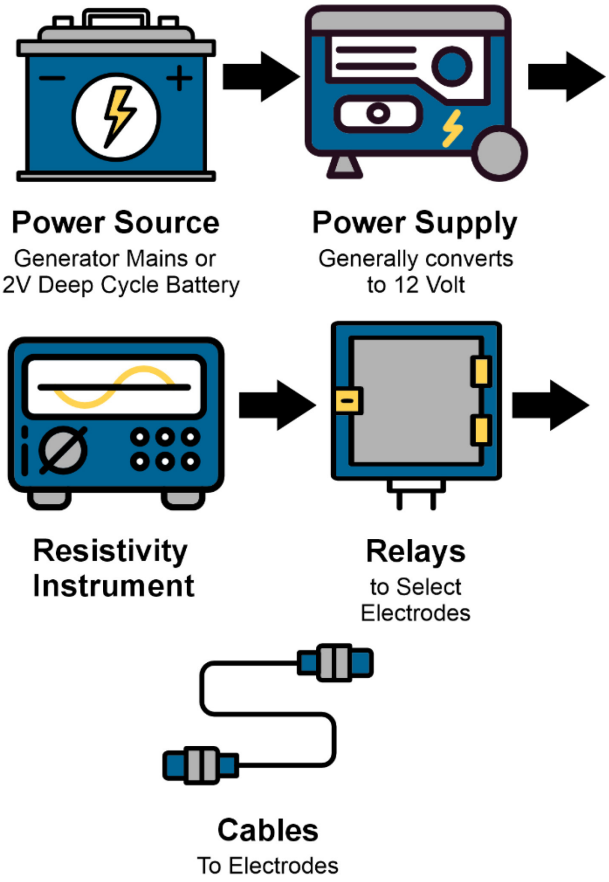


Figure 6-4. Instrumentation commonly associated with collecting ERI data. This includes a power source, a power supply to convert to instrument power (commonly 12V), an instrument for resistivity data acquisition, a relay switching system to select electrodes, and a cable with electrodes.

Source: Veronica Reed and Aestus, LLC. Used with permission.

The sensitivity of ERI to multiple subsurface physical and chemical properties makes ERI a highly versatile surface geophysical method. It can be used to image the hydrogeological framework controlling groundwater transport, the distribution of contaminants in groundwater, and variations of moisture content in the subsurface. The approach can also image the development of bioactivity for evaluating natural attenuation. The ER values that result from ERI or TERI have nonunique interpretations of subsurface properties, as multiple factors influence subsurface resistivity. A single value can correlate to a single parameter in a simple setting (homogeneous subsurface with a salt spill), but generally, confirmation sampling will be required to test interpretations, especially in electrically complex settings.

The technology is commonly deployed at the surface. ER data can be collected over all geologies and through urban areas, being careful of infrastructure. It can also be deployed on water, which allows for surveys to be deployed in places that are difficult to drill (**Figure 6-6** (left)). This approach can be combined with land-based surveys to evaluate groundwater and surface water interactions. The depth of investigation is one-fifth of the total survey length, so a 30-meter (~100 ft) depth of investigation requires a 150-meter (~500 ft) survey line. The technology generally requires a set of electrodes to couple to the ground, a multi-electrode cable, a switching system, and a measurement instrument (**Figure 6-4**). These instruments come in single-channel and multichannel configurations that allow multiple potential measurements to be collected at a single current pair injection period. Based on labor costs, these more expensive multichannel instruments are needed to limit data acquisition time.

6.2.3.2 Acquisition and Data Collection

Survey design is a combination of survey parameters that are well defined and site conditions that are highly variable. 2D surveys can be designed assuming the depth of investigation is 20% of total line length (Figure 6-4 and Figure 6-5). For shallow sites, this means lateral coverage is harder to obtain if resolution is increasing and line length is decreasing. Depending on the objective, it may be better to overshoot the depth to limit labor on lateral coverage. For deeper objectives, the constraint on line placement is generally approval for crossing property boundaries and roads.

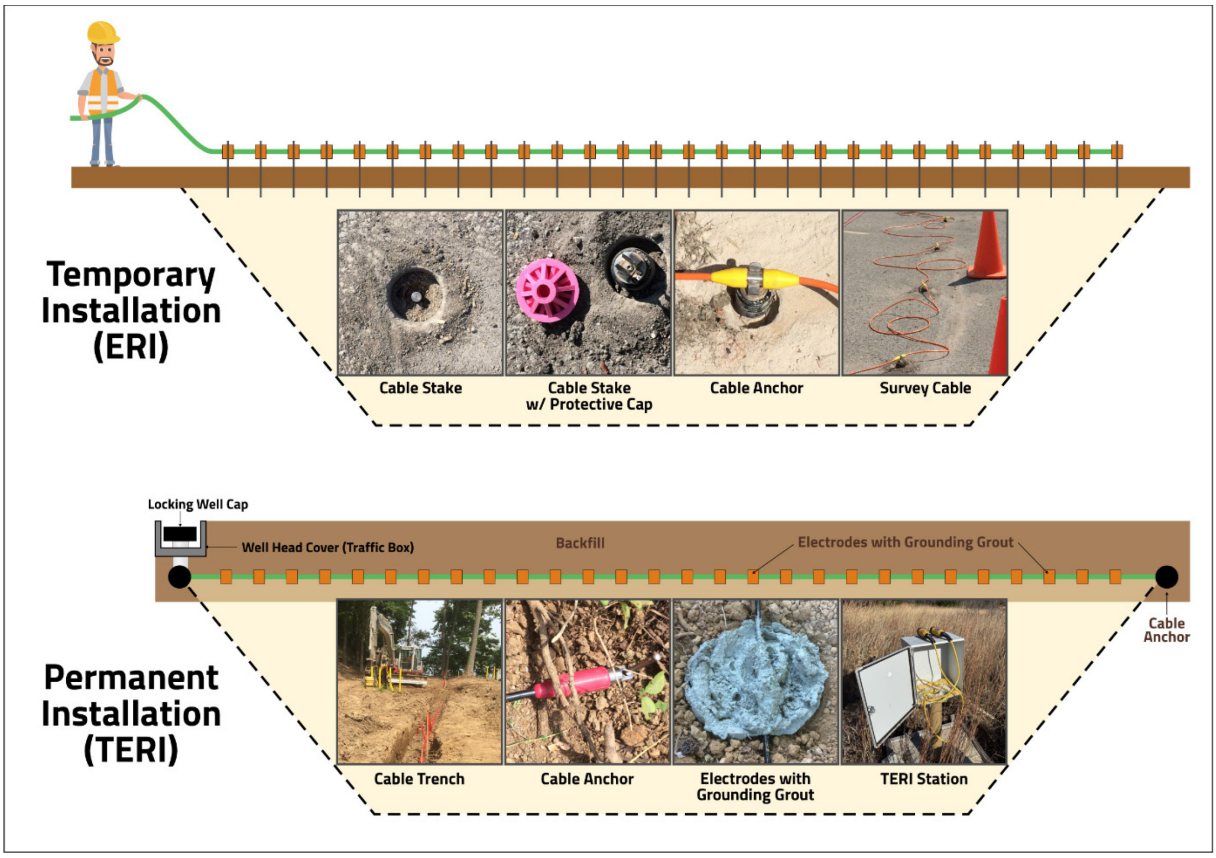


Figure 6-5. Configurations and photos for (upper) temporary electrode stakes for ERI surveys and (lower) permanent cable installation for TERI monitoring.

Source: Veronica Reed and Aestus, LLC.

For a typical site using 2D surveys, a minimum of six surveys is recommended to get data in multiple orientations and to see how parallel lines compare. A useful approach is to add contingency lines (2–4) so that adjustments can be made in the field to fill in between two parallel lines with significant variability or to chase a feature that is leaving the domain of another ERI image. Shorter lines of 300 meters (1,000 ft) or less should require a team of three people who are collecting ER data, surveying the electrode locations, and conducting QA/QC work. Longer lines targeting deeper objectives will require twice as many personnel to manage the workflow over the longer domain. Temporal datasets collected on permanently installed cables typically require fewer acquisition personnel (Figure 6-5). Only one person is required to collect data from temporal sites with permanently installed cables, but a second person can be deployed as a field safety protocol.

3D surveys or 2D surveys with a high number of electrodes are often of interest as an approach to improve the understanding of the subsurface. Increasing the number of electrodes increases equipment, acquisition time, and the number of QA checks to perform on additional electrode connections. When collecting ERI data for a 3D survey (often done in a grid pattern), the resolution decreases along an individual 2D plane for the same total number of electrodes, and personnel have to find an open area to fit the 3D electrode array. This relegates 3D work largely to academic purposes.

The biggest difference between various groups, both in industry and academia, acquiring ER datasets is QA/QC protocols. If equipment has rust or exposed wires, it is unlikely that quality QA/QC is being employed. Additionally, if questions regarding QA/QC protocols cannot be answered by field personnel, they are likely not following any. While these protocols have become entrenched in field chemical sampling fieldwork, the protocols are highly variable in geophysical fieldwork.

6.2.3.3 Data Processing

The primary rule of data processing of ER datasets is that bad field data cannot be magically improved in the processing stage. Poor quality field data provides a bad ER inverted data model. When reviewing ER data results, an evaluation of field QA/QC data provides tremendous insight into whether the data will provide a good dataset at the end of processing.

A key correction needed to process ER data is to accurately account for variable topography across the line (Loke et al. 2013). Topographic corrections are typically applied by adding terrain data to the data processing software. Terrain data can either be collected in the field using land survey equipment or extracted from high quality/high resolution digital elevation models (DEMs), such as those that can be generated from a drone-based LiDAR survey (Section 7.2.4). Inverse methods are used to process field resistivity datasets to compute a subsurface resistivity distribution that is consistent with acquired surface measurements. Typically, many more parameters than measurements are included in the subsurface resistivity model. As a result, inverse models generate nonunique solutions to the resistivity structure. Additional constraints on the model structure are included to favor certain models or images over others to narrow the plausible resistivity structure further. A common constraint is called smooth inversion or smoothness-constrained inversion because it produces models with smooth variations in physical properties (deGroot-Hedlin and Constable 1990). Another common constraint is called robust inversion (Sharma and Verma 2015).

Inverse methods involve an iterative approach in which a mathematical model is used to minimize the difference between the field measurements and the simulated values based on a numerical-forward model for a synthetic structure of the earth. Finite difference or finite element models are used in numerical forward modeling. Iterative parameter updates continue until these differences are less than a specified value defining a convergence criterion. At this point, the estimated model is considered a plausible representation of the resistivity structure of the subsurface. Because an inexperienced user can easily abuse it, the processing should be done by an experienced practitioner. To ensure the representation is plausible, experts use a variety of methods to assess the quality of the input data and information content of the inverted image and identify red flags. Unfortunately, geophysical contractors may not always use image appraisal tools to assess the realistic information content in the inverted images. Contractors should provide evidence of image appraisal as part of the delivery of ERI results. This can be in the form of root mean square error (RMSE) measurements for the datasets and sensitivity measurements to evaluate data quality with depth.

ERI data interpretation is best done as part of a multitechnology approach to refining the CSM. Interpretations of ERI survey images should be constrained by other information available at the site. Interpretations of resistivity images presented by a contractor should never be simply accepted without careful consideration of whether the interpretation is consistent with existing site information. Used

appropriately, the spatially rich information provided from an ERI survey significantly helps CSM refinement.

Another common error in the interpretation of resistivity images from a standard 2D survey is that the inversion routine solves for a 2D subsurface structure; no variation in resistivity is assumed in the direction perpendicular to the image. Although this is a reasonable assumption in some cases (for example, transects perpendicular to a pipeline or across a valley filled with sediments deposited in a low energy environment), 2D imaging is often done in complex 3D terrain (for example, over karst) where the 2D assumption is not valid. In this case, the image produced cannot be expected to represent full 2D reality and may contain image artifacts because 3D structures are being represented by a 2D model.

At various times, vendors and instrument manufacturers have attempted to separate acquisition companies and personnel in contracts from processing personnel to make processing more uniform and higher quality QA/QC. If strong field QA/QC protocols are employed so that questions of field variability can be addressed, this is a useful approach to take and can limit the expertise needed in the field acquisition team to only acquisition issues. Evaluating the data quality by processing while field teams are deployed is a useful, if not required, step to ensure that multiple mobilizations are not required. Project meetings before teams demobilize from sites can also be used as a decision point to add additional lines to fill in complicated domains or extend imaging to chase a plume.

6.2.3.4 Visualization

3D visualization of ERI data is required when collecting more than one 2D dataset on a site. Many vendors have 3D visualization software that can be used for this purpose. There are some tricks related to ER data that need to be addressed. The 3D visualization software can display the individual inverted data as points in space. This may overwhelm the software because a 2D dataset is commonly a kilopixel dataset that needs to have an order of magnitude of 1,000 datapoints to rotate or translate. Additionally, for a significant number of datasets, the cloud of data can be difficult to see effectively.

One option for managing these issues is to use software that allows fence diagrams of images of the dataset. This limits the number of objects that rotate and speeds up the use of the 3D model. Another option is to create depth or elevation slices through the dataset that can provide horizontal images to include that allow a good understanding of depth.

Finally, solid modeling of ERI datasets is a method to generate a 3D volume to evaluate, which is sometimes easier for stakeholders less familiar with ER data to understand. The issue for this effort is that most algorithms used to connect the points do not anticipate the high data density along the ER data planes in 2D. Thus, the solid model results in hundreds of “pipes” of data where a value is connected from one dataset to an adjacent dataset. This can be resolved by binning data into categories to improve the response of the visualization algorithm. If sufficient ER datasets are collected, someone will likely write an algorithm fit for this purpose.

6.2.3.5 QA/QC

Numerous quality control checks should be performed during the acquisition of field resistivity datasets. The repeatability of the recorded voltages in response to an injected current should be assessed by repeating individual measurements multiple times. A robust quantification of the error in the field measurement is achieved from a “reciprocal” measurement, whereby the electrode pairs being used for current injection and the electrode pairs being used for voltage measurement are switched over. The principle of reciprocity states that the normal and reciprocal measurement must be identical. Differences in the normal and reciprocal measurement provide a rigorous estimate of the measurement error. Use of reciprocal approaches will double the acquisition time for a survey if used on every measurement, limiting production rates.

Data errors depend on multiple factors, some of which can be addressed during the field survey. One factor is the contact resistance between the electrodes and the earth. This resistance limits the flow of current into the ground and consequently limits the magnitude of the recorded voltages. Poor contact resistances result from especially resistive ground (sand dunes or bedrock at surface), poorly placed and inserted electrodes, and bad contacts between the electrode and the resistivity instrument. Most resistivity instruments allow the user to assess contact resistances and correct issues prior to the start of a survey. High contact resistances resulting from the ground conditions can be reduced by watering the electrodes with an ion-rich water. Poor data quality also results from buried infrastructure, particularly electrical utilities. The site should be carefully evaluated for the presence of buried utilities, particularly at brownfield sites or within industrial complexes. Identifying the location of utilities helps to isolate anomalous electrical structures in the resistivity images caused by such infrastructure.

Accurate recording of the electrode locations is another important quality control consideration. Electrodes are typically placed with the intention of uniform spacing, which is sometimes prohibited by site conditions. When site conditions dictate that the electrodes be offset from the nominal spacing, exact electrode locations should be recorded. Incorrectly documented electrode locations result in model errors during inversion that manifest as artificial image structure at shallow depths close to the electrodes. The topography also should be recorded when the ground is not completely horizontal. Resistivity data modeling should account for the topography. All modern ERI processing software has the capability to account for topography during inverse modeling.

As previously noted, image appraisal is important in assessing the significance of the estimate of the resistivity structure; a measure of the depth of investigation to identify well-resolved regions of the subsurface is important. An additional simple but often overlooked quality control consideration during the data processing stage is the measure of misfit between the measured field data and the synthetic data determined using the estimated model for the resistivity structure. If this misfit criterion is not adequately minimized, the resulting image should not be considered the best possible estimate of subsurface resistivity. This can be evaluated as an RMSE between the field data and the inversion model data in the inversion process and the sensitivity matrix generated for the data. Inversion RMSEs below 10% generally represent good data that can be interpreted. Under 20% RMSEs have some noise issues and should be evaluated more closely. Inversion RMSEs above 20% for a dataset should not be used for interpretation unless the noise characteristics are well understood. For sensitivity data, a value (unitless) above $10^{-}3$ is strong, above $10^{-}5$ is reasonable, and below $10^{-}5$ is not able to “see” the subsurface.

A final quality control check comes from integrating subsurface data in the image domain. For example, boreholes collected within 15 ft (5 meters) of the survey line provide lithologic contacts or fault information that should be apparent in the ERI dataset. If image sensitivity is low, RMSE is high, or significant shallow noise is detected, the subsurface samples may indicate that the dataset is not providing a good sample of subsurface conditions where the boring was placed.

6.2.3.6 Integration into CSM

Integrating ER data into a CSM takes advantage of the high data density and spatial distribution of ER data by combining it with limited point data from wells, direct push instruments, and passive samplers. Insitu point data from boreholes can be used to calibrate the spatially extensive ER data and lead to a more robust CSM, particularly with targeted drilling. Similarly to how the medical industry calibrates medical scans by performing a biopsy of anomalous areas identified in the scan, ER data can be calibrated to geology, contaminant concentrations, and bioactivity levels by targeted drilling of anomalous electrical zones. The borehole data from these targeted features can inform the electrical signatures and can thus inform the CSM data gaps between the spatially limited boreholes.

Given that electrical signals result from a variety of subsurface influences (lithology, fluids, contaminants, etc.), a good approach is to separate CSM development into individual modules that can test hypotheses

against each other rather than looking at all CSM components against the ER data all at once. Testing a geology CSM for ER data against borehole logs or cores allows evaluation of geology without getting bogged down in ER signatures that may result from contaminants or bioactivity. Similarly, an additional CSM for hydrology, contaminants, bioactivity, and geotechnical risk can be developed.

The color scheme used to contour the ER data can be of great importance, because some color schemes can lead to a better understanding of what the data mean than others. This includes both data interpreters and other stakeholders. Often, creating a custom color scheme for each site that highlights the properties of the subsurface that are of greatest interest to stakeholders (shows various ranges of resistivity detected at the site using different colors) is helpful practice. The color modification process is like recontouring a topographic map (the elevation data points never change, but the contour interval is altered to produce different maps highlighting various features, or in this case, ranges of electrical resistivity). The use of various color schemes for the same ER data can help highlight the geometry of various signatures. In addition, taking the gradient of the ER data can highlight lithologic interfaces and the boundaries of subsurface features. These data can also find vertical pathways in ER datasets (Baines et al. 2002; Bowling et al. 2005; Halihan et al. 2013; de Pasquale et al. 2019).

6.2.4 What Are the Advantages?

6.2.4.1 Field Deployment

- Enables real-time evaluation of field data to adjust and optimize acquisition plans
- Applicable across a wide range of geologic settings and fluid types
- Effective in land-based, wetland, and open water environments, including surface water interfaces
- Capable of investigating depths up to 300 m (1,000 ft) in demonstrated applications

6.2.4.2 Low Environmental Impact

- Noninvasive, surface-based technology
- Low-carbon, sustainable method requiring minimal energy input
- Eliminates risk of cross-contamination between aquifers
- Proven and widely accepted in regulatory applications for decades when using strong QA/QC protocols

6.2.4.3 Technical Capabilities

- Provides continuous, high-resolution data coverage to minimize the risk of missing subsurface flow paths
- Images both vadose (unsaturated) and phreatic (saturated) zones
- Supports both static site characterization (ERI) and time-lapse monitoring of subsurface changes (TERI)
- Can directly detect NAPL products at concentrations above approximately 1 ppm (ERI)
- Can directly detect zones of bioactivity (ERI)
- Enables quantitative monitoring of injections and infiltration processes (TERI)

6.2.5 What Are the Limitations?

6.2.5.1 Contracting and Process

The use of ER methods varies widely from untrained personnel trying to use a rental tool without QA/QC protocols to ER vendors that do nothing else and have decades of experience in applying these tools. Clarity in a bid process requires a listing of needs as part of the project process. Sites typically have issues in contracting in QA/QC protocols used in data acquisition and processing under a USEPA Quality Assurance Project Plan (QAPP) process or similar. In practice ER results can have a broad range of outcomes based on site-specific conditions. Practitioners should consult contractors to determine the level of data integration and interpretation that are required.

6.2.5.2 Field Settings

ER methods have been applied in a variety of places, from flat grass fields with minimal human intervention to chemical plants and refineries that have seen over a century of contamination. While the versatility of ERI has been proven through its use in most any environment, limitations in field data collection settings have been identified. If grounding grids are in place at a site, these highly conductive surfaces cannot be imaged beneath from the surface. ER and other geophysical methods are not ideal at sites with grounding grids (such as at a substation).

Many ERI limitations are easily addressed and alleviated with proper data collection protocols in the field. If galvanic controls are active at a site, turning them off during data collection provides more assurance that a potential source of noise is not present. Survey designs that require straight lines of electrodes do not require straight cables, as the electrode stakes can be installed in the ground in a straight line and then cables with excess length between electrodes can be strung around obstacles such as large trees, industrial equipment, or full pallets.



Figure 6-6. Photo of ERI survey being conducted through a waterway (left). Photo of an ERI survey being conducted with a traffic crossing at a fueling station (right).

Source: Photos courtesy of Aestus, LLC. Used with permission.

For urban areas, data collection can be performed between and through buildings, and small holes can be drilled in the building floor if needed to make contact with the soil beneath the slab (**Figure 6-6**). Crossing roads and busy parking lots can be done () with traffic ramps that vehicles can drive over while protecting

cables and electrodes to keep traffic flowing with proper permitting. Survey lines can be run across and parallel to railroad tracks, and cables can often be threaded through the track ballast beneath the track which allows train traffic to continue during data collection.

In other terrains, over-the-water surveys require water safety protocols to be clearly defined and for boat traffic to be actively managed. Highly variable topography and dense vegetation do not adversely affect data collection provided that personnel have physical access, but additional safety protocols may be required in steeper terrains. Permafrost regions can strongly influence resistivity due to the high resistivity associated with the frozen portions of the imaging domain. This can make obtaining good contact difficult and may mask features that are in the frozen state because the resistivity will be much higher than the thawed zones in the subsurface.

6.2.5.3 Data Acquisition

Successful data acquisition requires far more than placing stakes, connecting cables, and collecting measurements. Just as groundwater sampling involves more than lowering a pump into a well and filling a bottle, reliable ERI acquisition depends on properly maintained equipment, rigorous quality assurance protocols, and experienced field practices. Faulty relays may continue to generate measurements while degrading data quality; corroded cables can produce data that cannot be processed effectively; and reversed cable connections can compromise entire datasets—an error that occurs more frequently than many realize.

Even when all quality assurance protocols are followed, data quality can vary with subsurface conditions. Cleaner datasets are generally obtained in conductive settings, such as clay-rich soils or conductive limestone. Noise may increase at highly bioactive sites or where significant buried metallic debris is present. High-resistivity settings can still provide good imaging when subsurface conditions are relatively homogeneous. The most challenging acquisition environments typically contain a wide range of electrical conditions within a single dataset, such as sites with both clay and gypsum geology or dry-cleaning sites exhibiting strong biological activity.

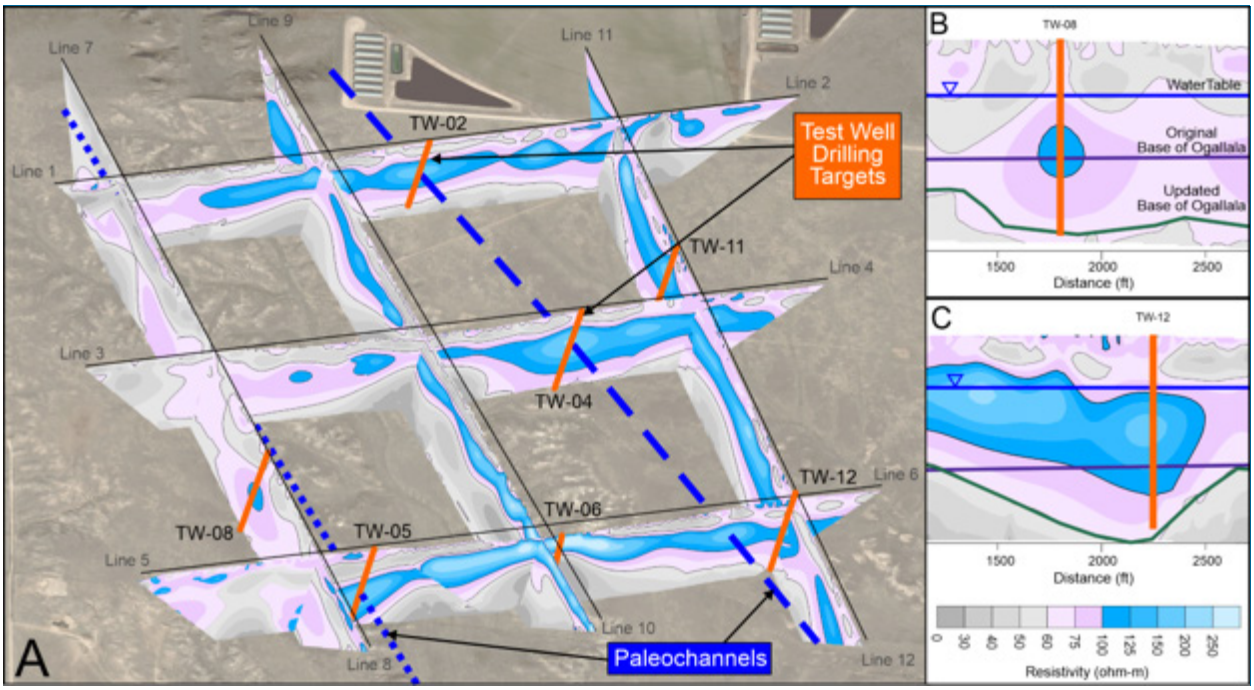
Quality ERI data can be obtained in complex settings when instrumentation components pass presurvey quality assurance testing and electrode contact resistance is measured, logged, and maintained within acceptable limits. All ERI datasets should also be topographically corrected and accurately surveyed to establish their proper geospatial position and orientation.

6.2.5.4 Resolution

The image resolution, or pixel size (the smallest interval where details can be distinguished), in ERI is equal to half of the spacing between the electrodes. For example, if the electrodes are spaced 1.5 meters (5 ft) apart, the resolution of the image will be 0.75 meters (2.5 ft). This is sometimes adjusted by managing poor datasets by making coarser grids to manage data loss. The resolution decreases (pixels get larger) as the total survey line length at the surface increases (if the number of electrodes stays constant). The depth of the investigation, or imaging depth, also increases with survey line length. Depth of investigation is generally equal to 20% of the total line length. Objects smaller than the resolution of the dataset can be imaged if they are more conductive than the image pixel. For a conceptual idea, if a thin metal plate was put through a 1-meter block, the block would still be imaged as highly conductive. So if a thin conductive bed is important to the CSM, it may be imaged effectively with ERI. Lab- and fieldwork have also shown that small resistors can generate signals by blocking pore throats in NAPL-impacted sites (Halihan et al. 2005, 2017).

An example of coarse resolution is provided in targeting water supply wells in the Ogallala aquifer (**Figure 6-7**). In this example, high resistivity coarser regions beneath the water tables are targeted for high hydraulic conductivity zones. Where the resistivity is high and the zones in blue are thicker, a higher

transmissivity zone was detected with test wells. These datasets used an electrode spacing of 15 meters (50 ft), giving a resolution of 7.5 meters (25 ft). This was still sufficient resolution to evaluate aquifer targets at this scale.



A. 12 electrical images with total length of 825 meters (2,700 ft) with a depth of investigation of 165 meters (540 ft) and a resolution of 7.5 meters (25 ft). High resistivity zones below the water table are shown in blue and test well drilling targets are orange.
B. Lower resistivity target showing greater thickness of aquifer than regional mapping suggested, but lower hydraulic conductivity sediments.
C. Higher resistivity target showing high total aquifer thickness and high hydraulic conductivity sediments. Color scheme changes from warm as electrically conductive to cool as electrically resistive because nontechnical readers do not visualize warm colors such as browns or grays as useful water supply well targets.

Figure 6-7. Water supply electrical imaging of mile section block of the Ogallala aquifer using higher-sensitivity GeoTrax Survey™ ERI.

Source: Courtesy of Aestus, LLC. Used with permission.

6.2.5.5 Noise Sources

The majority of ER instruments are designed to avoid signals near line voltage configurations (60 hertz in US) so that they avoid interference from powerlines or other leaks of grid power. Utilities can provide a source of noise if they are well coupled to the ground. This is commonly observed with old water mains or large metal well casings. Many modern utilities are no longer noise sources because external pipe coatings have limited the electrical coupling with the ground. Utility noise concerns can generally be managed by avoiding running ERI parallel with or on top of utility corridors. If that orientation is required, stepping off the corridor by 5 meters (~15 ft) is generally sufficient to avoid any noise. Metallic fences that are installed into concrete footers avoid having good coupling and typically do not cause noise issues. Barbed wire fences with metal fence posts just inserted into the soil can be a significant noise issue, so stepping off the fence line by at least 5 meters (~15 ft) is recommended.

Aboveground metallic structures are generally not issues for ERI datasets if they are not well coupled with the earth. Metal buildings on concrete or railroad tracks on nonconductive rock ballast remain isolated

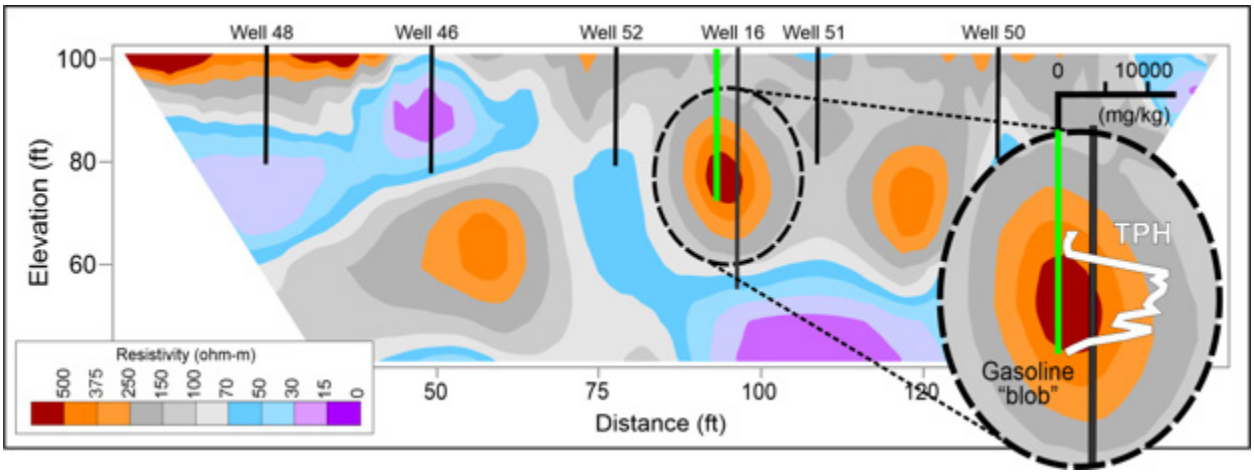
from images. When going through a building with a concrete foundation, the construction of the concrete determines the noise level. Drilling through the concrete can limit this issue, but some concrete has a significant amount of metal mesh, which can pose noise problems.

6.2.5.6 Multiple Signals

On electrically complex sites (such as most contaminated properties), bioactivity and remedial activities generate complex electrical subsurface structures. These sites will not have electrical structures where a single resistivity value will correspond to the extent of impacts. Instead, electrical signals from a variety of factors, including contaminants, bioactivity, injectate, etc., present at that point location in the subsurface will combine and overprint one another to create a total resistivity value that is not representative of any one factor. These multiple factors strongly affect the electrical resistivity signature, and it can be difficult to differentiate them with the ERI data alone. On these complex sites, integrating the spatially extensive ERI datasets with corresponding point data from direct push or drilling allows the resulting ER data to be calibrated and for a robust CSM to be constructed.

6.2.5.7 NAPL sites

NAPL sites are a common use of ER approaches because these sites have been shown to have spatially variable distribution of the separate phase material, LNAPL or DNAPL, and commonly have multiple source areas. The strong variations in electrical structure observed at these sites have caused controversy as to what a NAPL site should look like electrically. The current understanding is that as a liquid resistor, separate phase material, either LNAPL or DNAPL generates an electrically resistive signature from about 1 –10 mg/L concentration (Halihan et al. 2017). As bioactivity develops, electrically conductive signatures are generated by a biomass of a range of organisms and ions added to groundwater (Atekwana and Atekwana 2010; Stonecipher and McDonald 2011; Atekwana et al. 2024). Trapped biogenic gases such as methane and carbon dioxide can also generate electrically resistive structures at these sites that are generally more electrically resistive than the unweathered NAPL signatures (Halihan et al. 2017).



Resistive anomalies remaining after pump and treat and surfactant flush remedies were applied. Confirmation sampling through strong electrical resistor shown to correlate with TPH data. Additional sampling and testing illustrated in (Halihan et al. 2005).

Figure 6-8. Example of electrically resistive LNAPL anomalies (modified from data from Halihan et al. (2005)) using higher-sensitivity GeoTrax Survey™ ERI.

Source: Courtesy of Aestus, LLC. Used with permission.

Across instruments and vendors, the sensitivity of ERI datasets varies widely. The sensitivity provides a good indicator of whether an ERI dataset will effectively resolve NAPL signatures. Part of the quality assurance plan (such as a USEPA Quality Assurance Project Plan (QAPP)) should be an evaluation of dataset RMSE and image sensitivity for evaluating these targets.

Confirmation of these signatures requires testing to account for residual NAPL material because the material may generate a resistive signature but may not have sufficient ability to overcome capillary forces and enter a well. Additionally, common PID sampling on LNAPL sites will not detect methane pockets generated by bioactivity.

An example of electrically resistive LNAPL anomalies is shown in **Figure 6-8**. The figure (Halihan et al. 2005) shows USEPA sampling of a circular, resistive anomaly with residual LNAPL on a site that had pump and treat and surfactant flush remedies previously applied.

6.3 Ground Penetrating Radar

6.3.1 What Is the Technology?

Ground penetrating radar (GPR) is a high-resolution electromagnetic (EM) technique that has been developed over the past 40+ years to investigate the subsurface in environmental, engineering, and archaeological investigations (Daniels 2000). GPR is a widely accepted imaging and characterization tool. Its effectiveness depends strongly on site conditions. Similar to navigational radar, GPR identifies the location, shape, and size of subsurface features based on the reflection of high frequency [25 to 1,500 megahertz (MHz)] EM pulses or waves transmitted from a radar antenna (USEPA 2025c, 2016d).

6.3.2 How Is the Technology Used?

GPR equipment typically consists of a radar-control unit, transmitting and receiving antennas, electronics, and recording devices (**Figure 6-9**). The transmitting and receiving electronics are kept separate (Daniels 2000). The radar-control unit sends synchronized trigger pulses to the transmitting and receiving antennas at up to thousands of times per second (USEPA 2018b). The antenna is typically shielded to maximize the energy path to and from the subsurface target to reduce the energy transfer between the transmitter and receiver, as well as into the air, and to minimize external noise from interferences (Annan 2003). The system is digitally controlled, and data are digitally recorded for processing and display (USEPA 2025c). The GPR system contains a microprocessor, internal memory, and data storage.

Reflection profiling is the most common type of GPR deployment. Radar waves are transmitted, received, and recorded each time both antennas have been moved a fixed distance across the ground surface (USEPA 2018b). GPR is often deployed along linear transects. The number of transects is a function of the anticipated propagation of the EM wave in the geologic environment. The transects are completed in one direction and then an additional set is completed in a perpendicular direction to improve resolution. This collection technique is necessary because the reflected EM pulses are only acquired in the narrow band directly below the transect and could miss objects aligned parallel to the transects. Compiling responses along each transect line enables a clearer interpretation of the subsurface along a profile.

GPR applications in geologic studies include identifying the depth to bedrock, depth and thickness of soil strata, depth to the water table, and location of cavities or fractures in bedrock (USEPA 2016d, 2018b). GPR applications also include locating subsurface structures such as pipes, drums, waste and landfills, tanks, cables, trenches, pits, fill material, unexploded ordnance (UXO), and munitions. GPR may be used for quality control testing of soil surveys and archaeological surveys, or on road paving and asphalt projects (Annan 2009). GPR can operate as a stand-alone tool but is best when integrated with complementary tools such as electromagnetic (EM) locators, video pipe inspection, and electromagnetic

induction (EMI). For example, EM pairing allows the tracing of the energized metallic utilities that GPR would only record as a generic object. Incorporating GPR data into a broader CSM allows project managers to combine multiple lines of evidence for more accurate environmental and geological assessments. Paring the GPR with distinct subsurface tools offsets the inherent limitations of radar waves.

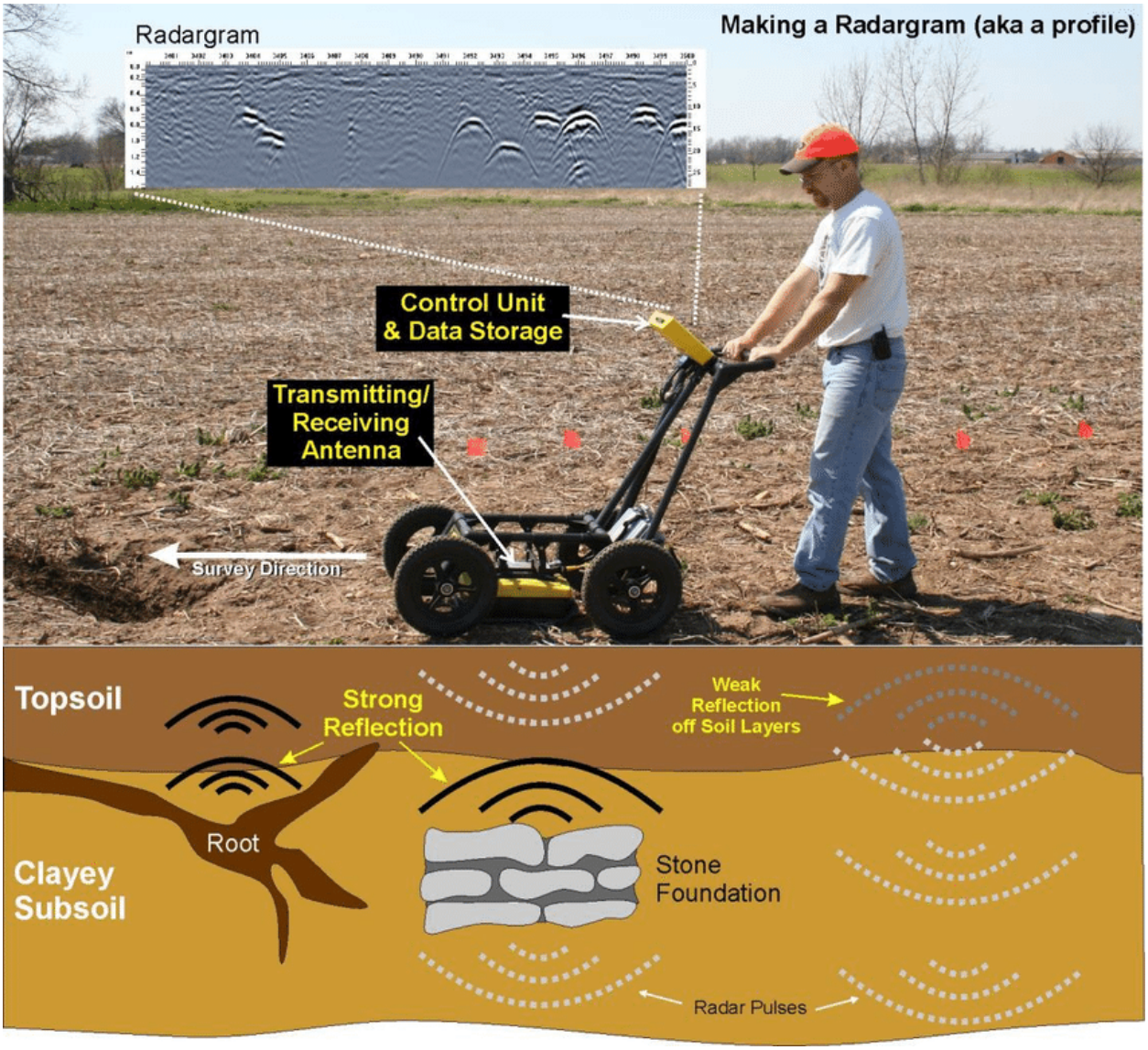


Figure 6-9. GPR implementation involves a pulse of EM energy traveling from a transmitter to a receiver antenna and contrasts in conductivity return a reflection in the GPR record.

Source: Jarrod Burks, Ph. D (Burks 2016). Used with permission.

In addition, GPR may be able to detect subsurface contamination provided the contaminant changes the dielectric permittivity to a detectable degree (for example, above background noise in the data). For example, the relative dielectric permittivity of a common organic solvent, trichloroethene, is 3.42, compared to 1.0 for air and 78 for water at 25°C; if such a contaminant displaces water sufficiently in the subsurface, a distinct change in the relative dielectric permittivity occurs for this region of the subsurface (Knight 2001). Similarly, the presence of an immiscible phase of liquid, such as NAPL, may provide an

even greater change in the dielectric constant than it would as a dissolved phase in the same media. When a pure NAPL displaces pore water, there is a reduction in conductivity and dielectric permittivity in the media, which translates to an increase in the EM wave velocity and decrease in attenuation (Redman 2009). However, in practice, NAPL identification with GPR is typically limited to recent releases that exhibit little weathering of the NAPL via biodegradation or other chemical interactions.

GPR works best in dry, coarse-grained materials such as sand and gravel. High conductivity soils and saltwater applications are highly detrimental to GPR application because of the high likelihood of EM attenuation (ASTM 2019). Because clayey fill (high conductivity) is frequently present in the shallow subsurface at industrial sites, penetration depths may be less than 30 ft (about 10 m) for environmental investigations (USEPA 2018b).

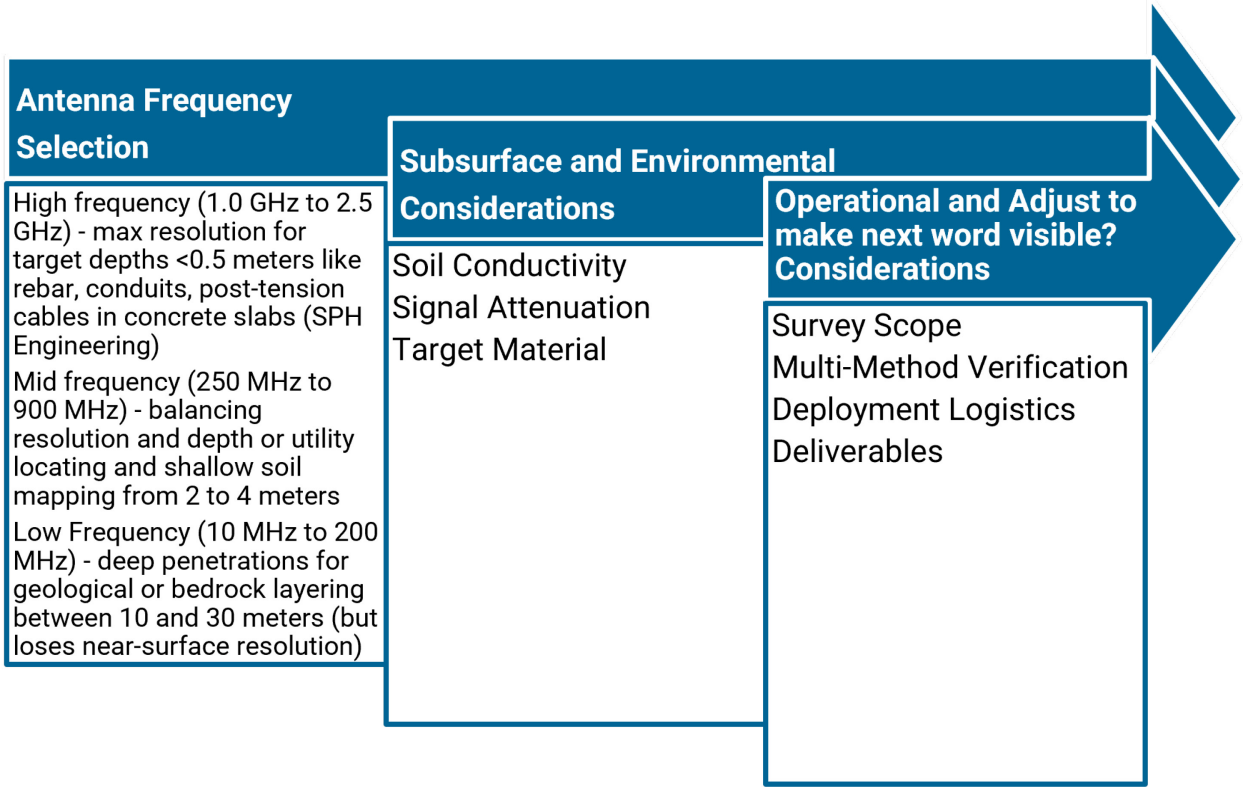


Figure 6-10. View of the GPR technology decision-making process for the application of GPR technology.

GPR equipment and software are complex, and technical training is needed for proper use, data filtering and processing, and interpretation. Technology users should discuss with the GPR service providers their QA/QC practices and competency guidelines to help the users understand the importance of qualified operators and data reviewers. The American Society for Testing and Materials (ASTM) published three primary standards for using GPR from the foundational guide (ASTM D6432) to specialized and focused guides for pavement and asphalt-covered concrete bridges (ASTM D4748 and ASTM D6087). ASTM D6432 outlines equipment, field protocols, and basic data interpretation for geological, engineering, and environmental site surveys (ASTM 2019). Training is particularly important for environmental applications of this technology. Users of GPR data should seek references and project examples from potential GPR providers to assess their experiences and backgrounds and minimum training expectations. Performing successful subsurface investigations requires defined deployment strategies and rigorous personnel standards. Training and quality assurances are needed from the GPR contractor to understand operator competency as it directly relates to interpretation accuracy. The American Society for Nondestructive

Testing (ASNT) issued guidance for GPR servicers to establish company-specific certification programs for the application of the use of nondestructive testing, such as GPR, in their 2011 Recommended Practice No. SNT-TC-1A (ASNT 2011). This guidance recommended that the minimum for certification is 8 hours of training with 60 hours of GPR practice to be certified as a Non-Destructive Technology (NDT) Level 1 in GPR. Subsurface Investigation Methodology (SIM) is an industry standard and training framework used specifically for locating underground utilities and scanning concrete (SIM 2025). SIM combines rigorous technician training, advanced dual technologies, and redundant verification methods to prevent property damage and job site accidents. SIM specifies 8 weeks of field mentoring, splitting time with 80 hours of classroom training. For additional information on accepted and recommended procedures for implementing GPR, please refer to (ASTM 2011).

Project objectives and GPR capabilities should be established with the contractor early in the project based on conditions and limitations at the site. To maximize field and technology effectiveness, the user should implement a structured decision-making process to screen site conditions, the utilization of varies GPR antenna frequencies for specific structural or environmental goals, and ascertainment of the training and experience of the GPS service provider. A decision-making process for the selection of applicable GPR antenna and complementary tools is shown in **Figure 6-10**. The initial step is for clients to discuss their subsurface project objectives to determine which frequency is needed. Next the client should communicate what is known about the site's soil and targeted materials, and finally, discuss operational and project considerations, such as deliverables, deployment logistics, or scope. GPR services are often contracted using a daily rate, particularly for short, well-defined projects.

6.3.3 Technology Implementation

Due to the wide range of frequency antennas that can be used, GPR is capable of a high degree of lateral and vertical resolution that often exceeds that of other surface geophysical methods(ASTM 2011). Large areas can be covered quickly in the field using GPR. When applied in the right setting, GPR is highly efficient and a reliable source of high-quality 2D and 3D data. The real-time capability of GPR allows a geophysicist to interpret the results qualitatively to evaluate site conditions and adjust the field program as needed (NJDEP 2005).

GPR detects changes in EM properties in the subsurface, such as dielectric permittivity, conductivity, and magnetic permeability, that are a function of soil and rock properties, water content, and bulk density (ASTM 2019). Dielectric permittivity (also known as dielectric constant) is a measure of the ability of a material to store an electric charge by separating opposite polarity charges in space; it effectively measures a material's ability to be polarized by electric displacement due to an electric field and has units of farads per meter (F/m) (ASTM 2019). It is more convenient in practice to use relative dielectric permittivity, which is the ratio of the dielectric permittivity of a material to the permittivity of a vacuum and is a dimensionless term (Annan 2003). The relative dielectric permittivity of geological materials varies from 1 for air to a maximum of around 80 (depending on the temperature) for water. Solid minerals or rocks have a low relative dielectric permittivity (less than 10). The relative dielectric permittivity of sediments and rocks varies widely depending on the porosity and the water content. Low-porosity rocks and dry unconsolidated sediments (for example, hydraulic conductivity whereas porous rocks and saturated sediments have high relative dielectric permittivity (Everett 2013; USEPA 2018b). Most geophysics textbooks include tables where representative values of hydraulic conductivity are published for different geologic materials; actual values strongly depend on porosity and water content.

GPR senses variations in hydraulic conductivity, which controls the velocity at which EM waves travel between a transmitter and receiver. The arrival time of the transmitted wave recorded at the receiver is usually stated in nano seconds (10^{-9} sec) (USEPA 2018b, 2025c). EM waves travel at 0.3 m/Ns (speed of light) through the air and less than 0.3 m/Ns through geologic media (USEPA 2018b, 2025c). Variations in the subsurface result in reflected EM waves that are returned to the instrument from interfaces or irregularities with hydraulic conductivity contrasts. Abrupt variations in water content and porosity are

usually the primary cause of reflections returned to the instrument. The returning portion of the EM wave is captured by the receiving antenna where its amplitude, wavelength, and two-way travel time are recorded for processing and interpretation (Dojack 2012). Short EM wavelengths (high frequency) yield a high resolution of interfaces and objects(USEPA 2025c).

GPR is most often a shallow subsurface tool (for example, 100 ft or less) due to the many variables that affect EM penetration, reflection, and scattering. Technology selection should be consistently made using a structured framework for decision making as discussed in the previous section. An inherent tradeoff between penetration depth and resolution must be evaluated critically and is discussed in greater detail in Section 6.3.3.1.

6.3.3.1 Acquisition and Data Collection

GPR is often one of the first tools employed at a site as the CSM is being developed but can be used alongside other technologies to bolster the CSM as well. Many factors at a site can attenuate the EM wave energy from GPR and, if not well understood and addressed in the investigation design, reduce the effectiveness of GPR. Three factors that should be understood prior to deploying GPR are the following: expected site stratigraphy and saturation data (including the types of sediments, stratigraphical order, depths, thicknesses, and water table depth) available from regional to local geologic literature and previous site characterization; presence of subsurface utilities and other potential interferences such as rebar-reinforced concrete, including their approximate locations based on aboveground indicators (for example, manholes, gas line markers), composition, depths, aboveground access, and interferences that could constrain equipment deployment; and locations of potential aboveground interferences such as fences, signs, and power lines. Having a solid grasp on these site characteristics is vital for the successful use of GPR.

The knowledge of the expected depth of investigation and relative suitability of soils can aid potential GPR users in refining their methods search. For example, the EC of near-surface sediments is a critical consideration as GPR is often rendered ineffective as a result of excessive signal attenuation by conductive soils (for example, clayey soils, high salinity soils). The USDA Natural Resources Conservation Service has used the soil attribute data from the State Soil Geographic (STATSGO) and the Soil Survey Geographic (SSURGO) databases to develop thematic maps showing relative suitability of soils for many GPR applications. GPR soil suitability maps (USDA 2009) can be generated for the site through the SSURGO data using the Web Soil Survey (WSS). In the WSS application, the GPR maps are located in the *Soil Data Explorer*, *Suitabilities and Limitations Ratings,* under the *Land Management* folder. Note that an area of interest needs to be created to access the *Soil Data Explorer.* GPR suitability ratings on WSS are in both numerical and verbal styles. The numerical ratings range from 0.01 to 1.00, indicating gradation of most negative impact (1.00, the lowest potential for GPR use) and the best impact (0.00, the highest potential for GPR use) on the application of GPR. Descriptive ratings for GPR penetration performance range from very high, high, very low, and unsuited.

Additional considerations include information gained by answering the following questions (Annan 2003):

- Is the target within the detection range of GPR regardless of the subsurface characteristics of the site?
- Will the target elicit a response that is detectable and discernible above background noise?
- Are multiple targets that need to be included in the study design likely to be present?
- Are there other conditions that would preclude using GPR?

A GPR study must be designed knowing the desired resolution and the depth of assessment that can be reliably attained for that level of resolution. The EM pulse frequency is inversely proportional to signal penetration and data resolution (the lower the frequency of the EM pulse, the deeper the signal

penetration but the poorer the data resolution, and vice versa). Two commonly used rules of thumb for evaluating the resolution of GPR are (1) the resolution may be approximated as the maximum depth of the investigation divided by 100 and (2) GPR will be ineffective if the actual target depth is greater than 50% of the maximum depth of the radar (Annan 2003). Additionally, when detecting subsurface utilities, the diameter of a conduit that may be detected is 1 inch per ft of burial (for example, 4-inch minimum diameter conduit located 4 ft bgs).

GPR data may be collected using two modes: moving and fixed. In the moving mode, the transmitter and receiver are maintained at a fixed distance and are moved together along a line to produce a profile (Daniels 2000; USEPA 2016d). The size of the target and survey objectives must consider the spacing between the traces received by the equipment (USEPA 2025c). This mode offers the advantage of rapid data acquisition (**Figure 6-9** and **Figure 6-11**). See technology experts for application of moving GPR paired with UAS. In fixed mode, the transmitting and receiving antennas are moved independently to different points to make discrete measurements. The EM wave is transmitted, the receiver is turned on to receive and record the signals, and then the receiver is turned off (Daniels 2000). The measurements recorded create a trace, a time history of the travel of an EM pulse from the transmitter to the receiver. This mode is more labor intensive but provides greater flexibility than moving mode.

6.3.3.2 Visualization

Collected GPR data require considerable iterative post processing to improve data quality prior to interpretation. This post processing is performed with specialty software and should be conducted by a competent and trained practitioner. Because advanced data processing often includes a higher degree of interpreter bias, it is important to discuss the assumptions made by the practitioner processing the data (Annan 2009).

The GPR trace recorded must be converted from two-way travel time to a depth. The travel time is a record of the changes in amplitude of the EM wave as it travels through the subsurface and encounters reflectors that send the wave back to the ground surface (**Figure 6-9**). The propagation velocity of the EM wave is calculated by dividing the propagation velocity of an EM wave in a vacuum (3×10^8 m/s) by the square root of the dielectric permittivity of the subsurface materials (obtained from literature sources). Once the propagation velocity has been estimated based on published values or professional judgment, it is multiplied by the measured two-way travel time to determine the equivalent depth (ASTM 2019).

The objective of GPR data presentation is to depict a visual image that approximates the subsurface and position of any anomalies. Oftentimes, GPR results include subtleties that do not produce sharp boundaries. These subtleties often represent gradational boundaries that can complicate GPR data interpretation. Examples include heterogeneous fill materials or the water table (Annan 2003). These subtleties in data interpretation should be carefully considered. A significant amount of data filtering is required to produce usable and unbiased GPR images of subsurface data. Corrections to the recorded EM wave are made to account for the effects of attenuation due to geometric spreading, removal of low-frequency energy that subsequently distorts the recorded waveform, and topography. More sophisticated processing includes a step known as migration to correct the location of reflections coming from interfaces that are not vertically below the instrument. Further details can be found in (Annan 2009).

GPR displays are most often presented as 2D cross sections showing travel times for reflection events. These plots depict distance at ground surface on the x-axis versus depth travel time (surrogate for depth bgs) on the y-axis. An example of a 2D image illustrating the location of a sewer line is shown in **Figure 6-11**. To collect the data, the GPR servicer walks a specific direction dragging a GPR unit consisting of a transmitter (Tx) that emits EM pulses and a receiver (Rx) that records returning signals. As the GPR unit approaches a buried object, the distance between the radar and the target decreases until the unit is directly overhead. Because the distance is greatest when the radar is far away and shortest when directly overhead, the graphed time delay creates an inverted curve known as a reflection hyperbola. The apex

(highest point) of the hyperbola indicates the exact location and minimum depth of the buried object. This figure also shows how dragging the GPR across a localized target (such as a sewer line) results in a characteristic hyperbola in the reflection record.

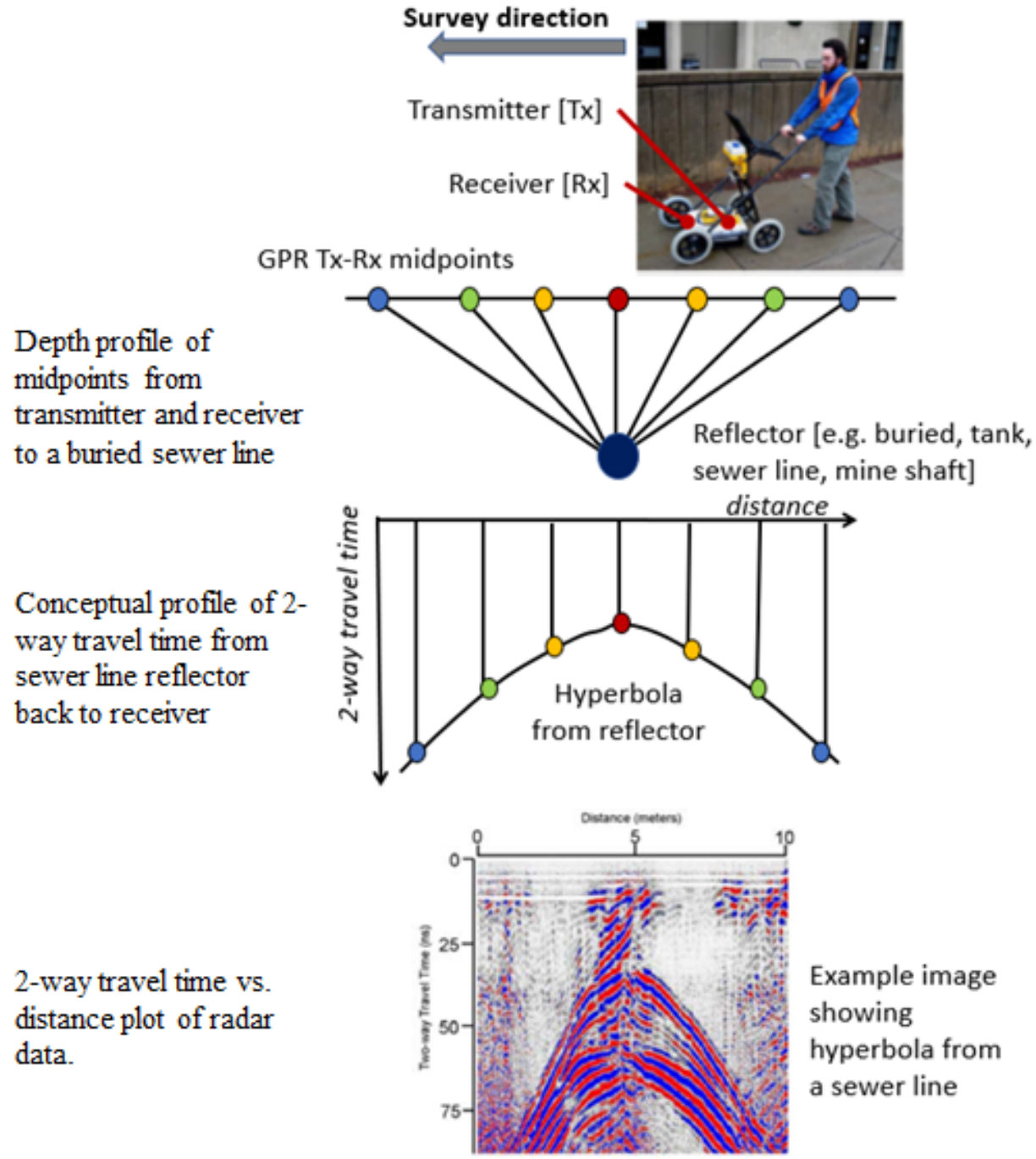


Figure 6-11. Schematic of a GPR survey of sewer line. The graphic illustrates how GPR detects buried features and creates a characteristic hyperbolic reflection pattern.

Source: Rutgers University Newark, Lee Slater. Used with permission.

Another useful representation of GPR datasets is a 3D block diagram showing relative amplitudes of EM energy at different levels or slices. These block diagrams are useful for identifying and isolating features of interest but can be more challenging for nontechnical reviewers to understand. For a 3D image to be useful, the amplitude color ranges should be assigned thoughtfully with a minimum number of colors. The viewing angle is another important visualization aspect to consider. A comparison of 2D and 3D images for the same target is shown in **Figure 6-12**.

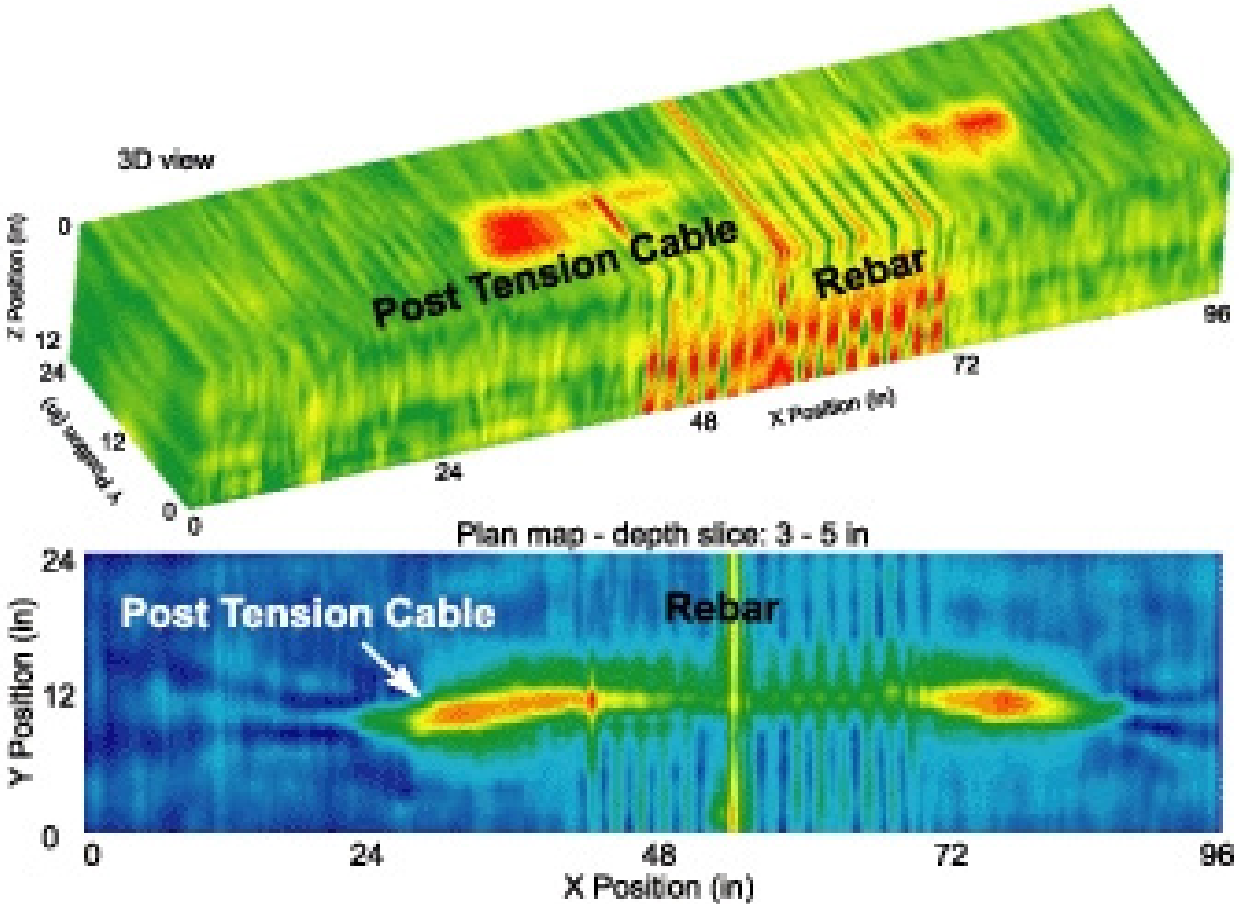


Figure 6-12. 3D GPR block view of response contrast for metallic objects in relation to 2D horizontal slices.

Source: USEPA (2016c).

6.3.3.3 Quality Control

Quality control procedures apply to GPR field procedures and data processing and interpretation activities. In the field, test lines are used to obtain the system settings that are optimal for the site. Field logs should be maintained to document system settings and field procedures and changes to either. Site conditions at the time of the survey (for example, weather, ambient conditions) should be recorded because they can influence test data. Equipment calibration is usually performed in accordance with manufacturer's specifications. Operational checks should be performed prior to use and throughout the day as a periodic check. Corrective actions taken to fix equipment or troubleshoot problems should also be recorded. Data should be reviewed as quickly as possible in the field so that scans can be rerun if necessary. It is good practice to rerun the test line to confirm proper system operation (ASTM 2019).

6.3.4 What Are the Advantages?

The advantages of GPR include:

- real-time results and data interpretation in the field
- real-time safety for workers and infrastructure (for example, locating utilities, clearing borehole locations)
- continuous display of data along a transect
- nondestructive
    - high spatial resolution
    - versatile across materials and environments

6.3.5 What Are the Limitations?

GPR has depth limitations depending on the contrast of electrical properties of the geologic formations and the variability in signal attenuation. These factors result in signal losses due to EC, the dielectric constant, and scattering (ASTM 2019). The effectiveness of a GPR survey strongly depends on the rate of attenuation of the EM energy as the signal propagates into the earth. At some distance, the attenuation is so excessive that the returned signal is no longer detectable above the EM noise levels. The attenuation of EM waves is largely from EM energy converting to thermal energy, an effect that increases with the EC of soil, rock, and fluids (USEPA 2018b). The attenuation rate determines the penetration depth of a GPR instrument at a site. In rocks and soil, the degree of saturation, content of pore fluid (for example, free ions in solution), clay mineralogy, and soil types strongly influence the bulk material's conductivity and ability to transmit an EM wave (ASTM 2019).

Unfortunately, site conditions often preclude optimal performance of GPR. The ionic strength of site groundwater and thickness of clay deposits reduce signal-penetration depth. In general, signal penetration is best in dry, sandy, or rocky soils and worse in moist, clayey, and conductive soils (USEPA 1993a). Signal attenuation can be 3 ft (1 m) or less in conductive materials such as seawater, mineral-rich clays, or metallic materials. Conversely, penetration depths have been reported up to 100 ft in water-saturated sands to nearly 1,000 ft in granite (ASTM 2019). In a quartz sand-rich environment with the water table at 15 ft, depths of 20 ft are easily obtainable.

Similarly, the presence of surface and buried conductive (metallic) debris on a site can severely hamper subsurface investigations. Radar waves are predominately attenuated by EC (Everett 2013). Reinforcing rods in concrete, buried railway tracks, and even metal underground tanks reduce radar wave energy, leaving little energy for the required detection of reflections.

Finally, accessibility issues on a site can limit effective GPR deployment. GPR equipment must be physically moved across the study area. Although the equipment is portable and often pushed manually by one person via a cart comparable in size to a shopping cart (**Figure 6-9**), heavily wooded sites, congested areas, or heavily sloped areas can limit GPR. Air-wave interferences are also problematic because they reflect the EM signal, which is then captured by the receiver. Air-wave reflections can occur from overhead power lines, telephone poles, walls, fences, and vehicles(Annan 2003). However, GPR may be paired with unmanned aerial systems (UAS) to overcome the abovementioned site limitations. Refer to the GPR subcontractor on the capabilities and limitations of using UAS with GPR technology. Also refer to Section 7.

6.4 Seismic Methods

6.4.1 What Is the Technology?

Seismic exploration methods are commonly used to determine site geology, stratigraphy, and rock and fluid properties. These techniques provide information about subsurface geology, and they make use of the properties of sound waves as they propagate through earth. The methods are based on geologic materials having different acoustic impedance (the product of density and seismic velocity). This difference results in body waves that reflect or refract at the interface of two strata, and surface waves that disperse (spread out) as they travel across the surface of the earth.

Seismic reflection and refraction techniques measure the travel time of two types of body waves from surficial shots (an energy source, usually in the form of a sledgehammer striking a metal plate flat on the ground). The primary wave (P wave), also called a compression wave, is the fastest traveling wave and, consequently, the first to arrive to a strata boundary. The secondary wave (S wave), also called the shear or transverse wave, travels slightly slower than the P wave and can be produced by the conversion of a P wave if it strikes a boundary at an oblique angle. Seismic-wave velocities depend on the elastic moduli and the densities of the geologic material that the wave travels through. Elastic moduli are a set of constants that define how a material responding to stress deforms, then recovers to its original shape after the stress stops. For example, a sound wave travels at a speed of 300 m/sec to 800 m/sec through unconsolidated sand, but travels at a speed between 4,600 m/sec and 7,000 m/sec through granite.

Multichannel analysis of surface waves (MASW) is a seismic technique that uses surface waves (specifically Rayleigh waves) from a similar energy source (for example, sledgehammer striking a metal plate) to determine shear-wave velocity (Vs) profiles in the subsurface. The basis of this technique is the dispersive characteristics of surface waves when traveling through a layered medium; different wavelengths propagate with different velocities depending on their penetration depth. There are two types of MASW techniques (passive and active); active MASW is the most common and is discussed in this section.

6.4.2 How Is the Technology Used?

Applications for seismic methods include mapping depth to bedrock and bedrock topography, mapping depth to groundwater, identifying and mapping faults, identifying geologic settings for NAPL transport, mapping stratigraphy, and mapping subsurface geologic structures. In addition, MASW is commonly used for mapping variation in soil stiffness (Vs is a direct indicator of ground stiffness) and identifying low-velocity anomalies (for example, karst terrain, voids and sinkholes, severely weathered bedrock, waste pits, and surface bedrock features).

Although seismic methods (especially reflection) can be more expensive than other geophysical methods, they are cost effective for the information they provide and areas that can be characterized compared to invasive drilling methods. Equipment is readily available, portable, and nonintrusive, and seismic measurements have good resolution and provide relatively rapid coverage of a large area. Some general applications and advantages for each of reflection, refraction, and MASW methods are provided below:

6.4.2.1 Seismic Reflection

Seismic reflection can define sequential stratigraphy to great depths (>1,000 m or 3,281 ft), although a thick sequence of dry gravel greatly affects the depth of penetration. Depending on the application,

seismic reflection can resolve layers down to 1 m (3 ft) thickness and is not affected by highly conductive electrical surface layers. Other advantages include:

- Data permit mapping of many horizons with each shot.
- The method can work regardless of velocity at depth (for example, reflection surveys are not hampered by a clay layer overlying a sand or gravel layer).
- Observations can be more readily interpreted in terms of complex geology.
- Observations use the entire reflected wavefield (the time history of ground motion at different distances between the source and the receiver).
- The subsurface is directly imaged from the acquired observations.

6.4.2.2 Seismic Refraction

Seismic refraction is often used in shallow areas (less than 30 meters or 100 ft) where the principal goal is to map bedrock topography beneath a single overburden unit. It also is employed to map weathered bedrock and fracture zones during water prospecting. If the velocity of the transmitting unit used with seismic refraction increases with depth, results may have to be modified or discarded. For example, a low-velocity thin-sand unit that is overlain by a high-velocity clay unit may not be resolvable with the refraction technique. Recent advances in inversion of seismic refraction data make it possible to image relatively small, nonstratigraphic targets such as foundation elements and perform refraction profiling in the presence of localized low-velocity zones such as incipient sinkholes. Other advantages include:

- Refraction observations generally employ fewer source and receiver locations than reflection and are thus relatively cheap to acquire.
- Little data processing is performed on refraction observations with the exception of trace scaling or filtering, which helps pick the arrival times of the initial ground motion.
- Because such a small portion of the recorded ground motion is used, developing models and interpretations is no more difficult than with other geophysical surveys.

6.4.2.3 MASW

MASW is a low-cost, noninvasive method that does not require heavy machinery for data measurement. Measuring geophones are placed in the ground and do not require coupling to the ground. Therefore, data are acquired relatively quickly without leaving lasting marks on the surface. Compared to seismic reflection and refraction methods, MASW is applicable in a wider range of field conditions but covers a generally smaller area.

The main advantage of the MASW method compared to seismic reflection and refraction is that it determines stiffness profiles with far greater precision. Surface waves have stronger energy than body waves; hence, higher signal-to-noise ratios are usually obtained in surface methods (Park et al. 2002; Gouveia et al. 2016). MASW is a primary method for determining the average shear-wave velocity in the top 30 meters of the subsurface (Vs30), which is a critical parameter for site classification under international building codes and for seismic hazard assessments (Foti et al. 2014).

6.4.3 Technology Implementation

A linear array of geophones (a recording device used to convert velocity into voltage) is typically established along the ground surface. Surficial shots (a seismic energy source, usually obtained by hitting a metal plate placed flat on the ground with a sledgehammer) are generated to provide a seismic wave in

the form of a strong vibration that is recorded by the geophones. Shots are fired, in turn, at each geophone, and active geophones are progressively added ahead of the shots in a roll-along fashion. The geophones receive and transmit data to a data processing unit where software algorithms process the signal. The data processed are used to produce an image of the subsurface stratigraphy.

6.4.3.1 Reflection

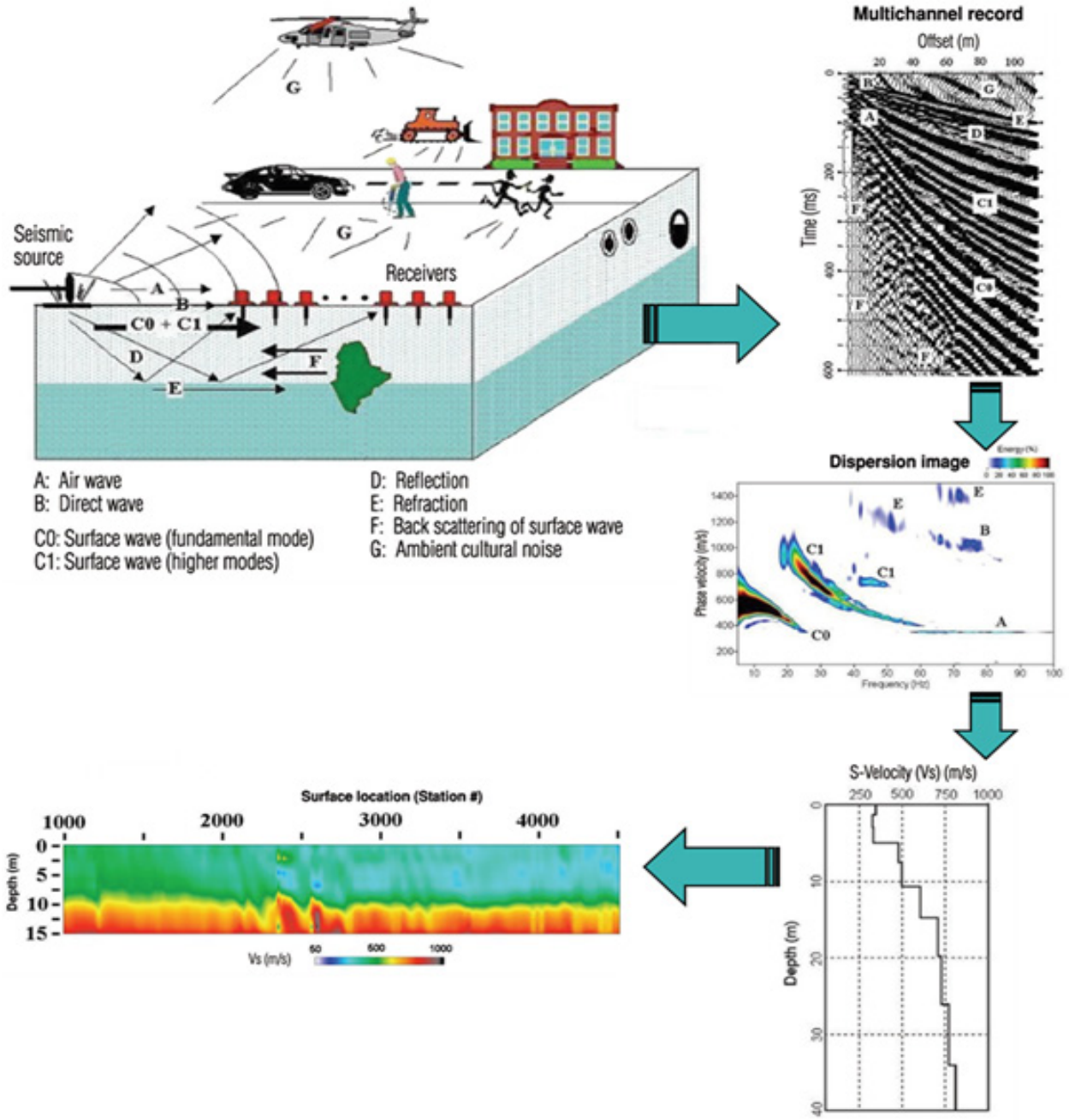


Figure 6-13. General seismic graphic depiction of an MASW field survey and field records imaging multiple types of seismic waves that can be distinguished and then showing how the data can be analyzed.

Source: Modified after Park et al. (2007). Used with permission.

Reflection surveys use geophones to record the arrival of the P waves after they have reflected from a subsurface horizon. As the first seismic wave (the P wave) generated by the shot source (for example, sledgehammer) travels through the geologic media, it propagates in three different ray paths. One path is along the ground surface (direct ray). The second path is represented by the reflected wave. The reflected wave consists of the wave that travels down to the interface layer, hits the interface, and travels upwardly from the refracting layer (reflected ray). The third path (critically refracted ray) is represented by the refracted wave, which has three legs. The first leg travels downwardly across the first layer and with an offset x from the downward reflected ray, hits the interface, and produces the second leg of the refracted wave that travels along the second layer (at the speed of the lower layer). The third leg travels upwardly through the refracting layer or refractor by critical refraction). A simplified diagram of the method is shown in **Figure 6-13**.

6.4.3.2 Refraction

The seismic refraction technique analyzes the refracted wave along the different stratigraphic interfaces by recording the signatures on each geophone in the spread implanted in the ground. Ray paths go downward to the boundary (depicted as the turquoise layer near label 'E' in **Figure 6-13**), are refracted along the boundary, and return to the surface. The recorded signal response is plotted and processed as a function of the distance (off set) from the source. The processed signal produces a cross section of the seismic wave velocity, which, in turn, conveys information about the geologic stratigraphy (Sheriff and Geldart 1995; National Research Council 2000). The seismic refraction technique generates an image of the subsurface impedance contrast for the area investigated. The image provides data related to the distance and travel time of the reflected wave (National Research Council 2000). **Figure 6-13** provides a schematic of a seismic refraction survey. First arrivals near the shot have paths directly from the shot to the detector. Rays traveling along the boundary are the first to arrive at receivers (geophones) away from the shot because the lower material (below the boundary noted above) has a higher velocity (V2 > V1).

6.4.3.3 MULTICHANNEL ANALYSIS OF SURFACE WAVES

In this method, the ground is struck multiple times with a sledgehammer to enhance the amplitude of the surface wave and minimize background noise. This process is called vertical stacking. Data are recorded and analyzed via dispersion and inversion analysis.

Because higher frequency signals are mostly refracted energy and refracted energy noise, low-frequency geophones are needed; low-frequency, vertically polarized geophones are commonly used to record surface wave data because they can record extremely low-frequency data and attenuate higher frequency signals. The desired surface-wave energy to analyze in MASW usually ranges between 5 Hz and 40 Hz. **Figure 6-13** illustrates an overview of the method, including:

- data acquisition and the multichannel record obtained (note that it contains multiple frequencies despite looking like only one)
- dispersion image generated from each record along with its extracted dispersion curve
- one-dimensional shear-wave velocity profile that is back-calculated from the curve
- final 2D shear-wave velocity profile map produced using an appropriate interpolation method

6.4.3.4 Data Collection Design

The maximum depth and resolution of the data depend on the energy and frequency of the initial pulse and arrangement (geometry) of the geophones. Factors to consider in deciding which energy source to

use include:

- its energy output (the stronger it is, the better the signal to noise ratio); for environmental work, possible energy sources include a 14- or 16-lb sledgehammer and accelerated weight drop
- frequency content (higher frequencies offer high resolution but decay more quickly than lower frequencies; this lowers the depth of investigation)
- should allow for stacking measurements to improve the signal to noise ratio (it should be repeatable)
- the source signature should be well-defined (the wave energy should be known exactly) to significantly enhance the imaging quality (GPG 2017).

Common geometries of survey designs include multichannel and common midpoint (CMP). A multichannel design can be a split spread, which has a central shot with receivers on both sides, or a single-ended spread where the receivers are always on one side of the source. Seismic traces belong to a single source, a common source gather. A CMP design uses multiple shots and receivers specifically so that some subsurface points are sampled more than once. The goal is to identify all reflections to a point on various profiles and stack them to get an enhanced signal-to-noise ratio. The degree of multiplicity from a particular location is known as fold. For example, a 24-channel seismograph is commonly used to gather 12-fold data.

MASW

For MASW investigations, the resolvable depth of investigation that can be obtained with the highest accuracy is related to the receiver spacing, which should be greater than 30% of the investigation depth but not exceed the investigation depth (MASW 2018). In practice, the length of spread is usually limited in the range of 10 ft to 300 ft and the maximum depth of investigation is less than 150 ft. Note that surface waves generated by most seismic sources are attenuated and are not usable at the end of a long receiver spread because they become noisy (Park et al. 1999).

6.4.3.5 Quality Control

To ensure seismic data are properly recorded, the geophones should have:

- a digital converter to convert electrical signals into a time series of numbers
- the ability to start digitizing at the same time the shot is initiated
- a computer to manage input and to plot signals so that data quality can be checked visually
- built-in software to carry out initial data interpretations (GPG 2017)

To acquire data of sufficient quality, the surveyor should ensure no noise is generated at the geophones by confirming that the geophone has good contact with the ground surface. In addition, ambient noise should be kept to a minimum during the survey. Avoid noise from people walking, cars, or heavy equipment movement in the proximity of the geophones.

Source offset (the distance between the source and first receiver) is an important consideration for MASW investigations because surface waves are formed at a certain distance from the source. If the first receiver is placed closer than this distance to the source, ambient noise is recorded rather than the surface waves. Source offset has been suggested to lie within the range of 25% to 50% of the receiver array length (MASW 2018; Park Choon B. and Carnevale Mario 2012; Park et al. 1999).

In addition to data-acquisition quality discussed above, the field data for MASW investigations require a number of preprocessing and processing considerations:

- Raw seismic data are converted into Kansas Geological Survey data processing format (KGS or SEG-Y), named for first developers of the method. Field geometry should be correctly assigned during data format conversion.
- Field data should be inspected, and bad records removed.
- Field data are inspected for consistency in the alignment of surface waves in neighboring records.
- Filtering and muting are used to identify and eliminate noise.
- Sometimes preliminary data processing is performed to investigate the optimum ranges of phase velocity and frequency.
- To improve the estimation of the optimum dispersion curve, multiple curves are extracted from several multichannel records and are combined into a single experimental curve.
- Inversion of the data further reduces the uncertainty associated with the experimental dispersion curve estimates.

The seismic reflection technique generates an image of the subsurface impedance contrast for the area investigated. The image provides data related to the distance and travel time of the reflected wave (National Research Council 2000). **Figure 6-13** provides a schematic of a seismic refraction survey. First arrivals near the shot have paths directly from the shot to the detector. Rays traveling along the boundary are the first to arrive at receivers (geophones) away from the shot because the lower material has a higher velocity (V2 > V1).

6.4.3.6 Data Processing and Visualization

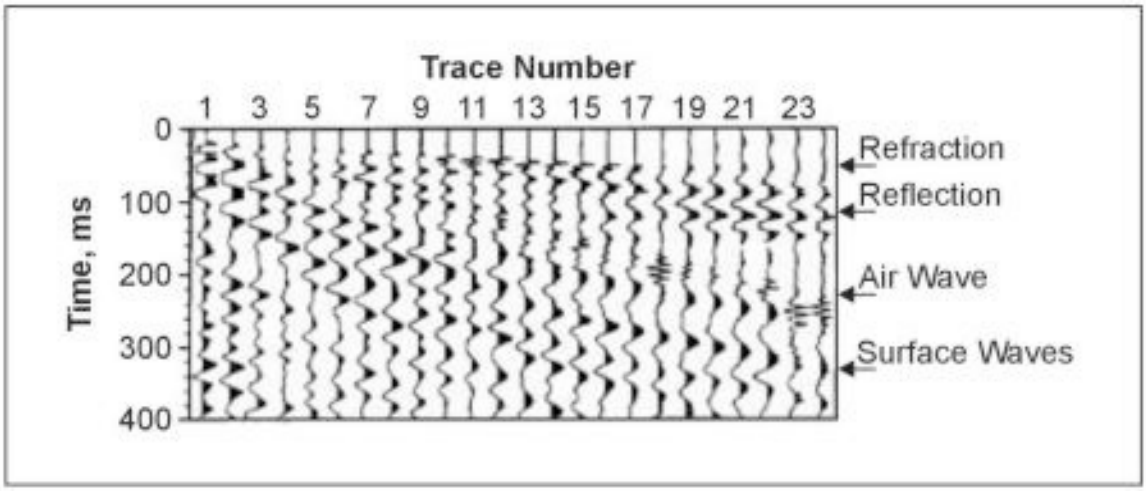


Figure 6-14. Simple seismic reflection record.

Source: (USEPA 2016c).

Qualified specialists referred to as geophysicists typically perform data processing. These individuals should have all available information (for example, well logs, known depths, results from ancillary methods, and the expected results). The data from seismic surveys are usually plotted on time distance graphs and as a profile of stacked data of distance versus time. Most seismic instrumentation is capable

of drawing a vertical cross section through the ground, or profiles, that are a layer-cake representation of depth to acoustic boundaries (stratigraphic horizons) and types of acoustic anomalies. Instrumentation obtains data that are used to create vertical cross sections or profiles. **Figure 6-14** provides a seismic reflection record. The receivers are arranged to one side of a shot, which is 15 m from the first geophone.

Data processing consists of three primary activities: deconvolution, CMP stacking, and migration. Deconvolution restores a waveshape to its form before filtering. CMP stacking uses a stack of common midpoints to gather traces. Migration performs an inversion so that reflections and diffractions are plotted at their true locations (Yilmaz 2001).

Seismic Reflection

The essential steps to process seismic reflection data (G. Baker 1999) are:

- Obtain common source-point gathers (collections of seismic data recorded by multiple receivers).
- Sort into CMP gathers. (Reflection events appear as hyperbolic trajectories, and the goal is to stack them to a single trace.)

1) Perform a velocity analysis for each event to find the stacking velocity.
2) Perform a normal moveout correction and stack to yield a single trace corresponding to a coincident source and receiver.
3) Composite the traces into a CMP-processed section.

These techniques can be expensive due to software cost and the need for a qualified specialist to interpret the results, but technically robust and excellent results can be achieved. An important outcome of the processing is obtaining a true depth section. This requires conversion of the times of the reflections to depths by derivation of a velocity profile. Well logs and check shots are often necessary to confirm the accuracy of this conversion.

Seismic Refraction

The generalized reciprocal method (GRM) is typically used to acquire, process, and interpret seismic refraction data. GRM is an interpretation method designed to accurately map undulating refractor surfaces from in-line refraction data using both forward and reverse shots. The method is related to the Hales and the reciprocal seismic refraction interpretation methods. In this method, it is crucial to acquire at least seven shots per spread. Assuming a 24-channel acquisition system, one center shot is required between geophones 12 and 13, one shot between each of geophone pairs 6 and 7 and 18 and 19, a near-offset shot from each end geophone (geophones 1 and 24), and one far-offset shot from each end of the spread. In practice, often 13 shots are used per spread for high-resolution investigations. To map the refractor surface, an off-end shot must be located at each end of the spread so that each first arrival on the geophone spread has enough signal to noise ratio to sufficiently identify the surface, generally the base of weathering.

Blind zones and hidden layers may be encountered. A hidden layer is an intermediate velocity, intermediate-depth layer whose thickness or velocity is such that rays from a deeper, higher velocity layer arrive at the ground surface sooner than rays from the hidden layer. Standard seismic refraction interpretation schemes yield significant errors in calculated refractor depths in the presence of blind zones or hidden layers. The GRM is the only method capable of overcoming this problem.

Data processing includes the selection of first-break arrival times, the generation of time-distance plots for each line, the assignment of selected portions of the travel-time data to individual refractors, and the

phantoming of travel-time data for the target (lower) refractor. Once this preprocessing work is complete, GRM processing begins. Layer thicknesses and velocities are calculated, and a geophysical interpretation of the geologic parameters is made. The end product is a seismic refraction profile that indicates the seismic layers detected, the depths to the interfaces between layers as they vary along the line, and the seismic velocities encountered.

MASW

After seismic data are uploaded into the MASW software (SurfSeis), the velocity at which each different frequency propagates is automatically analyzed. Each multichannel record is transformed from the space-time domain to the frequency domain, and a dispersion image (also called overtone image) is produced. The dispersion image shows fundamental and higher modes of the Rayleigh waves. A fundamental mode dispersion curve is then extracted from each dispersion image (Park 2006). Accurate extraction of the dispersion is the most critical step because it primarily determines the accuracy of the final shear-wave velocity profile. In a trial-and-error approach, the user can run the dispersion program several times for different phase velocity ranges and select the optimum dispersion curve. To improve the estimation of the optimum dispersion curve, multiple curves are extracted from several multichannel records and are combined into a single experimental curve.

The final step is developing the shear-wave velocity profile from the dispersion curve using an inversion process. Rayleigh waves are the product of interfering compressional and shear waves; therefore, inversion of the dispersion curve results in compressional and shear-wave velocities as a function of depth. In the inversion process, several possible soil models are estimated, and a dispersion curve model that best fits the experimental dispersion curve is selected. The theoretical dispersion curve of the models is first computed and compared to the experimental dispersion curve based on the RMSE between the two curves. If the calculated RMSE is greater than the specified minimum error, the soil model is modified and a new dispersion curve is calculated. The procedure is repeated until either the specified minimum error or the maximum number of iterations is reached. The shear-wave velocity profile of the model resulting in the best fit is the final output of dispersion-inversion analysis (Olafsdottir et al. 2018).

Spatial interpolation methods can be used to create a 2D shear-wave velocity map by assigning each 1D shear-wave velocity profile at the surface coordinate in the middle of the receiver spread used to acquire the corresponding record .

6.4.4 What Are the Advantages?

6.4.4.1 Seismic Reflection

Seismic reflection can define sequential stratigraphy to great depths (>1,000 m or 3,281 ft), although a thick sequence of dry gravel greatly affects the depth of penetration. Depending on the application, seismic reflection can resolve layers down to 1 m (3 ft) thickness and is not affected by highly conductive electrical surface layers. Other advantages include:

Data permit mapping of many horizons with each shot.

The method can work regardless of velocity at depth (for example, reflection surveys are not hampered by clay layer overlying a sand/gravel layer).

Observations can be more readily interpreted in terms of complex geology.

Observations use the entire reflected wavefield (the time history of ground motion at different distances between the source and the receiver).

The subsurface is directly imaged from the acquired observations.

6.4.4.2 Seismic Refraction

Seismic refraction is often used in shallow areas (less than 30 m or 100 ft) where the principal goal is to map bedrock topography beneath a single overburden unit. It also is employed to map weathered bedrock and fracture zones during water prospecting. If the velocity of the transmitting unit used with seismic refraction increases with depth, results may have to be modified or discarded. For example, a low-velocity thin-sand unit that is overlain by a high-velocity clay unit may not be resolvable with the refraction technique. Recent advances in inversion of seismic refraction data make it possible to image relatively small, nonstratigraphic targets such as foundation elements and perform refraction profiling in the presence of localized low-velocity zones such as incipient sinkholes. Other advantages include:

Refraction observations generally employ fewer source and receiver locations and are thus relatively cheap to acquire.

Little data processing is performed on refraction observations with the exception of trace scaling or filtering, which helps pick the arrival times of the initial ground motion.

Because such a small portion of the recorded ground motion is used, developing models and interpretations is no more difficult than with other geophysical surveys.

6.4.4.3 MASW

MASW is a low-cost, noninvasive method that does not require heavy machinery for data measurement. Measuring geophones are placed in the ground and do not require coupling to the ground. Therefore, data are acquired relatively quickly without leaving lasting marks on the surface. Compared to seismic reflection and refraction methods, MASW is applicable in a wider range of field conditions.

The main advantage of the MASW method compared to seismic reflection and refraction is that it determines stiffness profiles with far greater precision. Surface waves have stronger energy than body waves; hence, higher signal-to-noise ratios are usually obtained in surface methods (Park et al. 2002; Gouveia et al. 2016).

6.4.5 What Are the Limitations?

The disadvantages of seismic methods are in the interpretation of data, which requires ground-truthing, information from other tools, and substantial expertise to interpret. The performance of seismic methods can be significantly affected by cultural noises, such as highways and airports, as well as buried building foundations. Seismic methods do not perform well in heterogeneous settings where thin discontinuous layers may not be detected or resolved. Additionally, depth penetration may be sacrificed due to lack of low-frequency seismic energy . Other tool-specific limitations are discussed below.

6.4.5.1 Seismic Reflection

Seismic reflection costs more than refraction and is limited to penetration depths generally greater than approximately 50 ft. At depths less than approximately 50 ft, reflections from subsurface density contrasts arrive at geophones at nearly the same time as the much higher amplitude ground roll (surface waves) and air blast (the sound of the shot). Reflections from greater depths arrive at geophones after the ground roll and air blast have passed, making these deeper targets easier to detect and delineate. It is possible to obtain seismic reflections from shallow depths. The maximum depth and resolution of the

data depend on the energy and frequency of the initial pulse and arrangement (geometry) of the geophones. Factors to consider in deciding which energy source to use include:

- Vary field techniques depending on depth.
- Minimize impacts due to air blast and ground role to increase signal to noise ratio.
- Place shots and geophones near shallow or surface groundwater.
- Use severe low-cut filters and arrays of a small number (one to five) of geophones.
- Ensure reflections are visible on the field records after all recording parameters are optimized.
- Guide data processing by the appearance of field records; use extreme care to avoid stacking refractions or other unwanted artifacts as reflections.

Additional limitations are:

- frequency content—higher frequencies offer high resolution but decay more quickly than lower frequencies; this lowers the depth of investigation.
- Because many source and receiver locations must be used to produce meaningful images, reflection seismic observations can be expensive to acquire.
- A source should allow for stacking measurements to improve the signal to noise ratio (it should be repeatable).
- Reflection seismic processing requires appropriate software and a relatively high level of expertise. Thus, processing observation data is relatively expensive. The source signature should be well-defined (the wave energy should be known exactly) to significantly enhance the imaging quality .
- At later times in the seismic record, more noise is present, making the reflections difficult to extract from the unprocessed data.

6.4.5.2 Seismic Refraction

Seismic refraction is generally applicable only where the seismic velocities of layers increase with depth. Therefore, where higher velocity (for example, clay) layers may overlie lower velocity (for example, sand or gravel) layers, seismic refraction may yield incorrect results. Additionally, seismic refraction requires geophone arrays with lengths of approximately four to five times the depth to target of interest. This limits its application to mapping features at depths less than 100 ft. Greater depths are possible, but the required array lengths may exceed site dimensions, and the shot energy required to transmit seismic arrivals for the required distances may necessitate using large explosive charges. Furthermore, the lateral resolution of seismic refraction data degrades with increasing array length due to migration of seismic waves. Other limitations include:

Observations require relatively large source-receiver offsets. Seismic reflection surveys are typically designed to detect a reflection from a particular subsurface point multiple times. This approach improves the ability to detect and image a given event because the method makes it more difficult to discern direct arrivals and sound waves traveling through the air.

Observations are generally interpreted in terms of layers that can have dip and topography. Seismic refraction surveys are most useful at sites where velocities increase with depth (for example, a sand or gravel layer overlies a clay layer instead of a clay layer overlying a sand or gravel layer).

Observations use only the arrival time of the initial ground motion at different distances from the source (offsets). The depth of penetration is approximately one-fifth of the length of the geophone spread, including offset shots. For example, if the depth of investigation must be 10 m, at least 50 m (measured from offset shot to offset shot) must be available for the survey .

A model for the subsurface is constructed by attempting to reproduce the observed arrival times. Vertical resolution for seismic data is how thin a layer can be before the reflections from its top and bottom become indistinguishable. Vertical resolution is dependent on the signal wavelength, which is dependent on the frequency and velocity of the material. The theoretical minimum thickness is ¼ wavelength (for example, careful processing could extract the pulses if they overlap by half a wavelength).

6.4.5.3 MASW

Rayleigh wave amplitudes decrease exponentially with depth; therefore, resolution diminishes markedly with increasing depth. As a result, investigations using MASW are limited to much shallower depths than either reflection or refraction. For MASW investigations, topography influences the quality of the field measurements; surveying should be conducted on relatively flat ground for best results. The overall topographic variation might not affect the data, but the ground should be nearly flat, at least within the receiver span (Park 2006).

6.5 Electromagnetic Surveys

6.5.1 What Is the Technology?

EM methods use an energy source (either an electric field or a changing magnetic field) to excite ground current. The ground current follows two fundamental principles of EM induction. Faraday's law of electromagnetic induction estimates how a magnetic field interacts with an electric current to produce an electromotive force; Ampere's law states that electric currents generate magnetic fields. Together, these two tenets embody the most fundamental EM phenomena: that a varying magnetic field will result in a varying electric field that will create another varying secondary magnetic field. When an electrical current is inducted into the ground (a conductor), a varying magnetic field is generated. The induction of the electrical current varies depending on the composition of the subsurface, and the secondary magnetic field provides information about the EC of the subsurface. The main objective of EM methods is to extract this information from measured data and translate it to electrical resistivity or EC images of the subsurface.

This section describes two sets of tools: frequency domain electromagnetic (FDEM) surveys and time domain electromagnetic (TDEM) surveys. FDEM surveys measure the electrical response of the subsurface at several frequencies to obtain information about conductivity variations with depth. Primary FDEM methods include terrain conductivity, horizontal loop EM, very low frequency EM, EM induction and EM metal detectors, magnetotellurics (natural and controlled source), and electrical offset logging (EOL). TDEM surveys achieve the same results by measuring the electrical response of the subsurface to a pulsed wave at several time intervals after transmission.

6.5.2 How Is the Technology Used?

6.5.2.1 FDEM

FDEM instruments consist of a transmitter and receiver that use inductive coupling between electrical coils and subsurface conductors to identify subsurface targets (**Figure 6-15**). A primary alternating current magnetic field generates electrical currents (known as eddy currents) to flow in subsurface conductors. These eddy currents generate a secondary magnetic field. The receiver coil of the FDEM

instrument measures the resultant field (vector sum of the primary and secondary fields). FDEM instruments generally have two configurations. One configuration involves two loops or coils that consist of a transmitter coil and a receiver coil where one person carries each. The receiver coil receives the primary and secondary magnetic fields. A second FDEM configuration includes a single instrument that houses the transmitter and receiver and is typically used with a field computer and a GPS.

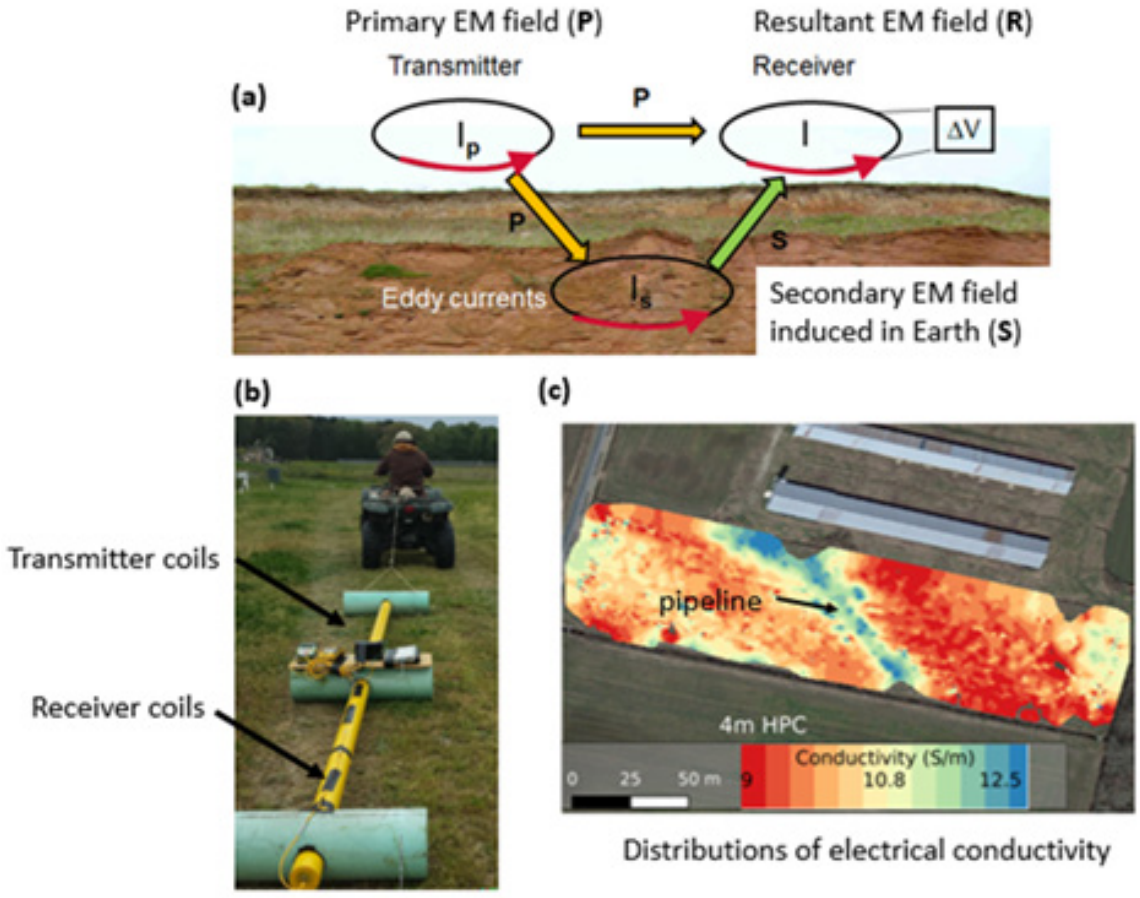


Figure 6-15. FDEM instrument components.

Source: Rutgers University Newark, Lee Slater. Used with permission.

Most EM equipment allows measurement of both the in-phase component and the 90° out-of-phase, or quadrature components of the resultant field. Common FDEM systems use a low-induction approximation where the out-of-phase component is proportional to the EC. In this case the instruments are often described as terrain conductivity meters. The instrument records apparent EC, which is typically reported in mS/m. The in-phase component is a ratio of the secondary magnetic field and primary field and is measured in parts per thousand. It is a strong indicator of metal content.

FDEM is often used as a reconnaissance tool to guide more detailed surface geophysical surveys. The inductive coupling of the instrument to the subsurface means that measurements can be acquired rapidly without the need for direct ground contact, which allows for quick and efficient data collection relative to galvanic electrical resistivity imaging surveys. FDEM surveys are typically used for lateral geologic and hydrogeologic profiling in the subsurface, contaminant plume mapping, fill and waste delineation, and locating tanks and buried drums, buried structures, and underground utilities.

6.5.2.2 TDEM

TDEM surveys measure variations of EC (inverse of resistivity) in the subsurface. EC correlates well with several physical and chemical properties of subsurface materials, including particle size, texture, porosity, and ionic content (salinity), so it provides a detailed picture of subsurface material. TDEM surveys measure the amplitude of a signal as a function of time; the signal is transmitted as an electric current pulse (for example, by turning off the current quickly), and measurements are obtained after the primary field disappears (only in the presence of the secondary field).

TDEM instruments consist of a transmitter and receiver that send and receive an electrical signal. An electrical current is passed through an ungrounded loop (which requires no direct contact with the ground) that generates a magnetic field that, in turn, generates electrical eddy currents in the subsurface. Eddy currents are dependent on the subsurface electrical conductivity and geometry of the layers and are measured using an induction coil [see **Figure 6-16(a)**]. The current diffuses more slowly in conductive materials compared to resistive materials. Soundings—information about the subsurface conductivity as a function of depth—are measured in the receiving coil.

Transient soundings can be conducted by placing a wire in a square loop on the ground. The wires are then connected to the transmitter, and the receiving coil is placed in the middle of the transmitter loop. The receiving coil is connected to the receiver, and the receiver is connected to the transmitter. These connections allow synchronization between the transmitter and receiver [see **Figure 6-16(b)**]. TDEM data recording is completed in time windows called gates. The gates are set from a few microseconds up to tens or even hundreds of milliseconds after the transmitter current has been turned off. The gates are arranged logarithmically, increasing time lengths to improve the signal-to-noise ratio at later times; these later signals provide information on deeper layers.

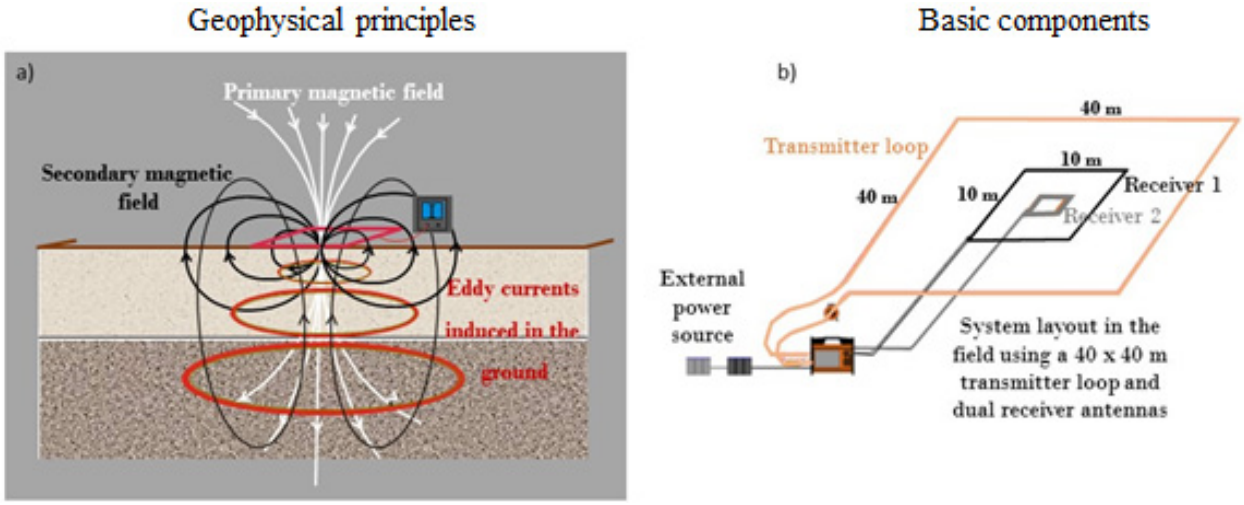


Figure 6-16. Example of duo central receiver coils with the WalkTEM system.

Source: Courtesy of MALÅ Geoscience/Guideline Geo. Used with permission.

TDEM equipment can be suspended from an aircraft (fixed wing or helicopter) for airborne EM methods, placed or pulled on the ground for ground-based surveys, or towed by a boat for waterborne surveys. TDEM ground arrays allow for larger transmitter loops that increase depths of measurement. Because towed arrays can cover considerably larger areas, they are often used in mineral prospecting for identifying conductive ore bodies or other large-scale projects. TDEM systems for environmental studies can sound the depth, thickness, and conductivity of layers down to about 300 m (about 1,000 ft) below surface (Sørensen and Auken 2004; Christiansen and Auken 2012; Auken et al. 2017).

6.5.3 Technology Implementation

6.5.3.1 Data Processing and Data Visualization

FDEM

FDEM resulting data should be used only for qualitative purposes. Data files are downloaded from the field computer following data collection. Depending on the instrument type and model, GPS measurements may be incorporated into the data file during the survey. Data are processed using various software programs and assessed for data quality. Data processing software interpolates data between actual measurement points. Data are then typically presented in a color-contoured, plan-view map showing the amplitude of the bulk conductivity and the in-phase modes for a specific approximate investigation depth. Data from multifrequency FDEM instruments can be inverted to produce 2D or 3D variations in EC across a site.

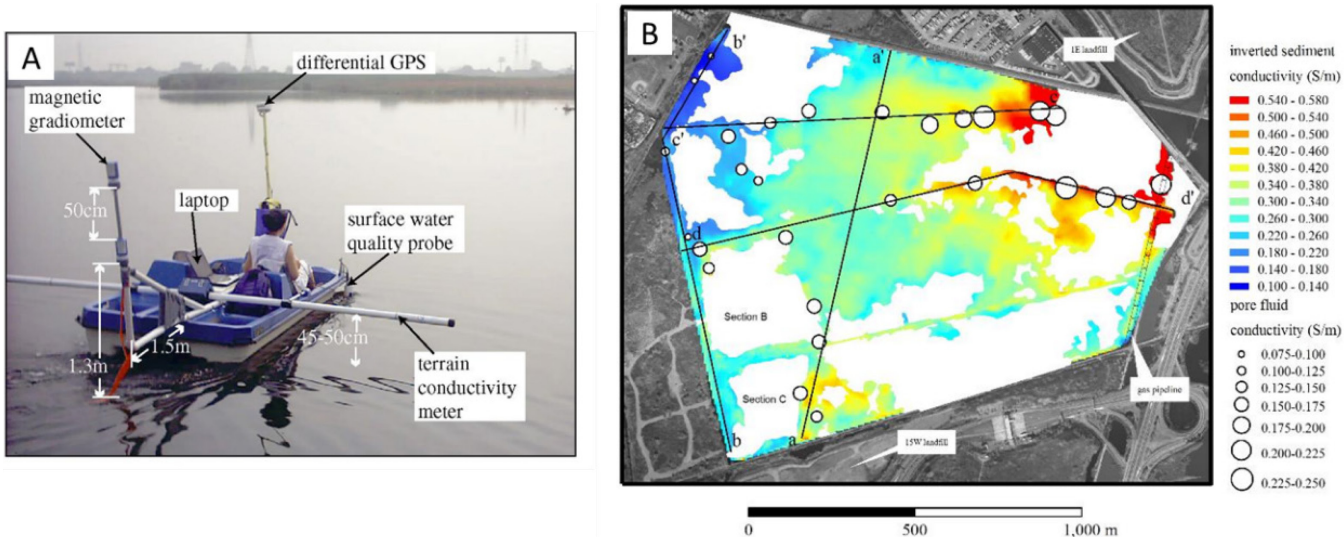


Figure 6-17. Example of an FDEM survey mapping variations in conductivity across a wetland impacted by leachate plumes from landfills.

Source: Modified from Mansoor (2006). Used with permission.

Figure 6-17 shows (a) a paddleboat equipped with terrain-conductivity meter, differential GPS, surface-water quality probe, and a magnetic gradiometer (for mapping metals) and (b) the resulting interpolated image of EC of the sediments from over 12,000 data points, with direct measurements of pore fluid conductivity extracted from sediment samples. The plume from the landfill in the northeast of the wetland is immediately obvious from the high EC of the sediments.

TDEM

TDEM systems allow the user to visualize the acquired data in the field with minimal preprocessing. For accurate presentation and interpretation of the subsurface model, noise removal and inversion of the raw data must be performed. To prepare the acquired data for geophysical inversion and interpretation, distorted or noisy data must be removed, and data should be averaged to improve the signal-to-noise ratio. Variations in topography (or elevation) should be incorporated when interpreting the sounding data. Accounting for topography and elevation will provide more accurate depths to subsurface features such as water-table interface throughout the sounding.

Noisy or distorted data are removed manually by visually assessing the data. Once the raw data are relatively free of noise, data are averaged to form soundings for inversion. Averaging is essential to improve the signal-to-noise ratio. Various averaging methods are available in different processing software. Averaging filter widths can range from small to large. A small averaging filter width is preferable where the signal-to-noise ratio is good and in situations where lateral resolution is a priority; a large averaging filter width improves the signal-to-noise ratio, especially when handling noisy data or mapping deeper geologic structures is a priority.

Inversion of the processed TDEM data is usually performed using computer algorithms. Currently, advanced computer software allows processed TDEM data to be automatically inverted to a layered earth model. The inversion results are usually presented as 2D cross sections, contour maps, and mean resistivity maps. For example, inversion results for TDEM data acquired in grid format should be presented in detailed, scaled 2D profile and contour maps, indicating the contour interval with scaled profile plots (traverses shown on map). Anomalous resistivity areas showing targeted features (for example, probable drum burial or contaminant plumes) should also be indicated on the contour map. Pertinent information related to the instrumentation (system technical specification), field operations, and site conditions and issues that may affect data quality, processing workflow, and interpretation techniques should be recorded.

A geophysical datum always consists of two numbers—the measurement itself and the uncertainty of the measurement, because the measured data consist of both the earth response and the background noise. When performing a single transient in a TDEM sounding, the signal can be significantly affected by noise sources. Some noise sources such as lightning and communications equipment can be effectively decreased through repeated measurements (for example, stacking) where noise is decreased and the signal is enhanced. Other noise sources such as human-made structures (high-voltage power lines, fences, pipelines, cables) can overwhelm the receiver and cause the data to be unusable. In those cases, the survey should take place further away from the noise source.

6.5.3.2 Data Collection Design

FDEM

FDEM surveys are generally performed by walking or towing an instrument behind a vehicle in even-spaced transects in a grid pattern (**Figure 6-17**). The lateral resolution of the data is determined by the spacing of data collection points; therefore, transect spacing should be selected based on the size of the desired target. For example, transect spacing can be greater for landfill or plume delineation and smaller for buried metallic debris identification.

The distance between the transmitter and receiver coils influences detection depth and data resolution. A greater coil separation allows for a greater depth of detection and, conversely, lower data resolution. Greater depths of detection are useful for profiling geologic and hydrogeologic features or identifying large-scale features that do not need high-resolution results. Features that warrant high-resolution profiling (such as buried utilities or minor changes in soil types) should generally be collected with smaller coil spacing; however, this limits the investigation depth. Generally, a coil spacing of 12 ft has an effective exploration depth of approximately 15–20 ft.

The instrument orientation (vertical dipole or horizontal dipole modes) can influence detection depths. In-phase and out-of-phase measurements are collected at greater depths and lower resolution when in vertical dipole mode. Measurements collected in horizontal dipole mode are shallower and higher resolution.

FDEM instrumentation commonly consists of a single transmitter and a single receiver that collects in-phase and out-of-phase measurements simultaneously. Newer FDEM instruments have multiple receiver

coils (at different separations and orientations) that can provide measurements of both the in-phase and quadrature-phase components at multiple depth ranges simultaneously.

TDEM

TDEM data can be collected in a rectangular grid pattern (for example, readings taken at the nodes of the grid) or along a traverse or profile. The survey configuration is site-specific and dependent upon site conditions and the size and orientation of the target. For example, mapping or searching buried metallic objects at a large site should be conducted by a grid configuration; mapping a fault line or a geologic contact requires completion of a profile. Generally, it is most beneficial to place the profiles perpendicular to known or expected geologic structures. The length of the profile and grid sizes are crucial parameters to conducting an effective investigation. Note that it is always recommended to extend data collection far enough beyond the conductive target to obtain background levels (NJDEP 2005). For airborne TDEM, flight speed is a tradeoff between lateral resolution, mapping depth, and costs. A low flight speed provides high data density, improved lateral resolution, and a higher mapping depth and vice versa.

To achieve the required depth of investigation and resolution, both the size of the side lengths of the transmitter and the amount of current carried by the loop should be established. Usually, most TDEM systems are equipped with software that is used in the field during data acquisition. Within the software, inputs such as antenna loop size, gate time, current, power-line frequency (for example, 50 Hz for Europe and 60 Hz for the US), and source of noise in EM data can be changed in the field. Generally, longer gate times are needed to investigate greater depths.

Obtaining proper sounding intervals during data acquisition is important to ensure high-lateral resolution. For example, if an electrically conductive contaminant plume is to be investigated, several stations should be within the plume. The sounding interval near the suspected edge of the plume should also be adjusted for an accurate resolution of the conductivity gradient. As a rule, the higher the spatial sampling density, the higher the lateral resolution. As with other geophysical surveys, elements such as monitoring wells, property lines, and potential sources of cultural interference should be noted. The surface topography should also be collected to aid in data interpretation.

6.5.3.3 Quality Control

FDEM

Most FDEM instruments need to be calibrated prior to data collection, typically more than once per day, to avoid significant data drift that occurs during an extended data collection period. Instrument calibration should be documented using standardized forms and procedures.

Survey pattern and orientation can have an impact on interpolated data results. For example, collecting data perpendicular to a linear anomaly (such as a utility) is preferred, and collecting data in a transect pattern versus a meandering, nonlinear pattern is preferred. It is good practice to periodically download data and check for quality issues. Field conditions and notable features should be recorded during the survey.

Several different data interpolation methods can be used to process FDEM data. There is not a single appropriate interpolation method; multiple methods may need to be considered to determine which one is most appropriate. Quality control may include reviewing daily static test data to verify calibration results, data repeatability, and reliability. Spatial variation between GPS and coils should be considered. Electronic lag time is also corrected during data processing, as well as drift.

Quality control for processing inverted data from multifrequency FDEM instruments may include reviewing inversion misfits and the robustness of the inversion parameters and comparing inverted results with validation data.

TDEM

QA/QC checks are essential and should be performed before, during, and after data collection. Prior to the survey, the TDEM system should be calibrated to establish the absolute time shift and data level to facilitate precise modeling. Prior site information (for example, existing boreholes or other reference models) can be used to correct leveling and drift during calibration modeling. Making these corrections prior to the survey ensures accurate data when estimating depth and mapping near-surface features.

An inventory of infrastructure close to, around, and buried at the site should also be conducted prior to surveying. Infrastructure is the major source of noise in TDEM data and can adversely affect data quality. Planning TDEM profiles parallel to and within 100 m (328 ft) of potential noise sources should be avoided.

Field-data processing and visualization are essential to identifying buried sources of noise for removal during final data processing. After data collection, readings must be evaluated as part of the quality control process. Readings should be considered inaccurate (unless determined otherwise) when the midpoint between the transmitter and receiver coils is within four coil separations from a metal fence, pipeline, power line, or other source of cultural noise (NJDEP 2005).

6.5.4 Cost Issues

6.5.4.1 FDEM

The cost of an FDEM survey depends on the type of instrument and site conditions. A standard FDEM survey includes one (single instrument) or two (separate coils) field personnel. A single person using a single instrument that houses both coils can survey approximately 2–3 acres (with 5-ft or greater line spacing) in a day under good site conditions. A two-person crew using separate coils can survey approximately 3acres to 4acres per day under good site conditions. Productivity declines in the presence of more complex terrain. An FDEM survey is expected to cost $2,000–$3,000 per day for field data acquisition. The cost involved in data processing varies, but approximately one-half day of data processing time per day of field acquisition is a reasonable estimate.

6.5.4.2 TDEM

The cost of a TDEM survey depends on the survey type (airborne or ground-based survey). For airborne surveys, the daily cost depends primarily on the survey size (line-km covered), location of the survey area, and the time of year. This information is used to estimate the cost of mobilizing and demobilizing the system and crew, daily fixed cost of the crew on site, helicopter availability and rate, equipment requirements, fuel requirement, system endurance, survey duration, and the applicable standby rate. For example, a survey that is close [<25 km (<16 mi)] to a base of operations (for example, ease of access to roads, fuel, hotel, landing site) is far less expensive than one performed in a remote area. A survey involving >1,000 line-km (>621 line-mi) is much less expensive on a line-km rate basis than a small survey [<100 line-km (>62 line-mi)]. Late fall and winter survey periods are more unpredictable and therefore more expensive than spring-summer surveys, specifically regarding weather-related standby. The cost to conduct an airborne survey is expected to range from $16,000/day to $25,000/day. Beyond survey charges, data quality control, processing, reporting, and sometimes interpretation are included in the survey price. Please note, most companies conducting airborne TDEM surveys provide a quote on a per job basis rather than a daily basis.

Ground-based TDEM surveys are quoted on a daily basis. A daily cost includes personnel, geophysical equipment, GPS, vehicle, and data processing and typically ranges from $1,800/day–$5,000/day. Ground-based TDEM surveys range from small (for example, shallow targets such as pipes and UXO) up to large, deep targets such as ore bodies for the minerals industry. As a result, typical daily costs have a large range, primarily depending on loop size, number of operators, and terrain. For example, at the smallest scale, one person operates the TDEM system mounted on a wheeled cart; at a larger scale, several people are needed to move the large transmitting loop. Overall, the size of the survey, site conditions, site location, and time of year are the deciding factors affecting the total cost for ground-based and airborne TDEM.

6.5.5 What Are the Advantages?

6.5.5.1 FDEM

Advantages of using FDEM technology (versus galvanic resistivity surveys) include relatively fast and easy collection of EM field measurements, nonintrusive data collection that can be done on foot or from a vehicle at low speeds (**Figure 6-15**), and minimal data processing. In general, FDEM can provide high-quality lateral resolution when collecting continuous measurements; the resolution is determined by the spacing between the transmitter and receiver coils, as well as the spacing between the measurements (ASTM 2018).

6.5.5.2 TDEM

The main advantages of TDEM surveys when compared to alternative direct current methods are that they provide high lateral resolution, deeper depth of penetration, and denser data coverage. In addition, TDEM is noninvasive and capable of resolving three or more layers in the subsurface. Finally, airborne TDEM surveys can be performed quickly and can produce large amounts of data over a relatively short period of time.

6.5.6 What Are the Limitations?

Misuse of these tools usually occurs when they are used beyond their limitations or because the physical limitations and disadvantages of the method are not understood. Electromagnetic surveys can be highly susceptible to interference (noise) when conducted near metallic objects, fences, and power lines.

6.5.6.1 FDEM

Limitations to consider include:

- geologic and cultural interference (utilities, metal fences, power lines)
- depth of detection limits
- data resolution expectations (generally, greater depths will have lower resolution, and shallower depths will have higher resolution)
- inadequate survey set up or poor-quality data collection
- data processing and interpolation require specialized knowledge
- significant labor for some methods
- variations in data resolution between survey methods

6.5.6.2 TDEM

Limitations to consider include (Wightman et al. 2004; ASTM 2020a):

- Poor response in highly resistive (very low conductivity) materials, because it cannot measure low values of conductivity
- Unable to detect nonconductive materials (PVC, fiber optics, etc.)
- Assumes that the subsurface layers are horizontal within the study area
- Requires a sufficient resistivity contrast between the background conditions and the structure being mapped.
- Interference from natural and cultural conditions
- Natural conditions (lightning, clayey soils, etc.)
- Noise (radar transmitters, radios, power lines, wind turbines, etc.)
- Interference with metallic structures (pipes, fencing, buried trash, etc.)
- Equipment is more costly due to greater complexity.

6.6 Other Surface Geophysics Tools

There are several other surface geophysics tools used in the investigations related to resources, industrial, environmental, structural, and other problems. These are specific methods used for specific purposes and do not have a common widespread application across remediation projects. Some of these are discussed below in an abbreviated manner and will add value to typical practitioners. Caution is recommended, such as with all remediation site investigation tools, when employing these methods and how they are used in the decision-making process, especially for complex projects. Some of these methods are critical to refining remediation CSMs and making critical project decisions.

6.6.1 Gravity

Every point on the earth's surface experiences slightly different gravitational force or acceleration (Dobrin and Savit 1988; Telford et al. 1990), depending on the density and distribution of the subsurface materials. Denser rocks (such as basalt or unweathered bedrock) exert a slightly stronger gravitational pull, while lower-density materials (such as sediments, voids, or landfilled waste) exert a weaker pull. By precisely measuring tiny variations in gravity, geophysicists can infer changes in subsurface density. Gravimeters are used to measure these slight variations and are capable of detecting sensitive variations, as little as a one part per billion. Gravity anomalies (typically as millgals or as microgals) are measured after applying correcting factors for elevation, latitude, terrain, tides, and instrument drift. This helps us in the interpretation of subsurface geologic structures. Interpreting these signatures helps build models of subsurface geology, identify buried structures or voids, and understand features that influence groundwater flow and remediation planning.

Gravimetry has three broad applications:

- mapping of subsurface stratigraphy and structure
- detecting voids, buried structures, and waste materials
- supporting remediation system design and risk reduction

High-resolution gravity surveys include measuring extremely small variations in the earth's gravity field, known as microgravity. This tool is useful in specific projects that include mapping of voids and sink holes, monitoring subsurface structural changes such as subsidence, infrastructure assessments, and locating buried waste pits and low-density fill areas.

These methods supplement information gathered from other surface geophysics methods such as GPR and ERT and help further refine our understanding of the subsurface with minimal disturbances.

Case studies where these were used include:

1) Internal Characterization of a Sealed Landfill (Ilhavo Landfill, Portugal) (Mantlík et al. 2009).

   Gravity surveys were used to map internal density variations within a sealed landfill installed in low-density Quaternary sand formations. Two gravity profiles—one across the landfill and one regional—were collected to identify lateral density differences linked to waste type, age, and compaction. The gravity results were jointly interpreted with resistivity profiles to constrain landfill depth and delineate internal zones, enabling better assessment of environmental risks and guiding monitoring and remediation approaches.

2) Sinkhole and Void Detection in Karst Terrain (Kentucky Highway Sites, USA) (Crawford et al. 1999)

   Microgravity surveys were employed extensively in Kentucky to investigate sinkhole collapses affecting major highways. The method successfully identified bedrock caves, voids in overburden, and irregular depth to bedrock—all critical for understanding collapse mechanisms and planning mitigation. In multiple cases, microgravity data informed route changes, emergency repair strategies, and long-term stabilization, reducing the risk of future failures and improving environmental safety around transportation corridors.

3) Depth to Bedrock Based on Modeling of Gravity Data of the Eastern Part of Edwards Air Force Base, California (Langenheim et al. 2019)

   USGS described a gravity survey acquired to determine the thickness of basin-fill deposits (depth to bedrock) and to delineate geologic structures that might influence groundwater flow beneath the eastern part of Edwards Air Force Base, California. Inversion of these gravity data combined with geologic maps and well information provides an estimate of the thickness of basin-fill deposits (defined here as Cenozoic sedimentary and volcanic rocks). After removing the gravitational effect of the basin-fill deposits, the inversion also results in a gravity map that reflects variations in the bedrock density. The depth to bedrock is generally less than 1 km in the map area, except for localized depressions north and south of Kramer Hills, northwest-trending pockets about 4 km northeast of Rogers Lake, and a large depression southwest of Rogers Lake. In the area near Leuhman Ridge, depth to bedrock is shallow. The Spring and Leuhman faults do not coincide with large variations in basin-fill thickness or with prominent gravity gradients, suggestive of minor vertical displacement and minor horizontal displacement at their southeastern mapped extents where they project across a large gravity low.

6.6.2 Magnetotellurics

Magnetotellurics (MT) is an electromagnetic geophysical method that uses naturally occurring variations in the earth's magnetic and electric fields to infer subsurface electrical conductivity. These natural EM fields originate from lightning activity (high-frequency band) and magnetospheric and ionospheric interactions driven by solar activity (low-frequency band). The MT sensors measure orthogonal electric and magnetic fields at the surface. The frequency-dependent impedance tensor calculated from these fields reveals how EM waves penetrate and attenuate in the subsurface—behavior controlled by contrasts in electrical resistivity. Conductive zones (for example, clays, saline groundwater, geothermal fluids, contamination pathways) produce different responses than resistive materials (for example, bedrock, dry sediments).

Telford, Geldart, and Sheriff (1990) emphasized MT's ability to investigate subsurface resistivity from tens of meters to crustal and upper-mantle depths, making it especially useful where seismic or potential-field methods face limitations. They described MT field systems as using electrodes to measure horizontal electric fields and magnetometers to measure magnetic fields, with data subsequently transformed into frequency-domain impedances. These impedances are then interpreted using 1D, 2D, or 3D conductivity models, though Telford noted the strong role of nonuniqueness and the need to incorporate supplementary geologic and geophysical constraints.

Magnetotellurics encompasses several related submethods distinguished primarily by frequency range, source characteristics, depth of investigation, and survey objectives. These variants allow MT to image from tens of meters to hundreds of kilometers into the earth.

Different methods of magnetotellurics (various USGS publications) include:

- **Long-Period Magnetotellurics (LMT)** focuses on very low-frequency natural electromagnetic variations, typically with periods from thousands of seconds down to about 1 Hz, which enables imaging of the deep crust and upper mantle. These long-period signals originate primarily from magnetospheric and ionospheric current systems, allowing LMT to penetrate tens to hundreds of kilometers into the earth. Because of this depth sensitivity, LMT is best suited for broad regional tectonic studies and for understanding major deep-seated structures that influence crustal evolution. Its utility lies in capturing slow-varying EM fields that traverse thick lithospheric sections, though this dependence on weak natural fields means LMT is sensitive to noise and must be recorded for long durations to extract usable signals.
- **Audio-Frequency Magnetotellurics (AMT)** occupies the higher-frequency end of the MT spectrum, typically from about 1 Hz to 10,000 Hz, which enables it to resolve shallow subsurface structures at depths ranging from a few tens of meters to several kilometers. These high frequencies are generated primarily by global lightning activity, producing strong natural EM signals that allow AMT to generate detailed resistivity images of near-surface groundwater systems, engineering sites, geothermal zones, mineralized bodies, and environmental contamination pathways. AMT is therefore widely used in hydrological, environmental, and remediation studies because it offers high spatial resolution in the shallow stratigraphy, precisely the depth range where anthropogenic impacts and shallow geologic hazards occur.
- **Broadband MT (BBMT)** integrates the frequency coverage of both MT and AMT, combining long-, intermediate-, and high-frequency natural sources into a single resistivity dataset that spans from about 1,000-second periods to 10,000 Hz. This merger allows geophysicists to simultaneously image shallow, intermediate, and deeper structures without the need for separate surveys. BBMT is especially valuable in multilayered or structurally complex environments, where shallow heterogeneity affects deeper interpretations and vice versa. The combined frequency range enhances inversion stability across depth scales and mitigates gaps associated with natural "dead bands," resulting in more continuous and interpretable resistivity models for resource assessment, groundwater management, and integrated environmental investigations.
- **Controlled-Source Audio-Frequency Magnetotellurics (CSAMT)** modifies the traditional MT approach by using an active electromagnetic transmitter placed at a distant location to generate a stable, high-frequency signal that mimics natural AMT fields. This method is particularly advantageous in areas where cultural or industrial EM noise masks natural signals, such as in urban settings, mining districts, or near infrastructure. CSAMT offers improved signal-to-noise ratios, better control of transmitter geometry, and multiple survey configurations, such as scalar, vector, and tensor modes. These are optimized for different geologic targets. With frequencies typically ranging from 5 Hz to 10 kHz, CSAMT produces high-resolution resistivity images ideal for mapping shallow contamination, investigating engineered subsurface structures, and characterizing near-surface hydrogeologic systems under challenging noise environments.

- **Continuous Profiling MT (CPMT)** relies on low-frequency (<1 Hz) magnetospheric source fields, similar to LMT, but is implemented as a dense, continuous measurement approach to map long-wavelength resistivity variations across broad regions. By acquiring MT data in a profiling mode rather than at sparse stations, CPMT enables more coherent mapping of deep crustal structures, structural boundaries, and regional conductivity trends associated with tectonic blocks, deep fault corridors, sedimentary mega-basins, or lithospheric discontinuities. Its operational efficiency and large-area coverage make CPMT well suited for reconnaissance-level subsurface characterization, geothermal province delineation, and foundational geologic framework studies that support further detailed MT or AMT surveys.

Case studies where these were used include:

1) Geothermal Fluid Pathway Mapping at Ain Al-Harrah Hot Spring, Saudi Arabia (Ashadi et al. 2024)

   Researchers collected broadband MT data (0.001–60 s) at 15 stations to characterize the geothermal reservoir underlying the Ain Al-Harrah hot spring.

Key Outcomes

- Identified a conductive anomaly related to the geothermal heat source (>3.5 km depth)
- Mapped fractures acting as fluid-flow conduits
- Located resistive and mixed-resistivity zones representing bedrock units and fluid pathways
- This information helped evaluate environmental impacts, groundwater interactions, and sustainable geothermal development.

2) Groundwater System Characterization Using Natural and Controlled-Source Magnetotellurics

   In a study focused on groundwater contamination and hydrogeologic structure, MT was used to produce detailed resistivity images supporting environmental assessment.(Agyemang 2022)

Key Outcomes

- Demonstrated that resistivity imaging with MT can delineate groundwater flow paths, salinity variations, and structural controls that affect contaminant transport
- The method's high sensitivity to resistivity variation proved valuable for nonintrusive monitoring of groundwater quality.

3) Geothermal Resource Assessment and Environmental Planning in Hubei Province, China (Jianshi County) (Simeng et al. 2025)

   Researchers used 51 broadband MT stations to develop a 2D resistivity model to support geothermal exploration and environmental resource planning.

Key Outcomes

- Mapped fault systems that influence subsurface fluid flow
- Identified low-resistivity zones corresponding to geothermal reservoirs
- Helped define the sustainable resource boundary and understand interactions with groundwater
- Though focused on geothermal development, the study informs broader hydrogeologic management and contamination risk assessment.

7 REMOTE SENSING

7.1 Introduction

Remote sensing is the process of collecting data from a distance for the purpose of measuring, analyzing, or assessing broad regions of the earth's surface, and in some cases, shallow subsurface. In the development of a CSM, remote sensing data can be a useful tool in establishing project site baseline information, such as detailed topography, current imagery, thermal anomalies, vegetation health, and soil characteristics. These data types are collected via specialized sensors that are attached to mobile aerial platforms, such as satellites, manned aircraft, or unmanned aerial systems (UAS). Throughout this section, UAS will be referred to as drones, as these terms are often used interchangeably in the industry.

Remote sensing systems are rapidly developing, as are the available tools (sensors and sample collection devices). One potential barrier to employing these tools is uncertainty about the skills needed and the time required to collect the data. Skill levels can vary based on the remote platform, sensors used, and the size of the area to be investigated.

When considering remote sensing data for a project, three criteria must be weighed in choosing the most appropriate data type:

- What data are needed?
- Which sensor will fulfill that need?
- What platform is best suited to obtaining the data?

When determining data needs, remote sensing data should not be considered as limited to a coarse, low-resolution dataset used only to provide an initial baseline. High-resolution data can be obtained from data sensors via platforms such as drones that have the ability to fly close to ground level and can rapidly collect data not otherwise feasible or deemed as unsafe (for example, rocky slopes, inaccessible areas, remote water bodies). To determine how best to fill that need, Section 7.2 will define the data associated with the four most commonly used sensors and select less commonly used sensors and monitoring devices. These are:

- **Red green blue (RGB) cameras** – These are typical visible spectrum photographic cameras that are used to capture still photos, orthographic photos for large areas, and photogrammetry for 3D results.
- **Thermal**–Thermal sensors, or forward-looking infrared sensors, can detect temperature signatures.
- **Multispectral and hyperspectral–**These sensors can identify material signatures based on their electromagnetic wavelengths.
- **Light detection and ranging (LiDAR)–**These sensors capture high-resolution renderings of topography or objects using an active approach by emitting laser pulses.
- **Less common sensors and drone-specific devices–**Magnetometers, ground penetrating radar, gamma ray, bathymetric LiDAR, multimeters, and air and water samplers.

To determine the final parameter and what platform will achieve the most beneficial dataset, Section 7.3 will present the platforms and the sensors they support. This section will focus primarily on drones due to the improvements in drone technology and accessibility, which have allowed project managers to self-perform or contract private companies to capture remote sensing data. This allows real-time results at a scale more suited to a project's specific needs and often at a cost much less than manned aircraft flights.

Figure 7-1 provides a brief overview of project data needs coupled with what platforms work with specific sensor types.

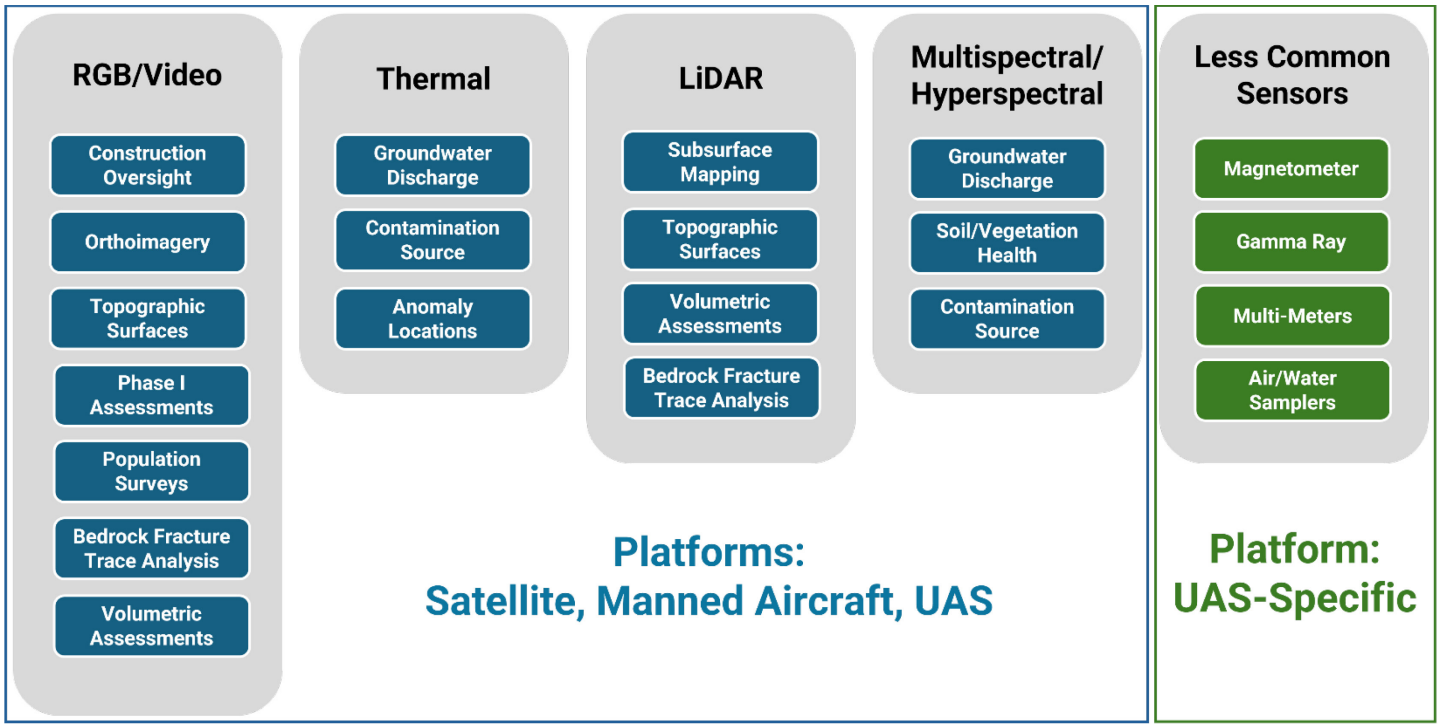


Figure 7-1. Overview of sensors with example project use cases.

Due to the increasing accessibility of drones and their ability to carry a variety of payloads, coupled with technological advancements in more conventional sensors, Section 7.4 will address some less common sensors and samplers that now can be carried by a drone to collect data or environmental media not otherwise possible using land-based methods.

7.1.1 Existing Remote sensing Data Availability

Due to the broad coverage of data collected via remote sensing sensors, there is a wide array of data types available via public and private agencies that can be downloaded free of charge from government websites or purchased from private entities. While a variety of data can be obtained from public or private sources, it should be noted that most data are limited in data type (sensor type), data resolution, and timeliness of the data. Data most frequently found via public sources would be light detection and ranging data (LiDAR), high-resolution orthomosaic imagery, multispectral data, or normalized difference vegetation index data (NDVI). However, this data may or may not meet specific time period or resolution requirements for the project. Some data types that would be difficult to find via public or private sources would be magnetometer data, gamma ray data, or orthomosaic imagery or LiDAR of remote areas. Therefore, contracting with a private company to fly a manned aircraft or a drone, or self-performing a drone flight of the project site, may be necessary.

A wide variety of satellite imagery data are available online. For example, NASA, NOAA, and USGS provide satellite data. It should be noted that although satellite data may have a lower resolution than drone-based data or manned aircraft, this is not always the case. Many satellites use a data capture method known as synthetic aperture radar (SAR). This active data collection method works by sending out a pulse of energy and then records the reflection from earth to provide a more detailed assessment of the substrate (for example, mountains, urban areas, sea ice). The sending of a pulse allows SAR to capture

terrestrial data even when there is cloud cover and provides a higher resolution dataset. Uses include urban monitoring, global mapping, change detection, monitoring of areas with low to moderate penetration, agricultural monitoring vegetation density, biomass and vegetation mapping. (source: https://www.earthdata.nasa.gov/learn/earth-observation-data-basics/sar)

Similarly, airborne LiDAR data are available from the US Interagency Elevation Inventory (NOAA 2019) state GIS Data repositories or even some local municipalities. **Appendix B. Remote Sensing Data Sources** provides an abbreviated listing of publicly available remote sensing data sources and includes the host agency, sensor, platform, brief description of its application, coverage, and data resolution details. It should be noted that these sources may become out-of-date based on changes to the public and/or private hosted sites and new sources are continuously becoming available.

Available data must be examined prior to collecting data to potentially narrow and focus additional data collection. When using satellite imagery data, note the timeframe of the imagery and how it corresponds to the timeframe of the proposed project. Although imagery data may be available, image processing may be required. Prior to purchasing imagery data, available data should be researched; many states have no-cost LiDAR data available. When weighing the option of employing available remote sensing data versus collecting drone data, it is crucial to know the needed temporal resolution, spatial resolution, and spectral resolutions required for the specific project.

7.2 Sensors

The sensors that capture data from the surface (or subsurface) areas of the earth can be divided into two categories: passive and active. Passive sensors include RGB (red, green, blue) or visible spectrum cameras, multispectral and hyperspectral cameras, and thermal cameras. They rely on natural energy emitted by a surface, which the sensor will detect and record. This energy is typically in the form of electromagnetic radiation, and the data are interpreted based on wavelength ranges detected by the sensor. Visible light sensors (RGB cameras) represent the approximate midrange of EMS wavelengths whereas gamma ray sensors detect short waves, infrared light (thermal cameras) detect longer waves, and multispectral and hyperspectral cameras detect a wide variety of wavelengths (350–2500 nanometers [nm]) in which the bands are isolated to produce material signatures (**Figure 7-2**).

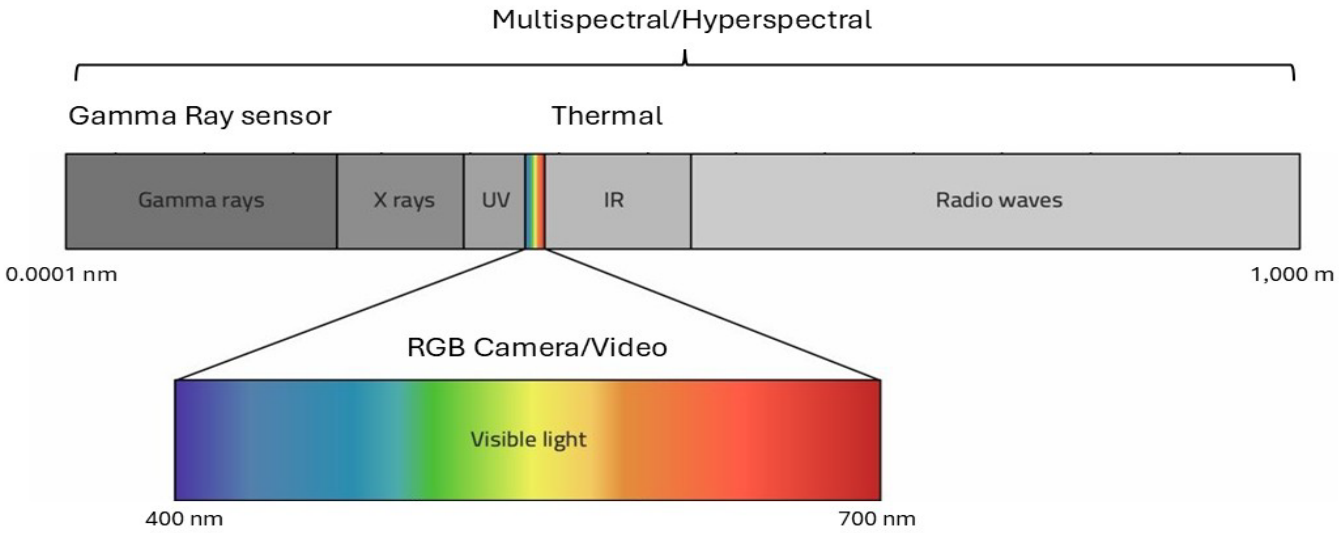


Figure 7-2. Electromagnetic spectrum.

Source: Courtesy of Mark Dhruv EA Engineering

Active sensors emit radiation in the form of laser pulses which, when directed at the earth's surface, receive a reflected pulse detected and measured by the sensor. In this section we will focus on LiDAR sensors as the most widely used active sensors. We will discuss the following three factors that should be considered when deciding on the best path forward in obtaining and analyzing remote sensing data for the project:

- Sensor type–The sensor type that will provide the data needed to support site characterization with examples of how the sensor can be used to enhance the site characterization to provide a basis of understanding which sensor to choose for a particular application.
- Data access–Options for obtaining the data from a selected sensor type (accessing publicly available resources, purchase options, self-performing)
- Data storage–Computer hardware requirements for housing the remote sensing data analysis and presentation software data processing software considerations if self-performing data collection and presenting results.

7.2.1 RGB camera

7.2.1.1 What Is the Technology?

RGB (red, green, blue) or visible spectrum cameras are the most commonly used sensors. While typically used for still images or videos, the advantage of RGB cameras on mobile platforms is their ability to collect high-resolution series of images, which are geometrically corrected to provide spatially accurate orthomosaic imagery of areas larger than what can be captured in a single photo (Section 7.2.3.2). Additionally, these images can be taken at precise angles with degrees of overlap to create 3D renderings of a structure or horizontally and vertically accurate topography to determine elevations or distances, a process known as photogrammetry (Section 7.2.3.3).

The cameras can range in size to accommodate the platform on which they will be used, and while satellites and manned aircraft have a much heavier payload and thus can carry higher resolution cameras, drones have proven to be able to carry a comparable product, albeit smaller in scale. Regardless of size, all modern cameras have the capabilities to capture high-resolution images. Specific data goals can help determine which camera is best suited for a particular need.

7.2.1.2 Sensor Size

The purpose of the camera's sensor is to capture light and convert it into an electronic signal, which is then processed to form a digital image. The larger the sensor, the greater the ability to capture more light and detail, leading to a high-resolution image quality, even at high altitudes. These large sensors also allow for a greater field of view, enabling each photo to capture a larger area without a loss of resolution. To accommodate the larger sensors and associated components (lens and filters), the camera housing is more suitable for manned aircraft and satellite platforms. Drone camera sensors, while much smaller in size, also can capture high-resolution images; however, due to the smaller size of the sensor and components, the field of view is limited.

7.2.1.3 Pixel Size and Density

Resolution and clarity are functions of the number of pixels. A high pixel count can result in a high-resolution image, but the size of the pixels must also be considered in relation to the size of the camera's sensor. So, a high pixel count can be tempered by a small lens or sensor. It is important to not simply rely on the number of pixels as a representation of image quality.

7.2.1.4 RGB Camera Data Types

Orthoimagery

With advancements in video technology, aerial video is becoming more popular. Oblique videos are commonly shot from drones to assist in site characterization. The unique perspective of aerial videography and photography allows for an unprecedented level of understanding at a variety of sites (large and small). In addition, using geospatial data embedded in information collected by the drone, video may be embedded with metadata and later synced with a video mapping program. Similarly, photos and videos may be georeferenced or attached to geotagged photo locations to provide assistance in site characterization. These basic methods are relatively inexpensive and use widely available software.

Beyond photo and video, the next most common application of drones is the collection of visible spectrum data as a collection of overlapping datasets. Software that can extract three-dimensional information from two-dimensional image data has transformed drones into powerful mapping and surveying tools.

The drone camera is the tool most often used in site characterization due to its low cost, high availability, and simplicity of the self-explanatory nature of a picture. Additionally, the operational requirements and technical knowledge required to use a camera are low relative to other sensors. Off-the-shelf camera drones can be purchased for as little as $1,000. Detailed technical information about these cameras is provided in Section 7.2.2 and Section 7.2.3. The abbreviated technical information available in **Appendix B** for common sensors provides remote sensing data sources providing categories, programs, agencies, sensor type, platform, and applications.

Photos and video can be used for inspection, documentation, change detection, and many other purposes. Low-altitude photos and videos can yield valuable information about a site that is not apparent from ground observations.

Drones flying less than 400 ft above the ground allow ground sampling distances of inches or less versus feet for conventional visible spectrum aircraft photography. Drones often use wide-angle lenses, which are less prone to distortion due to vibration than longer lenses. Using a gimbal to stabilize a wide-angle lens can yield focused images in a variety of lighting conditions. In many areas of the country, atmospheric haze is a common problem when obtaining aerial photographs. Drone sensors benefit from less atmosphere between the subject and sensor and, thus, less distortion from atmospheric interference or weakening of specific EM bands.

Furthermore, in most cases, uncorrected photographs are of less use than the post processed outputs. The most recognized post process image is the orthomosaic, which is geometrically corrected to remove distortion caused by topographic relief, lens distortions, and camera position. The orthomosaic can be used to measure true distances because it is an accurate representation of the earth's surface. Organizations should consider the need for and methods to archive not only the uncorrected photos but the processed products.

3D Photogrammetry

Software employing techniques such as georeferenced orthomosaic images, point clouds, triangulated irregular network (TIN) meshes, digital elevation models (DEM), and digital terrain models (DTM) can extract 3D information from 2D images. Images with a high level of overlap taken from various positions, even without spatial orientation, can thus be used to generate 3D models.

A typical workflow involves programming the drone to fly a series of flight lines back and forth over the subject, capturing images with overlap front to back and side to side. Overlap requirements vary

depending on the site and mapping objectives, but, as a rule of thumb, at least 60% overlap is needed to reconstruct terrain maps with a high degree of accuracy. Subjects with vertical facades or geologic features not visible in straight down (nadir) images can be reconstructed from photos taken at an angle that capture the facade. If a single structure is being captured, a series of circular orbits around the structure at two or more different altitudes is often combined with nadir images. Most drone flight-planning software automatically calculates the flight lines, image intervals, and camera gimbal positions from a polygon or point of interest to support such image development.

These techniques work best for subjects with adequate contrast and stationary features. Water or featureless surfaces such as sand cannot be modeled because they lack sufficient contrast to match pictures. Movement creates distortion because the sensor reads out the image one line at a time rather than all at once. These rolling shutter or electronic shutter sensors can introduce distortion as the camera-subject relationship changes during a single photo. Using fast mechanical shutters and gimbals help to compensate for the lack of adequate contrast and movement.

Drones have brought aerial mapping within reach due to the ability to scale costs and requirements to a site-specific nature.

7.2.1.5 Project Examples

Orthoimagery

Orthoimagery is a foundation data type in remote sensing. It applies to almost every project. It is used to develop basemap imagery, where features can be identified, distances measured, or images compared for temporal changes. The advantage of using orthorectified imagery is that it is spatially accurate (note that accuracy is dependent on the resolution and the rectifying based on ground control markers used to orient the orthoimage). The images can therefore provide spatially relevant information, such as distances and coordinates, not otherwise available from single aerial images or oblique photographs.

Photogrammetry

Similar to orthoimagery, photogrammetry-rendered images provide horizontal spatial accuracy as well as spatial accuracy in the vertical dimension. This element allows for viewing site topographic relief in 3D viewers to assess site safety concerns or calculating soil pile volumes, for example. While similar to LiDAR in respect to vertical capabilities, photogrammetry captures only what the camera “sees” and is not able to penetrate tree canopies to the extent that LiDAR data does—an important factor when considering the use of the more economical photogrammetry over the more expensive, density-rich LiDAR data.

7.2.2 Multispectral and Hyperspectral Cameras

7.2.2.1 What Is the Technology?

Multispectral and hyperspectral imaging technologies provide detailed insights into the earth’s surface and atmosphere by capturing reflected light at multiple wavelengths. The core principle is that every material on earth’s surface—whether it is vegetation, water, soil, or human-made—has a unique spectral signature. This signature is a distinctive pattern of absorption and reflection across the electromagnetic spectrum, functioning much like a fingerprint for identification. By analyzing these detailed spectral signatures, these technologies enable the identification and characterization of materials that might appear identical to the human eye or a standard camera.

Multispectral

Multispectral and hyperspectral cameras are differentiated by spectral resolution, which is a combination of bandwidth specificity and band number. Multispectral cameras typically collect data on several discrete and wide spectral bands (often between 3 to 10) (**Figure 7-3**). The bandwidth is typically on the order of ~100 nm. These bands are typically without severe atmospheric interference and designed to focus on particular parts of the electromagnetic spectrum, such as visible (400–700 nm), near-infrared (near-infrared reflectance (NIR), 700–1300 nm), or shortwave infrared (SWIR, 1300–2500 nm). It is commonly used for classification of different materials (for example, plant vs. nonplant).

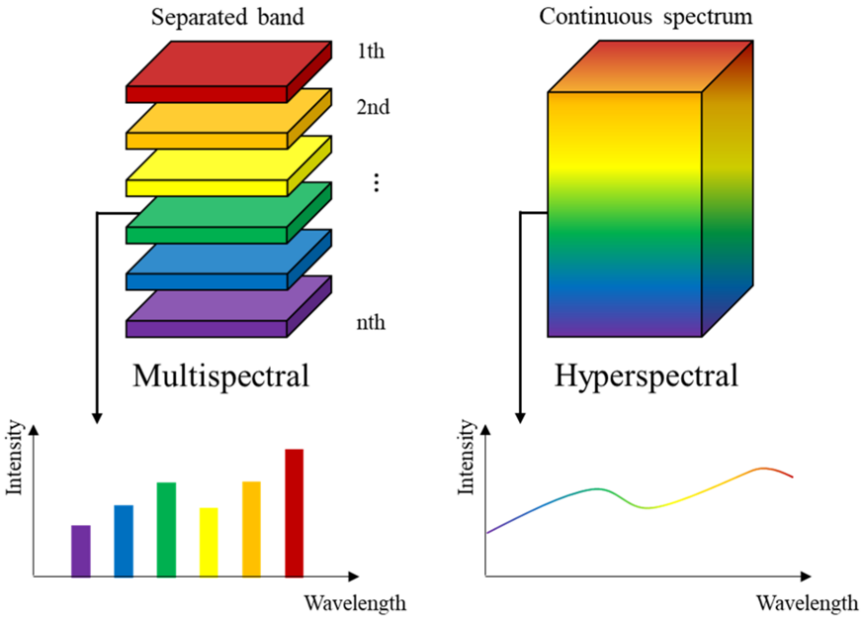


Figure 7-3. Multispectral data vs. hyperspectral data.

Source: Jung et al. (2024).

Hyperspectral

Hyperspectral cameras collect data on tens to hundreds of contiguous and narrow spectral bands, allowing for greater characterization of the area or items imaged (**Figure 7-3**). The wavelengths typically range from around 350 nm to around 2500 nm, with a bandwidth on the order of 1–10 nm. These cameras allow for the identification of materials (for example, plant species), detection of subtle differences in material composition, and determination of abundance or quantity of materials, as well as physical and biochemical properties not discerned by multispectral analysis (for example, mineral and surface chemical composition) (Hennessy et al. 2020).

7.2.2.2 How Is the Technology Used?

Multispectral and hyperspectral imaging technologies are used to characterize materials by measuring how surfaces reflect electromagnetic radiation across specific wavelength bands. Because each material has a distinct spectral response pattern, these sensors can be used to identify land use and land cover types (for example water, wetland, desert, forest, crop, urban) and vegetation types (for example, grasses, shrubs, trees); to detect plant stress; to distinguish minerals and soil types (for example, clays, sand, carbonates, sulfates); to map built surfaces (for example, asphalt, concrete, roofing materials); to identify debris (for example, drums, containers, waste metal, plastics); to support environmental management (for example, oil spill, forest fire); and to estimate biophysical and biochemical variables (for example, leaf area index, leaf water content, leaf chlorophyll, and leaf nitrogen content). These techniques have also been used to support contaminated land remediation (for example, presence of hydrocarbon and heavy metals) (Slonecker et al. 2010; Choe et al. 2008). These technologies can be applied to both terrestrial and aquatic systems.

Generally, multispectral sensors are suited for mapping applications where a coarser ground spatial resolution and broad spectral patterns are sufficient, such as general land cover classification, biomass

estimation, or identifying major vegetation changes. Spaceborne multispectral systems also provide long and consistent temporal datasets, making them particularly useful for tracing changes over time.

In contrast, hyperspectral sensors enable the detection of subtle spectral features that multispectral systems cannot resolve (**Figure 7-4**). Such fine spectral resolution supports applications such as distinguishing closely related plant species; differentiating between healthy and diseased plants; detecting changes in leaf biochemistry; identifying mineralogical and soil composition differences; and quantifying or mapping chemical constituents (for example, chlorophyll, colored dissolved organic matter, oil, suspended sediment).

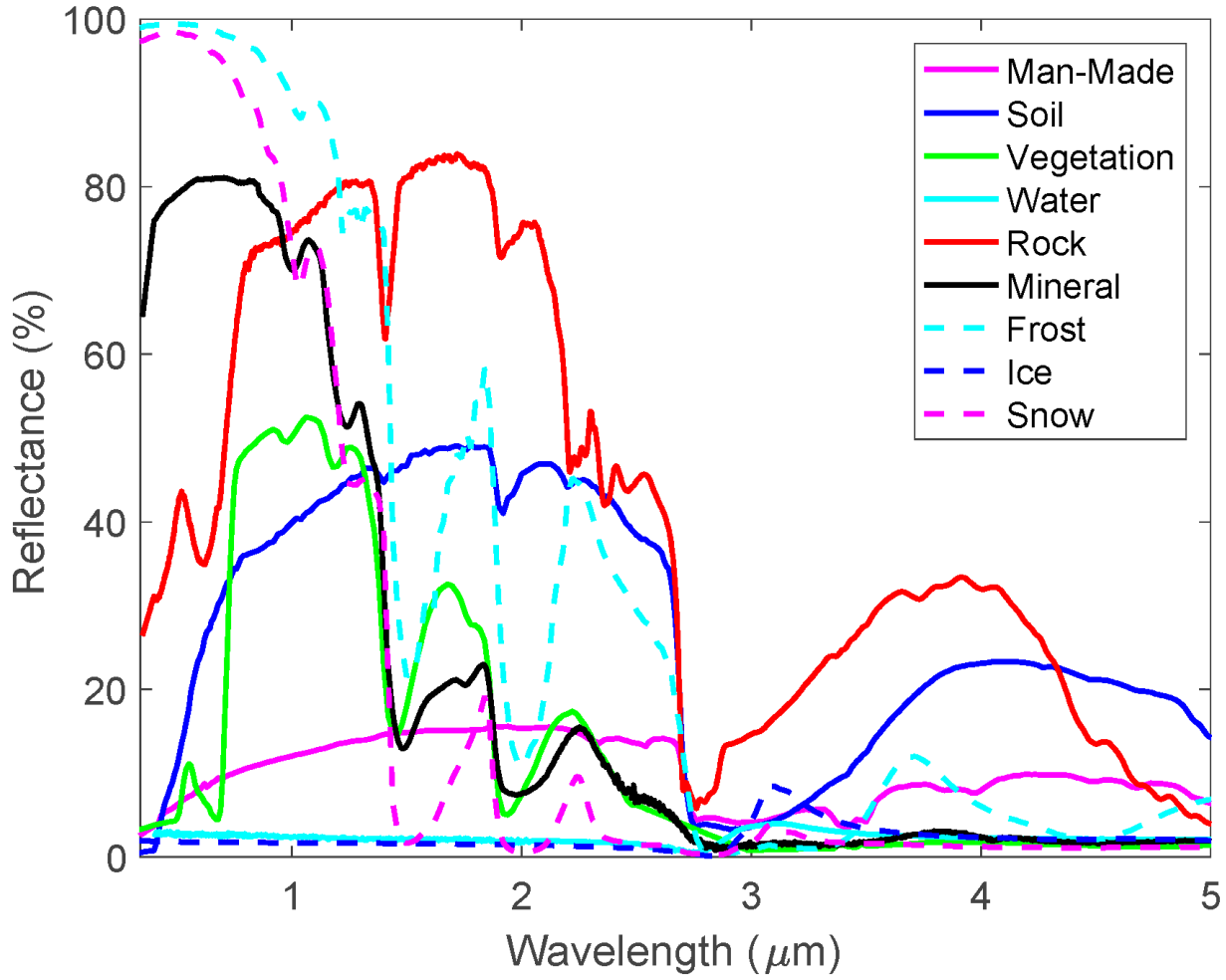


Figure 7-4. The typical reflective spectra for various land surface materials from the ASTER Spectral Library.

Source: Yanq, Liu, and Wu (2020).

Data Evaluation

A multispectral or hyperspectral imaging system produces a 3D dataset, with two spatial dimensions with one spectral dimension. Thus, every pixel contains a reflectance spectrum.

Analysis of multispectral and hyperspectral imagery can follow several pathways depending on the objectives. Image classification is one of the most widely used methods, but spectral data can also be evaluated using specialized spectral indices, spectral mixture analysis for estimating fractional abundances in mixed pixels, and quantitative retrieval models linking reflectance to biophysical or biochemical properties (for example, chlorophyll, colored dissolved organic matter, suspended sediment).

Image classification groups image pixels into a specific material or land cover category using supervised or unsupervised approaches. Supervised classification relies on user-defined training data. Pixel spectra are compared to known reference spectra collected from field measurements or publicly available spectral libraries. Unsupervised classification groups pixels into spectrally similar clusters without prior knowledge of class labels. Analysts then assign class names after examining cluster spectra.

There are two major groups of classification methods:

- Pixel-based (spectral) classifiers–rely solely on the spectral signature of each individual pixel. The pixel is treated as an independent observation, and classification depends on how closely its spectrum matches either known training spectra (in supervised classification) or spectral clusters identified by the algorithm (in unsupervised classification). This approach works best when pixel size is large relative to feature size or when spectral contrast among classes is strong. However, it struggles in heterogeneous landscapes where mixed pixels are common, and it ignores spatial context such as shape, texture, or neighborhood patterns. This method is useful for determining what things are made of, such as stressed plants, minerals, and moisture, but weak on shapes and individual features.
- Object-based classifiers–incorporate both spectral and spatial patterns for classification. Object classification is the process of identifying specific materials by matching their spectral signatures to a known reference pattern. This breaks the image into discrete identified objects—for example, “trees.” (2) classification of those objects. This method is particularly useful in applications where individual features (for example, trees, buildings, patches of vegetation) span multiple pixels.

Classification can be done through a variety of algorithms, such as adaptive coherence estimator, maximum likelihood, artificial neural network, support vector machine, and spectral angular mapper. The accuracy of each classifier should be evaluated. This requires use of a standard spectral library, which should include reflectance profiles for all material types expected at the site (for example, vegetation, soils, human-made materials). These libraries may come from public resources (for example, ENVI, ASTER, ECOSTRESS, USGS, university repositories) or be collected using on-site field spectroradiometer measurements. The accuracy assessment also requires the collection of ground truth data from various locations representing different material types within the site. Ground truth data should document the type of material, material coverage, and corresponding spectral reflectance profile at each location. A subset of ground truth data is used to train the algorithm (in supervised classification), while the remainder is used for validation. The accuracy is often evaluated by constructing an error (confusion) matrix, which compares the classification results against the ground-truth data. From this matrix, analysts compute key measures such as overall accuracy, and producer’s and user’s accuracy. Additional measures such as the kappa coefficient help quantify agreement beyond chance and allow statistical comparison among classification methods or spectral data obtained from different events.

When a single pixel contains multiple materials (for example, a pixel covering both soil and vegetation), it might be needed to analyze the contribution from different materials. Spectral mixing algorithms (for example, linear mixture models and artificial neural networks) can identify the pure spectral “endmembers” within a mixed pixel and estimate the fractional abundance of each material.

Besides using the spectra profile for analysis, many applications rely on specialized spectral indices that are calculated from a few specific narrow spectral bands. Spectral indices can be used for detection and

classification or to assess particular biophysical characteristics. One group of such indices is called (Yan et al. 2025)*vegetation indices* . For instance, vegetation indices based on reflectance at 705 nm and 750 nm have been used to estimate chlorophyll quantity (Wu et al. 2008). The water column corrected NDVI, defined as (NIR-Red)/(NIR+Red), was found to correlate with the percent cover of submerged vegetation in low turbidity water (up to 25 NTU) (Liew and Chang 2012).

Software for spectral data processing examples includes Google Earth Engine, Environment for Visualizing Images (ENVI), ERDAS IMAGINE, TerrSet liberaGIS, MATLAB Hyperspectral Image Processing Toolbox, MultiSpec, and Datum Workstation.

7.2.2.3 What Are the Advantages?

- Multispectral: Cost-effective, simpler to process, useful for broad monitoring, fairly high temporal resolution (days to weeks), greater accessibility due to the larger number of space-based multispectral sensors
- Hyperspectral: High precision enables detection of subtle material and biochemical variations that cannot be differentiated by multispectral cameras. The continuous spectrum allows for the creation of tailored spectral indices for specific applications

7.2.2.4 What Are the Limitations?

- Multispectral: Limited spectral resolution; cannot distinguish subtle spectral differences
- Hyperspectral: more expensive and often limited in spatial coverage; generates very large data volumes and require significant storage, processing and calibration efforts; low signal-to-noise ratio due to the narrow bandwidths, very sensitive to noise. The quality of hyperspectral data can be affected by site or acquisition conditions such as weather, illumination (for example, shadows), and atmospheric scattering.

7.2.2.5 Project Example

Vegetation

In terrestrial vegetation applications, vegetation appears green because chlorophyll absorbs red light (630–680 nm) and blue (450–520 nm) wavelengths and reflects green (520–600 nm); changes in this reflectance pattern can indicate stress or disease. Reflectance at these three wavelengths is employed as a measure of active plant chlorophyll. A sick plant reflects more red and blue relative to green due to reduced photosynthesis. When vegetation is dense, a near-infrared band, a.k.a. “red edge” (680 –730 nm) is often used to help with characterization. The cellular structure of vegetation causes NIR light to be reflected; this reflectance varies with plant cycle, season, climate, habitat, and other parameters (Adão et al. 2017). Stress and dead leaves significantly reduce NIR reflectance. Therefore, the ratios of the NIR reflectance to red reflectance can be used to indicate plant biomass, general health, and hydration status.

These technologies extend beyond terrestrial settings to aquatic environments. Because both water and water column constituents confound the signal from aquatic targets, multispectral and hyperspectral methods perform best in shallow waters of clear to moderate water type. The usable spectral region was limited to wavelengths less than 950 nm due to the strong absorption of radiation by water in the NIR. Based on the Worldview-2 satellite multispectral sensor (8 bands), (Liew and Chang 2012) found that at low turbidity level (0.5 NTU), the typical NIR peak (near 720 nm) in the vegetation spectra is preserved up to a depth of about 0.5 m, and is not visible for depth more than 1 m. While multispectral can be used to delineate the area of submerged vegetation, hyperspectral cameras can characterize chlorophyll, colored dissolved organic matter, and suspended sediment in suitable optical conditions. For example, hyperspectral camera imagery is being used to monitor cyanobacteria blooms in fresh water. The camera

can differentiate the reflected wavelength differences between chlorophyll a, contained by particular cyanobacteria, and chlorophyll b, typical of plants and green algae (Randolph et al. 2008).

7.2.3 Thermal Camera

7.2.3.1 What Is the Technology?

Thermal cameras work by detecting infrared (IR) radiation, or heat, emitted by a surface to produce an image that depicts the variation in temperatures. The lens of a thermal camera detects the energy in the form of an electromagnetic wavelength greater than 730 nm and focuses that energy onto a microbolometer sensor that converts the energy into electronic signals (Figure 7-5). An onboard processer translates these signals into a visual image, often displayed in a color palette to show temperature differences, allowing the drone to "see" heat signatures and temperature variations invisible to the human eye. Thermal sensors can vary in size depending on the platform it is used with and the resolution of the resulting image; however, the basic function of the camera is the same and thus suitable for drones, manned aircraft, or even satellites (Figure 7-5).



Figure 7-5. Example of a drone-based thermal camera.

Source: Ed Winner, PhD., Remediation Products, Inc.

Factors to consider when choosing a thermal camera for a drone are listed below. These specifications are dependent on one another. For example, larger fields of view (FOV) require higher image resolution to achieve the same result as a smaller FOV.

- FOV: Measurement of the area captured by the thermal lens
- Spectral band: Measurement of the infrared sensor's electromagnetic range
- Thermal sensitivity: The degree to which a sensor can measure the differences in relative temperature
- Image resolution: The level of detail based on the number of thermal pixels in the image. This should not be confused with an RGB camera whose image resolution is greater due to the shorter wavelengths in the visible light spectrum. Infrared data captured by a thermal camera result in lower resolution due to the longer wavelengths of infrared light.

A typical thermal sensor designed to be attached to a multirotor medium-lift drone (see Section 7.3 for information on drone types) has an FOV of 45°, a spectral band of 8 µm–14 µm, a thermal sensitivity of <50 milli-kelvins, and a thermal image resolution of 640 x 512.

It should be noted that thermal cameras use infrared emissions to convert into images, whereas infrared sensors do not have thermal imaging functionality. So infrared sensors should not be confused with thermal imaging cameras.

Processing thermal data is often conducted by someone trained in thermography; however, existing software has made the analysis of raw thermal data accessible to nontrained thermographers through the use of analysis software such as ArcGIS or proprietary thermal analysis software tools. Thermal data consists of 2D thermal images, resulting in an output such as a "heat map." The thermal images from the sensor can be draped onto point cloud data from a LiDAR, typically, to create 3D models of the thermal image.

7.2.3.2 What Are the Advantages?

Thermal data can help characterize a site by detecting changes in temperature from the surrounding environment that would not otherwise be seen by eyesight or an RGB camera.

7.2.3.3 What Are the Limitations?

While thermal cameras can detect the temperature of most surfaces, there are factors that may affect the results; highly polished or reflective surfaces (surfaces with low emissivity) do not absorb heat as well as nonreflective surfaces.

7.2.3.4 Project Examples

Thermal sensors can be used to detect variances in temperature on surfaces or to identify temperature anomalies from the surrounding environment. Examples include:

- Heat loss from infrastructure such as buildings, pipelines, containers, or cold spot identification in the case of solar panel assessments
- Temperature anomaly detection for identifying lifeforms or vegetation stress, seeps from landfills, or groundwater upwelling in streams or rivers.

7.2.4 LiDAR

7.2.4.1 What Is the Technology?

LiDAR sensors are active sensors that emit a series of laser pulses that reflect off surfaces to measure distances. These pulses are then translated into elevation or heights based on the position of the laser in relation to the object being measured (for example, ground surface or buildings). Practical applications include creating topological bare earth DEMs, generating highly accurate terrain mapping, performing infrastructure inspections, and creating a dynamic, virtual model that integrates live data to mirror the physical status of the terrain, creating a true-to-life digital replica referred to as digital twins.

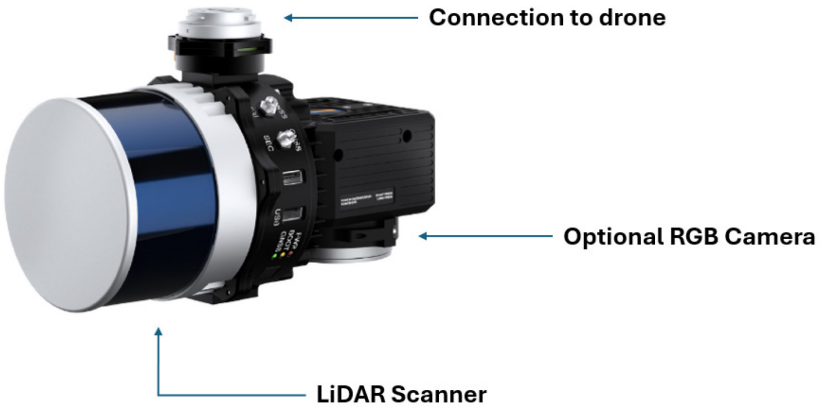


Figure 7-6. Example of a LiDAR sensor.

Source: Inertial Labs- Resepi XT-3. Used with permission.

Due to the density of frequency of the pulses and the accuracy of the reflected returns, LiDAR data can be measured with centimeter accuracy in both the vertical and

horizontal planes. LiDAR uses near-infrared light (around 1,000 nm) to image objects. Laser pulses are used to measure distances; lower cost LiDAR systems typically emit about 4,000 pulses per second, while advanced systems can emit hundreds of thousands or even millions of pulses per second.

A LiDAR sensor requires three components: the LiDAR scanner (**Figure 7-6**) that produces the laser pulses; the Global Navigation Satellite System (GNSS) GPS, which relays spatial positioning; and the inertial measurement unit (IMU), which tracks the drone's orientation, movement, acceleration, and angular velocity. These three components are computed to produce the highly accurate point cloud data.

When the laser light strikes an object, it is reflected back to a sensor, which records the time between the emission and the reflection of the laser pulse. This time is converted into a distance, and these measured distances are combined point-by-point to produce a 3D image called a point cloud. Each point in the cloud is assigned a classification such as ground, water, vegetation, human-made objects, etc., based on the laser pulse return. Lidar sensors configured for multiple returns can better develop bare earth surfaces by filtering out reflective data from trees or other objects that do not represent the ground surface. The last return reaches the forest floor which would be retained for developing a bare earth DEM. The waveform graph indicates the attenuation of laser energy as it propagates through the canopy (Salas 2021). **Figure 7-7** shows how a LiDAR sensor can penetrate the tree canopy. Classified point clouds can be easily manipulated, allowing undesired features to be filtered out. Initially, point clouds generated by LiDAR do not include color information; however, some manufacturers merge color image data from a camera to colorize the point cloud.

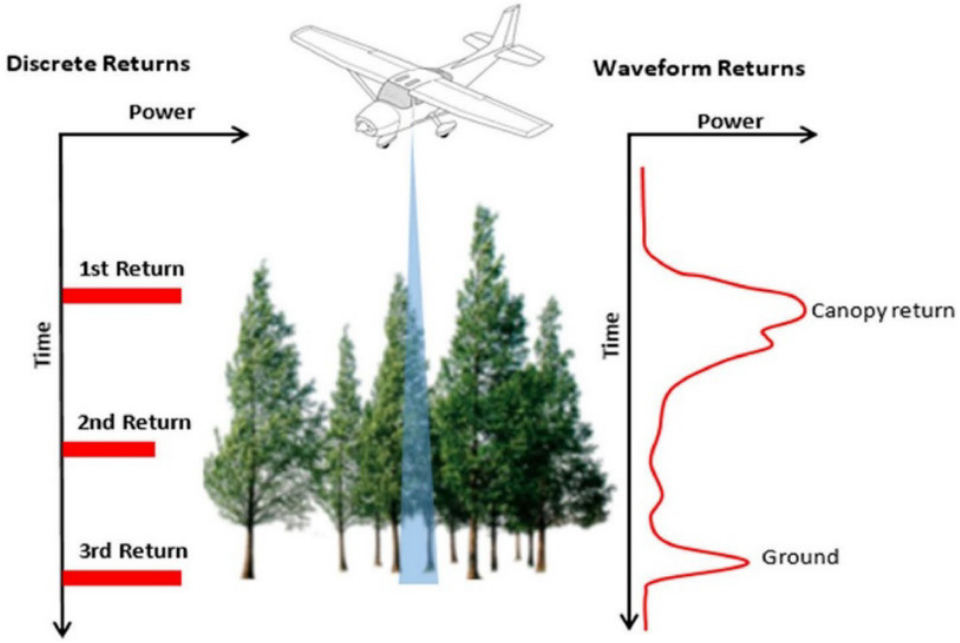


Figure 7-7. LiDAR pulse with different returns.

Source: Salas (2021)

7.2.4.2 What Are the Advantages?

Aerial drone LiDAR technology offers numerous advantages, making it increasingly popular in engineering, architecture, and environmental studies. It provides high-resolution, detailed data for accurate 3D maps and allows for swift coverage of large areas, reducing survey time compared to ground-based methods. Precise elevations can be captured using spatial positioning of the platform making LiDAR outputs for highly accurate planning purposes. Additionally, LiDAR point cloud data are capable of providing bare earth terrain models that can be useful in detecting topographic features hidden beneath vegetation cover.

7.2.4.3 What Are the Limitations?

Aerial drone LiDAR has several limitations. Initial costs for LiDAR systems, software, and training are

significant. In many cases, 3D photogrammetry may suffice if centimeter precision and bare earth DEMs are not required for project needs. LiDAR data also require substantial processing power and skilled personnel for point cloud classification and interpretation.

7.2.4.4 Project Examples

Topographical Survey–Due to its level of precision, LiDAR is often used as an alternative to traditional topographic surveys. In addition to its wide-area coverage, it has been used on project sites to monitor construction progress. For example, for wetland rehabilitation projects, a before and after survey using a drone or manned aircraft-mounted LiDAR can provide precise depth data for thin-layer sediment applications.

Landfill Site Volumetrics–3D mapping of a landfill can provide baseline volume information from which capacity assessments can be determined for planning purposes.

Digital Twin Development–A digital twin is a precise 3D replica of a physical asset or area generated using LiDAR sensor data. Capturing high-resolution point clouds enable simulation, monitoring, and predictive analytics for real-world objects in industries such as construction, urban planning, and manufacturing. While the development of a digital twin using LiDAR can be ground based or aerial based, the use of a drone to capture the asset greatly increases the efficiency of the data capture and increases access to all facets of the asset.

7.2.5 Less Common Sensors

7.2.5.1 Ground Penetrating Radar (GPR)

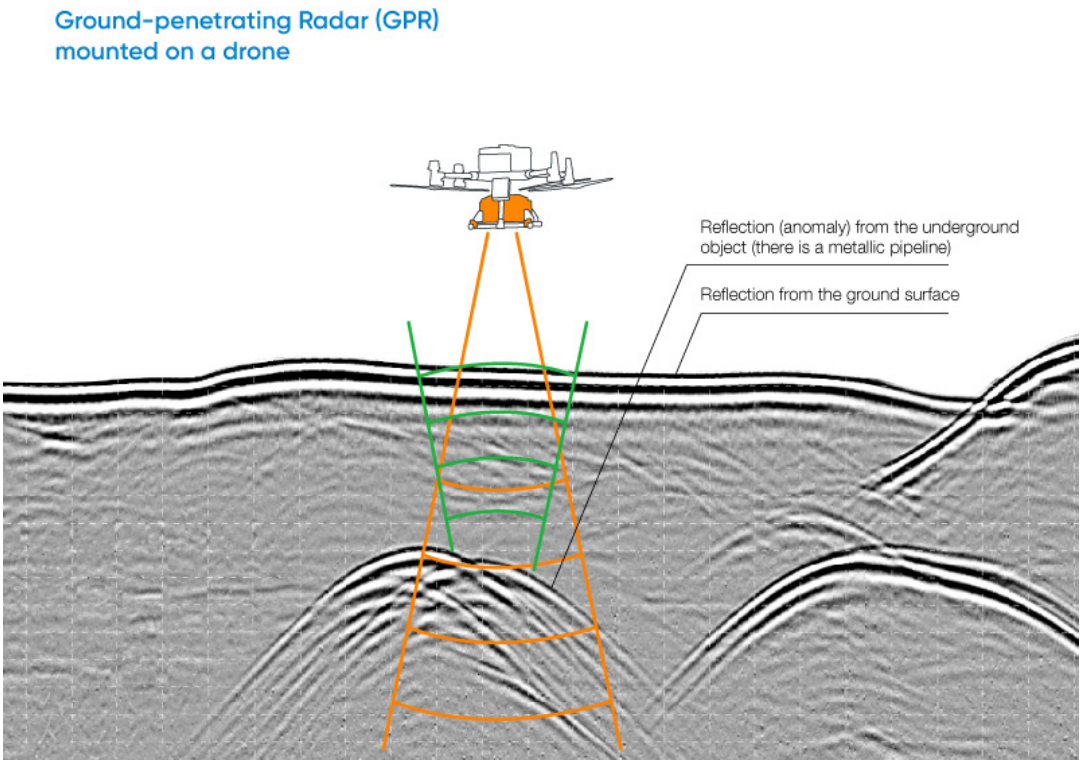


Figure 7-8. Schematic of drone-based GPR.

Source: SPH Engineering. Used with permission.

The drone-based (GPR) system operates by flying low and steadily over the survey area, maintaining a constant antenna height above the ground to ensure consistent subsurface penetration and high data quality (**Figure 7-8**). During flight, the radar transmitter emits short electromagnetic pulses toward the surface. These pulses propagate through subsurface materials at speeds governed by each material's tendency to polarize and conduct, dielectric permittivity, and conductivity, gradually attenuating as they travel deeper.

When the radar energy encounters buried objects or boundaries between materials with contrasting properties, a portion of the signal is reflected back to the surface and captured by the receiving antenna. The system records the amplitude and two-way travel time of these echoes, while onboard processing units log the raw radar data alongside GNSS and altimeter measurements, precisely time-stamping and georeferencing each trace. In post processing, specialized software converts the data into radargrams, where reflections, hyperbolic signatures, and contrast reveal subsurface features, and depths are calculated from the measured travel times using estimated wave velocities. See Section 6.3 for more information on GPR sensor specifications and project examples.

What are the Advantages?

Applying the use of a GPR sensor on a drone allows greater area coverage and allows access to areas that might be deemed unsafe or unsuitable for a ground-based GPR device.

What are the Limitations?

Some limitations of using a drone-based magnetometer sensor include:

- reduced data quality due to interference or "noise" from aboveground objects
- limited radar signal penetration due to flight height
- payload constraints limit the use of more robust deep-penetrating GPR sensors
- shorter operating time due to drone battery life
- regulatory limitations for using drones in flight-restricted areas



Figure 7-9. SPH Engineering SENSYS MagDrone R1 with rigid mount.

Source: SPH Engineering. Used with permission.

7.2.5.2 Magnetometer

Drone-based magnetometers are used widely in the site characterization industry to locate and map ferrous items across a wide area both at the surface and within the shallow subsurface. Examples where a magnetometer would be used to help characterize a site include to locate mineral deposits, buried utilities, unexploded ordnance, archaeological artifacts, industrial waste, or other ferrous metal items. Magnetometers work by detecting and measuring the magnetic field of a ferrous item. The sensors (for example, fluxgate coils or magnetoresistive sensors) detect variations in the object's magnetic strength and direction and translate these changes into electric signals. This information can inform the depth or the size of the object. Additionally, it can also indicate the direction of the item of interest as it lies in the ground.

Magnetometers are designed for detecting ferrous metal objects on or below the ground surface up to a certain depth. Sampling rates vary based on technology, but a typical magnetometer may collect

electromagnetic results at a rate of 1,000Hz, which allows drones to fly at approximately 10 meters per second and still collect samples at 1 cm intervals. Additionally, drone-based magnetometers may be self-contained and thus equipped with an internal GPS antenna and IMU module to provide precise location data results. Above and to the right are two examples of drone-based magnetometers. **Figure 7-9** shows a foldable rigid mount to reduce swing, and **Figure 7-10** shows a cable tether.



Figure 7-10. Geometrics MagArrow II.

Source: SPH Engineering. Used with permission.

Project Example—Military Munitions Response Program

Current or former military sites are required under the Department of Defense's rule regarding Closed, Transferred, and Transferring Ranges Containing Military Munitions to assess and remove military munitions from any site or property that is to be closed or transferred to public or private entities (65 FR 36423). To properly assess and locate munitions items throughout a formerly used military site, handheld or human-powered electromagnetic devices are used to locate any potential munition items for subsequent removal. To assist in this process, drone-based magnetometers have been used as a wide-area assessment tool to characterize an area of interest for density and extent of surface and buried munitions. Prior to recent developments in drone technology, magnetometers were affixed to helicopters and flown at heights 10–20 meters aboveground to capture coarse geophysical data results of potential buried or surface munitions. For additional information on wide-area assessments to identify areas of concentrated munitions use, refer to the ITRC document *Frequently Asked Questions about Wide-Area Assessment for Munitions Response Projects* (ITRC 2010b).

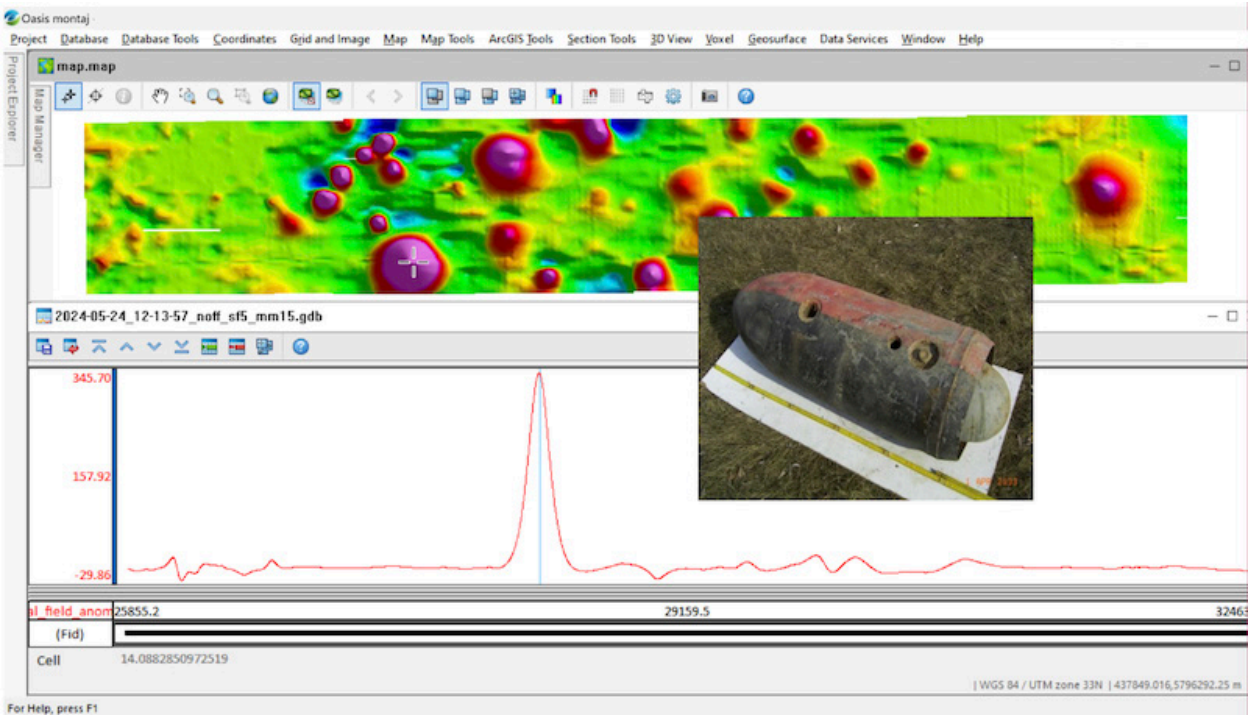


Figure 7-11. Magnetometer survey results as shown in geophysical software (Oasis-Montage).

Source: SPH Engineering. Used with permission.

However, due to advancements in drone technology and lightweight magnetometers designed specifically as a drone payload option, geophysical results have improved greatly. Finer data results and more precise location accuracy are due to the proximity a drone can fly to the surface and the speed at which it is flown. Typically, the magnetometer is suspended from the drone to allow for close contact to the ground and reduced electromagnetic interference produced by the drone. **Figure 7-11** illustrates the results of a drone-based magnetometer survey using geophysical processing software.

What Are the Advantages?

Applying the use of a magnetometer sensor on a drone provides greater area coverage and allows access to areas that might be deemed unsafe or unsuitable for a ground-based magnetometer device.

What Are the Limitations?

Some limitations of using a drone-based GPR sensor include:

- magnetic interference from drone motors, batteries, or other components on the drone
- altitude sensitivity—as altitude increases, weaker magnetic anomalies may be missed
- shorter operating time due to drone battery life
- regulatory limitations for using drones in flight-restricted areas

7.2.5.3 Bathymetry

Capturing bathymetry from drones is possible but currently only in coastal and nearshore environments up to depths of 50 meters depending on water clarity. Marine or aquatic bathymetrical surfaces can be obtained using a specialized LiDAR sensor that sends green laser pulses at approximately 532 nm (ideal wavelength to maximize water penetration with little absorption and scattering). Note that the ideal wavelength in water, 532 nm, is different from that in air, which is 1000 nm. To ensure precise depth measurements, advanced refraction correction techniques based on Snell's law are used to account for the bending of the laser beam at the air-water interface (Hydro-International 2025).

The LiDAR unit requires a medium- or heavy-lift drone to carry the LiDAR payload but otherwise functions the same as terrestrial LiDAR in that the main components are the laser scanner, GNSS GPS, and IMU.

If the project requires bathymetrical data in nearshore environs only, the use of a drone-based LiDAR could greatly reduce costs and enhance data collection efficiency, as nearshore or coastal areas can be difficult for watercraft to navigate due to shallow waters or heavy surf conditions.

7.2.6 Data Processing, Storage, and Analysis

7.2.6.1 Data Processing

The benefits of obtaining remote sensing data from public sources or privately contracted entities that will capture the data for the project is that the processing of the raw data is often done as part of the contract with the service collecting the data or is already processed before being posted for download on public data repositories. This means that the data can be incorporated into the analysis software, whether that is a computer-aided design (CAD) product, geographic information systems (GIS) product, or a thermal or spectral analysis software, without any additional processing. However, in the case where the remote sensing is self-performed, the raw data itself may have to be processed, which will require specialized software and training. Depending on the type of sensor that is being used for the project data needs, there are software packages that are "end-to-end," meaning that they handle the complete

workflow from start to finish. From drone flight mission planning to data collection, the processing, analysis, sharing, storage, and management of data are often integrated into a single software package or multiple software packages that work in tandem. The software and the licensing of the software can be included in the sensor and platform (drones) rental or purchase agreement.

Once sensor data have been obtained either through a public source or self-performed, the data must be assessed to determine whether additional processing should be performed. This requires staff with experience in processing the specific type of remote sensing data collected and the software needed for such operations. For example, processing aerial imagery requires software that is different from processing LiDAR or multispectral data. Additionally, some data types, such as multispectral data, require interpretation of the results necessitating a different skill set. Another example is processed versus unprocessed LiDAR data. The point cloud produced from a LiDAR flight will contain return data that needs to be processed and classified using specialized software and an understanding of that software to provide a complete bare earth DEM or similar output.

Table 7-1. Cloud-based versus desktop: Elements to consider when selecting cloud-based versus desktop data processing and storage.

Consideration	Cloud-based	Desktop-based
How often is data processed?	Many sites per month	Occasional, but data-heavy projects
Team size and geography	Multiuser, multisite	Single user or centralized team
Internet speed and reliability	Fast + reliable needed	Poor or offline fieldwork is required
Data sensitivity	An encrypted cloud is sufficient for data security	Sensitive or private data
Budget	Ongoing subscription	Upfront hardware and software costs
Needed speed	Speed linked to internet parameters	Faster if you use a high-end PC
File size	Large and may help with automated scaling	Limited

When processing and analyzing data from drones, all drone software must integrate two data streams. One stream originates from the sensor (for example, visual camera, LiDAR, thermal, multispectral, etc.). The second stream comes from the GPS and IMU, which provides location data. (Refer to Section 7.3.3.6. for additional information on GPS and IMU). All data streams must be precisely time-stamped because the software matches the data streams based on their time stamps. Most modern drones synchronize the data streams automatically, but verifying that system clocks are aligned before flying can save problems later. For imagery data, it is necessary to know if the software accepts RAW unprocessed data straight from the camera's sensor. RAW data allows the maximum amount of information to be used in post processing, thereby supporting the highest color and image detail fidelity. Some software accepts JPG files, which save storage space and are ideal for sharing; however, some information is lost during the file compression process. For the drone-collected data to be useful, whether in RAW or JPG format, EXIF metadata must be attached to the image files. EXIF metadata can record information such as the drone's GPS location, camera settings, time stamp, orientation, and resolution, along with the drone model, serial number, and other characteristics, all of which are necessary for mapping. The exact information recorded depends on the integration, so it is worth checking when working with new equipment. The imagery processing software then integrates the RAW and EXIF files by time stamp.

While imagery is used to explain drone software, sensor data from LiDAR also has similar considerations. LiDAR data are typically stored in .las files, which are raw data files, while .laz files are compressed versions of these .las files. The raw .las files are point clouds and meshes, which are typically multigigabyte files. The GPS and IMU trajectory data are commonly combined into a single output trajectory file, which is typically an SBET (Smoothed Best Estimate of Trajectory) that contains time-

stamped position and orientation data synchronized with laser pulses. So the SBET file serves a similar purpose to the EXIF files for imagery.

In either case, data processing software can be cloud-based or desktop. Cloud-based solutions are superior for sharing data and cost-effectively maintaining large datasets. Desktop solutions are better suited for areas with limited internet access, for integration into GIS or CAD workflows, and for processing sensitive or private data **Table 7-1**.

7.2.6.2 Data Analysis

When considering data analysis and presentation, think of the end user's needs. Surveyors, engineers, and GIS analysts will require point cloud data, while end users such as planners and the public will need orthomosaic maps. Each data type will have a format that best meets the needs of the end user.

For remediation, detailed datasets such as point clouds for terrain analysis, multispectral imagery for assessing vegetation health and metal contamination, and elevation models for evaluating drainage and erosion are required. Project managers, regulators, and stakeholders may require more accessible formats, such as interactive web maps showing contamination areas, annotated reports documenting cleanup progress, color-coded thermal maps that identify subsurface anomalies, or chronological visualizations that present site restoration progress. Presentations often combine multiple data types. Remote sensing data can be combined in a multilayered approach to provide a more robust CSM of the project site. For example, a LiDAR survey provides a high-resolution *bare earth* topography DEM that then an orthomosaic RGB image is draped over for visual context. A thermal layer is added to identify groundwater seeps or discharge points, which appear as temperature anomalies. A multispectral layer is used to create a vegetation health map (for example, NDVI), which can highlight areas where contaminant stress is impacting plant life. By combining these and other datasets, the GIS platform allows practitioners to identify correlations that would not be readily apparent from a single data source. The data can ultimately be delivered through cloud platforms, custom web portals, mobile apps, or printed reports for stakeholders. Ultimately, the presentation format must transform complex spatial data into clear and concise presentations that make complex data accessible to the audience.

7.2.6.3 Data Storage

It is safe to say that drone-collected data makes large files. File sizes can vary significantly depending on ground sampling distance (GSD), flight altitude, camera megapixel count, and overlap percentage. **Table 7-2** provides estimates for standard photogrammetry with approximately 75% overlap and a GSD of 1–3 cm/pixel from an RGB camera. LiDAR and multispectral cameras may have even larger files, depending on the camera and its settings. Storage capacity needs to be sufficient for files that may be gigabytes in size.

Table 7-2. Estimates for standard photogrammetry.

Data Type	File Size (20 acres)	Estimated Size (5 acres)
Raw images (RAW format)	10–30 GB	2.5–7.5 GB
Compressed images (JPG format)	2–5 GB	0.5–1.25 GB
Processed orthomosaic (GeoTIFF)	2–5 GB	0.5–1.25 GB
Point cloud (.las/.laz)	5–20 GB (.las); 1–4 GB (.laz)	1.25–5 GB (.las); 250–1000 MB (.laz)
3D mesh (OBJ/PLY)	1–3 GB	250–750 MB

Along with sufficient storage space, the files need to be organized in a way that allows them to be retrieved and their locations communicated to others. Naming should be standardized using a consistent

folder hierarchy (for example, Sitename_YYYYMMDD/MissionID/RAW/PROCESSED/REPORTS) with shared naming conventions for collaborative access. Finally, keep security in mind; encrypt sensitive data, and limit user permissions to stored data.

Given that the files are large, consideration should be given to the retention period for different files. For example, RAW images and flight logs may be retained for a short period, while compressed files might be maintained long-term. Regardless of the example, it is recommended that consideration be given to a retention policy before files are accumulated. Also, due to the large data size, cloud storage costs should be taken into consideration when collecting and storing remote sensing data.

7.3 Remote sensing Platforms

This section will provide an overview of the different remote sensing platforms with a focus on using unmanned aerial systems (UAS, drones) on a project-specific basis. Understanding these platforms will aid in determining what data source options would best fit project needs based on availability, cost, and spatial and temporal limitations. **Figure 7-12** summarizes the availability and spatial extent of the three types of platforms that are addressed in the following subsections.

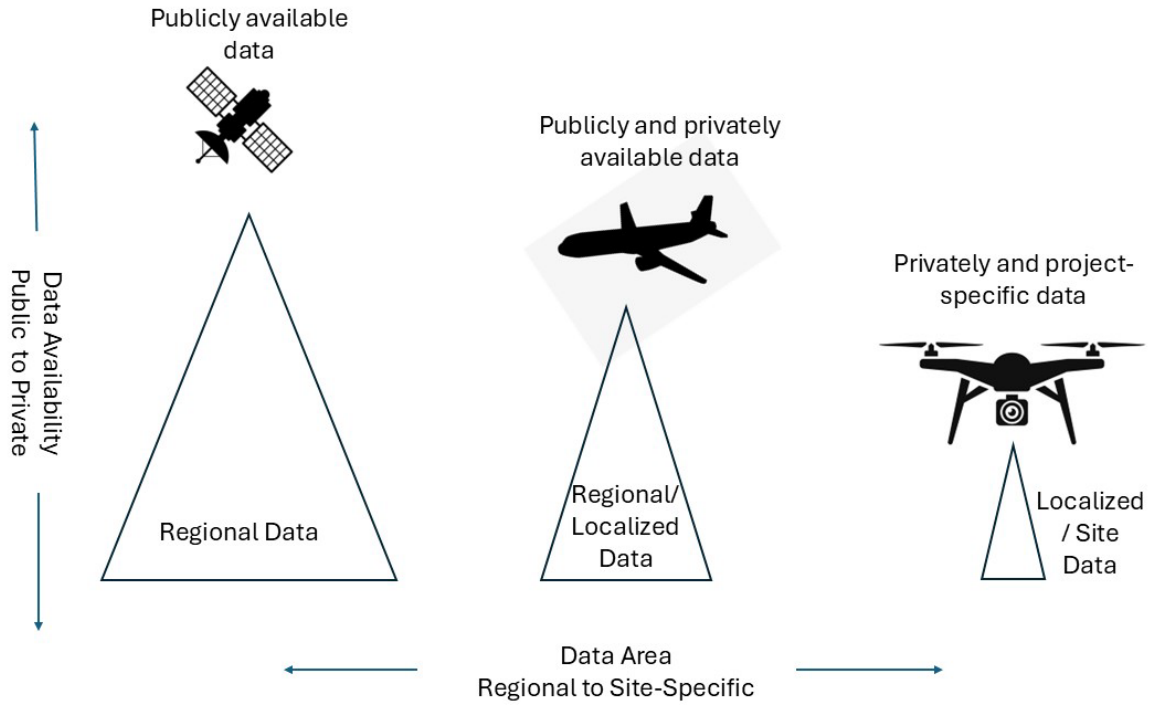


Figure 7-12. Availability and spatial extent of the three types of platforms.

Source: Courtesy of Mark Dhruv EA Engineering

7.3.1.1 What Is the Technology

Satellites are spacecraft designed to orbit a celestial body for the purpose of communication, observation, or remote sensing. They were first used for imaging earth's terrain in the mid-1960s and remain one of the primary sources of remote sensing data. Landsat 1, launched in 1972, became the world's first earth-observing satellite exclusively used for studying planet Earth. Equipped with a multispectral scanner, the satellite obtained 81,000 acres within the first few days after it launched.

Today, there are many satellites capturing data on a consistent basis with a variety of data sensor types, which will be described later in this section.

7.3.1.2 Platform Limitations

While widely used for capturing large areas for analysis of the earth's surface, satellites are somewhat limited for use as a data collection platform due to obstructed views (for example, cloud cover, atmospheric distortion), high monetary costs of obtaining specific data types, limitations in coverage and temporal requirements, and reduced resolution (Vorster, 2025). Additionally, satellite data are primarily captured on a prescribed schedule, and data are processed to be readily available for download from government or commercial websites, thus may not have the resolution required for specific project needs.

7.3.1.3 Platform Advantages

Remote sensing data obtained from satellites are often widely available on government websites (for example, USGS, NASA's Earthdata.gov) with commercial options available for greater specificity in data types and resolution. Additionally, satellite data typically cover larger regions that other platform types may not be able to achieve.

7.3.2 Manned Aircraft

7.3.2.1 What Is the Technology?

Remote sensing data obtained via manned aircraft typically consist of specialized planes equipped with high-end sensors. These flights can be contracted and flown for a specific area or may be part of an ongoing effort by a federal, state, or local government agency looking to increase their remote sensing information. While manned aircraft do not cover as wide an area as satellites, they are better suited to large areas than a drone.

7.3.2.2 What Are the Platform Limitations?

Perhaps the greatest limitation of using manned aircraft to capture remote sensing data is their high cost. Fuel, pilot time, and plane rental can often be cost-prohibitive for smaller projects. Additionally, planes do not have the capability for low altitude flights, which may eliminate many sensors that require a certain proximity to the ground to capture the highest quality data.

7.3.2.3 What Are the Platform Advantages?

Manned aircraft are suitable for large areas or areas smaller than are suitable from satellite data coverages. Since manned aircraft space and weight restrictions allow for the use of high-end mapping sensors, better spectral resolution is achieved, there are fewer flight restrictions than for UAS operations, and manned aircraft are safer than UAS operations.

7.3.3 Unmanned Aerial Systems (Drones)

7.3.3.1 What Is the Technology?

The use of unmanned aerial systems (UAS), or drones, equipped with remote sensors has become an established practice for site characterization across a wide range of projects. This advancement has been driven by key technological developments, including improved battery efficiency, compact high-

performance electric motors, and lightweight onboard computing systems with substantial data storage capacity. When paired with inexpensive, widely available, and reliable sensors (most notably high-resolution optical cameras), these platforms form a highly flexible and scalable data acquisition system.

As these systems have matured, dedicated drone software has further accelerated innovation. Capabilities such as autonomous flight now enable precise navigation along predefined flight paths with minimal operator input. Additionally, remote operations from fixed docking stations are increasingly feasible, although beyond-visual-line-of-sight deployments typically require regulatory waivers. Complementary advances in software for data collection, processing, mapping, and visualization have transformed raw sensor outputs into actionable site intelligence.

The integration of advanced platforms with streamlined data acquisition and processing workflows allows drones to collect information that previously required significant time, labor, and exposure to hazardous or inaccessible terrain. The relative ease of deployment also supports frequent and repeatable flight operations, enabling high-resolution temporal monitoring and a more robust understanding of site dynamics over time.

7.3.3.2 What Are the Platform Limitations?

Not ideal for larger projects; limited by weather conditions: winds greater than 25 miles per hour or rain. Drones can be limited by the type of sensor needed or the size of the area to be captured. Large areas may benefit from a fixed wing drone, which provides longer flight times but is not capable of hovering at a location for further inspection. If the project requires a heavier sensor payload, then a small drone equipped with only an RGB camera and/or thermal would not suffice. This imparts a cost versus capability trade-off that may dissuade companies from building a fleet of drones due to the various functionalities of the different drone types.

7.3.3.3 What Are the Platform Advantages?

Drones are well suited for inspections and small area coverage and easy to mobilize and deploy (**Table 7-3**).

Table 7-3. Platform attributes.

Platform	Data Extent			Cost			Resolution			Availability		
	Regional	Local	Site-Specific	Free	Purchased	Self-Performed	Low	Medium	High	Public	Private	Contracted or Self-Performed
Satellite	x			x	x		x	x		x	x	
Manned Aircraft	x	x	x	x	x	x	x	x	x	x	x	x
Drone		x	x		x	x			x		x	x

7.3.3.4 Drone Types

Drones can be grouped into two broad categories: sUAS (small unmanned aerial systems) and non-sUAS (large UAS). The key difference between the two categories is overall size and weight of the drone with payload. Non-sUAS drones are greater than or equal to 55 pounds (24.95 kg) and primarily used by

military organizations for long-distance reconnaissance and heavy payload capacity. Therefore, non-sUAS drones are not applicable to the majority of use cases in site characterization. The primary drones used for site characterizations are sUAS drones, which are less than 55 pounds with payload. Within the sUAS category, drones can range from micro or nano drones (<250 grams) up to heavy-lift drones that are under the 55-pound limit. This document will focus on sUAS drones for all applications described.

Key drone components include the airframe, propulsion system, navigation equipment and flight controller (often composed of GPS, onboard stabilization, and autonomous flight computer), and its payload (for example, camera). When selecting a drone for remote sensing, it is important to consider the basis of the intended payload and type of data collection needed to achieve project objectives and the size of the area to be covered. Drones are available in different types and configurations, each providing its own set of unique advantages and disadvantages. It is important to understand the capabilities and limitations of each type when selecting a drone for a specific application. The primary types of drones are fixed wing, rotary wing (helicopter), and multirotor.

Fixed-Wing

Fixed-wing drones are the most power-efficient platform type and can generally fly longer and carry more payload than other drones. The primary disadvantage of fixed-wing aircraft is their inability to hover in place, thus not well suited for inspecting specific locations. Many fixed-wing drones are now capable of a vertical takeoff pattern, thus eliminating the need for a runway. Fixed-wing drone sizes can vary greatly with some military-issue drones as large as small, manned aircraft. However, for use in commercially acquired remote sensing data, fixed-wing drones are comparable in size to multirotor drones.

Rotary Wing

Rotary-wing or helicopter configurations allow hovering and vertical take offs and landings. Rotary-wing drones are more efficient than multirotor drones due to their long and narrow rotor blades. Rotary-wing drones are often used to carry payloads that are too heavy for a multirotor. These drones are more mechanically complex because the rotor blades constantly change pitch through each rotation. Although electronic stabilization systems have reduced the complexity of some of these mechanisms, rotary-wing drones require more maintenance than other drones. One significant advantage of rotary-wing drones is that they can be powered by a single motor, making them well suited to internal combustion or turbine power, which allows the drones to fly much longer than battery-powered aircraft.

Multirotor

Multirotor drones, which dominate the current drone market, usually have an even number of electric motors that turn fixed pitch propellers. The four- and six-propeller configurations are most common. The torque of the propeller pairs turning one direction is countered by an opposing torque of propeller pairs turning the other direction. Pitch and roll are accomplished by varying the motor speed. Yaw (rotation around the vertical axis of the drone) is accomplished by varying the speed of propeller pairs to unbalance the torque in the desired direction. Multirotor drones are mechanically simple with as few as four moving parts. Mechanical complexity is replaced by electronics and software, making them reliable and easy to operate. Multirotor drones are generally battery powered and not as well suited to fuel power; they typically have a flying time duration of 30–40 minutes. although that may vary greatly based on payload, drone size, and weather. Sizes are referred to as heavy-lift, medium-lift, and light-lift drones. Light-lift drones are most often used for visual inspections and phase I assessments via thermal or RGB cameras, which are installed semipermanently and typically do not allow for swapping out sensor types. Medium and heavy-lift drones are primarily used for heavier payloads such as LiDAR or magnetometers, or for soil, sediment, water, and air sampling. These drones allow for swapping sensor types. **Table 7-4** describes the capabilities of each type of multirotor drone.

Table 7-4. Drone sizes and specifications.

Sensor Type Supported	Weight Class Description	Weight Class	Max. Payload	Flight Time	Typical Use
RGB camera (integrated) Metal-oxide sensors (MOS) (5–20 g) Light EC sensors	Ultra-light Exempt by Part 107	<250 g (micro-unmanned aerial vehicle (UAV))	50–100 g	15–30 min	Visual inspection, mapping, site reconnaissance, indoor/confined space work
RGB camera (integrated) Thermal sensor NDVI sensor (hyperspectral and/or multispectral) Electrochemical (20–150 g) Catalytic light explosive limit (LEL) Light particulate matter (PM) (100–150 g)	Small quadcopters	0.5–2 kg (small UAV)	200–800 g	20–35 min	Site surveys, fence-line monitoring, safety screening, orthomosaic mapping
LiDAR Gamma ray sensor PM (pumped) Multigas EC systems Non-dispersive infrared (NDIR) (basic modules) RGB + multisensor integration	Medium enterprise UAVs	2–5 kg (medium UAV)	0.5–2 kg	20–40 min	Air quality studies, environmental compliance, multiparameter monitoring
Magnetometers Water sampler/monitor PID (700–1000 g) NDIR (full payload ~1 kg) Compact tunable diode laser absorption spectroscopy (TDLAS) (250–800 g) Optical gas imaging (OGI) (uncooled 250–600 g) RGB + gas integration	Heavy-lift quadcopters	5–15 kg (heavy UAV)	2–6 kg	15–35 min	VOC surveys, methane detection, leak detection, regulatory monitoring
TDLAS (advanced, 0.75–2 kg) LiDAR–TDLAS (1–3 kg) Multisensor (RGB + LiDAR + gas)	Heavy-lift multirotor (octocopter)	15–25 kg (large UAV)	5–10 kg	15–30 min	Quantitative plume mapping, emissions inventory, large-site characterization
Cooled OGI (1.5–3.5 kg) Large LiDAR + gas systems RGB + full sensor fusion	Industrial UAV platforms	>25 kg (industrial UAV)	10–20+ kg	10–25 min	Refinery-scale monitoring, research-grade mapping, high-precision leak detection

Much like satellites and manned aircraft, spatial location information is delivered to the drone and thus, the sensor, from external global positioning systems (GPS) equipment. This information is obtained from either onboard real-time kinematic (RTK) GPS units or from ground control points (GCPs) that are placed at strategic locations on the ground that can be sensed by the sensor and used to tie the resulting data to the correct spatial position. At the end of this section is a summary of the GPS types used in conjunction with the drone and sensor.

7.3.3.5 How Can the Technology Be Used?

Flight Planning Software

Flight planning software focuses on developing flight plans and executing automated flight patterns and actions, such as taking pictures at defined intervals. It aids in preflight checks, weather planning, and identifying no-fly zones. The software may also store previous flight plans for future reuse. In short, flight planning software assists the pilot by instructing the drone on how and where to fly. Align the software package with the specific workflow.

When selecting flight planning software, align the platform with the type of mission. For mapping and surveying tasks—such as monitoring wells, visualizing chemical or biological gradients, capturing excavation volumes, acquiring aerial site imagery, or calculating stockpile volumetrics—look for software that supports grid-based flight planning, high image overlap, and smooth integration with post processing workflows. If the focus is on inspection and monitoring—such as regularly revisiting wellheads, checking infrastructure, or conducting thermal, infrared, or LiDAR imaging—prioritize tools that offer repeatable waypoint missions, terrain-following capabilities, and consistent flight path reproduction. For operations near regulated airspace or involving multiple pilots or aircraft, select platforms with robust airspace intelligence and management features. Finally, if nonstandard hardware is used or you anticipate expanding into technologies such as LiDAR or nonmainstream drone systems, opt for software that is flexible and compatible with a wide range of platforms rather than one tied to a specific manufacturer.

The list below outlines features included in many software packages. Consider these features when selecting flight-planning software for commercial drone operations:

- **Platform compatibility**–Does the software support the make and model drone? If you intend to use multiple drones for a mission, make sure that the software supports all the drones. It is helpful if different pilots using various devices and platforms can sync across devices and platforms to replicate missions.
- **Ease of planning and field workflows**–Desktop + mobile support, offline capability (important for remote sites), KML import and export, etc.
- **KML (Keyhole Markup Language) import and export**–Allows users to define a flight area on a computer using tools such as Google Earth, save it as a KML file, and then import it into drone software to generate a flight plan automatically. Conversely, it also allows one to export a completed mission to share with others or use the data in various applications. KML is a convenient way to plan complex missions on a larger screen with more up-to-date maps than planning directly in the drone's mobile app. Other languages that allow similar functions are the JSON-based plan file format and the DSL called "droneDSL," among others.
- **Plan flight paths**–The drone may be instructed to complete a flight pattern including waypoints, grids, crosshatch, terrain following, altitudes, and overlap percentages.
- **Waypoints** are user-defined points on a map. Each waypoint will be flown in a specific sequence and potentially has individual parameters configured, such as altitude, speed, gimbal angle, heading, and camera actions.
- **Execute automated missions**–The drone flies the pattern and takes images or sensor readings at defined intervals.
- **Manage airspace and safety**–The flight planning software should enable the operator to identify no-fly areas and ground hazards to ensure safe and regulatory-compliant operations. The software should provide preflight checks and airspace awareness and mark no-fly zones. Geofencing uses GPS to create virtual boundaries, preventing the pilot from entering restricted zones, such as airports. The software may prevent the operator from taking off, or it may alert the pilot.
- **Mission-type support**–LiDAR support, multispectral, inspection workflows, etc. Specific sensors may have unique requirements, such as operating at a constant altitude with LiDAR or being able to focus on relatively close objects, as seen with inspection cameras.
- **Post-mission and data integration**–For mapping or inspections: How does the planning tie into data capture, processing, and analytics?
- **Scalability and fleet management**–If there are multiple drones or pilots, does the software have the capacity to manage missions, allocate tasks, and share flight plans? Software that can manage multiple drone flights and pilots simultaneously is referred to as "full enterprise." For

example, a centralized controller dashboard allows tracking of multiple drones, pilots, flight missions, battery statuses, and other parameters, both in real time and as stored missions.

- **Store or repeat missions** for consistent data collection over time (for example, monthly monitoring).

Regulations and Policies

The Federal Aviation Administration (FAA) continues to integrate UAS into the National Airspace System (NAS) through a combination of regulations, authorizations, and programs designed for both public agencies and civil operators. The FAA presently supports two options for certifying public agency drone operations: fly under 14 CFR Part 107 as civil aircraft or conduct Public Aircraft Operations under a public Certificate of Waiver or Authorization (COA). The older Section 333 exemption (49 USC §44807, formerly "Section 333") that predated Part 107 has been largely superseded for small UAS and is no longer the routine mechanism for small UAS operations. Public COAs remain available for agencies that need to operate as public aircraft or conduct missions outside Part 107, and the FAA maintains expedited processes for urgent missions (for example, emergency COAs).

Part 107 applies to government entities and commercial operators alike. Requirements include remote pilot certification by the FAA (written exam and recurrent online training), drone registration, and compliance with operational limitations. Commercial operation includes work performed for compensation as well as work performed without compensation in the furtherance of a business or for research. Flying drones for educational or instructional purposes (for example, teaching a STEM class or a drone training program) may operate either under Part 107 or as a recreational flier (see FAA Educational Users (FAA 2026a)).

Part 107 rules allow UAS to operate a drone under specific conditions that are summarized in the bullet points below (see FAA Press Release – New FAA Rules for Small Unmanned Aircraft Systems Go into Effect (FAA 2026b).

- Maximum drone weight less than 55 pounds
- Maximum altitude of 400 ft above ground level
- Maximum speed of 100 mph (87 knots)
- Minimum visibility of 3 statute miles
- Flight only within unaided visual line-of-sight of the pilot
- Operation and/or visual observer of only one craft at a time
- Operation only in daylight or 30 minutes before official sunrise to 30 minutes after official sunset with anti-collision lighting
- Operations over people and vehicles prohibited
- Yield to manned aircraft required

The FAA's website is the official source of drone information and registration. Drone regulations are continually evolving, and it is important for pilots to stay up to date on current regulations. Useful resources for drone regulations and information include:

- FAA Unmanned Aircraft Systems web page (FAA 2026b)
- FAA DroneZone web page (FAA 2019)
- Know Before You Fly web page (KBYF 2015)

The document links below cover the material on the FAA Remote Pilot Airman Knowledge Test:

- Remote Pilot – Small Unmanned Aircraft Systems Study Guide (FAA 2016)
- US DOT Advisory Circular: Small Unmanned Aircraft Systems (FAA 2021)
- Part 107 Drone Exam Practice Tests Questions (3DInsider 2019)

Remote Identification

The FAA has instituted Remote identification requirements for all drones operating under Part 107 regulations. Remote ID serves as a digital license plate for drones, providing vital information such as the drone's identity, location, and control status to enhance airspace safety and security. This system allows authorities to locate and identify drones in real time, thus preventing unauthorized or potentially hazardous operations. Most Part 107 drones must now either be equipped with a Standard Remote ID system or a broadcast module, unless operating within an FAA-Recognized Identification Area. These requirements are part of the FAA's ongoing efforts to integrate drones into the National Airspace System (NAS) and ensure compliance with current and evolving regulations.

Blue UAS and NDAA Compliance

The Defense Innovation Unit's (DIU) Blue UAS program provides a standardized pathway for rapidly integrating commercially developed unmanned aircraft into US defense and government operations by vetting platforms and key components for cybersecurity, supply-chain integrity, and operational suitability. A central element is compliance with the National Defense Authorization Act (NDAA), which restricts procurement and operation of UAS, and certain critical subcomponents produced in "covered foreign countries" (for example, China, Russia, Iran, North Korea), helping mitigate risks of data exfiltration and hardware compromise. DIU maintains a Blue UAS Cleared List and an on-ramp process to add new platforms and components, enabling faster, more confident procurement while ensuring both performance and security criteria are met. For non-DOD users seeking similar assurances, DIU's complementary Green UAS program applies a parallel trust framework outside the DOD environment.

Legal Considerations

Flight operations should be planned and conducted in accordance with applicable airspace restrictions, property access requirements, and relevant federal, state, tribal, and local regulations. Although the FAA regulates the National Airspace System, additional requirements may apply regarding trespassing, privacy, park usage, and access to public or private property used for takeoff, landing, or mission support activities. Necessary coordination and permissions should be obtained prior to flight operations.

Drone work may require new service agreements or riders to existing agreements and changes in insurance policies, delaying work. It can take time to establish a new contract for drone water sampling owing to legal requirements. Client agreements or aircraft use policies within a company may not have anticipated drone use. Liabilities for aircraft may be based on the crash of a manned-helicopter or fixed-wing aircraft, which grossly overstates the liability related to a drone.

Best Operational Practices

The following operational practices were adapted from drone sampling as described in Castendyk et al. (2017). Drone operations are best performed by a two-person sampling team of a pilot and a spotter. The pilot is responsible for flying, defining a safe flight area, and ensuring equipment is operating properly. The spotter is responsible for ensuring no one enters the safe flight area, watching for changes in environmental conditions (for example, weather, birds, vehicle traffic), assisting the pilot in positioning the

drone over the sample point; and, when using the drone for sampling, collecting the sample(s) when the drone returns.

1. Upon arrival at the site, review weather conditions. Moderate to strong wind can make the drone difficult to control. Note that wind speeds are typically lower in the early morning. Precipitation and condensation from fog or clouds can damage exposed circuitry.
2. Establish the safe flight area, a 20-ft by 20-ft area delineated with cones or other brightly colored markers, where the drone takes off and lands. The safe flight area must have an unobstructed, line-of-sight view of media to be sampled or area from which data are collected. Avoid hazards such as the top of a cliff, the bottom of a highwall, trees, powerlines, and active vehicle traffic. During drone operations, only the pilot and the spotter are allowed to enter the safe flight area. Typically, the pilot and spotter stand just outside of the area when the drone is turned on and off.
3. Prior to flight, inspect batteries for cracks, swelling, or other defects prior to use. Install and secure fully charged batteries into the drone. Used batteries must be placed in a charging station.
4. As appropriate for planned operations, attach sampling equipment and check sensors, controls, and the condition of the drone.
5. Thereafter, raise the drone and payload, position the system relative to the sampling point or point at which sensor data collection is initiated. Initiate planned flight pattern or route to sampling point. As noted above, the selected flight pattern should be advantageous for data collection and safe navigation.
6. Once the allotted flight time has passed or data collection goals are met, land the drone within the safe flight area. For active sampling, such as water sampling, an experienced team can generally complete step 5 in approximately 15–20 minutes.
7. Replace the batteries with a fresh set and repeat step 5 until all samples or sensor data are collected. Always inspect batteries and drone rotors and blades for damage or defects prior to recommencing flight. Used batteries can swell and crack the housing.
8. Prepare the sampling report, which should include at a minimum: (1) notes regarding weather conditions, (2) the sampling and data collection coordinates, (3) the sampling point (in 3D for water sampling), and (4) justification for the selected sampling point(s) or data collection area.

Site-specific Considerations

Prior to implementing drone operations at a site, it is critical to evaluate site-specific physical characteristics that may either impede or improve data collection. Some common considerations include the following:

Topography changes may impede safe operations and must be considered in flight planning. For example, the amount of overlap needed to produce quality data for both active and passive sensors changes with topography, flight pattern, objects being imaged, and available light. In rugged mountains, the light available to illuminate the pixels on the sensor from a shady slope is relatively weak; the light illuminating the pixels on the sensor from a sunny slope is stronger. Additionally, different objects (for example, rocks versus vegetation) reflect more or less light. These ambiguities can significantly affect remote sensing data accuracy.

Sun position, cloud cover, and time of day may contribute to lighting effects that negatively impact data collection. Harsh midday light, for example, can cause excessive contrast, blown highlights, hard shadows, and washed images. Changing light conditions, such as dynamic cloud cover, may also cause issues with a passive sensor. Full cloud cover, on the other hand, may reduce shadowing and variations in light intensity. Too much cloud cover or fog may not only block reflected light but also pose operational safety hazards.

Ground-cover variations may lead to errors in photo stitching and processing. Ground cover such as snow, water, or tall grass moving in the wind may cause difficulty in finding tie points between images. Heavy vegetation may also reduce the effectiveness of active sensors in penetrating canopies and may obscure the ground surface from passive sensors.

Temperature variations in the air or between the ground and the air may influence gradients observed during thermal data collection efforts. Additionally, some sensors have a recommended operating temperature range. Operating outside that range may reduce sensor performance or cause the sensor to fail.

Water, including ponded water, may obscure active or passive sensors from an aerial platform. Many sensors have a limited ability to penetrate beyond a few centimeters of water.

Many drones are not designed for use in high winds or rain, and such conditions may influence operational safety and data collection.

Environmental Considerations

Incidents have been reported where birds, particularly large birds of prey, have directly attacked drones. Such attacks could result in damage to the drone and possibly fatal injuries to birds. To protect the drone and wildlife, a spotter equipped with binoculars can constantly scan the flight area to alert the pilot of bird activity. If birds are spotted, drone flight should cease until the birds have exited the area.

7.3.3.6 Positioning

Onboard Real-time Kinematic (RTK) Global Positioning System (GPS)

Onboard RTK GPS units use at least one additional GPS receiver at a nearby known static position to continuously correct the airborne GPS position. These corrections are transmitted from the base station to the drone via radio frequency; thus, the drone must be within range of the base station to receive the correction data. This method provides GPS horizontal accuracies of a few tenths of an inch. Drones using RTK GPS units can produce data with horizontal and vertical accuracies less than 0.5 inches without ground control. RTK has an additional benefit in that it enables the drone to fly and land precisely. When a short loss of communication between the fixed base and the aircraft occurs, the airborne GPS can revert to a less accurate floating mode, resulting in unusable image coordinates.

These methods are costly compared to using a navigational GPS or a navigational GPS paired with GCPs. When high-accuracy data are required but deployment of GCPs is dangerous or inconvenient relative to the data needs, RTK may be worth the cost.

Ground Control Points

GCPs are an effective way to georeference drone data and greatly improve accuracy for navigational GPS. This method can also be used with images that contain no geographic coordinates. This method involves manually identifying surveyed ground targets within the post processing software. Temporary targets are often used but features clearly visible in several photos can be used as GCPs. Products produced using ground control can achieve accuracy of less than 0.1 ft horizontally and vertically. Some software products allow extra targets to be designated as check points. Check points are not used by the software to georeference the point cloud but rather to measure error between calculated and surveyed coordinates.

Post-processed Kinematic (PPK)

Post-processed kinematic (PPK) GPS units have an advantage over RTK GPS units in that a continuous communication link between base and aircraft is not necessary. A base station must be set up prior to flight operations. PPK uses logs from the base station or a network of continuously operating reference system (CORS) receivers to correct image coordinates after the flight. Raw logs from the onboard GPS as well as PPK methods can provide equivalent accuracies to RTK methods but require post processing that may be complex.

7.3.3.7 Data Certification Requirements

Depending on the purpose of the georeferenced data, data generated from a drone flight should be verified by licensed professional surveyors or other professionals with mapping experience.

7.3.3.8 Data Collection Design

Data management and sharing should be considered early in the development of a drone program. Proper data management leverages data collected from multiple sources and allows data to be easily located and shared. Data sharing can enhance safety and lower costs by reducing the need for redundant flights. A drone can collect gigabytes of data in a single flight. Information technology resources and GIS may not be prepared for the vast amount of resulting data; cloud-based computing and data storage should be considered in these instances. A lack of preparedness may be due to the data infrastructure not sufficient to store and process this amount of data. Additionally, as mentioned in Section 7.2.6.3, a preplanned system for file naming should be employed as data is pulled off the drone memory card and saved to a laptop to keep the multiple files for large data collection efforts easy to manage and decipher for later processing.

7.4 Drone-based Environmental Monitoring and Sampling

In addition to collecting remote sensing data, drones can also be used to collect and monitor environmental media such as air, water, soil, and sediment. This section will describe use cases of some of the more widely used devices carried by drones to perform tasks in a more efficient and safer manner than traditional methods, as well as performing these tasks in areas that would otherwise be inaccessible. It is important to note that these sensor types may still be in the experimental or pilot stage and may not be commercially available for purchase or rent.

7.4.1 Environmental Media Sample Collection

When considering using a drone to collect media such as water, soil, or sediment, the capacity of the drone to carry an adequate amount of sample must be factored into the sampling device itself. The nature of such sample collection types may limit the types of drones one can use for this purpose.

Drone Payload Capacity

The drone used to collect water samples should be able to lift (1) the weight of the drone, (2) the weight of the environmental media sampling device, and (3) the weight of the sample itself. Small drones useful for photography may not have the lift required for these components nor have the functionality to swap payloads. As noted in **Table 7-4**, heavy- and medium-lift drones are best suited for collecting samples.

Flight Distance and Power Supply

An additional factor to consider when using a drone for sample collection is the limitations placed on the power supply (batteries or gasoline). Not only does the weight of the sample affect flight duration, but the distance between sample location and landing zone also needs to be factored into the flight plan. Typically, the company that designs the sampling device will have recommendations on which drone model is best suited to carrying that device. In some cases, the drone can be purchased from the sample device manufacturer and configured to carry that device.

7.4.1.1 Water Sampling

Multiple water-sampling devices have been developed and demonstrated for drones. In general, drone water-sampling devices fall into two categories: surface-water sampling devices, and deep-water sampling devices (**Figure 7-13**). While a simple internet search will turn up multiple companies that design water sampling devices, it is important that the criteria listed below are considered before purchasing a device:

- Has it been tested and demonstrated to work?
- Is it commercially available for rent or purchase?
- Can it collect water samples from the required depths?
- Does it collect the required sample volume in one flight?
- Will regulators accept water samples collected with this method (see below)?

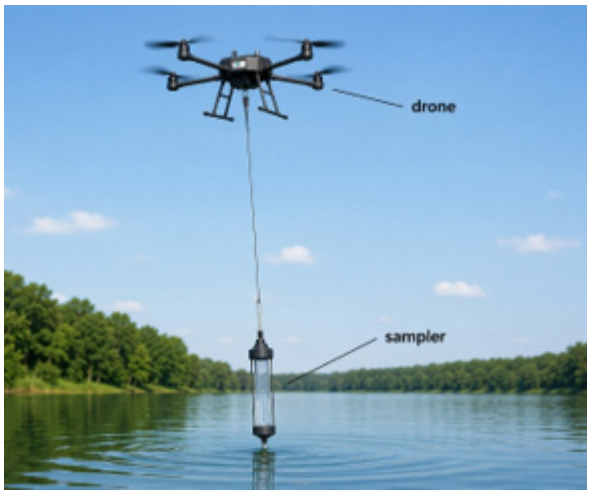


Figure 7-13. Water sampling using a drone.

Source: Ed Winner, PhD., Remediation Products, Inc.

The advantages of water sampling using drones include the following:

- Improve safety by eliminating the need for humans to work on or near water. Standard practices for water sampling involve a person filling water bottles from a shoreline or from a boat. Working on or near water presents several risks to human health. In addition to the obvious concern of drowning, some stratified basins can accumulate large quantities of dissolved gases (CO_2, H_2S, CH_4), and rapid degassing events can displace atmospheric oxygen, leading to asphyxiation or, in the case of hydrogen sulfide, causing acute toxicity.
- Reduce costs associated with water sampling (no need for a boat or an access road; fewer staff)
- Allow increased sampling frequency due to ease of sampling and reduced cost
- Enable better water quality management because of better understanding of water quality and shorter response time to changes in water quality

Drone water sampling has several disadvantages compared to boat-based practices. As the practice gains wider acceptance and regulatory approval, some of these disadvantages may be eliminated.

- Sample volume is limited due to the weight of a loaded water sampler.

- Sample depth is restrained by regulatory restrictions on drone height. Methods that involve suspending the sampler on a tether below the drone (D. Castendyk et al. 2017, 2018)() are restricted to maximally 400 ft below the drone and sampling can occur only to a depth of the tether.
- Drone water sampling is new and unfamiliar to regulators and the industry, leading to caution when adopting nonstandard techniques.
- Establishing legal approval to conduct drone water sampling may hinder its use.

In a field evaluation reported by (Straight et al. 2021), the Nevada Division of Environmental Protection evaluated drone-based water sampling during an August 2017 demonstration and concluded that the methodology was acceptable for regulatory purposes, allowing multiple samples to be collected while maintaining human and environmental safety. Subsequent research has reinforced this conclusion. Reviews of drone-assisted sampling cite improved operator safety, access to hazardous or otherwise inaccessible water bodies, reduced field logistics, and lower monitoring costs compared with boat- or wading-based methods(Lally et al. 2019; Walker et al. 2023). Validation studies have demonstrated that well-designed drone sampling systems produce samples and field measurements comparable to traditional methods across a wide range of chemical, physical, and microbiological analyses while reducing personnel exposure to hazards associated with pit lakes, steep shorelines, contaminated waters, and unstable terrain (Devin Castendyk et al. 2020; Graham et al. 2022; Horricks et al. 2022).

Operational limitations remain, including limited payload capacity and flight endurance, sensitivity to wind and precipitation, tether snagging, sample bottle oscillation, regulatory flight restrictions, and sampling-depth limitations imposed by drone altitude and tether length (Lally et al. 2019; Walker et al. 2023). Engineering advances—including autonomous multisample collection systems, longer flight endurance, increased payload capacity, and improved autonomous flight control—are steadily reducing these limitations, making drone-based sampling an increasingly practical tool for environmental monitoring and water-quality investigations (Walker et al. 2023).

7.4.1.2 Soil and Sediment Sample Collection

Soil and sediment collections from a drone work on the same principles as a water sampler; however, devices engineered for drones are less widely used than water samplers due to the limited ability of a device tethered to a drone to generate the necessary force to grab solid media such as soil or sediment. However, devices are available, most being experimental and not commercially available for purchase or rent.

7.4.2 Air Monitoring

The following sections are intended to orient the reader to drone-deployable systems (screening instruments) for sampling and monitoring. For each sensor or capture unit, a synopsis of how it works, what it samples, its sensitivity, and its weight will be addressed. The internal citations can guide readers interested in examining the topic in greater depth, as can these review articles (Burgués and Marco 2020; Jońca et al. 2022; Noh and Oh 2025).

Several drone-deployable systems, both commercially available and experimental, are used for air monitoring. The value of drone deployment for air sampling lies in avoiding the need for personnel to collect samples from stacks, flares, roofs, and elevated piping. They enable sampling over significant distances, such as landfills, and across potentially hazardous terrain. Drones also excel at collecting repeated samples over vast areas and at supporting data mapping. Drone-mounted air sensors support coverage between fence-mounted sensors or other fixed stations (EPA, 2020). They can fill coverage gaps by sampling streets, neighborhoods, and topographical features. Drones are advanced tools that can measure across 3D space, providing critical data on how local or regional pollutants are distributed

and behave. They enable the collection of previously uncollected samples and protect individuals by allowing work to be conducted at a safe distance.

The data collected fall into three categories: vertical and horizontal profiling of particulate matter (PM) and gases, leak detection and quantification, and targeted samples collected for laboratory analysis (Villa et al. 2016). While the sensors used may span multiple categories, we will present the sensor types as they are most often employed, with small (<3 kg) drones as the primary example.

7.4.2.1 Direct-reading Instruments (Real-time Measurements)

These instruments provide real-time or near-real-time measurements during flight and are primarily used for semiquantitative screening assessments, spatial mapping, and source localization.

Particulate Matter (PM)

The current industry standard is fixed ground monitors that collect horizontal PM measurements (Clements et al. 2022). These types of monitors are not well-suited for measuring PM in the vertical direction or over extensive areas (Liu et al. 2022). This is exacerbated when the target emissions are fine particles. Drones, however, can navigate the vertical component of emissions and repeatedly retrace flight paths, providing greater data density to support a better understanding of PM dispersion in the atmosphere and to improve the characterization of air quality.

Most commercially available PM sensors are laser-scattering optical particle counters, which range from low-cost modules to research-grade models (Clements et al. 2022). Sensor size varies by manufacturer, but typical dimensions are 0.5 cm x 0.25 cm, and weights range from the light category (100 to 150 grams) to the heavy category (500 to 800 grams). These sensors deliver real-time measurements of PM across three groups: particles with diameters equal to or smaller than 2.5 µm (PM2.5), particles with diameters equal to or smaller than 1 µm (PM1), and particles with diameters equal to or smaller than 10 µm (PM10) (Kuula et al. 2020). Ultra-fine particles X< 0.1 µm are too small for most commercial sensors. Thus, the data are presented as categories by particle size, enabling a comprehensive understanding of air quality across particle size ranges. PM2.5 is likely the most critical particle size (USEPA 2026). When selecting a sensor, verify its performance across a range of particle sizes.

Detection limits for laser-scattering sensors must be understood in relation to the sensor's operating principles. When a particle disrupts the laser beam, it is counted and sized. The flow rate and the time through the sensor determine the detection limits. If the flow rate is too high, the particles still disrupt the beam, but the data become noisier. The optimal approach is to adjust the flow rate to minimize noise, since the sensor can detect a single particle if necessary. Thus, particle counts over an interval (flow) are relative to error. The accuracy and precision of the counts must be matched to the specific sensor and flow rate. These factors should be considered when selecting a sensor; therefore, refer to the manufacturer's data sheet for more information.

Electrochemical Cells or Fuel-cell Gas Sensors

Electrochemical cells are the most common sensors used by drones for air monitoring of CO, NO, NO_2, O_3, CO_2, and SO_2 with ppb-level resolution (Mead et al. 2013; Spinelle et al. 2015). They can be used for environmental monitoring, pollution mapping, and detecting gas leaks. In these sensors, the gas diffuses through a porous membrane or capillary to reach an electrode. When the gas reaches the electrode, it causes an electrical current, proportional to its concentration, through oxidation or reduction. This type of sensor is susceptible to temperature and relative humidity. Electromagnetic fields and prop wash can also impact these sensors. In addition, the sensor is subject to drift due to electrolyte drying or water absorption, electrode contact with silicon and sulfides, and changes in the diffusion membrane. Once the electrode exhibits significant measurement drift due to factors inherent to the electrode, it must be

replaced. If drift is caused by external factors such as temperature or humidity, the sensor will return to normal operation once those factors are addressed. Despite these parameters that can cause drift, the sensors are accurate and reliable, and a small amount of drift can be accounted for in the collected data. They are also relatively inexpensive.

The elements of drift presented above are relevant to the discussion of detection limits. Typically, these sensors have a detection limit of 10–50 ppb, as tested in a laboratory setting. In the field, the detection limit ranges from 0.1 to 1 ppm (Spinelle et al. 2015). The differences are within the elements that are described as drift. Each gas type will have different detection limits and sensitivities to drift. For example, NO_2 sensors are very sensitive (5–20 ppb) (Mead et al. 2013), but in the field, humidity-induced drift can raise the detection limit by 5–10 times. Thus, each sensor needs to be selected based on the primary gases of interest, with consideration of both field sensitivity and performance.

Metal-oxide Semiconductors (MOS) Sensors

Metal-oxide sensors (MOS) have good sensitivity and quick response and recovery times. They detect oxidizing gases, such as NO_2 and O_3, and reducing gases, including BTEX, methane, propane, butane, hydrogen, CO, NH_3, and H_2S. However, MOS are not selective for specific gases; rather, they indicate that oxidizing or reducing gases are present within a range. Distinguishing similar gases in complex environments is challenging and remains an area of ongoing research and development.

Most MOS sensors consist of a metal-oxide semiconductor film, most often made of SnO_2 (tin dioxide), but other oxides, such as ZnO, WO_3, TiO_2, and CuO, are also used, depending on the target gases. The gas is drawn across the heated film, where, as in an electrochemical cell, an electron is adsorbed or desorbed. The changing resistance across the film is measured. For oxidizing gases, resistance increases, while for reducing gases, resistance decreases.

Sensor sizes vary by manufacturer and specific capabilities. However, micro-electro-mechanical systems (MEMS) MOS platforms dominate the drone market because they use less power, are smaller, have faster warm-up and response times, and cost less. As a result, only MEMS sensors are described here. The sensor is approximately 2 mm² and 1 mm thick, weighing about 0.3 grams before a housing and mount are added. Housed and ready for use, they are 25 mm x 25 mm and weigh approximately 5 grams.

The detection limits vary across gases and among sensor models and manufacturers. Like the electrochemical cells, humidity and temperature influence sensitivity. MOS sensitivity depends mainly on the chemical reactivity of the molecule at the metal-oxide surface. Practical detection limits for the oxidizing gases NO_2 and O_3 are about 10–100 ppb. Reducing gases vary in detection limits. As MEMS, MOS devices are very sensitive to alcohols and general VOC (detection limits around 50–200 ppb), moderately sensitive to gases such as H_2, CO, and NH_3 (1–10 ppm), and weakly sensitive to BTEX and methane.

Catalytic Sensors (LEL Sensor or Pellistor)

Catalytic LEL (lower explosive limit) sensors or pellistor sensors are used on small drones to detect and localize flammable gas plumes in real time. Drones may be used for safety screening, such as locating methane or propane leaks along pipelines, monitoring oil and gas infrastructure, surveying landfills, and inspecting confined spaces or hazardous areas. Because these sensors provide instantaneous readings expressed as a percentage of the LEL, they are used to locate sources and hot spots and map relative concentration gradients, particularly in unsafe environments.

The sensors work by oxidizing combustible gases on a heated catalyst bead. The sensor contains two types of beads: catalyst beads and reference beads. Both beads are electrically heated to a high temperature. When a flammable gas contacts the catalytic bead, it oxidizes at its surface, generating

heat. This heat increases the electrical resistance of the catalytic beads relative to the reference beads. The difference is converted into a signal proportional to the combusted gas's concentration. The signal is typically reported as percent LEL. Because the sensing principle depends on combustion, these sensors require oxygen to operate and cannot function in inert or oxygen-depleted atmospheres.

Catalytic LEL sensors are relatively compact and lightweight. The element weighs only a few grams, and a complete unit with housing, wiring, and optional airflow management falls within the 50–150gram range. Power consumption is higher than that of many electrochemical or optical sensors because the beads must remain heated, but the total power draw is usually manageable within the power budget of small drones.

Catalytic LEL sensors respond to most flammable gases and vapors with different response factors. They detect combustible gases at concentrations relevant to explosion risk, typically from a few percent of the LEL up to 100% LEL. This corresponds to concentrations in the hundreds to thousands of ppm for gases such as methane. So they are excellent for detecting flammable atmospheres but are not suitable for distinguishing between gases or for measuring trace-level concentrations. For small-drone applications, they are real-time safety sensors that require support from more specific analytical tools, such as PID sensors or laboratory-based analysis.

Photoionization Detection Sensors (PID)

PIDs are familiar tools in remediation; most people are acquainted with their use in the field to screen drill cores for VOC, providing semiquantitative results. PIDs on drones are typically used to do real-time monitoring of VOC in the air. They are helpful for HAZMAT response, industrial leaks, landfill and soil-gas screening, and indoor air quality.

A PID uses a UV lamp that emits photons with a known energy. If a gas molecule has an ionization potential lower than the lamp's photon energy, it will be ionized. The UV lamp's photon knocks an electron from that gas, and these electrons produce a current. The higher the concentration of the gas, the higher the probability of the photon striking the gas, leading to more current. There's no chemical specificity in the photon-molecule interaction, and no spectral or temporal information that could differentiate compounds.

The primary means of favoring certain types of compounds is by selecting the UV lamp's energy. Choose a lamp energy appropriate for the target chemicals. Typically, three lamp energies are available: 9.8 eV, which is narrowly focused on benzene and toluene; 10.6 eV, which covers aromatics, alkenes, and ethers (this is the most common general-use lamp); and 11.7 eV, which extends the compounds that can be detected to include, for example, chlorinated hydrocarbons.

A drone-based PID will be about 50 mm by 65 mm and weigh 40 grams. But depending on the intended use, a sampling stack and pump may be needed, raising the weight to between 700 and 1,000 grams. The sampling stack is an air inlet positioned to avoid turbulence from the drone's propellers. There are also air chambers or baffles that enclose the intake to deal with the same problem. These items and pumps add to the weight. The pump is needed to ensure a regulated flow to the PID, thereby increasing read accuracy.

Commercial field instruments typically provide detection limits ranging from a few ppb to ppm, depending on the target compound, lamp energy, calibration gas, sampling configuration, and environmental conditions. Response times are generally on the order of a few seconds to less than 1 minute, making PID sensors well suited for rapid airborne surveys (Spinelle et al. 2017; Xu et al. 2021). Under optimized laboratory conditions, sub-ppb detection limits have been demonstrated, although such sensitivity is not typical of handheld or drone-mounted field instruments (Pang et al. 2019).

Integrated Multisensor Units

In the above paragraphs, sensors were presented by individual types, yet many environmental applications require monitoring multiple gases. Multisensor units are commercially available and more common than single-sensor units. Multisensor units may be stand-alone or integrated. A stand-alone system includes its own GPS, power supply, and link to the operator. Integrated systems obtain these resources through the drone. These combined sensor systems typically include 5 to 10 sensors, weigh under 2 kg, and are housed in a single casing.

7.4.2.2 Optical and Spectroscopic Monitoring Systems

Optical and spectroscopic monitoring systems rely on interaction between light and matter and are typically used for plume visualization, leak detection, or quantitative gas measurements.

Optical Gas Imaging (OGI) Sensors

Optical gas imaging (OGI) sensors are used to visualize gas plumes of methane, alkanes, ammonia, refrigerants, and other industrial gases for leak detection, landfill monitoring, and industrial inspections. OGI cameras are passive infrared imaging systems that detect gases by exploiting their characteristic absorption of thermal infrared radiation (IR) emitted or reflected by the surrounding environment. Each gas exhibits unique absorption features at specific infrared wavelengths. Narrow-band spectral filters isolate these absorption bands, allowing the camera to distinguish a target gas from the background. For example, methane exhibits a strong absorption feature near 3.3 µm, while ammonia absorbs strongly near 10.3 µm. When a gas plume is present, absorption within the selected spectral band reduces the infrared radiation reaching the detector relative to the background, enabling the plume to be visualized (Varon et al. 2021; Ravikumar et al. 2017).

Because OGIs depend on thermal contrast, the strongest IR will be seen against objects that are either warmer or cooler than the gas in the plume. So, sun-warmed steel tanks, a cold sky, warm ground, pipes, and so on, may all help to provide contrast. The time of day one collects data can also help provide thermal contrast, such as during sunrise or sunset, with sun-heated objects, or contrasting snow-covered ground.

Infrared cameras are of two broad types: cooled and uncooled. Cryogenically cooled cameras are more sensitive; however, they are also more expensive and heavier for small drones. Cooled OGIs are 1.5–3.5 kg. For use with small drones, uncooled OGIs are cube-shaped and measure 8–12 cm on a side, weighing 250–600 grams (Ravikumar et al. 2017). For drones, uncooled OGIs dominate the market.

Detection limits depend on the gas of interest and various environmental parameters. Because the instrument is “seeing” a plume that the concentration of which is tied to the concentration, emission rate, wind speed, and gas dispersion, these elements determine the concentration that the OGI can detect. So, as a rule of thumb, the release needs to produce a plume having tens to hundreds of grams per hour of gas to be detected (Zimmerle et al. 2020). If lower detection limits are required, a cooled OGI may be preferable, but drone OGI are not as effective as handheld OGI at this time.

Laser-based Sensors (TDLAS)

Tunable diode laser absorption spectroscopy (TDLAS) supports quantitative detection of gases such as methane, CO_2, acetylene, and ammonia, leak detection, and plume characterization, particularly for methane emissions (Fosco et al. 2025). Unlike optical gas imaging (OGI), TDLAS provides quantitative measurements rather than qualitative visualization. Quantification requires that the target gas exhibit sharp absorption lines within the diode laser’s tuning range. Gases with strong absorption characteristics,

such as methane, carbon dioxide, acetylene, and ammonia, are therefore best suited to TDLAS. In current drone-based applications, methane is the primary target gas.

The TDLAS is an active sensor that emits light in a very narrow bandwidth matched to the absorption band of the target gas. IR light emitted by the drone strikes a target gas, and the gas absorbs some of the spectrum. A photo detector in the TDLAS measures the reduction in laser intensity in the return signal. The ratio of the absorbed light to the initial light is relative to the concentration of the gas by the Beer-Lambert law. Multiple measurements are made along the beam's path and integrated, so the concentrations are reported as ppm × meter, or as total absorption over the entire beam path. TDLAS does not depend on sunlight or thermal contrast, as does OGI, so it works day or night. The sensor response is measured in milliseconds, allowing for flyover measurements. It can also quantify gases from hundreds of meters away if the laser's path is unobstructed.

Unlike OGI, TDLAS can quantify the target gas. Quantification requires that the gases' emissions have sharp adsorption lines within the diode laser's range. Gases with strong absorption characteristics, such as methane, carbon dioxide, acetylene, and ammonia, are the most readily measured, but currently, TDLAS for drones is primarily focused on measuring methane.

The sensitivity of a TDLAS sensor depends strongly on the optical path length through the target gas, because absorption is proportional to the product of gas concentration and path length. Two sensor architectures are used to control this path length: open-path and closed-path designs. In an open-path TDLAS, the laser travels through ambient air outside the sensor, and the effective path length is the distance the beam propagates through the gas plume before it is reflected to the sensor. In a closed-path TDLAS, gas enters the sensor by diffusion or a small fan, and the laser's path is the internal measurement of the chamber. Closed-path designs may use mirrors to increase the effective path length within the chamber, thereby improving detection limits. Achieving lower detection limits in closed-path systems typically requires a larger detector and optical assembly.

TDLAS can selectively detect gases at ppb levels in the laboratory and at ppm levels in the field. Based on how the TDLAS sensor works, detection limits are typically reported in ppm, which is the integrated concentration over the beam path length. In this case, the drone is collecting samples within the plume. If the inlet is connected to a tube suspended just above the ground surface, ppm data can be collected that is comparable to that from a walkover survey (Abichou et al. 2023). Typical detection limits for small drones are in the 1–5 ppm range (Silva and Scott 2023).

From a size and weight perspective, laser diodes used in TDLAS are highly efficient and relatively low power. Most drone-mounted TDLAS units weigh between 250 and 800 g, making them compatible with small multirotor platforms. Larger, higher sensitivity closed-path systems may weigh 750 g to 2 kg and require larger drones. Gas-mapping LiDAR–TDLAS hybrid systems are also available, typically weighing 1–3 kg and requiring midsized drones. The addition of LiDAR to the TDLAS absorption supports 2D and 3D plume mapping. It can improve sensitivity by a factor of 10 because LiDAR data enables the determination of the gas plume geometry.

Nondispersive Infrared (NDIR) Sensors

Nondispersive infrared (NDIR) sensors are most often used on small drones for quantitative measurement of carbon dioxide and, less frequently, methane. Like TDLAS, NDIR is an active optical absorption method; however, it uses a broadband IR source rather than a laser and does not disperse the light into a spectrum, so these sensors are referred to as nondispersive. In current small-drone applications, CO_2 is the primary target due to its strong, well-defined IR absorption band. NDIR sensors are available for CH4, but they have a lower absorption coefficient and high cross-sensitivity to other hydrocarbons.

NDIR sensors operate by emitting broadband infrared radiation through a closed measurement chamber containing ambient air. An infrared lamp or LED produces IR radiation typically spanning the 2–5 μm wavelength range. The IR wave passes through a sample chamber, where the ambient air flows or diffuses. A band-pass optical filter allows only the target gas's absorption wavelength (4.26 μm for CO_2) to pass through to the sensor. The sensor measures the intensity of IR light that passes through the filter. As the gas concentration increases, the light intensity decreases because the gas in the chamber interacts with it. A second detector has a filter that does not block the wavelength of the gas. This detector serves as a control or reference. The ratio of the absorption of the specific wavelength of the gas to the absorption of the reference is relative to the concentration of the target gas by the Beer-Lambert law (Hodgkinson and Tatam 2012).

NDIR sensors are referred to as closed-path because the IR light is projected into a chamber rather than into the gas outside the sensor. Increasing the optical path within the sensor can lower detection limits, but this comes at the cost of increased sensor weight. If the path length in the sensor is increased using mirrors, the sensor is referred to as a multipass NDIR; otherwise, it is a single pass. The gas can enter the chamber by either passive diffusion or by active pumping.

Drone NDIRs typically use a pump in combination with either a single-pass or multipass sensor. The single-pass NDIRs have detection limits of 10–50 ppm for methane and weigh 40–120 g. The multipass NDIRs have detection limits of 1–20 ppm and weigh 150–400 g (Liu et al. 2022). But the weights cited are for the sensor only. Once the sensor is housed, powered, and mounted, the weight is about 1 kg.

7.4.2.3 Whole-Air Samples Collected for Laboratory Analysis

These methods collect air samples during flight for subsequent laboratory analysis. They do not generate real-time concentration data.

Tedlar Bags

Tedlar gas-sampling bags are widely used in environmental monitoring as a simple, low-cost method for collecting "whole-air" samples for laboratory analysis. They are most often used for "grab samples" during site characterizations, odor or VOC investigations, industrial fence-line monitoring, gas-leak response, or plume characterization following fires, spills, or accidental releases.

Mounting a Tedlar bag onto a small drone is a simple extension of existing air sampling practices. A basic drone-based Tedlar system consists of a small gas-tight bag (usually 250 mL to 1 L), a lightweight diaphragm pump, flexible tubing, and a bag with a septum to allow for gas extraction. During flight, the pump draws ambient air through an inlet, typically via a tube positioned outside the rotor wash, and transfers it into the bag. Once the bag is filled, the pump shuts off, the valve seals, and the drone returns with a sample.

Compared with direct-reading sensors or sorbent tubes, which target a defined list of compounds, a Tedlar bag captures all airborne constituents present at the time of sampling, including unexpected or unknown chemicals, making it useful when the plume composition is uncertain. A significant advantage is that Tedlar bag samples are analyzed using standard laboratory methods such as USEPA TO-3, TO-14A, and TO-15 for VOC and reduced sulfur compounds. This makes sample analysis easier for environmental laboratories.

Tedlar bags can deform under rotor-wash turbulence unless protected. They can also adsorb or off-gas certain VOC, so reactive or high-volatility target compounds may limit storage to a few hours. When collecting a single grab sample, the drones must hover long enough to fill the bag. Therefore, consideration must be given to the drone's location in the plume and the concentration of target gases within a plume. They are best used for sampling to confirm or characterize known hotspots.

A typical configuration uses a 250–1,000 mL bag (1–10 grams), a small pump weighing 80–150 grams, tubing and fittings (20–40 grams), and a simple mounting bracket. In total, most systems fall in the 125–250gram range, well within the payload capacity of popular small multirotor drones. Larger bags, protective frames, or dual-bag setups may push this toward 300–400 grams.

Sorbent Tube (Tenax, Carbopack, Activated Carbon)

Sorbent tubes are small, rigid containers, often of glass or stainless steel, that are packed with adsorbent. A pump typically pulls air through the tube. The tube is located to avoid prop wash. Air pumped through the tube encounters the adsorbent. It is a flow-through system. When sampling is complete, the tube is sealed and sent to the laboratory for analysis using standard methods, such as USEPA Method TO-17.

The adsorbent is selected to match the compound(s) of interest, so knowing the target compound in advance is advantageous. Typically, sorbent tubes are used for capturing VOC, greenhouse gases (CO_2, CH_4), pesticides, and particulates (PM2.5, PM10). The absorbent is selected for the gas of interest; whole-air samples, such as those collected in a Tedlar bag, are not collected. This method does not support analysis for unknown samples. Based on the mass of absorbent, the tubes have a limit on total absorption, so it is essential to carefully determine flow rates and sampling times that are consistent with the tube's capacity.

The sorbent tubes are light (1–5 g) and durable. With the pump, sorbent tube, brackets, and tubing, the system weighs between 80 and 150 grams. The light weight of the system has enabled commercial multitube systems to extend flight time and prevent adsorbent saturation (Leitner et al. 2023).

Canisters (Miniaturized Stainless or Silonite®)

Miniaturized canisters, such as small Summa canisters, quartz containers (Chang et al. 2016), and glass vials are increasingly considered for drone-based air sampling when high-integrity whole-air samples are required. These canisters are typically constructed of electropolished stainless steel or internally coated with an inert silicon-based material to control reactivity and adsorption. For small-drone applications, canister volumes are typically 250–500 mL, but canisters as small as 50 mL are available.

The canister is evacuated prior to flight and fitted with either a simple flow restrictor or a miniaturized mass-flow controller. When the inlet valve opens, ambient air flows into the canister. Depending on the restrictor design, the sample may be collected as a grab sample (seconds) or as a time-integrated sample (minutes). The inlet is extended away from the prop wash via tubing or a short mast. Once filled, the valve closes, preserving the whole-air sample for laboratory analysis.

These canisters are most often used for trace-level VOC analysis, particularly when sample stability and compound preservation are critical. Canisters offer superior chemical inertness; longer allowable holding times; and improved performance for light hydrocarbons, chlorinated solvents, reduced sulfur compounds, and oxygenated VOC as compared to Tedlar bags. Standard laboratory methods are used to analyze the sample. This makes canisters attractive for regulatory compliance or defensible investigations.

A 250–500 mL canister typically weighs 300–700 g, depending on wall thickness and valve configuration. When combined with a valve actuator, tubing, and optional flow controller, total payloads commonly fall in the 500–1,000 g range, pushing the upper limits for <3 kg drones. Quartz (SiO_2) canisters in a range of approximately 250–500 mL should weigh about 200–500 g empty, depending on wall thickness and valve hardware (Yanq et al. 2020).

Mass-flow Controller Samplers

A mass-flow controller is not a type of sampler, but it can be incorporated with sampling devices that actively collect a sample into a storage container. It acts as a gatekeeper for a collection device, such as a Summa canister, a Tedlar bag, or a sorbent tube. It is an active flow-control system that uses a pump and a controller to meter air at a precise, constant rate into a collection device. It allows for time-integrated sampling. When quantitative, time-integrated, defensible samples are needed, a mass-flow controller may be appropriate. While useful, they weigh 150–300 g, excluding the sample collection device. Due to their weight, they are not typically used on drones. When used, they are often coupled to Summa canisters and sorbent tubes. See **Appendix C. Remote Sensing Air Sampling Tools** for a summary table for air sampling tools.

8 CASE STUDIES

Case studies are provided in this section as examples of the applicability, benefits, and costs of ASCT in environmental site characterization, including tool selection, data interpretation, and understanding of potential pitfalls or shortcomings related to individual tools. In addition, the case studies demonstrate the use of ASCT in developing an understanding of geology and contaminant distribution, increasing confidence in corrective-action decision making, and potentially reducing the overall project costs and duration of site characterization and remedial action.

A summary of each case study is provided below with external links to view all case studies and additional information and references.

8.1 Case Study 1—Pre-excavation Scoping at the Satus Store, Washington

A USEPA investigation of a closed, abandoned UST system at the Satus Store site located near a private drinking water well identified petroleum-contaminated soil and residual LNAPL. A high resolution site characterization (HRSC) was conducted in October 2020 to determine the extent of residual light non-aqueous phase liquid (LNAPL), estimate the volume of petroleum-contaminated soil exceeding Washington State Model Toxics Control Act (MTCA) Method A cleanup levels, and support excavation planning in a cost-effective manner. The investigation consisted of three days of direct-push borings using the UVOST® tool, along with four confirmation soil samples used to correlate fluorescence responses with laboratory data. The original plan was to begin with UVOST to define the area of residual NAPL, then use MIP/HPT tools to characterize lower levels of contamination and aquifer conductivity; however, the extent of petroleum contamination was much greater than anticipated, so the entire investigation focused on UVOST. Confirmation samples were collected from locations identified based on the UVOST results.

The investigation, conducted over a three-day period, confirmed that excavation was a practical remediation approach and helped define excavation boundaries. Results were communicated through reports, maps, and visualization tools, and demonstrated that remaining residual contamination was not mobile and posed limited risk to human health and the environment, supporting the site's candidacy for no further action pending limited confirmatory monitoring.

The study concludes that it is important for project managers and/or fund managers to consider costs and cost-effectiveness comprehensively for a site. The results demonstrate that while HRSC can be expensive up front, the use of HRSC with ASCT technologies can be more cost-effective overall than traditional investigation methods, especially when project scopes allow flexibility and multiple tools can be deployed efficiently during a single mobilization.

View the full case study at: **https://itrcweb.org/wp-content/uploads/2026/11/2026.11-ITRC_ASCT-2_Sec8_Case-Studies-FINAL.pdf**

For more information see: **https://www.epa.gov/system/files/documents/2025-03/hrsc-indian-country-2025-03-04.pdf**

8.2 Case Study 2—Understanding Contaminant Pathways at Heflin's Garage, Fredericksburg, Virginia

A large gasoline release in the mid- to late-1980s resulted in LNAPL and a dissolved-phase groundwater plume extending across a four-lane highway influenced by pumping from domestic water supply wells. The LNAPL and dissolved plume impacted the water supply. In addition, impacts to an area stream and vapor impacts to several homes were identified. A pump and treat system was operated for approximately 20 years with some success, but vapor impacts and sheens on the stream continued.

The case study describes the use of ASCT technologies during two studies (specifically a 2007 study using MIP in combination with EC and a 2021 study using OIP and MIP in combination with HPT) to understand geologic controls on distribution of residual NAPL and the complex patterns of LNAPL and dissolved-phase petroleum migration. The result of these studies supported the design and installation of an adequate monitoring well network and passive remediation barrier in a complex, unconsolidated sequence of clay, silt, and sand, at a project site complicated by limited access along a state highway.

The case study demonstrates that for sites where the fuel type is known to be gasoline, the OIP is sufficient for showing the presence of LNAPL. In addition, HPT used with either the OIP or MIP probes was shown to be a popular choice, because only one direct-push drive had to be made at each location to gather both physical and contaminant subsurface data.

View the full case study at: https://itrcweb.org/wp-content/uploads/2026/11/2026.11-ITRC_ASCT-2_Sec8_Case-Studies-FINAL.pdf#page=7

For more information see: https://www.epa.gov/system/files/documents/2025-03/hrsc-indian-country-2025-03-04.pdf

8.3 Case Study 3—LNAPL Identification and Delineation, and Assessment of Petroleum Vapor Intrusion Risk at TJ's Quik Stop, Poplar, Montana

In 1985 a release of 8,000 gallons of gasoline from piping beneath a dispenser was reported. Remedial actions on the site included localized soil excavation. In 1989 petroleum odors were reported in several homes and were attributed to petroleum entering the sewer system as a result of heavy rain. In 1996, the UST system was removed, and soil excavation was completed. In 2016, petroleum-related constituents were identified in groundwater underlying the former UST site.

The case study describes the use of ASCT technologies to delineate the distribution of petroleum contamination and assess the need for further action in relation to potential residual petroleum vapor intrusion. The HRSC used nine OIP and 13 MIP locations with EC and HPT and with confirmatory soil sampling to characterize the site, successfully identifying and delineating residual contamination after a single 5-day field effort. The characterization identified no areas on LNAPL and limited distribution of residual LNAPL, and confirmed vapor intrusion to be unlikely. The case study notes that some uncertainty remains due to a data gap created by a road between the site and another potential source across the road and recommends sample locations in roadways between potential source areas to avoid significant data gaps.

View the full case study at: https://itrcweb.org/wp-content/uploads/2026/11/2026.11-ITRC_ASCT-2_Sec8_Case-Studies-FINAL.pdf#page=10

For more information see: https://www.epa.gov/system/files/documents/2025-03/hrsc-indian-country-2025-03-04.pdf

8.4 Case Study 4—Hydrogeologic Framework and Extent of Saltwater Intrusion in Kings, Queens, and Nassau Counties, Long Island, New York

This report is from a cooperative study by the USGS and the New York State Department of Environmental Conservation to evaluate the sustainability of Long Island's sole-source aquifer system through hydrogeologic mapping, compilation of groundwater chloride concentrations, and groundwater flow modeling. The case study details the use of borehole and surface geophysical data in combination with historic lithologic, hydrologic, geologic, water quality, and water-use data to evaluate the sustainability of the aquifer system in western Long Island. The incorporation of the older existing data, along with the use of new ASCT data, helped to better define the geologic model of the region and access the extent of saltwater intrusion.

Lithologic and geophysical logs were used as a framework supplemented with eighteen new borehole geophysical logs, including NMR, gamma ray, resistivity, temperature, and EM logs. Surface geophysical data collected included historic seismic reflection surveys, TDEM soundings, and horizontal-to-vertical spectral ratio (HVSR) soundings (a passive seismic method). These data were used to map the hydrogeologic boundaries of the aquifer system. These surfaces were then interpolated and integrated with the historic borehole and water quality data to better understand the evolution of saltwater intrusion into the aquifer systems under western Long Island.

While this study covers a large regional area (far larger than most environmental sites), the principles used to track a geochemical signature through a complex hydrogeologic system can be applied at any scale.

View the full case study at: https://itrcweb.org/wp-content/uploads/2026/11/2026.11-ITRC_ASCT-2_Sec8_Case-Studies-FINAL.pdf#page=13

For more information see: https://pubs.usgs.gov/sir/2024/5048/sir20245048.pdf

8.5 Case Study 5—Use of Multiple Direct sensing Technologies and 3D Visualization to Complete a High Resolution Site Characterization of a DNAPL Pool

This case study describes an HRSC investigation to rapidly identify and delineate the source of trichloroethylene (TCE) contamination at a small manufacturing facility on a 0.5-acre parcel in New Jersey. Initial characterization relied on the membrane interface probe (MIP) with an integrated EC sensor to generate continuous vertical profiles of subsurface VOC response and lithology. MIP borings across the site revealed discrete, high-concentration chlorinated volatile organic compounds (CVOC) intervals and stratigraphic controls on contaminant migration that had not been resolved by traditional monitoring well data, allowing the investigation to focus on a localized source area indicative of DNAPL presence.

Although TCE itself does not fluoresce under UV light, the investigation incorporated the Optical Image Profiler (OIP-UV) after MIP confirmatory sampling results suggested a DNAPL source composed of mixed waste containing sufficient PAHs to produce a measurable UV fluorescence response. This allowed the OIP-UV to confirm DNAPL presence and precisely delineate the geometry of the DNAPL pool. In these targeted source areas, investigation points were advanced at very close spacing, with some DNAPL delineation borings located within approximately 2 ft of one another, providing a level of resolution not

achievable with traditional methods. All HRSC data were integrated into a 3D CSM using 3D visualization software (Earth Volumetric Studio), with LiDAR-derived topographic data used to accurately reference ground surface elevations, improving depth control, spatial accuracy, and confidence in subsequent remedial decision making.

The study concludes that HRSC investigations using direct sensing tools such as MIP and OIP combined with 3D visualization have the potential to reveal and accurately delineate the subsurface configuration of NAPL source zones and/or dissolved VOC plumes that is typically not achievable with the use of conventional site characterization techniques (such as the installation and sampling of groundwater monitoring wells). Using these ASCT to delineate dissolved-phase CVOC allowed groundwater monitoring wells to be placed at appropriate locations and depths. The study demonstrates the need to evaluate data in the field and, if needed or appropriate, apply additional tools or modify the approach while in the field to evaluate (in this case) the size of the DNAPL plume.

View the full case study at: https://itrcweb.org/wp-content/uploads/2026/11/2026.11-ITRC_ASCT-2_Sec8_Case-Studies-FINAL.pdf#page=109

For more information see: https://www.battelle.org/docs/default-source/conferences/chlorinated-conference/proceedings/2018-chlorinated-conference-proceedings/h5-improvements-in-site-data-collection-data-management-and-data-visualization/h5_1210_-925_koester_with-video.pdf?sfvrsn=d9368788_0

8.6 Case Study 6—Surface Geophysics: Electrical Resistivity

In 2015, approximately 2,000 gallons of diesel fuel were released from two aboveground storage tanks located adjacent to a municipal water supply well in Ada, Oklahoma. The well draws from the Arbuckle-Simpson aquifer; a highly permeable, karstic dolomite system. There was significant concern that the diesel could rapidly migrate through fractures and conduits, potentially impacting the municipal drinking water supply.

A multidisciplinary team consisting of municipal staff, environmental consultants, drilling contractors, and university researchers was assembled to respond to the incident. Electrical resistivity imaging (ERI) and temporal ERI (TERI), combined with confirmation drilling, was used to delineate diesel contamination and identify fractures serving as preferential flow pathways.

Remediation efforts included soil vapor extraction and vacuum recovery wells to remove diesel from the vadose zone and perched groundwater. A surfactant flush was implemented to enhance contaminant recovery, and elevated carbon dioxide levels indicated that microbial biodegradation was occurring within the source area. All remediation activities and well system upgrades were completed by January 2017, allowing the well field to safely return to service within two years.

The success of the project was driven by a rapid response, HRSC, and strong collaboration among technical experts, regulators, and municipal leadership. These efforts effectively prevented contaminant migration and protected the city's drinking water supply.

Additional details are available in the following master's thesis evaluating mass recovery approaches: Comparison between model and field diesel mass recovery in dolomite karst (Pickens 2018).

View the full case study at: https://itrcweb.org/wp-content/uploads/2026/11/2026.11-ITRC_ASCT-2_Sec8_Case-Studies-FINAL.pdf#page=117

For more information see: https://hdl.handle.net/20.500.14446/330757

8.7 Case Study 7—Site Contamination Assessment of Legacy Groundwater Impacts to Inform Regulatory Action, Somerton Park, South Australia

The South Australian Environment Protection Authority adopted a stage assessment approach to underpin regulatory action to protect human health from the impacts of orphaned site contamination. The assessment was conducted to evaluate chlorinated hydrocarbon (CHC) contamination suspected of migrating away from a commercial/industrial precinct toward residential properties in the metropolitan coastal suburb of Somerton Park in June 2023.

The first two stages of assessment in Somerton Park focused on understanding the extent of groundwater contamination in the unconfined regional water table aquifer, including development and refinement of a supporting CSM and a vapor intrusion risk assessment. The assessment identified chlorinated hydrocarbon contamination (TCE) in groundwater that presented an exposure risk to people accessing groundwater from private wells in the area. A secondary health risk arose from the potential for vapor intrusion into buildings (based on soil vapor concentrations of TCE above national screening criteria) caused by volatilization of contaminants in groundwater, primarily trichloroethene. The second stage assessment, however, concluded that there was a poor correlation between concentration of TCE in groundwater and in soil vapor, which was inconsistent with the assumption that shallow groundwater impacts were the source of TCE in soil vapor.

To address data gaps identified in the Stage 2 investigation, the assessment area boundary was expanded and additional investigation conducted to assess the nature and extent of the chlorinated hydrocarbon contamination and determine the associated risk to human health. This additional assessment incorporated high-resolution vertical profiling using MiHPT to provide enhanced characterization of the local hydrogeological environment and downhole data for the presence and relative magnitude of volatile chlorinated hydrocarbons and to guide the deeper aquifer investigations.

The case study demonstrates how insights from high-resolution profiling tools, used in conjunction with traditional site contamination assessment techniques, improved the understanding of exposure pathways and contaminant migration posed by historic contamination.

The use of membrane interface and hydraulic pressure tool (MIP) direct-push technology ahead of the drilling and sampling program enabled screened intervals to target zones of highest impact.

Outcomes of the assessment identified clear interactions between stranded chlorinated hydrocarbon impacts in the vadose zone and water table fluctuations in addition to deeper contamination migration pathways facilitated by poorly designed private wells.

View the full case study at: https://itrcweb.org/wp-content/uploads/2026/11/2026.11-ITRC_ASCT-2_Sec8_Case-Studies-FINAL.pdf#page=126

For more information see:
https://www.epa.sa.gov.au/environmental_info/site_contamination/assessment_areas/somerton-park

8.8 Case Study 8—Managing a Catastrophic Release to Achieve Rapid Decision Making and Minimizing Long-term Impacts

In response to a significant gasoline release at a gas station in Northern Virginia, the Virginia DEQ instructed the owner/operator to conduct an HRSC to determine how gasoline had moved from the release site and affected surrounding basements. The objectives of the investigation were to determine

the distribution of LNAPL and dissolved-phase contamination in perched and deeper aquifer, provide information to design and locate monitoring and recovery wells, and help assess feasible remedial technologies. The investigation used UVOST-LIF, MIP, EC, and HPT to characterize the release and correlate results with soil and groundwater analyses.

This case study shows how using direct sensing HRSC was able to provide a better understanding of the distribution and movement of gasoline through the subsurface to points of exposure than was afforded by using traditional monitoring wells. The combination of data generated through the use of UVOST, MIP, EC, and HPT provided a more precise understanding of the LNAPL location and distribution and related subsurface soil types. The data generated provided the information to plan further investigation and remedial actions, including more accurately locating and designing monitoring, compliance, and vacuum recovery wells and confirming the need to abandon long screen monitoring wells that were not providing representative data. In addition, it provided a better understanding of the likely mechanisms for contaminant transport to the adjacent structures. This investigation demonstrated the effectiveness of ASCT in mapping the distribution of contaminants and providing a better understanding of subsurface transport mechanisms than afforded by the conventional borehole sampling and well construction.

View the full case study at: **https://itrcweb.org/wp-content/uploads/2026/11/2026.11-ITRC_ASCT-2_Sec8_Case-Studies-FINAL.pdf#page=142**

For more information see: **https://neiwpcc.org/wp-content/uploads/2018/10/Wardle.pdf**

ACKNOWLEDGMENTS

ITRC and the Advanced Site Characterization Tools (ASCT) Update Team were deeply saddened by passing of Kris McCandless in 2026. Kris was a longtime supporter and volunteer for ITRC. He was always willing to befriend and mentor anyone on the Team and in the ITRC community. Kris was an active member and contributor to the ASCT Update Team. He brought nearly 40 years as a geologist both in the private and public sectors, including the last 10 years at the Virginia Department of Environmental Quality (DEQ) to the Team. Kris was the Virginia POC on ITRC's State Engagement Program. He played a key role in promoting ITRC throughout the Commonwealth, recruiting new ITRC members, and mentoring other POCs.

The members of the ITRC ASCT Update Team wish to acknowledge the individuals, organizations, and agencies that contributed to this technical/regulatory guidance.

The ASCT Update team was led by: John Mitsdarfer of the Oklahoma Department of Environmental Quality and Crystal Pirozek of the New Jersey Department of Environmental Protection.

Team leaders were assisted by Program Advisors: Jim Rocco and Lesley Hay Wilson of Sage Risk Solutions LLC.

Specifically, the team recognizes the efforts and contributions of the following:

State and Local Government

Gerard Aarons	California Department of Toxic Substances Control
Jeffrey Bahling	Indiana Department of Environmental Management
Todd Birky	Missouri Department of Natural Resources
Ahmet Bulbulkaya	Tennessee Department of Environment and Conservation
Candice Cone	Arkansas Division of Environmental Quality
Brian Davis	Minnesota Pollution Control Agency
Christina Fiocco	New Jersey Department of Environmental Protection
Maile Gee	California Department of Toxic Substances Control
Vicki Hadwin	Louisiana Department of Environmental Quality
Michelle Hu	California Department of Toxic Substances Control
Ricardo Jaimes	District of Columbia Department of Energy and the Environment
Eric Johnson	New Hampshire Department of Environmental Services
Bethanie Kirby	Tennessee Department of Environment and Conservation
Andrew Leavitt	California Department of Toxic Substances Control
Yushan Li	New Mexico Environment Department
Gina Marinacci	Delaware Department of Natural Resources and Environmental Control
Caitlin Martinez	New Mexico Environment Department
Kris McCandless	Virginia Department of Environmental Quality
Morgan McGee-Soloman	Delaware Department of Natural Resources and Environmental Control
Christopher Newell	Indiana Department of Environmental Management
Mike Penzone	Delaware Department of Natural Resources and Environmental Control

Caroline Rice	Wisconsin Department of Natural Resources
Camille Rossiello	South Carolina Department of Health and Environmental Control
Shahroze Ali	Delaware Department of Natural Resources and Environmental Control
Alexander Short	Minnesota Pollution Control Agency
Thomas Richardson	Virginia Department of Environmental Quality
	Federal Government
Christopher Mew	Los Alamos National Laboratory
Grace Petersen	U.S. Navy
Mark Rodriguez	U.S. Air Force
Stephen Stacy	U.S. Army Corps of Engineers
Tom Walker	U.S. Environmental Protection Agency
Alexander Wardle	U.S. Environmental Protection Agency
	International Government
Melinda Morris	South Australian Environment Protection Authority
	Academia
Nicholas Albergo	University of South Florida
Todd Halihan	Oklahoma State University
Andrea Rhoades	Colorado State University
	Emeritus
Lloyd Dunlap	Emeritus
	Industry Affiliates
Bianca Abrera	TRC
Pam Barnett	Racer Properties, LLC
Rachel Bosch	AECOM
John Bracken	Verdantas LLC
Brad Cross	ERM
Joann Dyson	GHD
Jim Finegan	Kleinfelder
John Fontana	Vista Geoscience
Samantha M. Frandsen	Aestus, LLC.
Taylor Hochbein	Geosyntec Consultants
Mark Johannes	ERM
Patrick Kelly	Woodard & Curran
Thomas Koester	S2C2, LLC

Acknowledgements

Kyle Kohler	Ramboll
Matt Kyrias	BBJ Group LLC
Brent Lazenby	Geosyntec Consultants
Karla Leslie	Parsons
Erin Mack	Corteva
Sriram Madabhushi	AECOM
Todd Miller	Kennedy/Jenks Consultants
Christopher Mulry	Groundwater & Environmental Services, Inc.
Suzanne O'Hara	Geosyntec Consultants
Harry O'Neill	Beacon Environmental
Bob O'Neill	Brown and Caldwell
Ethan Paul	ERM
Heather Reccelli	Ramboll
Collin Schohn	BBJ Group LLC
Elizabeth Schwartz	TRC
Mark Shruve	EA Engineering, Science, Technology, Inc., PBC
Lizanne Simmons	Kleinfelder
John Sohl	Columbia Technologies, LLC
Randy St. Germain	Dakota Technologies
Dan Walker	EA Engineering, Science, Technology, Inc., PBC
Ying Wang	WSP
Edward Winner	Remediation Products Inc.
Michael Worden	Civil & Environmental Consultants, Inc.
Ryan Wymore	CDM Smith
Julio Zimbron	E-Flux

The Team thanks the many others who offered advice, suggestions, reviews, and comments.

GLOSSARY

Active sensors
A solid-state chip that collects the return of a transmitted signal from an emitting source; for example, the return signal from a radar or light detection and ranging (LiDAR) camera.

Advection
Transport of solutes by flowing groundwater.

Alluvial
Unconsolidated rock or sediment that has been shaped by water and redeposited in a nonmarine setting.

Alluvial channel
A feature formed by the scouring effect of a river, typically under high energy conditions. It is therefore often coarser grained and more permeable than adjacent geologic units.

Aperture
The opening that allows light into the camera or onto the sensor.

Bedrock
When applied to rocks, this term includes the complete spatial and geometrical configuration of all those components that make up the rock. It covers terms such as texture, structure, and preferred orientation and so is an all-encompassing term that describes the shapes and characters of individual parts of a rock mass and the manner in which the parts are distributed and oriented in space. The individual parts are considered as contributing to a bedrock only if they occur repeatedly in a reproducible manner form one sample of rock to another (Horst et al. 2018).

Capillary boundary
The pore spaces in soil just above the water table that may contain water above the static level from interactive forces between the water and soil.

Charged coupled device (CCD) sensors
A type of integrated circuit madeup of a capacitor array that accumulates electric charge relative to light intensity and converts the charge to voltage.

Complementary metal–oxidesemiconductor (CMOS) sensors or active-pixel sensor
A type of integrated circuit with amplifiers in each pixel capacitor that accumulates electric charge relative to light intensity and converts the charge to voltage.

Conceptual site model (CSM)
Representation of the site that summarizes and helps project planners visualize and understand available information. The CSM is the primary planning and decision-making tool used to identify the key issues and the data necessary to transition a project from characterization through post remedy. It documents current site conditions and serves to conceptualize the relationship between chemicals in environmental media, sources, and receptors through consideration of potential or actual migration and exposure pathways.

Constituents/contaminants of concern (COCs)
Chemicals, compounds, elements detected in environmental media (soil, groundwater, surface water, sediment, air) above regulatory criteria or that pose an unacceptable risk to human health and the environment, as identified in the risk assessments.

Continuously operating reference system (CORS)
A network of continuously operating ground stations, maintained by the US National Geodetic Survey, that provide global satellite data consisting of carrier phase and code range measurements to support 3D positioning throughout the United States, its territories, and a few foreign countries.

Cultural noise sources
Aeromagnetic data, especially in highly populated areas, are often masked by undesirable magnetic signals from near-surface human-made objects—known as "cultural noise"—making post-processing and interpretation of the aeromagnetic data difficult.

Dense nonaqueous phase liquid (DNAPL)
A liquid that has a density greater than water and is immiscible with water (for example, coal tars, creosote, tank bottoms, bunker (marine) 8675 fuel, and chlorinated solvents). DNAPL may also be referred to as heavy NAPL.

Diffusion
The process of ionic or molecular constituents moving from a region of high concentration to a region of low concentration caused by their molecular motion in the absence of turbulent mixing.

Digital elevation model (DEM)
A digital image in which each pixel has an elevation value that represents the ground surface terrain or relief, not the contour of trees, buildings, or other objects that may obscure the ground surface or protrude above the ground surface.

Digital surface model (DSM)
A digital image in which each pixel has an elevation value that represents the surface relief, such as the tree canopy, buildings, or bare ground when it is exposed.

Direct-push technology
Casing is pushed (usually with a hydraulic hammer) into the subsurface without drilling or auguring. Little or no annular space is created using this method.

Dispersion
The spreading of a solute from the expected groundwater flow path as a result of mixing of groundwater.

Drive rod
The sections of direct-push drilling rod added to the direct sensing probe to extend the depth.

Drone
The airframe, propulsion system, navigation equipment, and flight controller (often composed of GPS, onboard stabilization, and autonomous flight computer) and its payload (for example, camera).

Electrical resistivity
The intrinsic resistance of the subsurface to transport an electrical charge via conduction mechanisms.

Field of view (FOV)
A measure of the area on the surface of the ground that is observed by a single sensor.

Focal length
The distance between the lens and sensor when the camera is correctly focused on an object.

Gimbal
A camera mount that allows the camera to move up and down and left to right.

Ground control points (GCPs)
Manually surveyed ground targets that are clearly visible in the collected data and can be used to measure vertical and horizontal error between the calculated point coordinates and the surveyed coordinates.

Ground sampling distance (GSD)
A description of spatial resolution in terms of the dimension of a square pixel per area on the ground.

Halogenated
Natural and synthetic chemicals that contain one or more halogens (fluorine, chlorine, bromine, or iodine) combined with carbon and other elements.

High resolution site characterization (HRSC)
HRSC uses dynamic strategies and techniques and scale-appropriate spatial and temporal measurement and sample density to define contaminant distributions and the physical context in which they reside (such as geology, hydrostratigraphy, groundwater flow conditions, preferential pathways, matrix properties, source architecture, and other factors that control contaminant distribution, fate, and transport) with greater certainty, supporting faster and more effective site cleanup.

Hydraulic conductivity
The rate that water can move through a saturated porous medium; defined as a proportionality constant (which includes the intrinsic permeability, the fluid density, a gravitational constant, and the dynamic viscosity).

Hyperspectral camera
A camera that collects spectral data on tens to hundreds of narrow spectral bands over its coverage range.

Inertial measurement unit (IMU)
Electronic measurement of roll, pitch, and yaw, which is combined with GPS data to determine the drone's geolocation.

ISO
A scale of light sensitivity for a digital sensor that is comparable to ISO of film.

[Bedrock] Joint
A fracture or break in rock that lacks any visible or measurable movement parallel to the fracture surface.

Karst
Rock formations, typically limestone or dolomite, formed by dissolution of rock and often characterized topographically by sinkholes, sinking streams, and closed depressions and characterized in the subsurface and by porosity features such as bedding planes, pinnacles, conduits, and caves.

LiDAR
A camera that uses pulses of laser light, near-infrared (about 1,000 nm) to image objects and measure distances.

Light nonaqueous phase liquid (LNAPL)
A liquid (for example, petroleum oil, gasoline, diesel fuel) that has a density less than water and is immiscible with water.

Lines of evidence
Pieces of evidence organized to show relationships among multiple hypotheses or complex interactions among agents, events, or processes. A weight of evidence approach includes the assignment of a numeric weight to each line of evidence.

Lithology
Soil or rock type and origin.

Long-wave infrared camera (LWIR)
A camera having a sensor to detect wavelengths above 10,000 nm, a range that is referred to as thermal infrared.

Membrane
A semipermeable, thin film polymer that is permeable to gas but impermeable to liquids.

Multispectral camera
A camera that collects data on three to nine relatively wide bands in near-infrared and red spectra.

Navigational GPS
Satellite-based system that provides geolocation and time information to a global positioning system (GPS) receiver using four or more GPS satellites.

Nonaqueous phase liquid (NAPL)
A liquid that is immiscible with water.

Fracture orientation
The strike and dip of an inclined plane.

Orthomosaic
A consolidated image, built from a collection of aerial images, corrected to remove distortions caused by camera perspective.

Passive sensors
A solid-state chip that collects reflected, ambient light across a defined region of the electromagnetic spectrum—for example, the light collected by a camera.

Permeability
Intrinsic measure of the ability of a porous material to allow fluids to past through it.

Photo stitching
The combining of multiple photographic images, having overlapping fields of view, to produce a high-resolution image or panoramic image.

Pixel pitch
The width of an individual pixel on a sensor relative to the width of the whole sensor.

Plume
An elongated body of groundwater containing contaminants, emanating from a point source or multiple sources and migrating within a hydrogeologic unit(s). The shape and movement of the mass of the contaminated water is affected by the geology, biochemistry, geochemistry, contaminants, and the flow characteristics of the groundwater. Because they often travel through discrete fractures and fracture sets, bedrock plumes are commonly asymmetrical in shape. Therefore, in bedrock, it may be more appropriate to use the terms “contaminant distribution” or “area of impact.”

Point cloud
A collection of data points (latitude, longitude, and altitude) within a defined coordinate system that is assembled in digital space to represent a surface.

Porosity (primary, secondary)
The ratio of the void volume to the total volume in geologic material. For primary porosity the void volume is the intergranular or inter-crystalline space. For fracture porosity the void volume is the space within fractures.

Post-processed kinematic (PPK) GPS
The use of location data from a base station or a network of operating reference system receivers to correct image coordinates after the flight data collection.

Precipitation
The process of a chemical separating from a solution.

Preferential pathway
A high-permeability conduit for contaminant migration, such as utility penetrations, lines, or drains; building sumps or drainage pits; elevator shafts; fractures in bedrock; or gravel channels.

Probe
Direct sensing instrument attached to the lead end of a drilling rod.

Qualitative data
A measurement (for example, LIF and PID measurements) that provides a relative measure of absence or presence of a compound but is not suitable as stand-alone data for making remedy decisions.

Quantitative data
Compound-specific values in units of concentration based on traceable standards (for example, µg/l, ppm, ppbv).

Rayleigh waves
Surficial seismic waves that travel along the earth's surface or other solid medium. They are characterized by elliptical motion perpendicular to a surface. They possess generally larger amplitudes and more displacement than other surface waves.

Real-time kinematic (RTK) GPS
The use of at least one additional GPS receiver at a nearby known static position to continuously supplement the GPS data from a satellite-based system.

Receptor
An individual, plant, or animal that has the potential to be exposed to a contaminant in the environment media.

Remote sensing
Gathering of data from a distance by use of an airborne detector.

Saturated zone
Area below the unsaturated zone in which all the soil pores and rock fractures are filled with water.

Semiquantitative data
Compound-specific quantitative measurements based on traceable standards but in units other than concentrations (for example, ng or ug) or that provide measurements within a range.

Semivolatile organic compounds (SVOC)
A subgroup of volatile organic compounds that tend to have a higher molecular weight and higher boiling point temperature.

Sensor
A solid-state chip that converts an optical image to an electronic signal.

Site characterization
The process of developing an understanding of the geologic, hydrologic, and engineering properties at the site, including the soil, rock, groundwater and, in many cases, human-modified conditions in the subsurface (for example, utilities, structures, mines and tunnels) that can impact site conditions (Benson and Yuhr 2016).

Stakeholder
A person, a group, or an organization that is either affected or potentially affected, or has any interest in the project or in the project's outcome, either directly or indirectly (Congressional Commission 1997).

Stratigraphy
The sequence of soil and rock layers in the subsurface, typically informed by an understanding of the natural processes that led to that sequence (for example, deposited in a marine environment versus laid down by a river).

String potentiometer (a.k.a. String pot)
A transducer used to detect and measure linear position and velocity using a flexible cable and spring-loaded spool. Used to measure the depth of a probe in a borehole during advancement.

Surface geophysical tool
A class of nonintrusive geophysical instruments used to evaluate the subsurface. They indirectly measure physical properties of materials from signals produced by natural or generated sources and rely on contrasts in the properties of different materials.

Time-resolved
Activities measured with respect to time.

Transmissivity
The product of hydraulic conductivity and aquifer saturated thickness. For a discrete fracture, the aquifer saturated thickness is the effective aperture.

Trunk line
Cable connecting a probe instrument to the aboveground data acquisition instruments.

Unconsolidated formation
Loosely bound sediments such as sand, gravel, silt, and clay that have not been hardened by burial or geologic processes. Typically, easy to excavate and penetrate with direct-push tools but may collapse easily.

Unmanned aerial systems (UAS)
The airframe, propulsion system, navigation equipment, and flight controller (often composed of GPS, onboard stabilization, and autonomous flight computer) and its payload (for example, camera).

Unmanned aerial vehicle (UAV)
An airframe that is unmanned, often referred to as a "drone." The UAV is a component of a UAS, which includes all elements that enable the drone to fly and perform specific tasks.

Vadose zone
The portion of the subsurface above the groundwater table in which the pore space is filled with both air and water. The vadose zone is also referred to as the unsaturated zone.

Volatile organic compounds (VOC)
Organic chemicals that have a high vapor pressure at ordinary room temperature.

ACRONYMS

ASCT	advanced site characterization tools
ATV	acoustic televiewer
BTEX	benzene, toluene, ethylbenzene, and xylenes
CPT	cone penetrometer testing
CSM	conceptual site model
DFN	discrete fracture network
DNAPL	dense nonaqueous phase liquid
DyeLIF©	dye-enhanced laser induced fluorescence
EC	electrical conductivity
ECD	electron capture detector
EM	electromagnetic
EMFM	electromagnetic flow meter
ERI	electrical resistivity imaging
ERT	electric resistivity tomography
EXIF	exchange image file
FAA	Federal Aviation Administration
FACT	FLUTe activated carbon technique
FDEM	frequency domain electromagnetic
FID	flame ionization detector
FLUTe	Flexible Liner Underground Technology
FOV	field of view
GC	gas chromatograph
GCP	ground control point
GNSS	global navigation satellite system
gpm	gallons per minute
GPR	ground penetrating radar

GPS	global positioning system
GRM	generalized reciprocal method
GSD	ground sampling distance
HPFM	heat pulse flowmeter
HPT	hydraulic profiling tool
HPT-GWP	HPT groundwater profiler
HPT-GWS	HPT groundwater sampler
HRSC	high resolution site characterization
IMU	inertial measurement unit
IR	infrared
ISO	As used in this document, a defined term related to the sensitivity of a camera sensor to light
LED	light-emitting diode
LiDAR	light detection and ranging
LIF	laser-induced fluorescence
LNAPL	light nonaqueous phase liquid
LWIR	long-wave infrared
MASW	multichannel analysis of surface waves
MiHPT	membrane interface probe–hydraulic profiling tool (with electrical conductivity
MIP	membrane interface probe
MTBE	methyl tertiary-butyl ether
NAPL	nonaqueous phase liquid
NDVI	normalized difference vegetation index
NIR	near-infrared reflectance
NMR	nuclear magnetic resonance
NNLS	non-negative least squares
OIP	Optical Image Profiler
OIP-G	Optical Image Profiler-green

OTV	optical televiewer
PAH	polycyclic aromatic hydrocarbon
PCE	tetrachloroethene (also referred to as perchloroethene)
PID	photoionization detector
QA	quality assurance
QC	quality control
RADAR	radio detection and ranging
RE	reference emitter
%RE	response relative to a reference emitter calibration standard
ROST	Rapid Optical Screening Tool
RPAS	remotely piloted aircraft system
RTK	real-time kinematic
SEER	Scenario Evaluator for Electrical Resistivity
SVOC	semivolatile organic compound
TarGOST	Tar-Specific Green Optical Screening Tool
TCE	trichloroethene
TDEM	time domain electromagnetic
UAS	unmanned aircraft system
UAV	unmanned aerial vehicle
USEPA	US Environmental Protection Agency
USGS	US Geological Survey
UV	ultraviolet
UVOST	Ultraviolet Optical Screening Tool
VIS	visible spectrum
VOC	volatile organic compound
VRS	vertical resistivity sounding
Waterloo APS	Waterloo Advanced Profiling System

XRF	x-ray fluorescence
XSD	halogen-specific detector

REFERENCES

3DInsider. 2019. "Part 107 Drone Exam Practice Tests Questions." 3DInsider. https://3dinsider.com/part-107-test-questions/.

Abichou, Tarek, Nizar Bel Hadj Ali, Sakina Amankwah, Roger Green, and Eric S. Howarth. 2023. "Using Ground- and Drone-Based Surface Emission Monitoring (SEM) Data to Locate and Infer Landfill Methane Emissions." *Methane* 2 (4): 440–51. https://doi.org/10.3390/methane2040030.

Adamson, D. T., S. Chapman, N. Mahler, et al. 2014. "Membrane Interface Probe Protocol for Contaminants in Low-Permeability Zones." *Groundwater.* 52 (4): 550–65. https://doi.org/https://doi.org/10.1111/gwat.12085.

Adão, T., J. Hruška, L. Pádua, et al. 2017. "Hyperspectral Imaging: A Review on UAV-Based Sensors, Data Processing and Applications for Agriculture and Forestry." *Remote Sensing* 9 (11). https://doi.org/https://doi.org/10.3390/rs9111110.

ADEC. 2024. "Field Sampling Guidance." Alaska Department of Environmental Conservation. https://dec.alaska.gov/media/2kcbhgia/field-sampling-guidance-2024.pdf.

Agyemang, Victor Ofori. 2022. "Groundwater Exploration by Magnetotelluric Method within the Birimian Rocks of Mankessim, Ghana." *Applied Water Science* 12 (3): 26. https://doi.org/10.1007/s13201-022-01576-9.

Aldstadt, J. 2002. *An In-Situ Laser-Induced Fluorescence System for Polycylic Aromatic Hydrocarbon-Contaminated Sediments (Final Report – Project Number GL975149-01-0, Submitted to United States Environmental Protection Agency Great Lakes National Program Office, Chicago, Illinois).*

ALT. 2023. "OBI40-GR-2G Optical Borehole Imager." Advance Logic Technology. https://mountsopris.com/wp-content/uploads/2026/02/QL40-OBI-2G_OBI40-GR-2G.pdf.

Annan, A. P. 2003. *Ground Penetrating Radar: Principles, Procedures & Applications*. Sensors & Software Incorporated.

Annan, Peter. 2009. "Section 1. Electromagnetic Principles of Ground Penetrating Radar." In *Ground Penetrating Radar: Theory and Applications*. https://doi.org/DOI:10.1016/B978-0-444-53348-7.00001-6.

API. 2017. *API Publication 4784 Quantification of Vapor Phase-Related Natural Source Zone Depletion Processes*. American Petroleum Institute. https://standards.globalspec.com/std/10164963/api-publ-4784.

Apitz, Sabine, Lisa M. Borbridge, Kim Bracchi, and Stephen H. Lieberman. 1993. "Fluorescent Response of Fuels in Soils: Insights into Fuel-Soil Interactions." *Environmental Process and Treatment Technologies, SPIE* 1716.

Ashadi, Abdul Latif, Bulent Tezkan, Pritam Yogeshwar, et al. 2024. "Magnetotelluric Case Study from Ain Al-Harrah Hot Spring, Al-Lith, Saudi Arabia." *Arabian Journal for Science and Engineering* 49 (1): 899–912. https://doi.org/10.1007/s13369-023-08293-8.

ASNT. 2011. "Recommended Practice No. SNT-TC-1A Personnel Qualifications and Certification in Nondestructive Testing." The American Society for Nondestructive Testing. https://source.asnt.org/2071-snt-tc-1a-2011/.

ASTM. 2010. *D6187-10.* Standard Practice for Cone Penetrometer Technology Characterization of Petroleum Contaminated Sites with Nitrogen Laser-Induced Fluorescence. ASTM International.

ASTM. 2011. *D6429-99(2011)E1*. Standard Guide for Selecting Surface Geophysical Methods. (Withdrawn 2020). ASTM International.

ASTM. 2012. *D5778-12.* Standard Test Method for Electronic Friction Cone and Piezocone Penetration Testing of Soils. ASTM International.

ASTM. 2013. *D7242/D7242M - 06(2013)E1.* 2013 Standard Practice for Field Pneumatic Slug (Instantaneous Change in Head) Tests to Determine Hydraulic Properties of Aquifers with Direct Push Groundwater Samplers. ASTM International.

ASTM. 2017. *D7352-17.* Standard Practice for Direct Push Technology for Volatile Contaminant Logging with the Membrane Interface Probe (MIP). ASTM International.

ASTM. 2018. *D5753-18 Standard Guide for Planning and Conducting Borehole Geophysical Logging*. Standard Test Method for Electronic Friction Cone and Piezocone Penetration Testing of Soils. ASTM International.

ASTM. 2019. *D6432-19.* Standard Guide for Using Surface Ground Penetrating Radar Method for Subsurface Investigation. ASTM International.

ASTM. 2020a. *D6820-20*. Standard Guide for Use of the Time Domain Electromagnetic Method for Geophysical Subsurface Site Investigation. ASTM International.

ASTM. 2020b. *E1689-20.* Standard Guide for Developing Conceptual Site Models for Contaminated Sites. ASTM International. **https://store.astm.org/e1689-20.html**.

ASTM. 2022. *E3361-22.* Standard Guide for Estimating Natural Attenuation Rates for Non-Aqueous Phase Liquids in the Subsurface. ASTM International. **https://store.astm.org/e3361-22.html**.

Atekwana, Estella A., and Eliot A. Atekwana. 2010. "Geophysical Signatures of Microbial Activity at Hydrocarbon Contaminated Sites: A Review." *Surveys in Geophysics* 31 (2): 247–83. **https://doi.org/10.1007/s10712-009-9089-8**.

Atekwana, Estella A., Eliot A. Atekwana, Leonard O. Ohenhen, and Silvia Rossbach. 2024. "Biogeophysics for Optimized Characterization of Petroleum-Contaminated Sites." In *Advances in the Characterisation and Remediation of Sites Contaminated with Petroleum Hydrocarbons*, edited by Jonás García-Rincón, Evangelos Gatsios, Robert J. Lenhard, Estella A. Atekwana, and Ravi Naidu. Springer International Publishing. **https://doi.org/10.1007/978-3-031-34447-3_9**.

Auken, Esben, Tue Boesen, and Anders V. Christiansen. 2017. "Section Two - A Review of Airborne Electromagnetic Methods with Focus on Geotechnical and Hydrological Applications From 2007 to 2017." In *Advances in Geophysics*, edited by Lars Nielsen, vol. 58. Elsevier.

Baines, Dave, Derald G. Smith, Duane G. Froese, Paul Bauman, and Grant Nimeck. 2002. "Electrical Resistivity Ground Imaging (ERGI): A New Tool for Mapping the Lithology and Geometry of Channel-Belts and Valley-Fills." *Sedimentology* 49 (3): 441–49. **https://doi.org/10.1046/j.1365-3091.2002.00453.x**.

Baker, Gregory. 1999. "Processing Near-Surface Seismic-Reflection Data: A Primer." *Society of Exploration Geophysicists*, ahead of print. **https://doi.org/https://doi.org/10.1190/1.9781560802020**.

Baker, Michael. 2004. *Final Supplemental Groundwater Characterization Report Bishop Tube Site*. Harrisburg, Pennsylvania.

Beck, Frank P., Patrick J. Clark, and Robert Puls. 2000. "Location and Characterization of Subsurface Anomalies Using a Soil Conductivity Probe." *Ground Water Monitoring and Remediation - GROUND WATER MONIT REMEDIAT* 20: 55–59. **https://doi.org/10.1111/j.1745-6592.2000.tb00265.x**.

Becker, Matthew W., Francine Cason, Megan Ward-Baranyay, Craig Divine, Jonah Munholland, and Erik Zardouzian. 2025. "Monitoring Groundwater Thermal Treatment Using a Fiber-Optic Distributed Temperature Sensing Network." *Sensors* 25 (23): 7105. **https://doi.org/10.3390/s25237105**.

Benson, Richard, and Lynn Yuhr. 2016. "What Is Site Characterization." In *Site Characterization in Karst and Pseudokarst Terraines*. **https://link.springer.com/section/10.1007/978-94-017-9924-9_11**.

Berlman, I. B. 1971. *Handbook of Fluorescence Spectra of Aromatic Molecules.* Academic Press, New York. Academic Press.

Binley, Andrew, Susan S. Hubbard, Johan A. Huisman, et al. 2015. "The Emergence of Hydrogeophysics for Improved Understanding of Subsurface Processes over Multiple Scales." *Water Resources Research* 51 (6): 3837–66. **https://doi.org/10.1002/2015WR017016**.

Bowling, Jerry C., Antonio B. Rodriguez, Dennis L. Harry, and Chunmiao Zheng. 2005. "Delineating Alluvial Aquifer Heterogeneity Using Resistivity and GPR Data." *Groundwater* 43 (6): 890–903. **https://doi.org/10.1111/j.1745-6584.2005.00103.x**.

Bumberger, Jan, Dirk Radny, Andreas Berndsen, Tobias Goblirsch, Johannes Flachowsky, and Peter Dietrich. 2011. "Carry-Over Effects of the Membrane Interface Probe." *Ground Water* 50: 578–84. **https://doi.org/10.1111/j.1745-6584.2011.00879.x**.

Burgués, Javier, and Santiago Marco. 2020. "Environmental Chemical Sensing Using Small Drones: A Review." *Science of The Total Environment* 748 (December): 141172. **https://doi.org/10.1016/j.scitotenv.2020.141172**.

Burks, Jarrod. 2016. *The Highland County Gist Settlement (33Hi417): Archaeological Investigation into the Results of Manumission at a Settlement of Freedmen in Southern Ohio*. **https://doi.org/10.13140/RG.2.2.11869.61923**.

Butler Jr, James Johnson. 2019. *The Design, Performance, and Analysis of Slug Tests*. 2nd Edition. CRC Press. **https://doi.org/https://doi.org/10.1201/9780367815509**.

Carey, Dr. Grant R. 2016. "Mass Flux/Discharge: DNAPL and Back-Diffusion." USEPA 24th Annual NARPM Training Program. **https://porewater.com/docs/2016_NARPM_Carey-Grant_v2.pdf**.

Cascade. 2026. "WaterlooAPS." Site Characterization Technologies, Cascade. **https://www.cascade-env.com/site-characterization-technologies/waterlooaps/**.

Castendyk, D., B. Hill, P. Filiatreault, et al. 2018. "Experiences with Autonomous Sampling of Pit Lakes in North America Using Drone Aircraft and Drone Boats." Proc. 11th Inter. Conf. on Acid Rock Drainage (ICARD) & Inter. Mine Water Assoc. (IMWA) 2018 Ann. Conf., Pretoria, South Africa, September 10.

Castendyk, D., B. Straight, P. Filiatreault, and US Patent Office Application. 2017. Apparatus connecting a water sample bottle to an unmanned aerial vehicle (UAV) in order to collect water samples from below the surface of a water body. issued 2017.

Castendyk, Devin, Jimmy Voorhis, and Bradley Kucera. 2020. "A Validated Method for Pit Lake Water Sampling Using Aerial Drones and Sampling Devices." *Mine Water and the Environment* 39 (3): 440–54. https://doi.org/10.1007/s10230-020-00673-y.

Chang, Chih-Chung, Jia-Lin Wang, Chih-Yuan Chang, Mao-Chang Liang, and Ming-Ren Lin. 2016. "Development of a Multicopter-Carried Whole Air Sampling Apparatus and Its Applications in Environmental Studies." *Chemosphere* 144 (February): 484–92. https://doi.org/10.1016/j.chemosphere.2015.08.028.

Choe, Eunyoung, Freek van der Meer, Frank van Ruitenbeek, Harald van der Werff, Boudewijn de Smeth, and Kyoung-Woong Kim. 2008. "Mapping of Heavy Metal Pollution in Stream Sediments Using Combined Geochemistry, Field Spectroscopy, and Hyperspectral Remote Sensing: A Case Study of the Rodalquilar Mining Area, SE Spain." *Remote Sensing of Environment* 112 (7): 3222–33. https://doi.org/10.1016/j.rse.2008.03.017.

Christiansen, Anders Vest, and Esben Auken. 2012. "A Global Measure for Depth of Investigation." *Geophysics* 77 (4): WB171–77. https://doi.org/10.1190/geo2011-0393.1.

Christy, T. M. 1996. "Driveable Permeable Membrane Sensor for the Detection of Volatile Compounds in Soil." *Tenth National Outdoor Action Conference* (Las Vegas, NV), 169–77.

Clements, A., R. Duvall, D. Greene, and T. Dye. 2022. *The Enhanced Air Sensor Guidebook*. EPA/600/R-22/213. Washington, D.C. https://cfpub.epa.gov/si/si_public_record_report.cfm?Lab=CEMM&dirEntryId=356426.

Cohen, Robert M., Anthony P. Bryda, Scott T. Shaw, and Charles P. Spalding. 1992. "Evaluation of Visual Methods to Detect NAPL in Soil and Water." *Groundwater Monitoring & Remediation* 12 (4): 132–41. https://doi.org/10.1111/j.1745-6592.1992.tb00072.x.

Coleman, A. 2006. *Development of a Characterization and Assessment Framework for Coal Tar at MGP Sites.* EPRI Report 1010137. Palo Alto, CA.

Congressional Commission. 1997. *Framework for Environmental Health Risk Management: Final Report*. Volume 1. The Presidential/Congressional Commission on Risk Assessment and Risk Management. https://nepis.epa.gov/Exe/ZyPDF.cgi/9101K1C3.PDF?Dockey=9101K1C3.PDF.

Considine, Thomas, and Jr Albert Robbat. 2008. "On-Site Profiling and Speciation of Polycyclic Aromatic Hydrocarbons at Manufactured Gas Plant Sites by a High Temperature Transfer Line, Membrane Inlet Probe Coupled to a Photoionization Detector and Gas Chromatograph/Mass Spectrometer." *Environmental Science & Technology* 42 (4): 1213–20. https://doi.org/10.1021/es702252q.

Costanza, J., and W. M. Davis. 2000. "Rapid Detection of Volatile Organic Compounds in the Subsurface by Membrane Introduction into a Direct Sampling Ion-Trap Mass Spectrometer." *Field Analytical Chemistry & Technology* 4 (5): 246–54. https://doi.org/10.1002/1520-6521(2000)4:5%3C246::aid-fact4%3E3.0.co;2-w.

Crawford, Nicolas, M. A. Lewis, S. A. Winter, and J. A. Webster. 1999. "Microgravity Techniques for Subsurface Investigations of Sinkhole Collapses and for Detection of Groundwater Flow Paths through Karst Aquifers." *Seventh Multidisciplinary Conference on Sinkholes and the Engineering and Environmental Impacts of Karst* (Harrisburg-Hershey, Pennsylvania), 203–18.

CRCCare. 2018. *Technical Measurement Guidance for LNAPL Natural Source Zone Depletion*. Technical Report No. 44. Cooperative Research Centre for Contamination Assessment and Remediation of the Environment. https://crccare.com/wp-

content/uploads/2022/12/CRCCARETechnicalreport44_TechnicalmeasurementguidanceforLNAPLnaturalsourcezonedepletion.pdf.

Crumbling, Deana M. 2004. "The Triad Approach to Managing Decision Uncertainty for Better Cleanup Project." Region 3 RCRA CA Workshop, September 14. https://archive.epa.gov/epawaste/hazard/web/pdf/triad.pdf.

Daniels, Jeffrey J. 2000. *Ground Penetrating Radar Fundamentals.*

Day-Lewis, F. D., C. D. Johnson, L. D. Slater, et al. 2016. "A Fractured Rock Geophysical Toolbox Method Selection Tool." *Groundwater* 54 (3): 315–16. https://doi.org/10.1111/gwat.12397.

Devlin, J. F., and C. D. McElwee. 2007. "Effects of Measurement Error on Horizontal Hydraulic Gradient Estimates." *Groundwater* 45 (1): 62–73. https://doi.org/10.1111/j.1745-6584.2006.00249.x.

Devlin, J. F., P. C. Schillig, I. Bowen, et al. 2012. "Applications and Implications of Direct Groundwater Velocity Measurement at the Centimetre Scale." *GQ10: Groundwater Quality Management in a Rapidly Changing World* 127 (1): 3–14. https://doi.org/10.1016/j.jconhyd.2011.06.007.

Devlin, J. F., G. Tsoflias, M. McGlashan, and P. Schillig. 2009. "An Inexpensive Multilevel Array of Sensors for Direct Ground Water Velocity Measurement." *Groundwater Monitoring & Remediation* 29 (2): 73–77. https://doi.org/10.1111/j.1745-6592.2009.01233.x.

Divine, Craig, Shandra Justicia-León, Jennifer Martin Tilton, et al. 2023. "Min-Trap® Samplers to Passively Monitor In-Situ Iron Sulfide Mineral Formation for Chlorinated Solvent Treatment." *Groundwater Monitoring & Remediation* 43 (3): 57–69. https://doi.org/10.1111/gwmr.12595.

Dixon, J. M. 2005. "PhotochemCAD 2. A Refined Program with Accompanying Spectral Databases for Photochemical Calculations." *Photochem Photobiol* 81: 212–13.

Dobrin, M. B., and C. H. Savit. 1988. *Introduction to Geophysical Prospecting*. 4th Edition. McGraw Hill. https://webapps.unitn.it/Biblioteca/it/Web/EngibankFile/Introduction%20to%20geophysical%20prospecting.pdf.

Dojack, Lisa. 2012. *Ground Penetrating Radar Theory, Data Collection, Processing, and Interpretation: A Guide for Archaeologists.* University of British Columbia. ANTH 545B, edited by Vancouver: University of British Columbia Library. University of British Columbia.

Einarson, Murray, Adrian Fure, Randy St. Germain, Steven Chapman, and Beth Parker. 2018. "DyeLIF™: A New Direct-Push Laser-Induced Fluorescence Sensor System for Chlorinated Solvent DNAPL and Other Non-Naturally Fluorescing NAPLs." *Groundwater Monitoring & Remediation* 38 (3): 28–42. https://doi.org/10.1111/gwmr.12296.

Everett, Mark E. 2013. *Near-Surface Applied Geophysics*. Cambridge University Press.

FAA. 2016. "Remote Pilot – Small Unmanned Aircraft Systems Study Guide, FAA-G-8082-22." Federal Aviation Administration. https://www.faa.gov/sites/faa.gov/files/regulations_policies/handbooks_manuals/aviation/remote_pilot_study_guide.pdf.

FAA. 2019. "Welcome to the FAADroneZone." FAADroneZone, Federal Aviation Administration. https://faadronezone-access.faa.gov/#/.

FAA. 2021. "Small Unmanned Aircraft Systems (Small UAS) Advisory Circular, AC 107-2A." Federal Aviation Administration.

https://www.faa.gov/documentLibrary/media/Advisory_Circular/Editorial_Update_AC_107-2A.pdf.

FAA. 2026a. "Educational Users." Unmanned Aircraft Systems, Federal Aviation Administration. https://www.faa.gov/uas/educational_users.

FAA. 2026b. "Unmanned Aircraft Systems (UAS)." Drones, Federal Aviation Administration. https://www.faa.gov/uas.

Fabregat, Ivan, Francisco Gutiérrez, Carles Roqué, et al. 2017. "Reconstructing the Internal Structure and Long-Term Evolution of Hazardous Sinkholes Combining Trenching, Electrical Resistivity Imaging (ERI) and Ground Penetrating Radar (GPR)." *Geomorphology* 285 (May): 287–304. https://doi.org/10.1016/j.geomorph.2017.02.024.

Fiacco, Joe. 2010. "High Resolution Site Characterization: A Sustainable Risk Management Approach." *EHS Journal*. https://ehsjournal.org/joe-fiacco/high-resolution-site-characterization-a-sustainable-risk-management-approach/2010/.

Fields, J. Jr, T. Tandy, T. Halihan, et al. 2022. *Electrical Resistivity Imaging of an Enhanced Aquifer Recharge Site*. 19 (5). Geophys Eng. https://doi.org/doi:10.1093/jge/gxac073.

Folch, A., L. del Val, L. Luquot, et al. 2020. "Combining Fiber Optic DTS, Cross-Hole ERT and Time-Lapse Induction Logging to Characterize and Monitor a Coastal Aquifer." *Journal of Hydrology* 588 (September): 125050. https://doi.org/10.1016/j.jhydrol.2020.125050.

Fortune. 2026. "Oil & Gas/Geophysical Service Market Source." Fortune Business Insights, April. https://www.fortunebusinessinsights.com/industry-reports/geophysical-service-market-100105.

Fosco, D., M. De Molfetta, P. Renzulli, B. Notarnicola, C. Carella, and G. Fedele. 2025. "Innovative Drone-Based Methodology for Quantifying Methane Emissions from Landfills." *Waste Management* 195 (March): 79–91. https://doi.org/10.1016/j.wasman.2025.01.033.

Foti, Sebastiano, Carlo G. Lai, Glenn J. Rix, and Claudio Strobbia. 2014. "Surface Wave Methods for Near-Surface Site Characterization." https://api.semanticscholar.org/CorpusID:129683519.

Geoprobe. 1994. "A Percussion Probing Tool for The Direct Sensing of Soil Conductivity." Geoprobe Systems, A Division of KEJR, INC, March. https://geoprobe.com/direct-image/ec-electrical-conductivity.

Geoprobe. 2006. "Geoprobe® Screen Point 16 Groundwater Sampler, Standard Operating Procedure." Geoprobe Systems, A Division of KEJR, INC, November. https://geoprobe.com/sites/default/files/storage/pdfs/sp16_sop_mk3142_1106_0_0.pdf.

Geoprobe. 2015. "Geoprobe Systems® Electrical Conductivity (EC) System Standard Operating Procedure." Geoprobe Systems, A Division of KEJR, INC, January. https://geoprobe.com/sites/default/files/pdfs/EC_SOP_0115_0.pdf.

Geoprobe. 2019. "OIP Green Successfully Detects Coal Tar Fluorescence." Geoprobe Systems, A Division of KEJR, INC, January. https://geoprobe.com/articles/oip-green-successfully-detects-coal-tar-fluorescence.

Geoprobe. 2021a. "Geoprobe® Membrane Interface Probe (MIP) Standard Operating Procedure." Geoprobe Systems, A Division of KEJR, INC, March. https://geoprobe.com/sites/default/files/pdfs/MIP_SOP_mk3010_0321.pdf.

Geoprobe. 2021b. "Geoprobe® Optical Imaging Profiler (OIP) Standard Operating Procedure." Geoprobe Systems, A Division of KEJR, INC, October. https://geoprobe.com/sites/default/files/pdfs/OIP%20SOP%20rev.2.2.pdf.

Geoprobe. 2026a. "Hydraulic Profiling Tool." Geoprobe Environmental Technologies, Geoprobe Systems, A Division of KEJR, INC. https://www.geoprobe.be/en/products/direct-image/hpt-probe/.

Geoprobe. 2026b. "Hydraulic Profiling Tool - Groundwater Profilers." Geoprobe Environmental Technologies, Geoprobe Systems, A Division of KEJR, INC. https://geoprobe.com/direct-image/gw-profilers.

Gouveia, Fátima, Isabel Lopes, and Rui Carrilho Gomes. 2016. "Deeper VS Profile from Joint Analysis of Rayleigh Wave Data." *Engineering Geology* 202 (March): 85–98. https://doi.org/https://doi.org/10.1016/j.enggeo.2016.01.006.

GPG. 2017. "Geophysics for Practicing Geoscientists (GPG), Version 0.0.1." https://gpg.geosci.xyz/.

Graham, C. T., I. O'Connor, L. Broderick, M. Broderick, O. Jensen, and H. T. Lally. 2022. "Drones Can Reliably, Accurately and with High Levels of Precision, Collect Large Volume Water Samples and Physio-Chemical Data from Lakes." *Science of The Total Environment* 824 (June): 153875. https://doi.org/10.1016/j.scitotenv.2022.153875.

Hale, J. 2011. "Direct-Push, Laser Induced Fluorescence Application to Fractured Rock." Paper presented at Fractured Rock and Eastern Ground Water Regional Issues Conference.

Halihan, Todd, Andrew Love, Mark Keppel, and Volmer Berens. 2013. "Analysis of Subsurface Mound Spring Connectivity in Shale of the Western Margin of the Great Artesian Basin, South Australia." *Hydrogeology Journal* 21 (7): 1605–17. https://doi.org/10.1007/s10040-013-1034-8.

Halihan, Todd, Stuart W. McDonald, Phil Patey, and Marcy Stonecipher. 2012. "ERI Evaluation of Injectates Used at a Dry-Cleaning Site." *Remediation Journal* 22 (3): 79–91. https://doi.org/10.1002/rem.21322.

Halihan, Todd, Stanley T. Paxton, Ivy Anne Graham, Thomas R. Fenstemaker, and Matt Riley. 2005. "Post-Remediation Evaluation of a LNAPL Site Using Electrical Resistivity Imaging." *Journal of Environmental Monitoring: JEM* 7 4: 283–87. https://doi.org/10.1039/b416484a.

Halihan, Todd, Valina Sefa, Tom Sale, and Mark Lyverse. 2017. "Mechanism for Detecting NAPL Using Electrical Resistivity Imaging." *Journal of Contaminant Hydrology* 205 (October): 57–69. https://doi.org/10.1016/j.jconhyd.2017.08.007.

Hatfield, K., Michael D. Annable, and P. Rao. 2006a. "Field Demonstration and Validation of a New Device for Measuring Water and Solute Fluxes at Naval Base Ventura County, Port Hueneme, CA." https://api.semanticscholar.org/CorpusID:91768397.

Hatfield, K., Michael D. Annable, and P. Suresh C. Rao. 2006b. "Field Demonstration and Validation of a New Device for Measuring Groundwater and Perchlorate Fluxes at IHDIV-NSWC, Indian Head, MD." https://apps.dtic.mil/sti/tr/pdf/ADA468561.pdf.

Hatfield, K., and P. Rao. 2006a. "Field Demonstration and Validation of a New Device for Measuring Water and Solute Fluxes NASA LC-34 SITE." https://api.semanticscholar.org/CorpusID:117070192.

Hatfield, K., and P. Rao. 2006b. *Protocol Report - Demonstration and Validation of a Water and Solute Flux Measuring Device*. ESTCP Project ER-0114. https://www.serdpestcp.org/Program-Areas/Environmental-Restoration/Contaminated-Groundwater/Monitoring/ER-200114/.

Hedlin, C. deGroot-, and S. Constable. 1990. "Occam's Inversion to Generate Smooth, Two-Dimensional Models from Magnetotelluric Data." *GEOPHYSICS,* 55 (12): 1613–24.

Hennessy, Andrew, Kenneth Clarke, and Megan Lewis. 2020. "Hyperspectral Classification of Plants: A Review of Waveband Selection Generalisability." *Remote Sensing* 12 (1): 113. **https://doi.org/10.3390/rs12010113**.

Hodgkinson, Jane, and Ralph P. Tatam. 2012. "Optical Gas Sensing: A Review." *Measurement Science and Technology* 24. **https://api.semanticscholar.org/CorpusID:122312714**.

Horricks, Ryan A., Cody Bannister, Leah M. Lewis-McCrea, James Hicks, Kiersten Watson, and Gregor K. Reid. 2022. "Comparison of Drone and Vessel-Based Collection of Microbiological Water Samples in Marine Environments." *Environmental Monitoring and Assessment* 194 (6): 439. **https://doi.org/10.1007/s10661-022-10095-8**.

Horst, John, Nicklaus Welty, Robert Stuetzle, Rick Wenzel, and Randy St. Germain. 2018. "Fluorescent Dyes: A New Weapon for Conquering DNAPL Characterization." *Groundwater Monitoring & Remediation* 38 (1): 19–25. **https://doi.org/10.1111/gwmr.12261**.

Hydro-International. 2025. "Charting Depths from above with Airborne Bathymetric Lidar." *Hydro International* (The Netherlands), February. **https://www.hydro-international.com/content/article/charting-depths-from-above-with-airborne-bathymetric-lidar**.

ITRC. 2003. *Technical and Regulatory Guidance for the Triad Approach: A New Paradigm for Environmental Project Management, SCM-1*. Interstate Technology & Regulatory Council. **https://itrcweb.org/wp-content/uploads/2024/09/SCM-1.pdf**.

ITRC. 2008. *Enhanced Attenuation: Chlorinated Organic*. Interstate Technology & Regulatory Council. **https://itrcweb.org/wp-content/uploads/2024/09/EACO-1.pdf**.

ITRC. 2010a. *Decision Framework for Applying Monitored Natural Attenuation Processes to Metals and Radionuclides in Groundwater*. Interstate Technology & Regulatory Council. **https://itrcweb.org/wp-content/uploads/2024/09/APMR1.pdf**.

ITRC. 2010b. *Frequently Asked Questions about Wide-Area Assessment for Munitions Response Projects*. Interstate Technology & Regulatory Council. **https://itrcweb.org/wp-content/uploads/2024/09/UXO-6.pdf**.

ITRC. 2013. "Environmental Molecular Diagnostics. EMD-2." Interstate Technology & Regulatory Council, Washington, D.C. **https://projects.itrcweb.org/emd-2/**.

ITRC. 2015. *Integrated DNAPL Site Characterization and Tools Selection. ISC-1.* Interstate Technology & Regulatory Council. **https://projects.itrcweb.org/DNAPL-ISC_tools-selection/**.

ITRC. 2017. "Characterization and Remediation in Fractured Rock. FracRx-1." Interstate Technology & Regulatory Council, Washington, D.C. **https://fracturedrx-1.itrcweb.org/**.

ITRC. 2018. *LNAPL Site Management: LCSM Evolution, Decision Process, and Remedial Technologies" [LNAPL-3]*. Interstate Technology & Regulatory Council. **https://lnapl-3.itrcweb.org/**.

ITRC. 2021. "Use and Measurement of Mass Flux and Mass Discharge. Maf-1." Interstate Technology & Regulatory Council, Washington, D.C. **https://maf-1.itrcweb.org/**.

ITRC. 2024. "Passive Sampling Technology Update. PSU-1." Interstate Technology & Regulatory Council, Washington, D.C. **https://psu-1.itrcweb.org/**.

ITRC. 2026. "Vapor Intrusion Toolkit." Interstate Technology & Regulatory Council, Washington, D.C. https://itrcweb.org/vapor-intrusion-toolkit/.

Jońca, Justyna, Marcin Pawnuk, Yaroslav Bezyk, Adalbert Arsen, and Izabela Sówka. 2022. "Drone-Assisted Monitoring of Atmospheric Pollution—A Comprehensive Review." *Sustainability* 14 (18): 11516. https://doi.org/10.3390/su141811516.

Jung, Sung H., Siyoon Kwon, Il W. Seo, and Jun S. Kim. 2024. "Comparison between Hyperspectral and Multispectral Retrievals of Suspended Sediment Concentration in Rivers." *Water* 16 (9): 1275. https://doi.org/https://doi.org/10.3390/w16091275.

KBYF. 2015. "Know Before You Fly." https://knowbeforeyoufly.org/.

Keys, W. S. 1988. *Borehole Geophysics Applied to Ground-Water Investigations*. Report Nos. 87–539. Open-File Report. Denver, CO. USGS Publications Warehouse. https://doi.org/10.3133/ofr87539.

Keys, W. S., R. E. Crowder, and W. J. Henrich. 1993. "Selecting Geophysical Logs for Environmental Applications." *Report Number: CONF-9305192--*, 267–83. https://www.osti.gov/biblio/6207550.

Knight, Rosemary. 2001. "Ground Penetrating Radar for Environmental Applications." In *Annual Review of Earth and Planetary Sciences*, vol. 29. no. Volume 29, 2001. Annual Reviews. https://doi.org/https://doi.org/10.1146/annurev.earth.29.1.229.

Kram, Mark, Arturo A. Keller, and Lorne Everett. 2019. "Comments in Response to 'DyeLIF™: A New Direct-Push Laser-Induced Fluorescence Sensor System for Chlorinated Solvent DNAPL and Other Non-Naturally Fluorescing NAPLs.'" *Groundwater Monitoring & Remediation* 39 (1): 73–74. https://doi.org/10.1111/gwmr.12313.

Kram, Mark L., Arturo A. Keller, Steve M. Massick, and Leroy E. Laverman. 2004. "Complex NAPL Site Characterization Using Fluorescence Part 1: Selection of Excitation Wavelength Based on NAPL Composition." *Soil and Sediment Contamination: An International Journal* 13 (2): 103–18. https://doi.org/10.1080/10588330408984082.

Kuula, J., T. Mäkelä, M. Aurela, et al. 2020. "Laboratory Evaluation of Particle-Size Selectivity of Optical Low-Cost Particulate Matter Sensors." *Atmospheric Measurement Techniques* 13 (5): 2413–23. https://doi.org/10.5194/amt-13-2413-2020.

Labaky, W., J. F. Devlin, and R. W. Gillham. 2007. "Probe for Measuring Groundwater Velocity at the Centimeter Scale." *Environmental Science & Technology* 41 (24): 8453–58. https://doi.org/10.1021/es0716047.

Lakowicz, J. R. 1999. "Principles of Fluorescence Spectroscopy, 2nd Ed." *Kluwer Academic/Plenum Publishers, New York*.

Lally, H. T., I. O'Connor, O. P. Jensen, and C. T. Graham. 2019. "Can Drones Be Used to Conduct Water Sampling in Aquatic Environments? A Review." *Science of The Total Environment* 670 (June): 569–75. https://doi.org/10.1016/j.scitotenv.2019.03.252.

Langenheim, Victoria, Andrew Morita, Allen Christensen, Geoffrey Cromwell, and Christopher P. Ely. 2019. *Depth to Bedrock Based on Modeling of Gravity Data of the Eastern Part of Edwards Air Force Base, California*. Report Nos. 2019–1128. Open-File Report. Reston, VA. USGS Publications Warehouse. https://doi.org/10.3133/ofr20191128.

Leitner, S., W. Feichtinger, S. Mayer, et al. 2023. "UAV-Based Sampling Systems to Analyse Greenhouse Gases and Volatile Organic Compounds Encompassing Compound-Specific Stable Isotope

Analysis." *Atmospheric Measurement Techniques* 16 (2): 513–27. https://doi.org/10.5194/amt-16-513-2023.

Liew, S. C., and C. W. Chang. 2012. "Detecting Submerged Aquatic Vegetation with 8-Band WorldView-2 Satellite Images." *2012 IEEE International Geoscience and Remote Sensing Symposium*, July 22, 2560–62. https://doi.org/10.1109/IGARSS.2012.6350957.

Liu, Y., J. D. Paris, M. Vrekoussis, et al. 2022. "Improvements of a Low-Cost CO_2 Commercial Nondispersive Near-Infrared (NDIR) Sensor for Unmanned Aerial Vehicle (UAV) Atmospheric Mapping Applications." *Atmospheric Measurement Techniques* 15 (15): 4431–42. https://doi.org/10.5194/amt-15-4431-2022.

Loke, M. H., J. E. Chambers, D. F. Rucker, O. Kuras, and P. B. Wilkinson. 2013. "Recent Developments in the Direct-Current Geoelectrical Imaging Method." *Journal of Applied Geophysics* 95 (August): 135–56. https://doi.org/10.1016/j.jappgeo.2013.02.017.

Lunne, Tom, P. Robertson, and John Powell. 1997. "Cone Penetration Testing in Geotechnical Practice." *Soil Mechanics and Foundation Engineering* 46. https://doi.org/10.1007/s11204-010-9072-x.

Mansoor, Nasser. 2006. "High-Resolution Geophysical Characterization of Shallow-Water Wetlands." *Geophysics* 71 (4): B101–9. https://doi.org/https://doi.org/10.1190/1.2210307.

Mantlík, František, Manuel Matias, Jose Lourenço, Carlos Grangeia, and Hélder Tareco. 2009. "The Use of Gravity Methods in the Internal Characterization of Landfills—a Case Study." *Journal of Geophysics and Engineering* 6 (4): 357. https://doi.org/10.1088/1742-2132/6/4/003.

MASW. 2018. "Multichannel Analyses of Surface Waves (MASW) - Data Acquisition." Park Seismic LLC. https://www.masw.com/DataAcquisition.html.

McCall, Wesley. 2010. *Tech Guide for Calculation of Estimated Hydraulic Conductivity Log from HPT Data*. Geoprobe. https://geoprobe.com/sites/default/files/pdfs/tech_guide_estk_v5_0_0.pdf.

McCall, Wesley, Thomas M. Christy, and Mateus K. Evald. 2017. "Applying the HPT-GWS for Hydrostratigraphy, Water Quality and Aquifer Recharge Investigations." *Groundwater Monitoring & Remediation* 37 (1): 78–91. https://doi.org/10.1111/gwmr.12193.

McCall, Wesley, Thomas M. Christy, Daniel Pipp, et al. 2014. "Field Application of the Combined Membrane-Interface Probe and Hydraulic Profiling Tool (MiHpt)." *Groundwater Monitoring & Remediation* 34 (2): 85–95. https://doi.org/10.1111/gwmr.12051.

McCall, Wesley, Thomas M. Christy, Daniel A. Pipp, et al. 2018. "Evaluation and Application of the Optical Image Profiler (OIP) a Direct Push Probe for Photo-Logging UV-Induced Fluorescence of Petroleum Hydrocarbons." *Environmental Earth Sciences* 77: 374. https://doi.org/10.1007/s12665-018-7442-2.

MDEQ. 2013. *Montana Light Non-Aqueous Phase Liquid (LNAPL) Recovery and Monitoring Guidance*. Montana Department of Environmental Quality. https://deq.mt.gov/Files/Land/StateSuperfund/Documents/montana%20LNAPL%20Recovery%20and%20Monitoring%20Guidance%20FINAL%2007_15_13.pdf.

MDEQ. 2017. *Senate Bill 96 (2015) Status of $7,000,000 Appropriation from the Orphan Share Account Environmental Quality Council – Final Report July 1, 2015 to June 30, 2017*. Montana Department of Environmental Quality. https://deq.mt.gov/files/Land/LUST/Documents/downloadables/Final%20Report%20(July%202017).pdf.

Mead, M. I., O. A. M. Popoola, G. B. Stewart, et al. 2013. "The Use of Electrochemical Sensors for Monitoring Urban Air Quality in Low-Cost, High-Density Networks." *Atmospheric Environment* 70 (May): 186–203. https://doi.org/10.1016/j.atmosenv.2012.11.060.

Meng, Fansong, Jinguo Wang, Zhou Chen, Fei Qiao, and Dong Yang. 2023. "Shaping the Concentration of Petroleum Hydrocarbon Pollution in Soil: A Machine Learning and Resistivity-Based Prediction Method." *Journal of Environmental Management* 345 (November): 118817. https://doi.org/10.1016/j.jenvman.2023.118817.

Milsom, J., and A. Eriksen. 2011. *Field Geophysics, 4th Edition.* John Wiley & Sons Ltd. https://doi.org/DOI:10.1002/9780470972311.

Morozov, Darya, David Walsh, Cristina McLaughlin, et al. 2024. "High-Resolution Direct Push NMR Tools for Groundwater Investigations." *Groundwater Monitoring & Remediation* 44 (2): 39–54. https://doi.org/10.1111/gwmr.12645.

Murray, C. J., G. V. Last, and M. J. Truex. 2005. "Review of Geophysical Techniques to Define the Spatial Distribution of Subsurface Properties or Contaminants." Pacific Northwest Laboratory, August. https://www.pnnl.gov/main/publications/external/technical_reports/PNNL-15305.pdf.

Mussett, Alan E., and M. Aftab Khan. 2012. "Looking into the Earth: An Introduction to Geological Geophysics." *Cambridge University Press.*, ahead of print, June. https://doi.org/https://doi.org/10.1017/CBO9780511810305.

National Research Council. 2000. *Seeing into the Earth: Noninvasive Characterization of the Shallow Subsurface for Environmental and Engineering Applications*. 1st ed. National Academy Press.

Nielsen, B. J. 1995. *A New Site Characterization and Monitoring Technology, Environmental Monitoring and Hazardous Waste Site Remediation*. Environmental Monitoring and Hazardous Waste Site Remediation, edited by T. Vo-Dinh.

NJDEP. 2005. *Field Sampling Procedures Manual*. New Jersey Department of Environmental Protection. https://dep.nj.gov/srp/guidance/fspm/fspm-2005/.

NOAA. 2019. "United States Interagency Elevation Inventory." National Oceanic and Atmospheric Administration. https://coast.noaa.gov/inventory/.

Noh, Daegwon, and Eunsoon Oh. 2025. "Chemical Detection Using Mobile Platforms and AI-Based Data Processing Technologies." *Journal of Sensor and Actuator Networks* 14 (1): 6. https://doi.org/10.3390/jsan14010006.

Olafsdottir, Elin Asta, Bjarni Bessason, and Sigurdur Erlingsson. 2018. "Combination of Dispersion Curves from MASW Measurements." *Soil Dynamics and Earthquake Engineering* 113 (October): 473–87. https://doi.org/https://doi.org/10.1016/j.soildyn.2018.05.025.

Ozark. 2021. *Point Velocity Probe Handbook*. Ozark Underground Laboratory. https://ozarkundergroundlab.com/assets/point-velocity-probe-handbook.pdf.

Pang, Xiaobing, Haijun Nan, Jinping Zhong, Daiqi Ye, Marvin D. Shaw, and Alastair C. Lewis. 2019. "Low-Cost Photoionization Sensors as Detectors in GC × GC Systems Designed for Ambient VOC Measurements." *Science of The Total Environment* 664 (May): 771–79. https://doi.org/10.1016/j.scitotenv.2019.01.348.

Panthi, Jeeban, Thomas Boving, Soni M. Pradhanang, and Mamoon Ismail. 2024. "Time-Lapse Geophysical Measurements for Monitoring Coastal Groundwater Dynamics in an Unconfined Aquifer." *Groundwater* 62 (4): 513–26. **https://doi.org/10.1111/gwat.13382**.

Park, Choon B. 2006. "SurfSeis User's Manual V2.0." Kansas Geological Survey. **https://www.kgs.ku.edu/software/surfseis/Manuals/Manual20.pdf**.

Park Choon B. and Carnevale Mario. 2012. "Optimum MASW Survey?Revisit after a Decade of Use." In *GeoFlorida 2010*. Proceedings. **https://doi.org/10.1061/41095(365)130**.

Park, Choon B., Richard D. Miller, and Hidetoshi Miura. 2002. "Optimum Field Parameters of an MASW Survey." **https://api.semanticscholar.org/CorpusID:6668795**.

Park, Choon B., Richard D. Miller, and Jianghai Xia. 1999. "Multichannel Analysis of Surface Waves." *Geophysics* 64: 800–808. **https://doi.org/https://doi.org/10.1190/1.1444590**.

Park, Choon B., Richard D. Miller, Jianghai Xia, and Julian Ivanov. 2007. "Multichannel Analysis of Surface Waves (MASW) - Active and Passive Methods." Kansas Geological Survey, January 1. **https://www.masw.com/files/PAR-07-A.PDF**.

Parker, Beth. 2007. "Investigating Contaminated Sites on Fractured Rock Using the DFN Approach. 2007 NGWA/U.S." *EPA Fractured Rock Conference: State of the Science and Measuring Success in Remediation, Portland, ME*, 150–68.

Parker, Beth, and J. A. Cherry. 2011. "The Discrete Fracture Network (DFN) Approach for Contaminated Bedrock Site Characterization." Center for Applied Groundwater Research, April. **https://g360group.org/wp-content/uploads/2017/11/the-discrete-fracture-network-dfn-approach-for-contaminated-bedrock-site-characterization-articles1-9-2011-04-28_final-1.pdf**.

Pasquale, G. de, N. Linde, J. Doetsch, and W. S. Holbrook. 2019. "Probabilistic Inference of Subsurface Heterogeneity and Interface Geometry Using Geophysical Data." *Geophysical Journal International* 217 (May): 816–31. **https://doi.org/10.1093/gji/ggz055**.

Peterson, J. L. 2017. "Borehole Geophysical Logging – Applications for Environmental Site Remediation (New Jersey Site Remediation Professional Licensing Board Course No. 2015-2017)." Paper presented at Princeton Geoscience, Inc. to the New Jersey Licensed Site Remediation Professionals Association and the New York – Philadelphia Section of the Association of Environmental and Engineering Geologists.

Pickens, Cullen Mikael. 2018. "Comparison between Model and Field Diesel Mass Recovery in Dolomite Karst." Oklahoma State University. **https://hdl.handle.net/20.500.14446/330757**.

Puls, Robert W., and Michael J. Barcelona. 1996. "Low-Flow (Minimal Drawdown) Groundwater Sampling Procedures, EPA/540/S-95/504." United State Environmental Protection Agency. **https://www.epa.gov/sites/default/files/2015-06/documents/lwflw2a.pdf**.

Quinnan, J. A. 2010. "Re-Evaluating MIPs - Observations on Limitations Based on Comparison with Whole-Core and Vertical Profile Sampling." Paper presented at Battelle 7th International Conference: Remediation of Chlorinated and Recalcitrant Compounds. Oral Presentation.

Randolph, Kaylan, Jeff Wilson, Lenore Tedesco, Lin Li, D. Lani Pascual, and Emmanuel Soyeux. 2008. "Hyperspectral Remote Sensing of Cyanobacteria in Turbid Productive Water Using Optically Active Pigments, Chlorophyll and Phycocyanin." *Applications of Remote Sensing to Monitoring Freshwater and Estuarine Systems* 112 (11): 4009–19. **https://doi.org/10.1016/j.rse.2008.06.002**.

Ravikumar, Arvind P., Jingfan Wang, and Adam R. Brandt. 2017. "Are Optical Gas Imaging Technologies Effective for Methane Leak Detection?" *Environmental Science & Technology* 51 (1): 718–24. **https://doi.org/10.1021/acs.est.6b03906**.

Redman, J. D. 2009. "Section 8 - Contaminant Mapping." In *Ground Penetrating Radar Theory and Applications*, edited by Harry M. Jol. Elsevier. **https://doi.org/10.1016/B978-0-444-53348-7.00008-9**.

Robertson, P. K. 1990. "Soil Classification Using the Cone Penetration Test." *Canadian Geotechnical Journal - CAN GEOTECH J* 27: 151–58. **https://doi.org/10.1139/t90-014**.

Robertson, P. K., and K. L. Cabal. 2008. *Guide to Cone Penetration Testing for Geo-Environmental Engineering, 2nd Edition.* Signal Hill, California. **https://vdoc.pub/download/guide-to-cone-penetration-testing-for-geo-environmental-engineering-107ia4ap50c8**.

Robertson, P. K., John Sully, D. J. Woeller, Tom Lunne, John Powell, and D. G. Gillespie. 2011. "Estimating Coefficient of Consolidation from Piezocone Tests." *Canadian Geotechnical Journal* 29: 539–50. **https://doi.org/10.1139/t92-061**.

Robertson, Peter K. J., R. G. Campanella, Donald G. Gillespie, and Jw Greig. 1986. "Use of Piezometer Cone Data." **https://api.semanticscholar.org/CorpusID:132007304**.

Salas, Eric Ariel L. 2021. "Waveform LiDAR Concepts and Applications for Potential Vegetation Phenology Monitoring and Modeling: A Comprehensive Review." *Geo-Spatial Information Science* 24 (2): 179–200. **https://doi.org/10.1080/10095020.2020.1761763**.

Schillig, P. C. 2012. "VelProbePE: An Automated Spreadsheet Program for Interpreting Point Velocity Probe Breakthrough Curves." *Computers & Geosciences* 39 (February): 161–70. **https://doi.org/10.1016/j.cageo.2011.06.007**.

Schlumberger. 2009. *Log Interpretation Charts, 2009 Edition.* Sugar Land, Texas. **https://dn760106.eu.archive.org/0/items/2009EditionLogInterpretationCharts/chartbook.pdf**.

Schulmeister, Marcia, James Butler Jr, J. M. Healey, L. Zheng, D. A. Wysocki, and Wes McCall. 2003. "Direct-Push Electrical Conductivity Logging for High-Resolution Hydrostratigraphic Characterization." *Ground Water Monitoring and Remediation - GROUND WATER MONIT REMEDIAT* 23: 52–62. **https://doi.org/10.1111/j.1745-6592.2003.tb00683.x**.

ScienceDirect. 2016. "Cone Penetration Test." Elsevier B.V. **https://www.sciencedirect.com/topics/engineering/cone-penetration-test**.

SDPRCF. 2005. *A Study of Managing Uncertainties Using the Triad Approach*. South Dakota Petroleum Release Compensation Fund. **https://triadcentral.clu-in.org/ref/doc/sdprcfstudy.pdf**.

Sharma, Shrey, and Gunjan Kumar Verma. 2015. *Inversion Of Electrical Resistivity Data: A Review*. **https://doi.org/10.5281/zenodo.1106169**.

Sheriff, R. E., and L. P. Geldart. 1995. *Exploration Seismology.* Cambridge University Press.

Silva, Dane, and Mitchell Scott. 2023. "Advanced Gas Emission Detection Solutions." LMOP Webinar. Detecting Landfill Methane Emissions with Drones, September 28. **https://www.epa.gov/system/files/documents/2023-10/lmop_webinar_september_28_2023.pdf**.

SIM. 2025. "Subsurface Investigation Methodology." Simspec.org. **https://www.simspec.org/**.

Simeng, Peng, Xie Xingbing, Zhang Lianqun, et al. 2025. "Application of the Magnetotelluric Method in Geothermal Exploration in Jianshi County, Hubei Province, China." *Discover Geoscience* 3 (1): 70. https://doi.org/10.1007/s44288-025-00181-y.

Slonecker, Terrence, Gary B. Fisher, Danielle P. Aiello, and Barry Haack. 2010. "Visible and Infrared Remote Imaging of Hazardous Waste: A Review." *Remote Sensing* 2 (11): 2474–508. https://doi.org/10.3390/rs2112474.

Sørensen, Kurt, and Esben Auken. 2004. "SkyTEM – A New High-Resolution Helicopter Transient Electromagnetic System." *Exploration Geophysics* 35: 194–202. https://doi.org/10.1071/EG04194.

Spinelle, Laurent, Michel Gerboles, Gertjan Kok, Stefan Persijn, and Tilman Sauerwald. 2017. "Review of Portable and Low-Cost Sensors for the Ambient Air Monitoring of Benzene and Other Volatile Organic Compounds." *Sensors* 17 (7): 1520. https://doi.org/10.3390/s17071520.

Spinelle, Laurent, Michel Gerboles, Maria Gabriella Villani, Manuel Aleixandre, and Fausto Bonavitacola. 2015. "Field Calibration of a Cluster of Low-Cost Available Sensors for Air Quality Monitoring. Part A: Ozone and Nitrogen Dioxide." *Sensors and Actuators B: Chemical* 215 (August): 249–57. https://doi.org/10.1016/j.snb.2015.03.031.

Spurlin, Matthew S., Brent W. Barker, Bradley D. Cross, and Craig Divine. 2019. "Nuclear Magnetic Resonance Logging: Example Applications of an Emerging Tool for Environmental Investigations." *Remediation Journal* 29: 63–73. https://doi.org/10.1002/rem.21590.

St. Germain, R. 2008. "Remediation Technology Symposium." May 14.

St. Germain, R., and T. Martin. 2008. "North American Environmental Field Conference & Exposition - LIF Workshop Slides." https://clu-in.org/download/char/lif/Dakota-Technologies-LIF-Workshop.pdf.

St. Germain, Randy. 2011. "Laser-Induced Fluorescence (LIF) Primer." *Applied NAPL Science Review, Demystifying NAPL Science for the Remediation Manager.* 1 (9). https://www.dakotatechnologies.com/about/newsletters/article/2016/03/16/laser-induced-fluorescence-primer.html.

St. Germain, Randy. 2022. "Managing NAPL Heterogeneity's Hijinks Part 1." *ANSR* 10 (8). https://naplansr.com/managing-napl-heterogeneitys-hijinksvolume-10-issue-8-december-2022/.

St. Germain, Randy. 2023. "Managing NAPL Heterogeneity's Hijinks Part 2." *ANSR* 11 (1). https://naplansr.com/part-2-of-managing-napl-heterogeneitys-hijinksvolume-11-issue-1-march-2023/.

St. Germain, Randy. 2024. "High-Resolution Delineation of Petroleum NAPLs." In *Advances in the Characterization and Remediation of Sites Contaminated with Petroleum Hydrocarbons*, edited by Jonás García-Rincón, Evangelos Gatsios, Robert J. Lenhard, Estella A. Atekwana, and Ravi Naidu. Springer International Publishing. https://doi.org/10.1007/978-3-031-34447-3_8.

St. Germain, Randy. 2025. "Recently Discovered Trait in Coal Tar and Creosote Fluorescence Leads to Greatly Reduced Reliance on Validation Sampling." Group 2, Poster Board #46). Battelle 2025 Sediments Conference. https://www.dropbox.com/scl/fi/rq0zdl28wnbzygg5uiz7k/Bayou-Bonfouca-Creosote-NAPL-vs-False-Positives-Case-Study.pdf?rlkey=nczn527aictpfcoor02fyskq0&e=1&dl=0.

St. Germain, Randy, M. Einarson, A. Fure, S. Chapman, and B. Parker. 2014. "Dye Based Laser-Induced Fluorescence Sensing of Chlorinated Solvent DNAPLs." Paper presented at 3rd International Symposium on Cone Penetration Testing. https://www.dakotatechnologies.com/about/newsletters/article/2014/08/06/dye-based-laser-induced-fluorescence-sensing-of-chlorinated-solvent-dnapls.html.

Stonecipher, Marcy, and Stuart McDonald. 2011. "Correlation of High Resolution Eri Results to Geochemical Zonation at a Degraded LNAPL Site in Grand Junction, Colorado." https://api.semanticscholar.org/CorpusID:131112840.

Straight, Brian J., Devin N. Castendyk, Diane M. McKnight, Connor P. Newman, Pierre Filiatreault, and Americo Pino. 2021. "Using an Unmanned Aerial Vehicle Water Sampler to Gather Data in a Pit-Lake Mining Environment to Assess Closure and Monitoring." *Environmental Monitoring and Assessment* 193 (9): 572. https://doi.org/10.1007/s10661-021-09316-3.

Telford, W. M., L. P. Geldart, and R. E. Sheriff. 1990. *Applied Geophysics*. 2nd ed. Cambridge University Press. Cambridge Core. https://doi.org/10.1017/CBO9781139167932.

Tyler, Scott W., John S. Selker, Thom Bogaard, Nick van de Giesen, and Juan Aquilar-Lopez. 2022. *Distributed Fiber-Optic Hydrogeophysics*. The Groundwater Project. https://doi.org/https://doi.org/10.21083/978-1-77470-031-0.

Ulrich, Shannon, Jennifer Martin Tilton, Shandra Justicia-Leon, et al. 2021. "Laboratory and Initial Field Testing of the Min-Trap™ for Tracking Reactive Iron Sulfide Mineral Formation during in Situ Remediation." *Remediation Journal* 31 (3): 35–48. https://doi.org/10.1002/rem.21681.

USACE. 1995. "Engineering and Design: Geophysical Exploration for Engineering and Environmental Applications, Engineer Manual." Engineer Manual EM 1110-1-1802. Department of the Army, U.S. Army Corps of Engineers, August 31. https://www.publications.usace.army.mil/Portals/76/Publications/EngineerManuals/EM_1110-1-1802.pdf#:~:text=This%20manual%20provides%20an%20introduction%20to%20geophysical%20exploration,for%20geophysical%20methods%20typically%20used%20in%20these%20investigations.

USACE. 2008. *Former Kirksville Air Force Station, Missouri*. FUDS PROJECT NO. B07MO023204. U.S. Army Corps of Engineers.

USACE. 2023. *Conceptual Site Models*. Engineer Manual EM 200-1-12. US Army Corps of Engineers. https://www.publications.usace.army.mil/Portals/76/Publications/EngineerManuals/EM%2020 0-1-12_2023Aug11.pdf.

USDA. 2009. "Ground-Penetrating Radar Soil Suitability Maps." U.S. Department of Agriculture. http://websoilsurvey.sc.egov.usda.gov/.

USEPA. 1991. "Risk Assessment Guidance, Volume I Human Health Evaluation Manual (Part B, Development of Risk-Based Preliminary Remediation Goals)." United State Environmental Protection Agency, December. https://semspub.epa.gov/work/HQ/156739.pdf.

USEPA. 1993a. *Subsurface Characterization and Monitoring Techniques: A Desk Reference Guide.* Subsurface Characterization and Monitoring Techniques: A Desk Reference Guide. United State Environmental Protection Agency. https://nepis.epa.gov/Exe/ZyNET.exe/30004L8E.TXT?ZyActionD=ZyDocument&Client=EPA&Index=1991+Thru+1994&Docs=&Query=&Time=&EndTime=&SearchMethod=1&TocRestrict=n&Toc=&TocEntry=&QField=&QFieldYear=&QFieldMonth=&QFieldDay=&IntQFieldOp=0&ExtQFieldO

p=0&XmlQuery=&File=D%3A%5Czyfiles%5CIndex%20Data%5C91thru94%5CTxt%5C00000009%5C30004L8E.txt&User=ANONYMOUS&Password=anonymous&SortMethod=h%7C-&MaximumDocuments=1&FuzzyDegree=0&ImageQuality=r75g8/r75g8/x150y150g16/i425&Display=hpfr&DefSeekPage=x&SearchBack=ZyActionL&Back=ZyActionS&BackDesc=Results%20page&MaximumPages=1&ZyEntry=1&SeekPage=x&ZyPURL.

USEPA. 1993b. "Use of Airborne, Surface, and Borehole Geophysical Techniques at Contaminated Sites, A Reference Guide EPA/625/R-92/007." United State Environmental Protection Agency, September. https://www.epa.gov/system/files/documents/2024-11/epa-reference-guide-use-of-airborne-surface-borehole-geophysical-techniques-at-contaminated-sites.pdf.

USEPA. 2006. *Guidance on Systematic Planning Using the Data Quality Objectives Process*. EPA/240/B-06/001. United State Environmental Protection Agency. https://www.epa.gov/sites/default/files/documents/guidance_systematic_planning_dqo_process.pdf.

USEPA. 2007. *Management and Interpretation of Data Under a Triad Approach – Technology Bulletin*. EPA 542-F-07-001. United States Environmental Protection Agency. https://19january2021snapshot.epa.gov/sites/static/files/2015-05/documents/management_and_interpretation_of_data.pdf.

USEPA. 2008. "Triad Issue Paper: Using Geophysical Tools to Develop the Conceptual Site Model." United State Environmental Protection Agency, December.

USEPA. 2011. *Environmental Cleanup Best Management Practices: Effective Use of the Project Life Cycle Conceptual Site Model*. EPA 542-F-11-011. United States Environmental Protection Agency. https://www.epa.gov/sites/default/files/2015-04/documents/csm-life-cycle-fact-sheet-final.pdf.

USEPA. 2016a. *Expected Site Assessment Tools For Underground Storage Tank Sites: A Guide For Regulators*. United States Environmental Protection Agency.

USEPA. 2016b. *Expedited Site Assessment Tools for Underground Storage Tank Sites: A Guide for Regulators*. United State Environmental Protection Agency.

USEPA. 2016c. *Fifth Five-Year Review Report for Bayou Bonfouca Superfund Site, Slidell, St. Tammany Parish, Louisiana*. United State Environmental Protection Agency.

USEPA. 2016d. "Ground-Penetrating Radar." Environmental Geophysics, United State Environmental Protection Agency, May 24. https://archive.epa.gov/esd/archive-geophysics/web/html/ground-penetrating_radar.html.

USEPA. 2017. "Low Stress (Low Flow) Purging and Sampling Procedure for the Collection of Groundwater Samples from Monitoring Wells, EQASOP-GW4." United State Environmental Protection Agency; Region 1, January.

USEPA. 2018a. *Best Practices for Data Management Technical Guide*. Washington D.C.

USEPA. 2018b. "Ground Penetrating Radar." Geophysical Methods, United State Environmental Protection Agency. https://clu-in.org/characterization/technologies/default2.focus/sec/Geophysical_Methods/cat/Ground_Penetrating_Radar/.

USEPA. 2018c. "Membrane Interface Probe (MIP)." USEPA Clu-In, United State Environmental Protection Agency. https://cluin.org/characterization/technologies/mip.cfm.

USEPA. 2018d. "Smart Scoping for Environmental Investigations Technical Guide." United States Environmental Protection Agency. https://semspub.epa.gov/work/HQ/100001799.pdf.

USEPA. 2018e. *Smart Scoping for Environmental Investigations Technical Guide*. EPA ID # 542-G-18-004. United States Environmental Protection Agency. https://semspub.epa.gov/work/HQ/100001799.pdf.

USEPA. 2023. *High Resolution Site Characterization at Petroleum Underground Storage Tank Release Sites – Applicability, Benefits, and Costs*. United States Environmental Protection Agency. https://www.epa.gov/system/files/documents/2023-04/High%20Resolution%20Site%20Characterization%20Study%20Report.pdf.

USEPA. 2025a. "Characterization and Monitoring Technology Guides for Cleaning Up Contaminated Sites." Technologies for Cleaning Up Contaminated Sites, United States Environmental Protection Agency, October 2. https://www.epa.gov/remedytech/characterization-and-monitoring-technology-guides-cleaning-contaminated-sites.

USEPA. 2025b. "Fluid-Temperature and Fluid-Conductivity Logging." Environmental Geophysics, United States Environmental Protection Agency. https://www.epa.gov/environmental-geophysics/fluid-temperature-and-fluid-conductivity-logging.

USEPA. 2025c. "Ground Penetrating Radar (GPR)." Environmental Geophysics, United States Environmental Protection Agency. https://www.epa.gov/environmental-geophysics/ground-penetrating-radar-gpr.

USEPA. 2025d. *Implementing Direct Sensing High Resolution Site Characterization at EPA UST Release Sites in Indian Country*. EPA-510-R-25-001. U.S. Environmental Protection Agency Office of Underground Storage Tanks. https://www.epa.gov/system/files/documents/2025-03/hrsc-indian-country-2025-03-04.pdf.

USEPA. 2026. "Ground Penetrating Radar (GPR)." Environmental Geophysics, United State Environmental Protection Agency. https://www.epa.gov/environmental-geophysics/ground-penetrating-radar-gpr.

USGS. 2000a. "Geophysical Logs - Gamma Logs." https://www.usgs.gov/media/images/geophysical-logs-gamma-logs.

USGS. 2000b. "Geophysical Logs - Spontaneous-Potential Log." https://www.usgs.gov/media/images/geophysical-logs-spontaneous-potential-log.

USGS. 2000c. "Geophysical Logs - Temperature Logs." https://www.usgs.gov/media/images/geophysical-logs-temperature-logs.

USGS. 2007. *Borehole Geophysical Logging of Water-Supply Wells in the Piedmont, Blue Ridge, and Valley and Ridge, Georgia*. Department of the Interior, U.S. Geological Survey. https://pubs.usgs.gov/fs/2007/3048/pdf/fs2007-3048.pdf.

USGS. 2016a. "Fractured Rock Geophysical Toolbox Method Selection Tool (FRGT-MST)." USGS Software Releases. https://www.usgs.gov/software/fractured-rock-geophysical-toolbox-method-selection-tool-frgt-mst.

USGS. 2016b. "Vertical Flowmeter Logging." https://water.usgs.gov/ogw//bgas/flowmeter/.

USGS. 2018a. "FLASH: A Computer Program for Flow-Log Analysis of Single Holes." https://www.usgs.gov/node/279273.

USGS. 2018b. "Fractured Rock Geophysical Toolbox Method Selection Tool (FRGT-MST)." January 25. https://www.usgs.gov/software/fractured-rock-geophysical-toolbox-method-selection-tool-frgt-mst.

USGS. 2019a. "Earth Explorer." https://earthexplorer.usgs.gov/.

USGS. 2019b. "Fiber-Optic Distributed Temperature Sensing Technology for Surface-Water and Groundwater Studies." Water Resources Mission Area, Washington, D.C., February 24. https://www.usgs.gov/mission-areas/water-resources/science/fiber-optic-distributed-temperature-sensing-technology#overview.

Van de Putte, W., S. Van Herreweghe, W. Vansina, et al. 2012. "On-Site Component-Specific Detection of Volatile Organic Components with the EnISSA MIP." Battelle 8th International Conference: Remediation of Chlorinated & Recalcitrant Compounds, May.

Van Nostrand, Robert Gaige, and Kenneth L. Cook. 1966. *Interpretation of Resistivity Data*. Report No. 499. Professional Paper. Washington, D.C. https://pubs.usgs.gov/publication/pp499.

Varon, D. J., D. Jervis, J. McKeever, I. Spence, D. Gains, and D. J. Jacob. 2021. "High-Frequency Monitoring of Anomalous Methane Point Sources with Multispectral Sentinel-2 Satellite Observations." *Atmospheric Measurement Techniques* 14 (4): 2771–85. https://doi.org/10.5194/amt-14-2771-2021.

VDEQ. 2017. *DEQ's Northern Region Petroleum Program Current Understanding of the Robinson Terminal North – the Former Washington Post Paper Depot*. Virginia Department of Environmental Quality. https://www.deq.virginia.gov/Portals/0/DEQ/Land/Tanks/rtn_cssummary.pdf.

Villa, Tommaso F., Felipe Gonzalez, Branka Miljievic, Zoran D. Ristovski, and Lidia Morawska. 2016. "An Overview of Small Unmanned Aerial Vehicles for Air Quality Measurements: Present Applications and Future Prospectives." *Sensors* 16 (7): 1072. https://doi.org/10.3390/s16071072.

Walker, S. E., M. Sheaves, and N. J. Waltham. 2023. "Barriers to Using UAVs in Conservation and Environmental Management: A Systematic Review." *Environmental Management* 71 (5): 1052–64. https://doi.org/10.1007/s00267-022-01768-8.

Weston. 2014. *Remedial Investigation Report, Savage Municipal Water Supply, Superfund Site OU3, 621 Elm Street, Milford, New Hampshire*. Translated by Hazardous Waste Remediation Bureau. Concord, New Hampshire.

Wiedemeier, Todd H., John T. Wilson, David L. Freedman, and Brady Lee. 2017. *Providing Additional Support for MNA by Including Quantitative Lines of Evidence for Abiotic Degradation and Cometabolic Oxidation of Chlorinated Ethylenes*. Technical Report ER-201584. https://www.researchgate.net/publication/327160472_Providing_Additional_Support_for_MNA_by_Including_Quantitative_Lines_of_Evidence_for_Abiotic_Degradation_and_Co-metabolic_Oxidation_of_Chlorinated_Ethylenes.

Wightman, W., Frank Jalinoos, Kanaan Hanna, and Philip Sirles. 2004. *Application of Geophysical Methods to Highway Related Problems*. FHWA-IF-04-021. US Department of Transportation, Federal Highway Administration. https://rosap.ntl.bts.gov/view/dot/49856.

Williams, John H., and Carole D. Johnson. 2004. "Acoustic and Optical Borehole-Wall Imaging for Fractured-Rock Aquifer Studies." *Journal of Applied Geophysics* 55 (1): 151–59. https://doi.org/https://doi.org/10.1016/j.jappgeo.2003.06.009.

Winner, Edward. 2025. "Planning, Projecting, and Paying: How to Save Dollars through 'Risk-Informed' Decision Making." National Tank Conference, September 23. https://neiwpcc.org/wp-content/uploads/2025/10/5C_Winner_Controlling-Cost_Wednesday.pdf.

Wu, Chaoyang, Zheng Niu, Quan Tang, and Wenjiang Huang. 2008. "Estimating Chlorophyll Content from Hyperspectral Vegetation Indices: Modeling and Validation." *Agricultural and Forest Meteorology* 148 (8): 1230–41. https://doi.org/10.1016/j.agrformet.2008.03.005.

Xu, Wei, Yunfei Cai, Song Gao, et al. 2021. "New Understanding of Miniaturized VOCs Monitoring Device: PID-Type Sensors Performance Evaluations in Ambient Air." *Sensors and Actuators B: Chemical* 330 (March): 129285. https://doi.org/10.1016/j.snb.2020.129285.

Yan, Kai, Si Gao, Guangjian Yan, et al. 2025. "A Global Systematic Review of the Remote Sensing Vegetation Indices." *International Journal of Applied Earth Observation and Geoinformation* 139 (May): 104560. https://doi.org/10.1016/j.jag.2025.104560.

Yanq, Q., X. Liu, and W. Wu. 2020. *A Hyperspectral Bidirectional Reflectance Model for Land Surface*. Sensors. 2020; 20(16):4456. https://doi.org/https://doi.org/10.3390/s20164456.

Yilmaz, Ozdogan. 2001. *Seismic Data Analysis.* Society of Exploration Geophysicists. https://doi.org/https://doi.org/10.1190/1.9781560801580.

Zimbron, Julio. 2020. "Methods, Systems, and Devices for Measuring in Situ Saturations of Petroleum and NAPL in Soils." United States Patent Application. United States Patent and Trademark Office, September 24. https://patentimages.storage.googleapis.com/fe/be/43/7cf08ee3e20493/US20200300761A1.pdf.

Zimbron, Julio A., and Christian C. Rayo. 2025. "Repeatable Imaging of Soil Processes Through a Stabilized Port: Examples of (i) Soil Contaminants and (Ii) Plant Root Growth." *Sensors* 25 (3): 968. https://doi.org/10.3390/s25030968.

Zimmerle, Daniel, Timothy Vaughn, Clay Bell, Kristine Bennett, Parik Deshmukh, and Eben Thoma. 2020. "Detection Limits of Optical Gas Imaging for Natural Gas Leak Detection in Realistic Controlled Conditions." *Environmental Science & Technology* 54 (18): 11506–14. https://doi.org/10.1021/acs.est.0c01285.

APPENDIX A. SUMMARY AND SELECTION RESOURCE FOR THE PVP FAMILY OF TOOLS

Tool Type	Overview	Ideal Measurement Environment	Measurement Type	Calibration Required?	Average Measurement Duration
Point Velocity Probe (PVP)	The PVP is the oldest and most widely utilized tool in the PVP family. The PVP is a point-scale measurement device capable of collecting co-located groundwater velocity and water sample measurements. Installations of PVP require dedicated boreholes and permanent installations. PVP have been deployed with great success in transects along critical boundaries and at various areas of concern at industrial sites worldwide.	Unconsolidated, saturated, porous media. General rule of thumb is less than 20% silt and clay fraction.	Groundwater velocity with ability to measure horizontal, vertical, and composite flow directions (3-dimensions).	No additional measurements are required for determination of groundwater velocity.	0.5 - 48 hours
HRX·PVP	An adaptation of the PVP for measurement of groundwater velocity in one dimension, originally designed for use in the Horizontal Reactive Media Well (HRX Well[8]).	Unconsolidated, saturated, porous media. Designed and tested for use in cylindrical well casing or benchtop column experiments.	Groundwater velocity in one-dimension that is a function of the installation orientation of the tool	No additional measurements are required for determination of groundwater velocity	0.25 - 5 hours
Streambed PVP (SBPVP)	The SBPVP is a tool specifically designed to investigate groundwater surface water interactions. The tools sits on the base of a drivepoint that is inserted into upper 3 inches (7 cm) of lakebed and streambed sediments	Soft-bottomed lakebed and streambed environments	Groundwater velocity with the ability to measure strictly vertical groundwater surface water exchanges. Additionally, the SBPVP can measure the horizontal, vertical, or composite components of hyporheic flow	No additional measurements are required for determination of groundwater velocity	0.1 - 5 hours
In-Well PVP (IWPVP)	The IWPVP is a tool specifically designed for the rapid characterization of groundwater flux within the screened intervals of groundwater monitoring wells within porous media aquifers. IWPVPs are easily deployed and recovered from monitoring wells and are therefore not dedicated instruments.	New or existing groundwater monitoring wells that have recently been developed to ensure good hydraulic connection with surrounding formation.	Horizontal groundwater flux within the monitoring well that can be calibrated to estimate the groundwater flux and/or seepage velocity in the surrounding formation.	Yes, because the measurements are conducted within wells the measured flux must be transformed to groundwater flux outside the well via a calibration line. An estimate of effective porosity is also required to further transform the estimated fluxes to velocities.	0.01 - 0.75 hours
Fractured Rock In-Well PVP (F-IWPVP)	The F-IWPVP is a tool specifically designed for the rapid characterization of groundwater flux within the screened intervals of groundwater monitoring wells and competent boreholes within fractured rock aquifers. F-IWPVPs are easily deployed and recovered from monitoring wells and are therefore not dedicated instruments.	New or existing groundwater monitoring wells or boreholes that have recently been developed to ensure good hydraulic connection with surrounding formation and all drilling fluids have been flushed.	Horizontal groundwater flux within the borehole that can be calibrated to estimate the groundwater velocity in the corresponding fractures or rock matrix. A qualitative measure of vertical borehole flow may also be possible.	Yes, because the measurements are conducted within boreholes the measured flux must be transformed to groundwater flux outside the well via a calibration line. Due to the nature of fractured media, an estimate of fracture aperture is required for accurate calibration of fractures velocities.	0.01 - 0.75 hours

Source: Ozark 2021, used with permission; "Ozark Underground Laboratory's Point Velocity Probe Handbook".

APPENDIX B. REMOTE SENSING DATA SOURCES

Category	Program	Agency	Sensor	Platform	Application	Coverage	Resolution	Per-Sensor Resolution Details
Multispectral	Landsat Program	USGS / NASA	MSS; TM; ETM+	Satellite	Moderate-resolution land surface observation	Global land coverage	30 m multispectral; 15 m pan; thermal 60–100 m (resampled to 30 m)	MSS: ~60 m; TM: 30 m; ETM+: 30 m multispectral, 15 m pan; TIRS: 100 m (resampled to 30 m)
	USGS EarthExplorer	USGS	Landsat (MSS, TM, ETM+); AVHRR; Declassified imagery	Satellite	Data discovery & download for multispectral archives	Global & U.S. (varies by dataset)	Varies by dataset	Varies by sensor/product
	LP DAAC	USGS / NASA	MODIS; ASTER	Satellite	Land data distribution (multispectral products)	Global (varies by mission/data product)	Varies by mission (e.g., MODIS 250–1000 m; ASTER 15–90 m; ECOSTRESS ~70 m; GEDI footprint-scale)	MODIS: 250 m (bands 1-2), 500 m (bands 3-7), 1 km (thermal); ASTER: VNIR 15 m, SWIR 30 m, TIR 90 m; ECOSTRESS: ~70 m
	NASA Earthdata Search	NASA	MODIS; ASTER; others across DAACs	Satellite	Cross-DAAC search and access for Earth science data	Global (aggregates many missions)	Varies by dataset	Aggregates multiple missions; resolution varies by dataset
	PO.DAAC	NASA JPL	AVHRR (sea surface temperature)	Satellite	Physical oceanography (SST and related)	Global oceans & surface water	Varies (e.g., SST ~1 km; altimetry cm-level height grids)	AVHRR SST ~1 km; other ocean sensors vary (altimetry cm-level)
	NSIDC DAAC	NASA	Various cryosphere-related sensors	Satellite	Cryosphere data access	Polar regions & global cryosphere	Varies (snow/ice products from tens of m to km)	Cryosphere products vary: 25 km passive microwave to 30 m optical
	NESDIS	NOAA	AVHRR	Satellite	Weather/ocean monitoring data archive and access	Global (operational NOAA satellites)	Varies by instrument (e.g., VIIRS, AVHRR)	AVHRR: ~1.1 km; VIIRS: 375 m (I-bands), 750 m (M-bands)
	National Climatic & Oceanographic Data Centers	NOAA	Multiple (incl. remotely sensed products)	Satellite	Meteorological and oceanographic data access	Global & U.S. (NOAA archives)	Varies by product	Varies by sensor/product
	NAIP	USDA	Aerial cameras (leaf-on orthoimagery)	Airborne	Agriculture & forestry applications	CONUS (leaf-on seasons)	0.60 m (typ.); 0.30 m in some states/years	Aerial imagery: 0.60 m typical; 0.30 m in some states/years
	Environmental Dataset Gateway / RSIG	EPA	Various (access portals)	Various	Environmental datasets incl. remote sensing	U.S. environmental datasets (varies)	Varies	Varies by sensor/product
	Data.gov	US Federal (catalog)	Various	Various	Catalog of government datasets	U.S. Federal (catalog; varies)	Varies	Varies by sensor/product

Appendix B. Remote Sensing Data Sources

Category	Program	Agency	Sensor	Platform	Application	Coverage	Resolution	Per-Sensor Resolution Details
Hyperspectral	AVIRIS (incl. AVIRIS-NG) operations	NASA / JPL	AVIRIS; AVIRIS-NG	Airborne	Research-grade imaging spectroscopy	Airborne campaigns (site-specific)	Airborne; meter-scale pixels (campaign-dependent)	Airborne hyperspectral: ~4-20 m pixel size depending on altitude
	HyspIRI (planned)	NASA	HyspIRI	Satellite (planned)	Space-based hyperspectral (future)	Mission concept (not operational)	Mission concept; not operational	Planned: VNIR 30 m, SWIR 60 m (concept)
	NASA Earthdata Search	NASA	Hyperspectral datasets via DAACs	Satellite/ Airborne	Discovery and access to hyperspectral products	Global (aggregates many missions)	Varies by dataset	Aggregates multiple missions; resolution varies by dataset
	USGS EROS (hyperspectral facilitation)	USGS	Various (project-based hyperspectral)	Airborne	Access/support for hyperspectral applications	U.S. projects (as available)	Varies by project	Varies by sensor/product
	USGS Spectral Library	USGS	Reference spectra (materials)		Analysis support for imaging spectroscopy	N/A (reference library)		Varies by sensor/product
	CrIS (atmospheric sounder)	NOAA	CrIS	Satellite	Weather forecasting & climate monitoring	Global atmosphere	Sounder FOV (km-scale) varying by product	Spectral sounder: footprint ~14 km at nadir
	Data.gov (hyperspectral listings)	US Federal (catalog)	Various	Various	Dataset indexing across agencies	U.S. Federal (catalog; varies)	Varies	Varies by sensor/product
Photogrammetry	The National Map	USGS	Aerial cameras; satellite imagery (source data)	Airborne/ Satellite	Topographic data, orthoimagery, DEMs	United States	Product-dependent (e.g., DEM 1 m–10 m; imagery high-res)	Varies by sensor/product
	3D Elevation Program (3DEP)	USGS	LiDAR; photogrammetry in some areas	Airborne	High-resolution elevation (DEMs, point clouds)	United States (national program)	QL2 or better lidar; typical 1 m DEM / dense point clouds	Varies by sensor/product
	EarthExplorer	USGS	Historical aerial photos; modern orthoimagery	Airborne	Search & download of aerial/satellite imagery	Global & U.S. (varies by dataset)	Varies by dataset	Varies by sensor/product
	National Geodetic Survey (NGS)	NOAA	Aerial imagery for coastline/near-shore	Airborne	Coastal mapping & elevation	U.S. coasts & near-shore	High-accuracy coastal imagery/elevation (varies)	Varies by sensor/product
	Office for Coastal Management (OCM)	NOAA	Aerial imagery; elevation (photogrammetry-derived)	Airborne	Coastal resilience & habitat mapping	U.S. coasts	High-res coastal imagery & elevation (varies)	Varies by sensor/product
	NOAA Data Access Viewer	NOAA	Aerial imagery; elevation products	Airborne	Coastal GIS data discovery and download	U.S. coasts (coastal counties & near-shore)	High-res coastal imagery & lidar (varies)	Varies by sensor/product
	NAIP	USDA	Leaf-on aerial imagery	Airborne	Agriculture and resource management	CONUS (leaf-on seasons)	0.60 m (typ.); 0.30 m in some states/years	Aerial imagery: 0.60 m typical; 0.30 m in some states/years

Appendix B. Remote Sensing Data Sources

Category	Program	Agency	Sensor	Platform	Application	Coverage	Resolution	Per-Sensor Resolution Details
Photogrammetry	USACE (various)	USACE	Aerial & bathymetric surveys	Airborne	Flood risk, navigation, restoration	United States (project areas)	Engineering-grade topo/bathy (varies)	Varies by sensor/product
	FEMA (Mapping Information Platform)	FEMA	High-accuracy elevation (photogrammetry-derived)	Airborne	Flood insurance rate maps (FIRMs)	United States (flood mapping areas)	Elevation suitable for FIRMs (varies)	Varies by sensor/product
	Data.gov / GeoPlatform.gov	US Federal (catalog)	Various	Various	Centralized discovery of photogrammetry datasets	U.S. Federal (catalog; varies)	Varies	Varies by sensor/product
Orthoimagery	The National Map	USGS	NAIP (distributed); aerial & satellite sources	Airborne/ Satellite	Access to orthoimagery products	United States	Product-dependent (e.g., DEM 1 m–10 m; imagery high-res)	Varies by sensor/product
	EarthExplorer	USGS	NAPP; historical aerial; satellite ortho	Airborne/ Satellite	Search & download of orthoimagery	Global & U.S. (varies by dataset)	Varies by dataset	Varies by sensor/product
	High Resolution Orthoimagery (HRO)	USGS (with partners)	High-resolution aerial imagery	Airborne	High-resolution orthos for partnerships	U.S. urban/partner areas	High-resolution aerial orthos (sub-meter)	Varies by sensor/product
	NAIP	USDA	Leaf-on aerial imagery	Airborne	Nationwide agricultural orthoimagery	CONUS (leaf-on seasons)	0.60 m (typ.); 0.30 m in some states/years	Aerial imagery: 0.60 m typical; 0.30 m in some states/years
	NOAA Digital Coast / Data Access Viewer	NOAA OCM/NGS	Coastal high-resolution imagery	Airborne	Coastal management & emergency response	U.S. coasts	High-res coastal orthos & lidar (varies)	Varies by sensor/product
	NASA Earthdata Portal	NASA	Satellite imagery (e.g., Landsat)	Satellite	Access to satellite data used to generate orthos	Global (satellite missions)	Varies	Varies by sensor/product
Thermal Imagery	LP DAAC	USGS / NASA	ASTER (TIR); MODIS	Satellite	Thermal infrared & land surface temperature products	Global (varies by mission/data product)	Varies by mission (e.g., MODIS 250–1000 m; ASTER 15–90 m; ECOSTRESS ~70 m; GEDI footprint-scale)	MODIS: 250 m (bands 1-2), 500 m (bands 3-7), 1 km (thermal); ASTER: VNIR 15 m, SWIR 30 m, TIR 90 m; ECOSTRESS: ~70 m
	PO.DAAC & LP DAAC (ECOSTRESS)	NASA JPL / NASA	ECOSTRESS	ISS	Plant water use & heat stress	52°N to 52°S (ISS ground track)	~70 m pixels (ECOSTRESS)	Varies by sensor/product
	GES DISC	NASA	AIRS	Satellite	Atmospheric thermal data	Global (atmosphere & land; varies by product)	Varies by dataset	AIRS: ~13.5 km footprint; other atmospheric sensors vary

Appendix B. Remote Sensing Data Sources

Category	Program	Agency	Sensor	Platform	Application	Coverage	Resolution	Per-Sensor Resolution Details
Thermal Imagery	Landsat Program	USGS / NASA	TM (thermal); ETM+ (thermal); TIRS	Satellite	Surface temperature, water management, geothermal	Global land coverage	30 m multispectral; 15 m pan; thermal 60–100 m (resampled to 30 m)	MSS: ~60 m; TM: 30 m; ETM+: 30 m multispectral, 15 m pan; TIRS: 100 m (resampled to 30 m)
	NESDIS	NOAA	AVHRR; VIIRS	Satellite	Weather/climate & sea/land surface temperature	Global (operational NOAA satellites)	Varies by instrument (e.g., VIIRS, AVHRR)	AVHRR: ~1.1 km; VIIRS: 375 m (I-bands), 750 m (M-bands)
	NOAA Data Centers (NCEI/OCM)	NOAA	AVHRR; VIIRS	Satellite	Access to thermal sensor products	Global & U.S. (varies by product)	Varies	Varies by sensor/product
LiDAR	3D Elevation Program (3DEP)	USGS	Airborne LiDAR (QL2 or better)	Airborne	Nationwide high-resolution elevation data	United States (national program)	QL2 or better lidar; typical 1 m DEM / dense point clouds	Varies by sensor/product
	USGS Lidar Explorer / The National Map	USGS	LiDAR point clouds; DEMs	Airborne	Find, visualize, and download LiDAR data	United States (available project areas)	Point clouds (LAS); DEMs (often 1 m)	Airborne LiDAR: QL2 (~1 m DEM); point density ≥2 pts/m²
	NOAA Digital Coast / Data Access Viewer	NOAA OCM/NGS	Topographic & topobathymetric LiDAR	Airborne	Coastal elevation, flood modeling, erosion studies	U.S. coasts	High-res coastal orthos & lidar (varies)	Varies by sensor/product
	ICESat-2 (NSIDC DAAC)	NASA	ATLAS (ICESat-2)	Satellite	Ice sheet elevation, sea ice freeboard, canopy height	Global (satellite tracks)	Small-footprint photon-counting lidar (footprint-scale)	Photon-counting LiDAR: footprint ~11 m, along-track spacing ~0.7 m
	GEDI (LP DAAC)	NASA	GEDI	ISS	Forest canopy height & structure	52°N to 52°S (ISS ground track)	Footprint-scale canopy metrics (ISS-based)	LiDAR footprints ~25 m diameter; waveform vertical resolution ~1 m
	JALBTCX	USACE	Airborne topo-bathymetric LiDAR	Airborne	Coastal & inland waterway mapping	U.S. coasts & inland waterways	Topo-bathy lidar (sub-meter–meter scale)	Topo-bathymetric LiDAR: sub-meter horizontal accuracy
	USIEI (inventory)	NOAA / USGS	Inventory of high-accuracy elevation datasets	Various	Discover available topo/bathy LiDAR coverage	United States (inventory coverage)	Varies (inventory metadata)	Varies by sensor/product

APPENDIX C. REMOTE SENSING AIR SAMPLING TOOLS

Sensor or Sampler Category	Sensor Type	Technology Principle	Data Type	Gases / Media Detected	Quantitative?	Typical Use	Distinguishing Feature
Direct-Reading Instruments (Real-Time Measurements)	Optical Particle Counter (OPC)	Laser light scattering by airborne particles	Real-time particle counts by size bin	PM_1, $PM_{2.5}$, PM_{10}	Semi-quantitative	Vertical and horizontal PM profiling, dispersion studies	Mobile 3-D PM measurements unavailable from fixed monitors
	Electrochemical gas sensor	Electrochemical oxidation/reduction at electrode	Real-time concentration	CO, NO, NO_2, O_3, SO_2	Semi-quantitative	Ambient pollution mapping, fence-line surveys, leak screening	Low cost, ppb sensitivity, subject to drift
	MOS (metal-oxide semiconductor) sensor	Change in resistance of heated metal-oxide film	Real-time relative signal	Oxidizing gases (NO_2, O_3); reducing gases (VOCs, CO, H_2, NH_3, H_2S)	Qualitative / Semi-quantitative	Presence/absence screening, plume localization	Fast response, broad gas sensitivity, low selectivity
	Catalytic LEL sensor (pellistor)	Oxidation of combustible gas on heated catalyst bead	Real-time %LEL	Methane, propane, flammable gases	No (safety metric)	Safety screening, locating flammable gas plumes	Responds only at combustible concentrations
	Photo-Ionization Detector (PID)	UV photoionization of compounds below lamp IP	Real-time ion current	VOCs (lamp-dependent)	Semi-quantitative	VOC screening, HAZMAT response, landfill and soil-gas surveys	Broad VOC sensitivity, rapid screening
	Integrated multi-sensor unit	Combined electrochemical, MOS, PID, PM sensors	Multi-parameter real-time data	Multiple gases + PM	Semi-quantitative	Screening-level surveys and spatial mapping	Multiple sensors in a single payload
Optical & Spectroscopic Monitoring Systems	Optical Gas Imaging (OGI) camera	Passive IR absorption with narrow-band filtering	Visual plume imagery	Methane, alkanes, NH_3, refrigerants	No (qualitative)	Leak detection, source identification	Visualizes plumes without air contact
	TDLAS (open-path)	Laser absorption along atmospheric path	Path-integrated (ppm·m)	CH_4, CO_2, NH_3, C_2H_2	Yes	Quantitative plume characterization, leak detection	Long-range, rapid response
	TDLAS (closed-path)	Laser absorption in enclosed optical cell	Concentration or ppm·m	CH_4, CO_2, NH_3	Yes	Near-source quantification, controlled sampling	Increased sensitivity via internal path length
	LiDAR–TDLAS hybrid	Laser absorption + range finding	2-D / 3-D concentration fields	Primarily methane	Yes	Advanced plume mapping and emission analysis	Adds plume geometry to absorption data
	NDIR gas analyzer	Broadband IR absorption with optical filters	Real-time concentration	CO_2 (primary), CH_4 (limited)	Yes	Continuous CO_2 monitoring, plume transects	Robust, closed-path IR method
	Tedlar® bag sampler	Active pumping of whole air into polymer bag	Grab sample	VOCs, sulfur compounds, unknown mixtures	Yes (lab-based)	Confirmatory sampling, unknown plume characterization	Captures complete air mixture

Appendix C. Remote Sensing Air Sampling Tools

Sensor or Sampler Category	Sensor Type	Technology Principle	Data Type	Gases / Media Detected	Quantitative?	Typical Use	Distinguishing Feature
Whole-Air Sampling for Laboratory Analysis	Sorbent tube sampler	Adsorption of target compounds onto media	Integrated sample mass	Target VOCs, GHGs, pesticides, PM	Yes (lab-based)	Targeted compound analysis	Requires known analytes
	Miniaturized canister (stainless, Silonite®, quartz)	Evacuated container with controlled fill	Grab or time-integrated sample	VOCs, light hydrocarbons, sulfur compounds	Yes (lab-based)	Defensible or regulatory-grade sampling	High chemical stability and long holding times
Sampling Accessories	Mass-flow controller	Active metering of air flow into sampler	Time-integrated volume	Depends on paired sampler	N/A	Quantitative, defensible sample collection	Enables controlled sampling rates